ZooKeys 1228: 1–9 (2025)
DOI: 10.3897/zookeys.1228.127783

Research Article

A new genus and two new species of Opsiini leafhoppers (Hemiptera, Cicadellidae, Deltocephalinae) from China, with a key to genera

Shangmi Hu[1], Wenjun Cao[1], Jichun Xing[1]

1 *Institute of Entomology, The Provincial Special Key Laboratory for Development and Utilization of Insect Resources, Guizhou University, Guiyang, 550025, China*
Corresponding author: Jichun Xing (xingjichun@126.com)

Abstract

A new genus of the tribe Opsiini (Hemiptera, Cicadellidae, Deltocephalinae), *Odonaellus* **gen. nov.** and two new species, *O. serratus* **sp. nov.** (type species) and *O. expansus* **sp. nov.**, are described and illustrated; they are placed in the subtribe Eremophlepsiina. A key to subtribes and genera of Chinese Opsiini is provided. The type specimens of the new species are deposited in the Institute of Entomology, Guizhou University, Guiyang, China (GUGC).

Key words: Distribution, Homoptera, morphology, new taxa, taxonomy

Academic editor: Christopher H. Dietrich
Received: 18 May 2024
Accepted: 17 December 2024
Published: 13 February 2025

ZooBank: https://zoobank.org/8D398281-38EC-45FA-BC9B-EEBCC69F0EF5

Citation: Hu S, Cao W, Xing J (2025) A new genus and two new species of Opsiini leafhoppers (Hemiptera, Cicadellidae, Deltocephalinae) from China, with a key to genera. ZooKeys 1228: 1–9. https://doi.org/10.3897/zookeys.1228.127783

Introduction

The leafhopper tribe Opsiini belongs to the subfamily Deltocephalinae (Hemiptera, Cicadellidae) with *Opsius* Fieber, 1866 as its type genus. Until now, 42 genera and 353 species were known worldwide. The tribe is identified by the bifurcate aedeagus with two shafts and gonopores (Zahniser and Dietrich 2013). Sixty species belonging to 13 genera have been found in China (Cao and Xing 2022).

In this paper, a new genus *Odonaellus* gen. nov. and two new species from China are described and illustrated: *O. serratus* sp. nov. (type species; Yunnan) and *O. expansus* sp. nov. (Guangxi). Keys to Chinese genera of Opsiini and species of *Odonaellus* are provided. The type specimens of the new species are deposited in the Institute of Entomology, Guizhou University, Guiyang, China (GUGC).

Material and methods

Specimens used in this study were collected from Guangxi and Yunnan, China using a sweep net. Dry male specimens were used for the descriptions and illustrations. External morphology was observed under a stereoscopic microscope and characters were measured with an ocular micrometer. A Nikon SMZ1270 microscope was used to dissect the male genitalia. Color images for adult habitus and male genitalia were obtained using the Keyence VHX-6000 system. The genital segments of the examined specimen were macerated in 10% NaOH. Images were imported into Adobe Photoshop CS8 for labeling and plate composition. Morphological terminology follows Li et al. (2011).

Taxonomy

Tribe Opsiini Emeljanov, 1962

Key to subtribes and genera of Opsiini from China

Modified from Dai et al. 2010; Cao and Xing 2022.

1 Subgenital plates with macrosetae well developed and conspicuous **2**
– Subgenital plates with macrosetae absent or greatly reduced (**Eremophlepsiina**) **3**
2 Mesal margin of eye notched, single T-branched shaft arising from base of aedeagus, with shaft branches forming semicircle (**Circuliferina**) ...... ***Neoaliturus***
– Mesal margin of eye not notched, aedeagal shafts arising from base separately (**Opsiina**) **4**
3 Aedeagus shafts denticulate mesally on distal half .... ***Odonaellus* gen. nov.**
– Aedeagus shafts without denticulation ...... ***Pseudophlepsius***
4 Subgenital plate with an additional lateral plate at base ...... ***Alishania***
– Subgenital plate without additional lateral plate **5**
5 Pygofer with paired sharp lateral process arising ventrally ...... ***Norva***
– Pygofer without process **6**
6 Crown, pronotum, scutellum and forewings with a few, or no, brown spots **7**
– Crown, pronotum, scutellum and forewings with numerous scattered brown spots **9**
7 Aedeagal socle swollen and bulbous ...... ***Opsius***
– Aedeagal socle not swollen **8**
8 Aedeagal shafts with a subapical process ...... ***Japananus***
– Aedeagal shafts with three or four subapical processes ...... ***Japananoides***
9 Forewings with a triangular marble pattern forming in the middle of a darker rhomboidal spot when wings at rest ...... ***Hishimonus***
– Forewings without triangular marble pattern forming in the middle of a darker rhomboidal spot when wings at rest **10**
10 Aedeagus with atrium extending ventrad of shafts ...... ***Litura***
– Aedeagus with atrium not extending ventrad of shaft **11**
11 Aedeagus without basal process arising from socle **12**
– Aedeagus with basal process arising from socle **13**
12 Forewings with symmetrical longitudinal orange stripes ...... ***Yinformibus***
– Forewings without symmetrical longitudinal orange stripes ...... ***Orosius***
13 Aedeagus with two or three pairs of shafts ...... ***Hishimonoides***
– Aedeagus with pair of shafts divided near base ...... ***Introrsa***

Subtribe Eremophlepsiina Dmitriev, 2002

Odonaellus gen. nov.

https://zoobank.org/CDE39C57-F5A6-46C8-8556-424FB53F99E9

Type species. *Odonaellus serratus* sp. nov.

Description. Body yellowish-brown. Crown yellow, with white stripe and a pair of small black spots at apex of crown connected to a black transverse marginal band. Eyes dark brown; ocelli yellowish-brown and on anterior margin of head. Pronotum with anterior yellowish brown and posterior brown. Face pale brown. Forewing yellowish, with brown arched lines and patchy spots. Legs brownish yellow.

Body robust. Head including eyes narrower than pronotum; crown slightly produced medially, shorter than width between eyes; ocelli on anterior margin, separated from corresponding eye by approximately their own diameter; face slightly flattened, its width narrower than length; anteclypeus slightly expanded apically. Pronotum obviously longer than wide, anterior margin strongly and roundly produced, posterior margin slightly concave. Scutellum triangular, wider than long, slightly longer than pronotum, with transverse suture depressed. Forewing hyaline, about 3 times as long as wide, with 4 apical cells and 3 subapical cells; inner subapical cell closed. Fore femur with 2 dorsoapical setae; row IC with stout setae; row AV with short, stout setae; tibia with 2 rows of setae. Hind femur broadened distally and slightly bowed; apical setal formula 2+2+1; tibia flattened and nearly straight, row PD with 28 macrosetae decreasing in length toward base; row AD with approximately 13 long stout setae and 0–4 shorter stout setae between each long seta.

***Male genitalia*.** Male pygofer slightly longer than high, with paired ventral process or dorsal process, without macrosetae, and setae on posterior margin. Valve subtriangular. Subgenital plate without macrosetae or with a few small macrosetae and with wide base, slightly narrowed posteriorly, without digitiform apical extension. Aedeagal shaft arising from base with paired shafts, denticular, curved, U-shaped in ventral view, gonopore subapical. Connective Y-shaped, articulated with aedeagus. Style broad at base, subapically slightly concaved.

Remarks. This new genus is placed in subtribe Eremophlepsiina based on the following: crown concavely depressed, with a pair of apical black submedial maculae; head narrower than the pronotum; wings macropterous; macrosetae on the male subgenital plate reduced or absent, pygofer with paired posterior processes, aedeagus with shafts arising from the base; and the female ovipositor extending far beyond the pygofer apex. The genus is distinguished from other Eremophlepsiina by the lack of irregular brown markings on the head and pronotum, the much less prominent brown vermiculate markings on the forewing, and the apically denticulate shafts of the aedeagus. The two included species differ for some characters mentioned in the subtribal diagnosis provided by Zahniser and Dietrich (2013), suggesting that the genus may be intermediate between Eremophlepsiina and Opsiina (see Remarks for individual species below).

Etymology. The new genus name is derived from the Latin word "*odona*" and the diminutive suffix "*-ellus*", in reference to the denticulate (tooth-like) processes on the aedeagal shaft. Gender: masculine.

Distribution. Oriental region (China).

Key to species of *Odonaellus* gen. nov. from China (males)

1 Pygofer process arising from posterodorsal part of lobe (Fig. 5); aedeagus with base as long as shafts in ventral view (Fig. 10) ....***O. serratus* sp. nov.**

– Pygofer process arising from posteroventral part of lobe (Fig. 21); aedeagus with base much shorter than shafts in ventral view (Fig. 26) ....***O. expansus* sp. nov.**

***Odonaellus serratus* sp. nov.**

https://zoobank.org/F7F35958-C834-4091-8158-DD8F222FCE02
Figs 1–12

Description. Color pattern of anterior dorsum and face as in Figs 1–4. Face yellow with a few brown stripes (Fig. 4).

Other external features as in generic description. ***Male genitalia*.** Male pygofer with one pair of finger-like dorsal processes arising caudally and with a few macrosetae along caudal margin; ventral margin expanded (Figs 5, 6). Valve small (Fig. 7). Subgenital plate with a few stout setae (Fig. 8). Aedeagal shaft lamellar, apical tapered and apcial inner margin dentate; gonopore subapical (Figs 10, 11). Connective with arms shorter than stem (Fig. 9). Style curved, apical apophysis stout and subapically concaved (Fig. 12).

***Measurement*.** Length (including tegmen): ♂, 5.3–5.7 mm.

Type material. ***Holotype*:** • ♂, China: Yunnan, Mengla County, Mohan; 21°22'30"N, 101°75'46"E; 13 May 2015, coll. Qiang Luo (GUGC); ***paratypes*:** • 5 ♂♂, Yunnan, Mengla County, Mohan; 21°13'21"N, 101°44'59"E; 13 May 2015, coll. Qiang Luo; • 3 ♂♂, Yunnan, Mengla County, Menglun; 21°91'32"N, 101°26'83"E; 12 May 2015, coll. Qiang Luo (GUGC).

Etymology. The new species name is Latin adjective *serratus*, "serrate", used in reference to the apically aedeagal shaft toothed like a saw.

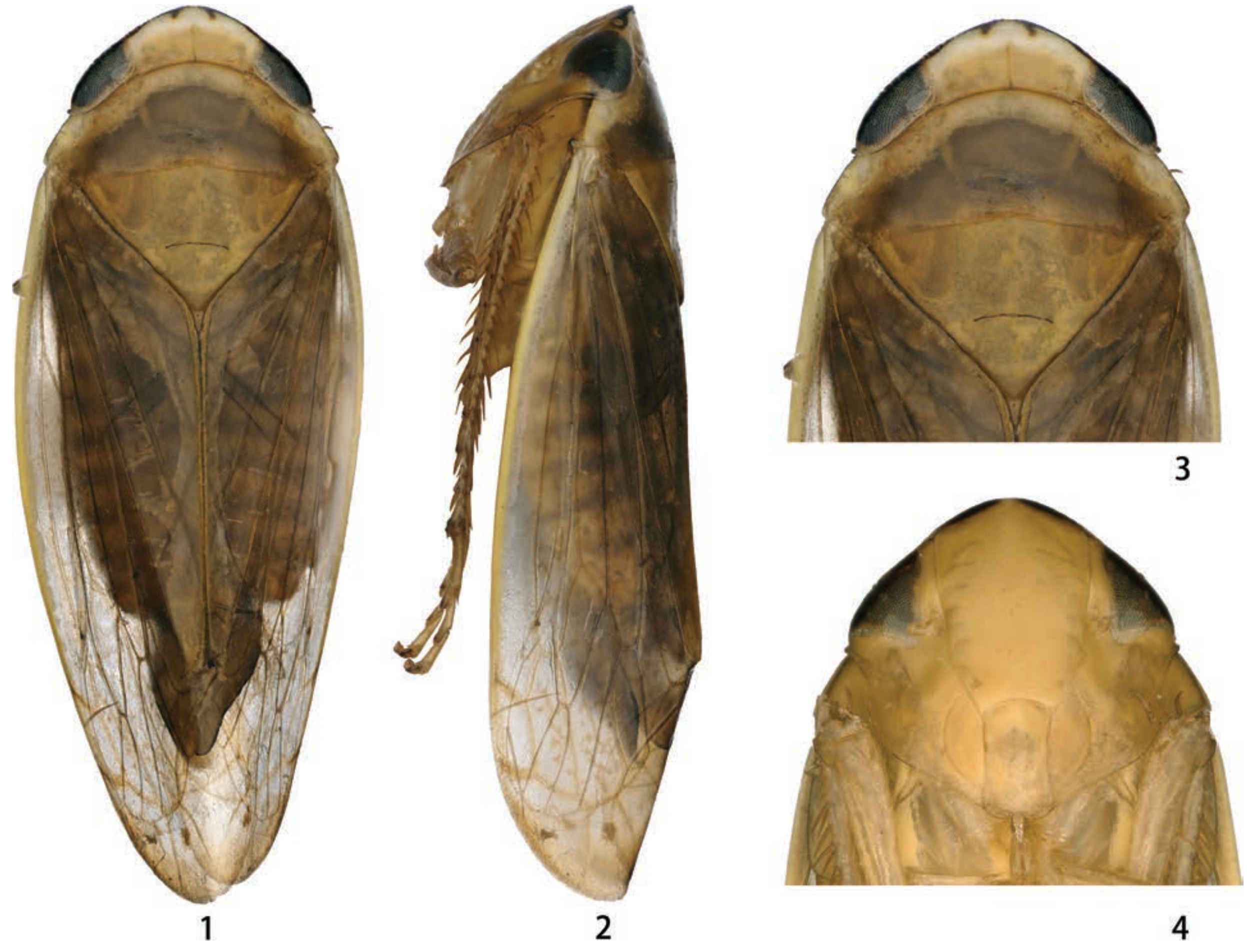

Figures 1–4. *Odonaellus serratus* sp. nov. **1** ♂, dorsal view **2** ♂, lateral view **3** ♂, head and thorax, dorsal view **4** ♂, face.

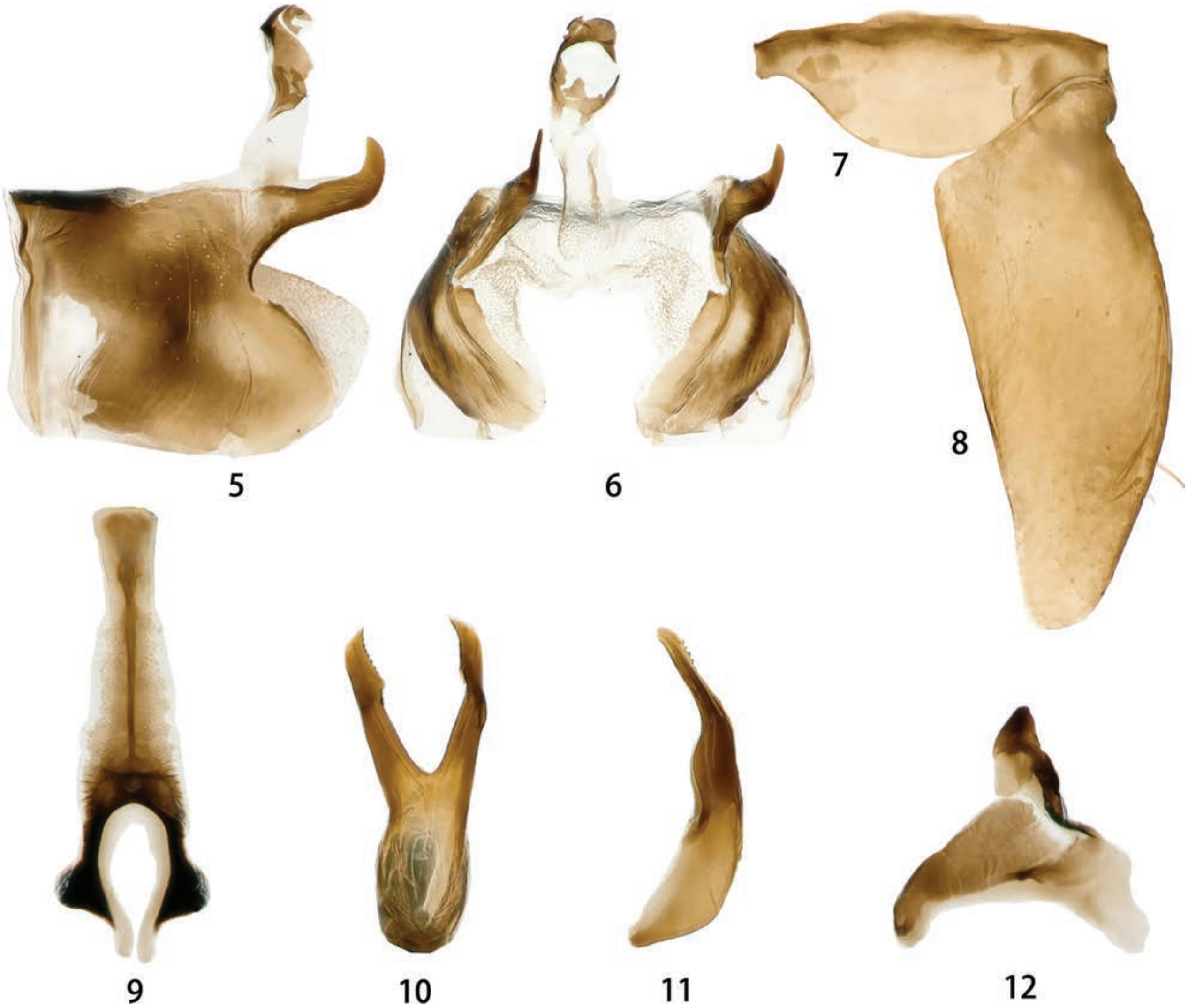

Figures 5–12. *Odonaellus serratus* sp. nov. **5** male pygofer side, lateral view **6** male pygofer side, ventral view **7** valve, ventral view **8** subgenital plates, ventral view **9** connective, ventral view **10** aedeagus, ventral view **11** aedeagus, lateral view **12** style, dorsal view.

Remarks. This species disagrees with the subtribal diagnosis of Eremophlepsiina, as provided by Zahniser and Dietrich (2013), in having small macrosetae present laterally on the male subgenital plate, the pygofer process arising dorsally rather than ventrally, and the valve distinctly shorter than wide.

***Odonaellus expansus* sp. nov.**
https://zoobank.org/662E89F3-915E-44F4-A0C3-3746755C2528
Figs 13–34

Description. Color pattern of anterior dorsum and face as in Figs 13–20. Male pronotum dark brown with irregular fuscous spots (Fig. 15); female pronotum yellowish brown, without spot (Fig. 19).

Other external features as in generic description. *Male genitalia*. Male pygofer with one pair of sharp ventral processes arising caudally and a pair of tiny posteroventral process grown in dorsal inner surface (Figs 21, 22). Valve large

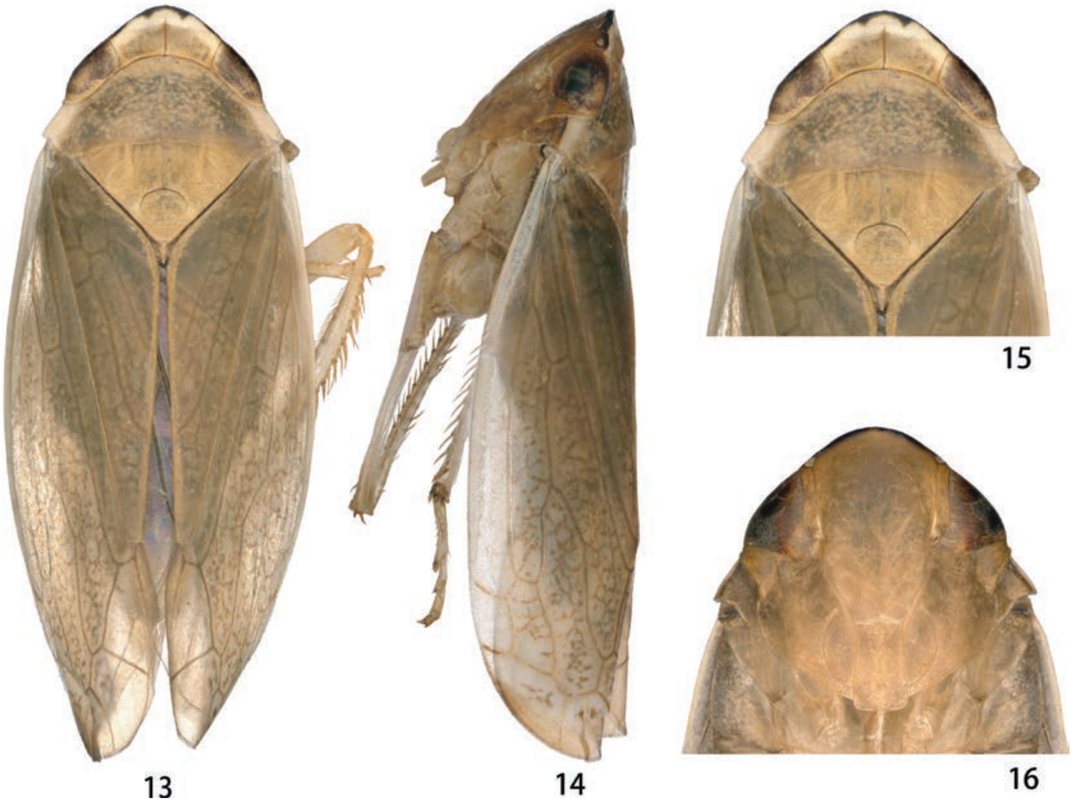

Figures 13–16. *Odonaellus expansus* sp. nov. **13** ♂, dorsal view **14** ♂, lateral view **15** ♂, head and thorax, dorsal view **16** ♂, face.

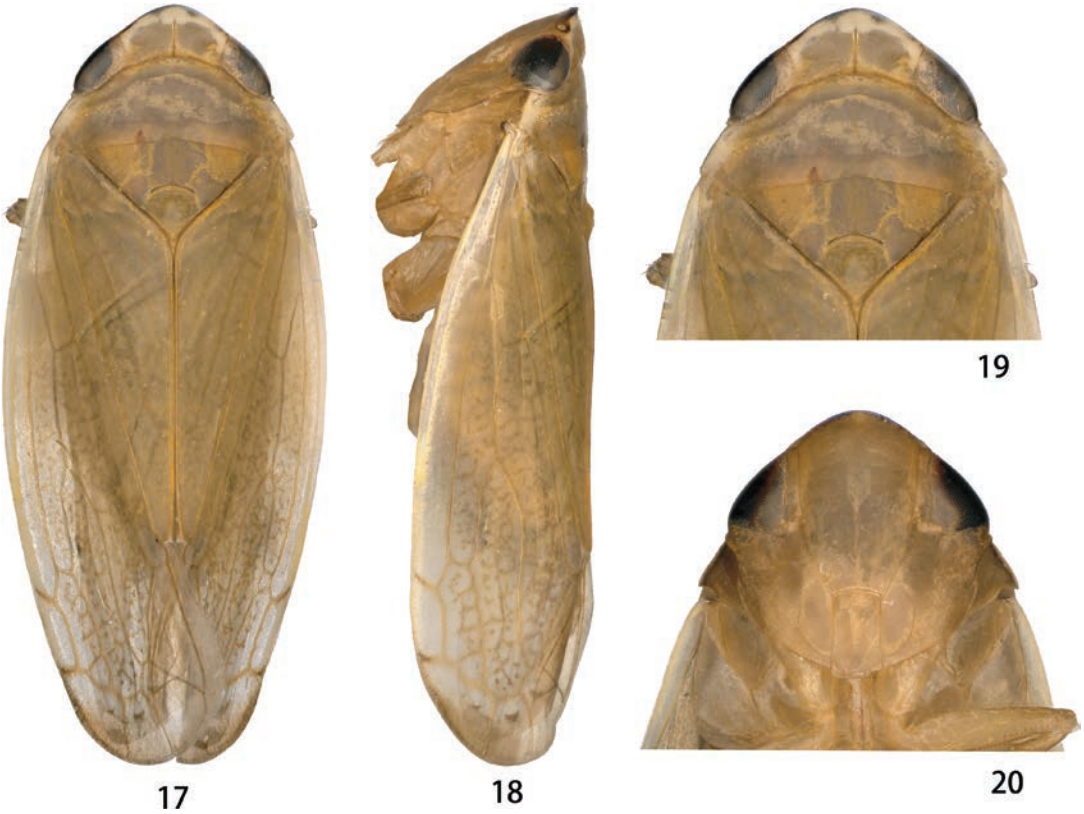

Figures 17–20. *Odonaellus expansus* sp. nov. **17** ♀, dorsal view **18** ♀, lateral view **19** ♀, head and thorax, dorsal view **20** ♀, face.

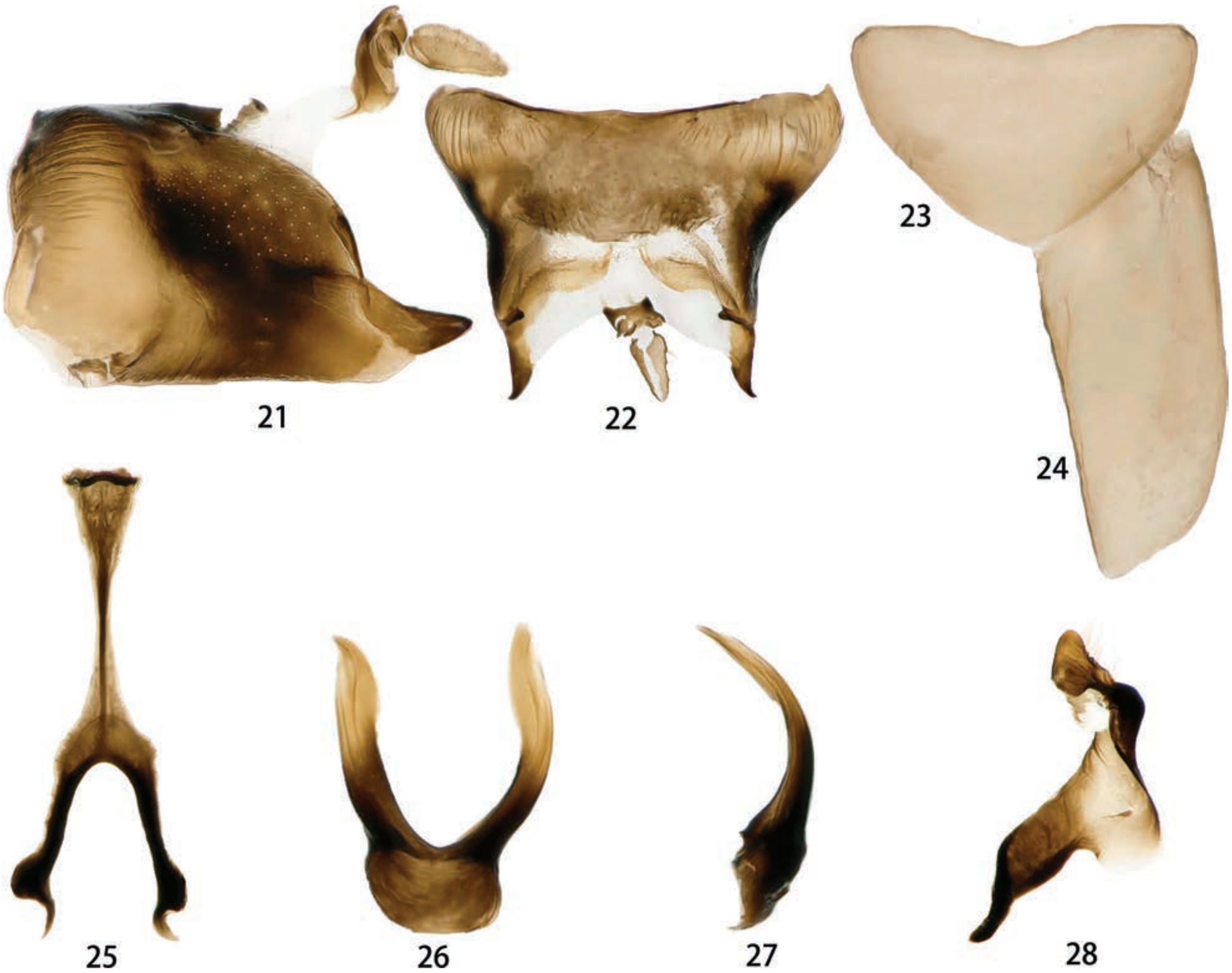

Figures 21–28. *Odonaellus* sp. nov. **21** male pygofer side, lateral view **22** male pygofer side, dorsal view **23** valve, ventral view **24** subgenital plates, ventral view **25** aedeagus, ventral view **26** aedeagus, lateral view **27** connective, ventral view **28** style, dorsal view.

(Fig. 23). Subgenital plate without macrosetae (Fig. 24). Aedeagal shaft auricular and subapical inner margin with a few small dentae; gonopore subapical (Figs 26, 27). Connective with arms shorter than stem (Fig. 25). Style curved; apical apophysis stout and subapically concave. (Fig. 28).

Female pygofer with ventroposterior margin sharply incurved (Fig. 29). Female seventh sternum posterior margin concave, resulting in projection on both sides (Fig. 30). First valvula of ovipositor slightly curved, attenuate to apex, with indistinct scale-like sculpture ventrally (Figs 31, 32). Second valvula with small teeth near apex (Figs 33, 34).

***Measurement*.** Length (including tegmen): ♂, 5.4–5.7 mm; ♀, 5.8–6.5 mm.

Type material. *Holotype*: • ♂, CHINA: Guangxi Autonomous Region, Longzhou County, Nonggang; 22°25'21"N, 106°97'27"E; 4 May 2014, coll. Qu Wu (GUGC); ***paratypes*:** • 4 ♂♂ 5 ♀♀, Guangxi Autonomous Region, Longzhou County, Nonggang; 22°49'97"N, 106°97'49"E; 8 May 2012, coll. Zhiwei Fan, Hu Li; • 3 ♂♂, Guangxi Autonomous Region, Longzhou County, Nonggang; 22°52'66"N, 106°96'94"E; 4 May 2014, coll. Qu Wu (GUGC).

Etymology. The new species name is Latin adjective *expansus*, “expanded”, which is in reference to the broadly expanded base of the aedeagal shaft.

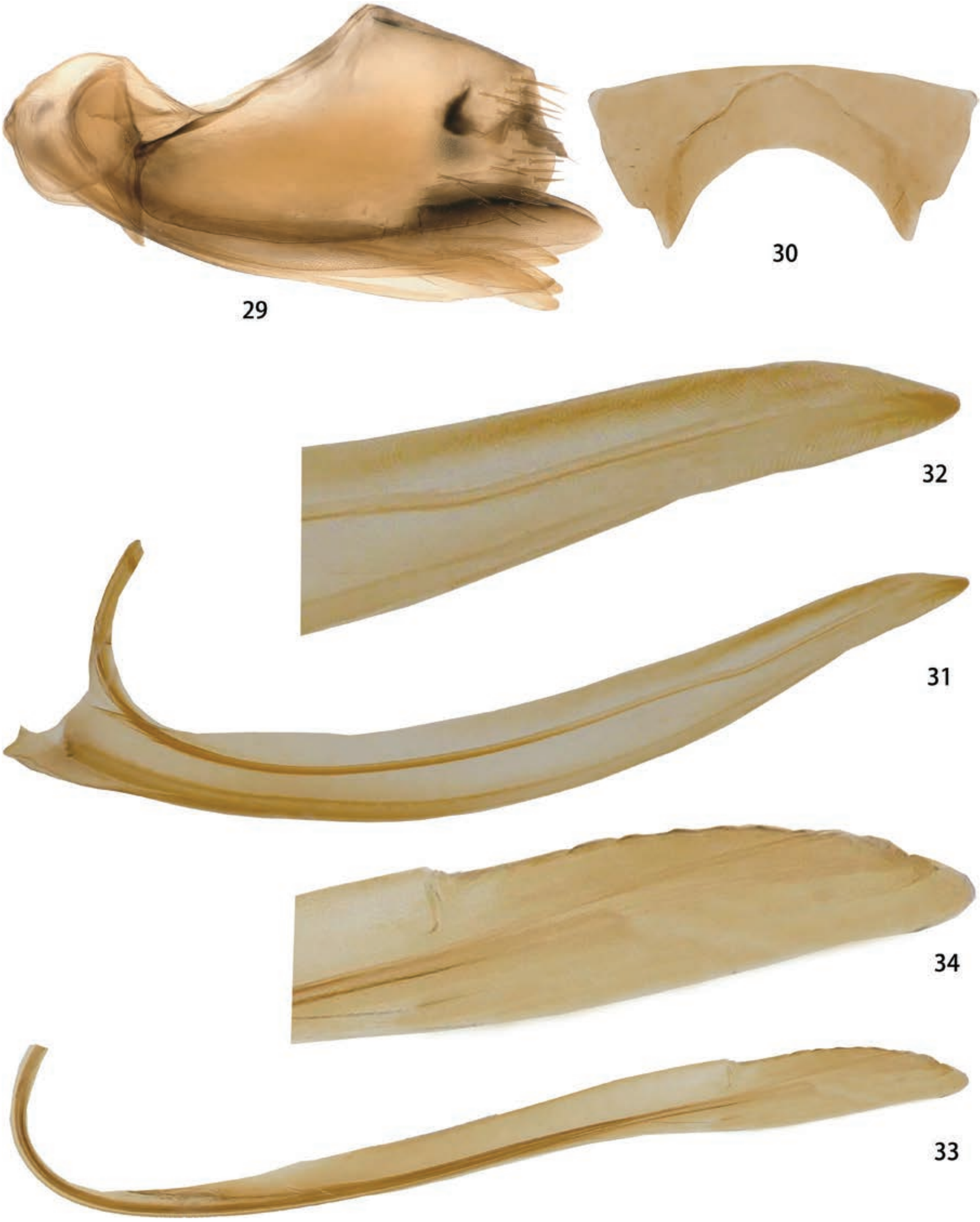

Figures 29–34. *Odonaellus expansus* sp. nov. **29** female genital capsule, lateral view **30** seventh sternite, ventral view **31** first valvula, lateral view **32** detail of sculptures of first valvula **33** second valvula, lateral view **34** detail of sculpture on second valvula.

Remarks. This species agrees more closely with the subtribal diagnosis of Eremophlepsiina (Zahniser and Dietrich 2013) than does the type species of the genus. Unlike *O. serratus*, *O. expansus* has the male valve nearly as long as wide, the pygofer process ventrally arising, and the subgenital plate lacking macrosetae as in other Eremophlepsiina.

Acknowledgements

We thank all of the academic editor, Dr Chris Dietrich (Illinois Natural History Survey, Champaign, U.S.A.) and Dr Saad El-Sonbati (King Saud University Museum of Arthropods, Saudi Arabia (KSMA)) for reading the manuscript and making some suggestions, and we thank the collectors for their gift of the specimens.

Additional information

Conflict of interest

The authors have declared that no competing interests exist.

Ethical statement

No ethical statement was reported.

Funding

This work was supported by the National Natural Science Foundation of China (32060123, 31301909), the key project of Science-technology basic condition platform from the Ministry of Science and Technology of the People's Republic of China (grant no. 2005DKA21402), and the data in this research comes from the database of the National Digital-Museum of Animal Specimens.

Author contributions

Conceptualization: SSH. Data curation: SSH. Formal analysis: SSH. Funding acquisition: JX, SSH. Investigation: WC. Methodology: WC. Resources: SSH. Software: WC. Validation: JX. Visualization: SSH. Writing - original draft: SSH.

Author ORCIDs

Shangmi Hu https://orcid.org/0009-0007-3824-5993
Wenjun Cao https://orcid.org/0000-0002-1865-2598
Jichun Xing https://orcid.org/0000-0002-3738-7996

Data availability

All of the data that support the findings of this study are available in the main text.

References

Cao WJ, Xing JC (2022) *Japananoides*, a new leafhopper genus from China (Hemiptera: Cicadellidae: Deltocephalinae). Zootaxa 5154: 345–354. https://doi.org/10.11646/zootaxa.5154.3.7

Dai W, Cui W, Xiao B, Zhang YL (2010) A new genus and species of Old World Opsiini (Hemiptera: Cicadellidae: Deltocephalinae), with a key to genera and species checklist for the tribe. Zootaxa 2607: 55–68. https://doi.org/10.11646/zootaxa.2607.1.2

Li ZZ, Dai RH, Xing JC (2011) Deltocephalinae from China (Hemiptera: Cicadellidae). Popular Science Press, Beijing, 336 pp. [in Chinese with English summary]

Zahniser JN, Dietrich CH (2013) A review of the tribes of Deltocephalinae (Hemiptera: Auchenorrhyncha: Cicadellidae). European Journal of Taxonomy 45: 1–211. https://doi.org/10.5852/ejt.2013.45

ZooKeys 1228: 11–52 (2025)
DOI: 10.3897/zookeys.1228.138773

Research Article

Lysathia flavipes and *Lysathia cilliersae* Cabrera sp. nov. (Coleoptera, Chrysomelidae): genetic and morphological unravelling of biocontrol agents for two invasive aquatic plants

Ana C. Faltlhauser[1,2], Nora Cabrera[3], M. Cristina Hernández[1], Andrés F. Sánchez Restrepo[1], Martin Hill[4], Alejandro J. Sosa[1,2]

1 *Fundación para el Estudio de Especies Invasivas (FuEDEI), Hurlingham, Argentina*
2 *Consejo Nacional de Investigaciones Científicas y Técnicas, CABA, Argentina*
3 *Facultad de Cs. Naturales y Museo, Universidad de La Plata, La Plata, Argentina*
4 *Department of Zoology and Entomology, Centre for Biological Control (CBC), Rhodes University, Makhanda, South Africa*
Corresponding author: Ana C. Faltlhauser (anafaltlhauser@gmail.com)

Abstract

In the search for specific natural enemies to control two invasive aquatic plants (IAP) from South America, *Ludwigia grandiflora* subsp. *hexapetala* (Onagraceae) and *Myriophyllum aquaticum* (Haloragaceae), taxonomic challenges associated with two *Lysathia* Bechyné, 1959 (Chrysomelidae; Alticini) species had to be resolved. *Lysathia flavipes* (Boheman, 1859) exhibits significant morphological variation, causes heavy damage to both IAPs, and may represent more than one species due to the phylogenetic gap between hosts. Additionally, an undescribed *Lysathia* species (previously published as *Lysathia* sp.), sourced from Brazil, has been successfully used as a control agent for *M. aquaticum* in South Africa since 1994. An integrative taxonomic approach combining genetic and morphological analyses was employed. A lectotype and paralectotypes for *Graptodera flavipes* Boheman, 1859 are here designated. Phylogenetic studies revealed that *L. flavipes* had greater genetic and morphological variation than originally described, and no evidence suggested that *L. flavipes* represented a species complex associated with its host plants. As a result, the species description was expanded. On the other hand, genetic and morphological differences such as body size, colouration, and genital structures further supported the description of *Lysathia cilliersae* Cabrera, **sp. nov.** and its differentiation from other closely related species, including *L. flavipes* and *L. ludoviciana* (Fall, 1910). Specimens of *L. cilliersae* **sp. nov.** collected in Misiones, Argentina, matched those from South Africa. Genetic sequences correlated with morphological vouchers, images, and illustrations of morphology and genitalia, as well as new distribution records, are provided. This research contributes to the taxonomic knowledge of the *Lysathia* genus and supports accurate species identification in applied entomological contexts, such as biological control programmes.

Key words: Alticini, biological control, DNA barcoding, haplotype, integrative taxonomy, Parrot's feather, Water primrose

Academic editor: Ron Beenen
Received: 16 October 2024
Accepted: 30 December 2024
Published: 13 February 2025

ZooBank: https://zoobank.org/4F80626D-A365-4139-9797-3ED099878CBF

Citation: Faltlhauser AC, Cabrera N, Hernández MC, Sánchez Restrepo AF, Hill M, Sosa AJ (2025) *Lysathia flavipes* and *Lysathia cilliersae* Cabrera sp. nov. (Coleoptera, Chrysomelidae): genetic and morphological unravelling of biocontrol agents for two invasive aquatic plants. ZooKeys 1228: 11–52. https://doi.org/10.3897/zookeys.1228.138773

Introduction

Invasive aquatic plants (IAP) have both ecological and economic impacts that threaten ecosystems (Hussner et al. 2017). Reduction of biodiversity and water quality, disruption of ecosystems by outcompeting native species, and altering habitats are some of the various challenges that these types of species pose (Stiers et al. 2011; Thouvenot et al. 2013). Traditional approaches to managing IAP often involve mechanical and chemical methods (Andreu et al. 2009); however, they can have limitations such as non-specificity, short-term effectiveness, and environmental concerns (Hussner et al. 2017). Given these challenges, biological control, which involves introducing monophagous natural enemies (insects, pathogens, or herbivores) to manage invasive species by reducing their population sizes or limiting their spread (Cruttwell McFadyen 1998), has gained attention as a control method (Sankaran et al. 2023). This approach offers several advantages, including long-term effectiveness, reduced environmental impact compared to chemical methods, and potential for self-sustaining control (Culliney 2005; McFadyen 2008; Hinz et al. 2020).

Water primrose (*Ludwigia grandiflora* subsp. *hexapetala* (Hook. & Arn.) G.L. Nesom & Kartesz; Onagraceae) and parrot's feather (*Myriophyllum aquaticum* (Vell.) Verdc.; Haloragaceae) are aquatic plants native to South America (Raven and Axelrod 1974; Orchard 1981; Sutton 1985; Sytsma et al. 2004; Wagner et al. 2007). In its native range in Argentina, they typically coexist in their natural environment (Fig. 1A, B), growing in shallow waters across the centre and north of the country, reaching northern Patagonia (Sabbatini et al. 1998). Conversely, they are considered aggressive IAPs in North America (Reddy et al. 2021b), Europe (Di Pietro et al. 2007; Thouvenot et al. 2013), Africa (Hill and Coetzee 2017), and Oceania (Hussner et al. 2017), where they obstruct water flow and cause various environmental and economic problems by forming dense mats that cover water bodies, streams, and irrigation channels (Pelella et al. 2023; Rojas-Sandoval 2024).

Figure 1. *Ludwigia grandiflora* subsp. *hexapetala* and *Myriophyllum aquaticum* coexisting in the same environment in Argentina, localities of **A** Calabacillas (Entre Ríos) and **B** Plottier (Neuquén) **C** Damage of *Lysathia flavipes* on *L. g.* subsp. *hexapetala* **D** *L. flavipes* larval damage on *M. aquaticum*.

Chemical or mechanical strategies against *L. g.* subsp. *hexapetala* and *M. aquaticum* have proven to be inefficient. For this reason, several projects are either developing integrated management approaches that include biological control or have already implemented biological control programmes against these weeds (Cilliers 1999a; Sheppard et al. 2006; Oberholzer et al. 2007; Scott et al. 2020; Reddy et al. 2021b; Lesieur et al. 2023; Pessina et al. 2024).

In the search of specific natural enemies for *L. g.* subsp. *hexapetala* and *M. aquaticum*, there is a particular interest to solve taxonomic challenges associated with two flea beetle species (Coleoptera: Chrysomelidae: Galerucinae: Alticini) within the genus *Lysathia* Bechyné, 1959. Surveys in Argentina have revealed frequent and abundant damage (Fig. 1C, D) in both weed species produced possibly by *Lysathia flavipes* (Boheman, 1859) (Cordo and DeLoach 1982; Hernández and Cabrera Walsh 2014; Reddy et al. 2021a). On the other hand, an undescribed *Lysathia* was collected in 1991 from near the town of Penedo (Rio do Janeiro state, Brazil), and imported into quarantine in South Africa where it was studied and released as a biocontrol agent for *M. aquaticum* (Cilliers 1999b). It is important to note that while the collection site coordinates of this *Lysathia* sp. was originally reported as Penedo (10.1700S, 36.3600W) in Cilliers (1999b), these correspond to a different location, also called Penedo, in the Alagoas State. Based on confirmation from the original collection research team, the correct coordinates for Penedo, Rio do Janeiro, are 22.4383S, 44.5270W.

Lysathia flavipes, initially studied by Cordo and DeLoach (1982) as a potential control agent for *Ludwigia g.* subsp. *hexapetala*, *Ludwigia peploides* subsp. *montevidensis* (Spreng.), and *M. aquaticum*, showed a limited host range to species of *Ludwigia* and *Myriophyllum*. Later, in the USA, Reddy et al. (2021a) investigated its biological parameters with a population collected in Uruguay, and concluded that this flea beetle was not a suitable candidate due to its lack of specificity. However, recent field observations showed morphological variability (e.g., variations in body and leg colouration, body size), its highly damaging capacity to the target species, and phylogenetic distance between these two main hosts suggest that *Lysathia flavipes* could represent more than one species.

The unidentified species of *Lysathia*, published in earlier works as *Lysathia* sp., from now on the biocontrol (BC) agent *Lysathia* sp., has proven to be a highly effective biological control agent against *M. aquaticum* in South Africa for the past 30 years (Coetzee et al. 2011; Martin et al. 2018). Following its collection in 1991 (S. Neser, Plant Protection Research Institute, Pretoria, 1992 pers. comm.) David. G. Furth (Smithsonian Institute in Washington) analysed a sample of the beetle and established that it differed from the known species *L. flavipes* and *L. ludoviciana* (Fall, 1910), also found on the same host plant and suggested that the beetle likely represented a new species (Cilliers 1999b). Subsequent testing conducted under quarantine conditions at the ARC Plant Protection Research Institute revealed that *Lysathia* sp. fed exclusively on the emergent leaves of *M. aquaticum* and it was released in 1994. No other taxonomists were working on this genus and the beetle remained undescribed. Recent findings in Argentina (Misiones Province) of specimens collected on *M. aquaticum* that resemble the BC agent *Lysathia* sp., provided a new opportunity to describe this species.

Apart from *L. flavipes* and the BC agent *Lysathia* sp., *L. ludoviciana*, has been reported to feed on both *Ludwigia g.* subsp. *hexapetala* and *M. aquaticum* (Habeck and Wilkerson 1980). This species is considered native in North America, distributed from southeastern New York to Florida and westward to Texas and parts of Mexico (Chester and Holt 1990). It has been studied for its potential as a biological control agent in the USA; however, its efficacy may vary depending on the target plant species and environmental conditions and further research is needed (Campbell and Clark 1983; McGregor et al. 1996). Given the similarity in host plants, the lack of information available for the genus, and that *L. ludoviciana* is the only *Lysathia* species that has genetic information available in databases; it is an essential species that can contribute to both morphological and genetic comparisons in the search for unravelling the identities of *L. flavipes* and the BC agent *Lysathia* sp.

The genus *Lysathia* is taxonomically complex. It was proposed by Bechyné (1959) with seven species transferred from the genus *Altica* Geoffroy, 1762, with *L. flavipes* as the type species. The morphological characteristics upon which Bechyné based this separation were considered subtle by Scherer (1962), who subsequently combined *Lysathia* in his *Altica* key. However, as mentioned by Reid and Beatson (2015), Scherer's action is not considered a nomenclatorial act and *Lysathia* remains a separate genus from *Altica*. As Bechyné (1959) described, *Lysathia* species are smaller than the ones catalogued within *Altica*, and characterised by the particularly incrassate femora, the feeble to sometimes indistinct basal transverse groove on the pronotum, and the male with a very short central lobe on the last abdominal sternite. Many species of *Lysathia* display a metallic body with fulvous legs, while in typical *Altica* the legs are usually metallic in colour. The aedeagus is of the same general type as in *Altica*, including the sculpture on its ventral side; however, rather large differences are observed in certain species, such as a strongly developed central ridge (Medvedev 2001). The genus includes species distributed in the Neotropic (South and Central America) and the south of the Nearctic region. According our bibliographical survey, there are 22 *Lysathia* species. Organised alphabetically, they are:

L. aenea (Oliver, 1808),
L. arapata Bechyné, 1959,
L. atrocyanea (Phil. & Phil., 1864),
L. bohumilae (Bechyné, 1954),
L. chaparensis Bechyné, 1959,
L. comasagua Bechyné & Bechyné, 1960,
L. flavipes,
L. hygrobia (Bechyné, 1955),
L. integricollis (Harold, 1876),
L. jacobyi (Csiki, 1939),
L. louella (Bechyné, 1955),
L. ludoviciana,
L. muriensis (Bechyné, 1954),
L. occidentalis (Suffrian, 1868),
L. patagonica Bechyné, 1957,
L. philippi (Csiki, 1939),
L. rockefelleri (Pallister, 1953),

L. simplex (Jacoby, 1891),
L. siolii Medvedev, 2001,
L. viedma Bechyné, 1957,
L. virescens (Blanchard, 1851),
L. volcanica Bechyné & Bechyné, 1960

(Bechyné 1957a, 1959; Bechyné and Springlová-Bechyné 1960, 1977; Furth and Savini 1996; Jerez 1988; Medvedev 2001; Scherer 1960; Virkki 1979). The species specifically distributed in Brazil and Argentina are *L. aenea*, *L. muriensis*, *L. siolii*, *L. bohumilae*, *L. flavipes*, *L. louella*, *L. viedma*, and *L. patagonica*.

To this date, there is no general systematic revisions focused on this genus and hence there is no current comprehensive key to differentiate these species. However, Bechyné (1954, 1955, 1959) contributed to the organisation of some of these species, particularly those distributed in southern South America, by referring to them in his publications as the *flavipes* group. Bechyné (1954) described two new *Altica* species, *A. bohumilae* and *A. muriensis*, grouping them with *A. flavipes*. Subsequently, in 1955, while describing additional *Altica* species from South America, he explicitly referenced *A. hygrobia* and *A. louella* as part of the "*A. flavipes* group" (Bechyné 1955). Since then, the term *flavipes* group has been used in publications, such as Bechyné (1959) including *L. arapata* and Medvedev (2001) with *L. siolii*. Other *Lysathia* species, such as *L. philippi*, *L. viedma*, and *L. patagonica*, are also described for southern South America but Bechyné does not include them in *flavipes* group since, apart from having a Patagonic distribution, they differ in morphological traits, such as having an opaque colouration and a different type of elytral punctation (Bechyné 1957a).

Precise taxonomic identification of biological control agents ensures that the selected species is effective against the target weed and does not pose risks to native or beneficial species. Misidentification of either the weed or the biological control agent can lead to ineffective control measures and unintended consequences such as damage to non-target species or ecosystems. The objective of this paper was to elucidate the inter- and intra-specific relationships of *L. flavipes* and the BC agent *Lysathia* sp. by performing phylogenetic analyses, subsequently, analysing these species through an integrative taxonomic approach, and establishing a one-to-one correlation between the morphological and genetic descriptions. In this study, the brief original description of *L. flavipes* is expanded, and the illustrations, distribution, and host plants updated. We also describe the BC agent *Lysathia* sp. against *M. aquaticum* as *Lysathia cilliersae* sp. nov.

Materials and methods

Study area and sample acquisition

Specimens (males and females) of *Lysathia flavipes* were collected during several field trips across eastern and central Argentina where *Ludwigia* spp. and *Myriophyllum aquaticum* are most commonly distributed. Collections occurred between 2018 and 2023 in the Argentine provinces of Neuquén, Río Negro, Buenos Aires, Entre Ríos, Corrientes, and Misiones. Plants were inspected for characteristic damage caused by larvae or adults (Fig. 1C, D). Specimens were primarily collected as adults, except in locations where both plant species coexisted; in these cases, larvae were collected to ensure they were feeding on the host plant, then reared in laboratory until adults emerged. Also, preserved specimens of *L. flavipes* from Uruguay, evaluated in Reddy et al. (2021a), were included in the study. Since the BC agent *Lysathia* sp., originally sourced from Brazil, is used as a biological control agent against *M. aquaticum* in South Africa, specimens were obtained from a colony released in the 1990s from the Waainek mass rearing facility (Centre for Biological Control (CBC), Makhanda, South Africa). In addition, specimens suspected to be the same BC agent *Lysathia* species were collected in Misiones and Entre Ríos provinces (Argentina) while feeding on *M. aquaticum*. Lastly, preserved specimens of *L. ludoviciana* collected on *Ludwigia* sp. in Louisiana (USA) were obtained from a donation to the Coleoptera collection at the La Plata Museum.

All collected samples were preserved with 99% ethanol and stored at −20 °C. For each individual, a unique identification code, geographic coordinates (latitude and longitude), external physical characteristics (body and leg colour), sex, host plant, and collection date were recorded (Suppl. material 1: table S1). Specimens used for genetic and morphological analysis were dry-mounted and photographed using a Canon EOS 90D DSLR camera attached to a Leica S9 D stereomicroscope. Images were processed using focus stacking in Adobe Photoshop 2020.

Genetic study

Genetic data

Individuals were selected for genomic DNA extraction using the Qiagen DNAeasy Blood & Tissue kit. To preserve reference specimens of each sample and allow for later correlation with their morphological descriptions, non-destructive extractions were performed using whole bodies, with a small puncture made in the left pleura using a fine needle. Specimens were subsequently recovered from the extraction process. Additionally, to increase DNA yield, a single left hind leg from each specimen was extracted and crushed. Only for two specimens from Uruguay, complete destruction of the specimens was necessary to enhance DNA extraction yield due to inadequate preservation. Two unlinked loci were sequenced (mitochondrial and ribosomal), to improve phylogenetic analyses. We were not successful in obtaining nuclear sequences. The Cytochrome c Oxidase Subunit I (COI) (~ 764 bp) and a ribosomal fragment corresponding to the 16S rRNA fragment (~ 524 bp), were amplified through polymerase chain reactions (PCR) in both directions. All samples were sequenced with primers C1J2195 (5’-TTGATT(CT)TTTGGTCA(CT)CC(AT)GAAGT-3’) and TL2N3014 (5’-TC(CT)A(AT)TGCA(CT) TAATCTGCCATATT-3’) (Simon et al. 1994). These primers have been previously used to amplify COI fragments of other flea beetles (Jenkins et al. 2009). Samples were also sequenced with 16sar-L (5’-CGCCTGTTTATCAAAAACAT-’3) and 16sbr-H (5’-CCGGTCTGAACTCAGATCAC-3’) primers after Salvi et al. (2019) targeting the fragment encompassing the domains IV and V of the16S rDNA. Details on PCR protocol are provided in the Suppl. material 1: PCR protocols. Sanger sequencing service from Macrogen was used.

In addition to the new sequences obtained, sequences previously published and available in the GenBank nucleotide database (https://www.ncbi.nlm.nih.gov/genbank/) were included. Specifically, the sequences downloaded were for *L. ludoviciana* from the mitochondrial COI gene (*n* = 10) and the ribosomal 16S (*n* = 2). Additionally, sequences from closely related taxa to *Lysathia* were retrieved to serve as outgroups: COI (*n* = 20) and 16S (*n* = 10); *Altica*, *Diorhabda*, *Longitarsus*, *Monolepta*, *Podontia*, *Psylliodes*, *Systena* and a specimen of the Galerucinae subfamily (likely *Paleosepharia* sp.) (Suppl. material 1: table S2). This study provides the first genetic sequences for *L. flavipes*. No previously published sequences were available for the analysis.

Sequences were inspected, trimmed, and aligned using GENEIOUS PRO v. 4.8 (http://www.geneious.com/), with the MUSCLE alignment algorithm (Edgar 2004). Each sequence was verified to correspond to a coding region, without gaps that could alter the reading frame. All new sequences obtained in this study were deposited in GenBank.

Phylogenetic reconstruction

Initially, a provisional morphological identification was conducted to group the collected specimens into the species to which they were suspected to belong. To examine the inter- and intra-specific phylogenetic relationships among the *Lysathia* species under study and to evaluate the correspondence between the obtained sequences and the morphological groupings, phylogenetic trees were constructed using new sequences from *L. flavipes*, the BC agent *Lysathia* sp., and *L. ludoviciana*. Sequences published in GenBank for *L. ludoviciana* and species from genera closely related to *Lysathia* were incorporated as outgroup. Several species of the genus *Altica* were specifically used to assess the proximity between the two genera, as some taxonomist question the separation of *Lysathia* proposed by Bechyné (1959). Phylogenetic trees were estimated for both individual and combined genes. Including a more conserved gene along with a more variable one can enhance branch resolution during reconstruction. Phylogenies were inferred using maximum likelihood (ML) analysis in RAxML-NG (Kozlov et al. 2019). The ML analysis was performed with bootstrap support values (BS) on 1,000 replications, using a GTRGAMMAI substitution model and standard parameters suggested by the software. Runs were conducted on the CERES HPC clusters server of the SCINet High-Performance Computer Systems of the ARS-USDA. The resulting trees were visualised using Figtree v. 1.4.4 software (http://tree.bio.ed.ac.uk/software/figtree/). Nodes with BS values exceeding 70% were considered sufficiently resolved (Hillis and Bull 1993).

Genetic diversity

To assess genetic variability within the species under study, *L. flavipes*, the BC agent *Lysathia* sp., and *L. ludoviciana*, a genetic diversity analysis was conducted using only mitochondrial data. Relationships between haplotypes were established by constructing a maximum parsimony network using the TCS inference algorithm implemented in PopArt v. 1.7. (Leigh and Bryant 2015), where haplotypes are connected by branches whose lengths are proportional to the number of mutations that differentiate them.

Morphological study

We reviewed original descriptions and relevant literature for all species of the genus *Lysathia* (Olivier 1808; Blanchard 1851; Boheman 1859; Philippi and Philippi 1864; Harold 1876; Fall 1910; Heikertinger and Csiki 1939; Pallister 1953; Bechyné 1954, 1955, 1957a, 1959; Bechyné and Springlová-Bechyné 1960; Medvedev 2001; Peck et al. 2014). We focused on comparing the species of interest for this research with those inside the *flavipes* group or overlapping geographic distributions, as these were the most relevant candidates for potential misidentification. We also examined all available images of type species and specimens deposited at MLP.

In the morphological descriptions, traits shared between male and female are not repeated after their initial mention. Terminology for the cephalic capsule follows Konstantinov (1998b) and Reid and Beatson (2015); venation of the hind wing is based on Kukalová-Peck and Lawrence (1993), the metanotum and metaendosternite follow Konstantinov (1998b) and Lingafelter and Konstantinov (2000). Nomenclature of female and male genitalia is based on Konstantinov (1987, 1998a), Lingafelter and Konstantinov (2000), and Reid and Beatson (2015).

Measurements were taken with an ocular micrometre on an Olympus dissecting microscope and are expressed in millimetres (mm), with mean (X) and standard deviation (SD). Body measurements include: total length (from the base of the antennae to the tip of the elytron), elytral width at the height of the humeri, and maximum elytral width in the basal third. The drawings were made with a camera lucida on a Leitz compound microscope and a Wild dissecting microscope.

Specimens were compared with photographs of the type series of *L. flavipes* provided by the Swedish Museum of Natural History (Naturhistoriska riksmuseet, Stockholm-**NHRS**) under the Creative Commons Attribution 4.0 International Public License. Additionally, images of type specimens of *L. bohumilae* and *L. muriensis* Bechyné were provided by Frey Beetle Collection (Frey Naturhistorisches Museum Basel, Biowissenschaften). Finally, a bibliographical revision was conducted to locate any evidence of designation of the type series for *L. flavipes* with the aim to verify whether a lectotype had previously been designated or if the status of the series remained as originally described by Boheman (1859). This revision included searches in Zoological Records, Scopus, and relevant databases.

The studied specimens were deposited in the following institutions: Museo de La Plata (**MLP**), Buenos Aires, Argentina; Sala de Colecciones "Moisés Bertoni" (**SLP-art**), Misiones, Argentina; South African National Collection of Insects (**SANC**), Pretoria, South Africa; and the private collection of the Foundation for the Study of Invasive Species (**FuEDEI**).

Results

Study area and sample acquisition

The samplings conducted followed the distribution of the known host plants: *Ludwigia grandiflora* subsp. *hexapetala*, *L. peploides* subsp. *montevidensis*, and *Myriophyllum aquaticum* in Argentina (Fig. 2).

A total of 35 specimens, initially assigned to *L. flavipes*, were collected from the central-east region of Argentina (from the northeast of Corrientes to the northernmost part of Patagonia). Additionally, nine specimens collected in

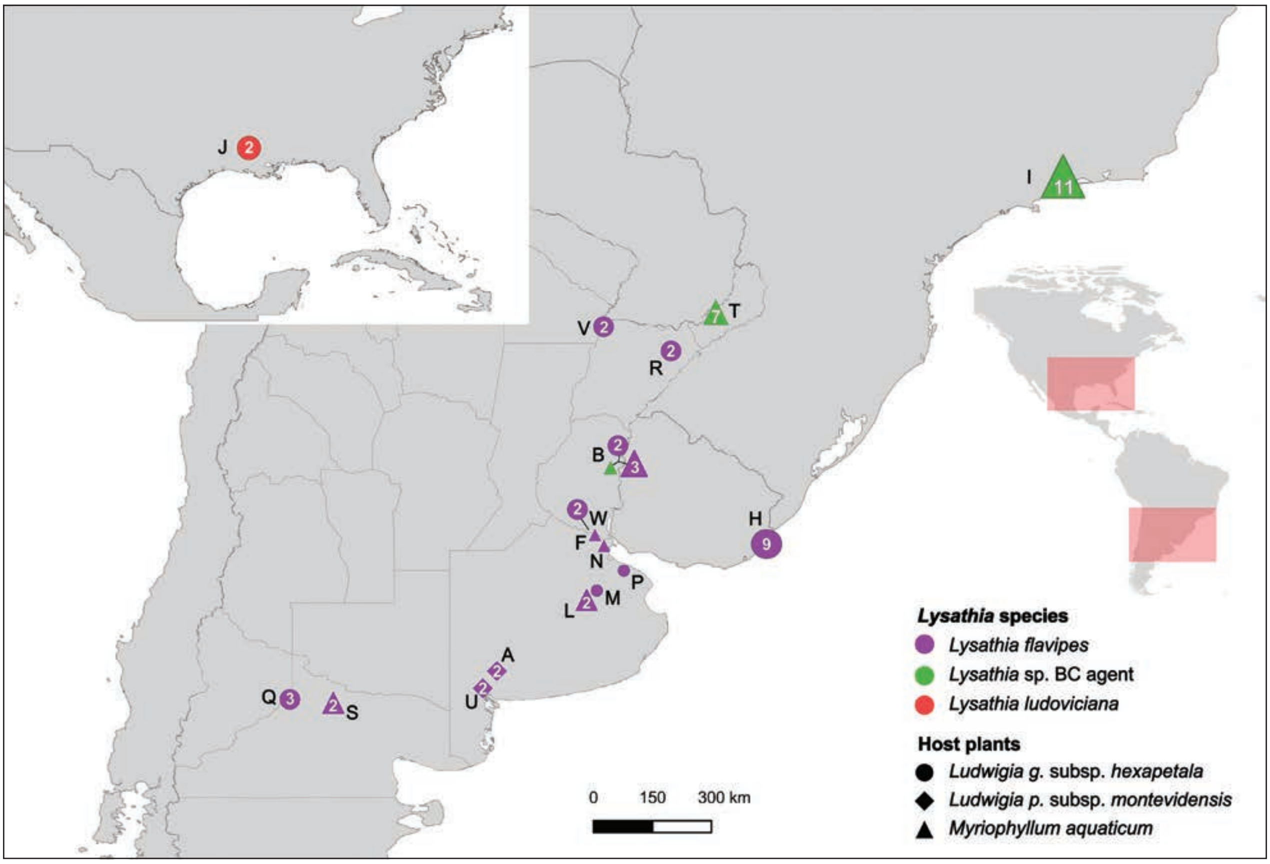

Figure 2. Collection sites for *Lysathia* specimens used in genetic and morphological studies. Colours on the map represent different *Lysathia* species, while shapes denote the host plants from which specimens were collected. Numbers within the shapes indicate the number of specimens, and letters correspond to the different localities. Additional information on localities are provided in Suppl. material 1: table S2.1.

Uruguay and studied in Reddy et. al (2021a), were donated from collaborators. For the BC agent *Lysathia* sp., 11 specimens were obtained from the mass rearing centre in South Africa (plotted at their origin site in Brazil, in Fig. 2) and eight specimens from Argentina. Lastly, two samples of *L. ludoviciana* were obtained from MLP. As a result, a total of 65 specimens were considered in our study.

Genetic study

Phylogenetic analyses

Of the 65 specimens from which DNA was extracted, 47 yielded successful sequences of the mitochondrial COI (presumed *L. flavipes* [*n* = 23], *L. ludoviciana* [*n* = 2], and presumed BC agent *Lysathia* sp. [*n* = 17]). Of the ribosomal 16S gene, 23 sequences were obtained (*L. flavipes* [*n* = 10], *L. ludoviciana* [*n* = 2], and BC agent *Lysathia* sp. [*n* = 11]) (Table 1).

Although DNA amplification of the nuclear Wingless gene was achieved, the obtained sequences exhibited very low signal in the chromatogram, making their accurate interpretation difficult. Consequently, these sequences were not considered reliable, and the use of this locus was discarded. Therefore, including the sequences obtained from GenBank, the final alignment consisted of 52 total sequences for COI and 23 for 16S.

Table 1. *Lysathia* specimens used in genetic analyses. Sample: respective sample codes; Species: initially assigned species, *Lysathia flavipes*, *L. ludoviciana* and the biocontrol (BC) agent *Lysathia* sp.; Sex: ♂= male ♀= female; Host plant: *Ludwigia p.* subsp. *montevidensis*, *L. g.* subsp. *hexapetala* and *M. aquaticum*; Sites of collection with their respective Code (letters), locality (Loc.), province (Prov.), and Country (ARG = Argentina, UY = Uruguay, SA = South Africa, and USA = United States of America). Accession number with which the sequences were entered into GenBank for Cytochrome Oxidase I (COI) and 16S ribosomal. (*) indicates that the specimen was later found not to be the initially assigned species.

Sample	Species	Sex	Host Plant	Site		GenBank	
				Code	Loc., Prov., Country	COI	16S
LM_A_02	*L. flavipes*	♂	*L. p. montevidensis*	A	V. Ventana, BA, ARG	PQ558504	
LH_B_01	*L. flavipes*	♂	*L. g. hexapetala*	B	Calabacillas, ER, ARG	PQ558491	
LH_B_02	*L. flavipes*	♀	*L. g. hexapetala*	B	Calabacillas, ER, ARG	PQ558492	PQ621632
MA_B_01	*L. flavipes*	♂	*M. aquaticum*	B	Calabacillas, ER, ARG	PQ558507	
MA_B_02	*L. flavipes*	♀	*M. aquaticum*	B	Calabacillas, ER, ARG	PQ558508	PQ621637
MA_B_03	*L. flavipes*	♂	*M. aquaticum*	B	Calabacillas, ER, ARG	PQ558509	PQ621638
MA_F_01	*L. flavipes**	♀	*M. aquaticum*	F	Otamendi, BA, ARG	PQ558510	PQ621639
LH_H_08	*L. flavipes*	♀	*L. g. hexapetala*	H	P. del Diablo, RO, UY	PQ558493	
LH_H_09	*L. flavipes*	♂	*L. g. hexapetala*	H	P. del Diablo, RO, UY	PQ558494	
MA_L_01	*L. flavipes*	♂	*M. aquaticum*	L	Las Flores, BA, ARG	PQ558511	PQ621640
MA_L_02	*L. flavipes*	♀	*M. aquaticum*	L	Las Flores, BA, ARG	PQ558512	
LH_M_01	*L. flavipes**	♀	*L. g. hexapetala*	M	Gorchs, BA, ARG	PQ558495	PQ621633
LH_P_01	*L. flavipes*	♀	*L. g. hexapetala*	P	La Plata, BA, ARG	PQ558496	
LH_Q_01	*L. flavipes*	♀	*L. g. hexapetala*	Q	Plottier, NQ, ARG	PQ558497	
LH_Q_02	*L. flavipes*	♀	*L. g. hexapetala*	Q	Plottier, NQ, ARG	PQ558498	
LH_Q_03	*L. flavipes*	♂	*L. g. hexapetala*	Q	Plottier, NQ, ARG	PQ558499	
LH_R_01	*L. flavipes*	♂	*L. g. hexapetala*	R	Galarza, CR, ARG	PQ558500	PQ621634
MA_S_02	*L. flavipes*	♀	*M. aquaticum*	S	V. Regina, RN, ARG	PQ558513	
LM_U_01	*L. flavipes*	♀	*L. p. montevidensis*	U	B. Blanca, BA, ARG	PQ558505	
LM_U_02	*L. flavipes*	♂	*L. p. montevidensis*	U	B. Blanca, BA, ARG	PQ558506	
LH_V_01	*L. flavipes*	♂	*L. g. hexapetala*	V	L. Brava, NQ, ARG	PQ558501	PQ621635
LH_V_02	*L. flavipes*	♀	*L. g. hexapetala*	V	L. Brava, CR, ARG	PQ558502	
LH_W_02	*L. flavipes*	♂	*L. g. hexapetala*	W	B. Largo, ER, ARG	PQ558503	PQ621636
MA_I_01	*L.* sp. BC agent	♀	*M. aquaticum*	I	Makhanda, EC, SA	PQ558476	PQ621621
MA_I_02	*L.* sp. BC agent	♂	*M. aquaticum*	I	Makhanda, EC, SA	PQ558477	PQ621622
MA_I_03	*L.* sp. BC agent	♀	*M. aquaticum*	I	Makhanda, EC, SA	PQ558478	PQ621623
MA_I_04	*L.* sp. BC agent	♀	*M. aquaticum*	I	Makhanda, EC, SA	PQ558479	
MA_I_05	*L.* sp. BC agent	♂	*M. aquaticum*	I	Makhanda, EC, SA	PQ558480	PQ621624
MA_I_06	*L.* sp. BC agent	♂	*M. aquaticum*	I	Makhanda, EC, SA	PQ558481	
MA_I_07	*L.* sp. BC agent	♀	*M. aquaticum*	I	Makhanda, EC, SA	PQ558482	PQ621625
MA_I_08	*L.* sp. BC agent	♂	*M. aquaticum*	I	Makhanda, EC, SA	PQ558483	PQ621626
MA_I_09	*L.* sp. BC agent	♂	*M. aquaticum*	I	Makhanda, EC, SA	PQ558484	PQ621627
MA_I_10	*L.* sp. BC agent	♀	*M. aquaticum*	I	Makhanda, EC, SA	PQ558485	PQ621628
MA_I_11	*L.* sp. BC agent	♀	*M. aquaticum*	I	Makhanda, EC, SA	PQ558486	PQ621629
MA_T_01	*L.* sp. BC agent	♂	*M. aquaticum*	T	D. Savio, MS, ARG	PQ558487	PQ621630
MA_T_02	*L.* sp. BC agent	♂	*M. aquaticum*	T	D. Savio, MS, ARG	PQ558488	PQ621631
MA_T_03	*L.* sp. BC agent	♂	*M. aquaticum*	T	D. Savio, MS, ARG	PQ556198	
MA_T_04	*L.* sp. BC agent	♀	*M. aquaticum*	T	D. Savio, MS, ARG	PQ556199	
MA_T_05	*L.* sp. BC agent	♂	*M. aquaticum*	T	D. Savio, MS, ARG	PQ558489	
MA_T_07	*L.* sp. BC agent	♂	*M. aquaticum*	T	D. Savio, MS, ARG	PQ558490	
MA_J_01	*L. ludoviciana*	♀	*Ludwigia sp.*	J	Kaplan, LU, EEUU	PQ558514	PQ621641
MA_J_02	*L. ludoviciana*	♂	*Ludwigia sp.*	J	Kaplan, LU, EEUU	PQ558515	PQ621642

The tree estimated using RAxML based on the mitochondrial COI gene fragment (Fig. 3) showed a higher level of discrimination compared to the ribosomal 16S tree (Suppl. material 1: fig. S1). The samples of the genus *Altica* used

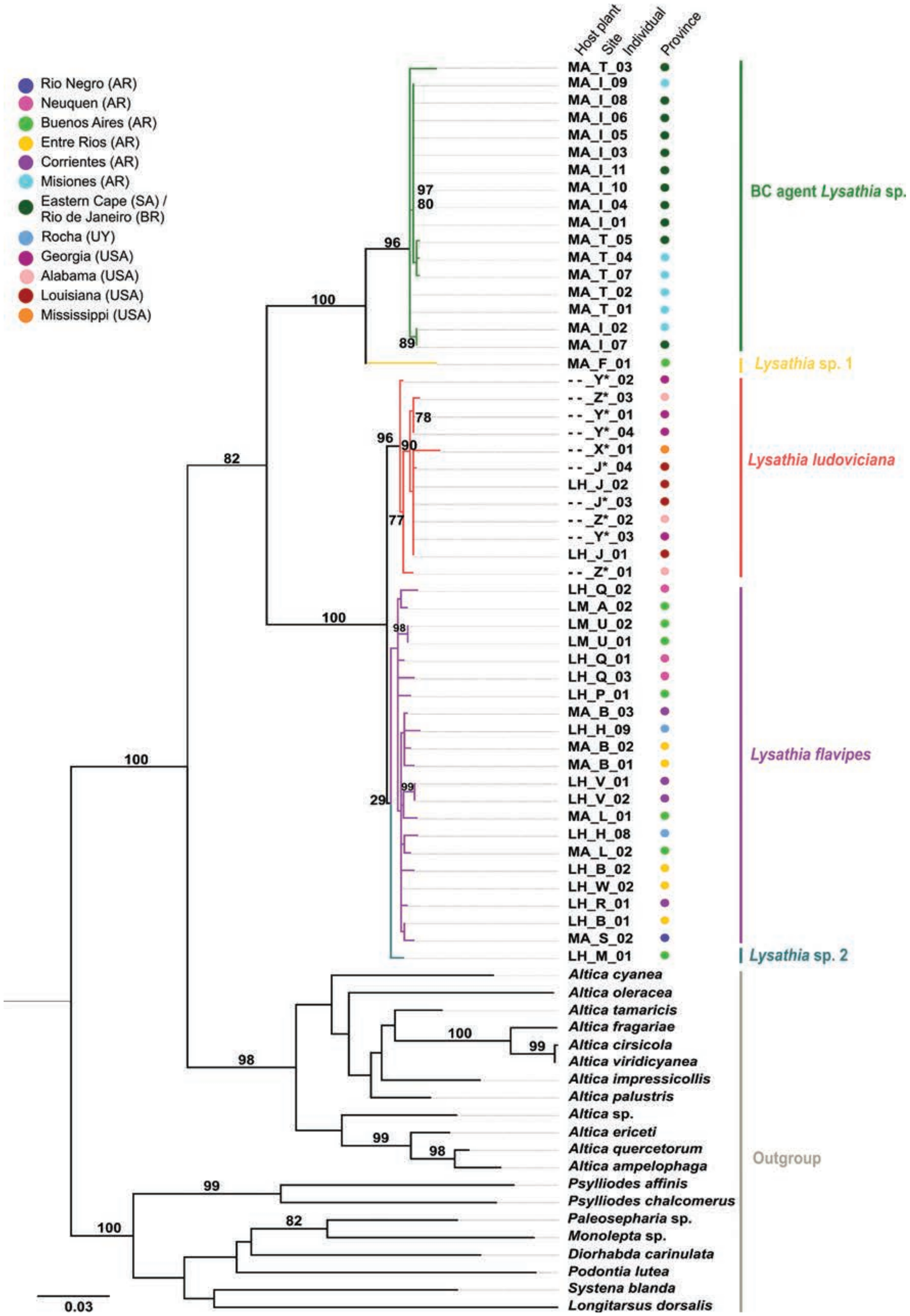

Figure 3. Best tree generated in RAxML for the *Lysathia* species studied, based on the mitochondrial Cytochrome Oxidase I (COI) gene. Names at the end of each terminal indicate the collection code (host plant_collection site code_number of individual). Abbreviation of host plants: *Myriophyllum aquaticum* (MA), *Ludwigia* g. subsp. *hexapetala* (LH), *Ludwigia p.* subsp. *montevidensis* (LM), and unknown plant (--). Collection site code: see Table 1. The coloured circles refer to the provinces/states where the specimens were collected. Specimens marked with * correspond to sequences obtained from GenBank.

as an outgroup were deeply rooted in the tree, with high bootstrap support (BS) value of 98% at the nodes separating them from the *Lysathia* species (Fig. 3). This high support was also observed for the other genera evaluated as outgroups (BS = 100%). The phylogenetic tree revealed that the *Lysathia* species studied form a well-defined group which does not contradict the hypothesis of monophyly for the genus (BS = 82%). The collected specimens were organised into two main clades, one comprising the BC agent *Lysathia* sp. and *Lysathia* sp. 1, and the other consisting of *L. ludoviciana*, *L. flavipes*, and *Lysathia* sp. 2. Originally identified as *L. flavipes*, *Lysathia* sp. 1 and sp. 2 were reclassified due to their distinct grouping from *L. flavipes*. Both the mitochondrial gene tree and the combined tree with the ribosomal gene, showed well-resolved branch values (BS = 100%) (Figs 3, 4).

The specimens collected as *L. flavipes* (purple subclade), despite exhibiting morphological variations, different host plants, and diverse geographical distribution, were mostly grouped into a single subclade with the exception of the two specimens, *Lysathia* sp. 1 and *Lysathia* sp. 2. This subclade also included the specimens from Uruguay, evaluated in the USA as potential biological control agents. The phylogenetic support for *L. flavipes* was weak (BS = 29%) (Fig. 3) although it was consistent for both genes and improved in the combined tree (BS = 52%) (Fig. 4). *Lysathia* sp. 1, is a single specimen from Otamendi, Buenos Aires. In both trees, it was positioned as a sister species to the BC agent *Lysathia* sp. with good support (Figs 3, 4). Conversely, *Lysathia* sp. 2, from Gorchs (Buenos Aires) showed uncertain placement. In the mitochondrial gene tree, *Lysathia* sp. 2 was positioned as a sister species to *L. flavipes* (Fig. 3), while in the combined tree, it positioned as a sister species to *L. ludoviciana* (Fig. 4).

The specimens of *L. ludoviciana*, both samples obtained from GenBank and the newly sequenced ones, grouped into a well-defined subclade with a high BS support value (96%; Fig. 3, red colour). This indicates strong phylogenetic support for the morphological correspondence of this group. In the combined tree, although based on fewer specimens, good branch support was also obtained (Fig. 4). In both cases, *L. ludoviciana* was the species phylogenetically closest to *L. flavipes* compared to the BC agent *Lysathia* sp.

The specimens identified as the BC agent *Lysathia* sp., including those from the mass rearing centre in South Africa and originally from Penedo (Rio de Janeiro, Brazil), as well as those collected in Misiones (Argentina), grouped into a single subclade with high BS support value (COI: BS = 96%; COI+16S: BS = 99%) (Figs 3, 4, green clade). This strong phylogenetic support indicates that specimens from both locations (Rio de Janeiro and Misiones) belong to the same species, the BC agent *Lysathia* sp.

Genetic diversity

Of the 53 sequences analysed, 28 haplotypes were identified, grouped into five clusters, three of which correspond to the *Lysathia* species studied (Fig. 5). The cluster associated to the specimens collected as *L. flavipes* consisted of 22 sequences and 18 haplotypes, demonstrating considerable haplotype diversity.

The H18 haplotype, consisting of specimens from Buenos Aires and Entre Ríos provinces (Fig. 5), appears to be the most ancestral within the cluster due to its multiple connections with other haplotypes and its central position. Similar to

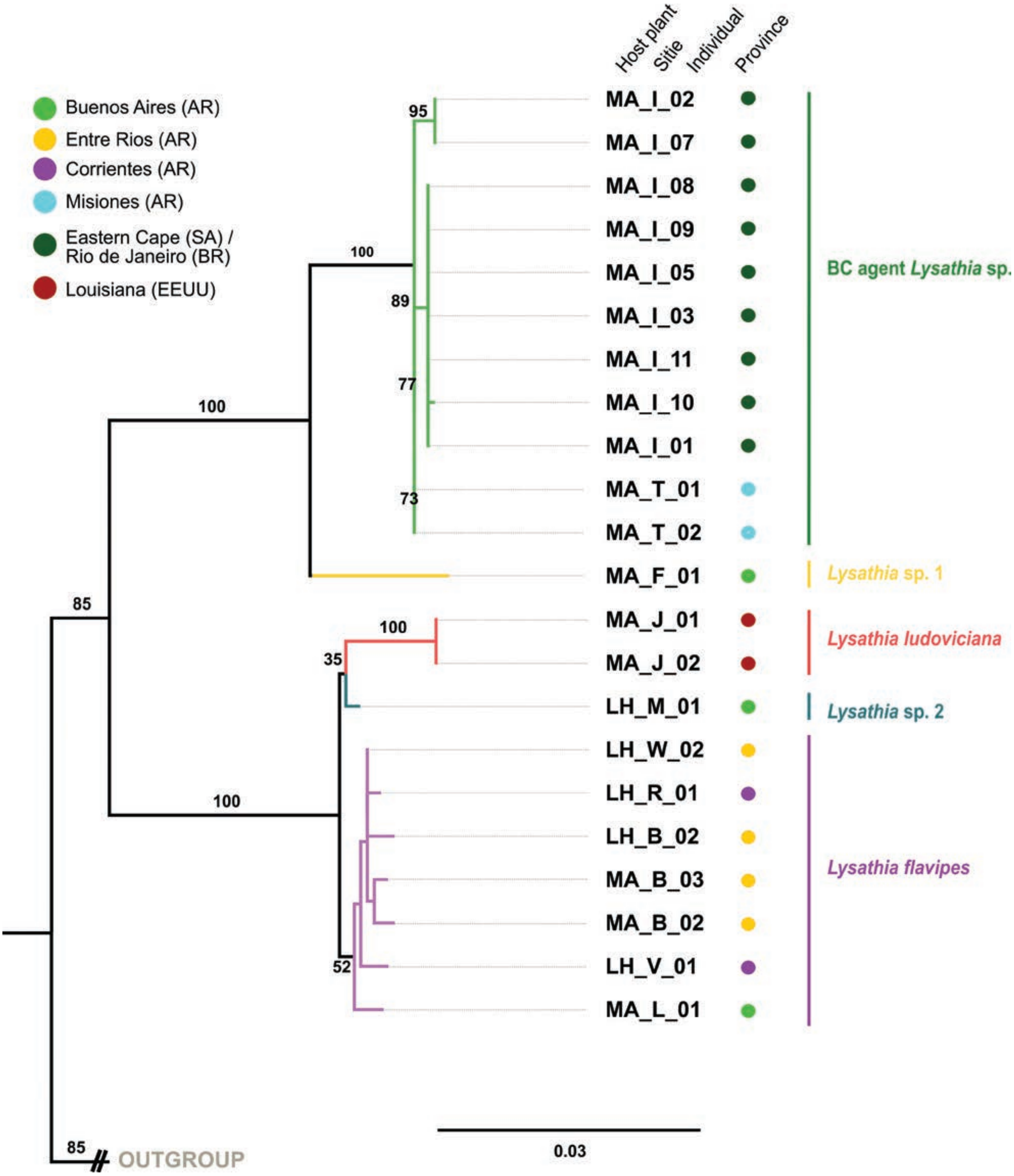

Figure 4. Best tree generated in RAxML for the *Lysathia* species studied, based on the combined mitochondrial (COI) and ribosomal (16S) genes. Names at the end of each terminal indicate the collection code (host plant_collection site code_ number of individual). Abbreviation of host plants: *Myriophyllum aquaticum* (MA), *Ludwigia g.* subsp. *hexapetala* (LH), *Ludwigia p.* subsp. *montevidensis* (LM). Collection site code: see Table 1. The coloured circles refer to the provinces/ states where the specimens were collected. The outgroup has been removed for clarity. The complete tree is presented in Suppl. material 1: figure S4.2.

observations in the phylogenetic trees (Figs 3, 4), the H14 haplotype, represented by a specimen collected in Gorchs (Buenos Aires Province), shows distinctiveness, suggesting it may represent a distinct or new species (*Lysathia* sp. 2).

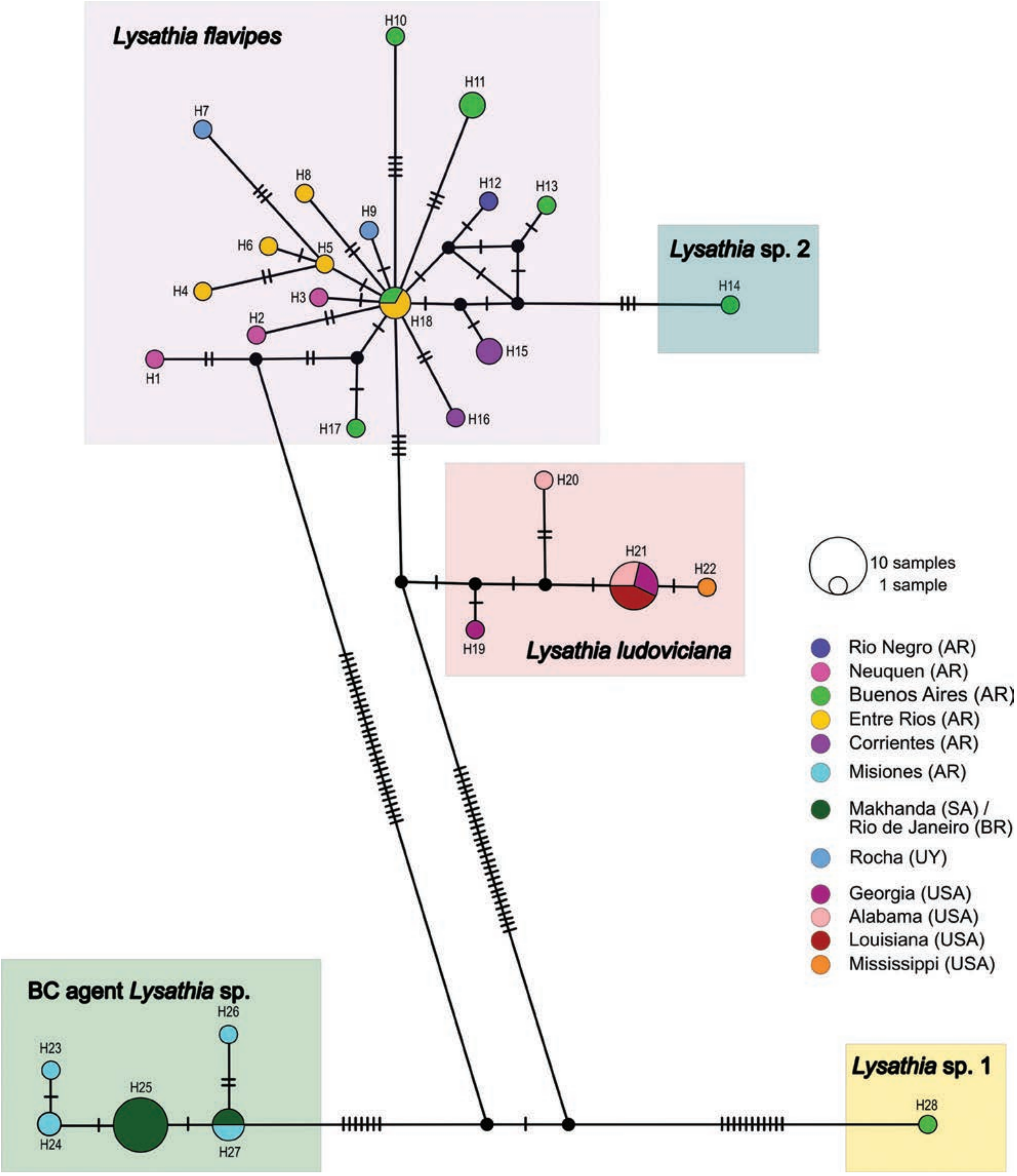

Figure 5. Mitochondrial haplotype network (COI) for *Lysathia* species estimated using the TCS algorithm in PoPArt. Each circle represents a haplotype, with its size proportional to its frequency. Colours indicate the province or state where the specimens were collected.

The cluster corresponding to specimens collected as the BC agent *Lysathia* sp. consisted of 17 sequences and five haplotypes. This cluster includes specimens from Misiones and South Africa (derived from insects collected in Rio de Janeiro, Brazil), which supports the observed morphological similarity in the field among these specimens. Notably, haplotype H27 was found in specimens from both locations (Fig. 6), suggesting they belong to the same species.

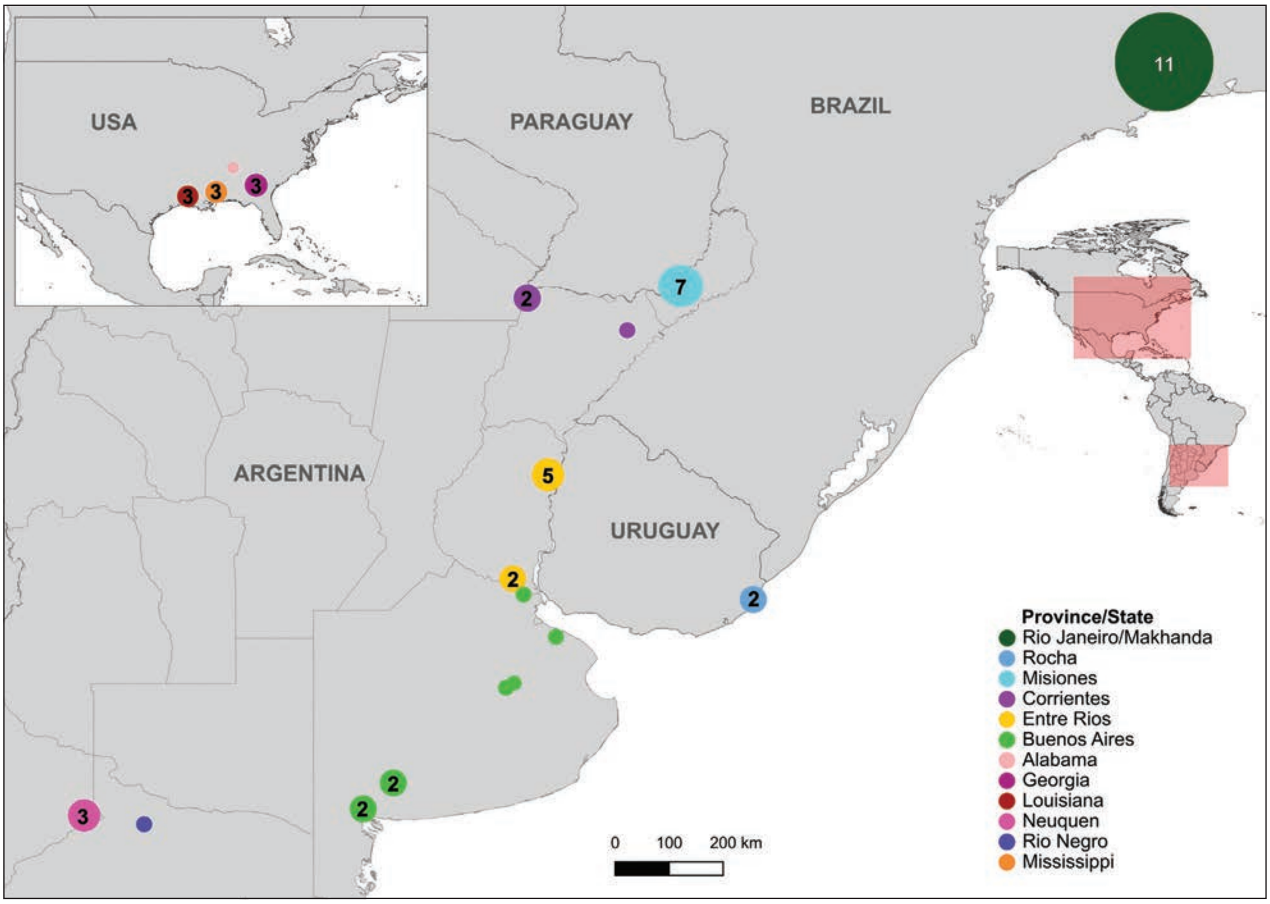

Figure 6. Map showing collection sites where DNA samples of *Lysathia* spp. were obtained. Circles represent collection sites, with their size proportional to the number of sequences collected (numbers inside the circles). Colours represent provinces or states where samples were collected, matching those shown in the haplotype network. Additional details are provided in Table 1.

The cluster comprising specimens collected as *L. ludoviciana* consisted of ten sequences and four haplotypes. Among these, haplotype H21 was the most frequent, including specimens distributed in Louisiana, Alabama, and Georgia. The haplotype network indicates a close relationship between *L. flavipes* and *L. ludoviciana*.

Finally, a unique haplotype (H28) from Buenos Aires Province (Otamendi locality) was observed. This haplotype, originally identified as a specimen of *L. flavipes*, did not group with other *L. flavipes* haplotypes and was thus reclassified as *Lysathia* sp. 1. Haplotype H28 was found to be highly differentiated from the clusters of *L. flavipes* and *L. ludoviciana* and, to a lesser extent, although still highly differentiated, from the BC agent *Lysathia* sp. This observation, supported by the phylogenetic study, suggests that *Lysathia* sp. 1 likely represents a distinct species from the three evaluated in this analysis.

Morphological studies

Previous knowledge of the morphology of some of these species, combined with the results from phylogenetic reconstruction and genetic diversity analysis of collected specimens, provided robust support for the morphological characterisation of *L. flavipes* and the BC agent *Lysathia* sp. Since all specimens used for genetic studies were preserved, the 47 individuals were morphologically compared. For *L. flavipes*, this comparison allowed for the incorporation of new information to expand upon Boheman's (1859) brief description. For the BC agent *Lysathia* sp., the morphological analysis enabled us to provide a detailed description of a new species, *Lysathia cilliersae* sp. nov.

Taxonomic account

Lysathia flavipes **(Boheman, 1859)**
Figs 7–10

Graptodera flavipes Boheman, 1859: 188.
Altica flavipes (Boheman): Weise 1888: 825.
Lysathia flavipes (Boheman), Bechyné 1959: 303.

Lectotype designation. Boheman (1859) did not specify a holotype specimen or number of specimens included in the original type series. To stabilise the nomenclature and provide a clear reference point, we designate here as the lectotype the female specimen labelled NHRS-JLKB 000073986 from Montevideo, Uruguay, housed at the Swedish Museum of Natural History. The remaining specimens from the original series are hereby designated as paralectotypes: NHRS-JLKB 000073987 (from Montevideo, Uruguay), NHRS-JLKB 000073988 (from Buenos Aires, Argentina), and NHRS-JLKB 000073989 (also from Buenos Aires, Argentina).

Material examined. ***Lectotype*****:** Photographs of the lectotype with labels. Uruguay • 1♀, pinned; Montevideo; 1859; "Kinb.", "flavipes Bhn.; NHRS-JLKB000073986. ***Paralectotypes*****:** Photographs of Paralectotypes with lables. Argentina • 1♂ pinned; "Buen. Ayr." [Buenos Aires]; "Kinb."; NHRS-JLKB000073988 • 1♂, pinned; "Buen. Ayr." [Buenos Aires]; "Kinb."; NHRS-JLKB000073989. Uruguay • 1♀, pinned; Montevideo; "Kinb."; NHRS-JLKB000073987 (Fig. 7).

Other material examined. Specimens used in genetic and morphological studies. Argentina – **Buenos Aires prov.** • ♀; Bahía Blanca; -38.699335, -62.329274; 28 Feb. 2021; A. Faltlhauser leg.; on *Ludwigia p*. subsp. *montevidensis*, chemically treated for DNA extraction; GenBank: PQ558505; Collectors code (C.c.): LFLMU01 (47); MLP • ♂; same data as preceding; GenBank: PQ558506; C.c.: LFLMU02 (48); MLP • ♂; Villa Ventana; -38.069774, -61.925423; 28 Feb 2021; A. Faltlhauser leg.; on *Ludwigia p*. subsp. *montevidensis*, chemically treated for DNA extraction; GenBank: PQ558504; C.c.: LFLMA02 (38); MLP • ♀; same locality and date as preceding; A. Faltlhauser leg.; on *Ludwigia p*. subsp. *montevidensis*; C.c.: LFLMA01 (16); MLP • ♂; Las Flores; -35.955143, -59.011231; 6 May 2022; A. Faltlhauser leg.; on *Myriophyllum aquaticum*, chemically treated for DNA extraction; GenBank: PQ558511, PQ621640; C.c.: LFMAL01 (12); MLP • ♀; same data as preceding; GenBank: PQ558512; C.c.: LFMAL02 (35); MLP • ♀ La Plata; -35.002000, -58.0256321; 21 Dic 2021, A. Faltlhauser leg; on *Ludwigia g*. subsp. *hexapetala*, chemically treated for DNA extraction; GenBank: PQ558496; C.c.: LFLHP01 (8); MLP • ♀ Dique Luján; -34.36496, -58.67688; 23 Sep 2021; on *Myriophyllum aquaticum*, chemically treated for DNA extraction; C.c.: LFMAN01 (10); MLP • ♀; R. Otamendi; -34.098854, -58.796713; 26 Jan 2021; A. Faltlhauser leg.; on *Myriophyllum aquaticum*, chemically treated for DNA extraction; GenBank: PQ558510,

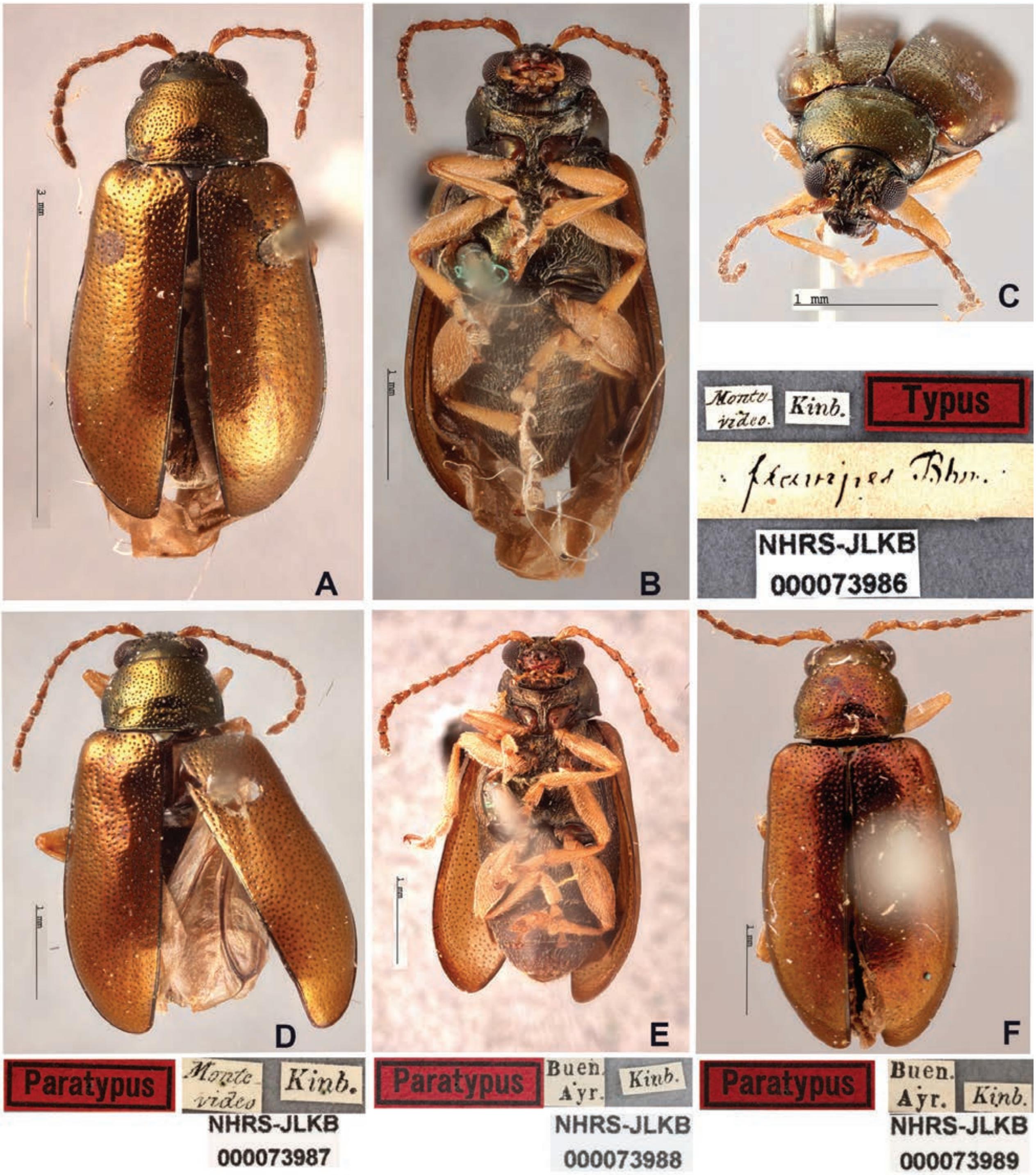

Figure 7. *Lysathia flavipes* (Boheman) **A–C** lectotype, female **A** dorsal **B** ventral **C** head **D** paralectotype, Montevideo **E** paralectotype Buenos Aires, male, ventral **F** paralectotype Buenos Aires, male, dorsal. Photographed by Anna Jerve (© 2022 Naturhistoriska Riksmuseet). Original photographs provided by the Swedish Museum of Natural History under Creative Commons Attribution 4.0 International Public License, CC-BY 4.0 (https://creativecommons.org/licenses/by/4.0/legalcode).

PQ621639; C.c.: LFMAF01 (11); MLP. – **Corrientes prov.** • ♂; Galarza; -28.090452, -56.709842; 01 Dic 2021; A. Faltlhauser leg; on *Ludwigia g*. subsp. *hexapetala*, chemically treated for DNA extraction; GenBank: PQ558500, PQ621634; C.c.: LFLHR01 (13); MLP • ♀; same data as preceding; C.c.: LFLHR02 (39); MLP • ♂; Laguna Brava; -27.49034, -58.71573; 29 May 2022; A. Faltlhauser leg; on *Ludwigia g*. subsp. *hexapetala*, chemically treated for DNA extraction; GenBank:

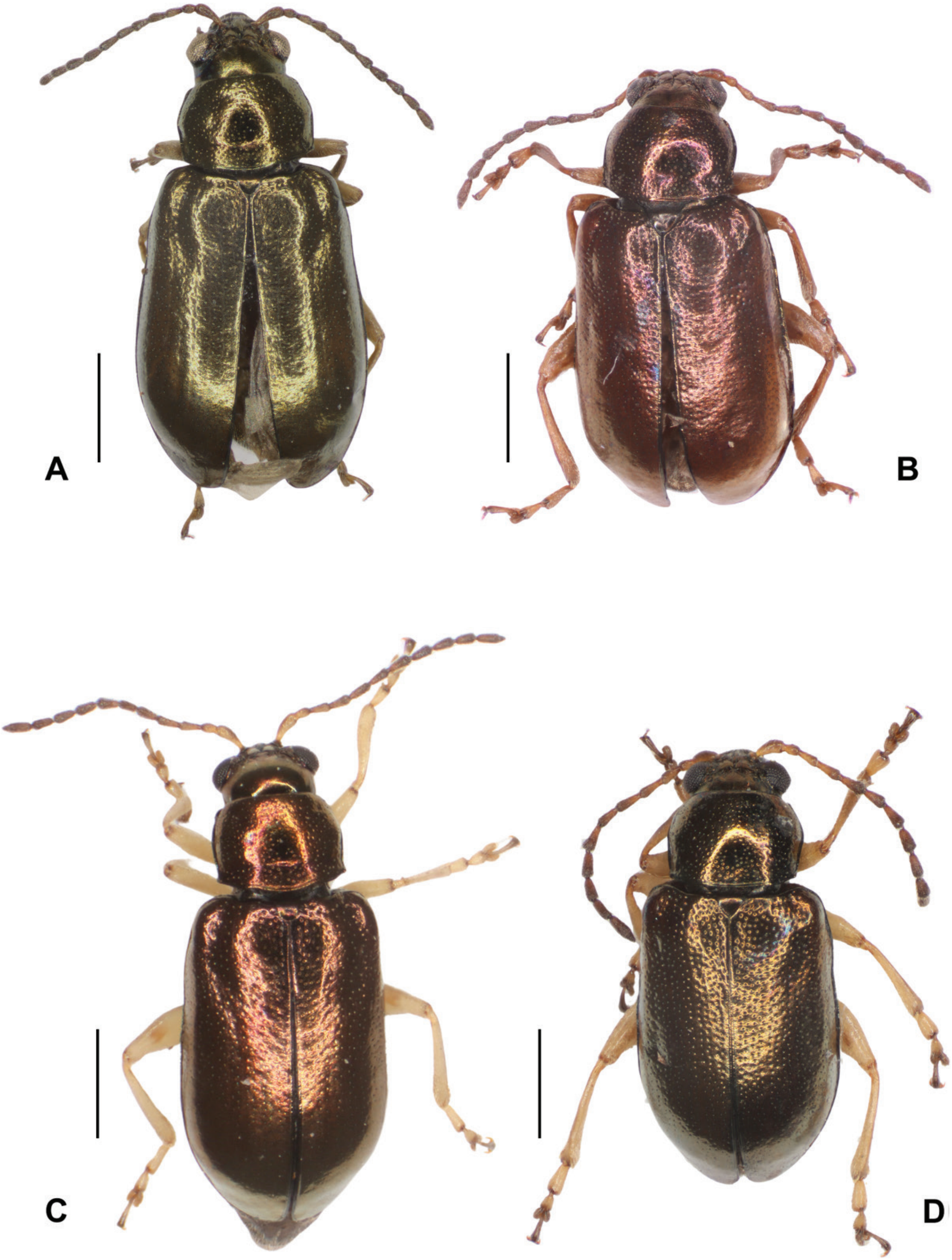

Figure 8. *Lysathia flavipes*, examples of colour variability **A** bronze-piceous dorsum (code MA_N_01) with a golden-green metallic sheen. Female. Dique Luján, Argentina **B** purplish piceous dorsum. Legs pale brown (code LM_U_01). Female. Bahía Blanca, Arg **C** copper-piceous dorsum. Whitish yellow legs. Female. Dique Luján, Arg **D** bronze -piceous dorsum. Legs whitish yellow. Male. La Plata, Arg.

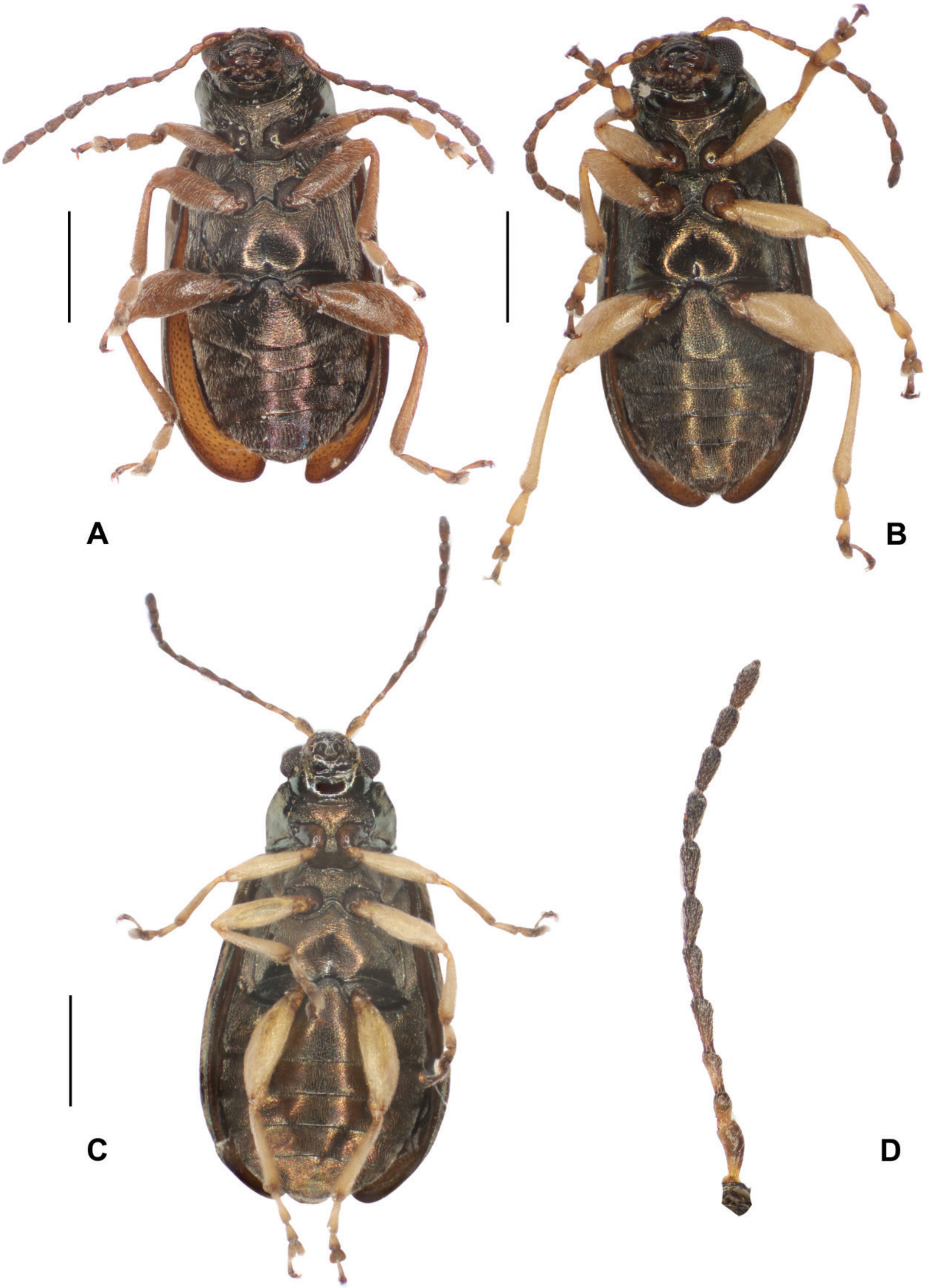

Figure 9. *Lysathia flavipes*, ventral, piceous colour. Variability in leg colouration **A** pale brown legs (code LM_U_01). Female. Bahía Blanca, Arg **B** whitish yellow legs. Male. La Plata, Arg **C** whitish yellow legs. Female. Dique Luján, Arg **D** left antenna. Female, La Plata, Arg.

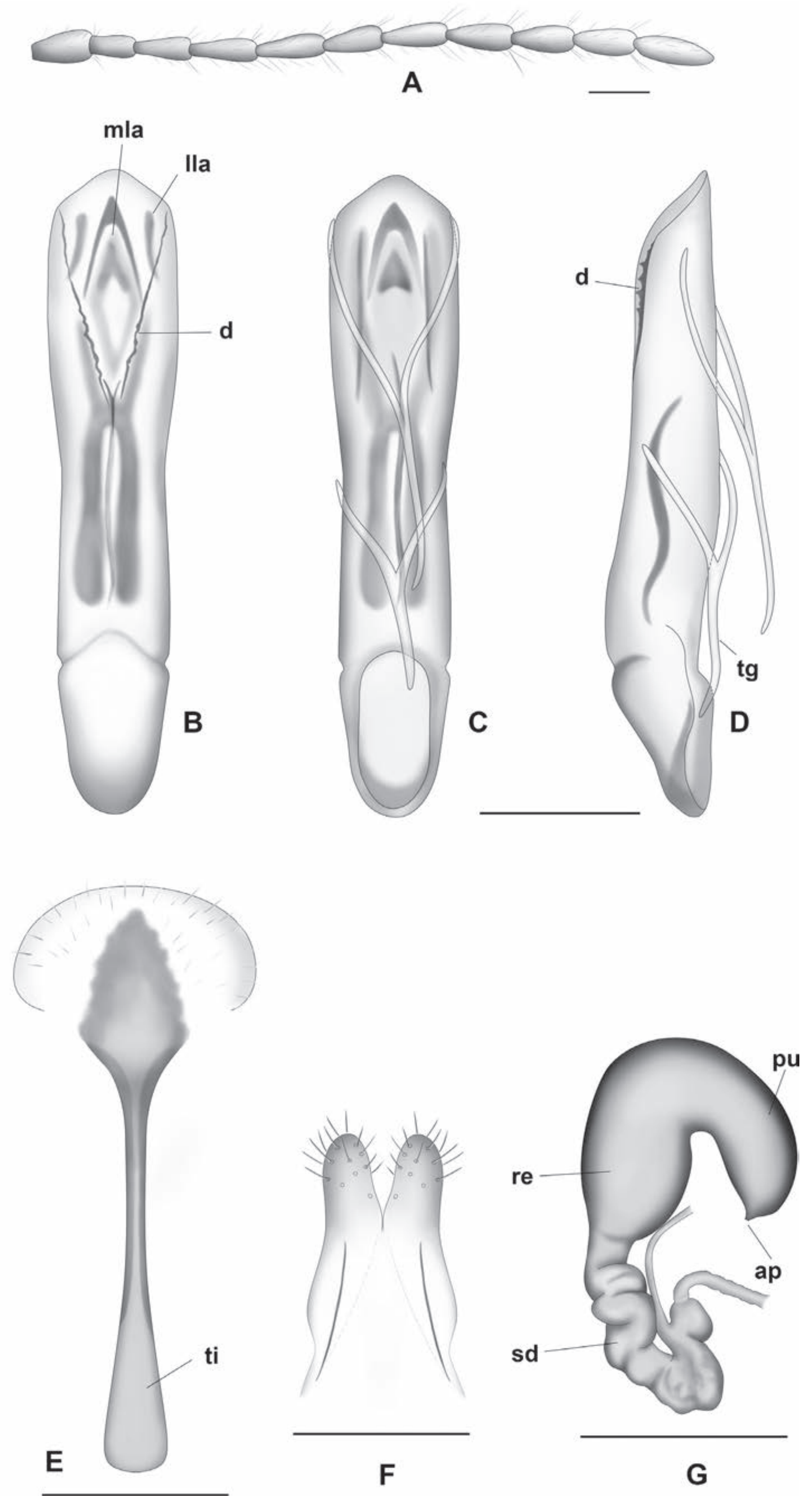

Figure 10. *Lysathia flavipes* **A** antenna **B–D** median lobe of aedeagus **B** dorsal view **C** ventral view **D** lateral view **E** sternite 8 **F** vaginal palpi **G** spermatheca. Abbreviations: **ap**: appendix, **d**: denticles, **lla**: lateral lamella, **mla**: median lamella, **pu**: pump, **re**: receptacle, **sp**: spermathecal duct, **tg**: tegmen, **ti**: tignum. Illustrations by Dr. Julia Rouaux. Scale bars: 0.1 mm.

PQ558501, PQ621635; C.c.: LFLHV01 (14); MLP • ♀; same data as preceding; GenBank: PQ558502; C.c.: LFLHV02 (19); MLP. – **Entre Ríos prov.** • ♂; Calabacillas, Cañada Venancio; -31.54152, -58.18974; 11 Jan 2022; A. Faltlhauser leg; on *Ludwigia g*. subsp. *hexapetala*, chemically treated for DNA extraction; GenBank: PQ558491; C.c.: LFLHB01 (40); MLP • ♀; same data as preceding; GenBank: PQ558492, PQ621632; C.c.: LFLHB02 (41); MLP • ♂; same location and collector as preceding; on *Myriophyllum aquaticum*, chemically treated for DNA extraction; GenBank: PQ558507; C.c.: LFMAB01 (42); MLP • ♀; same data as preceding; GenBank: PQ558508, PQ621637; C.c.: LFMAB02 (43); MLP • ♂; same data as preceding; GenBank: PQ558509, PQ621638; C.c.: LFMAB03 (44); MLP • ♀; Brazo Largo; -33.865303, -58.88294; 5 Feb 2022; A. Faltlhauser leg; on *Ludwigia g*. subsp. *hexapetala*, chemically treated for DNA extraction; C.c.: LFLHW01 (15); MLP • ♂; same data as preceding; GenBank: PQ558503, PQ621636; C.c.: LFLHW02 (20); MLP. – **Neuquén prov**. • ♀; Plottier, Río Limay; -38.969486, -68.185343; 21 Feb 2021; A. Faltlhauser leg; on *Ludwigia g*. subsp. *hexapetala*, chemically treated for DNA extraction; GenBank: PQ558497; C.c.: LFLHQ01 (9); MLP • ♂; same data as preceding; GenBank: PQ558498; C.c.: LFLHQ02 (36); MLP • ♂; same data as preceding; GenBank: PQ558499; C.c.: LFLHQ03 (37); MLP. – **Río Negro prov.** • ♂; Villa Regina; -39.09821, -67.075377; 29 Mar 2022; A. Faltlhauser leg.; on *Myriophyllum aquaticum*, chemically treated for DNA extraction; C.c.: LFMAS01 (31); MLP • ♀; same data as preceding; chemically treated for DNA extraction; GenBank: PQ558513; C.c.: LFMAS02 (32), MLP. URUGUAY – **Rocha prov.** • 5♀, 2♂; Punta del Diablo; -34.0130556, -53.598305; 10 Mar 2019; P. Pratt leg.; on *Ludwigia g*. subsp. *hexapetala*, chemically treated for DNA extraction; C.c.: LFLHH01-07 (17,18,21–23,33,34); MLP • ♀; same data as preceding; GenBank: PQ558493; C.c.: LFLHH08 (UY1) • ♂; same data as preceding; GenBank: PQ558494; C.c.: LFLHH09 (UY2).

Diagnosis. The characters that identify this species are: predominant bronze colour with golden, greenish, or purple reflections and piceous abdomen. Antennae brown, antennomere 1–3 yellowish. Antennomere 2 oval. Antebasal sulcus of prothorax slightly impressed. Lamina of sternite 8 subtriangular, spatular or with irregularly expanded sides; vaginal palpi short, conical. Median lobe broadened anteriorly from medial length, margins of dorsal depression with small denticles.

Description. Female. The description is based on photographs of the lectotype and paralectotypes, and on specimens collected in Argentina and Uruguay. Length: 4.3 (0.13); elytral base width: 1.7 (0.04); max. elytral width: 2.1 (0.13) ($n = 7$). ***Colour*.** Head bronze. Antennae brown, antennomeres 1–3 pale brown or yellowish. Mandibles, labium, and maxillae brown. Scutellum piceous. Thorax and dorsal elytra bronze with golden, greenish, or purple reflections. Abdomen, piceous. Legs whitish yellow, coxae chestnut, tarsomeres 1–3 yellowish, distal part dark brown. Ventral surface piceous (Figs 7–9). ***Head*** (Fig. 7C). Vertex glabrous, coarse setiferous punctures located above posterior margin of eyes, others located between inner margin of eyes and antennal calli. Post antennal calli barely raised, trapezoidal; antennal sockets closed to anterior margin of eyes, distance between them greater than transverse diameter of antennal sockets. Frontal ridge moderately convex; anterofrontal ridge lower than frontal ridge in lateral view, with small setae on each side, two or three short setae below antennal sockets and two long setae near base of clypeus. Antennae 11-segmented, inserted below midline of eyes, extended less than half of elytral length; antennomere 2 short, oval, longer than half the length of antennomere

3, antennomere 3 elongate, barely shorter than antennomere 4; antennomeres 4–7 cylindrical, similar in length, antennomeres 8–10 somewhat shorter, antennomere 11 acuminate at apex. Antennomeres 1–3 scarcely setose, from 4–11 densely setose over entire surface; all antennomeres with stiff, spreading setae at apex (Figs 9D, 10A). Eyes convex, inner margin slightly concave. ***Thorax*** (Figs 7, 8). Pronotum slightly convex, with irregular punctation, maximum width near mid-width. Antebasal sulcus slightly impressed, not reaching lateral margins; anterior lateral angles rounded, posterior angles acuminate, each with a long seta. Prosternum convex, finely pubescent, narrow prosternal process, rounded at apex, extending beyond the procoxal cavities; these are rounded and open posteriorly. Mesosternum with dense pubescence, short and wide mesosternal process; mesocoxal cavities inserted at the posterior margin. Metasternum usually longer than wide, central area finely striated, densely pubescent laterally, metacoxal cavities transverse, inserted at the posterior margin. Elytra convex, broader than pronotum; maximum width near the posterior third. Surface uniformly punctate in the basal half, with punctures similar but sparser than those on the pronotum, and more finely punctate towards the apex. Discal punctures aligned in two short rows near the elytral suture, humeral calli rounded, smooth. Epipleura subvertical, broad at the base, gradually narrowed towards the middle of the elytral length. Legs with the pro-mesofemora fusiform, moderately broadened; metafemora broader, dorsal margin slightly convex, anterior margin nearly straight. Apical margins of all tibiae with short spurs; trochanters, femora, and tibiae of all legs sparsely setose; ventral and lateral margins of metalegs densely setose. Tarsomere 1 of prolegs triangular, shorter than tarsomeres 2+3 combined; tarsomere 2 triangular; tarsomere 3 deeply bilobed. Tarsomeres 1 of meso-metalegs elongated, longer than tarsomeres 2+3 combined, claws appendiculate. ***Abdomen*** (Figs 7B, 9). Margin of fifth sternite convex.

Male. The specimens examined are similar in colour and sculpturing to the female. Body smaller, length: 3.9 (0.21); elytral base width: 1.5 (0.06); maximum elytral width: 1.7 (0.10) (n = 8). Similar to female in colour and morphology. Abdomen with margin of fifth sternite truncated (Figs 7E, 9B).

Description of genitalia in specimens from Argentina. *Female genitalia*. Sternite lamina 8 (Fig. 10E) subtriangular, lateral margins irregular, distal third of lamina sclerotized, tignum thin ~ 2.5 × lamina length, basal portion widened, broad. Vaginal palpi (Fig. 10F) short, conical, slightly divergent. Spermatheca (Fig. 10G) V-shaped, receptacle and pump sclerotised, receptacle oval, distal half narrow, subcylindrical, shorter than receptacle, with a very small appendix at apex. Basal portion of spermathecal duct short, cylindrical, distal part coiled.

Male genitalia (Fig. 10B–D). Aedeagus with median lobe sclerotised, symmetrical, in dorsal view widened from middle of aedeagus, tapering towards end, apex ventrally inclined with small projection, in lateral view slightly curved. Dorsal depression long, ~ 1/2 of median lobe, margins with denticles, one median lamella and two lateral, median lamella triangular, broad and long, ~ 5 × the width of laterals. Ventral depression ~ ¾ of aedeagus. Internal sac with broad U-shaped sclerite, lateral arms broader at the base, connected by a slightly sclerotised area. Tegmen Y-shaped, manubrium and arms of similar length.

Variations. The paralectotypes and other specimens of *L. flavipes* examined are similar to the lectotype specimen; however, there is variation in colouration, punctation, and details of the genitalia. It is necessary to consider the possible colour variations of the type series specimens that were collected before 1859. The colouration variations observed in mature, living specimens are often related to light incidence due to cuticle reflection. For example, the colouration of the Montevideo paralectotype specimen (Fig. 7D) shows variation in the colour of the pronotum that is metallic greenish; the ventral surface of antennomere 1 and the apex of the remaining antennomeres are somewhat darker than in the type, while the elytra are a paler bronze. In the paralectotype from Buenos Aires, the general colour is metallic bronze (Fig. 7F) and the yellow legs are paler. Some specimens collected in Argentina display a darker colour on the antennae and pronotum.

Punctation may vary due to the depth and distance between them. The greatest variation is observed in the punctation near the humeral calli where, in some specimens, is arranged in two rows surrounding the humeral calli. Female genitalia show minor variations. The lamina of sternite 8 is the most variable structure, its shape being highly irregular in some specimens, while in others there may be slight differences in the degree of divergence of the vaginal palpi and development of spermatheca.

Geographic distribution. *Graptodera flavipes* was originally described from Argentina (Buenos Aires) and Uruguay (Montevideo). Later Bechyné (1954, 1957b, 1959) recorded it in other Argentine provinces (Entre Ríos, Misiones, Corrientes, and Córdoba), Brazilian states (Mato Grosso, Santa Catarina, and Rio Grande do Sul), Bolivia, and Paraguay. Scherer (1960) recorded it for Amazonas (Brazil) and Río Negro province (Argentina). In this work, its distribution is expanded to more localities of the mentioned Argentine provinces and the southern limit of distribution is extended to the province of Neuquén (38°S).

Host plants. *Lysathia flavipes* was found feeding on *Ludwigia grandiflora* subsp. *hexapetala*, *Ludwigia peploides* subsp. *montevidensis* (Onagraceae) and *Myriophyllum aquaticum* (Haloragaceae).

Comments. Bechyné (1954) described two new species, *Altica bohumilae* and *Altica muriensis*, and included them in a key with *A. flavipes*. He grouped these species, later transferred to the genus *Lysathia*, based on their general copper to purplish colouration, with yellow legs and antennae (Bechyné 1959). *Lysathia flavipes* and *L. bohumilae* share the tarsomere of the male prolegs being less developed than that of *L. muriensis*. *Lysathia bohumilae* (cited for Argentina: Buenos Aires, Entre Ríos; Paraguay; and Brazil: Rio Grande do Sul) is a robust species, 4.5–5.5 mm, dark brown in colour, with very fine body punctation that decreases in the apical region of the elytra. *Lysathia muriensis*, cited for Rio de Janeiro (Brazil), differs from the other two species by the the tarsomere 1 of the male prolegs that is as wide as the base of the tibia. Other differentiating characters include a yellow general body colour with pale brown lateral areas on the elytra, and dense pubescence on the apical part of the elytra.

Bechyné included a new species, *L. louella*, in the *"flavipes* group" (Bechyné 1954), cited for Argentina (Tucumán and Salta), which so far does not share its distribution with the species mentioned above. Similar in size to *L. flavipes*, it differs from the other species by the structure of the elytra and its general brown colour with steel blue reflections and reddish antennae. Later, Bechyné (1957a) described *L. viedma* and *L. patagonica* for southern Argentina, relating them to the *Lysathia* species reported for Chile due to their dark (sombre) colouration in legs and antennae (sometimes reddish), in contrast to those of *L. flavipes* group.

In (1959), Bechyné described *L. chaparensis*, *L. arapata*, and *L. hygrobia* for Bolivia, associating these three species with the "*flavipes* group". The broad development of the tarsomere 1 of the male prolegs relates these species to *L. muriensis*.

Much later, Medvedev (2001) described *Lysathia siolii* from specimens collected on *Ludwigia natans* for the Pantanal region (alluvial plain shared by Mato Grosso do Sul, Mato Grosso, part of Bolivia and Alto Paraguay). He placed this species in the *flavipes* group, close to *L. bohumilae*, *L. flavipes*, and *L. hygrobia* (Bechyné 1959) from Bolivia because of its general bronze colouration and piceous antennae with dark ochre inner part. However, *L. siolii* differs by the dense and deep punctation of the elytra and a well-developed ventral ridge of the median lobe of aedeagus.

***Lysathia cilliersae* Cabrera, sp. nov.**

https://zoobank.org/4557971C-2EBD-4581-AFFE-D09BACCEE39A
Figs 11–15

Type material. *Holotype*: Argentina – **Misiones prov.** • 1♂ pinned; Domingo Savio (Ruta 6, 32 km E de Gob. Roca); -27.25561, -55.29895; 15 Nov 2022; A. Faltlhauser leg.; on *Myriophyllum aquaticum*, chemically treated for DNA extraction, left hind leg missing; GenBank: PQ558487, PQ621630; Collectors code: LCMAT01 (45); MLP. ***Paratypes*:** Argentina – **Misiones prov.** • 1♀; Domingo Savio (Ruta 6, 32 km E de Gob. Roca); -27.25561, -55.29895; 7 Jan 2024; A. Faltlhauser leg.; blue, on *Myriophyllum aquaticum*, chemically treated for DNA extraction; GenBank: PQ556199; Collectors code (C.c.): LCMAT04 (50); MLP • 1♀,1♂; same locality as for preceding; 7 Jan 2024; A. Faltlhauser leg.; on *Myriophyllum aquaticum*; MLP • 1♂ with genitalia in a separate microvial; same locality as preceding; 7 Jan 2024; A. Faltlhauser leg.; blue, on *Myriophyllum aquaticum*, chemically treated for DNA extraction; GenBank: PQ556198; C.c.: LCMAT03 (49); SANC. • 1♀ with genitalia in a separate microvial; same locality as preceding; 7 Jan 2024; A. Faltlhauser leg.; bronze, on *Myriophyllum aquaticum*, chemically treated for DNA extraction; C.c.: LCMAT06 (52); SANC. • 1♂; same locality as preceding; 15 Nov 2022; A. Faltlhauser leg.; bronze, on *Myriophyllum aquaticum*, chemically treated for DNA extraction; GenBank: PQ558488, PQ621631; C.c.: LCMAT02 (46); FUEDEI • 1♂; same locality as preceding; 7 Jan 2024; A. Faltlhauser leg.; bronze, on *Myriophyllum aquaticum*, chemically treated for DNA extraction; GenBank: PQ558489; C.c.: LCMAT05 (51); FUEDEI. – **Entre Ríos prov.** • 1♂; Calabacillas, cañada Venancio, (Rt.14, km 236); -31.5444953, -58.1873180; 8 Jan 2024; A. Faltlhauser leg.; blue, on *Myriophyllum aquaticum*; C.c.: LCMAB01 (53); MLP. South Africa – **Eastern Cape.** • 1♀; Makhanda, Waainek Mass Rearing Facility (CBC); -22.438539, -44.531849; 25 Nov 2019; A. Faltlhauser leg.; bronze, couple A, on *Myriophyllum aquaticum*; GenBank: PQ558476, PQ621621; C.c.: LCMAI01 (1); MLP • 1♂; same locality and date as for preceding; A. Faltlhauser leg.; bronze, couple A, on *Myriophyllum aquaticum*, chemically treated for DNA extraction; GenBank: PQ558477, PQ621622; C.c.: LCMAI02 (2); MLP • 1♀; same locality and date as for preceding; A. Faltlhauser leg.; couple B, on *Myriophyllum aquaticum*, chemically treated for DNA extraction; GenBank: PQ558478, PQ621623; C.c.: LCMAI03 (3); MLP • 1♂; same locality and date as for preceding; A. Faltlhauser leg.; bronze,

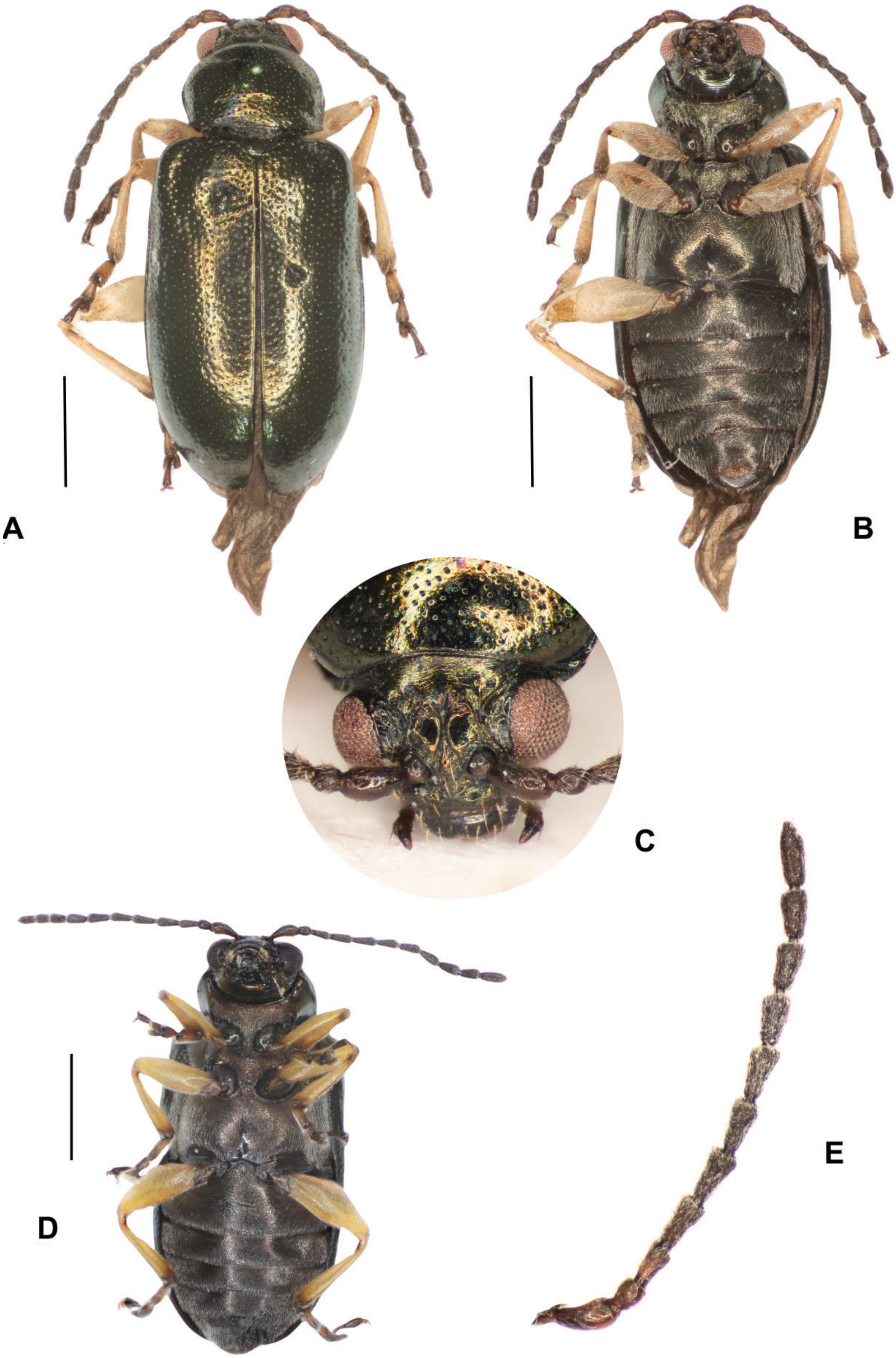

Figure 11. *Lysathia cilliersae* sp. nov. holotype. male (code MA_T_01) **A** dorsal view **B** ventral **C** head. The eye colour of this specimen is altered by the treatment for DNA extraction **D** ventral view of fresh specimen **E** antenna. Scale bars: 1 mm.

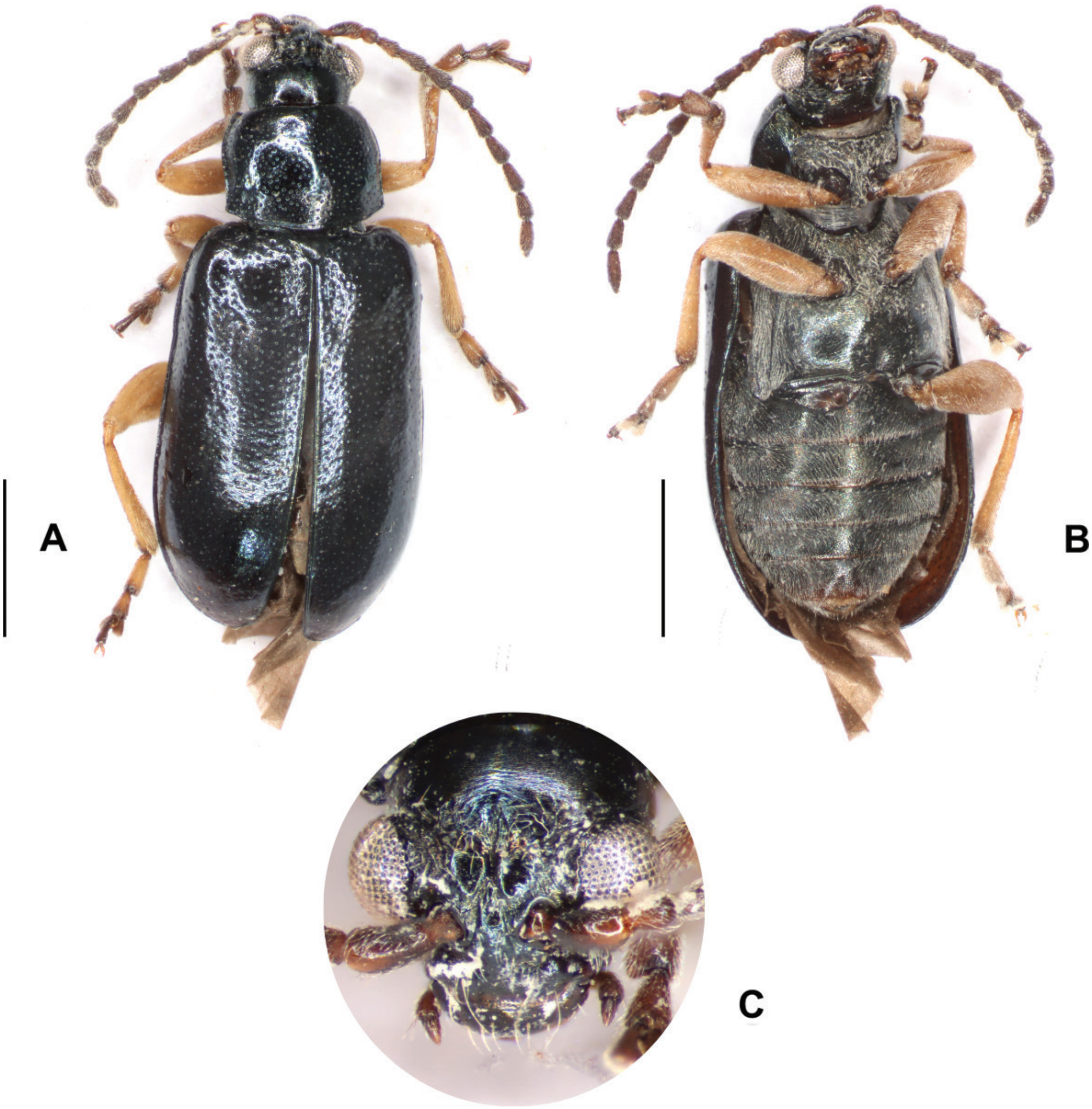

Figure 12. *Lysathia cilliersae* sp. nov. male (code MA_T_03). Colour variability in habitus **A** piceous back with silver-blue reflections **B** ventral, piceous colour **C** head. Scale bars: 1 mm.

couple B, on *Myriophyllum aquaticum*, chemically treated for DNA extraction; GenBank: PQ558479; C.c.: LCMAI004 (4); MLP • 1♀; same locality and date as for preceding; A. Faltlhauser leg.; bronze, couple D; on *Myriophyllum aquaticum*, chemically treated for DNA extraction; GenBank: PQ558482, PQ621625; C.c.: LCMAI007 (26); SANC • 1♂; same locality and date as for preceding; A. Faltlhauser leg.; bronze, couple D; on *Myriophyllum aquaticum*, chemically treated for DNA extraction; GenBank: PQ558483, PQ621626; C.c.: LCMAI08 (27); SANC • 1♀; same locality and date as for preceding; A. Faltlhauser leg.; bronze, couple C; on *Myriophyllum aquaticum*, chemically treated for DNA extraction; GenBank: PQ558480, PQ621624; C.c.: LCMAI05 (5); FUEDEI • 1♂; same locality and date as for preceding; A. Faltlhauser leg.; bronze, couple C; on *Myriophyllum aquaticum*, chemically treated for DNA extraction; GenBank: PQ558481; C.c.: LCMAI06 (6); FUEDEI • 1♂; same locality and date as for preceding; A. Faltlhauser

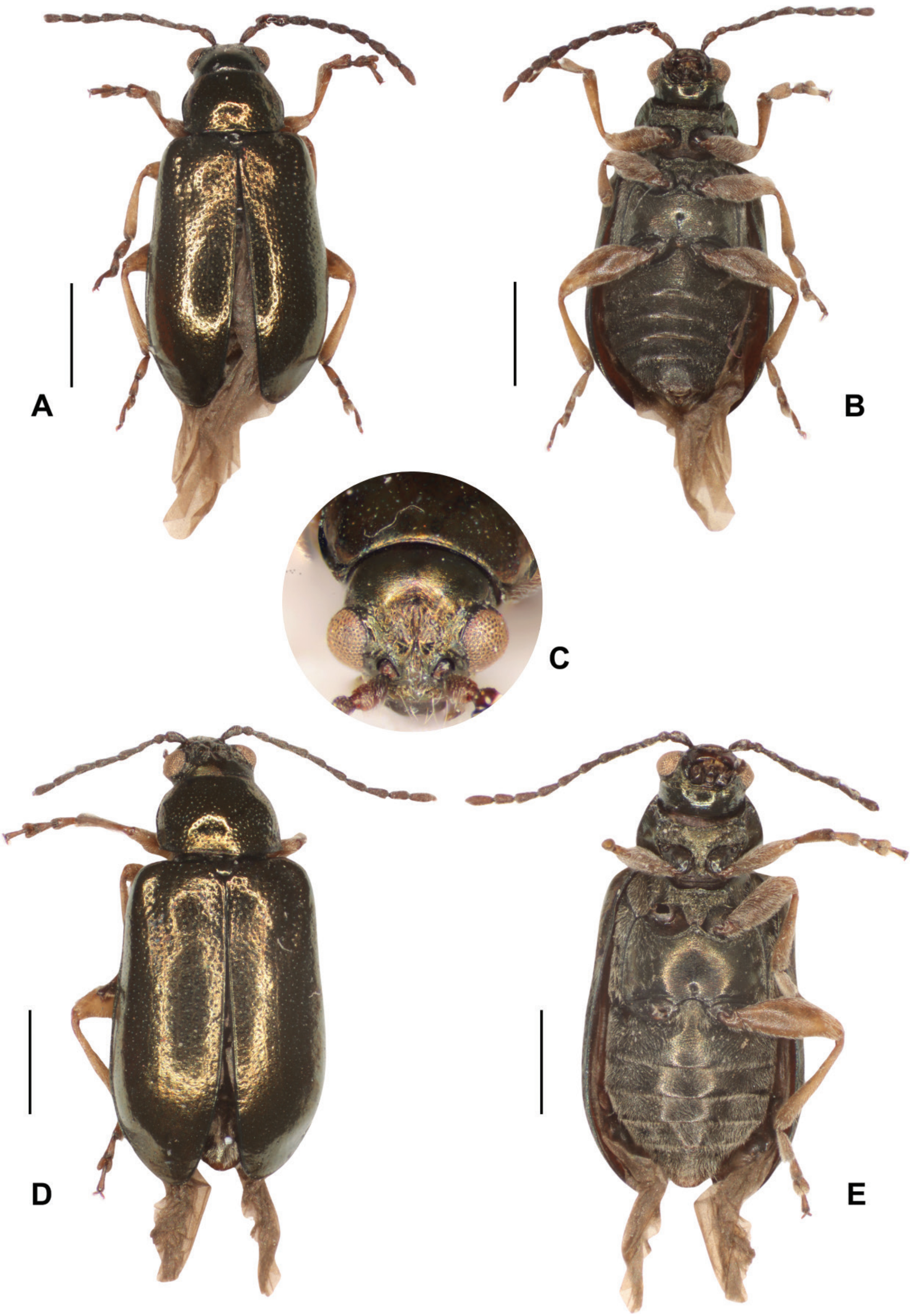

Figure 13. *Lysathia cilliersae* sp. nov. Specimens from mass rearing at the Centre for Biological Control (CBC), Makhanda, South Africa. Male specimen (code MA_I_02) **A** dorsal view **B** ventral view **C** head. Female specimen (code MA_I_01) **D** dorsal view **E** ventral view. Scale bars: 1 mm.

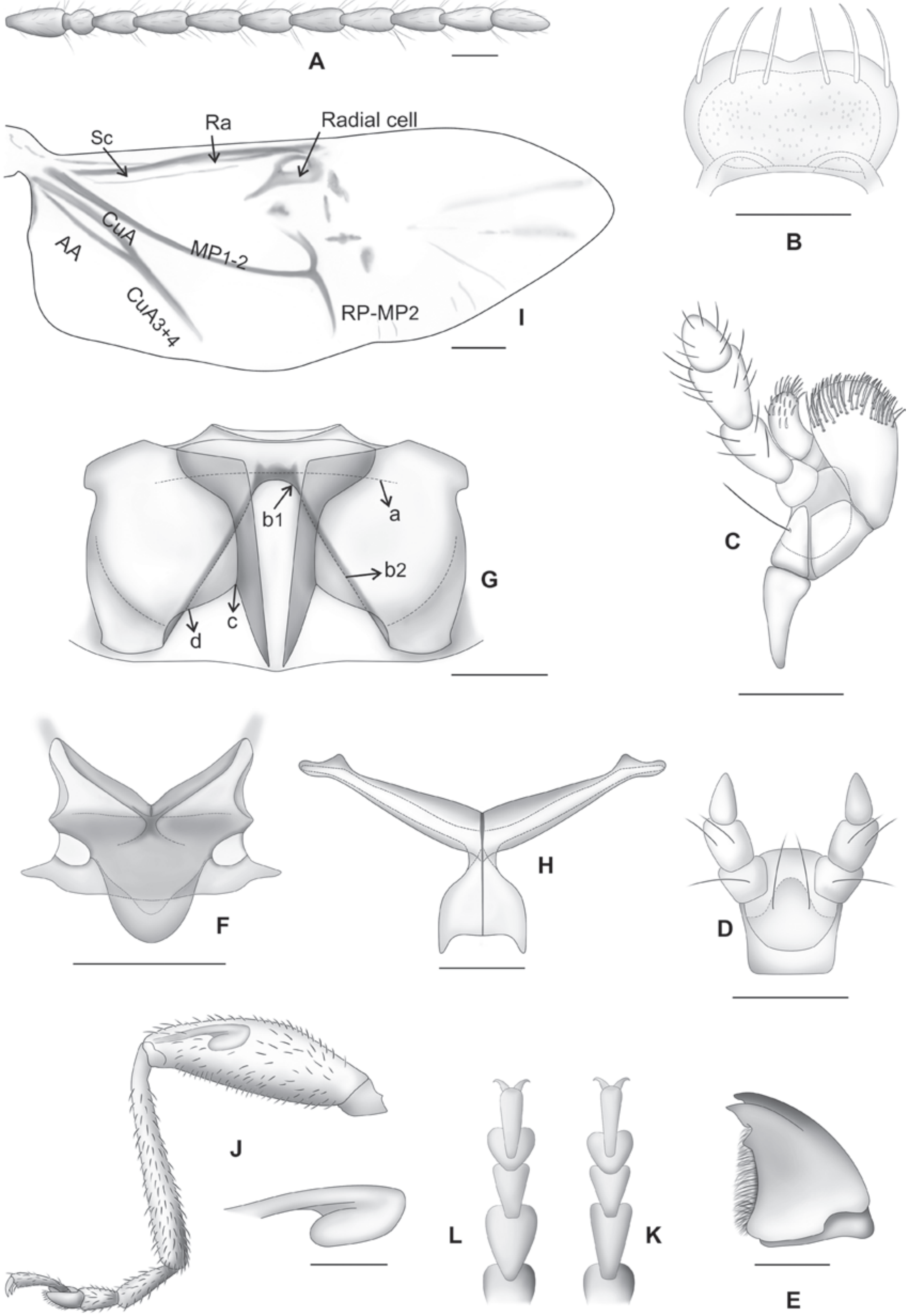

Figure 14. *Lysathia cilliersae* sp. nov. **A** antenna **B** labrum, dorsal view **C** maxilla, ventral view **D** labium, ventral view **E** mandible, external view **F** scutellum **G** metanotum **H** metendosterite, dorsal view **I** hind wing **J** leg and jumping organ of the metafemur **K** tarsitus of female proleg **L** tarsitus of male proleg. Abbreviations: **a**, metanotal bridge; **b1**, metanotal bridge b1; **b2**, metanotal bridge b2; **c**, metanotal bridge c; **d**, metanotal bridge d; **AA**, anal vein AA. **CuA**, cubital anal vein; **CuA 3+4** cubital anal vein 3+4; **MP 1+2**, posterior medial vein 1+2; **RA**, radial vein; **RAc**, radial cell; **SC**, subcostal vein. Illustrations Dr. Julia Rouaux. Scale bars: 0.1 mm.

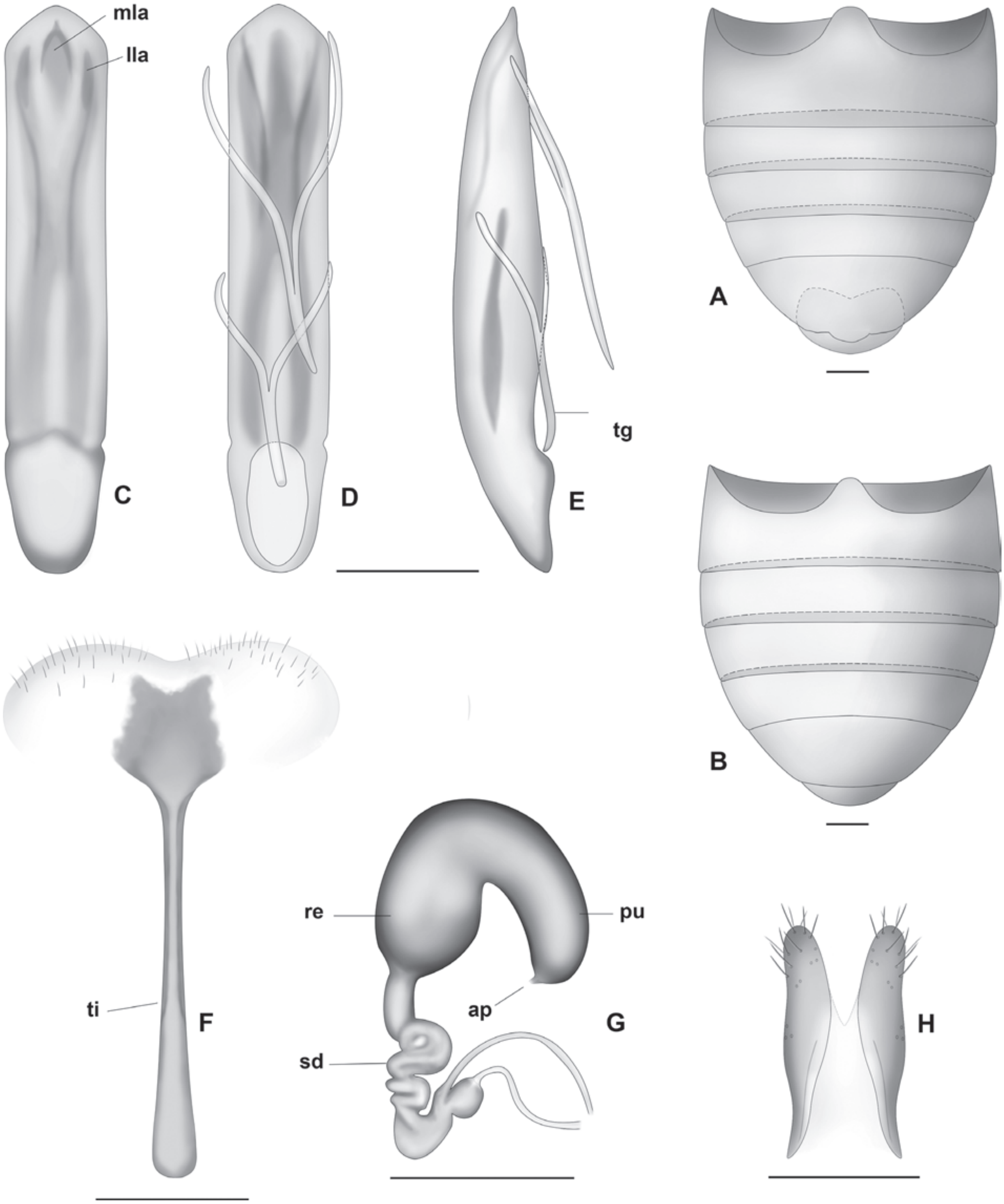

Figure 15. *Lysathia cilliersae* sp. nov. **A, B** abdomen, ventral view **A** male **B** female **C–E** median lobe of aedeagus **C** dorsal view **D** ventral view **E** lateral view **F** sternite 8 **G** spermatheca **H** vaginal palpi. Abbreviations: **ap**: appendix, **lla**: lateral lamella, **mla**: median lamella, **pu**: pump, **re**: receptacle, **sp**: spermathecal duct, **tg**: tegmen, **ti**: tignum. Illustrations Dr. Julia Rouaux. Scale bars 0.1 mm.

leg.; bronze, couple E; on *Myriophyllum aquaticum*, chemically treated for DNA extraction; GenBank: PQ558484, PQ621627; C.c.: LCMAI09 (28); SLP-art • 1♀ same locality and date as for preceding; A. Faltlhauser leg.; bronze, couple E; on *Myriophyllum aquaticum*, chemically treated for DNA extraction; GenBank: PQ558485, PQ621628; C.c.: LCMAI10 (29); SLP-art.

Other material examined. Argentina • 10♂, 10♀; Domingo Savio, Misiones (Ruta 6, 32 km E de Gob. Roca); -27.25561, -55.29895; 7 Jan 2024; A. Faltlhauser leg; on *Myriophyllum aquaticum*; FUEDEI, SLP-art. South Africa • 10♂, 10♀; Waainek Mass Rearing Facility (CBC), Makhanda, Eastern Cape; 25 Nov 2020; A. Faltlhauser leg; on *Myriophyllum aquaticum*; FUEDEI, SANC.

Diagnosis. This species can be identified by the following characteristics: general colouration piceous or dark brown with golden to green reflections (Fig. 11), dark bronze reflections (Fig. 13), or black with silver to bluish reflections (Fig. 12); Antenna piceous in colour, antennomere 2 globose. Antebasal ridge of pronotum very weakly impressed. Lamina of sternite 8 with lateral margins irregular; coxites long, thin, divergent; baculi weakly developed. Median lobe widened and tapering slightly towards the apex, margins of dorsal depression without denticules. Distal end of tibias and tarsomeres brown.

Description of the holotype male (Fig. 11). Length, 3.9 (0.13); elytra base width: 1.7 (0.03); maximum elytral width: 1.9 (0.07); (*n* = 5). Dorsal habitus piceous, or dark brown, with golden to green reflections. Ventral, dark brown (Fig. 11A, B). Antennae dark brown, basal 1/2 of antennomere 1 and inner margin of antennomere 1–3 yellowish. Distal portion of mandibles and labrum tinged with yellow. Legs yellowish white, trochanters tinged with chestnut near coxae, apex of femora and tibiae tinged with brown; tarsomeres 1 and 2 yellowish, with distal portion dark brown, tarsomere 3 brown (Fig. 11D).

Head (Fig. 11C) Vertex glabrous, more or less convex in lateral view; coarse punctures situated between posterior margin of antennal calli, inner margin of eyes and at least a pair of large supraorbital punctures; two or three pairs of long supraorbital setae; postantennal calli barely raised, trapezoidal, touching in the inner posterior angles; supracallinal sulcus strongly impressed; antennal sockets closed to anterior margin of eyes, distance between them slightly greater than transverse diameter of antennal sockets, two or three short setae below antennal sockets and two long setae near base of clypeus. Frontal ridge, moderately convex, anterofrontal ridge slightly lower than frontal ridge in lateral view, with row of small setae on each side. Antennae (Figs 11E, 14A) inserted below midline of eyes, extending 1/2 length of elytra; antennomere 2 short, globose, ~ 2 × the length of 3, antennomere 3 elongate, a little shorter than 4, antennomeres 4–7 elongate, similar in length, antennomeres 8–10 rather shorter, antennomere 11 apically acuminate. Antennomeres 1–3 scarcely setose, antennomeres 4–11 densely setose throughout, all antennomeres with erect, sparse setae at apex. Eyes convex, inner margin straight. Labrum (Fig. 14B) rectangular, distal margin slightly emarginated, with a row of six long setae near distal margin. Mandibles (Fig. 14E) symmetrical, 4-toothed apically, teeth 2–3 visible on external face, teeth 2–3 acute, subequal, tooth 4, short, acute. Maxillae (Fig. 14C) cardo apically broadened; galea subconical and lacinia cylindrical, both with fringelike pilosity, scarcer and shorter in galea. Maxillary palpi 4-segmented, palpomere 1 quadrangular, short; palpomeres 2 subcylindrical, equal, palpomere 3 subconical, rather shorter than 2, palpomere 4 subconical short, with wide base, tapering apically. Labium (Fig. 14D) with two setae between bases of palps, ligula rounded at apex; labial palp 3-segmented, palpomere 1 rectangular; palpomere 2 subconical, > 2 × longer than 1; palpomere 3 subconical with narrow base.

***Thorax*.** Pronotum slightly convex, shiny, finely punctate (1.2 wide × 0.8 mm long, *n* = 5), maximum width near the middle of the pronotum; antebasal sulcus very weakly impressed, scarcely visible, not reaching lateral margins; anterior lateral angles rounded and posterior lateral angles acuminate with a long, thin seta on each one. Surface with scattered punctures, more abundant at the base. Prosternum convex; finely pubescent, prosternal process narrow, rounded at apex, extending beyond posterior margin of procoxae, procoxal cavities oblong, open behind. Mesosternum densely microsculptured and pubescent, mesosternal process broad and short; mesocoxal cavities rounded inserted on posterior margin. Scutellum (Fig. 14F) triangular, smooth, rounded at apex. Metanotum (Fig. 4G) transverse, wider than long; metanotal ridge *d* intersecting *c* posteriorly to midpoint of *c*. Metasternum transverse, slightly concave centrally, with slightly pronounced bidentate projection between metacoxae; metacoxal cavities transverse, inserted at posterior margin. Metasternum usually broader than long, central area finely striate, densely pubescent in lateral areas, metasternal longitudinal suture visible near base of metacoxae, metacoxal cavities transverse inserted on posterior margin. Meta-endosternite (Fig. 14H) T-shaped, stalk wider at base, shorter than lateral arms, meso- and metafurcal tendons well developed, inserted near apex of lateral arms. Elytra oval, convex, slightly wider than pronotum, greatest width near the posterior one-third of elytra; humeral calli rounded, strongly produced. Surface densely, uniformly punctate; punctures somewhat coarser than on pronotum, more finely punctate at apex; discal punctures partly aligned in short rows, close sutura elytral. Hind wings (Fig. 14**I**) with veins RA, MP well sclerotised whereas veins SC, CuA, RP-MP2, and AA scarcely sclerotised. Vein SC connected to RA less than half its length, radial cell darkly pigmented, elongate, subtriangular; AA connected to CuA3+4 more than one-half the distance from origin of CuA; cubital anal cell closed, elongate. Legs with trochanters triangular, pro-and mesofemora almost parallel-sided, metafemora larger, dorsal margin evenly convex, ventral margin almost straight; apical margins of all tibiae with short spurs; trochanters, femora and tibiae of all legs sparsely setose; femora of metalegs densely setose ventrolaterally. Hind legs with metafemoral jumping organ (Fig. 14J). Tarsomere 1 of prolegs wider in male than in female (Fig. 14L, K), suboval, broad, shorter than tarsomeres 2+3 together, tarsomere 2 triangular, tarsomere 3 deeply bilobed; tarsomere 1 of meso- and metalegs elongate, longer than tarsomeres 2+3 together; tarsal claws appendiculate.

***Abdomen*.** (Fig. 15A) apex of ventrite 5 with a middle truncate lobe on posterior margin. Genitalia. Median lobe (Fig. 15C, D) thin, sclerotised, symmetrical, widened in dorsal view, tapering slightly toward the apex, scarcely deflexed, apically with a small projection scarcely visible in dorsal view, evenly curved in lateral view, slightly constricted at the basal ~ ¼. Dorsal depression usually long, ~ ¾ length of the median lobe, two lateral and a median lamella, median lamella wide at base, longer than laterals; ventral depression long, almost 3/4 its length margins slightly elevated. Internal sac with a large U-shaped sclerite, each lateral arms long, strongly sclerotised, anterior connecting portion weakly sclerotised. Tegmen Y-shaped, manubrium a little shorter than arms.

Female. The specimens studied are similar in size to males, length: 3.9 (0.18); elytral base width: 1.6 (0.07); maximum elytral width: 1.8 (0.19); (*n* = 7). Similar to males in colour and body sculpture. Tarsomere 1 of prolegs (Fig. 14K) triangular, narrower than in males. Abdomen (Fig. 15B) broader than in males, apical region of sternite 5 slightly convex. Genitalia: lamina of sternite 8 subtrapezoidal (Fig. 15F), irregular margins, distal half of lamina sclerotised, tignum very thin, little > 3 × the length of lamina, basal part slightly enlarged. Vaginal palpi (Fig. 15H) long, thin and divergent. Spermatheca (Fig. 15G) V-shaped, receptacle and pump sclerotised, receptacle rounded, pump subcylindrical, narrow, and somewhat longer than receptacle, with a very small appendix at apex. Basal portion of spermathecal duct cylindrical, narrow and long, distal part coiled.

Variations. In *Lysathia cilliersae* sp. nov. differences are observed among specimens in body colouration and punctation. The body colour primarily varies in the tone of reflections, ranging from bronze-gold, bronze-green, to metallic blue (Figs 11–13). A distinctive feature observed in the specimens from Misiones is the leg colouration: a very pale yellow that contrasts with the darker areas of the coxae, trochanters, distal part of the tibiae, and tarsomeres (Figs 11D, 16C, D). However, in one female, the legs appeared a somewhat "dirtier" and darker yellow, similar to most specimens from the mass rearing in CBC, South Africa (Fig. 13).

Variation in the punctation of the pronotum and elytra was noted in specimens of both sexes from South Africa and Misiones, making it difficult to establish a definitive punctation pattern. The variation observed in the pronotum refers to some specimens having deeper and denser punctation in the basal region. In some specimens, the elytral punctation is slightly deeper than in the pronotum. In all specimens, the punctation of the elytra decreases towards the distal portion. However, differences are evident in the basal region of the elytra: in some specimens, the punctation is faint and disorganised, while in others, one or two rows of less pronounced punctures are aligned parallel to the elytral suture in the upper part. The rounded and prominent humeri are bare, and in some specimens, there is a more elevated area near the humeri, where the punctures are fainter and scattered. In contrast, in others, the punctures are more robust and arranged in a row parallel to the humeri.

Etymology. The name of this species is dedicated to Dr. Carina J. Cilliers, ARC, Plant Protection Research Institute, South Africa, who studied and released this species as a biological control agent of *Myriophyllum aquaticum*.

Geographic distribution (Fig. 2). *Lysathia cilliersae* sp. nov. is currently known from Argentina, near the locality of Domingo Savio (-27.25561, -55.29895) in Misiones province. It was also recorded further south in Calabacillas, Entre Ríos (-31.5444953, -58.1873180). Additionally, genetic studies revealed that the specimens reared in South Africa, originally sourced from Penedo, Rio de Janeiro, Brazil, share the same haplotype as those from Misiones. Thus, it is inferred that the distribution of *L. cilliersae* sp. nov. extends between these two localities.

Biological notes. Laboratory crosses were carried out between specimens of *Lysathia cilliersae* sp. nov. exhibiting different colouration to observe whether they produced offspring and of which colouration. Naive females from Misiones and Calabacillas, Entre Ríos (locality not included in the genetic studies) were used. In a cross between a black female with silver-blue reflections from Misiones and a male with gold-green reflections from Entre Ríos, offspring of both colours were obtained: one male and three black females, and one male and three greenish gold females. In another cross between a golden-green pair from Misiones, 27 offspring were obtained, all golden-green. Finally, a black pair produced 29 black and seven green-gold offspring. Although these crosses are preliminary, it can be concluded that the different colouration does not indicate the existence of different biological species.

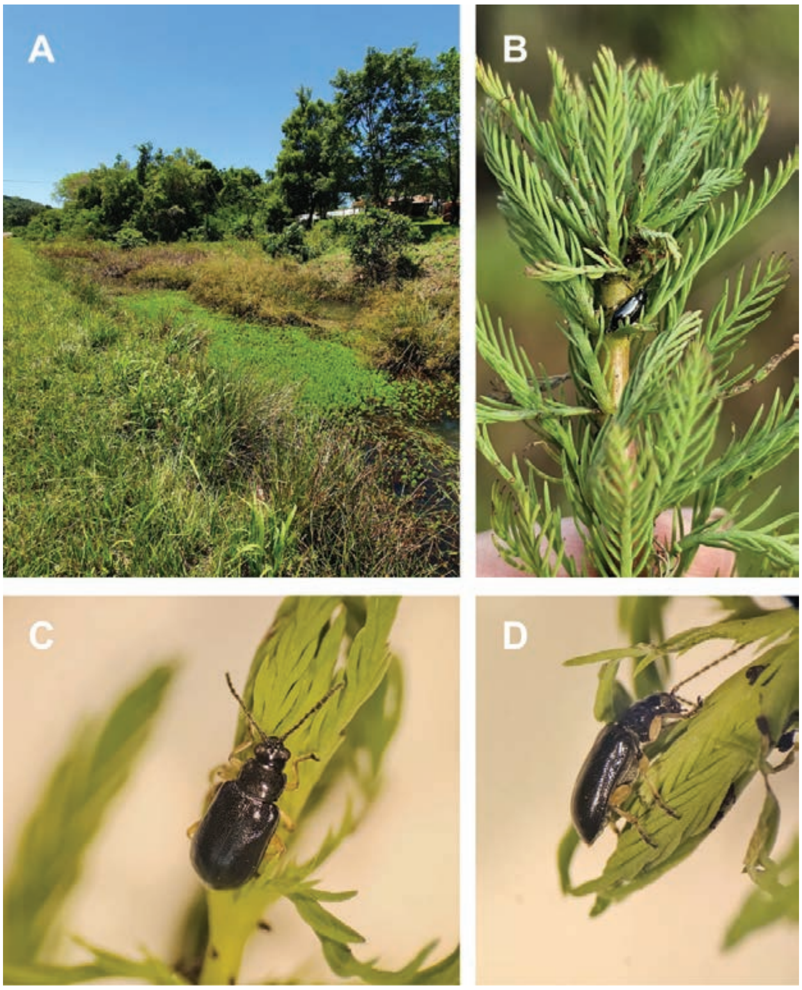

Figure 16. A type locality where *Lysathia cilliersae* sp. nov. was collected on *Myriophyllum aquaticum* (Misiones, Rt. prov. 6, Domingo Savio) **B** field-collected specimen of *L. cilliersae*. Live specimens of *L. cilliersae* sp. nov. **C** dorsal view **D** lateral view.

Comments. The small size of *L. cilliersae* sp. nov. as well as its colouration and punctation are similar to species in the *L. flavipes* group. Nevertheless, *L. cilliersae* sp. nov. can be distinguished from the *L. flavipes* group by their dark brown to black antennae, the globose antennomere 2, and the barely perceptible antebasal ridge of the pronotum, whereas in some species of the *flavipes* group, this ridge is more pronounced. Additionally, the leg colouration in some specimens is very pale, almost whitish yellow. The genital structures provide useful characters for species identification; however, more research is required for species within *Lysathia*, except for the aedeagus of *L. siolii* and the male and female genitalia of *L. flavipes*. Regarding the female genitalia, the shape of sternite 8 varies in both species, with the lamina having irregular margins. Some differences are also observed in the vaginal palpi and spermatheca. Although the degree of divergence in the inner margin of the vaginal palpi is variable, the baculi in females of *L. cilliersae* sp. nov. are barely perceptible, whereas in *L. flavipes*, they are heavily sclerotised. In the spermatheca of *L. cilliersae* sp. nov., the distal part reaches the base of the receptacle, while in *L. flavipes*, the receptacle is rounded and the distal part does not reach the base. In males, one of the most notable characteristics is the absence of a denticle on the margin of the dorsal depression and the development of the median sulcus on the ventral surface of the median lobe.

Discussion

In this study, an integrative taxonomic approach was applied combining genetic and morphological analysis to expand the description of *Lysathia flavipes* and describe a new species, *Lysathia cilliersae* sp. nov. The research revealed morphological and genetic variation within the *L. flavipes* specimens studied and extended its known distribution in Argentina, providing a more comprehensive description of the species. No evidence was found to suggest that *L. flavipes* represents a species complex associated with its different host plants, *Ludwigia g.* subsp. *hexapetala*, *Ludwigia p.* subsp. *montevidensis*, and *M. aquaticum*. On the other hand, *L. cilliersae* sp. nov. was formally described, further contributing to the understanding of this successful biological control agent against *M. aquaticum* and expanding its range from Brazil to Argentina.

The phylogenetic trees constructed in this study support the taxonomic revision made by Bechyné (1959), which separated *Lysathia* from *Altica*. Distinct and well-supported clades of *Lysathia*, as well as the clear separation from the included *Altica* species, show that the *Lysathia* species evaluated here form a cohesive and monophyletic group. Jenkins et al. (2009) had previously identified *Altica* as genetically separate from *Lysathia* although they only studied a single species (*Lysathia* sp.), likely *L. ludoviciana*. The results obtained here support this generic distinction, which has been questioned in the past by taxonomists due to the "subtle" morphological differences (Scherer 1962) and biological similarities with some species of *Altica* (McGregor et al. 1996; Takizawa 2005).

This genetic study has helped in revealing the genetic variability and potential species differentiation within the genus *Lysathia*. Accurate identification at species level within this genus is particularly challenging due to the significant morphological variability and the limited detail and illustration in the existing descriptions. Although molecular techniques alone do not resolve taxonomic challenges, they facilitate the identification of lineages, the comparison of different populations, and offer additional insights alongside morphological analysis (Jenkins et al. 2009). Such taxonomic difficulties are also observed in the related genus *Altica*, where traits generally considered constant in other alticines, like the antennal calli, oviscapt, and spermatheca, display substantial variation across species (Döberl 2010).

The phylogenetic and morphological analyses conducted in this study revealed that *L. flavipes* is a species with greater morphological and genetic variation than originally assumed. Although the bootstrap value obtained from the RAxML tree for the COI gene was low, the consistency in the positioning of the specimens in the combined COI and 16S gene tree and the improved bootstrap value provided additional support for the monophyly of *L. flavipes*. Based on both analyses, we can consider that, with the exception of two samples, all specimens belong to the same species. However, more data, including incorporating other genetic markers and more specimens, are recommended for further confirmation. For example, in this work the amplification of the nuclear gene Wg was not successful, but future research could benefit from the information this gene provides. The morphological variations observed in the collected specimens do not seem to be indicators of different species. This could be consistent with the significant number of haplotypes observed for *L. flavipes*. Of the 22 sequences analysed, 18 different haplotypes were observed. Although this study did not focus on the species' phylogeography, the haplotype network suggests that Buenos Aires and Entre Ríos could be a centre of origin with more ancestral haplotypes and that the species may have spread outward from this region. Another interesting result is the confirmation that the specimens collected in Uruguay and evaluated in USA (Reddy et al. 2021a) are, indeed, *L. flavipes* and therefore the studies on its biology and reproductive characteristics can be applied to the general characterisation of the species.

On the other hand, the initial hypothesis that the host plants on which each specimen was found feeding could indicate a possible species complex was not confirmed. No genetic or morphological groupings were observed related to the host plants *Ludwigia g*. subsp. *hexapetala* or *M. aquaticum*. Nor were there differences among specimens collected in sites where these plants are found in sympatry or allopatry. This, on the one hand, supports that *L. flavipes* is not a suitable candidate as a control agent for *L. g*. subsp. *hexapetala*, but it also raises several questions regarding the chemical similarities between these two plants, that are not phylogenetically related but to which, according to previous studies, *Lysathia flavipes* restricts its diet (Cordo and DeLoach 1982).

Of the specimens collected as *L. flavipes*, only two specimens consistently fell outside the species. Specimen MA_F_01 (referred to as *Lysathia* sp. 1 in the phylogenetic trees and haplotype network), from Otamendi, Buenos Aires, appeared in both trees as a sister species of *L. cilliersae* sp. nov. Its differentiation was also evidenced morphologically in its antennae, legs, and female genitalia. As only one specimen was available, a formal description of a new species was not made, although a morphological description and mitochondrial COI and 16S ribosomal genes sequences were provided for future studies (Suppl. material 1: Partial morphological description for *Lysathia* sp.1 (code MA_F_001)). On the other hand, specimen LH_M_01 (*Lysathia* sp. 2) from Gorchs, Buenos Aires, proved inconclusive regarding its phylogenetic placement. Depending on the gene studied, it positioned as a sister species to either *L. flavipes* or *L. ludoviciana*, in both cases with low branch support values. It is likely that, with the inclusion of additional genes and more specimens from both localities, the ambiguities observed here could be resolved.

Although the results suggest dismissing *Lysathia flavipes* as a potential control agent for *Ludwigia g*. subsp. *hexapetala*, the research conducted to reach this conclusion yielded valuable information to make the description of a new species, *Lysathia cilliersae* sp. nov. This result is noteworthy not only because it addresses questions regarding the genus *Lysathia* and its host plants, but also contributes to the understanding of the Neotropic biodiversity. Based on genetic and morphological analyses of *L. cilliersae* sp. nov., it was possible to corroborate that the specimens originally collected in Brazil and later exported as biological control agents for *M. aquaticum* in South Africa, are the same species as those found in Domingo Savio, Misiones, Argentina. The cohesion observed in the clades suggests that, despite the geographical separation, the specimens are genetically very similar, to the extent that the same haplotype was found in both countries, supporting their identification as a single species. Morphologically, polymorphisms are observed as in *L. flavipes*. A feature to highlight is the variation in colouration of *L. cilliersae* sp. nov. between both countries. In Argentina, the studied specimens exhibit variability in dorsal colouration, varying from bronze-gold, bronze-green, to metallic blue. However, the South African specimens are homogeneously bronze coloured. This difference may be due to the fact that, although South Africa has successfully maintained a colony of *L. cilliersae* sp. nov. for many years, the population is the result of a single introduction, which can lead to genetic drift, increased inbreeding and bottleneck effects. These reduces not only genetic variability but also potentially the effectiveness of the agent over time. In this context and after thirty years of its first release as a control agent in South Africa (Cilliers 1999a; Cilliers 1999b), the description of *L. cilliersae* sp. nov. is fundamental.

The lack of taxonomic identification of a biocontrol agent can not only delay the development of new biological control program (Maddox et al. 1992; Zucchi 2002), but also hinder those that are already underway. Insect taxonomy, particularly that of herbivores associated with invasive plants that are not considered agricultural weeds, have certain complications. For example, the amount of information on species of non-economic importance is, as expected, much scarce than other species with direct importance to humans (Shimbori et al. 2023). Integrative taxonomy studies are becoming more frequent and the incorporation of molecular diagnoses based on genetic markers are rapidly increasing in importance within taxonomy, especially used as complementary tools to morphological, behavioural or biological studies in general (Marvaldi 2024).

Although this study is not a revision of the genus, the significance of this work lies in the contribution of information within the context of applied entomology. Because taxonomic validation is essential for both taxonomy and biological control, all the genetic information obtained here is correlated with their respective morphological vouchers and are deposited in public data-bases and public collections.

Acknowledgments

We thank Dr. Tobias Malm, Collection Manager, and Anna Jerve from the Swedish Museum of Natural History in Stockholm, Dr. Christoph Germann, Curator of Frey Beetle Collection at the Natural History Museum in Basel, for providing photos of *Lysathia* specimens. We also thank the Instituto Misionero de Biodiversidad – Recursos Naturales de la provincia de Misiones (IMiBio) for the collection permits: Expediente 9950-11-2024-1. We also thank Dr. Julia Rouaux for the illustrations. Finally, we sincerely thank the reviewers and subject editor for their valuable feedback, which significantly enhanced this work.

Additional information

Conflict of interest

The authors have declared that no competing interests exist.

Ethical statement

No ethical statement was reported.

Funding

The study was financially supported by PICT 2015-1910 FONCYT (Argentina), Bilateral Agreement Argentina–South Africa (Ministry of Science, Technology and Productive Innovations from Argentina and NRF from South Africa), and Fundación para el Estudio de Especies Invasivas (FuEDEI). This research used resources provided by the SCINet project and/or the AI Center of Excellence of the USDA Agricultural Research Service, ARS project numbers 0201-88888-003-000D and 0201-88888-002-000D.

Author contributions

Ana C. Faltlhauser: Conceptualization, Data curation, Formal Analysis, Funding acquisition, Investigation, Methodology, Project administration, Resources, Supervision, Validation, Writing – original draft, Writing – review & editing. Nora Cabrera: Conceptualization, Data curation, Formal Analysis, Investigation, Methodology, Project administration, Validation, Visualization, Writing – review & edition. M. Cristina Hernández: Investigation, Data curation, Methodology, Software, Writing – review & editing. Andrés Sánchez Restrepo: Data curation, Software, Methodology, Writing – review & editing. Martin Hill: Funding acquisition, Resources, Investigation, Writing – review & editing. Alejandro J. Sosa: Conceptualization, Formal Analysis, Funding acquisition, Investigation, Project administration, Resources, Supervision, Writing – original draft, Writing – review & editing.

Author ORCIDs

Ana C. Faltlhauser https://orcid.org/0000-0003-3121-3650
M. Cristina Hernández https://orcid.org/0000-0003-4382-773X
Andrés Sánchez Restrepo https://orcid.org/0000-0001-7514-068X
Martin Hill https://orcid.org/0000-0003-0579-5298
Alejandro J. Sosa https://orcid.org/0000-0002-1680-8712

Data availability

All of the data that support the findings of this study are available in the main text or Supplementary Information.

References

Andreu J, Vilà M, Hulme PE (2009) An assessment of stakeholder perceptions and management of noxious alien plants in Spain. Environmental Management 43(6): 1244–1255. https://doi.org/10.1007/s00267-009-9280-1

Bechyné J (1954) Über die in Matto Grosso von F. Plaumann gesammelten Chrysomeloidea (Col. Phytophaga). Entomologische Arbeiten aus dem Museum G. Frey. Bd. 5: 116–580. https://www.biodiversitylibrary.org/page/45932795#page/128/mode/1up

Bechyné J (1955) Reise des Herrn G. Frey in Südamerika: Alticidae (Col. Phytophaga). Entomologische Arbeiten aus dem Museum G. Frey 6: 74-266. https://www.zobodat.at/pdf/Entomologische-Arbeiten-Museum-Frey_6_0074-0266.pdf

Bechyné J (1957a) Alticides neotropicaux de la collection du Museo Civico di Storia Naturale “Giacomo Doria” di Genova. Annali del Museo Civico di Storia Naturale di Genova. 69: 51–74. https://www.biodiversitylibrary.org/page/34909361#page/467/mode/1up

Bechyné, J (1957b) Provisorische Liste der Alticiden von Rio Grande do Sul (Col. Phytoph. Chrysomeloidea). Iheringia 3: 1–52. https://www.biodiversitylibrary.org/item/107738#page/80/mode/1up

Bechyné J (1959) Beiträge zur kenntnis der alticidenfauna boliviens. Beitrage Zur Neotropischen Fauna 1(4): 269–381. https://doi.org/10.1080/01650525909380619

Bechyné J, Springlová-Bechyné B (1960) Beiträge zur Kenntnis der Salvadorenischen Chrysomeloidea (Col. Phytoph.). Pesquisas, Zoologia 6: 5–73.

Bechyné J, Springlová-Bechyné B (1977). Zur Phylogenesis einiger neotropischen Alticiden (Col. Phytophaga). Studies on Neotropical Fauna and Environment 12(2): 81-145. https://doi.org/10.1080/01650527709360514

Blanchard E (1851) Fauna Chilena. Insectos. Coléopteros. In Gay Historia Física y Política de Chile 5: 522–558. https://doi.org/10.5962/bhl.title.16172

Boheman CH (1859) Coleoptera. Species novas descripsit. In: Kongliga Svenska Fregatten Eugenies Resa omkring jorden under bef äl af CA Virgin (Eds), Zoologi, 2 (1), Insecta. Svenska Vetenskaps Akademien Stockholm, Sweden, 113–218. https://doi.org/10.5962/bhl.title.2467

Campbell JM, Clark WJ (1983) Observations on host selection by *Lysathia ludoviciana* (Chrysomelidae), a beetle with potential for biological control of certain aquatic weeds. Texas Journal of Science 35(2): 165–167.

Chester EW, Holt SE (1990) The Uruguayian water-primrose (*Ludwigia uruguayensis*) in Tennessee and Kentucky. Journal of the Tennessee Academy of Science 65(1): 9–12.

Cilliers CJ (1999a) Biological control of parrot's feather, *Myriophyllum aquaticum* (Vell.) Verdc. (Haloragaceae), in South Africa. African Entomology Memoir 1: 113–118.

Cilliers CJ (1999b) *Lysathia* n.sp. (Coleoptera: Chrysomelidae), a host-specific beetle for the control of the aquatic weed *Myriophyllum aquaticum* (Haloragaceae) in South Africa. Hydrobiologia 415: 271–276. https://doi.org/10.1023/A:1003809011936

Coetzee JA, Hill MP, Byrnes MJ, Bownes A (2011) A review of the biological control programmes on *Eichhornia crassipes* (C. Mart.) Solms (Pontederiaceae), *Salvinia molesta* D. S. Mitch. (Salviniaceae), *Pistia stratiotes* L. (Araceae), *Myriophyllum aquaticum* (Vell.) Verdc. (Haloragaceae) and *Azolla filiculo*. African Entomology 19(2): 451–468. https://doi.org/10.4001/003.019.0202

Cordo H, DeLoach JC (1982) The Flea Beetle, *Lysathia flavipes*, that attacks *Ludwigia* (Water Primrose) and *Myriophyllum* (Parrotfeather) in Argentina. The Coleopterists Bulletin 36(2): 298–301.

Cruttwell McFadyen RE (1998) Biological control of weeds. Annual Review of Entomology 43: 369–393. https://doi.org/10.1146/annurev.ento.43.1.369

Culliney TW (2005) Benefits of Classical Biological Control for Managing Invasive Plants. Critical Reviews in Plant Sciences 24(2): 131–150. https://doi.org/10.1080/07352680590961649

Di Pietro R, Misano G, Wagensommer R (2007) Notulae alla checklist della flora vascolare italiana. Informatore Botanico Italiano 39: 401–403.

Döberl M (2010) Contribution to the knowledge of the Afrotropical species of *Altica* Geoffroy, 1762, excluding the species of Madagascar (Coleoptera: Chrysomelidae, Alticinae). Entomologische Zeitschrift mit Insekten-Börse 120(2): 51–72. https://www.cabidigitallibrary.org/doi/full/10.5555/20103139501

Edgar RC (2004) MUSCLE: multiple sequence alignment with high accuracy and high throughput. Nucleic Acids Research 32(5): 1792–1797. https://doi.org/10.1093/nar/gkh340

Fall HC (1910) Miscellaneous notes and descriptions of North American Coleoptera. Transactions of the American Entomological Society 36(2): 89–197. https://www.jstor.org/stable/25076873

Furth DG, Savini V (1996) Checklist of the Alticinae of Central America, including Mexico (Coleoptera: Chrysomelidae). Insecta Mundi 10: 45–68. https://digitalcommons.unl.edu/insectamundi/10

Habeck DH, Wilkerson R (1980) The life cycle of *Lysathia ludoviciana* (Fall)(Coleoptera: Chrysomelidae) on parrotfeather, *Myriophyllum aquaticum* (Velloso) Verde. The Coleopterists Bulletin 34(2): 167–170. https://www.jstor.org/stable/4000124

Harold E (1876) Diagnosen neuer Arten. Coleopterologischa Hefte 15: 118–124. https://www.zobodat.at/pdf/Coleopterologische-Hefte_15_0118-0124.pdf

Heikertinger F, Csiki E (1939) Chrysomelidae, Halticinae. Coleopterorum Catalogus. Vol. XXV, Pars 166: 1–336, Pars 169: 337–635. Uitgeverij Dr. W. Junk, Gravenhage.

Hernández MC, Cabrera Walsh G (2014) Insect Herbivores Associated with *Ludwigia* species, Oligospermum Section, in their Argentine distribution. Journal of Insect Science 14(1): 201. https://doi.org/10.1093/jisesa/ieu063

Hill MP, Coetzee J (2017) The biological control of aquatic weeds in South Africa: Current status and future challenges. Bothalia 47(2). https://doi.org/10.4102/abc.v47i2.2152

Hillis DM, Bull JJ (1993) An empirical test of bootstrapping as a method for assessing confidence in phylogenetic analysis. Systematic biology 42(2): 182–192. https://doi.org/10.1093/sysbio/42.2.182

Hinz H, Winston RL, Schwarzländer M (2020) A global review of target impact and direct nontarget effects of classical weed biological control. Current Opinion in Insect Science 38: 48–54. https://doi.org/10.1016/j.cois.2019.11.006

Hussner A, Stiers I, Verhofstad MJ, Bakker ES, Grutters BMC, Haury J, van Valkenburg JLCH, Brundu G, Newman J, Clayton JS, Anderson LWJ, Hofstra D (2017) Management and control methods of invasive alien freshwater aquatic plants: A review. Aquatic Botany 136: 112–137. https://doi.org/10.1016/j.aquabot.2016.08.002

Jenkins TM, Braman SK, Chen Z, Eaton TD, Pettis GV, Boyd DW (2009) Insights into Flea beetle (Coleoptera: Chrysomelidae: Galerucinae) Host specificity from concordant mitochondrial and nuclear DNA phylogenies. Annals of the Entomological Society of America 102(3): 386–395. https://doi.org/10.1603/008.102.0306

Jerez VR (1988) Estados preimaginales y biología de *Lysathia atrocyanea* (Phil. y Phil., 1864) (Chrysomelidae, Alticinae). Boletín de la Socociedad de Biología de Concepción, Chile 59: 95–103.

Konstantinov AS (1987) On the morphological structures used for identification of female Altica (Coleoptera, Chrysomelidae). Zoological Journal 54(1): 42–50.

Konstantinov AS (1998a) On the structure and function of the female genitalia in flea beetles (Coleoptera: Chrysomelidae: Alticinae). Proceedings of the Entomological Society of Washington, April 1998 100 (2): 353–360.

Konstantinov AS (1998b) Revision of the palearctic species of *Aphthona* Chevrolat and cladistic classification of the Aphthonini (Coleoptera: Chrysomelidae: Alticinae). Memoirs on Entomology, International. Vol. 11. Associated Publishers, Gainesville, Florida, 429 pp.

Kozlov AM, Darriba D, Flouri T, Morel B, Stamatakis A (2019) RAxML-NG: a fast, scalable and user-friendly tool for maximum likelihood phylogenetic inference. Bioinformatics 35(21): 4453–4455. https://doi.org/10.1093/bioinformatics/btz305

Kukalová-Peck J, Lawrence JF (1993) Evolution of the hind wing in Coleoptera. The Canadian Entomologist 125(2): 181–258. https://doi.org/10.4039/Ent125181-2

Leigh JW, Bryant D (2015) POPART: full-feature software for haplotype network construction. Methods in Ecology & Evolution 6(9): 1110–1116. https://doi.org/10.1111/2041-210X.12410

Lesieur V, Sforza RFH, Sheppard AW, Shaw RH (2023) Prioritising environmental invasive weeds of European concern for classical biological control: A reanalysis. Weed Research 63(4): 218–231. https://doi.org/10.1111/wre.12582

Lingafelter SW, Konstantinov AS (2000) Revision of PEDETHMA Weise (Coleoptera: Chrysomelidae). The Coleopterists Bulletin 54(4): 413–458. https://doi.org/10.1649/0010-065X(2000)054[0413:ROPWCC]2.0.CO;2

Maddox JV, McManus ML, Jeffords MR, Webb RE (1992) Exotic insect pathogens as classical biological control agents with an emphasis on regulatory considerations. In: Kauffman WC, Nechols JR (Eds) Selection criteria and ecological consequences of importing natural enemies. Entomological Society of America, 27–39. https://doi.org/10.4182/WNHY6280.1992.27

Martin G, Coetzee J, Hill M, Weyl P (2018) Ten years of post-release evaluation on *Myriophyllum aquaticum*, what have we learned? In: Hinz HL et al. (Eds) Proceedings of the XV International Symposium on Biological Control of Weeds, Engelberg, Switzerland, 250 pp. https://www.cabidigitallibrary.org/doi/pdf/10.5555/20203127158#page=269

Marvaldi AE (2024) Phylogenetic systematics and integrative taxonomy contribute to weed biological control. Biological Control 197: 105599. https://doi.org/10.1016/j.biocontrol.2024.105599

McFadyen R (2008) Return on investment: determining the economic impact of biological control programmes. In: Julien MH, Sforza R, Bon MC, Evans HC, Hatcher PE, Hinz HL, Rector BG (Eds) Proceedings of the XII International Symposium on Biological Control of Weeds, La Grande Motte (France), 22–27 April 2007. CAB International, Wallingford, 67–74. https://doi.org/10.1079/9781845935061.0067

McGregor MA, Bayne DR, Steeger JG, Webber EC, Reutebuch E (1996) The potential for biological control of water primrose (*Ludwigia grandiflora*) by the water primrose flea beetle (*Lysathia ludoviciana*) in the Southeastern United States. Journal of Aquatic Plant Management 34(2): 74–76. https://apms.org/wp-content/uploads/japm-34-02-074.pdf

Medvedev LN (2001) A new species of *Lysathia* Bechyne, 1959 from the Pantanal, Brazil (Insecta, Coleoptera, Chrysomelidae, Alticinae). Amazoniana 16(3/4): 417–420.

Oberholzer IG, Mafokoane DL, Hill MP (2007) The biology and laboratory host range of the weevil, *Listronotus marginicollis* (Hustache) (Coleoptera: Curculionidae), a natural enemy of the invasive aquatic weed, parrot's feather, *Myriophyllum aquaticum* (Velloso) Verde (Haloragaceae). African Entomology 15(2): 385–390. https://doi.org/10.4001/1021-3589-15.2.385

Olivier AG (1808) Entomologie, ou histoire naturelle des insectes, avec leur caractères génériques et spécifiques, leur description, leur synonymie, et leur figure enluminée. Coléoptères. Tome sixieme. Desray, Paris, 613–1104 [+ 46 plates]. https://doi.org/10.5962/bhl.title.61905

Orchard A (1981) A revision of South American *Myriophyllum* (Haloragaceae) and its repercussions on some Australian and North American species. Brunonia 4(1): 27. https://doi.org/10.1071/BRU9810027

Pallister JC (1953) The leaf beetles of North Central Mexico collected on the David Rockefeller Mexican Expedition (Coleoptera, Chrysomelidae). American Museum Novitates 1623: 1–95. https://core.ac.uk/reader/18224850

Peck SB, Thomas MC, Turnbow RH Jr (2014) The diversity and distributions of the beetles (Insecta: Coleoptera) of the Guadeloupe Archipelago (Grande-Terre, Basse-Terre, La Désirade, Marie-Galante, Les Saintes, and Petite-Terre), Lesser Antilles. Insecta Mundi 357. http://digitalcommons.unl.edu/insectamundi/857

Pelella E, Questino B, Luzi B, Mariani F, Ceschin S (2023) Impact of the Invasive Alien Macrophyte *Ludwigia hexapetala* on Freshwater Ecosystems: Evidence from Field Data. Biology 12(6). https://doi.org/10.3390/biology12060794

Pessina A, Humair L, Naderi R, Röder G, Seehausen ML, Rasmann S, Weyl P (2024) Investigating the host finding behaviour of the weevil *Phytobius vestitus* for the biological control of the invasive aquatic weed *Myriophyllum aquaticum*. Biological Control 192: 105509. https://doi.org/10.1016/j.biocontrol.2024.105509

Philippi RA, F Philippi (1864) Beschreibung einiger neuen chilenischen Káfer. Entomologische Zeittung Stettinger 25(1–12): 382–401.

Raven PH, Axelrod DI (1974) Angiosperm Biogeography and Past Continental Movements. Annals of the Missouri Botanical Garden 61(3): 539. https://doi.org/10.2307/2395021

Reddy AM, Pratt PD, Grewell BJ, Harms NE, Cibils-Stewart X, Cabrera Walsh G, Faltlhauser A (2021a). Biological and host range characteristics of *Lysathia flavipes* (Coleoptera: Chrysomelidae), a candidate biological control agent of invasive *Ludwigia* spp. (Onagraceae) in the USA. Insects 12(5): 471. https://doi.org/10.3390/insects12050471

Reddy AM, Pratt PD, Grewell BJ, Harms NE, Walsh GC, Hernández MC, Faltlhauser AC, Cibils-Stewart, X. (2021b) Biological control of invasive water primroses, *Ludwigia* spp., in the United States: A feasibility assessment. Journal of Aquatic Plant Management 59: 67–77.

Reid CAM, Beatson M (2015) Disentangling a taxonomic nightmare: A revision of the Australian, Indomalayan and Pacific species of *Altica* Geoffroy, 1762 (Coleoptera: Chrysomelidae: Galerucinae). Zootaxa 3918(4): 503–551. https://doi.org/10.11646/zootaxa.3918.4.3

Rojas-Sandoval J (2024) *Myriophyllum aquaticum* (parrot's feather). CABI compendium. https://doi.org/10.1079/cabicompendium.34939

Sabbatini MR, Murphy KJ, Irigoyen JH (1998) Vegetation–environment relationships in irrigation channel systems of southern Argentina. Aquatic Botany 60(2): 119–133. https://doi.org/10.1016/S0304-3770(97)00086-7

Salvi D, D'Alessandro P, Biondi M (2019) Host plant associations in Western Palaearctic *Longitarsus* flea beetles (Chrysomelidae, Galerucinae, Alticini): a preliminary phylogenetic assessment. ZooKeys 856: 101–114. https://doi.org/10.3897/zookeys.856.32430

Sankaran KV, Schwindt E, Sheppard AW, Foxcroft LC, Vanderhoeven S, Egawa C, Peacock L, Castillo ML, Zenni RD, Müllerová J, González-Martínez AI, Bukombe JK, Wanzala W, Mangwa D (2023) Chapter 5. Management, challenges, opportunities and lessons learned. In: Roy HE, Pauchard A, Stoett P, Renard Truong T (Eds) Thematic Assessment Report on Invasive Alien Species and their Control of the Intergovernmental Science-Policy Platform on Biodiversity and Ecosystem Service. IPBES secretariat, Bonn, Germany. https://doi.org/10.5281/zenodo.7430733

Scherer G (1960) Beitrag zur kenntnis der Alticiden fauna Brasiliens (Coleoptera: Phytoph.) Entomologische Arbeiten Aus Dem Museum G. Frey. Bd. 11(1): 180–272. https://www.biodiversitylibrary.org/item/173245#page/12/mode/1up

Scherer G (1962) Bestimmungsschlüssel der neotropischen Alticinen-Genera (Coleoptera: Chrysomelidae: Alticinae). Entomologische Arbeiten Aus Dem Museum G. Frey 13(Series 2): 497–607. https://www.biodiversitylibrary.org/item/173047#page/9/mode/1up

Scott D, Scholes JD, Randrianjafizanaka MT, Randriamampianina JA, Autfray P, Freckleton RP (2020) Mapping the drivers of parasitic weed abundance at a national scale: a new approach applied to *Striga asiatica* in the mid-west of Madagascar. Weed Research 60(5): 323–333. https://doi.org/10.1111/wre.12436

Sheppard AW, Shaw RH, Sforza R (2006) Top 20 environmental weeds for classical biological control in Europe: a review of opportunities, regulations and other barriers to adoption. Weed Research 46(2): 93–117. https://doi.org/10.1111/j.1365-3180.2006.00497.x

Shimbori EM, Querino RB, Costa VA, Zucchi RA (2023) Taxonomy and biological control: new challenges in an old relationship. Neotropical Entomology 52(3): 351–372. https://doi.org/10.1007/s13744-023-01025-5

Simon C, Frati F, Beckenbach A, Crespi B, Liu H, Flook P (1994) Evolution, weighting, and phylogenetic utility of mitochondrial gene sequences and a compilation of conserved polymerase chain reaction primers. Annals of the Entomological Society of America 87(6): 651–701. https://doi.org/10.1093/aesa/87.6.651

Stiers I, Crohain N, Josens G (2011) Impact of three aquatic invasive species on native plants and macroinvertebrates in temperate ponds. Biological Invasions 13: 2715–1726. https://doi.org/10.1007/s10530-011-9942-9

Suffrian E (1868) Verzeichniss der von Dr. Gundlach auf der Insel Cuba gesammelten Chrysomelinen. Archiv für Naturgeschichte 34(1): 164–252.

Sutton D (1985) Biology and ecology of *Myriophyllum aquaticum*. In: 1st International Symposium on Watermilfoil (*Myriophyllum spicatum*) and Related Haloragaceae Species, Vancouver (Canada), July 1985. The Aquatic Plant Management Society, Mississippi, 59–71.

Sytsma KJ, Litt A, Zjhra ML, Pires JC, Nepokroeff M, Conti E, Walker J, Wilson PG (2004) Clades, clocks, and continents: Historical and biogeographical analysis of Myrtaceae, Vochysiaceae, and relatives in the southern hemisphere. International Journal of Plant Sciences 165: S4. https://doi.org/10.1086/421066

Takizawa H (2005) Supra-generic subdivislons of the subfamily Atticinae based on larval characters, with descriptions of larvae of hispaniolan species (Coleoptera: Chrysomelidae). Insecta matsumurana. New series: Journal of the Faculty of Agriculture Hokkaido University, Series entomology 62: 187–206.

Thouvenot L, Haury J, Thiebaut G (2013) A success story: Water primroses, aquatic plant pests. Aquatic Conservation: Marine and Freshwater Ecosystems 23(5): 790–803. https://doi.org/10.1002/aqc.2387

Virkki N (1979) Brief Notes on the cytology of Neotropical Coleoptera III. “Luperodes Antillarum Blake” = *Lysathia ludoviciana* (Fall). The Journal of Agriculture of the University of Puerto Rico 63(1): 100–101. https://doi.org/10.46429/jaupr.v63i1.10317

Wagner WL, Hoch PC, Raven PH (2007) Revised Classification of the Onagraceae. Systematic Botany Monographs 83: 1–240.

Weise J (1888) Naturgeschichte der Insecten Deutschland, VI Band. Chrysomelidae. Berlin, 825–825. https://www.biodiversitylibrary.org/item/105313#page/847/mode/1up

Zucchi RA (2002) A taxonomia e o controle biológico de pragas. In: Parra JRP, Botelho PSM, Correa-Ferreira BS, Bento JMA (Eds) Controle biológico no Brasil: parasitóides e predadores. Manole, São Paulo, 17–24.

Supplementary material 1

Supplementary file

Authors: Ana C. Faltlhauser, Nora Cabrera, M. Cristina Hernández, Andrés Sánchez Restrepo, Martin Hill, Alejandro J. Sosa

Data type: docx

Explanation note: This file contains genetic protocols for PCR extraction, Lysathia species geographical information of ocurrences, gentic sequences codes, phylogenetic trees and preliminar morphological description for undescribed species.

Link: https://doi.org/10.3897/zookeys.1228.138773.suppl1

ZooKeys 1228: 53–67 (2025)
DOI: 10.3897/zookeys.1228.136718

Research Article

Discovery of the males of *Lasioglossum* (*Eickwortia*) *hienae* and *L.* (*E.*) *alexanderi*, with new distributional records for the species (Apoidea, Halictidae)

Ismael A. Hinojosa-Díaz[1], Ana Celeste Martínez Cervantes[1,2], Jason Gibbs[3]

1 *Departamento de Zoología, Instituto de Biología, Universidad Nacional Autónoma de México (UNAM), Tercer Circuito s/n, Ciudad Universitaria, Coyoacán, A.P. 70-153, Ciudad de México, C.P. 04510, Mexico*
2 *Posgrado en Ciencias Biológicas, Universidad Nacional Autónoma de México, Unidad de Posgrado, Circuito de Posgrados, Edificio D, Ciudad Universitaria, Coyoacán, Ciudad de México, C.P. 04510, Mexico*
3 *Department of Entomology, University of Manitoba, 12 Dafoe Road, Winnipeg, MB, R3T 2N2, Canada*
Corresponding author: Ana Celeste Martínez Cervantes (celeste.martinez@st.ib.unam.mx)

Abstract

Within the diverse genus *Lasioglossum*, the subgenus *Eickwortia* as currently understood, encompasses three characteristic species from mountainous areas in Mexico and Central America. Prior to this work only *Lasioglossum* (*Eickwortia*) *nycteris* had descriptions for both male and female. Here we describe and illustrate the previously unknown males of *L*. (*E*.) *hienae* and *L*. (*E*.) *alexanderi*, providing new distributional data for both species, and an updated species identification key for the group.

Key words: Costa Rica, description, identification key, Mexico, taxonomy

Academic editor: Thorleif Dörfel
Received: 10 September 2024
Accepted: 2 December 2024
Published: 14 February 2025

ZooBank: https://zoobank.org/CF87D575-79B1-4DEF-898F-E26CF06AF78D

Citation: Hinojosa-Díaz IA, Martínez Cervantes AC, Gibbs J (2025) Discovery of the males of *Lasioglossum* (*Eickwortia*) *hienae* and *L.* (*E.*) *alexanderi*, with new distributional records for the species (Apoidea, Halictidae). ZooKeys 1228: 53–67. https://doi.org/10.3897/zookeys.1228.136718

Introduction

The bee genus *Lasioglossum* Curtis, 1833 stands out in terms of species richness and morphological challenges to discriminate groups of species within it (Michener 2007; Gibbs et al. 2013). While the over 1800 species (Ascher and Pickering 2024) in the genus can be assigned to two informal series, *Lasioglossum* series and *Hemihalictus* series (Danforth et al. 2003; Michener 2007), the subgeneric classification is still in flux (Gibbs et al 2012; Gibbs 2018; Gardner 2023). The *Hemihalictus* series is characterized by the weakening or loss of vein 1rs-m of the forewing. The subgenus *Eickwortia* is a Neotropical member of the *Hemihalictus* series (Michener 2007; Gibbs and Dumesh 2013; Gardner 2023), originally described as a separate genus (McGinley 1999) for two species, *L. nycteris* (Vachal, 1904) and *L. alexanderi* (McGinley, 1999), the latter known only from the holotype, which is currently lost (Gibbs and Dumesh 2013). Both species occur in mountainous areas in Mexico and Central America. A third species, *L. hienae* Gibbs & Dumesh, 2013, was described based on a single female from the state of Colima, Mexico. *Lasioglossum* (*Eickwortia*) as conceived for the inclusion of the three mentioned species can be characterized by black integument, infuscate wings, and females with noticeably bidentate mandibles (McGinley 1999; Gibbs and Dumesh 2013). Only the male of *L. nycteris* has been described and is characterized by a slender metasoma, reminiscent of *Neocorynura*, and a slender hind basitarsus (McGinley 1999).

Recent phylogenetic evidence based on molecular data (Gardner 2023) shows that *Eickwortia* (*sensu stricto*) is nested within a clade of metallic, Neotropical species leading to an expanded definition of the subgenus, *Eickwortia* (*sensu lato*). This larger clade includes the so called *Augochlora*-like *Dialictus* (Gardner 2023), a distinctive group of species defined by Engel et al. (2007) as the "*aurora* species group". These metallic *Eickwortia* have generally been treated as *Lasioglossum* (*Dialictus*), although their position outside of *L.* (*Dialictus*) has been understood for some time (Danforth et al. 2003; Gibbs et al. 2012, 2013). Here we provide the description for the previously unknown males of *Lasioglossum* (*Eickwortia*) *hienae* and *L.* (*E.*) *alexanderi*, with new distributional records for the species.

Material and methods

Material examined for this study corresponded to 44 specimens, including the five newly described males. The *Lasioglossum* (*Eickwortia*) *hienae* specimens are all held in Mexican institutions: Colección Nacional de Insectos, Instituto de Biología, Universidad Nacional Autónoma de México (CNIN) (1 ♂, 3 ♀♀); Colección Himenopterológica, Museo de Zoología "Alfonso L. Herrera", Facultad de Ciencias, Universidad Nacional Autónoma de México (MZFC) (2 ♂, 21 ♀♀); Colección de la Estación de Biología Chamela, Instituto de Biología, Universidad Nacional Autónoma de México (EBCh) (3 ♀♀). *Lasioglossum* (*E.*) *nycteris* males were examined from the Snow Entomological Collection, Lawrence, Kansas, USA (2 ♂♂) and Colección Nacional de Insectos, Instituto de Biología, Universidad Nacional Autónoma de México (CNIN) (2 ♂♂). The new *L.* (*E.*) *alexanderi* records are deposited in the J.B. Wallis / R.E. Roughley Museum of Entomology (WRME), University of Manitoba, Winnipeg, Canada (2 ♂♂, 7 ♀♀) and Bee Biology and Systematics Laboratory (BBSL), Logan, Utah, USA (1 ♀).

The new males were associated to the female by the strong morphological similarity and the co-occurrence of both sexes during the same collecting events. Males of *L. hienae* can be identified as *L.* (*Eickwortia*) based on their remarkable similarity to *L. nycteris*. Males of *L. alexanderi* were collected with the female, which was readily identified using the description and photographs in McGinley (1999).

Morphological terminology for the male descriptions follows that of McGinley (1999) for the male of *L.* (*E.*) *nycteris* (the only *Eickwortia* male known before this work), as well as the description provided by Gibbs and Dumesh (2013) for the female of *L.* (*E.*) *hienae*. The interpretation of some characters is based on other sources (Michener and Fraser 1978; Brooks 1988; Michener 2007). Surface sculpture follows Harris (1979) terminology. Length measurements for *L.* (*E.*) *hienae* are presented as the average of the three available male specimens, showing individual lower and higher measurements in parenthesis, while for *L.* (*E.*) *alexanderi* meassurements for the two available specimens are shown. Length ratios are presented as the average for the measured specimens. Lengths of body setae are referred as comparison to ocellar diameter (OD). The genitalia were dissected from one male *L. hienae* and cleared in a solution of sodium hydroxide (NaOH) at room temperature for 12 hours. Photomicrographs were produced through a Zeiss Axio Zoom V16 microscope with an Axiocam MRC5 camera or a Canon EOS 7D camera with MPE-65 lens mounted on a copy stand with a StackShot system.

Results

***Lasioglossum* (*Eickwortia*) *hienae* Gibbs & Dumesh**
Figs 1–8

Lasioglossum (*Eickwortia*) *hienae* Gibbs and Dumesh 2013: 3 (♀).

Material examined. 30 specimens (3 ♂♂ previously unknown, 27 ♀♀). Mexico • 1 ♂; Oaxaca, Putla Villa de Guerrero, Entre Asunción Atoyaquillo y Cerro Campana; 16.71075°N, 97.80907°W; 1730 m a.s.l.; 07 Nov. 2015; I. Hinojosa/ C. Martínez leg.; Red aérea; OAX165; CNIN • 1 ♂; Oaxaca, Pluma Hidalgo, Ranchería San Isidro; 15.94056°N, 96.40083°W; 1255 m a.s.l.; 19 Sep. 2007; Omar Ávalos Hernández leg.; ejemplar_id: 1088 catálogo: 31964; OAH -215 [pencil/handwritten]; MUSEO DE ZOOLOGIA HYMENOPTERA 31964; MZFC • 1 ♂; Oaxaca, Pluma Hidalgo, Cascada mayor; 15°55'11"N, 96°23'34"W; 900 m a.s.l.; 19 Sep. 2007; E. Suaste leg.; ES01; MUSEO DE ZOOLOGIA HYMENOPTERA, 31873; 9–10 am; MZFC • 1 ♀; Oaxaca, Putla Villa de Guerrero, Entre Asunción Atoyaquillo y Cerro Campana; 16.71075°N, 97.80907°W; 1730 m a.s.l.; 07-Nov-2015; Red aérea; Col. I. Hinojosa, C. Martínez leg.; OAX162; CNIN • 1 ♀; Oaxaca, Putla Villa de Guerrero, Entre Asunción Atoyaquillo y Cerro Campana; 16.71075°N, 97.80907°W; 1730 m a.s.l.; 07-Nov-2015; Red aérea; Col. I. Hinojosa, C. Martínez leg.; OAX163; CNIN • 1 ♀; Oaxaca, Putla Villa de Guerrero, Entre Asunción Atoyaquillo y Cerro Campana; 16.71075°N, 97.80907°W; 1730 m a.s.l.; 07-Nov-2015; Red aérea; Col. I. Hinojosa, C. Martínez leg.; OAX164; CNIN • 1 ♀; Oaxaca, Pluma Hidalgo, Ranchería San Isidro; 15.94056°N, 96.40083°W; 1255 m a.s.l.; 19 Sep. 2007; Omar Ávalos Hernández leg.; ejemplar_id: 1089 catálogo: 31965; OAH -215 [pencil/handwritten]; MUSEO DE ZOOLOGIA HYMENOPTERA 31965; MZFC • 1 ♀; Oaxaca, Pluma Hidalgo, Ranchería San Isidro; 15.94056°N, 96.40083°W; 19 Sep. 2007; Andrés Ressendiz Flores leg.; ejemplar_id: 1080 catálogo: 31956; AR -03 [pencil/handwritten]; MUSEO DE ZOOLOGIA HYMENOPTERA 31956; MZFC • 1 ♀; Oaxaca, Pluma Hidalgo, Ranchería San Isidro; 15.94056°N, 96.40083°W; 19 Sep. 2007; Marycarmen Jiménez de Loera leg.; ejemplar_id: 1100 catálogo: 31976; MJ 04 [pencil/handwritten]; MUSEO DE ZOOLOGIA HYMENOPTERA 31976; MZFC • 1 ♀; Oaxaca, Pluma Hidalgo, Ranchería San Isidro; 15.94056°N, 96.40083°W; 19 Sep. 2007; Marycarmen Jiménez de Loera leg.; ejemplar_id: 1105 catálogo: 31981; MJ 06 [pencil/handwritten]; MUSEO DE ZOOLOGIA HYMENOPTERA 31981; MZFC • 1 ♀; Oaxaca, Pluma Hidalgo, Ranchería San Isidro; 15.94056°N, 96.40083°W; 19 Sep. 2007; Marycarmen Jiménez de Loera leg.; ejemplar_id: 1108 catálogo: 31984; MJ 06 [pencil/handwritten]; MUSEO DE ZOOLOGIA HYMENOPTERA 31984; MZFC • 1 ♀; Oaxaca, Pluma Hidalgo, Ranchería San Isidro; 15.94056°N, 96.40083°W; 1255 m a.s.l.; 19 Sep. 2007; Marycarmen Jiménez de Loera leg.; ejemplar_id: 1113 catálogo: 31989; MJ 10 [pencil/handwritten]; MUSEO DE ZOOLOGIA HYMENOPTERA 31989; MZFC • 1 ♀; Oaxaca, Pluma Hidalgo, Ranchería San Isidro; 15.94056°N, 96.40083°W; 1255 m a.s.l.; 19 Sep. 2007; Marycarmen Jiménez de Loera leg.; ejemplar_id: 1114 catálogo: 31990; MJ 10 [pencil/handwritten]; MUSEO DE ZOOLOGIA HYMENOPTERA 31990; MZFC • 1 ♀; Oaxaca, Pluma Hidalgo, La Soledad; 15°58'18"N, 96°31'54"W; 1550 m a.s.l.; 21 Sep. 2007; Marycarmen Jiménez de Loera leg.; ejemplar_id: 1119 catálogo: 31995; MJ 15 [pencil/handwritten]; MUSEO DE ZOOLOGIA HYMENOPTERA 31995; 09:30 h; MZFC • 1 ♀; Oaxaca, La Soledad; 15°58'18"N, 96°31'54"W; 1550 m

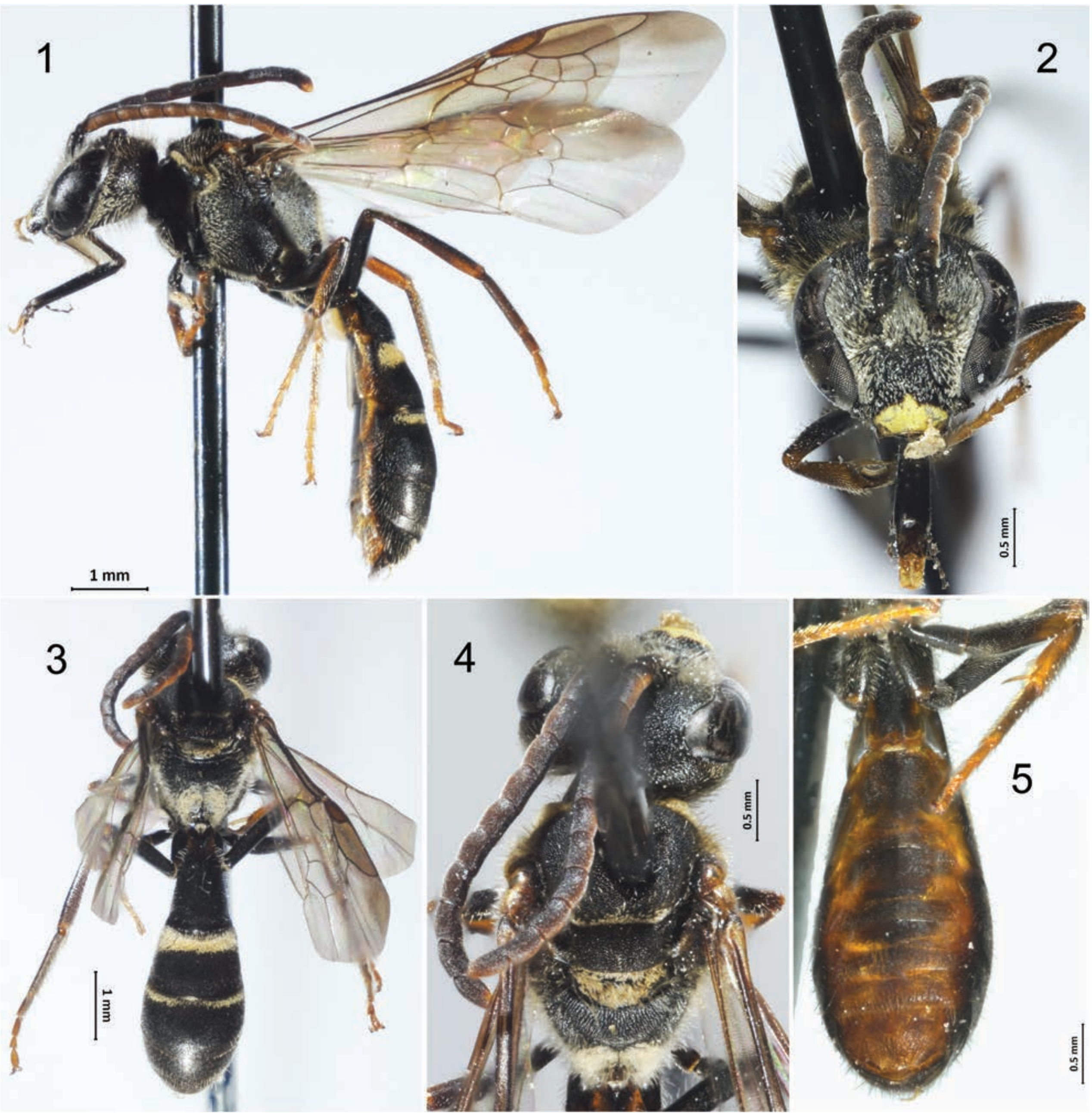

Figures 1–5. Male of *Lasioglossum* (*Eickwortia*) *hienae* **1** lateral habitus **2** face **3** dorsal habitus **4** dorsal view of mesosoma **5** ventral view of metasoma.

a.s.l.; 19 Sep. 2007; E. Suaste leg.; ES07; MUSEO DE ZOOLOGIA HYMENOPTERA 32002; 11:30 am-12:30 pm; MZFC • 1 ♀; Oaxaca, Rancho San Isidro; 15.94056°N, 96.40083°W; 1255 m a.s.l.; 19 Sep. 2007; Y. Ramírez leg.; YR07; MUSEO DE ZOOLOGIA HYMENOPTERA 29804; 13:00–14:00 hrs; MZFC • 1 ♀; Oaxaca, La Soledad; 15°58'18"N, 96°31'54"W; 1550 m a.s.l.; 21 Sep. 2007; Y. Ramírez leg.; YR10; MUSEO DE ZOOLOGIA HYMENOPTERA 29801; 9:00–10:00 am; MZFC • 1 ♀; Oaxaca, La Soledad; 15°58'18"N, 96°31'54"W; 1550 m a.s.l.; 21 Sep. 2007; Y. Ramírez leg.; YR10; MUSEO DE ZOOLOGIA HYMENOPTERA 29802; 9:00–10:00 am; MZFC • 1 ♀; Oaxaca, La Soledad; 15°58'18"N, 96°31'54"W; 1550 m a.s.l.; 21 Sep. 2007; Y. Ramírez leg.; YR10; MUSEO DE ZOOLOGIA HYMENOPTERA 29803; 9:00–10:00 am; MZFC • 1 ♀; Oaxaca, La Soledad; 15°58'18"N, 96°31'54"W; 1550 m a.s.l.; 21

Figures 6–8. Male genitalic capsule of *Lasioglossum* (*Eickwortia*) *hienae* **6** ventral aspect **7** dorsal aspect **8** lateral aspect.

Sep. 2007; Y. Ramírez leg.; YR11; MUSEO DE ZOOLOGIA HYMENOPTERA 29805; 10:00–11:00 am; MZFC • 1 ♀; Oaxaca, La Soledad; 15°58'18"N, 96°31'54"W; 1550 m a.s.l.; 21 Sep. 2007; Y. Ramírez leg.; YR11; MUSEO DE ZOOLOGIA HYMENOPTERA 29806; 10:00–11:00 am; MZFC • 1 ♀; Oaxaca, La Soledad; 15°58'18"N, 96°31'54"W; 1550 m a.s.l.; 19 Sep. 2007; E. Suaste leg.; ES05; MUSEO DE ZOOLOGIA HYMENOPTERA 31814; 9:30–10:30 am; MZFC • 1 ♀; Oaxaca, Pluma Hidalgo- Ranchería San Isidro "cafetal"; 15.94056°N, 96.40083°W; 1255 m a.s.l.; 19 Sep. 2007; A. Díaz leg.; DIMA03; MUSEO DE ZOOLOGIA HYMENOPTERA 31854; 9:03 am; MZFC • 1 ♀; Oaxaca, Pluma Hidalgo, Cascada mayor; 15°55'11"N, 96°23'34"W; 900 m a.s.l.; 19 Sep. 2007; E. Suaste leg.; ES01; MUSEO DE ZOOLOGIA HYMENOPTERA, 31868; 9–10 am; MZFC • 1 ♀; Oaxaca, Pluma Hidalgo, Cascada mayor; 15°55'11"N, 96°23'34"W; 900 m a.s.l.; 19 Sep. 2007; E. Suaste leg.; ES01; MUSEO DE ZOOLOGIA HYMENOPTERA, 31870; 9–10 am; MZFC • 1 ♀; Oaxaca, Pluma Hidalgo, Cascada mayor; 15°55'11"N, 96°23'34"W; 900 m a.s.l.; 19 Sep. 2007; E. Suaste leg.; ES01; MUSEO DE ZOOLOGIA HYMENOPTERA, 31871; 9–10 am; MZFC • 1 ♀; Oaxaca, Pluma Hidalgo, Cascada mayor; 15°55'11"N, 96°23'34"W; 900 m a.s.l.; 19 Sep. 2007; E. Suaste leg.; ES01; MUSEO DE ZOOLOGIA HYMENOPTERA, 31872; 9–10 am; MZFC.• 1 ♀; Colima, Hacienda San Antonio; 19.45192°N, 103.71394°W; 1190 m a.s.l.; 26 Oct. 2015; R. Ayala leg.; a15; EBCH • **1** ♀; Colima, Hacienda San Antonio; 19.45192°N, 103.71394°W; 1190 m a.s.l.; 26 Oct. 2015; R. Ayala leg.; a16; EBCH • 1 ♀; Colima, Hacienda San Antonio; 19.45192°N, 103.71394°W; 1190 m a.s.l.; 26 Oct. 2015; R. Ayala leg.; EBCH.

Diagnosis. Males of *L. hienae* resemble male *Neocorynura* due to the slender T1, but they can be distinguished by the characteristics of the tribe Halictini, which include the reflexed apex of T7, with a subapical ridge creating a false apex. Male *L. hienae* can be recognized by their black integument, yellow clypeal mark, anteriorly infuscate wings, and distinct tomentum on the metanotum, posterior propodeum, and base of T2. There is currently no reliable way to distinguish the males of *L. hienae* and *L. nycteris*.

Both species share unique characters within male *Lasioglossum* in the Western Hemisphere: inner metatibial spur short or absent entirely, T1 narrow (distinctly longer than wide), and hind legs long and slender.

Description. Male: Length 8.39 mm (8.14–8.62 mm).

Head length 2.03 mm (1.91–2.17 mm). Head width 2.13 mm (2.05–2.19 mm). Intertegular span 1.47 mm (1.39–1.58 mm).

Forewing length (Total) 6.53 mm (6.34–6.76 mm), forewing length (M-2rm) 2.39 mm (2.28–2.55 mm).

Maximum metasomal width (T3) 1.64 mm (1.58–1.72 mm).

Structure. Head approximately as long as wide (length/width ratio = 0.95). Gena width at midlength 0.74 × width of contiguous section of compound eye in lateral view. Supraclypeal area weakly protuberant. Clypeus width approximately twice length, width/length ratio = 2.04, projecting approximately 0.65 its length below lower margin of eyes; clypeal protuberance 0.26 mm (0.21–0.32 mm).

Ocellocular distance 2.60 × lateral ocellar diameter, approximately equal to distance between lateral ocellus and hind margin of vertex, and slightly longer than interocellar distance. Compound eyes convergent below, upper ocular distance 1.30 × lower ocular distance (Fig. 2). Hypostomal carinae subparallel, anterior angle acutely rounded (seemingly orthogonal in females). Antennal scape short, barely reaching midway between antennal socket and median ocellus; pedicel wider than long, two-thirds length of flagellomere 1; flagellomere 1 approximately half as long as flagellomere 2. Labrum short without apical process. Mandible simple, reaching opposing clypeal angle (Fig. 2). Pronotum maximum width 1.93 mm (1.86–2.03 mm); dorsolateral angle orthogonal as in the female (described as obtuse by Gibbs and Dumesh 2013); pronotal ridge uninterrupted carina mostly straight but with slight sinuation on lower half; pronotal lobe at most with a round projection (Fig. 1).

Inner metatibial spur absent. Tegula and forewing as in female except veins 1rs-m and 2rs-m not noticeably weak; hamuli arranged 4-1-3. Propodeum as in female. T1 width 0.71 × T2 width (Figs 3, 4). Hind leg noticeably slender, metafemur about six times as long as wide, metatibia about eight times as long as wide.

Surface sculpture. Face as in female, except frontal areas somewhat more granular (Fig. 2). Lower part of gena and subgena striolate on oblique view [described as striolate in female by Gibbs and Dumesh 2013]. Mesoscutum and mesoscutellum similar to female, slightly more granular (Fig. 4). Mesepisternum coarsely granular-imbricate throughout, except shiny anteriorly contiguous to pronotal ventral extension. Metepisternum as in female, but transverse carinulae stronger. Propodeum noticeably striolate on entire basal area (Figs 3, 4). Terga surface sculpture as in female.

Color. Body blackish brown, as described for the female in the original description, with the following remarks: apical half of clypeus bright yellow (Fig. 2), mandible bright yellow on outer surface except edges and basal outer interspace dark brown and apical tooth reddish amber. Posterior surface of entire flagellum and apex of flagellomere 11 amber. Tegula light brown to amber, translucid (Fig. 4). Legs proximally dark brown, lighter starting on distal third of femur and continuing on tibia, becoming yellow-amber on basitarsus and remaining tarsomeres, particularly on front and middle legs, pretarsal claws brown on distal half (Fig. 1). Forewing membrane hyaline, amber-ish, with green, yellow, and purple highlights; anterior margin infuscate, not as deeply as originally described for female; wing veins and pterostigma brown to amber-brown (Fig. 1). Terga blackish brown, with anterior margins (apical impressed areas) slightly reddish and lateral extensions translucid amber (Fig. 4); T1 with yellowish integument proximal to propodeum; sterna 1–4 brown to dark-brown with some underlying yellow-brown coloration basally and laterally, sterna 5–6 amber (Figs 3–5).

Pubescence. As described for the female, with the following remarks: facial setae longer on frontal, antennal scape and lower gena (1.5–2.5 OD); tomentum dense on paraocular and supraclypeal areas, less dense but noticeable on upper clypeal section (Fig. 2). Mesepisternum and metepisternum with denser, shorter (as compared to female) subappressed setae; lower metepisternal and lateral surface of propodeum tomentose, posterior surface of propodeum densely tomentose. Coxae with long (1.0–1.5 OD) setae, otherwise legs with short, subappressed setae. T2–T4 with bands as in female; metasomal sterna with long (1.5–2.5 OD), subappressed setae, appearing simple, arranged in bands coming off gradulus.

Genitalia. Sterna VII–VIII where not dissected. Genital capsule similar to that of *L.* (*E.*) *nycteris*, except as noted; gonobase short; gonocoxite noticeably strigulate, streaks not depicted in original description of *L.* (*E.*) *nycteris*; gonostylus moderately elongate, with two processes, trapezoidal apical process with scattered setae on its inner facing surface (a few long ones) appearing simple as opposed to the branched ones showed for *L.* (*E.*) *nycteris* in drawing by McGinley (1999), and retrorse membranous lobe about two-thirds length of gonocoxite, covered with minute moderately dense setae on its outer surface; volsella seemingly with prominent lateral lobe (Figs 6–8).

New distributional records. The single female used for the original description of the species by Gibbs and Dumesh (2013) was collected from the southern slope of the Colima volcano, state of Colima in west-central Mexico. In this study we present specimens, including the three previously unknown males, that expand the distribution of *L.* (*E.*) *hienae* east and south within Mexico; all are from localities in the state of Oaxaca with elevations ranging from around 900 to 1730 m (Fig. 9).

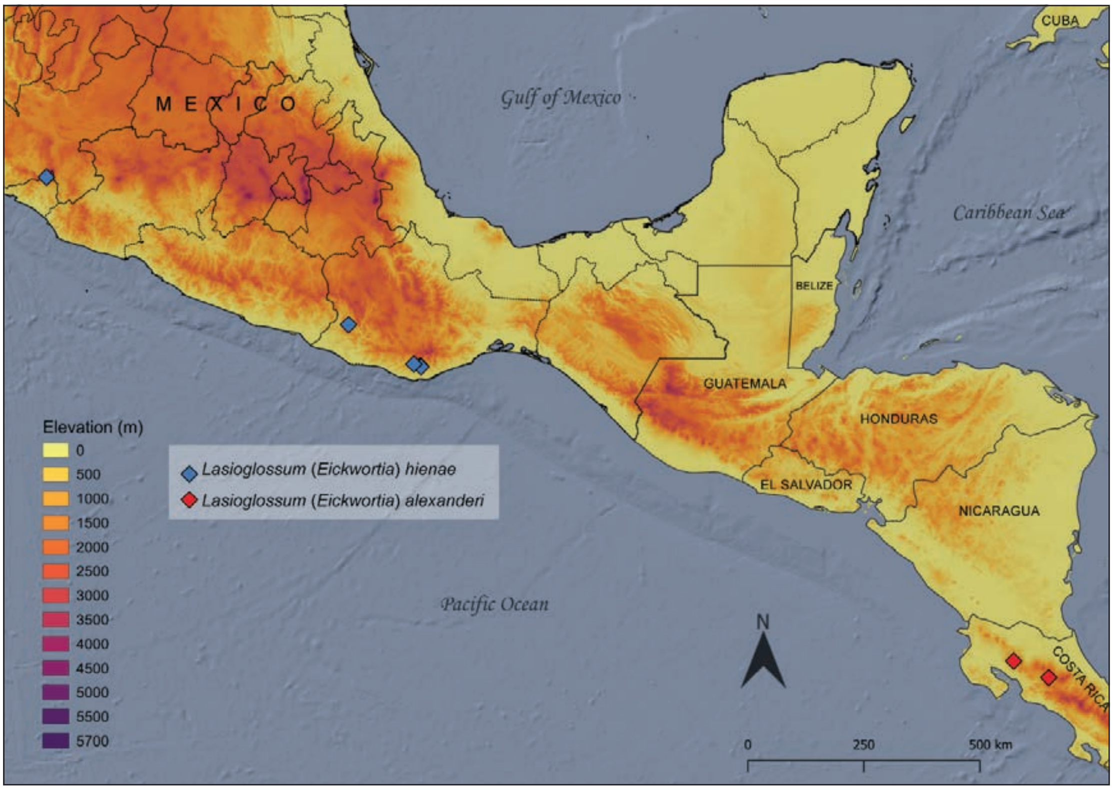

Figure 9. Known localities of *Lasioglossum* (*Eickwortia*) *hienae* and *L.* (*E.*) *alexanderi*.

***Lasioglossum* (*Eickwortia*) *nycteris* (Vachal)**

Halictus nycteris Vachal, 1904: 119 (♀).

Material examined. Mexico • 2 ♂♂; Hidalgo; 38 mi. NE Jacala; 10 Jul 1961; 3100'; U. Kans. Mex. Exped. leg.; SEMC; 1 ♂; Hidalgo; 10 kme E Otanga; 10 Nov 1991; 1110 m; R. Ayala leg.; CNIN; 1 ♂; Hidalgo; Tenango de Doria, El Dano; 20.235, −98.227; 11 Mar 1993; 1680 m; L. Godinez leg.; CNIN;

***Lasioglossum* (*Eickwortia*) *alexanderi* (McGinley)**

Figs 10–21

Eickwortia alexanderi McGinley 1999: 118 (♀).

Material examined. 10 specimens (2 ♂♂, 8 ♀♀). Costa Rica • 2 ♂♂, 7 ♀♀; Puntarenas, Monteverde, 10.3181, −84.8025; 09 Feb2020; T. McMahon leg; on yellow composite;WRME; 1 ♀; Puntarenas; Monteverde: 20/24 Jun 1986; W. Hanson | G. Bohart leg.; BBSL.

Diagnosis. The male of *L.* (*E.*) *alexanderi* is unique among all known Western Hemisphere *Lasioglossum* for the thickened apex of the clypeus above the labrum. The broad hind basitarsus is also unlike any *Lasioglossum* in the region. The female is entirely brown-black, mandibles bidentate, and wings entirely infuscate. The metapostnotum is crescent-shaped, defined apically by a sharp edge, and covered by subparallel. longitudinal carinulae (Fig. 21; McGinley 1999: fig. 13). An undescribed female collected simultaneously is remarkably similar, but the metapostnotum has a smooth apicolateral area, not sharply defined from the carinulate portion. This undescribed female is notably smaller, with varying levels of golden-green reflections and the apical terga are orange.

Description. Male:

Length 8.3–9.2 mm.

Head length 2.4–2.5 mm. Head width 2.8–2.9 mm. Intertegular span 2.0–2.2 mm.

Forewing length 7.7–8.3 mm.

Maximum metasomal width (T3) 2.3–2.35 mm.

***Structure*.** Head wider than long (length/width ratio = 0.85–0.91). Gena width at midlength 1.1–1.2 × width of contiguous section of compound eye in lateral view (Fig. 10). Supraclypeal area weakly protuberant. Clypeus width approximately twice length, width/length ratio = 2.2, projecting approximately half its length below lower margin of eyes (Fig. 11). Clypeal apex thickened, half-length of labrum (Fig. 13). Ocellocular distance 2.5 × lateral ocellar diameter, slightly greater than distance between lateral ocellus and hind margin of vertex, and 1.3 × interocellar distance (Fig. 12). Compound eyes convergent below, upper ocular distance 1.4 × lower ocular distance (Fig. 2). Hypostomal carinae strong, subparallel; anterior angle rounded. Antennal scape short, not reaching median ocellus; pedicel wider than long, three quarters length of flagellomere 1 (subsequent flagellomeres missing). Labrum short without apical process. Mandible simple, relatively broad

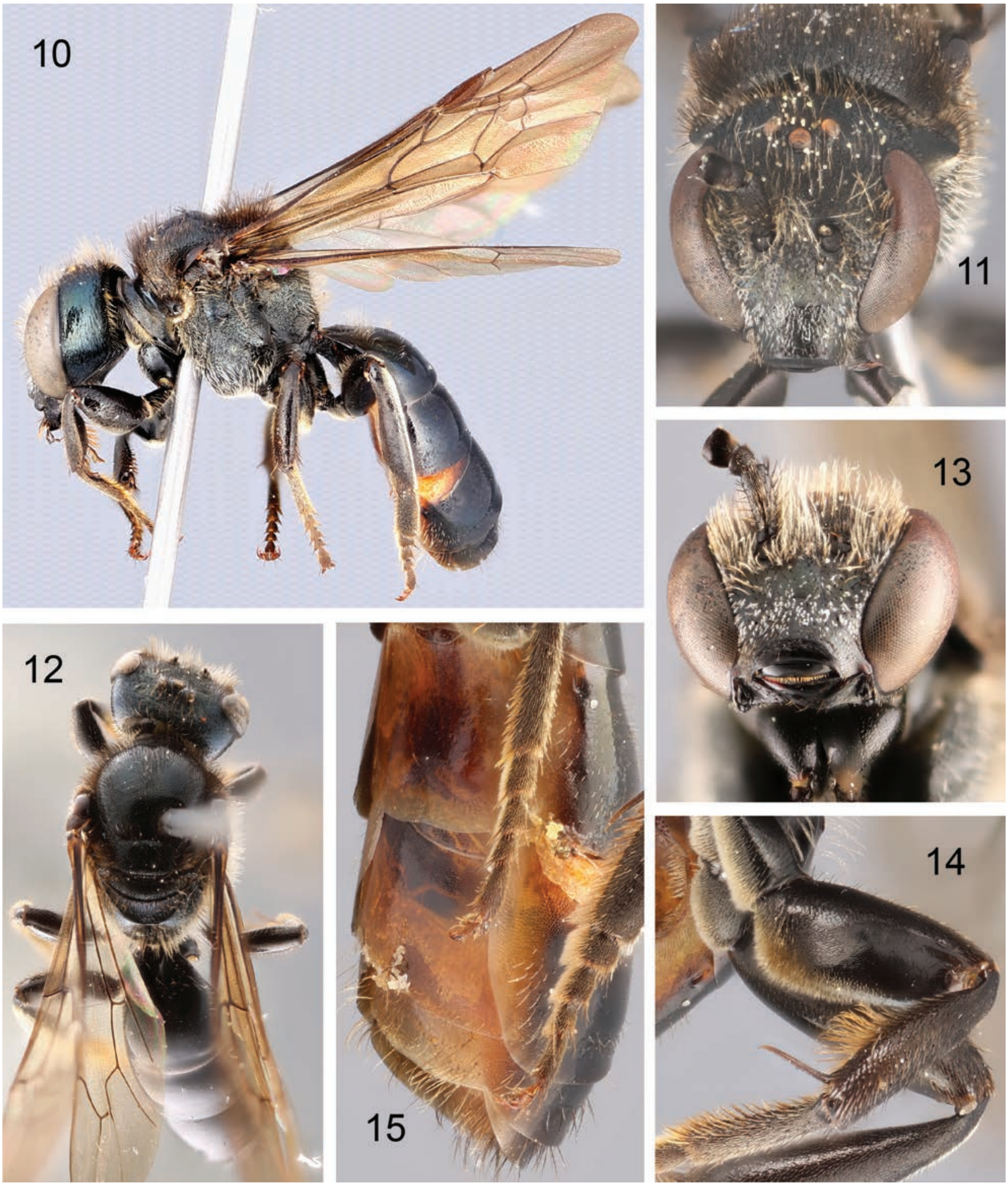

Figures 10–15. Male of *Lasioglossum* (*Eickwortia*) *alexanderi* **10** lateral habitus **11** face **12** dorsal habitus **13** mandibles and lower section of head **14** anterior surface of mesofemur **15** view of sterna.

at midlength, nearly reaching opposing clypeal angle (Fig. 13). Pronotum maximum width 2.7–2.8; dorsolateral angle orthogonal; pronotal ridge strongly angled, interrupted by oblique sulcus; pronotal lobe with anterior carina. Inner metatibial spur ciliate, subequal in size to outer metatibial spur. Tegula ovoid. Forewing veins 1rs-m and 2rs-m not noticeably weak; hamuli arranged 3-1-2.

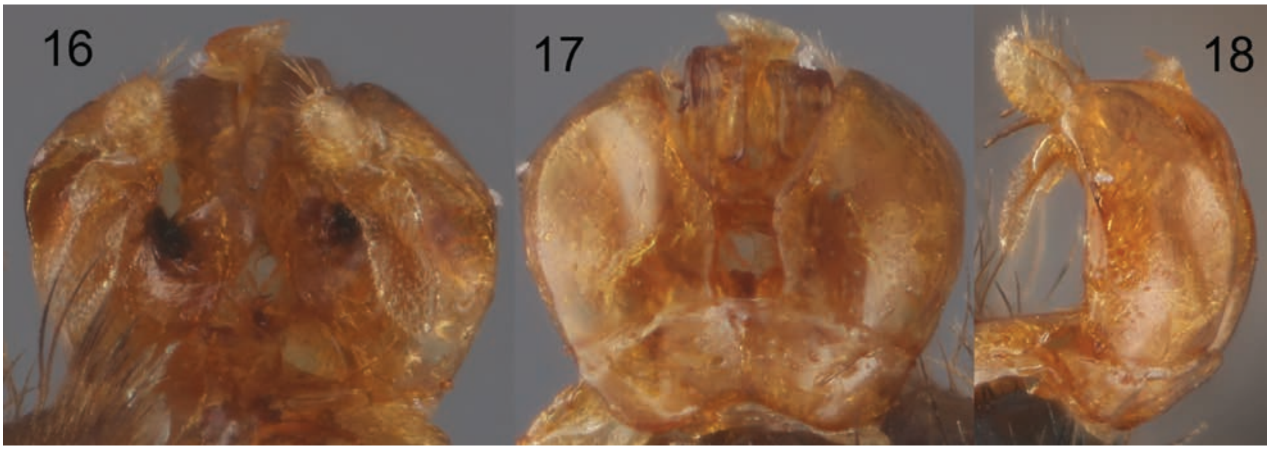

Figures 16–18. Male genitalic capsule of *Lasioglossum* (*Eickwortia*) *alexanderi* **16** ventral aspect **17** dorsal aspect **18** lateral aspect.

Surface sculpture. Face tessellate-granular below antennal sockets, scabriculous above (Fig. 11), Gena and subgena striolate in oblique view, outer subgena polished. Mesoscutum and mesoscutellum polished, anteromedial mesoscutum imbricate, becoming striolate anterolaterally (Fig. 13). Metapostnotum with dense, regular carinulae, slightly depressed at apex (Fig. 13). Mesepisternum transversely striolate on upper half, vertically striolate on anterior lower half, more irregularly sculptured towards mesocoxa. Metepisternum transverse carinulae above, imbricate, irregularly sculptured below.

Propodeum lateral surfaces similar to lower metepisternum, posterior surface tessellate noticeably.

Terga polished.

Color. Body blackish brown, with the following remarks: supraclypeal area with dull golden-green reflections, gena hints of green in certain lights, posterior surface of flagellomere 1 dark. Tegula dark brown (Fig. 12). Legs dark brown, pretarsal claws reddish brown (Fig. 15). Forewing membrane weakly infuscate throughout, with green and purple highlights; wing veins and pterostigma brown (Fig. 10). Metapostotum with blue tinge between carinulae. Terga blackish brown, with narrow rims reddish brown and ventrally reflexed portions amber; sterna amber (Fig. 15).

Pubescence. Head and mesosoma with erect branched setae (1.5–2.5 OD); tomentum sparse on clypeus, paraocular and supraclypeal areas (Fig. 11). Pronotal collar, lobe and adjacent pre-episternum with tomentum. Meso- and metacoxae and trochanters ventrally with dense velvety setae, extending onto ventral surface of mesofemur (Fig. 14), otherwise legs with short subappressed setae. Apical half of pro- and mesotibiae with long setae ventrally, somewhat curved apically becoming straight towards apex. T1 anterior face with erect setae, remaining terga with sparse short setae, except longer on premarginal lines of T5–T6. S1–S4 nearly bare, S5–S6 with long setae.

Genitalia. As in Figs 16–18. S7 with slender median process, S8 broadly rounded apically. Gonocoxite dorsally with inner edge subparallel for length approximately equal to gonobase (Fig. 17); gonostylus moderately elongate, rounded apically (Fig. 18); retrorse lobe present, moderately long, slender, rounded apically (Fig. 16); volsella with prominent lateral lobe.

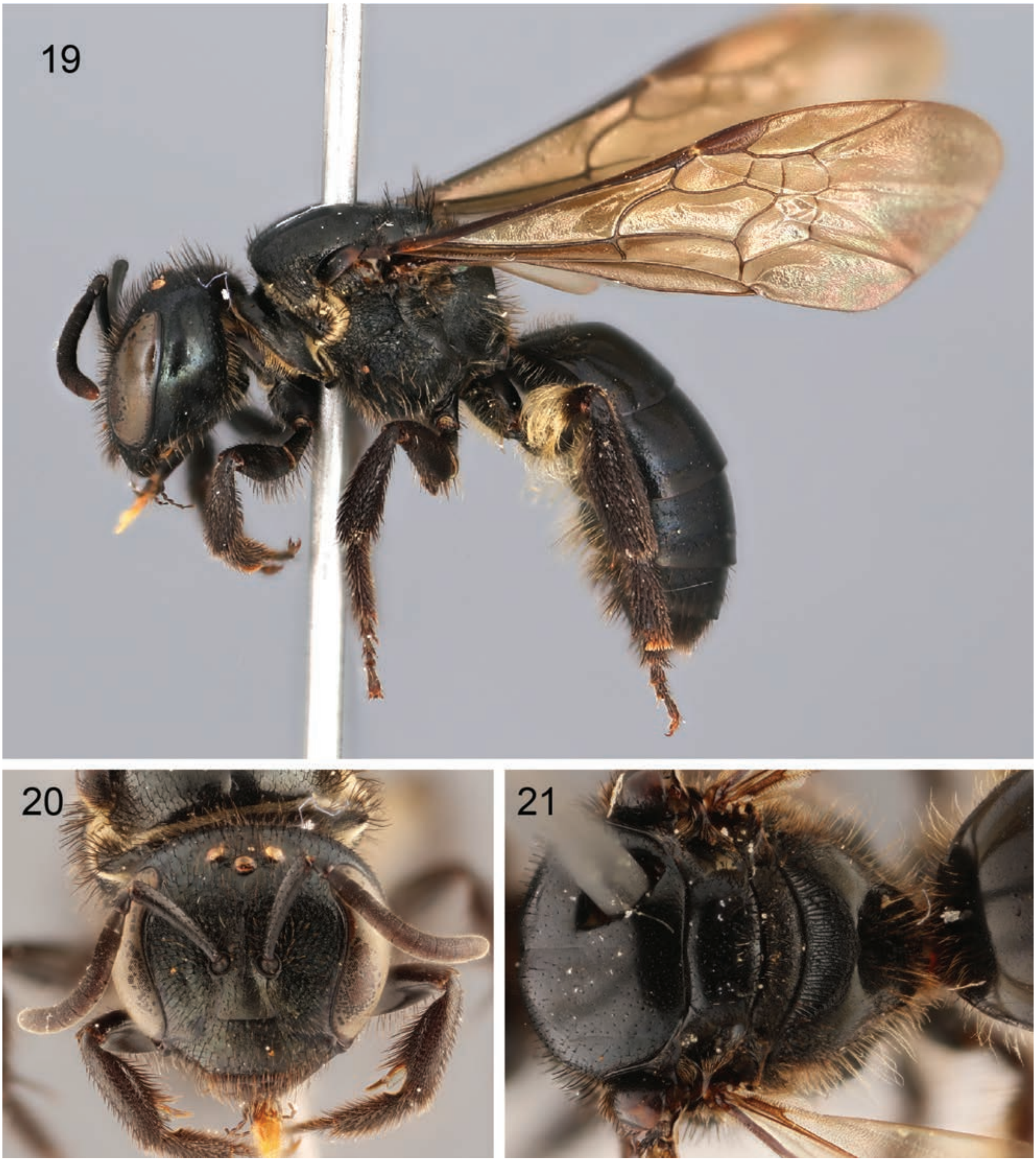

Figures 19–21. Female of *Lasioglossum* (*Eickwortia*) *alexanderi* **19** lateral habitus **20** face **21** dorsal view of mesosoma.

New distributional records

Although the holotype of *L. alexanderi* is lost, the description and figures are sufficient to recognize this unique species. At this point a neotype designation is not needed, and there is still hope the holotype may reemerge once more material in the former possession of McGinley is examined. The novelty of the male and co-occurrence with the female supports the association. The undescribed female co-occurring with *L. alexanderi* is unlikely to be the female based on the similar structure of the male and female metapostnotum, in addition to body color and size. The new collection site is approximately 70 km west of the type locality (Costa Rica; Heredia; 8.7 km N Varablanca).

Revised key to *Lasioglossum* (*Eickwortia*) *sensu stricto*

Modified from Gibbs and Dumesh 2013. Characters to distinguish males of *L. hienae* and *L. nycteris* are not currently known.

1 Both sexes: forewing complete infuscate; mesoscutum polished with subtle tessellation, distinct punctures; pronotal dorsolateral angle not carinate; metapostnotum distinctly carinulate. Males: posterior surface of propodeum without tomentum; T1 not slender; inner metatibial spur normal sized; hind basitarsus less than 3 × longer than wide .... ***L. alexanderi***

– Both sexes: forewing anterior third infuscate; mesoscutum dull with dense, fine punctures and scattered coarser ones; pronotal dorsolateral angle carinate; metapostnotum smooth, with scarcely visible carinulae. Males: posterior surface of propodeum covered by tomentum; male T1 slender; inner metatibial spur short or absent; hind basitarsus greater than 6 × longer than wide **2**

2 Female mesoscutum granulate, obscurely doubly punctate.........***L. hienae***

– Female mesoscutum tessellate with distinct double punctures (fine punctures separated by 1–2 diameters, coarse punctures separated by 5–10 diameters).. ***L. nycteris***

Discussion

Lasioglossum is by far the most diverse genus of bees (Ascher and Pickering 2024), with the number of species possibly reaching 2000 given the numerous undescribed species in several areas of the world. The mountainous regions of Mexico are a good example of areas where many *Lasioglossum* species remain unassigned to a known taxon (i.e. Fierros-López 1998; Hinojosa-Díaz 2003; Godínez-García et al. 2004; Bonet Ferrer and Vergara 2019; Razo-León et al. 2024). The present contribution adds to the knowledge of a characteristic group of species within *Lasioglossum*. The subgenus *Eickwortia* in its restricted sense includes only three very apomorphic species occurring in mountainous areas of Mexico and Central America, two of them known by a scarce number of female specimens. With the description of the males of *L.* (*E.*) *hienae* and *L.* (*E.*) *alexanderi*, we increase the knowledge on the morphological circumscription of this singular assemblage of species within the highly diverse *Lasioglossum*. Some of the features found in *Eickwortia* (*sensu stricto*) (i.e. apically bidentate mandibles of females), as traditionally understood, are also present in some Neotropical *Lasioglossum* recently found to be phylogenetically closely related (Gardner 2023), which leads to the possibility of reconsideration of the taxonomic definition of the group.

The male of *L. alexanderi* has unique features but lacks the autapomorphic characters of *L. nycteris* and *L. hienae*. However, its clypeus and hind leg characters are unlike other *Lasioglossum* known to us. In some ways, *L. alexanderi* seems intermediate between *L. nycteris* and the apparently related metallic species. This is further highlighted by the undescribed female found, which is so similar to *L. alexanderi* that a plausible hypothesis would be that it is a caste of the same species, with associated structural and color differences. Under certain lighting, *L. alexanderi* shows signs of metallic reflections on the gena and metapostnotum. Future study of this broader definition of *Eickwortia* is needed to contextualize the patterns seen in the females. Males of the metallic species share some similarities to *Eickwortia* (*sensu stricto*), but they seem to have fewer evident unique characters than the three species traditionally included.

In terms of distribution, most of the 30 *L.* (*E.*) *hienae* specimens here studied expand the known range of the species east, along the Sierra Madre del Sur range in the state of Oaxaca, Mexico. While the type locality given by Gibbs and Dumesh (2013) set the species in the mountains of the Transmexican volcanic belt. These two mountainous assemblages are biogeographic provinces of a major biogeographical assemblage, the Mexican transition zone, an area characterized by a mix of taxa with affinities to the Nearctic and Neotropical regions (Morrone 2019). For this region a few distributional patterns have been recognized (Morrone 2019), depending on the affinities of the species assemblages found in them. The series of *L.* (*E.*) *alexanderi* examined here were recorded at elevations above 1500 m, as was the holotype. *Eickwortia*, either in its current sense or in an expanded redefinition, seems to be allied to high elevations in the area, but more distributional records are needed for the included species.

Males of *L.* (*E.*) *nycteris* currently held at WRME (in the material examined above, referred to as deposited at CNIN) were compared to *L.* (*E.*) *hienae* males using photographs and discussion between the co-authors with reference to the detailed description of McGinley (1999). Available male *L.* (*E.*) *nycteris* have had the genitalia removed, but they are not associated with the specimens. Our statements of the seemingly lack of morphological differentiation of our newly described *L.* (*E.*) *hienae* males with those of *L.* (*E.*) *nycteris* are based on the comparison with the detailed original description of this (McGinley 1999). The newly described males were collected during the same collecting events as the females morphologically matching *L.* (*E.*) *hienae*, while no specimen of *L.* (*E.*) *nycteris* is known from those events.

The allometric variability observed in females of *L.* (*E.*) *nycteris* is also seen in the several females revised for this study. However, details of such variation are to be examined in future studies by the authors. The strongly bidentate mandible has been speculated to be an adaptation for nesting in wood, although given the moderate degree of macrocephaly it could potentially be related to intraspecific interactions. There is no evidence of nesting biology for these species; however, the *Hemihalictus* series displays a wide range of nesting behaviour (Michener 1974). *Lasioglossum figueresi* Wcislo is closely related and shows both solitary nesting and some low-level social nesting (Wcislo et al. 1993). A lot of work remains to be done to understand the biology and taxonomy of *Lasioglossum* (*Eickwortia*), but with this study we hope to contribute to a better understanding of the behavior, morphology, and distribution of the group.

Acknowledgements

We are grateful to Olivia Yáñez, Armando Luis (Museo de Zoología “Alfonso L. Herrera”, Facultad de Ciencias, UNAM), Ricardo Ayala (Estación Chamela, Instituto de Biología, UNAM), and Timothy McMahon for facilitating the use of specimens and data for this study. Susana Guzmán (Laboratorio de Microscopía y Fotografía de la Biodiversidad, Instituto de Biología, UNAM) assisted with the production of high-resolution stereomicroscope photos, and Chris Lambarri helped with some image production.

Additional information

Conflict of interest

The authors have declared that no competing interests exist.

Ethical statement

No ethical statement was reported.

Funding

Support for this study came from DGAPA-UNAM (PAPIIT IN223724) and National Sciences and Engineering Research Council of Canada Discovery Grant RGPIN-2018-05353. ACMC received support through a doctoral scholarship from Consejo Nacional de Humanidades, Ciencias y Tecnologías (CONAHCYT- Mexico).

Author contributions

Conceptualization: IAHD. Data curation: IAHD, JG, ACMC. Investigation: ACMC. Methodology: JG, IAHD.

Author ORCIDs

Ismael A. Hinojosa-Díaz https://orcid.org/0000-0002-5493-850X
Ana Celeste Martínez Cervantes https://orcid.org/0000-0001-5707-1051
Jason Gibbs https://orcid.org/0000-0002-4945-5423

Data availability

All of the data that support the findings of this study are available in the main text.

References

Ascher JS, Pickering J (2024) DiscoverLife bee species guide and world checklist (Hymenoptera: Apoidea: Anthophila). http://www.discoverlife.org/mp/20q?guide=Apoidea_species [Last accessed 24 May 2024]

Bonet Ferrer M, Vergara CH (2019) Abejas Silvestres de un Cafetal Orgánico en Veracruz, México. UDLAP, San Andrés Cholula, Puebla, Mexico, 517 pp.

Brooks RW (1988) Systematics and phylogeny of the anthophorine bees (Hymenoptera: Anthophoridae; Anthophorini). The University of Kansas Science Bulletin 53: 436–575.

Danforth BN, Conway L, Ji S (2003) Phylogeny of eusocial *Lasioglossum* reveals multiple losses of eusociality within a primitively eusocial clade of bees (Hymenoptera: Halictidae). Systematic Biology 52: 23–36. https://doi.org/10.1080/10635150390132687

Engel MS, Hinojosa-Díaz IA, Yáñez-Ordóñez O (2007) The *Augochlora*-like *Dialictus* from Guatemala and Southern Mexico (Hymenoptera: Halictidae). Acta Zoológica Mexicana (n.s.) 23: 125–134. https://doi.org/10.21829/azm.2007.233596

Fierros-López HE (1998) Abejas silvestres (Hymenoptera: Apoidea) del Volcán de Tequila, Jalisco, México. Folia Entomologica Mexicana 102: 21–70.

Gardner J (2023) Bees of the subgenus *Lasioglossum* (*Dialictus*) of the western Nearctic region (Hymenoptera: Halictidae: Halictini). Ph.D. thesis, University of Manitoba, Winnipeg.

Gibbs J (2018) DNA barcoding a nightmare taxon: assessing barcode index numbers and barcode gaps for sweat bees. Genome 61: 21–31. https://doi.org/10.1139/gen-2017-0096

Gibbs J, Dumesh S (2013) A new species, *Lasioglossum* (*Eickwortia*) *hienae*, from Mexico (Apoidea: Halictidae). Journal of Melittology 13: 1–11. https://doi.org/10.17161/jom.v0i13.4518

Gibbs J, Brady S, Kanda K, Danforth BN (2012) Phylogeny of halictine bees supports a shared origin of eusociality for *Halictus* and *Lasioglossum* (Apoidea: Anthophila: Halictidae). Molecular Phylogenetics and Evolution 65: 926–939. https://doi.org/10.1016/j.ympev.2012.08.013

Gibbs J, Dumesh S, Packer L, Danforth BN (2013) Revision and reclassification of *Lasioglossum* (*Evylaeus*), *L.* (*Hemihalictus*) and *L.* (*Sphecodogastra*) in eastern North America (Hymenoptera: Apoidea: Halictidae). Zootaxa 3672: 1–117. https://doi.org/10.11646/zootaxa.3672.1.1

Godínez-García LM, Hinojosa-Díaz IA, Yáñez-Ordóñez O (2004) Melitofauna (Insecta: Hymenoptera) de algunos bosques mesófilos de montaña. In: Luna I, Morrone JJ, Espinosa D (Eds) Biodiversidad de la Sierra Madre Oriental. Universidad Autónoma de México, Mexico, 321–337.

Harris RA (1979) A glossary of surface sculpturing. Occasional Papers in Entomology 28: 1–31.

Hinojosa-Díaz IA (2003) Abejas silvestres (Hymenoptera: Apoidea) del declive sur de la sierra del Chichinautzin, Morelos, México. Folia Entomológica Mexicana 42: 1–20.

McGinley RJ (1999) *Eickwortia* (Apoidea, Halictidae), a new genus of bees from Mesoamerica. University of Kansas Natural History Museum, Special Publication 24: 111–120.

Michener CD (1974) The Social Behaviour of the Bees. Harvard University Press, Cambridge, MA, 404 pp.

Michener CD (2007) The Bees of the World (2nd edn.). Johns Hopkins University Press, Baltimore, 953 pp.

Michener CD, Fraser A (1978) A comparative anatomical study of mandibular structure in bees (Hymenoptera: Apoidea). The University of Kansas Science Bulletin 51: 463–482. https://doi.org/10.5962/bhl.part.17245

Morrone JJ (2019) Regionalización biogeográfica y evolución biótica de México: encrucijada de la biodiversidad del Nuevo Mundo. Revista Mexicana de Biodiversidad 90: 1–68. https://doi.org/10.22201/ib.20078706e.2019.90.2980

Razo-León AE, Huerta-Martínez FM, Moya-Raygoza G, Muñoz-Urias A (2024) Bees (Hymenoptera: Apoidea) diversity and synanthropy in a protected natural area and its influence zone in western Mexico. Florida Entomologist 107: 20240005. https://doi.org/10.1515/flaent-2024-0005

Wcislo WT, Wille A, Orozco E (1993) Nesting biology of tropical solitary and social sweat bees, *Lasioglossum* (*Dialictus*) *figueresi* Wcislo and *L.* (*D.*) *aeneiventre* (Friese) (Hymenoptera: Halictidae). Insectes Sociaux 40: 21–40. https://doi.org/10.1007/BF01338830

ZooKeys 1228: 69–97 (2025)
DOI: 10.3897/zookeys.1228.142202

Research Article

A cryptic new species of tiger swallowtail (Lepidoptera, Papilionidae) from eastern North America

Charles J. DeRoller[1], Xi Wang[2], Julian R. Dupuis[3], B. Christian Schmidt[4]

1 *PO Box 374, Victor, New York, 14564, USA*
2 *Kingston, Ontario, Canada*
3 *Department of Entomology, University of Kentucky, Lexington, KY, 40546, USA*
4 *Canadian National Collection of Insects, Arachnids, and Nematodes, Biodiversity Program, Agriculture and Agri-Food Canada, Ottawa, ON, Canada*
Corresponding author: B. Christian Schmidt (christian.schmidt@agr.gc.ca)

Abstract

In the eastern Great Lakes region of North America, two tiger swallowtail species have previously been recognized, *Papilio glaucus* Linnaeus, 1758 and *Papilio canadensis* Rothschild & Jordan, 1906. A third entity, the Midsummer Tiger Swallowtail, has been treated as a *P. glaucus* × *canadensis* hybrid, and exhibits a mosaic of both intermediate and unique morphological and biological traits. Here we demonstrate that rather than being a localized, historically recent hybrid phenomenon, the Midsummer Tiger Swallowtail maintains its morphological and physiological distinctness over a large geographic region in the absence of one or both putative parental species, and was first documented in the literature nearly 150 years ago. *Papilio solstitius* **sp. nov.** is physiologically unique in delaying post-diapause development, which results in allochronic isolation between the spring flights of *P. glaucus* and *P. canadensis*, and the late summer flight of *P. glaucus*. Similarly, the geographic range of *Papilio solstitius* spans the region between the northern terminus of *P. glaucus* and southern limits of *P. canadensis*, remaining distinct in areas of sympatry. Defining the taxonomic identity of this unique evolutionary lineage provides an important baseline for further inquiry into what has served as an exemplary species group in evolutionary study.

Key words: cryptic species, hybrid, *Papilio glaucus*, Papilionidae, *Pterourus*, speciation

OPEN ACCESS

Academic editor: Shinichi Nakahara
Received: 19 November 2024
Accepted: 14 January 2025
Published: 14 February 2025

ZooBank: https://zoobank.org/F0AEECC8-82AD-48E3-8FBE-5CA6F883420F

Citation: DeRoller CJ, Wang X, Dupuis JR, Schmidt BC (2025) A cryptic new species of tiger swallowtail (Lepidoptera, Papilionidae) from eastern North America. ZooKeys 1228: 69–97. https://doi.org/10.3897/zookeys.1228.142202

Introduction

The North American *Papilio glaucus* species group (Lepidoptera: Papilionidae) is a model study system in insect evolutionary biology. The recognition and delimitation of *P. glaucus* L., 1758 and *P. canadensis* as a classic sibling species pair (Hagen et al. 1991; Sperling 1993) led to three decades of study in speciation, host plant adaptation, hybridization, and molecular evolution (e.g., Ryan et al. 2017 and references therein). More recently, the discovery of a third species, *P. appalachiensis* Pavulaan & Wright, 2002, has provided unprecedented insight into speciation via hybridization (Scriber and Ording 2005; Kunte et al. 2011; Cong et al. 2015; Vernygora et al. 2022). *Papilio appalachiensis* is now recognized as a homoploid hybrid species with origins from *P. glaucus* × *P. canadensis* crosses some 0.4 million years ago (Cong et al. 2015; Kunte et al. 2011).

The *Papilio glaucus* group previously comprised nine species (Kunte et al. 2011; Pavulaan 2024), and the five eastern North American species discussed herein are termed the *glaucus* complex. All are very similar in external appearance, and prior to 1991, were included within the concept of a single species, *P. glaucus*. Subsequently, three species were recognized: The Eastern Tiger Swallowtail (*P. glaucus*) which occurs across most of eastern USA and as far north as southwestern Ontario, and south of the Adirondack and Catskill Mountains in New York; the more northern Canadian Tiger Swallowtail (*P. canadensis*) that occurs across the boreal region from Newfoundland to Alaska, and as far south as southern Ontario and the northern Appalachians; and the Appalachian Mountains endemic *P. appalachiensis*, found from Pennsylvania to Georgia (Pavulaan and Wright 2002). The recently described New England Swallowtail, *Papilio bjorkae* Pavulaan, 2024, may be conspecific with *P. canadensis* or *P. glaucus*; as detailed below in “Comparative morphology of the *Papilio glaucus*-complex,” incomplete knowledge of *P. bjorkae*’s morphology, range, biology, and taxonomic status currently precludes full comparison to the remainder of the *P. glaucus* group.

The *Papilio glaucus* group is part of a larger, predominantly New World clade of swallowtails of the subgenus *Pterourus* Scopoli, sometimes recognized as a distinct genus (e.g., Pelham and Pohl 2023). The broader concept of the genus *Papilio* L. is used herein, in agreement with the results and reasoning presented by Condamine et al. (2023).

Each of the *glaucus*-complex species show adaptation to different thermal niches that can be broadly characterized as warm (*P. glaucus*), intermediate (*P. appalachiensis*), and cool (*P. canadensis*) climatic regions; all have broad larval host plant diets, and are not restricted by the distributions thereof. At coarse geographic scales, species distributions appear parapatric, but at finer spatial scales, multiple taxa can overlap (Fig. 1). The transition or contact zone between *P. glaucus* and *P. canadensis* has received considerable study. West of Lake Michigan, introgression and hybridization have been well-documented through morphometric and molecular studies (Luebke et al. 1988; Ryan et al. 2016, 2017, 2018). Here, a narrow hybrid zone (50–100 km wide) is maintained by strong selective pressure for adaptation to either warm or cool thermal regimes, with a rapid geographic shift from *P. glaucus* to *P. canadensis* across a threshold thermocline (Fig. 1; Scriber 2010; Ryan et al. 2016, 2017, 2018).

In the topographically and climatically complex region of eastern Ontario and adjacent New York, the relationship between *P. canadensis* and *P. glaucus* is less straightforward. Unlike the central Great Lakes region to the west, the ranges of *P. canadensis* and *P. glaucus* are more poorly defined as a result of confusing phenotypes and phenologies, making identification difficult. In northern New York, Vermont and eastern Ontario, univoltine tiger swallowtails with a July flight period have variously been called *P. glaucus* (Shapiro 1974; Layberry et al. 1998; Hall et al. 2014), “false second generation” (Hagen and Lederhouse 1985), “late flight *P. canadensis*” (Scriber and Ording 2005; Kunte et al. 2011), “hybrid types” (Scriber 1990), “late flight” (Scriber 2010), “late flight hybrids” (Wang 2018), “delayed ‘late flight’ hybrid swarm” (Scriber 2010), “a stable hybrid” (Zhang et al. 2013), “intermediate individuals” (Vernygora et al. 2022), “midsummer tiger swallowtail” (Schmidt 2020), and “divergent ecomorphs” (Vernygora et al. 2022). Hagen and Lederhouse proved that this taxon is not the second annual generation of any spring-flying swallowtails, instead representing a single-brooded

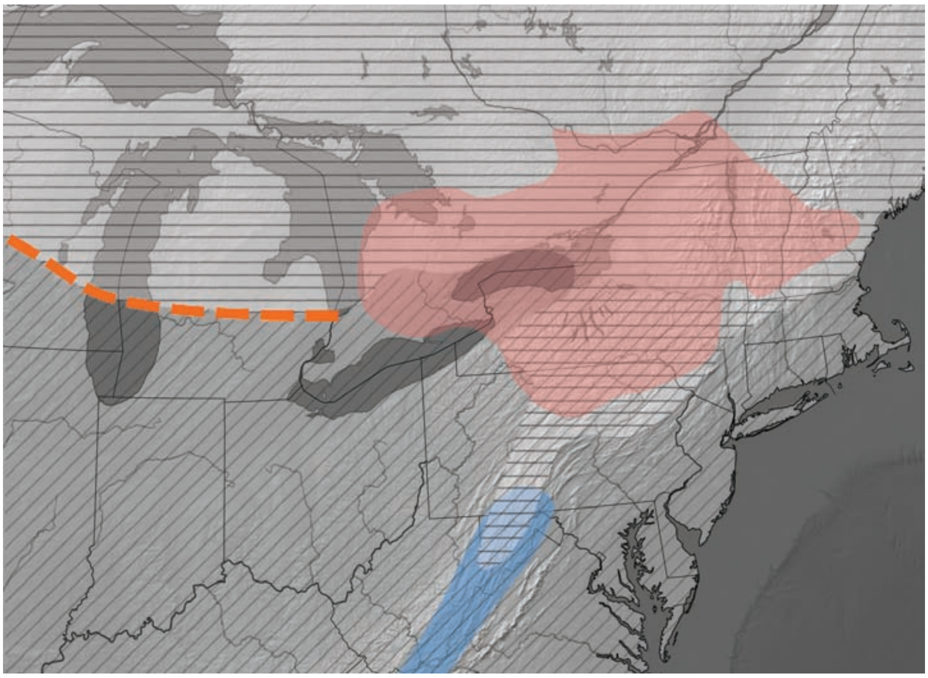

Figure 1. Geographic ranges of the *Papilio glaucus*-complex in eastern North America. *Papilio glaucus* (diagonal lines), *P*. *canadensis* (horizontal lines), *P*. *appalachiensis* (blue), and *P*. *solstitius* sp. nov. (red). In the central Great Lakes region, a sharp transition or hybrid zone occurs between *P. glaucus* to the south and *P. canadensis* to the north, indicated by the orange dashed line. In the northern Appalachian region this transition zone is much larger as a result of topography-induced climatic variation, with elevational rather than latitudinal separation. Considerable uncertainty exists in the northern range limit of *P. glaucus* in NY (see "Habitat and distribution" section). Distribution data based on Luebke et al. (1988); Stump et al. (2003); Pavulaan and Wright (2002); Mcnaughton et al. (2020) and specimens verified in this study (Suppl. material 1).

taxon physiologically distinct from *P. glaucus* and *P. canadensis* (Hagen and Lederhouse 1984; Scriber and Ording 2005). This taxon is now referred to by the common name Midsummer Tiger Swallowtail (MST; Schmidt 2020).

Here, we present evidence that MST is not the result of historically recent hybridization between *P. glaucus* and *P. canadensis* as suggested by Kunte et al. (2011); literature and specimen records of MST date back 150 and 50 years, respectively. MST was also previously thought to be geographically localized to areas of *P. glaucus* - *P. canadensis* overlap, but this is also not the case. MST exhibits a large geographic range that includes regions where one or even both putative parent species are absent (Fig. 1). Lastly, the unique late-season flight acts as an allochronic reproductive barrier between MST and other tiger swallowtails. Based on combined molecular, phenological, morphological, and natural history data, the Midsummer Tiger Swallowtail is described as a new species, *Papilio solstitius* sp. nov.

Methods and materials

Field studies and specimen collections were carried out from 1999 to 2023 in Pennsylvania, Virginia, Kentucky, and the Finger Lakes region of New York (CJD); and from 2008 to 2023 in eastern Ontario (XW, BCS). Host plant suitability, larval development, and adult emergence were studied based on *ex ova* and *ex larva* rearings from 2008 to 2011 in Hamilton, Ontario, and from 2015 to 2022 in Kingston, Ontario (XW). All larvae were reared indoors at a constant 23 °C under outdoor ambient light conditions. Larvae were provided with cuttings of the host they were found on, either green ash (*Fraxinus pennsylvanicus* Marshall) or black cherry (*Prunus serotina* Ehrhart), held in small vials of water. Pupae that were entering diapause rather than direct development did not exhibit melanization of the eyes (visible by transillumination) after 2–3 weeks and were placed in cold storage, either in a conventional refrigerator or unheated garage. After removal from cold storage, they were again kept at a constant 23 °C and time to eclosion recorded. Adult genitalia were prepared following the protocol detailed in Schmidt (2018) and imaged using a Leica DFC 450 camera mounted on a Leica M205C stereo microscope.

Where confident identification was possible, distribution and phenology data were augmented with records from iNaturalist (inaturalist.org), eButterfly (e-butterfly.org), and the Ontario Butterfly Atlas (Macnaughton et al. 2020). Manual calipers precise to the nearest 0.1 mm were used for wing measurements. Occurrence maps were created with SimpleMappr (https://www.simplemappr.net). Voucher specimens examined in this study (Suppl. material 1) are found in the following collections:

CNC	Canadian National Collection of Insects, Arachnids and Nematodes, Ottawa, CAN
CMNH	Carnegie Museum of Natural History, Pittsburgh, PA, USA
CJDC	Charles J. DeRoller Collection
XWC	Xi Wang Collection

Molecular datasets

Publicly available sequences and previous DNA barcoding efforts in the *P. glaucus* group have focused on both the 5' region of the mitochondrial *cytochrome oxidase subunit I* (COI) gene (the standard barcode region (Hebert et al. 2003) using primers LCO1490 and HCO2198 (Folmer et al. 1994)) and the 3' region of COI (primers Jerry and Pat, as used in Kunte et al. 2011; Vernygora et al. 2022). Unfortunately, few, if any, specimens have been sequenced for both regions, so we are limited to considering these regions separately and hereafter refer to them as COI5 and COI3, respectively. Fourteen MST specimens were sent to a private COI5 barcoding service; Sanger sequencing was performed by Azenta Life Sciences (Chelmsford, Massachusetts, United States), and consensus sequences were constructed using de novo assembly in Geneious Prime v. 2024.0 (uploaded to BOLD with accessions provided in the associated figure). Additionally, COI5 barcodes were generated for two *P. appalachiensis* (UASM400650 and UASM400651, also sequenced by Vernygora et al. 2022), to ensure representation of that species in the COI5 dataset (NCBI GenBank accessions: PQ578215.1 and PQ578216.1). Sequencing and analysis were conducted as in Vernygora et al. (2022). COI5 and COI3 sequences were retrieved from GenBank (September 2024) for all species in the *glaucus*-complex and aligned to a complete *P. glaucus* mitogenome (NC_027252.1). Outgroup taxa were also selected as in Vernygora et al. (2022). Unique and pertinent COI5 sequences in the BOLD database (i.e., those of *P. glaucus* and *P. canadensis* from NE USA and SE Canada) were added to this dataset, and we used AliView v1.28 (Larsson 2014) to align sequences either manually or using default settings with MUSCLE (Edgar 2004). We used IQ-Tree v. 2.3.5 (Nguyen et al. 2015) to conduct maximum likelihood tree searches using the best model identified by Bayesian Information Criterion with ModelFinder (Kalyaanamoorthy et al. 2017). One thousand replicates of ultra-fast bootstrap (ufBS, Hoang et al. 2018) and the Shimodaira-Hasegawa approximate likelihood ratio test (SH-aLRT, Guindon et al. 2010) were used to assess nodal support. The genomic phylogeny using 3,733 single nucleotide polymorphisms (SNPs) from Vernygora et al. (2022) was also considered (we focused on the majority rule consensus tree generated from MrBayes (Ronquist et al. 2012), although see Vernygora et al. (2022) for more details on their thorough analysis), and we reevaluated the morphology of those specimens noted as “intermediates” in their analyses. All trees were visualized with FigTree v. 1.4.4 (Rambaut and Drummond 2010).

Results

Taxonomic names currently in synonymy under *P*. *glaucus* and *P*. *canadensis* were reviewed and revised by Pavulaan and Wright (2002). Our review of these synonymies confirms that all taxon names are correctly attributed to their respective species, and do not apply to the Midsummer Tiger Swallowtail. As such, a new name is proposed here.

Papilio solstitius **sp. nov.**

https://zoobank.org/A9B99C5C-E8EC-4AA1-A6E6-B09E610E3389
Figs 3a, 4, 5, 6a, 7a, 8a, 9c-d, 10a, 11

Type locality. Canada, Ontario, Ottawa-Carleton District, Long Swamp, Old Almonte Rd., 45.249°N, 76.079°W.

Type material. ***Holotype*** (Fig. 4a) • male. Ontario, Ottawa-Carleton Dist., Old Almonte Rd. at Long Swamp, 45.249°N, 76.079°W, 3.Jul.2020, B.C. Schmidt, CNC voucher # CNCLEP00342771 [CNC]. ***Allotype*** (Fig. 4b) • female. Ontario, Frontenac Co., Vanalstine Lake, 44.858°N, 76.847°W, 5.Jul.2021, B. C. Schmidt, observed ovipositing on *Prunus serotina* [CNC]. ***Paratypes*** • 53 in CNC, 9 in XWC, 8 in CJDC; complete data and specimen deposition are given in Suppl. material 1.

Etymology. The epithet solstitius is derived from solstitium, the Latin term for solstice. The species’ unique midsummer flight period commences near the summer solstice.

Differential diagnosis. *Papilio solstitius* is closely related to *P*. *glaucus*, *P*. *canadensis* and *P*. *appalachiensis*, but differs from all in a suite of characters (Table 1). The most significant differences are apparent in developmental biology and phenology. *Papilio solstitius* is unique in its long post-diapause emergence delay, with adult eclosion beginning in late June to early July, compared to May for all other species (Fig. 2). Unlike the facultatively multivoltine *P*. *glaucus*, *P*. *solstitius* is obligately univoltine (like *P*. *canadensis* and *P*. *appalachiensis*). In the northern part of its range, *P. solstitius* overlaps with *P.*

Table 1. Comparison of morphological traits among species of the *Papilio glaucus*-complex. FW = forewing; DFW = dorsal forewing; VFW = ventral forewing; HW = hindwing; DHW = dorsal hindwing; VHW = ventral hindwing. Forewing length is geographically variable in *P. canadensis* and *P. glaucus*, and values are based on Ontario specimens.

Trait	***P. solstitius* sp. nov.**	***P. canadensis***	***P. glaucus***	***P. appalachiensis***	***P. bjorkae****
Head - setation of frons	intermediate, compact	long and diffuse	short and compact	intermediate, compact	short and compact
Average FW length (range): male	51 mm (42–57 mm)	46 mm (41–50 mm)	spring: 50 mm (43–52 mm); summer: 54 mm (45–58 mm)	50–62 mm	male and female combined: 49.2 mm (43–55 mm)
Average FW length (range): female	53 mm (48–56 mm)	48 mm (47–50 mm)	spring: 53 mm (50–55 mm); summer: 57 (49–64 mm)	50–65 mm	(unknown)
FW shape - distal margin	usually straight to slightly concave; concave frequency 40–50%	usually straight to slightly convex; concave frequency 25–30%	usually concave; concave frequency >80%	usually straight	concave
DFW - frequency of medial band black scales extending beyond Cu2 (male)	10–15%	55–70%	< 15%	< 20%	(unknown)
VFW margin: submarginal band	broadly coalescent lunules, usually with scalloped inner border	continuous band with straight inner and outer border; varying to coalescent rounded-rectangular elements, but lunules never well-separated by black	discrete lunules distinctly separated by black line along veins; varying to coalesced lunules with scalloped inner and outer margin	broadly coalescent lunules, usually with scalloped inner border	continuous band, sometimes with coalescent lunules anteriorly
VFW margin: inner (proximal) border	moderate amount of yellow dusting over black inner half	extensive yellow dusting over black inner half	extensive yellow dusting over black inner half	extensive yellow dusting over black inner half	extensive yellow dusting over black inner half
HW shape	elongate	broad / rounded	elongate	more triangular than *glaucus*	more angular than *glaucus*
HW tails	spatulate	aspatulate to slightly spatulate	spatulate	aspatulate to slightly spatulate	slightly to well-spatulate
HW margin	less scalloped	less scalloped	scalloped	less scalloped	less scalloped
HW anal cell black band width (male)	40–50%	55–90%	10–40% (summer); 20–50% (spring)	average ~50%	40–50% (based on 2 illustrated specimens)
DHW (female) submarginal orange lunule in cell Sc+R1	Smaller than remaining lunules, sometimes a mere dot	Smaller than remaining lunules, sometimes a mere dot	Much larger than remaining lunules	Slightly larger than remaining lunules	Slightly larger than remaining lunules
DHW female blue scaling	sparse	none to minimal	sparse to extensive	sparse	sparse
VHW marginal lunules	lunules rectangular to slightly crescentic	lunules more rectangular	crescentic lunules	lunules more rectangular	lunules rectangular to slightly crescentic
VHW marginal lunule ScR1 of female	length less than that of other lunules, often much more so	length less than that of other lunules, often much more so	conspicuously larger/ deeper than other lunules	similar in size to other lunules	conspicuously larger/ deeper than other lunules
VHW submarginal black band: inner border of 3 interspaces between Sc to M2	slightly scalloped	more linear than scalloped	scalloped	slightly scalloped	scalloped
VHW anal margin setation	sparse setation	long, dense setation	sparse to very sparse setation	sparse setation	(not given)
Abdomen shape	narrow, attenuated anteriorly	shorter, broad anteriorly	narrow, attenuated anteriorly	moderately attenuated anteriorly	(not given)
Abdomen subdorsal yellow stripe	broad, bright yellow, lateral black line well defined but narrow	narrower, less vivid yellow; sublateral black line wide	broad, bright yellow, sublateral black line faint or partially absent	broad, bright yellow, lateral black line well defined but narrow	(not given)
Male valve scales	solid yellow scales; clasper same shade abdomen	yellow with sparse black scales, clasper often appearing darker than abdomen	solid yellow scales; clasper same shade abdomen	solid yellow scales; clasper same shade abdomen	(not given)
Larva: 1st instar posterior white patch	usually present; rarely absent or faint	always present and well-developed	absent	absent or faint (tan)	unknown
Larva: 1st instar anterior white patch	usually present; rarely absent or faint	always present and well-developed	absent	absent	unknown

* based on images and information in Pavulaan (2024a).

canadensis, and in the south with *P. glaucus*; it is not known to overlap with *P. appalachiensis* (Fig. 1). Identification difficulties are therefore largely limited to confusion with either *P. canadensis* or *P. glaucus*. In combination with location and date, the comparative morphological characters summarized in Table 1

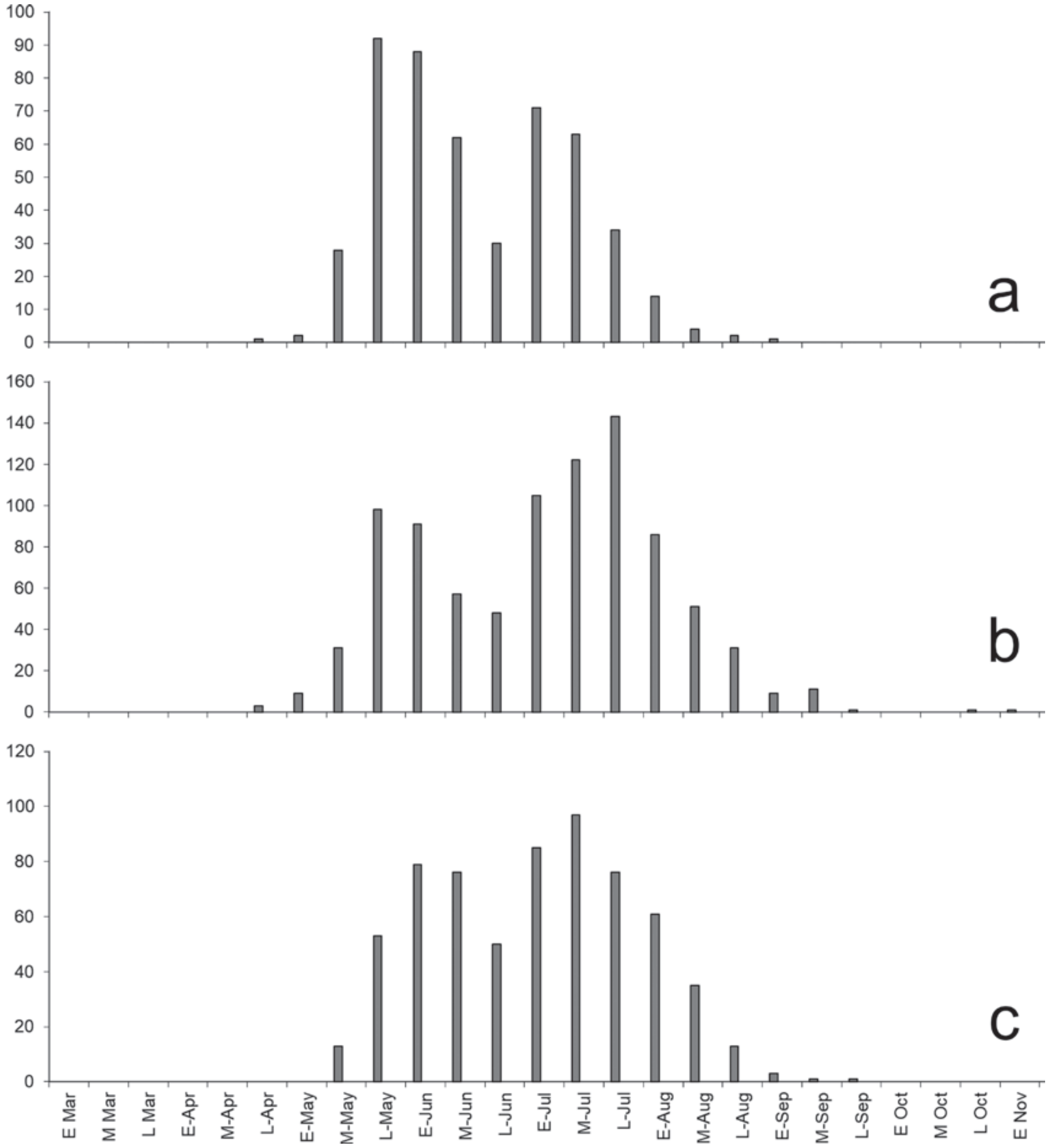

Figure 2. Phenology of *Papilio glaucus* group species from three regions, based on combined observations for all species and grouped by 10-day intervals **a** eastern Ontario (Hastings Co., Frontenac Co.; Mcnaughton et al. 2020), with *P. canadensis* peaking in late May – early June and *P. solstitius* in early to mid-July **b** finger Lakes region, New York (iNaturalist), with a late May – early June peak of spring *P. glaucus* and a July – August peak of *P. solstitius* and summer *P. glaucus*; note later seasonal persistence and late-shifted peak resulting from summer *P. glaucus*, which is absent in eastern Ontario (2a) **c** Greater Toronto region, with a spring peak comprised of *P. canadensis* and spring brood *P. glaucus*, and a July peak of *P. solstitius*; summer brood (August) *P. glaucus* are very rare.

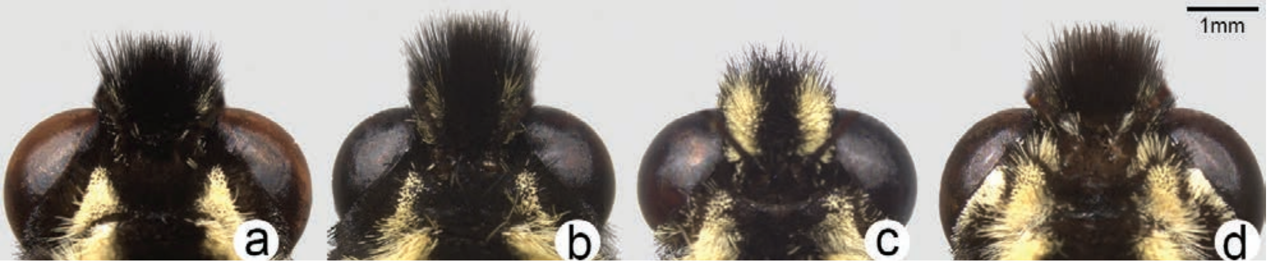

Figure 3. Dorsal view of head (antennae removed for clarity) comparing profile of frontal setae in **a** *P. solstitius* **b** *P. canadensis* **c** *P. glaucus* and **d** *P. appalachiensis*. Scale bar: 1 mm.

Figure 4. a dorsum of *Papilio solstitius*, male, holotype, ventrum on right. Long Swamp, Old Almonte Rd., Ottawa, Ontario, CAN. CNC voucher # CNCLEP00342771 **b** dorsum of *Papilio solstitius*, female allotype, ventrum on right. Vanalstine Lake, Frontenac Co., Ontario, CAN; ovipositing on *Prunus serotina*. Scale bar:10 mm.

and discussed in the “Comparative Morphology” section below will serve to identify most specimens.

Description of adult. Head (Fig. 3) and thorax: setation of frons of moderate length, intermediate between *P. canadensis* and *P. glaucus*; dorsum of

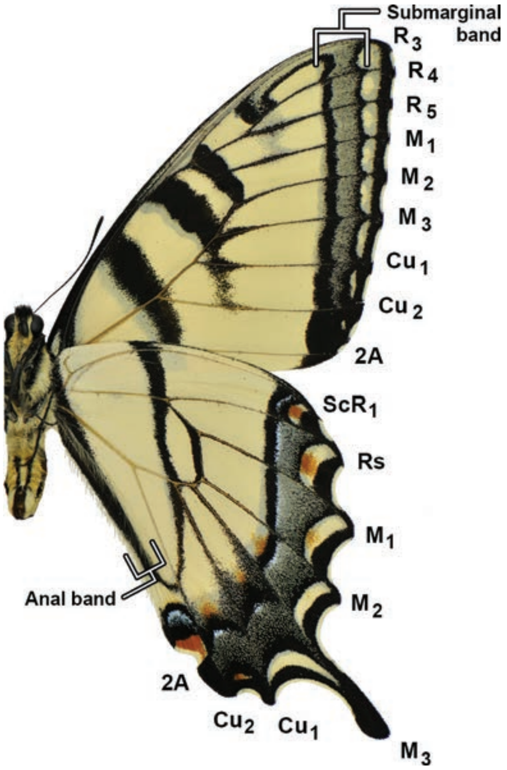

Figure 5. *Papilio solstitius*, ventrum, wing vein and pattern terminology.

head and thorax with limited sublateral yellow scaling; ventral thorax vestiture pale lemon yellow, legs black. Forewing (Figs 4, 5, 6): Male forewing length 50.7 mm (46.7–55.0 mm; *n* = 17), female 53.4 mm (47.7–57.0 mm; *n* = 8); dorsal ground color of male mustard yellow (Ridgway 1912), of female light orange yellow (Ridgway 1912), like that of *P. glaucus* but slightly richer in tone than *P. canadensis*; female mimetic dark phase absent; all pattern elements flat black; antemedial band an elongate wedge variable in thickness and edge, on average attenuating more strongly between Cu and anal margin than in *P. canadensis*; medial band an irregular rectangular bar across discal cell, variably extending as far as vein Cu$_2$ or slightly beyond (in *P. canadensis* the medial band is more extensive, more frequently extending past Cu$_2$ and sometimes to 2A); subapical black bar well-defined in cell R$_3$-R$_4$, diminishing across R$_5$-M$_1$, more strongly so than in *P. canadensis*; costa and subapical bar with diffuse yellow streaking, generally more so than in *P. canadensis*; females with wider, more diffuse transverse black bands than males; marginal band solid black with 6–8 yellow rounded-ovoid submarginal spots in interspaces; pattern elements repeated on ventral forewing, but ground color paler yellow, and black elements of distal half of wing with a flush of yellow scales; submarginal band variable but comprised of essentially D-shaped yellow spots usually separated by black lines along veins; yellow spots wider and more confluent than in *P. glaucus*, but more discrete and irregular than the essentially continuous, even-bordered band of *P. canadensis*. Hindwing: (Figs 4, 5, 7): Like *P. glaucus*, the scalloping of the hindwing outer margin is more pronounced than in *P. canadensis*, as a result of the disc margins oriented closer to the perpendicular of the long axis of the hindwing; the tail and Cu$_2$ angle are slightly more lunate/lobate than in *P. canadensis*; ground color identical to that of forewing; inner margin bordered

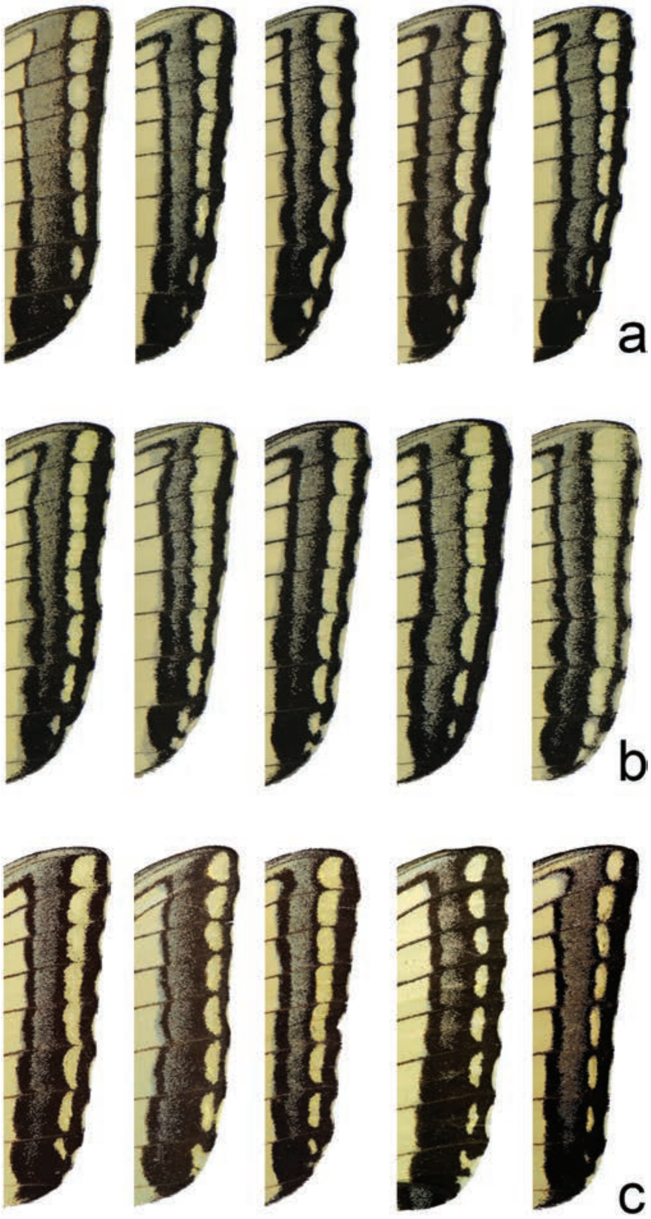

Figure 6. Comparison of variation in ventral forewing submarginal band in **a** *P. solstitius* **b** *P. canadensis* and **c** *P. glaucus*.

in black across 35–50% of cell 2A-Cu_2; narrow, straight medial line attenuating towards juncture with anal band near Cu_2; end of discal cell veins black-scaled; black marginal band extending along distal quarter of wing, with diffuse yellow dusting from vein M_2 to anal angle; yellow submarginal lunules in the four cell spaces between Rs and Cu1; lunules of cell ScR_1-Rs and Cu_2-Cu_1 (i.e., the uppermost and lowermost lunules) reduced or absent, orange or orange and yellow when present; anal angle with orange crescent capped proximally with blue, black bordered crescent; males with diffuse blue crescent in cell Cu_1-Cu_2, often faint, rarely traces of blue crescent in adjacent cell Cu_1-M_3; females with more extensive blue scaling, often with diffuse crescents extending to costal edge of submarginal band; ventral hindwing paler than dorsum, and with dusting of yellow scales across marginal band, and with more prevalent orange scaling in submarginal lunules and basad of marginal band in cells M_3-2A; yellow setae

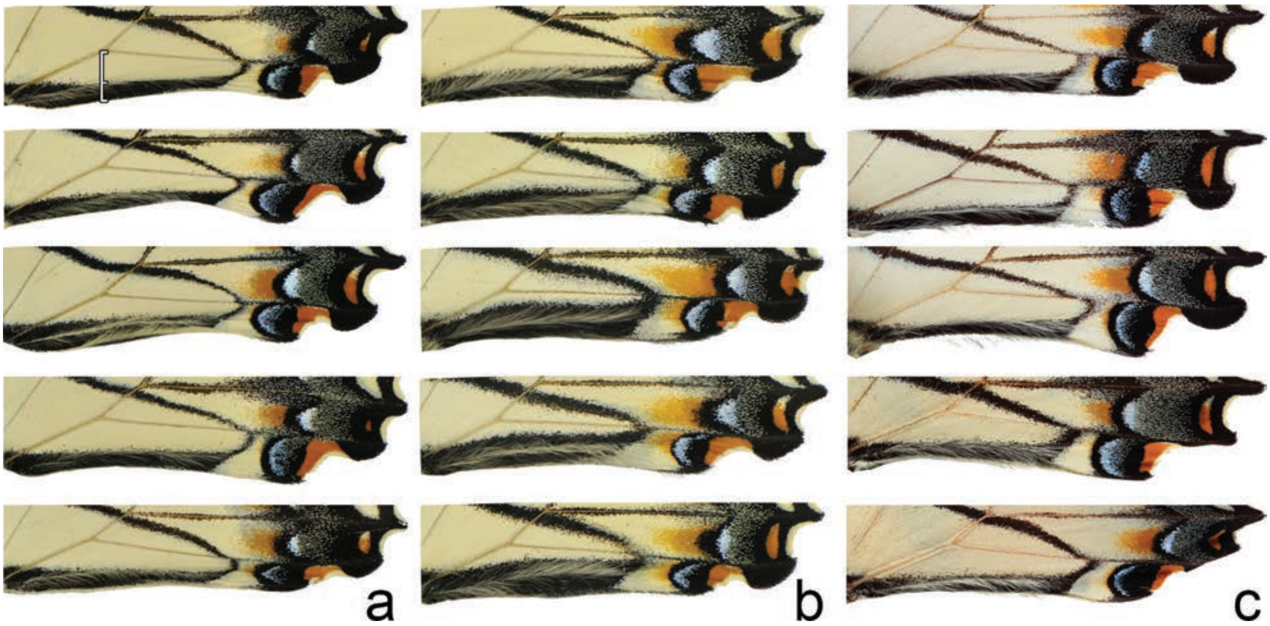

Figure 7. Comparison of variation in ventral hindwing anal band in **a** *P. solstitius* and **b** *P. canadensis* and **c** *P. glaucus*.

along anal band shorter and sparser than in *P*. *canadensis*. Abdomen: dorsum black, pale yellow laterally and ventrally with black sublateral line; vestiture of mixed yellow and black fine, setae; scales of male clasper entirely yellow (Fig. 8); clasper of male valve with two dorsal tines (Fig. 9).

Description of larva. First instar (Fig. 10) with well-developed white medial saddle, comprised of predominantly white dorsal pigmentation of segments A3-A4; three additional, variably developed white bands, one each comprised of T1 and T3, and a posterior band formed by A8; Anterior and posterior bands rarely absent (entirely brown pigmentation); mature larva (Fig. 11) indistinguishable from that of *P. glaucus* and *P. canadensis*.

Comparative morphology of the *Papilio glaucus*-complex

Adult morphology of all eastern North American species in the *glaucus*-complex can be deceivingly similar, and any single morphological character should not be relied upon for identification. Most similar to *P*. *solstitius* are *P*. *glaucus*, *P. canadensis* and potentially *P*. *bjorkae*, another new species in the *glaucus*-complex proposed in 2024 (Pavulaan 2024). Given its recency, the taxonomic status of *P. bjorkae* has not yet been scrutinized by the scientific community, but it is necessary to do so here. For the reasons detailed below the recognition and diagnosis of *P*. *bjorkae* is currently problematic, although based on the spring flight period and comparison of the figures in the original description (Pavulaan 2024), it is certain the name does not apply to MST.

The justification for treating *P*. *bjorkae* as a distinct species hinges on recognition of three distinct, partially sympatric, spring-flying taxa, recognized by adult phenotypes (*P*. *glaucus*, *P*. "near *canadensis*," *P*. *bjorkae*) which correlate with slightly different flight periods (Pavulaan 2024). No diagnostic differences in immature stages, biology, larval hosts, or molecular markers of *P*. *bjorkae* have been documented to date (Pavulaan 2024), nor is there evidence in previous research that might hint at the existence of such (e.g., Ording et al. 2010;

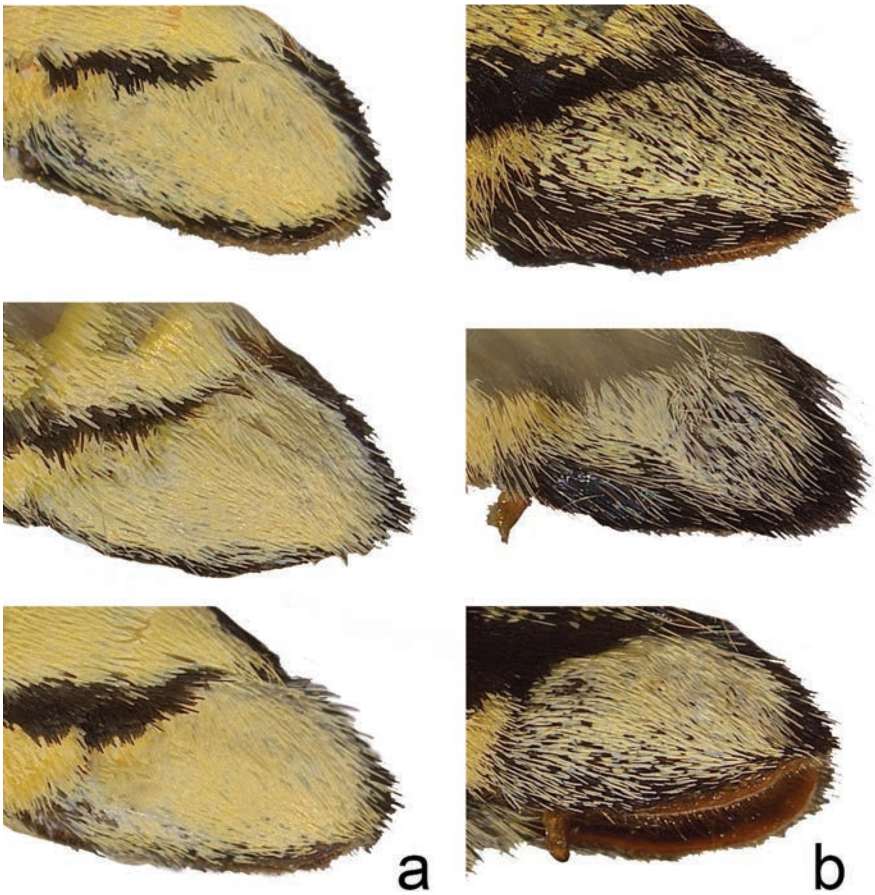

Figure 8. Comparison of scale coloration of male valve in **a** *P. solstitius* and **b** *P. canadensis*. Clasper color in *P. glaucus* (not shown) is identical to *P. solstitius*

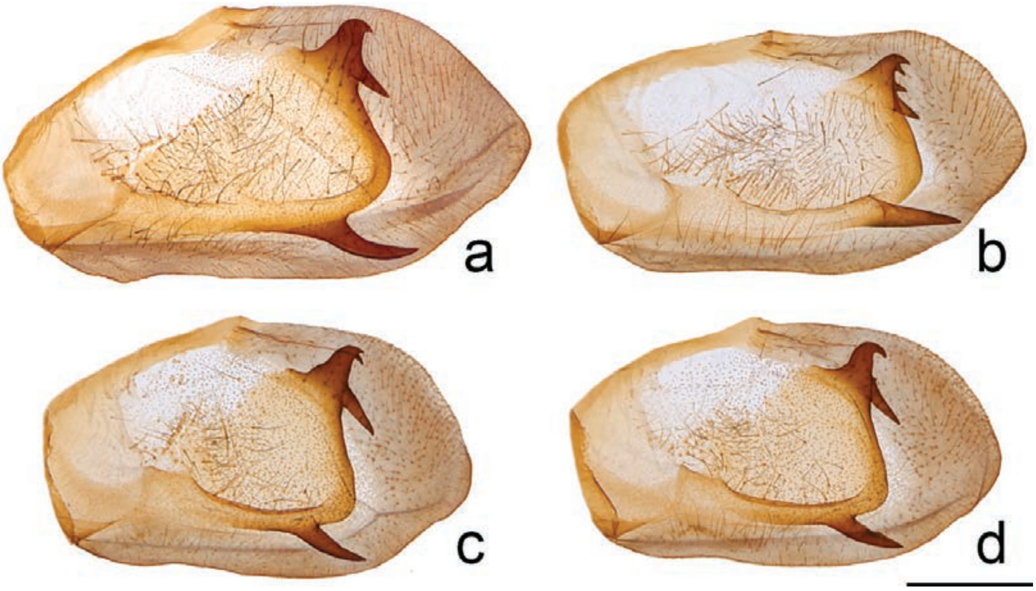

Figure 9. Inner surface of male right valve of **a** *P. solstitius* **b** *P. glaucus* **c, d** *P. canadensis* **c** and **d** show variation in dorsal clasper tines from the same individual (image of left valve (**d**) is flipped for ease of comparison).

Kunte et al. 2011). Using seasonal adult abundance peaks combined across the *glaucus*-complex, flight phenologies for taxa present within the range of *P. bjorkae* are attributed to spring (*P. glaucus*, *P. canadensis*, and *P. bjorkae*), summer (midsummer swallowtail), and late summer (second-generation *P*. *glaucus*) (Pavulaan 2024: figs 3–5). During spring (May through June), *P*. *bjorkae* flies in "late spring," versus "early spring" for *P*. *glaucus* and *P*. *canadensis*. However, only a single spring abundance peak is evident and attributed to *P*. *bjorkae*, whereas neither *P*. *glaucus* nor *P*. *canadensis* peaks are distinguishable due to the relative scarcity of observations for these species (Pavulaan 2024: 7, figs 3, 4). No additional data are provided to define late- versus early spring, leaving it unclear to what extent the phenology of *P*. *bjorkae* differs. Life history data that could corroborate such a difference are currently lacking.

The differential diagnosis of *P*. *bjorkae* is based largely on differences in wing pattern and shape, especially of the female (Table 1). Males are described as intermediate between *P*. *glaucus* and *P*. *canadensis*; comparative differences are given compared to *P*. *appalachiensis* and *P*. *canadensis*, but not *P*. *glaucus* (Pavulaan 2024: 16). Without an indication of sample size and a full description of male and female morphology, it is currently difficult to gauge intra- versus interspecific variation. Lastly, *P. bjorkae* is stated to be larger than spring *P*. *glaucus* and *P*. *canadensis*, but conflicting information on p. 9 states that *P*. *glaucus* is the largest species in the study region. No size measurements specific to male or female are given for *P*. *bjorkae* (including the holotype), nor is it possible to infer size of specimens from figures since scale bars are not given; size as a diagnostic trait for *P*. *bjorkae* therefore remains undefined.

The adult phenotype of *P. bjorkae* is very similar to that of *P*. *canadensis* and *P*. *glaucus*, so attributing phenotypic variation to three different putative taxa requires careful assessment. A potential additional source of phenotypic variation which remains unstudied stems from seasonal polymorphism in *P. glaucus*. Contrary to the assumption that *P*. *glaucus* is obligately bivoltine at the northern range edge (Pavulaan 2024), Ryan et al. (2016) demonstrate that it can be uni- or bivoltine depending on thermal constraints. In other words, temperature and day length experienced during the larval stage of *P*. *glaucus* dictate whether or not pupae develop directly into second generation adults, or enter winter diapause to emerge the following spring (Ryan et al. 2016). Since adult phenotype of *P. glaucus* is influenced by different temperature-photoperiod profiles (different spring and summer forms are well-known in *P*. *glaucus*, e.g., Pavulaan and Wright 2002), populations that comprise uni- and bivoltine cohorts would be expected to exhibit bimodal spring phenotypes (i.e., those developed from previous year's spring versus summer adults). If proven, phenotypic variation driven by facultative voltinism in *P.*

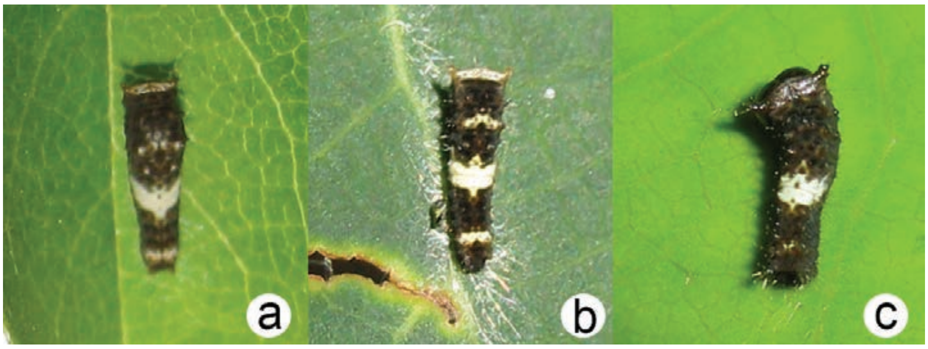

Figure 10. First instar of **a** *P. solstitius* **b** *P. canadensis* and **c** *P. glaucus*

Figure 11. Mature larva of *P. solstitius* on hop-tree (*Ptelea trifoliata*), Ottawa, Ontario, CAN (H. Goulet, photograph).

glaucus could account for the perception of phenotypes that are unaccounted for with existing taxonomy.

It is evident that the descriptive and diagnostic information defining *P*. *bjorkae* is currently incomplete and partially contradictory, and corroborating evidence for its distinctness as a species, outside of adult morphology, is lacking. This renders the recognition of *P*. *bjorkae* as a valid species tenuous at best. To spur further inquiry and study, we nevertheless include the known comparative phenotypic traits in Table 1.

Despite the overall similarity of *P. solstitius* to *P. glaucus*, we have found that it is possible to confidently identify the vast majority of individuals when multiple diagnostic traits are assessed. *Papilio solstitius* is most similar to the northernmost populations of spring generation *P*. *glaucus*, and some specimens are not distinguishable based on wing pattern alone. *Papilio solstitius* differs from *P*. *glaucus* in smaller overall size, greater tendency for the ventral forewing submarginal band to be band-like (broken into rounded crescents interrupted by black veins in typical *P*. *glaucus*); less scalloped outer border of the ventral hindwing submarginal band, and the absence of dark phase females (present in both *P. glaucus* and *P. appalachiensis*). The forewing outer margin is less frequently concave than in *P*. *glaucus*. Variation in these wing pattern traits often overlap with those of *P*. *glaucus*, and specimen identification requires consideration of seasonal timing and location. In *P. solstitius*, the tuft of setae projecting from the frons is much more prominent than in summer generation *P. glaucus*, where it is greatly reduced (Fig. 4); spring generation *P. glaucus* have similar setation to that of *P. solstitius*. The spring generation of *P. glaucus* can have some *P. canadensis*-like traits (Scriber 1990) that make it more difficult to differentiate from *P. solstitius* based on adult morphology alone. However, throughout much of the range of *P*. *solstitius*, there is no overlap with the more southern *P*. *glaucus*. Male genitalic structure is generally regarded as being homogenous among the *glaucus*-complex (Brower 1959; Hagen et al. 1991), but our limited sample suggests that there may be quantitative differences in the number of dorsal tines on the clasper, with *P*. *canadensis* and *P*. *solstitius* ranging from one to two spines and *P*. *glaucus* from one to three (Fig. 9).

Compared to sympatric *P. canadensis* populations, *P*. *solstitius* can usually be separated with confidence. It is larger with less extensive black markings, most consistently so in the narrower black border of the hindwing anal margin (Fig. 7; Table 1). The narrower margin also results in the large black V (formed by the medial line bridging to the distal part of the anal margin) appearing more U-shaped, versus more sharply V-shaped in *canadensis* (Fig. 7). The ground color is a slightly richer yellow tone. The body vestiture and color differ significantly between the two: the setation of *P. solstitius* is more sparse and shorter, particularly evident on the frons (Fig. 3), the dorsal thorax, and along vein 2A through the black anal margin band of the ventral hindwing (Fig. 7). The head and dorsal thorax are brighter yellow, as is the abdomen. The abdominal subdorsal yellow band is also wider, the male clasper is solid yellow, not interspersed with grey-black scales as in *P. canadensis* (Fig. 8).

Best observed on the underside of the hindwings, the anal margin black band relative to the width of the entire cell containing the band is approximately 10–40% wide in *P. glaucus* and 55–90% wide in *P. canadensis* (Scriber and Ording 2005). The band width averages greater in females than males, but the relative difference between species persists. In *P. solstitius*, this width ranges between approximately 30–55%. Also, on the underside of the hindwings, the lateral interface separating the basal yellow from the black submarginal region is typically somewhat straight in *P. canadensis* (though a common exception being in cell Rs-M_1 where the line can be bowed inward), noticeably scalloped in *P. glaucus*, with *P. solstitius* demonstrating intermediacy. The hindwing underside submarginal lunules tend toward those of *P. canadensis* in being more rectangular than crescentic.

Comparison of the larval morphology indicates that the color pattern of the first instar is diagnostic for *P*. *glaucus* and *P*. *canadensis* (Hagen et al. 1991; Scriber 1998). *Papilio solstitius* differs from *P. glaucus* and *P. canadensis* in the white dorsal banding pattern (Fig. 10). The prominent white medial saddle, comprised mostly of segments A3-A4, is present in all species. In *P. canadensis*, there are three additional, smaller white bands: two anterior bands formed by white pigmentation on T1 and T3, and a posterior band formed by A8. This banding pattern, with additional anterior-posterior (AP) bands, is consistent in *P. canadensis*. In *P*. *glaucus*, only the A3-A4 medial saddle is present, and AP bands are absent, the pigmentation on T1, T3, and A8 being dark brown. *Papilio solstitius* shows intermediacy and variability in the development of the AP bands. Typically, the AP bands are not as prominently white as in *P. canadensis*, but not completely brown as in *P*. *glaucus*. Development of the AP patterns varies and can be absent (*glaucus*-like) or highly developed (*canadensis*-like), although such variants are rare (< 10% of individuals reared). However, *canadensis*-like larvae never express the same intensity of white pigmentation as that species, although dark variants are essentially undistinguishable from *P*. *glaucus*. Examples of *glaucus*-like first instars are limited to one field-collection event on a single ash sapling (Kingston, 22.Jul.2023), where five of nine larvae were *glaucus*-like. Clearly, further study of larval variation is needed.

Larval host plants

In the southern range parts, *Papilio solstitius* seems to prefer ovipositing on tulip tree (*Liriodendron tulipifera* L.) and hoptree (*Ptelea trifoliata* L.), like *P. glaucus*. Larvae can occur regularly on hoptree where it is planted as an ornamental shrub outside of the natural range (Fig. 12). North of the native ranges of both of these plants (approximately north and east of the region of Toronto, Ontario), *P. solstitius* feeds on *Fraxinus pennsylvanica* and *Prunus serotina*, based on wild-collected ova and larvae and observation of oviposition (Fig. 4b). Larvae demonstrate high survival rates on tulip tree, unlike *P. canadensis*, and also demonstrate survival on quaking aspen (*Populus tremuloides* Michaux), unlike *P. glaucus*, but at a rate lower than that of *P. canadensis* (Mercader et al. 2009).

Diapause and phenology

Papilio solstitius exhibits delayed post-diapause pupal development, producing a single summer flight. In Ontario, the flight period commences in late June to early July, peaking in the first half of July (Fig. 2a). Studies on the effect of temperature on pupal development show a similar phenology in New York (Ording et al. 2010). Rearing field-collected ova and larvae from the Kingston region of Ontario further confirm that *P. solstitius* is univoltine with obligate diapause like *P. canadensis*, differing from *P. glaucus* which is facultatively multivoltine (Scriber 2013). Notably, some lab reared pupae overwintered twice, not eclosing until the second year.

Pupae removed from cold storage to a constant temperature of ~23 °C eclosed after 30.4 +/- 5.5 days (male and female combined), or an average of 699 degree-days (DD). *Papilio canadensis* pupae emerged 19.4 +/- 4.2 days ($p < 0.0001$), or 446 DD, under the same conditions. In eastern Ontario, accumulated degree-days (above a minimum threshold of 6 °C) for these values corre-

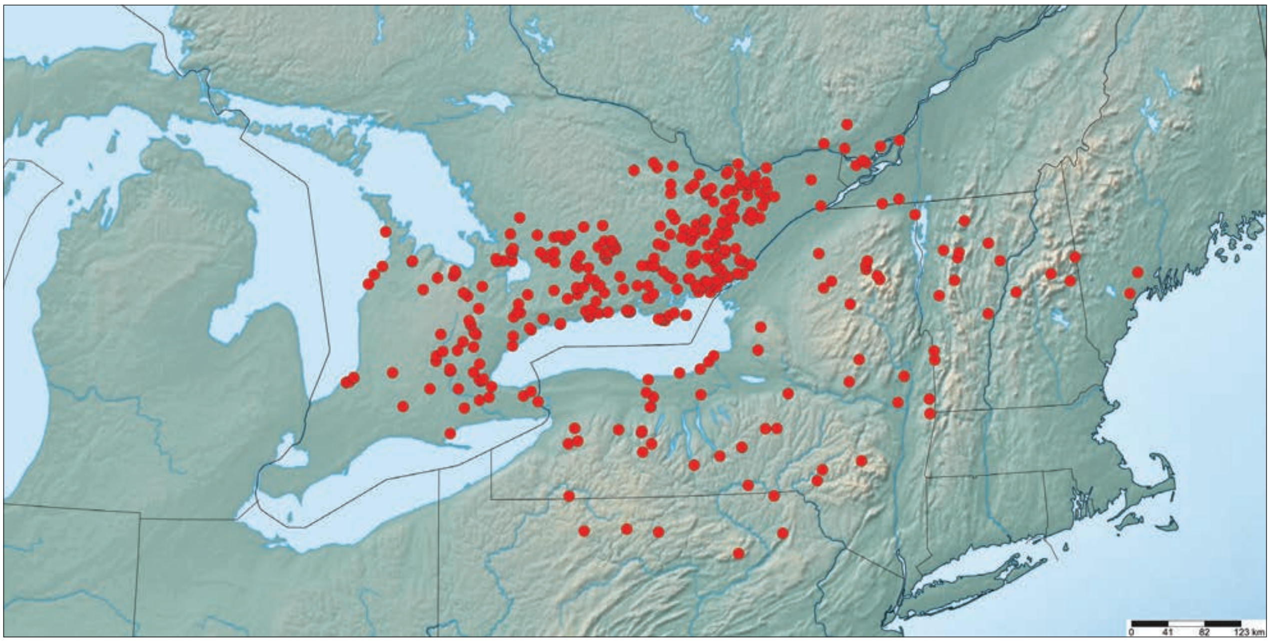

Figure 12. Distribution of examined specimens of *P. solstitius* (voucher data in Suppl. material 1).

spond to the second week of June (446 DD) and the first week of July (699 DD) (Schmidt and Layberry 2016), precisely when peak emergences of *P*. *canadensis* and *P*. *solstitius* are occurring (Fig. 2a). Difference in post-diapause pupal emergence therefore perfectly accounts for the staggered emergence peaks between *P. canadensis* and *P. solstitius* in eastern Ontario. Male and female *P. solstitius* differ in the length of post-diapause development delay. On average, males required approximately 26.6 +/- 3.2 days to eclose compared with 34.2 +/- 4.2 days for females (p = 0.02; *n* = 10; two-tailed T-test). In the wild, this would be expected to translate to a difference in peak flight times between the sexes of approximately 15 days, which matches well with field observations (Fig. 2).

Bivoltine *P. glaucus* populations occur primarily to the south of the range of *P. solstitius*. However, *P*. *glaucus* is facultatively univoltine or bivoltine at the northern range periphery, contrary to the initial hypothesis that it is unable to switch to univoltinism and limited to regions where it can undergo two annual generations (Hagen et al. 1991). In Ohio and Michigan populations, pupae are induced to enter winter diapause when 4th-5th instars experience photoperiods of less than 14 hours (Ryan et al. 2017). Facultative uni- vs. bivoltinism is also demonstrated by our rearing results from the Hamilton, Ontario region, which is north of the bivoltine thermal threshold (Scriber 2013). Lab-reared larvae of spring *P. glaucus* on *L*. *tulipifera* developed directly into a second generation of adults, despite the rarity of naturally occurring second-flight *P. glaucus* here. Univoltine *P. glaucus* populations probably occur more widely than previously recognized and have added to the complexity of defining the taxa involved in the *glaucus*-complex. Indeed, this could explain the perception of two spring-flying phenotypes (Pavulaan 2024) in regions where both uni- and bivoltine *P. glaucus* occur: offspring developing from either spring-flight (univoltine) or summer-flight (bivoltine) parents experience differing temperature-photoperiod profiles as larvae (known to influence adult phenotype), but both cohorts emerge the following spring. In southern Ontario and the Finger Lakes region of New York, the presence of both spring and summer *P*. *glaucus* likely accounts for a longer spring abundance peak and a more protracted late summer abundance peak (Fig. 2a, c; see also Schmidt 2020: fig. 7).

Habitat and distribution

Since *Papilio solstitius*, like its congeners, uses a range of unrelated host plants, it has a similarly broad habitat tolerance for a range of forest, forest edge and woodland habitats. Although habitats of *P. solstitius* and *P. canadensis* overlap widely, the former reaches its highest abundance in or near mesic or moist woodlands, particularly ash-dominated swamps, where ash is common. Conversely, *P. canadensis* is most common in drier upland habitats where trembling aspen is common.

The core range of *Papilio solstitius* includes eastern and southcentral Ontario, northern and central New York and adjacent Vermont, New Hampshire, and Pennsylvania (Fig. 12), encompassing a minimum land area of approximately 174 000 km^2 (by comparison, the range extent of *P*. *appalachiensis* is ~ 140,000 km^2). In New York, *P. solstitius* inhabits most of the state except the southeast and greater New York City area. In Canada, *P. solstitius* extends from the Montréal, Québec region west to the Bruce Peninsula of Ontario, south to the Niagara region (Fig. 12; Wang 2018; Schmidt 2020; Macnaughton et al. 2020). The western limit appears to be the eastern shores of Lake Huron; we have not seen any verifiable specimens west of there. The *glaucus*-complex has received considerable study in the lower peninsula of Michigan and in Wisconsin, and there is no evidence of delayed flight (July) swallowtails there (Luebke et al. 1988; Stump et al. 2003).

The northern range limit of *P. solstitius* is easily defined since adult morphology and phenology differ considerably from *P. canadensis*. Furthermore, the range limit is climatically constrained since *P. solstitius* larval development is shifted about a month later than *P. canadensis*, and development must be completed before autumnal leaf abscission and frost. The current northern limit is the southern edge of the Algonquin Dome, the lower Ottawa River valley, and the southern edge of the Gatineau/Laurentide escarpment as far east as the Montréal region.

Papilio solstitius has undergone a northward range expansion of several hundred kilometers since the 1970s (Schmidt 2020), as has *P*. *glaucus* elsewhere (Scriber et al. 2014). In 2022, *P. solstitius* was recorded for the first time near Montebello, Québec. Continuous monitoring at this location since 1994 indicates that *P. solstitius* was not present prior to 2022 (P. Legault, pers. comm). Based on the climatic zones given in Scriber et al. (2014), the distribution of *P*. *solstitius* approximates the 1300–1400 degree-day (°C) climatic envelope. For context, the northern limit of bivoltine *P*. *glaucus* is ~1444 DD. The southern (warm) limit of *P. canadensis* appears to be slightly north of this, and is possibly limited by pupal mortality due to prolonged high summer temperatures (Kukal et al. 1991). The northern range limit of *Papilio solstitius* is likely determined by minimum thermal requirements, given the late seasonal phenology of a July flight period that dictates a shorter window for larval development before autumnal host plant senescence.

The southern range limits of *P. solstitius* are currently difficult to define owing to overlap and confusion with single- and double-brooded *P*. *glaucus*, and the uncertainty in the northern range limit of *P*. *glaucus*. Swallowtails that are morphologically consistent with *P. solstitius* and eclosing in the first half of July, when *P. glaucus* is between flights, extend south to approximately 41, 42°N to the eastern seaboard (Fig. 12). In Pennsylvania, the southern extent of *P. solstitius* coincides approximately with the northern limit of *P. glaucus* containing dark morph females (Scriber 1996), extending from Erie to just north of Pittsburgh and east to New York City. It may also extend to the Atlantic coast through Connecticut and Rhode Island based on the phenology information in Pavulaan (2024), but this warrants further study.

The occurrence of *P*. *canadensis* at the southern range edge, near that of *P. solstitius*, may be more limited than depicted in some range maps (e.g., Pavulaan and Wright 2002; Cech and Tudor 2005; Monroe and Wright 2017). Our examination of putative *P. canadensis* photos from New York and Pennsylvania indicate that most are spring flight *P. glaucus*; CJD has been unable to verify the presence of typical *P*. *canadensis* in New York state south of the Adirondacks. It is possible and indeed expected that *P*. *canadensis* is undergoing a northward range contraction with warming climates (Scriber 2013), but this remains unexamined. In the Finger Lakes region of New York, members of the *glaucus*-complex can be observed continuously from mid-May to early September (Fig. 2b). In this region, a pale *canadensis*-like phenotype emerges first, followed by a tiger swallowtail in late May which has historically been referred to as "spring form" *P. glaucus*, and then finally *P. solstitius* in late June to July, and possibly a partial second flight of *P*. *glaucus* in August (although not all taxa are sympatric everywhere).

Phylogenetic analyses

Both regions of COI recover the same general relationships between members of the *P*. *glaucus* group, including *P. multicaudata* Kirby, 1884, *P. eurymedon* Lucas, 1852, *P. rutulus* Lucas, 1852, and the *glaucus*-complex clade of *P. glaucus*, *P. canadensis*, and hybrid taxa (*P. appalachiensis*, *P. solstitius*, etc.) (Figs 13, 14). Within the latter, *P. glaucus* and *P. canadensis* almost form reciprocally monophyletic clades in both COI5 and COI3, but in each gene, a handful of specimens fall in the opposing clade (marked with asterisks in Figs 13, 14), and *P. appalachiensis* falls throughout the *P. glaucus* clades in both genes. *Papilio solstitius* clusters within the *P. canadensis* clade, as does a handful of *P. glaucus*. Notably, there are few nodes with strong branch support within this clade of *P. glaucus*/*P. canadensis*/*P. appalachiensis*/*P*. *solstitius*, indicating close genetic similarity between all of these entities in their mitochondrial genomes. Excluding specimens with missing data in the 5' or 3' ends of their sequences, pairwise sequence identity for haplotypes in this *P. glaucus*/*P. canadensis* clade were > 98% for COI3 and > 97.5% for COI5.

We re-evaluated identification of specimens sequenced in Vernygora et al. (2022) and conclude that specimens noted as "intermediate" therein are mostly *P. glaucus*, but one is *P. solstitius* (samples annotated with asterisks in Fig. 15). In their SNP-based phylogeny (remade in Fig. 15), these specimens form a paraphyletic grade between typical (and more geographically distant) *P. canadensis* and *P. glaucus*; *Papilio appalachiensis* also falls out in this grade, and as with COI, only a handful of nodes within this broad clade were strongly supported and many of these specimens appeared admixed in Vernygora et al.'s population genetics-oriented analyses.

Discussion

Comparison of physiological and morphological traits of the *P. glaucus*-complex taxa in the eastern Great Lakes – northern Appalachian region reveals that the midsummer tiger swallowtail, *Papilio solstitius* sp. nov., is a distinct, locally common species rather than occasional F1 hybrid individuals between *P*. *glaucus* × *canadensis*. It is geographically widespread over thousands of square kilometers outside of established hybrid zones and is allochronically isolated from its sibling species. Nevertheless, the evolutionary origin of *P*. *solstitius* through hybridization between *P*. *glaucus* and *P*. *canadensis* is likely, as is continued hybridization between the three.

How has a large, conspicuous swallowtail butterfly gone unrecognized in a well-studied region of North America for so long? In hindsight, an earlier study of two univoltine tiger swallowtail populations near Ithaca, NY established the existence of a taxon that was clearly not attributable to either *P. glaucus* or *P. canadensis*, although both entities were referred to as *P. glaucus* (Hagen and

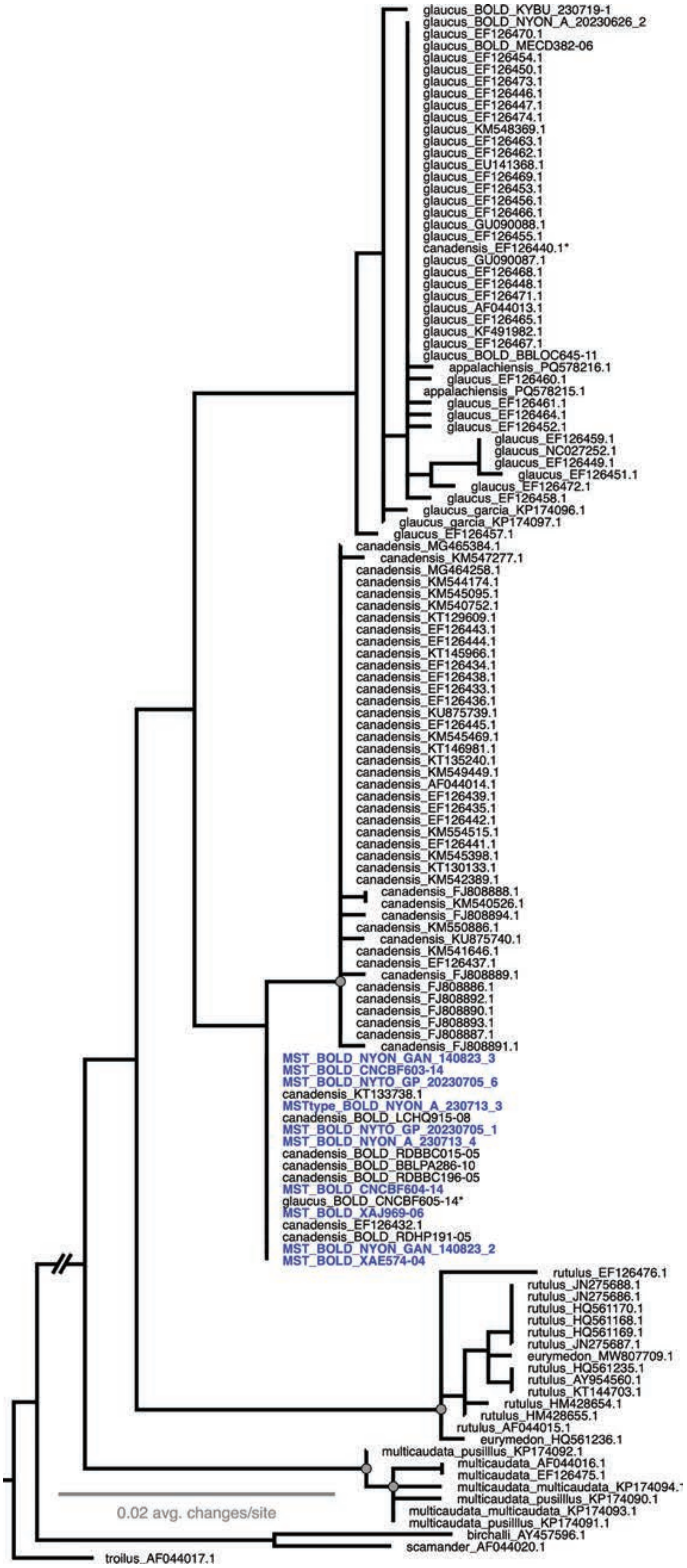

Figure 13. Maximum likelihood tree for COI5. Specimens are labeled with a species epithet determination and NCBI or BOLD accession numbers. *Papilio solstitius* samples indicated in blue as "MST." Specimens with asterisks indicate those that fell outside of their typical respective clade. Grey circles indicate strong node support (> 0.95 ufBS and > 0.8 SH-aL-RT). All outgroup branch lengths have been edited for space.

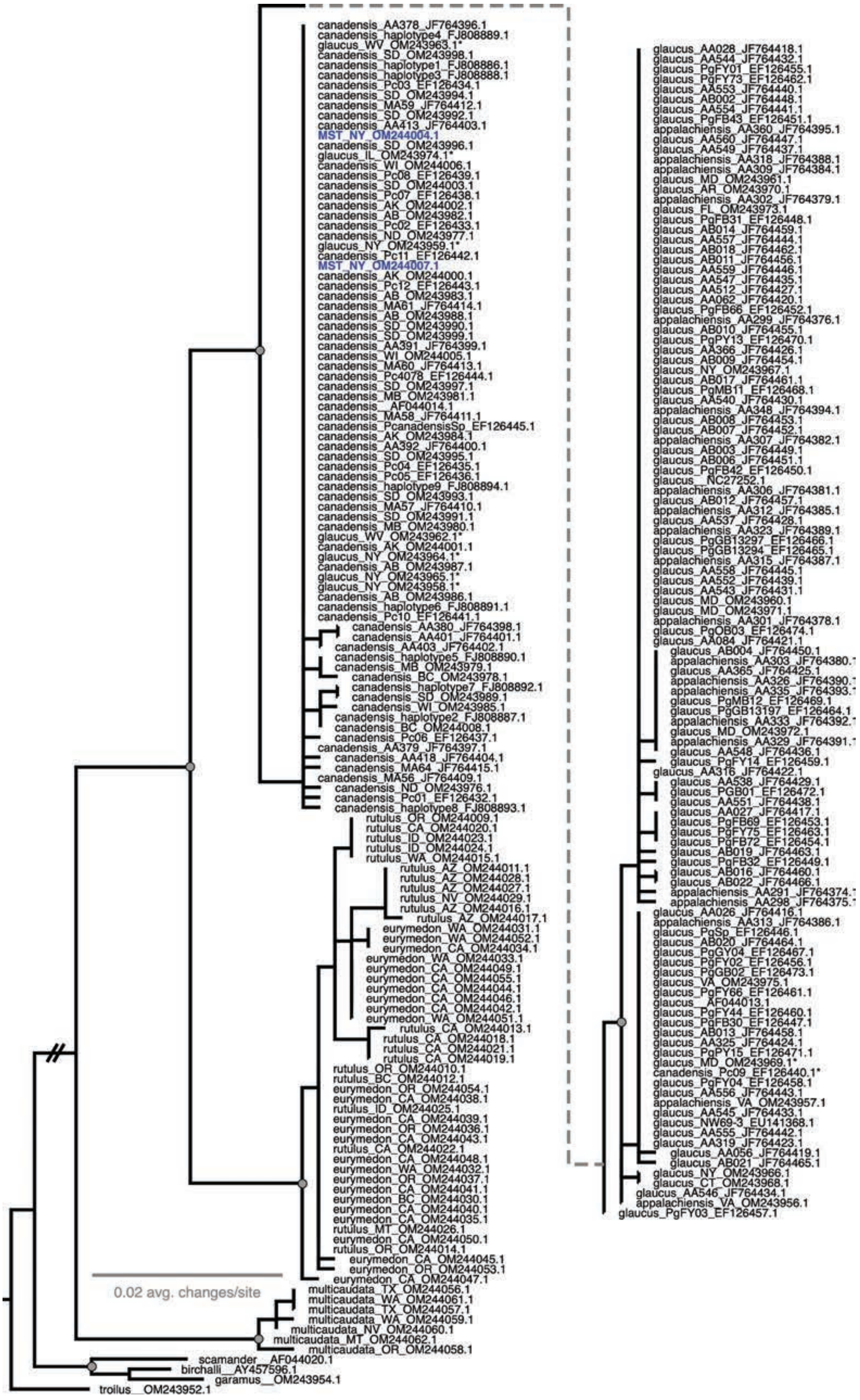

Figure 14. Maximum likelihood tree for COI3. Specimens are labeled with a species epithet determination, state/province, or additional unique identifier, and NCBI accession numbers. *Papilio solstitius* samples indicated in blue as "MST." Specimens with asterisks indicate those that fell outside of their typical respective clade. Grey circles indicate strong node support (> 0.95 ufBS and > 0.8 SH-aLRT). All outgroup branch lengths have been edited for space and dotted grey line is a visual link between independently shown parts of the tree.

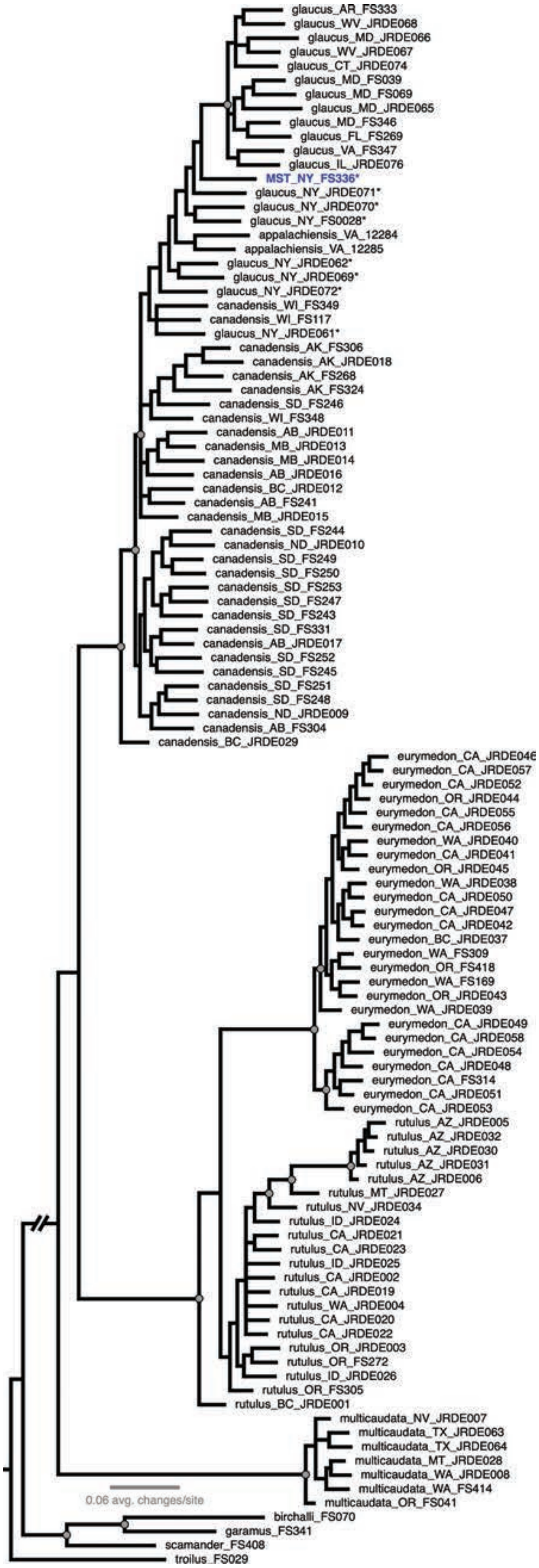

Figure 15. Majority rule consensus tree generated from 3,733 SNPs from Vernygora et al. (2022). Specimens are labeled with a species epithet determination, state/province, and unique identifier, and specimens with asterisks indicate those called "intermediates" in the original publication, including one we identify now as *P. solstitius* ("MST" in blue). Grey circles indicate strong node support (> 0.9 posterior probability support). All outgroup branch lengths have been edited for space.

Lederhouse 1985). *Papilio canadensis* was subsequently recognized as a distinct species (Hagen et al. 1991), but the late-flight tiger swallowtails remained a taxonomic enigma and were attributed to a hybrid zone phenomenon (Scriber 1990; Ording et al. 2010; Kunte et al. 2011). *Papilio solstitius* was documented as early as the 1970s in upstate New York (Hagen and Lederhouse 1985) and eastern Ontario (CNC specimens). However, the earliest literature reference to *P. solstitius* that we could find dates to the mid-1800s from southcentral Ontario. Saunders (1874) noted: "[The tiger swallowtail] appears first on the wing from the middle to the latter end of May, but becomes much more plentiful in July. Whether these July insects are a second brood, or whether the bulk of the chrysalids which have wintered do not mature until about this time we are unable to determine." As it were, it was not until 1984 that it was proven that the July swallowtails are in fact not a second generation (Hagen and Lederhouse 1985). At the time located near London, Ontario, Saunders' observations are now easily explained by what would have been either May-flying *P. canadensis* or *P. glaucus* (likely the latter based on current ranges), and *P. solstitius* with its unique July flight time.

Although *P. solstitius* exhibits a mosaic of characters of both *P. glaucus* and *P. canadensis* (Table 1) which might suggest that it is a hybrid, it differs from artificial hybrids in several significant ways (Table 2). Based on the novel detection of late-emerging populations in western Vermont, Ording et al. (2010) suggested *Papilio solstitius* to be of very recent hybrid origin mediated by climatic amelioration. The historic documentation and large geographic range, much of it beyond the contact zone between *P. glaucus* and *P. canadensis*, counter this hypothesis. Notably, the delayed pupal emergence with a single summer flight differs from lab hybrids which emerge in the spring (Ording et al. 2010). Our data for post-diapause pupal development of Ontario *P. solstitius* are comparable to values given by Ording et al. (2010) from Vermont

Table 2. Comparison of genetic and ecological traits among species of the *Papilio glaucus*-complex. Sourced from Kunte et al. (2011), Scriber and Ording (2005), and this paper. The recently described *P. bjorkae* is excluded because most traits remain undefined or unknown (see Introduction).

Trait	*P. glaucus*	*P. appalachiensis*	*P. solstitius* sp. nov.	*P. canadensis*	*F1* lab hybrid
Thermal habitat	warm	intermediate	intermediate	cool	na
Pupal diapause	facultative	obligatory	obligatory	obligatory	Z-linked
Voltinism	bivoltine	univoltine	univoltine	univoltine	photoperiod (Z)
Larval survival: aspen	low	high	high	high	high
Larval survival: tuliptree	high	high	high	low	high
Body size	large	large	intermediate	small	intermediate
Female polymorphism	mimetic	mimetic	non-mimetic	non-mimetic	W-linked
Pupal emergence	early	early	delayed	early	heterozygous (Z)
Flight season	early + late	early	mid	early	n.a.
mtDNA	*glaucus*-like	*glaucus*-like	*canadensis*-like	*canadensis*-like	maternal
Z: Kettin	*glaucus*	*canadensis*	*canadensis*	heterozygous	heterozygous (Z)
Z: TH	*glaucus*	*canadensis*	*canadensis*	*canadensis*	heterozygous (Z)
Z: Tpi	*glaucus*	*canadensis*	*canadensis*	*canadensis*	heterozygous (Z)
Z: Period	*glaucus*	*canadensis*	*canadensis*	*canadensis*	heterozygous (Z)
Z: PAH	*glaucus*	*canadensis*	*canadensis*	*canadensis*	heterozygous (Z)
LDH allozyme	100	80 / 40	80 / 40	80 / 40	heterozygous (Z)
LDH20 "hybrizyme"	-	+	+	-	n.a.
PGD allozyme	100 / 50	100 / 50	100/50 (40-50%)	125/80/150	heterozygous (Z)

populations: under controlled laboratory conditions, post-diapause pupae of *Papilio solstitius* and *P. canadensis* emerged after an average of 828 DD and 450 DD, respectively (Ording et al. 2010), versus our results for Ontario populations of both species at 690 DD and 437 DD. In eastern Ontario, the average peak flight period of *Papilio solstitius* is 11–20 July, compared to 1–10 June for *P. canadensis* (Fig. 2a). *Papilio solstitius* is distinct from artificial F1 hybrids and both parental species in this regard, which emerge in the spring (Ording et al. 2010). Importantly, this difference results in temporal reproductive isolation between *P. solstitius* and *P. canadensis*/*glaucus*. Within the *P. glaucus* group, delayed pupal emergence is unique to *P. solstitius*, and understanding the adaptive significance of this may provide key insights into its evolutionary history. Possibly it is a mechanism to escape pupal mortality due to summer heat, to which *P. canadensis* is susceptible (Kukal et al. 1991).

Hybridization between *P. glaucus* and *P. canadensis* has been well-documented using molecular and morphological evidence, and only some purported hybrid populations can be attributed to *Papilio solstitius*. The most extensively studied hybrid zone between *P. glaucus* and *P. canadensis* is a narrow geographic zone across Michigan's lower peninsula and into Wisconsin (Luebke et al. 1988; Hagen et al. 1991). Here, the hybrid zone is dictated by a narrow band of the thermal landscape that limits the occurrence of *P. canadensis* to the north and *P. glaucus* to the south. There is no evidence that *Papilio solstitius* occurs this far west. To the east, the biogeography of the *P. glaucus* group is more difficult to untangle, influenced by the complex topography of the northern Appalachians, Frontenac Arch, Alleghany Plateau, and Adirondack Mtns with the added complexity of Great Lakes weather effects. Unlike the region west of Lake Michigan, large gaps occur between the ranges of *P. glaucus* and *P. canadensis* here, but there is undoubtedly ongoing gene flow between *P. solstitius* and its sibling species and is fertile ground for future molecular study.

Some of the initial genetic work on the *glaucus*-complex included samples of *P. solstitius* and indicated different allele frequencies of alpha-galactosaminidase compared to *P. canadensis* (Hagen and Lederhouse 1985). *Papilio solstitius* also possesses a unique allozyme, LDH-20, not present in other *P. glaucus* group species (Scriber and Ording 2005). The presence of molecular traits unique to *P. solstitius* not known from either putative parent species cannot easily be explained by ongoing hybridization.

Considering recent genetic data together, it is clear that the standard barcoding gene, COI, is unable to confidently separate *P. solstitius* from *P. canadensis*. The handful of specimens falling outside their respective clades for COI may be indicative of geographic variation that has been historically unsampled/unsequenced, or more varied hybrid interactions between *P. glaucus* and *P. canadensis*. Ignoring these specimens that fall outside of their respective clades, *P. solstitius* clearly has more *P. canadensis* maternal influence, but its nuclear genome is less clear as our sampling is more limited and shows a paraphyletic grade in phylogenetic analyses (Fig. 15) and varied signals of admixture in the results of Vernygora et al. (2022). More comprehensive population genomic sampling will be required to tease apart the genetic situation of *P. solstitius*, *P. appalachiensis* (Cong et al. 2015), and the other hybrids/entities documented in this species group (Ryan et al.

2016, 2017, 2018; Pavulaan 2024). Although Scriber and Ording (2005) and Kunte et al. (2011) potentially addressed *P. solstitius* with other putative hybrids within the *P. glaucus* group, modern genomic methods should be used to properly characterize population-wide genetic variation throughout this broad geographic region and other hybrid entities within the *P. glaucus* group (Ryan et al. 2016).

Current evidence is consistent with the possibility that *P. solstitius* has a recombinant evolutionary origin similar to that of *P. appalachiensis*. However, most questions regarding the evolutionary origin of this taxon, and its role within the speciation of the *P*. *glaucus*-complex, remain to be answered. It is our hope that recognizing and defining the taxonomic identity of this unique evolutionary lineage provides a staging point in the fertile grounds for future research.

Acknowledgements

Whitney Carleton of New York State Office of Parks, Recreation and Preservation permitted study by CJD within NY state parks. Michael Galban, Historic Site Manager of Ganondagan State Historic Site Seneca Art & Culture Center, approved study on Haudenosaunee traditional lands. Dr. Mark Scriber provided insights resulting from his vast studies. Henri Goulet and Pierre Legault kindly provided new records and photographs of *P. solstitius*, and Christi Jaeger provided technical and field assistance. We also thank Rick Cavasin, Ross Layberry, Peter Hall, Ricky Patterson, and Alan McNaughton for providing feedback, discussion, additional data, and specimens that significantly aided the research presented here. Dr. Felix Sperling and an anonymous reviewer provided suggestions that improved the manuscript.

Additional information

Conflict of interest

The authors have declared that no competing interests exist.

Ethical statement

No ethical statement was reported.

Funding

No funding was reported.

Author contributions

All authors have contributed equally.

Author ORCIDs

B. Christian Schmidt https://orcid.org/0000-0003-4160-7629

Data availability

All of the data that support the findings of this study are available in the main text or Supplementary Information.

References

Brower LP (1959) Speciation in butterflies of the *Papilio glaucus* group. I. Morphological relationships and hybridization. Evolution 13(1): 40–63. https://doi.org/10.2307/2405944

Cech R, Tudor G (2005) Butterflies of the East Coast: an observer's guide. Princeton University Press, Princeton, New Jersey, 234 pp. https://doi.org/10.1515/9780691261164

Condamine FL, Allio R, Reboud EL, Dupuis JR, Toussaint EFA, Mazet N, Hu SJ, Lewis DS, Kunte K, Cotton AM, Sperling FAH (2023) A comprehensive phylogeny and revised taxonomy illuminate the origin and diversification of the global radiation of *Papilio* (Lepidoptera: Papilionidae). Molecular Phylogenetics and Evolution 183: 107758. https://doi.org/10.1016/j.ympev.2023.107758

Cong Q, Borek D, Otwinowski Z, Grishin NV (2015) Tiger swallowtail genome reveals mechanisms for speciation and caterpillar chemical defense. Cell Reports 10(6): 910–919. https://doi.org/10.1016/j.celrep.2015.01.026

Edgar RC (2004) MUSCLE: multiple sequence alignment with high accuracy and high throughput. Nucleic Acids Research 32(5): 1792–1797. https://doi.org/10.1093/nar/gkh340

Folmer O, Black M, Hoeh W, Lutz R, Vrijenhoek R (1994) DNA primers for amplification of mitochondrial cytochrome c oxidase subunit I from diverse metazoan invertebrates. Molecular Marine Biology and Biotechnology 3(5): 294–299.

Guindon S, Dufayard JF, Lefort V, Anisimova M, Hordijk W, Gascuel O (2010) New algorithms and methods to estimate maximum-likelihood phylogenies: assessing the performance of PhyML 3.0. Systematic Biology 59(3): 307–321. https://doi.org/10.1093/sysbio/syq010

Hagen RH, Lederhouse RC (1985) Polymodal emergence of the tiger swallowtail, *Papilio glaucus* (Lepidoptera: Papilionidae): source of a false second generation in central New York State. Ecological Entomology 10(1): 19–28. https://doi.org/10.1111/j.1365-2311.1985.tb00531.x

Hagen RH, Lederhouse RC, Bossart JL, Scriber JM (1991) *Papilio canadensis* and *P. glaucus* (Papilionidae) are distinct species. Journal of the Lepidopterists' Society 45(4): 245–258.

Hall PW, Jones C, Guidotti A, Hubley B (2014) The ROM field guide to butterflies of Ontario. Royal Ontario Museum, Toronto, Ontario, 488 pp.

Hebert PD, Cywinska A, Ball SL, deWaard JR (2003) Biological identifications through DNA barcodes. Proceedings of the Royal Society B: Biological Sciences 270(1512): 313–321. https://doi.org/10.1098/rspb.2002.2218

Hoang DT, Chernomor O, von Haeseler A, Minh BQ, Vinh LS (2018) UFBoot2: improving the ultrafast bootstrap approximation. Molecular Biology and Evolution 35(2): 518–522. https://doi.org/10.1093/molbev/msx281

Kalyaanamoorthy S, Minh BQ, Wong TKF, von Haeseler A, Jermiin LS (2017) ModelFinder: fast model selection for accurate phylogenetic estimates. Nature Methods 14(6): 587–589. https://doi.org/10.1038/nmeth.4285

Kukal O, Ayres MP, Scriber JM (1991) Cold tolerance of the pupae in relation to the distribution of swallowtail butterflies. Canadian Journal of Zoology 69(12): 3028–3037. https://doi.org/10.1139/z91-427

Kunte K, Shea C, Aardema ML, Scriber JM, Juenger TE, Gilbert LE, Kronforst MR (2011) Sex chromosome mosaicism and hybrid speciation among tiger swallowtail butterflies. PLOS Genetics 7(9): e1002274. https://doi.org/10.1371/journal.pgen.1002274

Larsson A (2014) AliView: a fast and lightweight alignment viewer and editor for large data sets. Bioinformatics 30(22): 3276–3278. https://doi.org/10.1093/bioinformatics/btu531

Layberry RA, Hall PW, Lafontaine JD (1998) The Butterflies of Canada. Toronto: University of Toronto Press, Toronto, Ontario, 354 pp. https://doi.org/10.3138/9781442623163

Linnaeus C (1758) Systema Naturae, 10th edn., Vol. 1, Stockholm, 824 pp.

Luebke HJ, Scriber JM, Yandell BS (1988) Use of multivariate discriminant analysis of male wing morphometrics to delineate a hybrid zone for *Papilio glaucus glaucus* and *P. g. canadensis* in Wisconsin. The American Midland Naturalist 119(2): 366–379. https://doi.org/10.2307/2425819

Macnaughton A, Layberry R, Cavasin R, Edwards B, Jones C (2020) Ontario butterfly atlas. https://www.ontarioinsects.org/atlas/

Mercader RJ, Aardema ML, Scriber JM (2009) Hybridization leads to host-use divergence in a polyphagous butterfly sibling species pair. Oecologia 158(4): 651–662. https://doi.org/10.1007/s00442-008-1177-9

Monroe JL, Wright DM (2017). Butterflies of Pennsylvania: a field guide. University of Pittsburgh Press, Pittsburgh, Pennsulvania, 336 pp.

Nguyen LT, Schmidt HA, von Haeseler A, Minh BQ (2015) IQ-TREE: a fast and effective stochastic algorithm for estimating maximum-likelihood phylogenies. Molecular Biology and Evolution 32(1): 268–274. https://doi.org/10.1093/molbev/msu300

Ording GJ, Mercader R, Aardema ML (2010) Allochronic isolation and incipient hybrid speciation in tiger swallowtail butterflies. Oecologia 162(2): 523–531. https://doi.org/10.1007/s00442-009-1493-8

Pavulaan H (2024) Determination of a new spring-flying species of the *Pterourus glaucus* complex (Papilionidae) in southern New England. The Taxonomic Report of the International Lepidoptera Survey 12(1): 1–26. https://doi.org/10.5281/zenodo.13952895

Pavulaan H, Wright D (2002) *Pterourus appalachiensis* (Papilionidae: Papilioninae), a new swallowtail butterfly from the Appalachian Region of the United States. The Taxonomic Report of the International Lepidoptera Survey 3(7): 1–20.

Pelham JP, Pohl GR (2023) Family Papilionidae Latreille, [1802] (apollos and swallowtails). In: Pohl GR, Nanz SR (Eds.) Annotated taxonomic checklist of the Lepidoptera of North America, North of Mexico. Wedge Entomological Research Foundation, Bakersfield, California, 193–196.

Rambaut A, Drummond AJ (2010) FigTree v1.4.4. Institute of Evolutionary Biology, University of Edinburgh. http://www.treebioedacuk/software/figtree

Ridgway R (1912). Color Standards and Color Nomenclature. Washington, DC. https://doi.org/10.5962/bhl.title.144788

Ronquist F, Teslenko M, Van Der Mark P, Ayres DL, Darling A, Höhna S, Larget B, Liu L, Suchard MA, Huelsenbeck JP (2012) MrBayes 3.2: efficient Bayesian phylogenetic inference and model choice across a large model space. Systematic biology 61(3): 539–542. https://doi.org/10.1093/sysbio/sys029

Rothschild W, Jordan K (1906) A revision of the American papilios. Novitates Zoologicae 13: 411–744. https://doi.org/10.5962/bhl.part.22801

Ryan SF, Valella P, Thivierge G, Aardema ML, Scriber JM (2016) The role of latitudinal, genetic and temperature variation in the induction of diapause of *Papilio glaucus* (Lepidoptera: Papilionidae). Insect Science 25(2): 328–336. https://doi.org/10.1111/1744-7917.12423

Ryan SF, Fontaine MC, Scriber JM, Pfrender ME, O'Neil ST, Hellmann JJ (2017) Patterns of divergence across the geographic and genomic landscape of a butterfly hybrid zone associated with a climatic gradient. Molecular Ecology 26(18): 4725–4742. https://doi.org/10.1111/mec.14236

Ryan SF, Deines JM, Scriber JM, Pfrender ME, Jones SE, Emrich SJ, Hellmann JJ (2018) Climate-mediated hybrid zone movement revealed with genomics, museum collection, and simulation modeling. Proceedings of the National Academy of Sciences of the United States of America 115(10): E2284–E2291. https://doi.org/10.1073/pnas.1714950115

Saunders WH (1874) On some of our common insects. II. The tiger swallow tail – *Papilio turnus*, L. The Canadian Entomologist 6(1): 2–5. https://doi.org/10.4039/Ent62-1

Schmidt BC (2018) Cryptic species among bumblebee mimics: an unrecognized *Hemaris* hawkmoth (Lepidoptera: Sphingidae) in eastern North America. Zootaxa 4399(1): 32–48. https://doi.org/10.11646/zootaxa.4399.1.2

Schmidt C (2020) More on Ontario tiger swallowtails. In: Hockley L, Macnaughton A (Eds) Ontario Lepidoptera 2019. Toronto Entomologists' Association Occasional Publication #51-2020, Toronto, Ontario, 3–11. https://www.ontarioinsects.org/publications/Summaries/2019.pdf

Schmidt BC, Layberry RA (2016) What Azure blues occur in Canada? A re-assessment of *Celastrina* Tutt species (Lepidoptera, Lycaenidae). ZooKeys 26(584): 135–164. https://doi.org/10.3897/zookeys.584.7882

Scriber JM (1990) Interaction of introgression from *Papilio glaucus canadensis* and diapause in producing "spring form" eastern tiger swallowtail butterflies, *P. glaucus* (Lepidoptera: Papilionidae). The Great Lakes Entomologist 23(3): 127–138.

Scriber JM (1996) Tiger tales: natural history of native North American swallowtails. American Entomologist 42(1): 19–32. https://doi.org/10.1093/ae/42.1.19

Scriber JM (1998) The inheritance of diagnostic larval traits for interspecific hybrids of *Papilio canadensis* and *P. glaucus* (Lepidoptera: Papilionidae). The Great Lakes Entomologist 31(2): 113–124. https://doi.org/10.22543/0090-0222.1955

Scriber JM (2010) Impacts of climate warming on hybrid zone movement: Geographically diffuse and biologically porous "species borders." Insect Science 18(2): 121–159. https://doi.org/10.1111/j.1744-7917.2010.01367.x

Scriber JM (2013) Climate-driven reshuffling of species and genes: potential conservation roles for species translocations and recombinant hybrid genotypes. Insects 5(1): 1–61. https://doi.org/10.3390/insects5010001

Scriber JM, Ording GJ (2005) Ecological speciation without host plant specialization; possible origins of a recently described cryptic *Papilio* species. Entomologia Experimentalis et Applicata 115(1): 247–263. https://doi.org/10.1111/j.1570-7458.2005.00285.x

Scriber JM, Elliot B, Maher E, McGuire M, Niblack M (2014) Adaptations to "thermal time" constraints in *Papilio*: latitudinal and local size clines differ in response to regional climate change. Insects 5(1): 199–226. https://doi.org/10.3390/insects5010199

Shapiro AM (1974) The butterflies and skippers of New York (Lepidoptera: Papilionoidea, Hesperioidea). Search 4(3): 1–60.

Sperling FAH (1993) Mitochondrial DNA variation and Haldane's rule in the *Papilio glaucus* and *P. troilus* species groups. Heredity 71(3): 227–233. https://www.nature.com/articles/hdy1993130

Stump AD, Sperling FA, Crim A, Scriber JM (2003) Gene flow between Great Lakes region populations of the Canadian tiger swallowtail butterfly, *Papilio canadensis*, near the hybrid zone with *P. glaucus* (Lepidoptera: Papilionidae). The Great Lakes Entomologist 36: 41–52. https://scholar.valpo.edu/tgle/vol36/iss1/8/

Vernygora OV, Campbell EO, Grishin NV, Sperling FAH, Dupuis JR (2022) Gauging ages of tiger swallowtail butterflies using alternate SNP analyses. Molecular Phylogenetics and Evolution 171: 107465. https://doi.org/10.1016/j.ympev.2022.107465

Wang X (2018) An update on tiger swallowtails in Ontario. In: Cavasin R, Linton JE (Eds) Ontario Lepidoptera 2017. Toronto Entomologists' Association Occasional Publication #48-2018, Toronto, Ontario, 25–29. https://www.ontarioinsects.org/publications/Summaries/2017_tigers.pdf

Zhang W, Kunte K, Kronforst MR (2013) Genome-wide characterization of adaptation and speciation in tiger swallowtail butterflies using de novo transcriptome assemblies. Genome Biology and Evolution 5(6): 1233–1245. https://doi.org/10.1093/gbe/evt090

Supplementary material 1

Voucher data for examined specimens of *Papilio solstitius*

Authors: Charles J. DeRoller, Xi Wang, Julian R. Dupuis, B. Christian Schmidt

Data type: xlsx

Link: https://doi.org/10.3897/zookeys.1228.142202.suppl1

ZooKeys 1228: 99–114 (2025)
DOI: 10.3897/zookeys.1228.129419

Research Article

Three new species of Polleniidae (Diptera) from China

Shixin Liu[1], Honghu Ji[2], Wenliang Li[1], Gang Yao[3]

1 *College of Horticulture and Plant Protection, Henan University of Science and Technology, Luoyang, Henan 471023, China*
2 *Jinhua Academy of Agricultural Sciences, Jinhua 321000, China*
3 *College of Agriculture, Jinhua University of Vocational Technology, Jinhua 321007, China*
Corresponding authors: Wenliang Li (wenliangli@haust.edu.cn); Gang Yao (likygang@163.com)

Abstract

Dexopollenia guangxiensis Liu, Li & Yao, **sp. nov.**, *Dexopollenia chongqingensis* Liu, Li & Yao, **sp. nov.** and *Xanthotryxus huapingensis* Liu, Li & Yao, **sp. nov.** from the Guangxi Zhuang Autonomous Region and Chongqing are described and illustrated. Keys to species of the genera *Dexopollenia* and *Xanthotryxus* from China are provided. Photographs of the habitus and male genitalia of the new species are also provided.

Key words: Calyptratae, cluster flies, *Dexopollenia*, identification key, Oestroidea, taxonomy, *Xanthotryxus*

Academic editor: Pierfilippo Cerrett
Received: 12 June 2024
Accepted: 3 November 2024
Published: 18 February 2025

ZooBank: https://zoobank.org/D8201D9E-0B59-4F8C-9EC3-83C44A030BC4

Citation: Liu S, Ji H, Li W, Yao G (2025) Three new species of Polleniidae (Diptera) from China. ZooKeys 1228: 99–114. https://doi.org/10.3897/zookeys.1228.129419

Introduction

The genus *Pollenia* Robineau-Desvoidy, 1830 was erected for the type species *Musca rudis* Fabricius, 1794, the earliest recorded cluster fly. The Polleniidae family group name was originally proposed by Brauer and Bergenstamm (1889) to include the single genus *Pollenia* (Gisondi et al. 2020). Later, *Pollenia*, *Dexopollenia* Townsend, 1917, *Xanthotryxus* Aldrich, 1930 and *Anthracomyia* Malloch, 1927 were treated as composing the subfamily Polleniinae (or tribe Polleniini) in Calliphoridae (Hall 1965; Dear 1986; Schumann 1986; Kurahashi 1989; Gisondi et al. 2020). The taxonomic status of Polleniinae has been debated. Over the past few years, molecular data consistently retrieved Polleniidae as sister to Tachinidae and phylogenetically distant from the 'core' Calliphoridae, but this sister-group relationship has remained practically without support from morphological evidence (Singh and Wells 2013; Kutty et al. 2019; Gisondi et al. 2020). Until the study of Cerretti et al. (2019), molecular-based phylogenetic analyses retrieved members of the former calliphorid subfamily Polleniinae as sister to Tachinidae; also, this clade is consistently reconstructed as distinct from the non-polleniine calliphorid clades with strong statistical support. On the other hand, a sister-group relationship between the former calliphorid subfamily Polleniinae and Tachinidae is supported by one non-homoplastic synapomorphy: ventral and ventrolateral surface of distalmost parts of the distiphallus smooth. All existing evidence shows that Polleniidae is monophyletic. Johnston et al. (2023) found in their study of subfamilial phylogenetic relationships within Polleniidae, that *Pollenia* forms a monophyletic clade, which is sister to the genera *Melanodexia*-*Morrinia*-*Dexopollenia*, and recovered *Dexopollenia-Xanthotryxus* Aldrich as sister to the remaining Polleniidae comprising *Pollenia* and sister-group *Morinia-Melanodexia*. Gisondi et al. (2023) studied the phylogenetic relationships within Polleniidae and obtained a morphological topology that is largely consistent with the findings of Johnston et al. (2023), particularly, that *Pollenia* is the sister taxon of the *Morinia-Melanodexia* clade, and suggested that Polleniidae be divided into Moriniinae and Polleniinae.

The family Polleniidae may be diagnosed as follows: Small to medium-sized oestroid flies varying from yellow to black in ground colour. Stem vein bare dorsally. Anal vein not reaching wing margin. Posterodorsal margin of hind coxa bare. Prosternum and proepisternal depression bare. Female: ovipositor sclerite length moderate; sternite 8 of ovipositor elongate with apex entire; cerci long and narrow. Male: ventral and ventrolateral surface of distalmost parts of distiphallus smooth (Cerretti et al. 2019).

Polleniidae accounts for around 150 described species in eight genera worldwide (Cerretti et al. 2019; Gisondi et al. 2020; Xue et al. 2020; Gisondi et al. 2023). Five of the eight genera (and 30 species) are known from China (Fan 1992; Fan 1997; Xue and Zhao 1996; Xue et al. 2020; Xue and Du 2022). *Dexopollenia* comprises 21 species (Cerretti et al. 2019; Gisondi et al. 2020; Xue and Du 2022), and the following nine species are known to occur in China: *D. aurantifulva* Feng, 2004; *D. disemura* Fan & Deng, 1993; *D. flava* Aldrich, 1930; *D. geniculata* Malloch, 1935; *D. luteola* Villeneuve, 1927; *D. maculata* Villeneuve, 1933; *D. nigriscens* Fan, 1992; *D. tianmushanensis* Fan, 1997; and *D. uniseta* Fan, 1992. *Xanthotryxus* comprises seven species, all distributed in China (Gisondi et al. 2020; Xue et al. 2020): *X. aurata* Séguy, 1934; *X. bazini* Séguy, 1934; *X. draco* Aldrich, 1930; *X. ludingensis* Fan, 1992; *X. melanurus* Fan, 1992; *X. mongol* Aldrich, 1930; and *X. uniapicalis* Fan, 1992. *Dexpollenia* and *Xanthotryxus* are distinct from West Palaearctic *Pollenia*, but preimaginal stages of *Dexopollenia* and *Xanthotryxus* are almost unknown in comparison to West Palaearctic Polleniidae (Kurahashi 1967; Szpila 2003; Grzywacz et al. 2012; Szpila et al. 2023).

In this article, two new species belonging to *Dexopollenia* and one new species belonging to *Xanthotryxus* are described, and updated keys of the two genera are provided.

Material and methods

The specimens were photographed under a Canon EOS 5DsR camera (Tokyo, Japan) with a Laowa FF 100 mm F2.8 CA-Dreamer Macro 2× lens (Hefei, China) and stacked with Helicon Focus ver. 7 software. The male genitalia were photographed under a Canon EOS 5DsR camera (Tokyo, Japan) with Mitutoyo, M Plan Apo 10× (Japan). Photographs were edited with Adobe Photoshop CC 2017. Morphological terminology mainly follows Cumming and Wood (2017) and McAlpine (1981).

Abbreviations used are as follows: **acr**—acrostichal setae; **dc**—dorsocentral setae; **ial**—intra-alar setae; **h**—humeral setae; **ph**—posthumeral setae; **pra**—prealar setae; **sal**—supraalar setae; **pal**—postalar setae; **mpl**—mesopleural setae; **spl**—sternopleural setae; **ppl**—pteropleural setae; **a**—anterior setae; **v**—ventral setae; **d**—dorsal setae; **p**—posterior setae; **ad**—anterodorsal setae; **pd**—posterodorsal setae; **av**—anteroventral setae; **pv**—posteroventral setae; **r-m**—radio-medial cross-vein; **2R$_5$**—distal fifth radial cell; **T**—tergite; **ST**—sternite.

Depositories cited in this work are as follows:

HAUST Insect Collection of Henan University of Science and Technology, Luoyang, Henan, China. Curator: Wenliang Li

Results

Taxonomy

Genus *Dexopollenia* Townsend, 1917

Dexopollenia Townsend, 1917: 201. Type species: *Dexopollenia testacea* Townsend, 1917 (original designation).

Diagnosis. Adults of this genus can be recognized by the combination of the following characters: body length 5–10 mm; eyes with hairs or bare; males frons narrow, interfrontalia surface disappears at narrowest part parafacial bare, arista plumose, vibrissa approaches epistoma; thorax with golden tomentum or soft hairs, propleura and basisternum of prothorax bare; postalar declivity with hairs, spl 1+1; subcostal sclerite with yellow hairs but no black setulae; radial stem vein and subalar knob bare, 2R_5 open, M_{1+2} tip gently curved forward in a wide obtuse angle or very gently in an arc, lower calypter bare; T_{3-5} with strong marginal bristles on the backside (Fan 1997).

Distribution. Australasian, Oriental and Palaearctic.

Key to Chinese species of genus *Dexopollenia* Townsend, 1917 (males)

Modified from Fan (1997).

1 Leg mostly yellow (Figs 3, 13), palpus yellow (Fig. 14)............................**2**
– Leg black, palpus black............................**9**
2 Discal scutellar setae present............................**3**
– Discal scutellar setae absent............................**5**
3 Thorax black (Figs 1, 11), tarsus yellow (Fig. 13)............................**4**
– Thorax mostly yellow, tarsus dark yellow............................***D. aurantifulva***
4 Interfrontalia reddish-brown (Fig. 14), T_5 black (Fig. 12), ST_1 hairs black, mid tibia 1 pd............................***D. chongqingensis* Liu, Li & Yao, sp. nov.**
– Interfrontalia orange (Fig. 4), T_5 mostly yellow (Fig. 2), ST_1 hairs yellow, mid tibia 2 pd............................***D. tianmushanensis***
5 Femur end and tibia base black............................**6**
– Femur end and tibia base yellow............................**7**
6 T_{3-5} mostly black, except for a narrow yellow trailing edge band at the end............................***D. geniculata***
– T_{1-5} mostly yellow (Fig. 2), except for dark spots in the middle............................***D. maculata***
7 Tarsus black (Fig. 3), ial 0+1............................**8**
– Tarsus end brown, rest yellow, ial 0+2............................***D. flava***
8 Thorax yellow, mpl 0+2, abdomen yellow only, T_5 brown............................***D. uniseta***
– Thorax black (Fig. 1), mpl 0+3, tergites except T_5 with black trailing edge band, T_{3-5} with a black ovate spot medially (Fig. 2)............................***D. guangxiensis* Liu, Li & Yao, sp. nov.**

9 Presutural acr 1 .... ***D. disemura***
– Presutural acr 0 ....**10**
10 Without facial carina, ph 1 .... ***D. nigriscens***
– Facial carina developed, ph 2 .... ***D. luteola***

Dexopollenia guangxiensis Liu, Li & Yao, sp. nov.

https://zoobank.org/C184C0F4-76C0-4E66-980E-394BF9AAB9C3
Figs 1–5, 6–10

Type material. ***Holotype*** • (dissected), male (HAUST), China: Guangxi Zhuang Autonomous Region, Guilin City, Lingui District, Huangsha Yao Township, Anjiangping, 25°55'6"N, 109°94'4"E, 1. VI. 2023, 1340 m, leg. Shixin Liu. ***Paratype*** • 1 male (HAUST), same data as holotype.

Diagnosis. Eyes with sparse short hairs; first and second antennal segments dark yellow, third antennal segment black except base dark yellow; facial carina not particularly developed; eyes 2 times higher than gena; thorax black, with dense white pollen; acr 1+2, ial 0+1, ppl absent; legs yellow except tarsus black; subcostal sclerite yellowish, bare; radial stem vein and subalar knob bare; abdomen with a mediodorsal dark vitta interrupted mediodorsally; cercus broad, terminal tip in dorsal view; paraphallus tip curved forward; hypophallus and acrophallus membranous.

Description. Male. Thorax appears black in ground colour, slightly white pollinose. Wing brownish-yellow. Legs yellow, tarsus black. Abdomen largely yellow, with a mediodorsal dark vitta interrupted mediodorsally.

Head (Figs 1, 3, 4). Eyes red, with sparse short hairs; post-ocellar setae and post-vertical setae present, eyes holoptic; Frons narrow, interfrontalia surface disappears at narrowest part; parafrontal yellow, with six pairs of frontal setae; parafacial and ocellar triangle dark yellow, with yellowish-white tomentum; gena yellow, with dense black setae; lunule bare; first and second antennal segments dark yellow, third antennal segment black except base dark yellow, first and second antennal segments with black setae, third antennal segment about 2 times longer than second antennal segment, arista plumose, arista longer than third antennal segment, but not more than epistome; mid-facial plate dark yellow, facial carina not particularly developed; palpus yellow; eyes 2 times higher than gena; postgena concolorous with gena, all yellow; hairs on postgena mostly black, yellowish hairs posteriorly.

Thorax (Figs 1, 3) black, with slightly white pruinescence; prodorsum and dorsum of mesothorax with crinkly golden hair; acr 1+2, dc 2+3, ial 0+1, h 2, ph 1+0, pra 1, sal 1, pal 2; scutellum black, with a tuft of crinkly golden hairs; anterior and posterior spiracles yellow, proepimeral setae present; anepisternum black, with crinkly golden hairs, mpl 0+3, spl 1+1; ppl absent, with a tuft of crinkly golden hairs; inferior laterotergite bare.

Wings (Fig. 5) brownish-hyaline; epaulet and basicostal scale dark yellow, subcostal sclerite yellowish, bare; radial stem vein and subalar knob bare; $2R_5$ open, width 1/2 the length of r-m; upper calypter and lower calypter dark yellow, halter yellow.

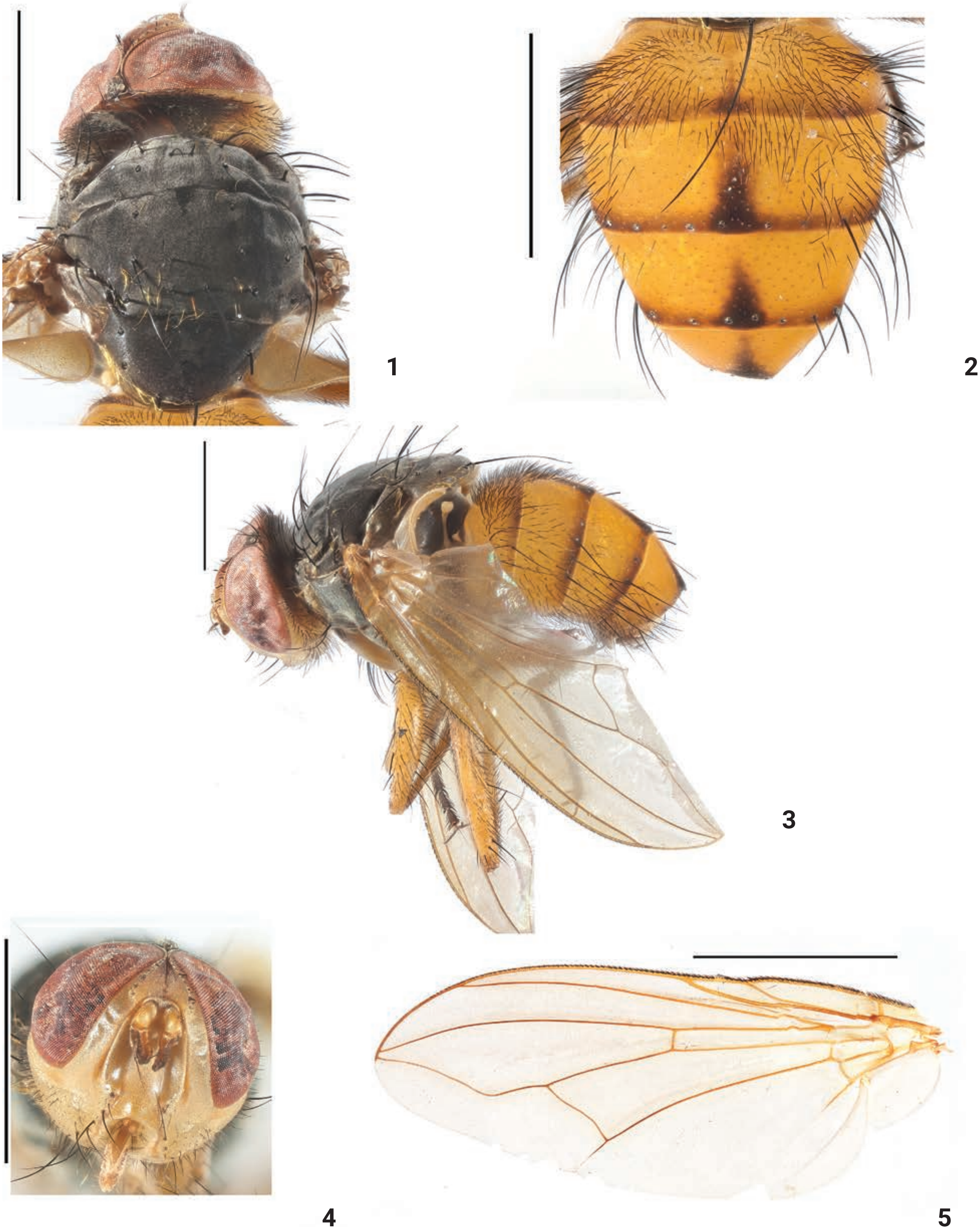

Figures 1–5. *Dexopollenia guangxiensis* Liu, Li & Yao, sp. nov. male (holotype) **1** head, thorax, dorsal view **2** abdomen, dorsal view **3** habitus, lateral view **4** head, anterior view **5** wing. Scale bars: 3 mm.

Legs (Fig. 3) yellow except tarsus black, fore femur with 10 pv, 4 pd; fore tibia with 3 ad, 2 pd; mid femur with 2 a; mid tibia with 2 ad, 2 p, 1 d, 2 pd; hind femora with 8 ad, 4 pd; hind tibia with 3 ad, 3 pd.

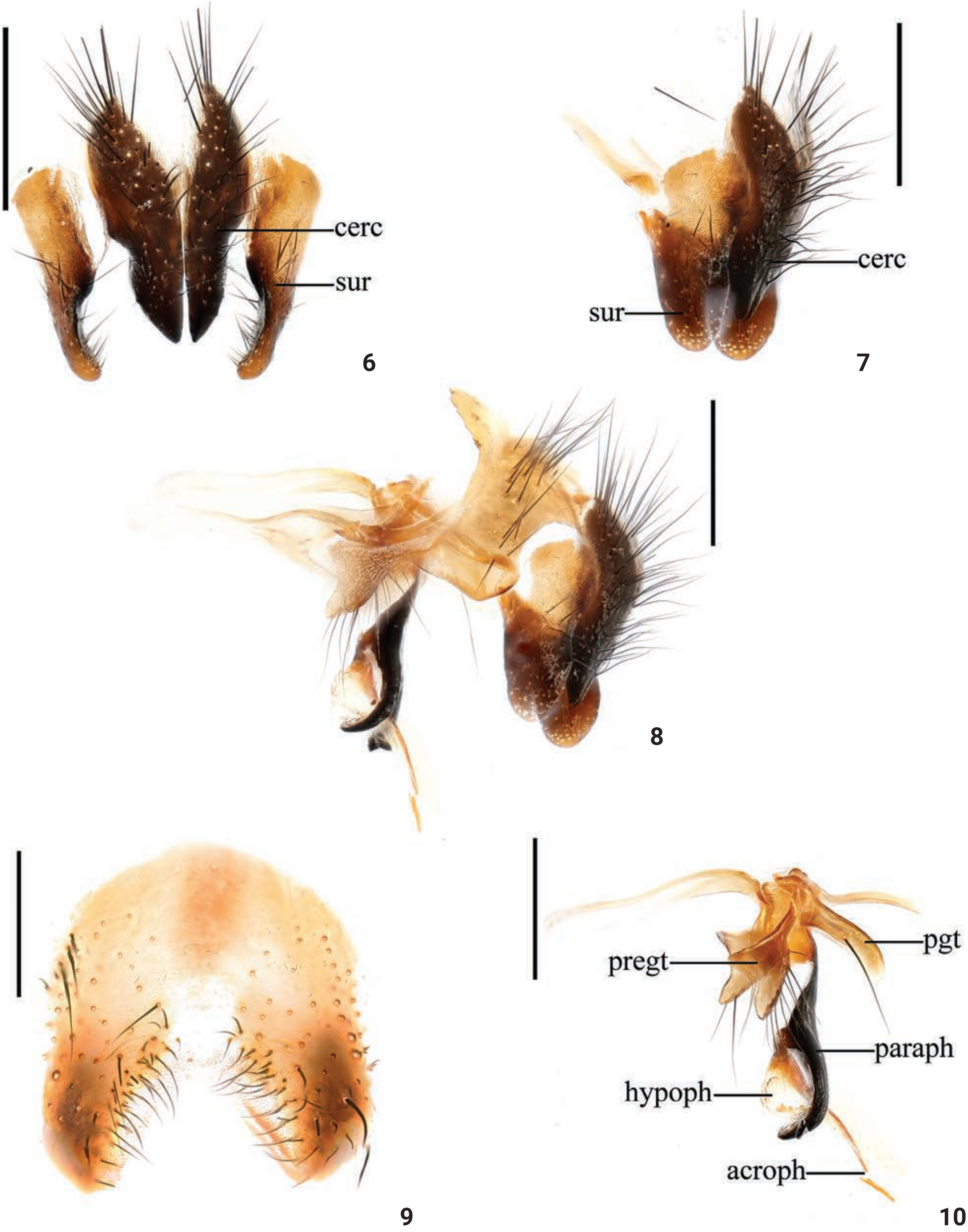

Figures 6–10. *Dexopollenia guangxiensis* Liu, Li & Yao, sp. nov. male terminalia **6** cercus and surstyli, posterior view **7** cercus and surstyli, lateral view **8** terminalia lateral view **9** ST_5 ventral view **10** phallic complex, lateral view. Scale bars: 0.3 mm. Abbreviations: acroph: acrophallus; cerc: cercus; hypoph: hypophallus; paraph: paraphallus; pgt: postgonites; pregt: pregonites; sur: surstyli.

Abdomen (Figs 2, 3) largely yellow, with a mediodorsal dark vitta interrupted mediodorsally; ST$_{1-4}$ with long black setae, terminal margin of lateral lobe of ST$_5$ with a black spot (Fig. 9); epandrium with long dense black setae. Male terminalia: medial side of surstyli with dense black hairs in posterior view (Fig. 6); cerci broad, terminal tip in posterior view (Fig. 6); surstyli broad and terminal rounded in lateral view (Figs 7, 8); pregonite with a row of black setae, and postgonites with one black seta; paraphallus terminal curved forward; hypophallus and acrophallus membranous (Figs 8, 10).

Female. Unknown.

Measurements. Male. Body length 5.1–8.6 mm.

Etymology. The specific epithet is chosen after Guangxi Province where the holotype was collected.

Distribution. China (Guangxi).

Remarks. This new species is similar to *D. maculata* Villeneuve, 1933, but differs in the following points: ial 0+1, ad 2, T$_{1-4}$ with a mediodorsal dark vitta interrupted mediodorsally, and cerci broad in dorsal view. Further, the new species paraphallus is slightly wider and rounded terminally compared to the *D. maculata* paraphallus, and the new species postgonites is longer than the *D. maculata* postgonites.

Dexopollenia chongqingensis **Liu, Li & Yao, sp. nov.**

https://zoobank.org/79D82223-F59A-407F-8AEC-EC05BE4350A1
Figs 11–15, 16–20

Type material. ***Holotype*** • (dissected), male (HAUST), CHINA: Red flag guard station, Yintiaoling, Wuxi County, Chongqing, 31°30'32.2972"N, 109°49'10.8334"E, 16. VIII. 2023, 1125 m, leg. Xulong Chen. ***Paratypes*** • 2 males (HAUST), same data as holotype.

Diagnosis. Eyes bare; interfrontalia reddish-brown; parafrontal gray, with seven pairs of frontal setae; parafacial and ocellar triangle reddish-brown, parafacial base gray; first and second antennal segments brown, third antennal segment reddish-brown except base brown, third antennal segment about 2.5 times longer than second antennal segment, arista plumose; eyes 3 times height of gena. Thorax black, acr 1+2, dc 2+3, ial 0+2, h 2, ph 1+0, pra 1, sal 1, pal 2; scutellum dark reddish-brown. T$_{1+2}$ all yellow, T$_{3-4}$ with a dark stripe in the middle, T$_4$ almost black, T$_5$ all black; surstyli end bends to both sides in posterior view; cercus slender, terminal tip bottom 2/5 black in dorsal view; surstyli broad in lateral view.

Description. Male. Thorax appears black in ground colour, slightly white pollinose. Wing brownish-yellow. Legs yellow. Abdomen largely yellow, T$_{1+2}$ all yellow, T$_{3-4}$ with a dark stripe in the middle, T$_4$ almost black, T$_5$ all black.

Head (Figs 11, 13, 14). Eyes red, bare; eyes holoptic; frons narrow, interfrontalia surface disappears at narrowest part, interfrontalia reddish-brown; parafrontal gray, with seven pairs of frontal setae; parafacial and ocellar triangle reddish-brown, parafacial base gray; gena yellow, with dense black setae; lunule bare; first and second antennal segments brown, third antennal segment reddish-brown except base brown, third antennal segment about 2.5 times

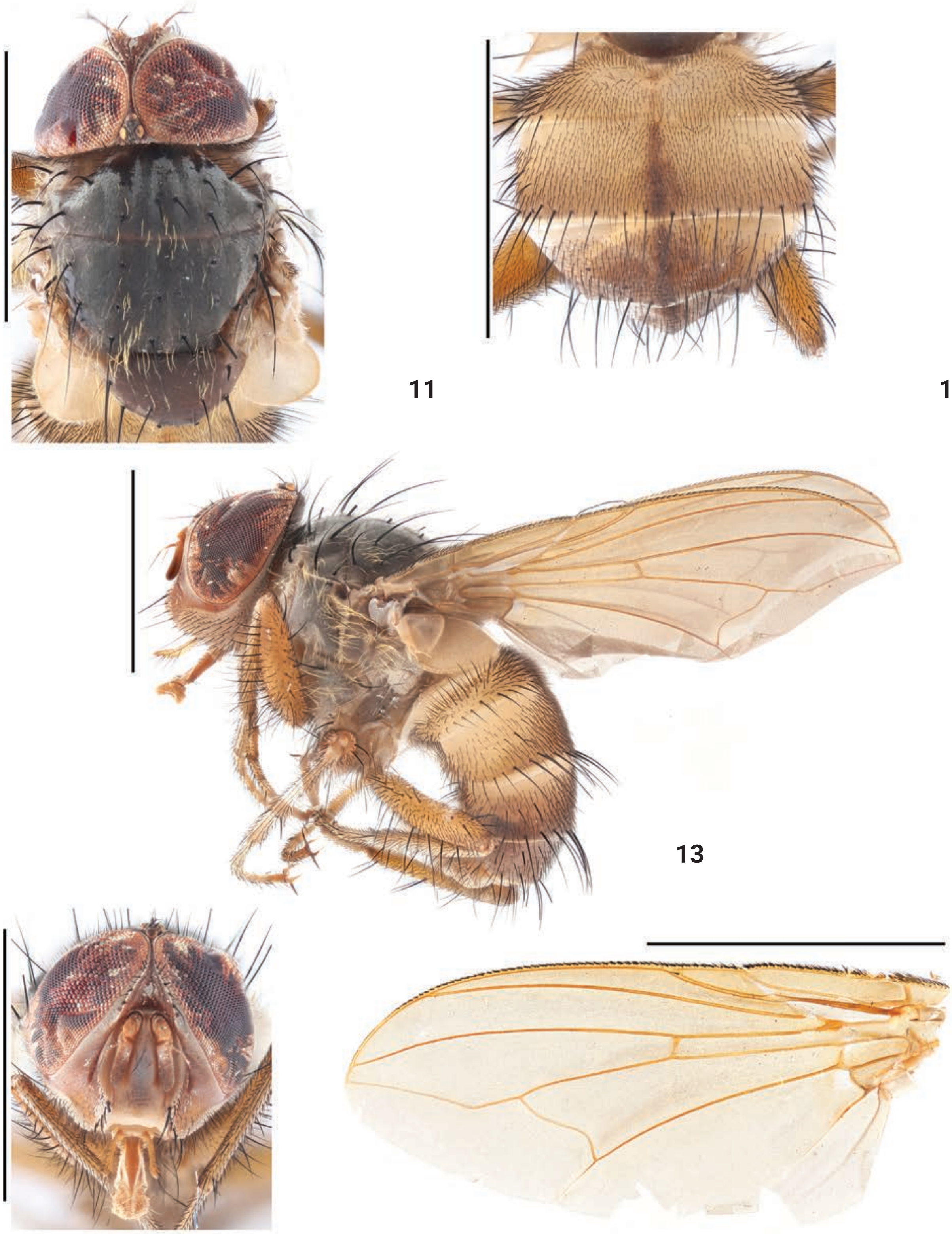

Figures 11–15. *Dexopollenia chongqingensis* Liu, Li & Yao, sp. nov. male (holotype) **11** head, thorax, dorsal view **12** abdomen, dorsal view **13** habitus, lateral view **14** head, anterior view **15** wing. Scale bars: 3 mm.

longer than second antennal segment, arista plumose; mid-facial plate dark reddish-brown, facial carina not particularly developed; palpus yellow; eyes 3 times higher than gena; postgena concolorous with gena, all yellow.

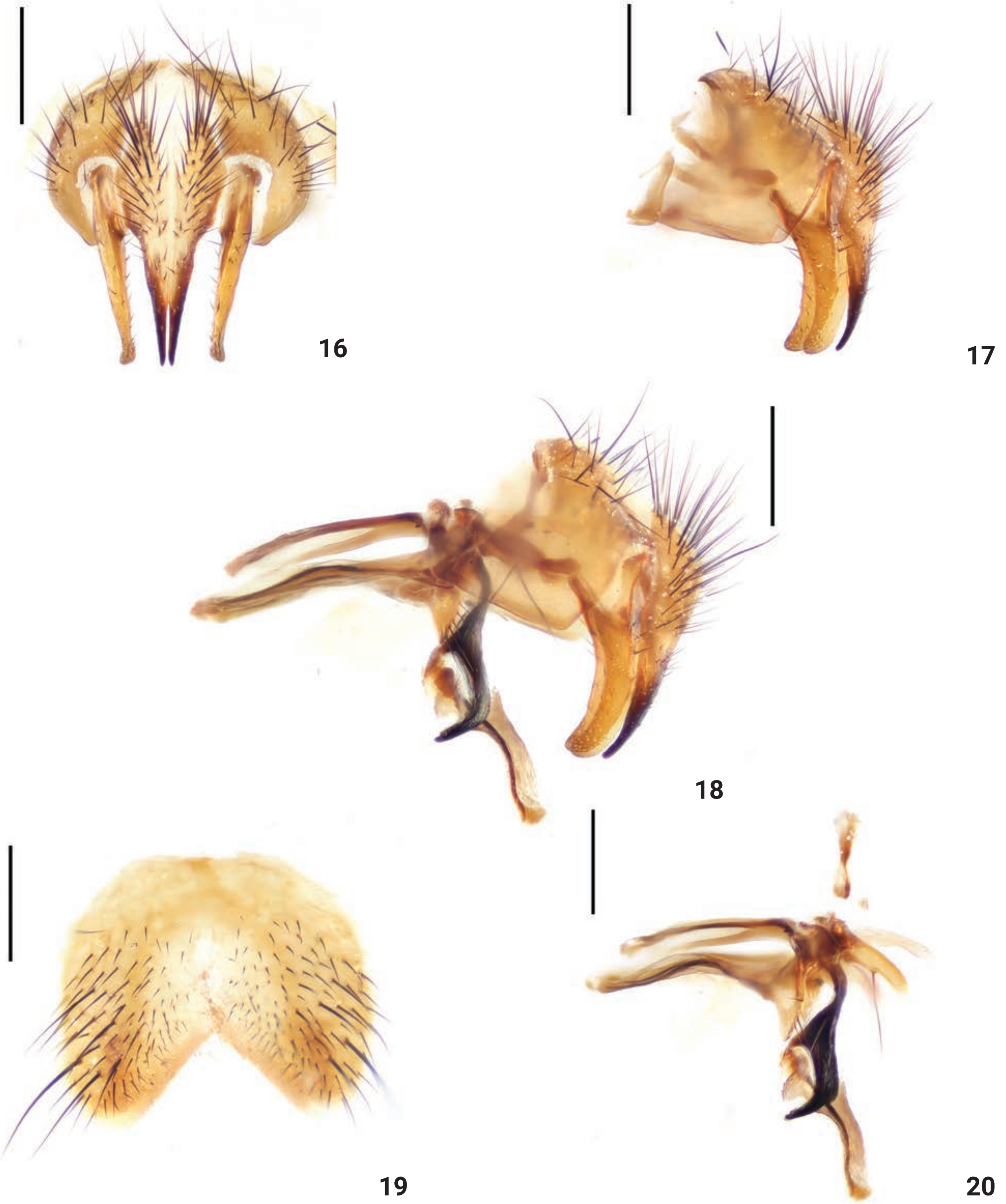

Figures 16–20. *Dexopollenia chongqingensis* Liu, Li & Yao, sp. nov. male terminalia **16** cercus and surstyli, posterior view **17** cercus and surstyli, lateral view **18** terminalia lateral view **19** ST$_5$ ventral view **20** phallic complex, lateral view. Scale bars: 0.3 mm.

Thorax (Figs 11, 13) black, with slightly white pruinescence; prodorsum and dorsum of mesothorax with crinkly golden hair; acr 1+2, dc 2+3, ial 0+2, h 2, ph 1+0, pra 1, sal 1, pal 2; scutellum dark reddish-brown; anterior and posterior spiracles yellow, proepimeral setae present; anepisternum black, with crinkly golden hair, mpl 0+4, spl 1+1; ppl absent, with a tuft of crinkly golden hair; inferior laterotergite bare.

Wing (Fig. 15) brownish-hyaline; epaulet and basicostal scale yellow, subcostal sclerite yellowish, bare; radial stem vein and subalar knob bare; $2R_5$ open; upper calypter and lower calypter brown, halter yellow.

Legs (Fig. 13) yellow, fore femur with 10 pv, 4 pd, 3 p; fore tibia with 3 p, 2 ad; mid femur with 3 pv, 2 av; mid tibia with 1 ad, 1 pd; hind femora with 7 ad, 7 av, 5 pd; hind tibia with 3 ad, 2 pd.

Abdomen (Figs 12, 13) largely yellow, with dense black hairs; T_{1+2} all yellow, T_{3-4} with a dark stripe in the middle, T_4 almost black, T_5 all black; ST_{1-4} with long black seta, ST_5 tip with long black seta (Fig. 19). Male terminalia: surstyli end bends to both sides in posterior view (Fig. 16); cercus slender, terminal tip bottom 2/5 black in posterior view (Fig. 16); surstyli broad in lateral view (Figs 17, 18); pregonite with a row of black seta anteriorly, and one black seta posteriorly; paraphallus terminal curved forward; hypophallus and acrophallus membranous (Figs 18, 20).

Female. Unknown.

Measurements. Male. Body length 3.4–8.6 mm.

Etymology. The specific epithet is chosen after Chongqing where the holotype was collected.

Distribution. China (Chongqing).

Remarks. This new species is similar to *D. maculata* Villeneuve, 1933, differing in the following points: tarsus yellow, T_4 mostly black, and T_5 all black. The cerci are slender and the basal 2/5 is black in posterior view. Surstyli are more slender than *D. maculata* in lateral view. The terminal paraphallus in the new species is approximately angular and curved; in *D. maculata* the terminal paraphallus is arc-shaped and bent. The lower part of the paraphallus in the new species is wide and in *D. maculata* it is slender.

Genus *Xanthotryxus* Aldrich, 1930

Xanthotryxus Aldrich, 1930: 3. Type species: *Xanthotryxus mongol* Aldrich, 1930 (original designation).

Diagnosis. Adults of this genus can be recognized by the combination of the following characters: bulk size, body length 9–13 mm, body totally black; eyes bare; parafacial bare or with hairs, facial carina broadly flat or slightly round, not angular; antennae black, arista plumose, vibrissa far from epistoma; scutum, scutellum and tergite with crinkly golden hairs; propleura and basisternum bare, suprasquamal ridge bare, postalar declivity with tomentum; basal tubercle of R_{4+5} with small black setae, subcostal sclerite with a tuft of setae and yellow villi; legs black; abdomen with golden tomentum, cerci slender, acrophallus well developed and hypophallus not well developed (Fan 1997).

Distribution. Palaearctic, Oriental.

Key to Chinese species of genus *Xanthotryxus* Aldrich, 1930 (males)

Modified from Fan (1997).

1 Discal scutellar setae present, ST_1 hairs all yellow or partially yellow.......**2**
– Discal scutellar setae absent, ST_1 hairs all black........................... ***X. bazini***

2 Presutural acr 1 or 0 .... **3**
– Presutural acr 2 .... **4**
3 Presutural acr 1, parafacial with hairs, $2R_5$ open (Fig. 25) .... ***X. aurata***
– Presutural acr 0, parafacialia bare, $2R_5$ closed .... ***X. ludingensis***
4 $2R_5$ open (Fig. 25), opening length approximately equal to the length of r-m **5**
– $2R_5$ narrow opening, opening length approximately 1/3 of the length of r-m .... ***X. melanurus***
5 Apex of cerci separated in posterior view **6**
– Apex of cerci united in posterior view .... ***X. uniapicalis***
6 Parafacialia bare (Fig. 24), h 4, ppl 3 .... ***X. huapingensis* Liu, Li & Yao, sp. nov.**
– Parafacialia with hairs, h 3, ppl 2 .... **7**
7 Frontal setae 15, T_{2-5} hairs all black .... ***X. mongol***
– Frontals setae 10, T_{2-5} hairs partially yellow .... ***X. draco***

***Xanthotryxus huapingensis* Liu, Li & Yao, sp. nov.**

https://zoobank.org/9FC00353-209C-4EF0-833F-C29BF84B410C
Figs 21–25, 26–30

Type material. ***Holotype*** • (dissected), male (HAUST), CHINA: Guangxi Zhuang Autonomous Region, Guilin City, Lingui District, Huangsha Yao Township, Anjiangping, 25°55'6"N, 109°94'4"E, 1. VI. 2023, 1340 m, leg. Shixin Liu. ***Paratypes*** • 2 males (HAUST), same data as holotype.

Diagnosis. Eyes bare; third antennal segment about 2.5 times longer than second antennal segment, third antennal segment as long as distance from vibrissa to epistoma; eyes 3 times higher than gena; palpus black; h 4, ppl 3, with a tuft of crinkly golden hairs; postalar declivity with a dense tuft of crinkly golden hairs; legs black; subcostal sclerite yellowish, with dense yellow tomentum and 2–3 setae; surstyli terminal extension and hook-like in lateral view.

Description. Male. Black species. Thorax black with crinkly golden hairs. Wing brownish-yellow. Legs black. Abdomen black tessellate yellow sarcophagids markings.

Head (Figs 21, 23, 24). Eyes red, bare; frons black, with sparse short black hair, eminence near antennae; interfrontalia surface linear at narrowest part; parafacial and mediane dull red, bare, with yellowish-white tomentum; lunule bare; antennae brownish, with yellowish-white tomentum, third antennal segment about 2.5 times longer than second antennal segment, arista plumose; facial carina well developed; third antennal segment as long as distance from vibrissa to epistoma; gena black, with dense black hairs; eyes 3 times higher gena; palpus black.

Thorax (Figs 21, 23). black, with dense crinkly golden hairs; acr 2+3, dc 2+3, ial 0+2, h 4, ph 3+0, pra 1, sal 2, pal 2; anterior and posterior spiracles black, proepimeral bristles present; anepisternum with a dense tuft of crinkly golden hairs on the posterior margin, mpl 0+6, spl 1+1, ppl 3, with a tuft of crinkly golden hairs; postalar declivity with a dense tuft of crinkly golden hairs.

Wing (Fig. 25) brownish-hyaline; epaulet and basicostal scale black; subcostal sclerite yellowish, with dense yellow tomentum and 2–3 setae; radial stem vein bare, radial vein knob with yellow tomentum; upper calypter and lower calypter reddish-brown.

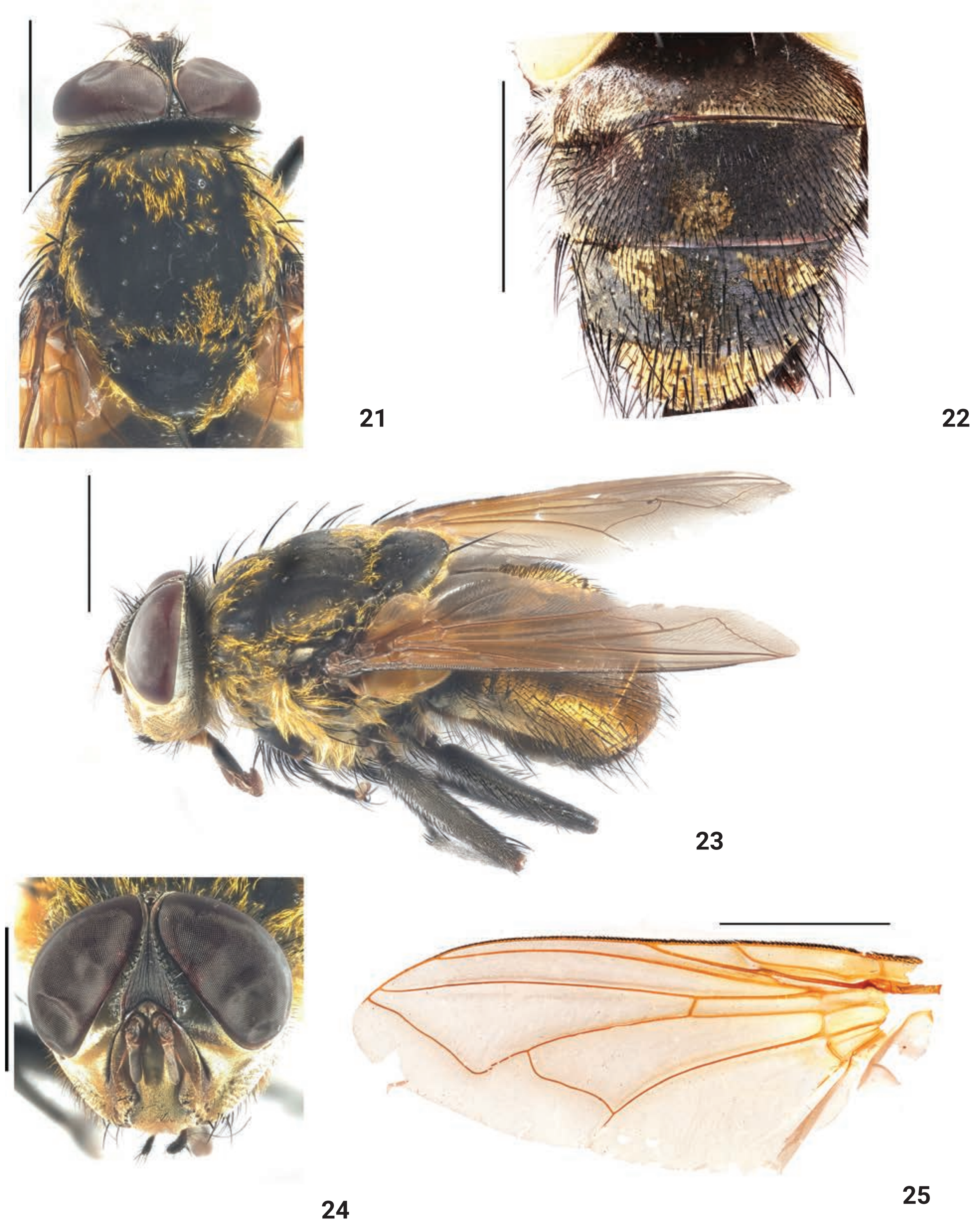

Figures 21–25. *Xanthotryxus huapingensis* Liu, Li & Yao, sp. nov. male (holotype) **21** head, thorax, dorsal view **22** abdomen, dorsal view **23** habitus, lateral view **24** head, anterior view **25** wing. Scale bars: 3 mm.

Legs (Fig. 23) black, femora with white tomentum; tarsi with dense short yellow hairs on ventral surface; fore femur with 11 d, 13 pd, 14 v; mid femur with 11 v; mid tibia with 1 ad, 2 pd; hind femora with 1 d, 14 ad, 1 pd, 10 v, 7 av; hind tibia with 3 ad, 5 pd.

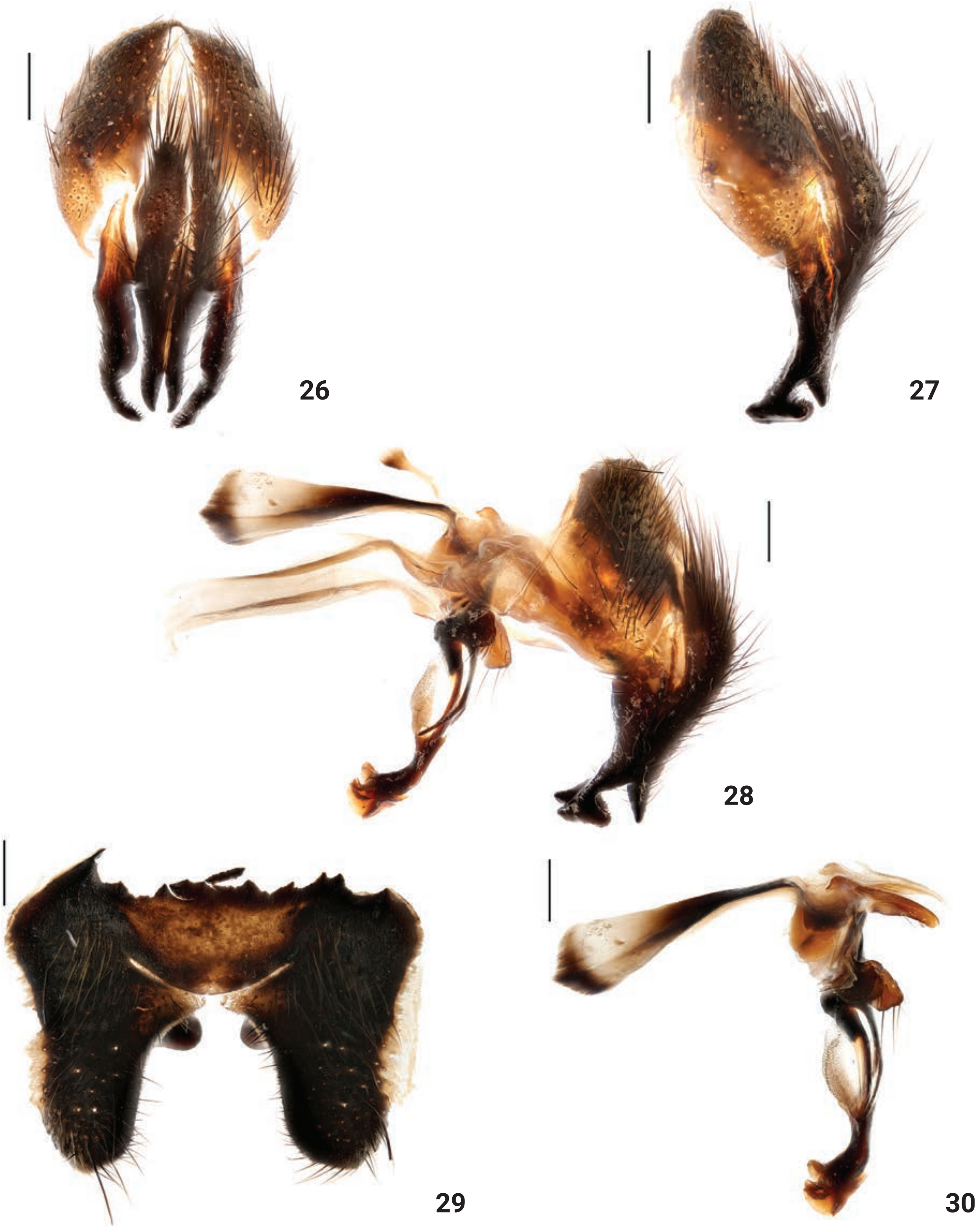

Figures 26–30. *Xanthotryxus huapingensis* Liu, Li & Yao, sp. nov. male terminalia **26** cerci and surstyli, posterior view **27** cerci and surstyli, lateral view **28** terminalia lateral view **29** ST_5 ventral view **30** phallic complex, lateral view. Scale bars: 0.3 mm.

Abdomen (Figs 22, 23) black, tessellate yellow sarcophagids markings; ST_1 with yellow setae, ST_{2-5} with black setae and yellow setae; ST_5 two prominences on the ventral surface (Fig. 29). Male terminalia: end of surstyli curved inward in posterior view (Fig. 26); end of cerci sharp and curved backward in posterior view (Fig. 26); surstyli hook-like in lateral view (Figs 27, 28); pregonites with a row of black setae, postgonites bare; paraphallus slender and curved forward; hypophallus membranous; acrophallus well developed and terminal trumpet (Figs 28, 30).

Female. Unknown.

Measurements. Male. Body length 11.3–14.5 mm.

Etymology. The specific epithet is chosen after Huaping National Nature Reserve, Guangxi Province where the holotype was collected.

Distribution. China (Guangxi).

Remarks. The new species is similar to *X. draco* Aldrich, 1930, but it differs by the following points: h 4, ph 3+0, ppl 3, base of the antennae distinctly separated, terminal extension of surstyli hook-like in lateral view. The new species paraphallus is slender, and the acrophallus is not as developed as in *X. draco*. The new species phallus is rather similar to that of *X. mongol* and *X. uniapicalis*, but can be separated from the latter two as follows: the end of the *X. mongol* paraphallus is approximately angular curved, while in the new species the paraphallus terminal is arc-shaped and bent; moreover, the new species paraphallus is thinner than that of *X. mongol*; the new species paraphallus does not bend forward beyond the hypophallus in lateral view, whereas the *X. uniapicalis* paraphallus bends forward over the hypophallus in lateral view.

Acknowledgements

We are grateful to Mr Xiaohan Ye, Mr Xulong Chen and Ms Pengyan You for their help in collecting specimens.

Additional information

Conflict of interest

The authors have declared that no competing interests exist.

Ethical statement

No ethical statement was reported.

Funding

The research was funded by the National Natural Science Foundation of China (31970435), Investigation and assessment of priority areas for terrestrial biodiversity conservation in Guangxi (GXZC2022-G3-001173-JGJD).

Author contributions

Conceptualization, G.Y. and W.L.; Methodology, G.Y.; Software, S.L.; Validation, G.Y.and W.L.; Analyses, S.L., G.Y. and W.L.; Investigation, S.L., H.J.; Resources, G.Y.; Data Curation, S.L., H.J.; Writing – Original Draft was written by S.L. and G.Y.; Writing – Review & Editing, G.Y. and S.L.; Visualization, S.L., and H.J.; Supervision, G.Y. and W.L.; Project Administration, G.Y. and W.L.; Funding Acquisition, G.Y.

Author ORCIDs

Shixin Liu https://orcid.org/0009-0007-7102-9061
Honghu Ji https://orcid.org/0009-0001-8217-7293
Wenliang Li https://orcid.org/0000-0001-9019-1223
Gang Yao https://orcid.org/0000-0002-3551-5878

Data availability

All of the data that support the findings of this study are available in the main text.

References

Aldrich JM (1930) New two-winged flies of the family Calliphoridae from China. Proceedings of the United States National Museum 78(1): 1–5. https://doi.org/10.5479/si.00963801.78-2844.1

Brauer F, Bergenstamm JE von (1889) Die Zweiflügler des kaiserlichen Museums zu Wien. IV. Vorarbeiten zu einer Monographie der Muscariae Schizometopa (exclusive Anthomyidae). Pars I. Denkschriften der Kaiserlichen Akademie der Wissenschaften. Wien. Mathematisch-Naturwissenschaftliche Klasse 56: 69–180.

Cerretti P, Stireman III JO, Badano D, Gisondi S, Rognes K, Lo Giudice G, Pape T (2019) Reclustering the cluster flies (Diptera: Oestroidea, Polleniidae). Systematic Entomology 4: 957–958. https://doi.org/10.1111/syen.12369

Cumming JM, Wood DM (2017) Adult morphology and terminology [chapter 3]. In: Kirk-Spriggs AH, Sinclair BJ (Eds) Manual of Afrotropical Diptera: Vol. 1, Suricata 4, SANBI Publications, Pretoria, 89–133.

Dear JP (1986) Calliphoridae (Insecta: Diptera). Fauna of New Zealand 8: 1–86.

Fabricius JC (1794) Entomologia systematica emendata et austa secundum classes, genera, species adiectis synonymis, locis, observationibus, descriptionibus. Pt 4. [vi +] 472 pp. Hafniae [=Copenhagen].

Fan ZD (1992) Calliphoridae. In: Key to the common flies of China. 2nd Edn. Science Press, Beijing, 523–530.

Fan ZD (1997) Diptera: Calliphoridae, 407–438. In: Fauna Sinica Insecta Vol. 6. Science Press, Beijing, 1–707.

Feng Y (2004) Five new species of the tribe Polleniini from Sichuan, China (Diptera, Calliphoridae, Calliphorinae). Acta Zootaxonomica Sinica 29(4): 803–808.

Gisondi S, Rognes K, Badano D, Pape T, Cerretti P (2020) The world Polleniidae (Diptera, Oestroidea): key to genera and checklist of species. Zookeys 971: 106–108. https://doi.org/10.3897/zookeys.971.51283

Gisondi S, Buenaventura E, Jensen AR, Stireman III JO, Nihei SS, Pape T, Cerretti P (2023) Phylogenetic relationships of the woodlouse flies (Diptera: Rhinophorinae) and the cluster flies (Diptera: Polleniidae). PLOS ONE 18(9): 1–14. https://doi.org/10.1371/journal.pone.0285855

Grzywacz A, Szpila K, Pape T (2012) Egg morphology of nine species of *Pollenia* Robineau-Desvoidy 1830 (Diptera: calliphoridae). Microscopy Research & Technique 75(7): 955–967. https://doi.org/10.1002/jemt.22020

Hall DG (1965) Family Calliphoridae. In: Stone et al. (Eds) A catalog of the Diptera of America north of Mexico. Agricultural Research Service, United States Department of Agriculture, Washington D.C., Agriculture Handbook 276: 922–932.

Johnston NP, Piwczyński M, Trzeciak P, Walczak K, Szpila K (2023) Integration of mitogenomic and morphological data disentangles the systematics of *Pollenia* and establishes a revised phylogenetic hypothesis for the Polleniidae. Systematic Entomology 48(2): 296–315. https://doi.org/10.1111/syen.12576

Kurahashi H (1967) Studies of the calyptrate muscoid flies from Japan. VI. Revision of the tribes Bengaliini and Polleniini of the subfamily Calliphoridae and the subfamilies Chrysomyinae and Rhiniinae (Diptera, Calliphoridae). The Science Reports of the Kanazawa University 12(2): 255–302.

Kurahashi H (1989) Family Calliphoridae. In: Evenhuis NL (Ed.) Catalog of the Diptera of the Australasian and Oceanian Regions, Vol. 86, Bishop Museum Serial Publication, Honolulu, Hawaii, 702–718. [Including updated online version available at] http://hbs.bishopmuseum.org/aocat/calliphoridae.html

Kutty SN, Meusemann K, Bayless KM, Marinho MAT, Pont AC, Zhoyu X, Misof B, Wiegmann BM, Yeates D, Cerretti P, Meier R, Pape T (2019) Phylogenomic analysis of Calyptratae: resolving the phylogenetic relationships within a major radiation of Diptera. Cladistics 35: 605–622. https://doi.org/10.1111/cla.12375

Malloch JR (1927) Notes on Australian Diptera, No. XI. Proceedings of the Linnean Society of New South Wales 52: 299–335.

Malloch JR (1935) Diptera Calyptratae chiefly from Malaya and North Borneo. Journal of the Federated Malay States Museum 17(4): 646–685.

McAlpine JF (1981) Morphology and terminology - Adults. Chapter 2. In: McAlpine JF, Peterson BV, Shewell GE, Teskey HJ, Vockeroth JR, Wood DM (Eds) Manual of Nearctic Diptera, Vol. 1. Agriculture Canada Monograph, 27, Canadian Government Publishing Centre, Quebec, 9–63.

Robineau-Desvoidy JB (1830) Essai sur les Myodaires. Mémoires Présentés par Divers Savans à l'Académie Royale des Sciences de l'Institut de France 2(2): 1–813.

Schumann H (1986) Family Calliphoridae. In: Soós Á, Papp L (Eds) Catalogue of Palaearctic Diptera. Vol. 12. Calliphoridae-Sarcophagidae. Budapest: Academy Press, 11–58.

Séguy E (1934) Diptères de Chine de la collection de M. J. Hervé-Bazin. Encyclopédie Entomologique, Série B. Mémoires et notes. II. Diptera 7[1933]: 1–28.

Singh B, Wells JD (2013) Molecular systematics of the Calliphoridae (Diptera: Oestroidea): evidence from one mitochondrial and three nuclear genes. Journal of Medical Entomology 50: 15–23. https://doi.org/10.1603/ME11288

Szpila K (2003) First instar larvae of nine West-Palaearctic species of *Pollenia* Robineau-Desvoidy 1830 (Diptera: Calliphoridae). Entomologica Fennica 14: 193–210. https://doi.org/10.33338/ef.84188

Szpila K, Piwczynski M, Glinkowski W, Lutz L, Akbarzadeh K, Baz A, Johnston NP, Grzywacz A (2023) First molecular phylogeny and species delimitation of West Palaearctic *Pollenia* (Diptera: Polleniidae). Zoological Journal of the Linnean Society 197: 267–282. https://doi.org/10.1093/zoolinnean/zlac035

Townsend CHT (1917) XII. Indian flies of the subfamily Rhiniinae. Records of the Indian Museum 13(4): 185–202. https://doi.org/10.5962/bhl.part.5859

Villeneuve J (1927) Myodaires supérieurs nouveaux de l'ile de Formose. Revue de Zoologique et Botanique Africaine 15(3): 387–397.

Villeneuve J (1933) Myodaires supérieurs asiatiques nouveaux. Bulletin et Annales de la Société Royale d'Entomologique de Belgique 73: 195–199.

Xue WQ, Du J (2022) Six new species of Calliphoridae (Diptera) from China. Acta Parasitologica Et Medica Entomologica Sinica 29(3): 177–190.

Xue WQ, Zhao JM (1996) Calliphoridae, 1455–1460. In: Flies of China Vol. 2. Liaoning Science and Technology Press, Shenyang, 1367–2425.

Xue WQ, Li WL, Liu XY (2020) Calliphoridae. In: Yang D, Wang MQ, Li WL (Eds), Species Catalogue of China. Vol. 2. Animals INSECTA (VI). Diptera (3). Cyclorrhaphous Brachycera. Science Press, Beijing, 732–760.

ZooKeys 1228: 115–126 (2025)
DOI: 10.3897/zookeys.1228.137496

Short Communication

Barbastella caspica (Chiroptera, Vespertilionidae) in China: first record and complete mitochondrial genome

Zhong-Yu Wang[1], Shamshidin Abduriyim[1]

1 *College of Life Science, Shihezi University, Shihezi 832003, Xinjiang, China*
Corresponding author: Shamshidin Abduriyim (shamshidin@shzu.edu.cn)

Abstract

The Caspian barbastelle, *Barbastella caspica*, has spread widely in the Caspian region, Iran, and Central Asia; however, there is no evidence of its occurrence in China so far. During a field investigation, we collected a single specimen of *B. caspica* in China's Xinjiang Uyghur Autonomous Region. At the same time, we obtained the free-flight echolocation calls of the bat. It omitted signals with start frequency of 33.15 ± 1.43 kHz, end frequency of 29.82 ± 0.40 kHz, frequency of most energy 31.48 ± 0.40 kHz, duration of 2.43 ± 0.24 ms, and a pulse interval of 246.57 ± 9.48 ms, which are probably type-I sounds emitted through the mouth. We also sequenced its entire mitochondrial genome to elucidate the genomic structure and its evolutionary relationships with closely related *Barbastella*. The mitochondrial genome of *B. caspica* spans 16,933 bp, comprising 13 protein-encoding genes, 22 transfer RNA genes, two ribosomal RNA genes, and a displacement loop/control region. Consistent with previous bat mitogenome reports, the majority of mitochondrial genes are encoded on the heavy chain. A phylogenetic analysis based on 13 protein-coding genes revealed that *Rhogeessa*, *Plecotus*, and *B. caspica* formed a clade within Vespertilionidae. *Barbastella caspica* was found to be a sister species to *B. beijingensis* and *B. leucomelas* in phylogenetic trees using the cytochrome *b* and *ND1* gene sequences. This is the first report of the mitogenome of a member of the genus *Barbastella*, as well as the first record of the distribution of *B. caspica* in China and first documentation of its echolocation calls.

Key words: Echolocation calls, phylogenetic analysis, Xinjiang

This article is part of:
Biology of Pangolins and Bats

Academic editor: Wieslaw Bogdanowicz
Received: 25 October 2024
Accepted: 11 January 2025
Published: 18 February 2025

ZooBank: https://zoobank.org/E3C990CC-7911-43EA-9116-44CB754C4227

Citation: Wang Z-Y, Abduriyim S (2025) *Barbastella caspica* (Chiroptera, Vespertilionidae) in China: first record and complete mitochondrial genome. ZooKeys 1228: 115–126. https://doi.org/10.3897/zookeys.1228.137496

Introduction

The *Barbastella* genus is widely distributed from Northeast Africa to across Eurasia to Taiwan and Japan. Currently, only six species are recognized: *B. barbastellus* Schreber, 1774, *B. beijingensis* Zhang et al., 2007, *B. caspica* Satunin, 1908, *B. darjelingensis* Hodogson, 1855, *B. leucomelas* Cretzschmar, 1826, and *B. pacifica* Kruskop et al., 2019 (https://www.checklistbank.org/). In China, distributional records exist only for *B. beijingensis* and *B. darjelingensis* (http://www.sp2000.org.cn/).

The Caspian barbastelle, *B. caspica*, primarily inhabits drier habitats and is occasionally found in caves, crevices, and mines. Its main distribution encompasses northern Iran, the Caucasus region (Armenia, Azerbaijan, and Dagestan in Russia), Uzbekistan, and Tajikistan (Kruskop 2015). Research on this species is relatively limited, with a few studies focusing on taxonomic status and distribution (Kruskop et al. 2019). Furthermore, genomic studies on species of *Barbastella* have been lacking, and the phylogenetic position of this genus within the family Vespertilionidae has not been explored.

In this study, we used mist nets to capture and ultrasound recording equipment to record *B. caspica* echolocation calls. Furthermore, we conducted a comprehensive assembly and analysis of the complete mitochondrial genome of *B. caspica*, thus establishing the first genomic resource of *Barbastella*. Specifically, we analyzed the nucleotide composition of the entire mitochondrial DNA molecule, investigated the codon usage patterns and selective constraints of protein-coding genes (PCGs), and described the secondary structure of each identified tRNA gene. Finally, based on mitochondrial PCGs, cytochrome *b* (*Cytb*), and *ND1* sequences, we examined the phylogenetic position of *Barbastella* among other representative species of Vespertilionidae and of *B. caspica* within its genus. On the one hand, the complete assembly of mitochondrial genome markers was a significant step toward advancing our understanding of the genomic evolutionary biology and systematics of *Barbastella* species. On the other hand, this study also reported the first documentation of this species in China and the features of echolocation calls during flight.

Materials and methods

A bat individual was captured using mist nets during a survey of chiropteran resources in Yarkand County (37°54'24.75"N, 76°47'2.86"E), Xinjiang Uygur Autonomous Region of China, in July 2023 (Fig. 1). The specimen (SC230705005) is currently stored at the College of Life Sciences, Shihezi University. Morphological identification revealed that the bat had short, wide ears with the front ends of both ears connected, indicating that it belongs to a species of barbastelles bat, *Barbastella* genus (https://www.checklistbank.org/). A Song Meter SM4BAT FS ultrasonic recording device (Wildlife Acoustics, USA) was placed next to the mist net to record bat echolocation calls. Subsequently, the recorded echolocation sound waves were analyzed using sound analysis software (Kaleidoscope v. 5.4.8).

In the laboratory, total genomic DNAs were extracted from muscle tissues using the Tiancheng Genomic DNA Extraction Kit (Tiangen Biotech, Beijing, China). The mitochondrial genome of *B. caspica* was amplified using PCR with 11 pairs of custom-designed primers (Suppl. material 1). Products that met quality-control criteria were purified and commercially sequenced. Sequencing data were processed and assembled using SeqMan software (Tamura et al. 2013). The annotation of the mitochondrial genome was performed using the GeSeq organelle genome annotation server (Tillich et al. 2017) (https://chlorobox.mpimp-golm.mpg.de/geseq.html). Annotation refinement and adjustment of start/stop codons were performed using MEGA X (Kumar et al. 2018). The finalized mitochondrial sequence has been deposited in NCBI GenBank under accession number PP963575.

Results and discussion

The echolocation call of *Barbastella caspica* is characterized by frequency modulation (FM) (Fig. 2a, b). In free-flight outdoor conditions, the pulses are composed of a single harmonic. The peak frequency is notably low, with the highest

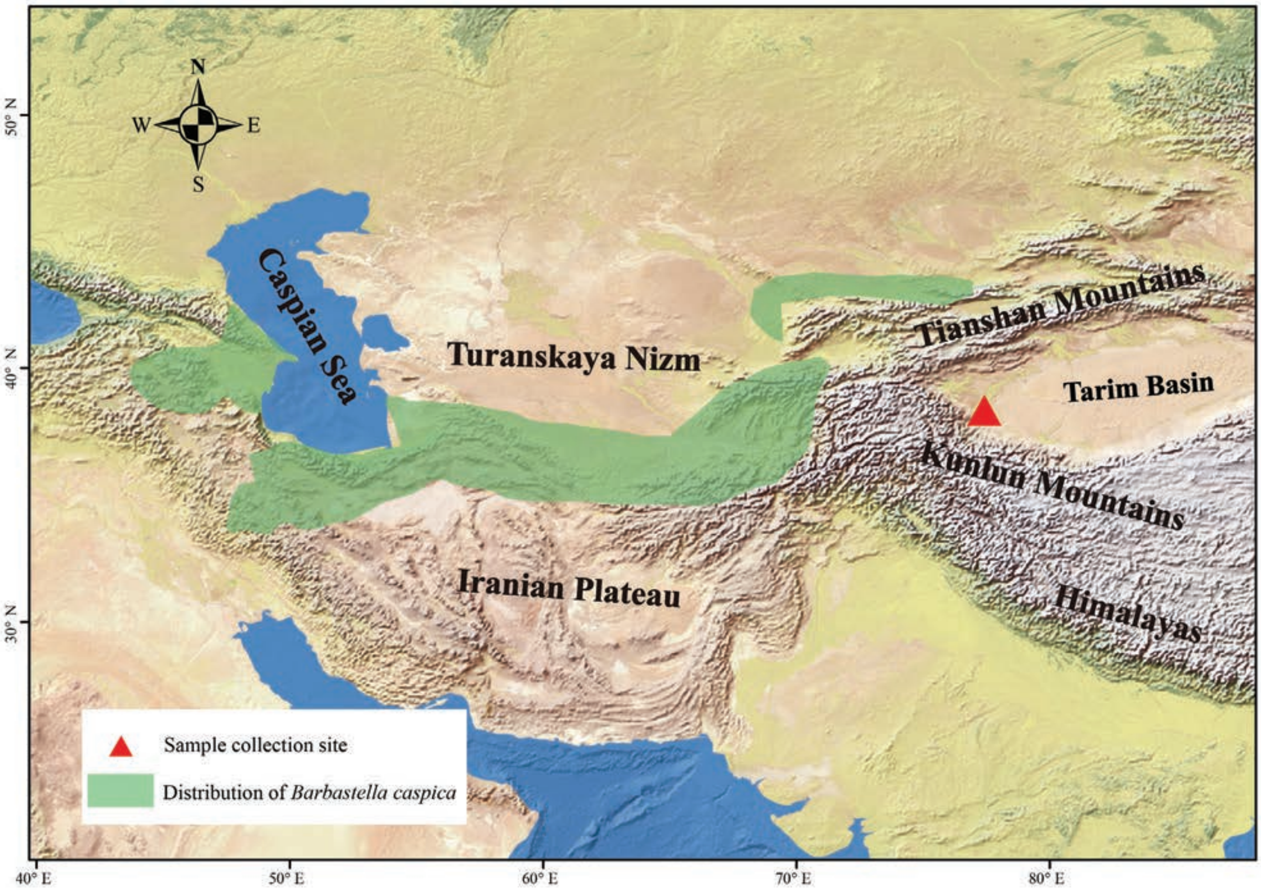

Figure 1. Map of Central Asia showing the geographic range of *Barbastella caspica* (green) and sampling site (red triangle) in southern Xinjiang, China.

energy peak occurring at 31.48 ± 0.40 kHz (Fig. 2c). The frequency bandwidth is narrow, measuring only 5.79 ± 1.04 kHz. The initial frequency is at 33.15 ± 1.43 kHz and the final frequency is at 29.82 ± 0.40 kHz. The pulse duration is relatively short, approximately 2.43 ± 0.24 ms, with an interpulse interval of 246.57 ± 9.48 ms (Table 1). These characteristics closely resemble the sound waves emitted by other species of *Barbastella* while foraging (Zhang et al. 2007) and were similar to the type-I sounds of *Barbastella* species (Denzinger et al. 2001). However, considering that certain species of horseshoe bat consistently emit two different types of sound waves during foraging (Seibert et al. 2015), it is possible that our sound-wave detector failed to capture type-II sounds. Alternatively, it is likely that *B. caspica* does not produce this particular sound during foraging or that the frequency of the emitted sound waves is lower than in other *Barbastella* species. These possibilities should be confirmed in future studies.

The mitochondrial genome of *B. caspica* is a circular DNA molecule with a length of 16,933 base pairs (Fig. 3). The genome encompasses a total of 37 genes, consisting of 13 PCGs, 22 transfer RNA genes (tRNAs), two ribosomal RNA genes (rRNAs), and one D-loop region. The size and organization of these mitochondrial genes (Table 2) are consistent with previous reports of other vespertilionid species (Guo et al. 2021; Martínez-Cárdenas et al. 2024; Valencia M. et al. 2024). Among the 13 PCGs (11,408 bp), they exhibit similarities with other species of Vespertilionidae, such as being located on the heavy strand except for *ND6* (Martínez-Cárdenas et al. 2024; Valencia M. et al. 2024). The

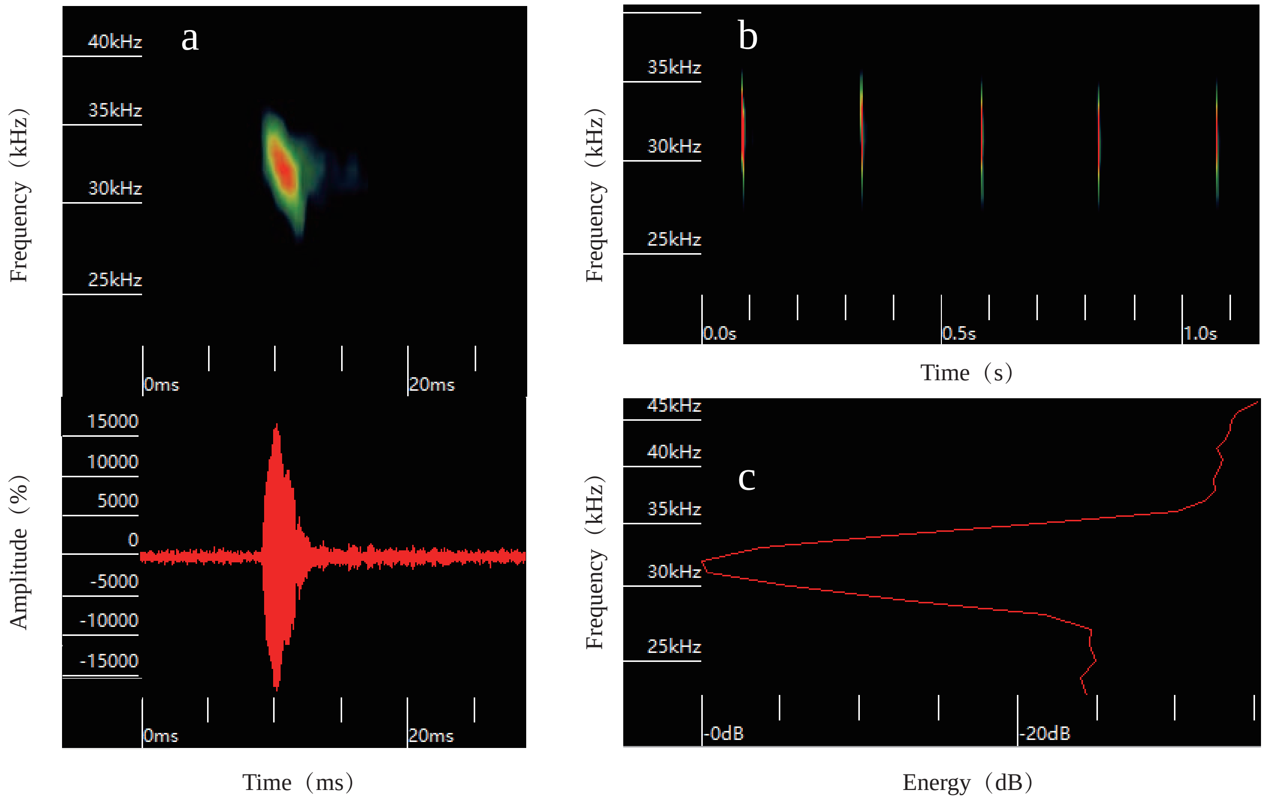

Figure 2. Echolocation calls features of *B. caspica* in free flight conditions: the spectrogram and waveform with time unit in milliseconds (**a**), the spectrogram with a time unit of seconds (**b**) and the energy spectrum (**c**).

Table 1. Echolocation calls features of *Barbastella caspica* in free-flight conditions.

Items	Range	Mean ± SD
Initial frequency (kHz)	29.97–34.63	33.15 ± 1.43
Terminate frequency (kHz)	28.99–30.19	29.82 ± 0.40
Frequency bandwidth (kHz)	4.02–7.27	5.79 ± 1.04
Main frequency (kHz)	31.07–31.96	31.48 ± 0.40
Duration time (ms)	2.05–2.74	2.43 ± 0.24
Interval time (ms)	232.29–266.43	246.57 ± 9.48

average A+T content of PCGs in mitochondria is 59.92%, ranging from 56.31% (*COX1*) to 64.73% (*ATP8*), which is higher than the G+C content (40.08%) of the 13 PCGs. Furthermore, they show similar negative AT skew and CG skew, as well as a high A+G content (60.03%) (Suppl. material 2) (Guo et al. 2021; Martínez-Cárdenas et al. 2024; Valencia M. et al. 2024). All PCGs start with ATG or ATA codons and terminate with TAA or truncated T residues, except for the *Cytb* gene, which terminates with AGA (Table 2).

Suppl. material 3 shows the codon counts and RSCU values of *B. caspica*. The 33 codons are used more frequently (RSCU > 1, Suppl. material 4). The codons AAU-Asn (158), ACA-Thr (133), CCA-Pro (130), ACU-Thr (121), and CUA-Leu (118) are the most frequently used. There are 22 typical tRNA genes, ranging in length from 59 bp (tRNA-Ser1) to 75 bp (tRNA-Leu2). Eight of these genes are located on the L strand, while 14 are on the H strand. In total, they span 1520 bp. Except for tRNA-Ser (Table 2, Suppl. material 5), all these tRNA

Table 2. Composition and organization of the mitochondrial genome of *Barbastella caspica*.

Gene	Strand	Location	Size(bp)	Start Codon	Stop Codon	Anticodon	Continuity
tRNA-Phe	H	1–72	72	–	–	GAA	0
12S Rrna	H	72–1031	960	–	–	–	−1
tRNA-Val	H	1032–1100	69	–	–	TAC	0
16S rRNA	H	1101–2668	1569	–	–	–	0
tRNA-Leu2	H	2669–2743	75	–	–	TAA	−1
ND1	H	2749–3705	957	ATG	TAA	–	5
tRNA-Ile	H	3705–3772	68	–	–	GAT	−1
tRNA-Gln	L	3770–3843	74	–	–	TTG	−3
tRNA-Met	H	3844–3911	68	–	–	CAT	0
ND2	H	3912–4953	1042	ATA	T−−	–	0
tRNA-Trp	H	4954–5020	67	–	–	TCA	0
tRNA-Ala	L	5028–5095	68	–	–	TGC	7
tRNA-Asn	L	5096–5168	73	–	–	GTT	0
tRNA-Cys	L	5200–5266	67	–	–	GCA	31
tRNA-Tyr	L	5267–5332	66	–	–	GTA	0
COX1	H	5334–6878	1545	ATG	TAA	–	1
tRNA-Ser2	L	6882–6950	69	–	–	TGA	3
tRNA-Asp	H	6958–7024	67	–	–	GTC	7
COX2	H	7025–7708	684	ATG	TAA	–	0
tRNA-Lys	H	7711–7779	69	–	–	TTT	2
ATP8	H	7780–7983	204	ATG	TAA	–	0
ATP6	H	7941–8621	681	ATG	TAA	–	−43
COX3	H	8621–9404	784	ATG	T−−	–	−1
tRNA-Gly	H	9404–9472	69	–	–	TCC	−1
ND3	H	9472–9818	347	ATA	TA−	–	−1
tRNA-Arg	H	9819–9889	71	–	–	TCG	0
ND4L	H	9891–10187	297	ATG	TAA	–	1
ND4	H	10181–11558	1378	ATG	T−−	–	−7
tRNA-His	H	11559–11627	69	–	–	GTG	0
tRNA-Ser1	H	11628–11686	59	–	–	GCT	0
tRNA-Leu1	H	11688–11758	71	–	–	TAG	1
ND5	H	11759–13579	1821	ATA	TAA	–	0
ND6	L	13563–14090	528	ATG	TAA	–	−17
tRNA-Glu	L	14091–14158	68	–	–	TTC	0
Cytb	H	14164–15303	1140	ATG	AGA	–	5
tRNA-Thr	H	15304–15375	72	–	–	TGT	0
tRNA-Pro	L	15373–15441	69	–	–	TGG	−3
D-loop	H	15442–16933	1492	–	–	–	0

molecules have the classical cloverleaf structure. This phenomenon has been mentioned in previous studies and is common among metazoans (Vivas-Toro et al. 2021; Basaldúa et al. 2023). However, more research is needed to determine the functionality of these features in *B. caspica*.

Based on 13 PCG sequences, we successfully constructed the phylogenetic topology of 31 species from the vespertilionid subfamilies Myotinae and Vespertilioninae. Consequently, *Rhogeessa*, *Plecotus*, *Pipistrellus*, *Glischropus*, *Hypsugo*, and *Barbastella* formed the subfamily Vespertilioninae, with *Barbastella* being a sister genus to *Plecotus* (Fig. 4). Consistent with previous results based

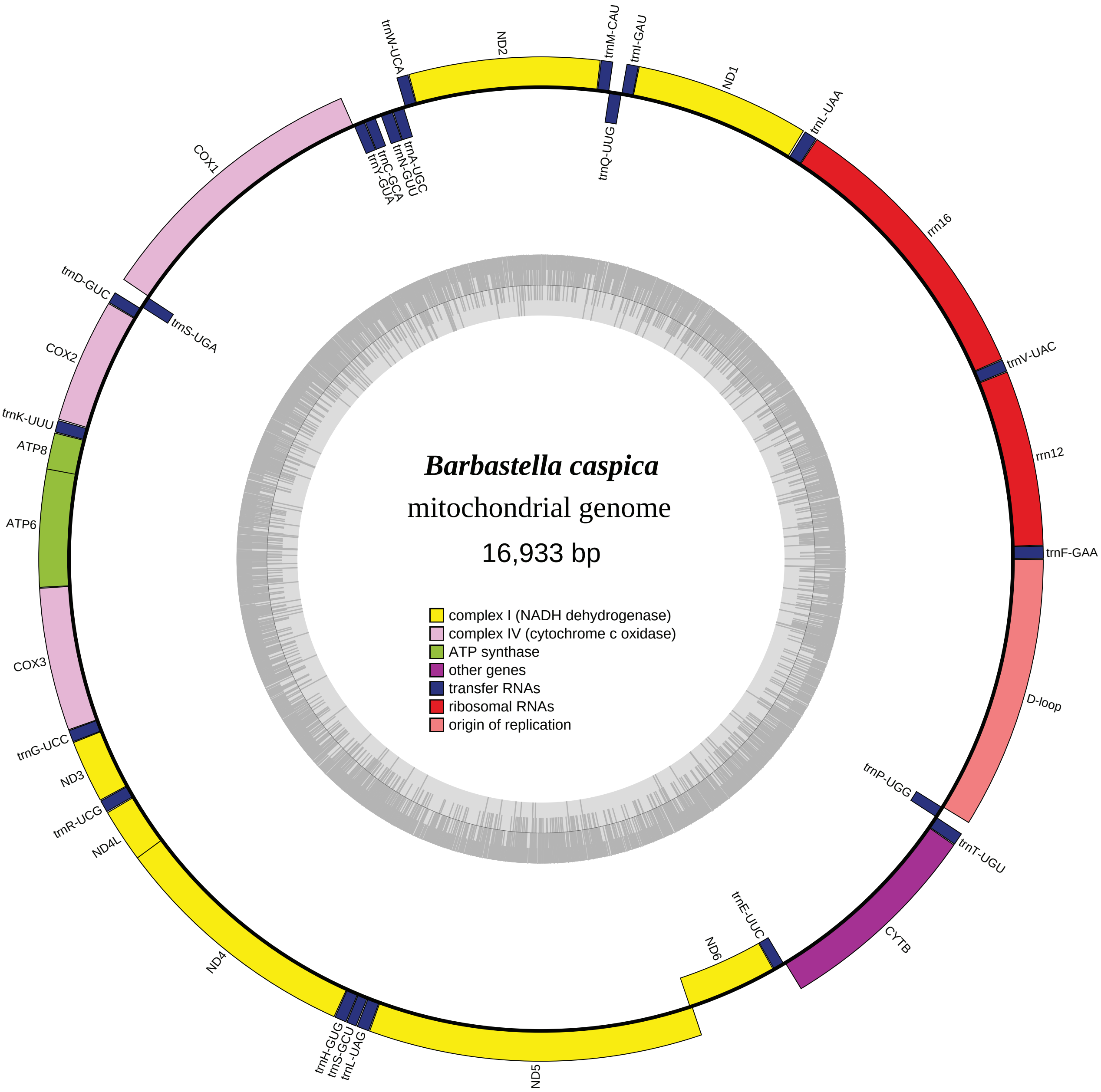

Figure 3. Mitochondrial genome map of *B. caspica*. The mitochondrial DNA of *B. caspica* is 16,933 base pairs long, consisting of different segments: 22 blue segments representing tRNA coding regions, 2 red segments corresponding to 12SrRNA and 16SrRNA, 7 yellow segments for *ND1*, *ND2*, *ND3*, *ND4L*, *ND4*, *ND5*, and *ND6*, 3 pink segments for *COX1*, *COX2*, and *COX3*, 1 purple segment for the *Cytb* gene, and 1 light red segment for the D-loop region.

on the *COI* gene (Chakravarty et al. 2020), we found that *Plecotus* and *Barbastella* belonged to the same tribe, Plecotini, which also includes four other genera (Wilson and Mittermeier 2019; https://www.checklistbank.org/), implying that more genome-based phylogeny is required to understand the intergeneric evolutionary relationships within the Plecotini.

Phylogenetic trees were constructed to elucidate the evolutionary relationship of *B. caspica* with other species of vespertilionids, based on the *Cytb* and *ND1* genes along with all PCGs. Within *Barbastella*, *B. caspica* is identified as a distinct species. However, differential topological structures were observed in the phylogenetic trees constructed based on the *ND1* and *Cytb* genes (Fig. 5).

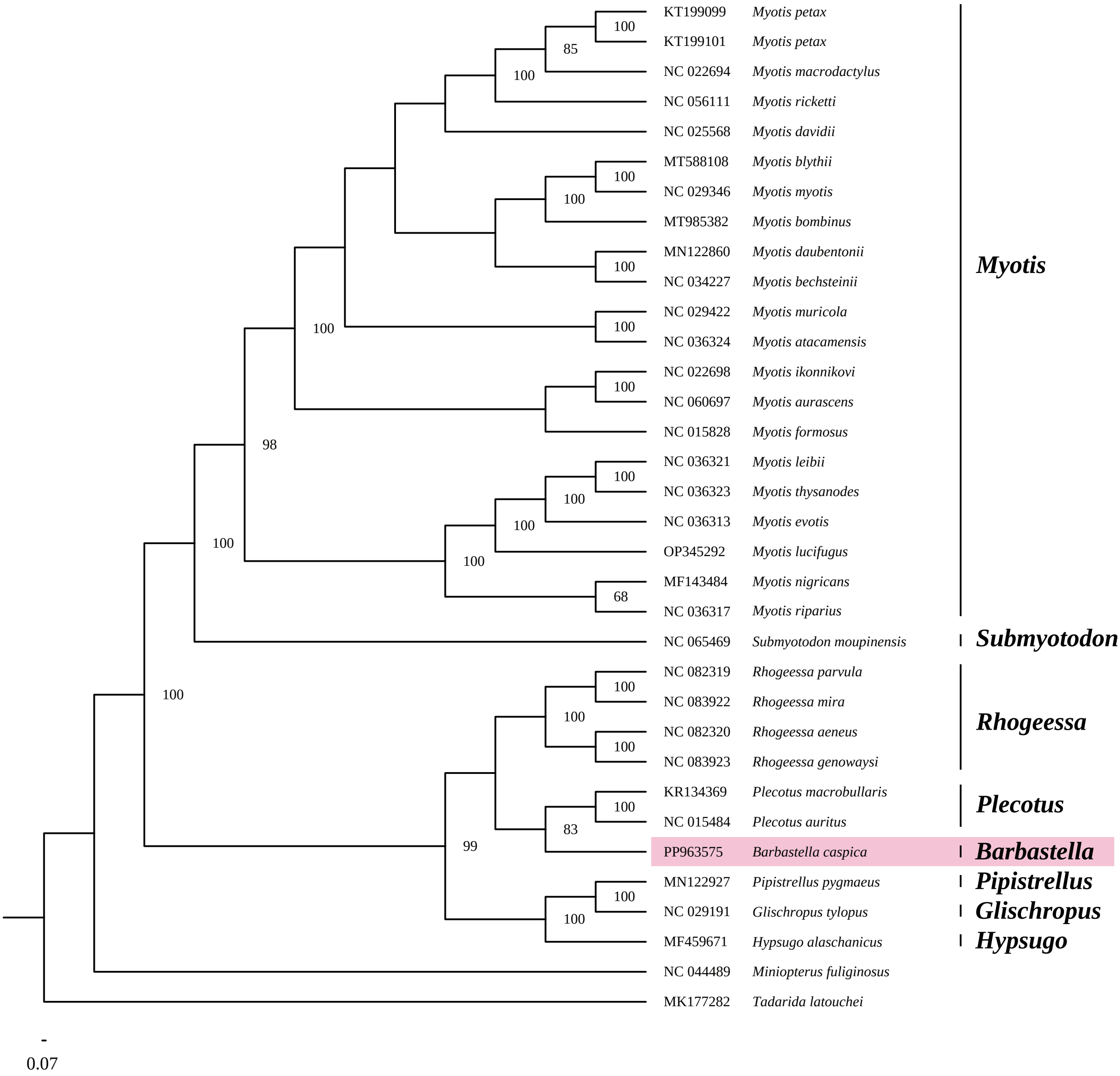

Figure 4. The phylogenetic relationships of the Vespertilionidae based on 13 protein-coding genes using the maximum-likelihood method with 1,000 bootstrap replicates. *Tadarida latouchei* and *Miniopterus fuliginosus* were designated as outgroups. Nodes with support values ≥ 80 are indicated.

Namely, *B. caspica* was a sister species to *B. leucomelas* in the *ND1* phylogenetic tree, but sister to *B. beijingensis* in the *Cytb* phylogenetic tree.

The pairwise distances (Table 3) shows that the smallest genetic distances (3.7% based on the *ND1* gene) are between *B. caspica* and *B. leucomelas*. However, the direct pairwise distance between the two species based on the *Cytb* gene is 13.4%, which is consistent with the results of the phylogenetic tree.

The systematic construction of the *ND1* phylogenetic tree, as well as the *ND1* genetic distances within *Barbastella*, consistently indicate a close genetic relationship between *B. caspica* and *B. leucomelas*, which agrees with the results of Smirnov et al. (2020). In contrast, the findings of the *Cytb* analyses are conflicting (Fig. 5, Table 3). Phylogenetic tree inconsistencies are common among mammals, especially due to important evolutionary events (Rokas and Chatzimanolis 2008).

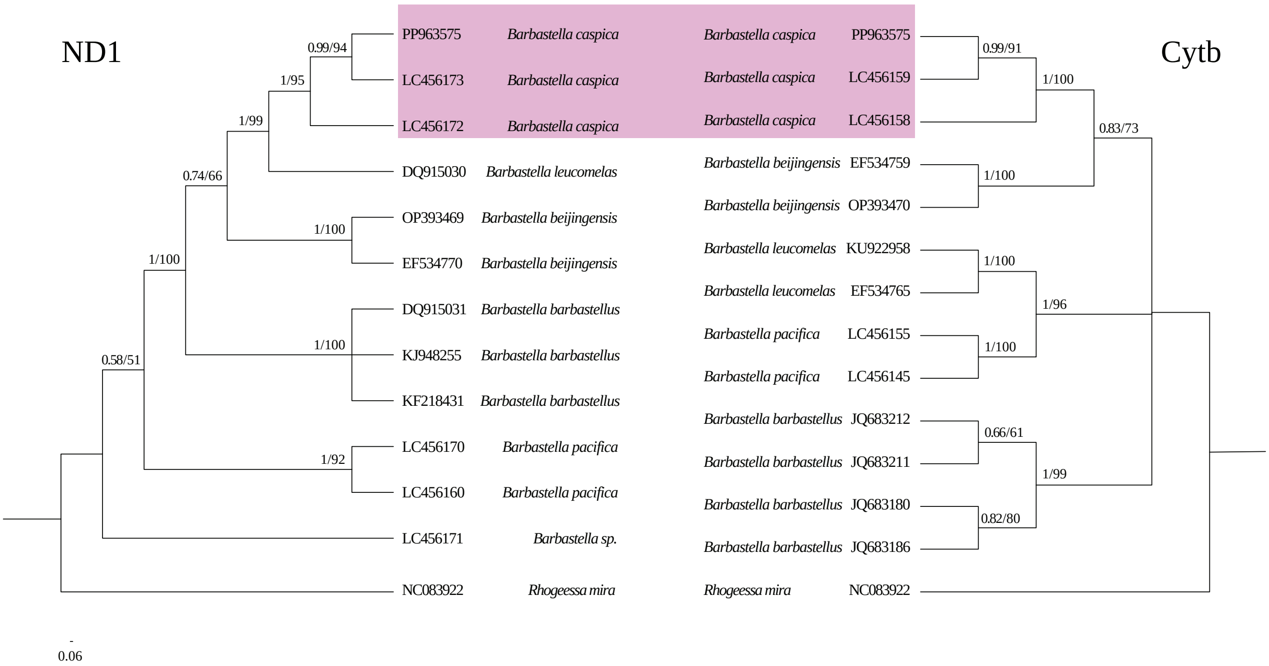

Figure 5. The Bayesian analyses of phylogenetic relationships of members of the *Barbastella* genus based on 806 bp *ND1* (left) and 1140 bp *Cytb* (right) sequences using Bayesian-inference (BI) and maximum-likelihood (ML) methods. *Rhogeessa mira* is used as the root, and nodes with support values of ≥ 0.7 (BI) and 80 (ML) are labeled.

Table 3. ML distances (above the diagonal) and *p*-distances (below the diagonal) (in %) for *ND1* and *Cytb* sequences of *Barbastella caspica*.

Species	*B. caspica*	*B. leucomelas*	*B. beijingensis*	*B. barbastellus*	*B. pacifica*
B. caspica	–	5.0 / 15.4	12.8 / 13.6	14.1 / 16.1	16.9 / 16.0
B. leucomelas	3.7 / 13.4	–	13.2 / 15.3	14.7 / 16.6	18.2 / 14.9
B. beijingensis	9.4 / 12.0	9.6 / 18.0	–	15.4 / 18.4	17.1 / 17.6
B. barbastellus	10.6 / 13.9	10.8 / 14.2	11.1 / 15.7	–	17.9 / 15.2
B. pacifica	12.6 / 13.8	13.5 / 13.1	12.6 / 14.9	13.3 / 17.9	–

These discrepancies can be attributed to factors such as inadequate gene sampling, hybridization events, gene introgression, or horizontal transfer. Although these findings provide enough evidence to consider *B. caspica* as an independent species (Fig. 5, Table 3), our understanding of its evolutionary relationship with other *Barbastella* species remains limited. Furthermore, the Central Asian species is named *B. walteri* (Smirnov et al., 2021). Hence, to obtain more comprehensive information, it is necessary to explore the genomic aspects of all species rather than confining our study solely to partial genes.

Previous reports have indicated that *B. caspica* is distributed from the Caucasus region through Iran to Tajikistan (Kruskop 2015), excluding China. This report has expanded our understanding of the geographic distribution of *B. caspica*. Combining these findings with previous research, we infer that the eastern edge of the *B. caspica* distribution extends to Xinjiang, China. Before this discovery, only two species of barbastelles (*B. darjelingensis* and *B. beijingensis*) had been documented in China, and *B. darjelingensis* was found exclusively in Xinjiang. Therefore, our report adds an additional species of barbastelle bats to the Chinese biodiversity.

Conclusions

This study highlights the presence of *B. caspica* in Xinjiang, China, for the first time and presents the first complete assembly of the mitochondrial genome, providing valuable genetic resources for investigating inter- and intraspecific evolutionary relationships. In addition, we describe for the first time free-flight echolocation calls, possibly of type-I sounds omitted through the mouth. Taking the collection site of our specimen of *B. caspica* into account, it is necessary to conduct further ecological and genetic studies at the population level on a whole distributional scale.

Acknowledgements

We express our sincere appreciation to subject editor and reviewer for their constructive comments and suggestions on our manuscript. We thank Chai Guanghou and Zhang Yan for their indispensable support during the two-month field sampling period. We acknowledge financial support from the National Natural Science Foundation of China (grant no. 32260328). We thank the editor, Wieslaw Bogdanowicz, and the reviewers for their constructive comments on the manuscript.

Additional information

Conflict of interest

The authors report that they have no conflicts of interest.

Ethical statement

The Biology Ethics Committee of Shihezi University approved all sample handling and experimental procedures (Approval: 2023-221). All bat treatment procedures were in accordance with the Bat Workers' Manual (Mitchell-Jones and McLeish 2004).

Funding

This study received financial support from the National Natural Science Foundation of China (no. 32260328).

Author contributions

Conceptualization: SA. Data curation: SA. Formal analysis: ZYW. Investigation: ZYW. Methodology: SA. Project administration: SA. Software: ZYW. Funding Acquisition: SA. Writing – original draft: ZYW. Writing – review and editing: SA, ZYW.

Author ORCIDs

Zhong-Yu Wang https://orcid.org/0009-0002-6277-942X
Shamshidin Abduriyim https://orcid.org/0000-0002-7038-077X

Data availability

The mtDNA sequences we obtained have been deposited in the NCBI GenBank databases under accession numbers PP963575.

References

Basaldúa S, Rodriguez-Pilco M, Gutiérrez-Guerrero Y, Ortega J, Baeza JA (2023) The mitochondrial genome of the endemic and endangered trumpet-nosed bat *Musonycteris harrisoni* (Chiroptera: Phyllostomidae). Journal of Natural History 57: 1206–1219. https://doi.org/10.1080/00222933.2022.2150581

Chakravarty R, Ruedi M, Ishtiaq F (2020) A recent survey of bats with descriptions of echolocation calls and new records from the western Himalayan region of Uttarakhand, India. Acta Chiropterologica 22: 197. https://doi.org/10.3161/15081109ACC2020.22.1.019

Denzinger A, Siemers B, Schaub A, Schnitzler H-U (2001) Echolocation by the barbastelle bat, *Barbastella barbastellus*. Journal of Comparative Physiology A: Sensory, Neural, and Behavioral Physiology 187: 521–528. https://doi.org/10.1007/s003590100223

Guo W, Liang X, Wu Y, Yu W (2021) The complete mitochondrial genome of *Tylonycteris fulvida* (Chiroptera: Vespertilionidae) in South China. Mitochondrial DNA Part B 6: 3274–3275. https://doi.org/10.1080/23802359.2021.1993103

Kruskop SV (2015) Dark and pale: taxonomic status of the barbastelle (*Barbastella*: Vespertilionidae, Chiroptera) from Central Asia. Acta Chiropterologica 17: 49–57. https://doi.org/10.3161/15081109ACC2015.17.1.004

Kruskop SV, Kawai K, Tiunov MP (2019) Taxonomic status of the barbastelles (Chiroptera: Vespertilionidae: *Barbastella*) from the Japanese archipelago and Kunashir Island. Zootaxa 4567. https://doi.org/10.11646/zootaxa.4567.3.3

Kumar S, Stecher G, Li M, Knyaz C, Tamura K (2018) MEGA X: Molecular Evolutionary Genetics Analysis across computing platforms. Molecular Biology and Evolution 35: 1547–1549. https://doi.org/10.1093/molbev/msy096

Martínez-Cárdenas A, Becerril V, Ortega J, López-Cuamatzi IL, Arroyo-Cabrales J, Díaz-Pacheco I, Antonio Baeza J (2024) Comparative mitochondrial genomics of endemic Mexican vesper yellow bats genus *Rhogeessa* (Chiroptera: Vespertilionidae) and insights into internal relationships in the family Vespertilionidae. Gene 918: 148492. https://doi.org/10.1016/j.gene.2024.148492

Rokas A, Chatzimanolis S (2008) From gene-scale to genome-scale phylogenetics: the data flood in, but the challenges remain. In: Murphy WJ (Ed.) Phylogenomics. Methods in Molecular Biology. Humana Press, Totowa, NJ, 1–12. https://doi.org/10.1007/978-1-59745-581-7_1

Seibert A-M, Koblitz JC, Denzinger A, Schnitzler H-U (2015) Bidirectional echolocation in the bat *Barbastella barbastellus*: different signals of low source level are emitted upward through the nose and downward through the mouth. PLoS ONE 10: e0135590. https://doi.org/10.1371/journal.pone.0135590

Smirnov DG, Vekhnik VP, Dzhamirzoyev GS (2020) On the taxonomic status of the "Asian" barbastelle (Chiroptera: Vespertilionidae: *Barbastella*) in the Eastern Caucasus. Plecotus et al. 23: 3–12. [In Russian]

Smirnov DG, Khabilov TK, Tadzhibaeva DE (2021) Modeling the potential distribution range of *Barbastella walteri* (*Barbastella*: Chiroptera, Vespertilionidae) in the Central Asian region based on Bioclimatic Data. Arid Ecosystems 11: 262–269. https://doi.org/10.1134/S2079096121030136

Tamura K, Stecher G, Peterson D, Filipski A, Kumar S (2013) MEGA6: Molecular Evolutionary Genetics Analysis version 6.0. Molecular Biology and Evolution 30: 2725–2729. https://doi.org/10.1093/molbev/mst197

Tillich M, Lehwark P, Pellizzer T, Ulbricht-Jones ES, Fischer A, Bock R, Greiner S (2017) GeSeq – versatile and accurate annotation of organelle genomes. Nucleic Acids Research 45: W6–W11. https://doi.org/10.1093/nar/gkx391

Valencia MP, Baeza JA, López-Cuamatzi IL, Ortega J (2024) Characterization of the mitochondrial genomes of the Mexican endemic bats *Corynorhinus mexicanus* and *Corynorhinus leonpaniaguae* (Chiroptera: Vespertilionidae). Molecular Biology Reports 51: 760. https://doi.org/10.1007/s11033-024-09700-5

Vivas-Toro I, Ortega J, Baeza JA (2021) The complete mitochondrial genome of the Honduran white bat *Ectophylla alba* (Allen 1982) (Chiroptera: Phyllostomidae). Gene 802: 145868. https://doi.org/10.1016/j.gene.2021.145868

Wilson DE, Mittermeier RA (2019) Handbook of the Mammals of the World. 9. Bats. Lynx Edicions, Barcelona.

Zhang J-S, Han N-J, Jones G, Lin L-K, Zhang J-P, Zhu G-J, Huang D-W, Zhang S-Y (2007) A new species of *Barbastella* (Chiroptera: Vespertilionidae) from north China. Journal of Mammalogy 88: 1393–1403. https://doi.org/10.1644/07-MAMM-A-114R2.1

Supplementary material 1

PCR primers designed for mitochondrial genome analysis of *B. caspica*

Authors: Zhong-Yu Wang , Shamshidin Abduriyim

Data type: docx

Link: https://doi.org/10.3897/zookeys.1228.137496.suppl1

Supplementary material 2

Base composition of the mitogenomes of *B. caspica*

Authors: Zhong-Yu Wang , Shamshidin Abduriyim

Data type: docx

Link: https://doi.org/10.3897/zookeys.1228.137496.suppl2

Supplementary material 3

RSCU values of protein-coding genes in mitochondrial genome of *B.caspica*

Authors: Zhong-Yu Wang , Shamshidin Abduriyim

Data type: pdf

Link: https://doi.org/10.3897/zookeys.1228.137496.suppl3

Supplementary material 4

Frequency and RSCU values of codon in protein coding genes in the mitogenome of *B. caspica*

Authors: Zhong-Yu Wang , Shamshidin Abduriyim

Data type: docx

Link: https://doi.org/10.3897/zookeys.1228.137496.suppl4

Supplementary material 5

The secondary structure of tRNA gene

Authors: Zhong-Yu Wang , Shamshidin Abduriyim

Data type: pdf

Link: https://doi.org/10.3897/zookeys.1228.137496.suppl5

ZooKeys 1228: 127–138 (2025)
DOI: 10.3897/zookeys.1228.138309

Research Article

Carulaspis silvestrii Lupo (Hemiptera, Coccomorpha, Diaspididae): redescription and neotype designation, with a key to *Carulaspis* MacGillivray species

Salvatore Nucifora[1], Gaetana Mazzeo[1], Mehmet B. Kaydan[2], Michele Ricupero[1], Agatino Russo[1]

1 *Department of Agriculture, Food and Environment, University of Catania, Catania, Italy*
2 *Biotechnology Development and Research Centre, Çukurova University, Adana, Turkiye*
Corresponding author: Salvatore Nucifora (salvatore.nucifora@unict.it)

Abstract

The insect genus *Carulaspis* MacGillivray, associated with Pinidae and Magnoliidae, includes six species: *C. juniperi*, *C. minima*, *C. visci*, *C. atlantica*, *C. taxicola* and *C. silvestrii*. The first description of *C. silvestrii* lacks key morphological features that are of paramount importance for species identification. *Carulaspis silvestrii* type specimens also remain undiscovered, suggesting a potential loss of taxon information. This study provides a detailed redescription of *C. silvestrii*, including drawings, SEM images and neotype designation for taxonomic stability. For the first time, molecular characterization of *C. silvestrii* was made using a partial 28S ribosomal gene. In addition, a morphological key for distinguishing species of *Carulaspis* is provided to aid the scientific community in taxonomic and identification endeavors.

Key words: 28S ribosomal gene, armored scale insects, *Cupressocyparis*, identification key, *Juniperus*, molecular characterization, Sicily

Academic editor: Takumasa Kondo
Received: 4 October 2024
Accepted: 5 December 2024
Published: 20 February 2025

ZooBank: https://zoobank.org/3935E645-0532-4B33-8DEB-D7E945E04FA4

Citation: Nucifora S, Mazzeo G, Kaydan MB, Ricupero M, Russo A (2025) *Carulaspis silvestrii* Lupo (Hemiptera, Coccomorpha, Diaspididae): redescription and neotype designation, with a key to *Carulaspis* MacGillivray species. ZooKeys 1228: 127–138. https://doi.org/10.3897/zookeys.1228.138309

Introduction

The genus *Carulaspis* MacGillivray, 1921 (Hemiptera: Coccomorpha: Diaspididae), is closely associated with Pinophyta (Cephalotaxaceae, Cupressaceae, Pinaceae, Taxaceae) and Santalaceae (Watson 2002; García Morales et al. 2016), and considered to be of Palearctic origin (Williams and Watson 1988; Miller and Davidson 2005; Suh and Evans 2016). The genus comprises six species, half of which are currently reported outside their area of origin, probably because they have spread with the international trade of their host plants which include ornamental plants of economic interest. These species are *C. juniperi* (Bouché, 1851), *C. minima* (Signoret, 1869), and *C. visci* (Schrank, 1781) (García Morales et al. 2016). The other species are present in a more restricted area, as follows: *Carulaspis atlantica* (Lindinger, 1911), reported in Algeria (Biche et al. 2022), Canary Islands (Lindinger 1911), Morocco (Balachowsky 1954), Spain (Gómez-Menor Ortega 1960); *C. taxicola* (Vayssière, 1913), reported only in Algeria (Vayssière 1913; Biche et al. 2022); *C. silvestrii* Lupo, 1966, reported only in Italy (Lupo 1966; Nucifora and Watson 2001).

Carulaspis silvestrii was collected by Professor Vincenzo Lupo (1966) on needle-like leaves and cones of *Juniperus macrocarpa* Sm. (= *J. oxicedrus* L. ssp. *macrocarpa* Boll.) in Bosco Gravina, Donnalucata (province of Ragusa, Sicily, Italy) and dried specimens were deposited in the Department of Agriculture, Food and Environment (Di3A), University of Catania (Italy). Lupo dedicated the new species *C. silvestrii* to the entomologist Filippo Silvestri, one of the founding fathers of Italian entomology (Barbagallo 2000), and published the original species description in the journal of the Italian Academy of Entomology (Lupo 1966), which today suffers from low visibility in the international scientific community.

The original description of *C. silvestrii* lacks the description of some morphological characters that are necessary to facilitate differentiation among the other *Carulaspis* species. In addition, the name-bearing type specimens of *C. silvestrii* were never found. This study provides a detailed redescription of *C. silvestrii*, supported by drawings and photographs, with the designation of a neotype for taxonomic stability. Molecular characterization of *C. silvestrii* was also made by using a partial 28S ribosomal gene. The taxonomic position of the genus *Carulaspis* is discussed, focusing mainly on widespread species, with the aim of improving the taxonomy of the genus and providing morphological keys for species identification.

Materials and methods

Morphological examination

Male and female individuals of *C. silvestrii* were examined under a stereomicroscope, and details of some adult females, naturally dried and not metallised, were observed by SEM (Phenom XL G2 Desktop Thermo Fisher Scientific). Some adult females were individually mounted in Canada balsam on slides according to the method described by Watson (2002) and observed under a compound optical microscope (ZEISS Axiolab 5) at magnifications between 50 and 630×. Slide-mounted specimens of *C. silvestrii* were compared with slide-mounted specimens of *C. juniperi*, *C. minima*, *C. visci*, *C. atlantica* and with two syntypes of *C. taxicola* (Table 1).

Table 1. Specimens of other *Carulaspis* species studied for comparison purposes.

Species	Specimens	Host plant	Locality / Collection data	Depository
C. atlantica (Lindinger)	1 adult female (HOLOTYPE)	*Juniperus sabina*	Sabinosa, Canary Islands - El Hierro - Spain / 6 May 1901 - G. Lindinger *leg.*	Zoologisches Museum von Hamburg - Germany
	4 adult females (topotypes)		Sabinosa, Canary Islands - El Hierro - Spain / 13 Jul. 2023 - S. Nucifora *leg.*	Di3A, University of Catania - Italy
C. juniperi (Bouché)	15 adult females	*J. hemisphaerica*	Mount Etna, Sicily - Italy / 17 Jul. 2005 - S. Nucifora *leg.*	Di3A, University of Catania - Italy
	8 adult females		Mount Etna, Sicily - Italy / 21 Mar. 2023 - S. Nucifora *leg.*	
C. minima (Signoret)	13 adult females	Cupressaceaee sp.	Donnalucata, Sicily - Italy / 16 Mar. 2023 S. Nucifora *leg.*	Di3A, University of Catania - Italy
C. visci (Schrank)	15 adult females	*Viscum album*	Mount Etna, Sicily - Italy / 21 Mar. 2023 - S. Nucifora *leg.*	Di3A, University of Catania - Italy
C. taxicola (Vayssière)	2 adult females (of 5 SYNTYPES)	*Taxus baccata*	l'Atlas de Blida - Algeria / 7 Jun. 1913 - M. Maire *leg.*	Museum National d'Histoire naturelle, Paris - France

The morphological description and terminology follow the scheme proposed by Miller and Davidson (2005). The neotype and the other studied slide-mounted specimens are deposited at the following institutions: Department of Agriculture, Food and Environment, University of Catania, Italy (**Di3A UNICT**); Muséum nationale d'Histoire naturelle, Paris, France (**MNHN**); The Natural History Museum, London, U.K. (**BMNH**); Zoologisches Museum von Hamburg, Germany (**LIB-ZMH**), and Çukurova University Scale insect collection (**CU-Sic**).

Molecular characterization

Carulaspis silvestrii was molecularly characterized by sequencing ≈800 bp of the 28S gene, as proposed by Normark et al. (2019). *Carulaspis juniperi* was included in the molecular characterization because it is considered the type species for the genus *Carulaspis* and has closer morphological similarities to *C. silvestrii*. DNA was extracted from three sets of 30 specimens each using the E.Z.N.A.® Tissue DNA Kit (Omega Bio-tek, Inc., Norcross, GA, USA) with a destructive extraction protocol. Primer pairs were 28s_s3660 5'- GAG AGT TMA ASA GTA CGT GAA AC -3' and 28s_a335 5'- TCG GAR GGA ACC AGC TAC TA -3' as described in Normark et al. (2019). PCR was carried out according to the protocol described in Ricupero et al. (2021) with slight modifications. Each reaction was performed in 20 µL volume with 0.85X FailSafe™ PCR 2X Pre-Mix F (Lucigen Corporation, Middleton, WI, USA), 0.5 µM of each primer, 1.5 units of Taq DNA Polymerase (Invitrogen, Thermo Fisher Scientific, Waltham, MA, USA) and 2 µL of DNA template. The cycling conditions were: 96 °C for 5 min, 35 cycles at 96 °C for 65 s, 45 °C for 1 min, 72 °C for 1 min, followed by a final cycle at 72 °C for 10 min. Reactions and cycling conditions were performed in Applied Biosystems™ MiniAmp™ Plus thermal cycler. PCR amplificates were first checked by electrophoresis on 1% agarose gel. Successful PCR products were then purified and sequenced by BMR Genomics sequencing service (Padova, Italy) using the Sanger method. For each species, the coding regions were checked for errors and trimmed for low quality. Since the sequences were identical, they were merged into a single one using Unipro UGENE version 1.26.1. The resulting FASTA files were aligned to reference sequences from the National Center for Biotechnology Information (NCBI) GenBank® using the Basic Local Alignment Search Tool for species identification (Altschul et al. 1990). The sequences of *C. juniperi* and *C. silvestrii* were deposited in GenBank under the following accession numbers: PP910166 and PP910167, respectively.

Taxonomy

Carulaspis silvestrii Lupo, 1966

Figs 1–6

Neotype designation. Having established that there are no type specimens of *Carulaspis silvestrii* Lupo, 1966 that bear the name, a neotype of this taxon was designated in accordance with the provisions of Article 75 of The International Code of Zoological Nomenclature (International Commission on

Zoological Nomenclature 1999). The qualifying reasons for this proposal are as follows: (i) the neotype is designed to clarify the taxonomic status of *C. silvestrii* compared to other species of the same genus; (ii) data (i.e., labelled text on the permanent microscopic slide of the neotype) and morphological description of *C. silvestrii* given in the present paper are appropriate to ensure recognition of the specimen here designed as neotype; (iii) most co-authors of the present publication belong to the Department of Agriculture, Food & Environment (formerly Faculty of Agriculture), University of Catania, where Prof. V. Lupo worked and where his collection of Diaspididae scales is deposited; they acquired here the certainty that the name-bearing type specimens of *C. silvestrii* have never been found, so assuming they were lost; (iv) the proposed neotype is designated from the type locality and host plant from which this species was recorded; it is obtained from a dry original sample collected and labelled by Prof. V. Lupo on November 3, 1964, mounted by us on a permanent microscopical slide using Canada balsam medium; (v) it is thereby declared that the designated neotype is the property of the University of Catania, where it is preserved at the Section of Applied Entomology, the Department of Agriculture, Food & Environment (Di3A), where a research entomological collection is available, with facilities for the preservation of name-bearing type specimens which are accessible for their study.

Material examined. ***Neotype*** (here designated): Italy, Sicily • adult female, neotype of *Carulaspis silvestrii*; right label [red label]: on *Juniperus* / *macrocarpa* Sm. / Sicily, ITALY / Bosco Gravina [currently part of The Irminio River Nature Reserve] / Donnalucata (RG) / 3.xi.1964 / V. Lupo leg.; left label [red label]: *Carulaspis silvestrii* / Lupo, 1966 / NEOTYPE / Di3A UniCT / S. Nucifora, des.; deposited at Di3A UNICT (Fig. 1).

Other material. Italy, Sicily • 13 adult females (topotypes); 3 Nov. 1964; Ragusa province, Donnalucata, Bosco Gravina; V. Lupo leg.; on *Juniperus macrocarpa*; 8 specimens deposited at Di3A UNICT, 1 specimen at LIB-ZMH, 1 specimen at MNHN, 1 specimen at BMNH, 2 specimens at CU-Sic • 2 adult females (topotypes); 7 Oct.1997; Ragusa province, Donnalucata, The Irminio River Nature Reserve; S. Nucifora leg.; on *J. macrocarpa*; deposited at Di3A UNICT • 2 adult females (topotypes); 16 Jan. 2023; S. Nucifora leg., Ragusa province, Donnalucata, The Irminio River Nature Reserve; 36°46.46'N, 14°35.68'E; alt. ca 5 m a.s.l.; on *J. macrocarpa*; deposited at Di3A UNICT • 5 adult females; 16 Mar. 2023; S. Nucifora leg.; Ragusa province, Donnalucata; 36°46.58'N, 14°36.42'E; alt. ca 18 m a.s.l.; on × *Cupressocyparis leylandii* (A.B. Jacks. & Dallim.) Dallim (new host association); deposited at Di3A UNICT.

Figure 1. The slide of the neotype of *Carulaspis silvestrii* Lupo, 1966.

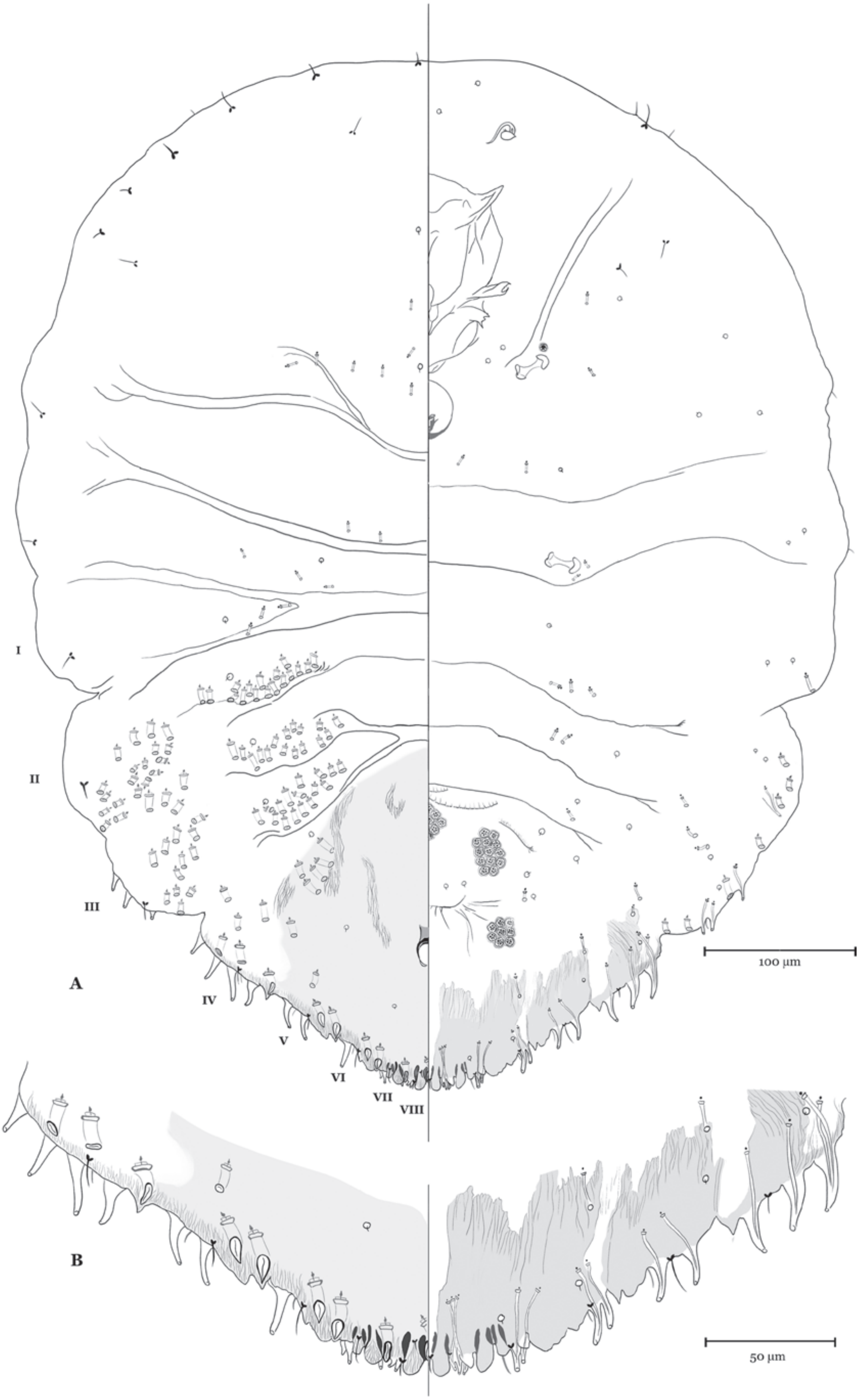

Figure 2. *Carulaspis silvestrii* Lupo, 1966, neotype, adult female showing features of the dorsum on the left side and those of the venter on the right **A** habitus **B** detail of pygidial margin and submargin.

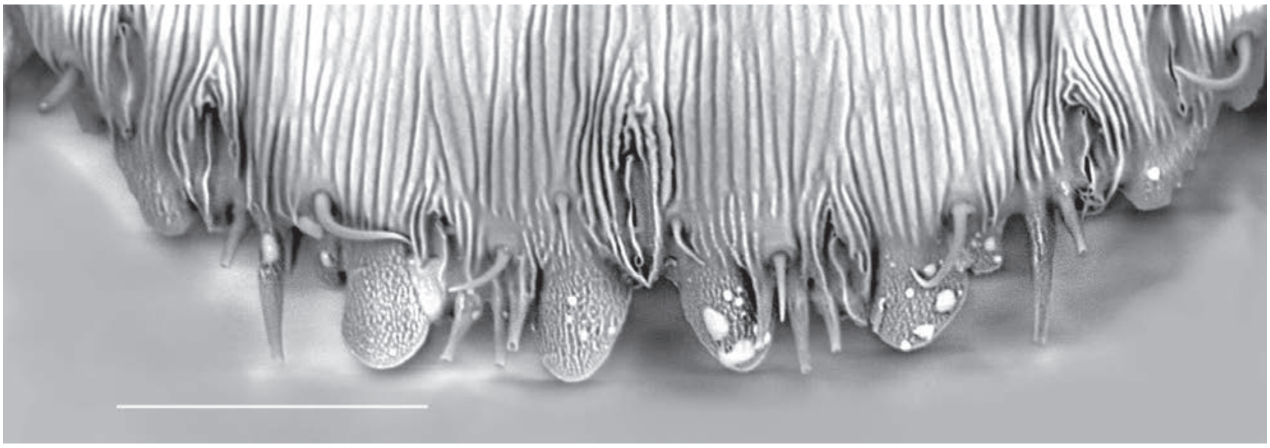

Figure 3. *Carulaspis silvestrii* Lupo, 1966, specimen showing detail of pygidial margin, dorsal side, segments 6–8. Scale bar: 25 µm. (a few drops of hardened glue are visible on the sample).

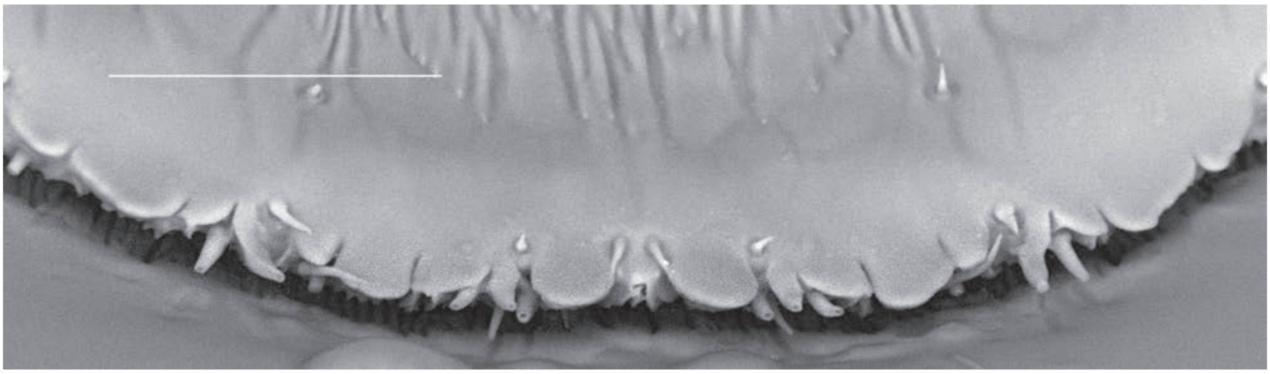

Figure 4. *Carulaspis silvestrii* Lupo, 1966, specimen showing detail of pygidial margin, ventral side, segments 6–8. Scale bar: 25 µm**.**

Redescription of *Carulaspis silvestrii* adult female. *Appearance in life*. Adult female cover rather circular, slightly convex, white; with central exuviae, yellow; ventral veil often absent, sometimes reduced to a thin white partial residue. Male cover elongate, white, felted and with 1 or 3 longitudinal ridges, with apical exuvia, yellow. Body of adult female yellow or reddish-brown. On needle-like leaves and cones.

Slide-mounted characters of the adult female (Figs 2–6). Body oval, longer than wide, slightly turbinate. The greatest width of the body is generally at the level of metathorax. Segment 1 of the abdomen and the thorax generally of similar width. Stronger intersegmental narrowing at margin between abdominal segments 1–2 and 3–4. The first and second pairs of ***lobes*** well-developed; third and fourth lobes represented by sclerotized raised areas. Median lobes not yoked, generally a little bit longer than wide, with medial and lateral margins parallel or diverging slightly, without evident notches, separated by space 0.4–0.9 times width of median lobe. Second lobes bilobed, without notches, with medial lobule about same size as median lobe. Third lobes reduced to a projecting ridge, sometimes with few light serrations on lateral margin, with two rounded apices as trace of lobules, without medial notches. Fourth lobes as a marginal thickening with only one rounded distal apex, sometimes with a light trace of lobules and with few small serrations on lateral margin; small ***paraphyses*** on the developed lobes. Dorsal seta laterad

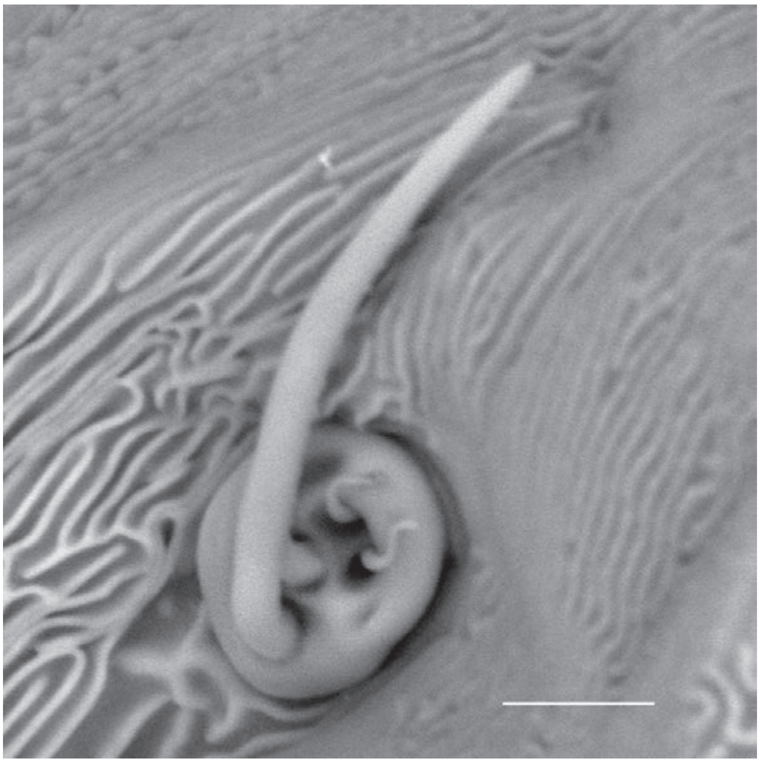

Figure 5. *Carulaspis silvestrii* Lupo, 1966, specimen showing antenna. Scale bar: 5 µm.

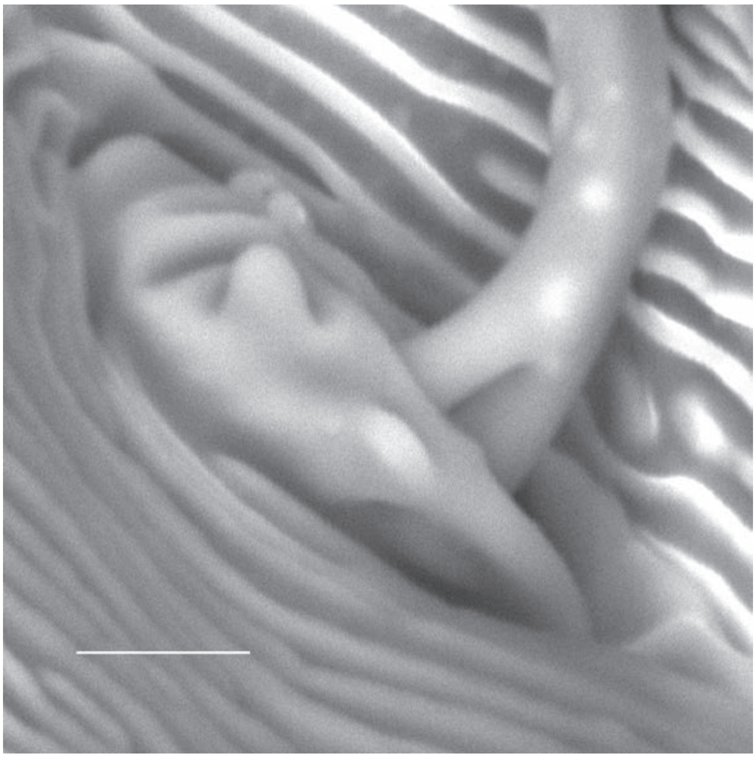

Figure 6. *Carulaspis silvestrii* Lupo, 1966, specimen showing antenna detail. Scale bar: 2.5 µm.

of median lobes never extending beyond apex of lobes. Anal opening located 2.2–4.0 times length of anal opening from base of median lobes, anal opening 8–13 µm long. ***Macroducts*** located in body margin and submarginal and submedial areas of abdomen, with total of 50–120 ducts on each side of body, counting all macroduct orifices anterior to anal opening. Dorsal macroducts of 2 sizes, larger size macroducts present in marginal areas of segments 4 to 8, smaller size macroducts located near body margin in submarginal areas and in submedial areas of segments 2–5, generally absent on submarginal and submedial areas of segments 6 or 7; with one macroduct between median lobes 10–13 µm long, one macroduct in first space 11–15 µm long, with 8–13 on each side of pygidium on segments 5 to 8. ***Microducts*** in dorsal surface located in medial area among head and prothorax, with a cluster of 7–13 ducts and in medial or submedial areas, from mesothorax to segment 1, and with 5–10 ducts on each side of body. Pygidial microducts absent on dorsum. ***Ventral microducts*** on pygidium located in submarginal areas of segments 5 and 6, with 2–4 ducts on each side of body, and in submedial areas on segment 5, at level of the vulva, with 1 or 2 ducts, on each side of body; present in medial and submedial areas of thorax and prepygidium, with 9–16 ducts. ***Macroducts in ventral side***, similar to small-size macroducts on dorsum, located on margin and submargin of any of segments 3, 2 or 1. ***Vulva*** opening lies 0.5–0.6 times of the length of the ventral side of the pygidium at the beginning of the free margin. ***Perivulvar pores***, in 5 rounded groups, 19–34 pores on each side of body. ***Crenulae*** present on ventral side of pygidium in median position, anteriorly to the vulva opening. Hardly noticeable crenulae sometimes present on medial area of prepygidial sternites. ***Spiracles*.** Anterior, with 1 or 2 perispiracular pores, posterior without pores. ***Antennae*.** Tubercle-like, with 2 short, thin setae, and 1 conspicuous curved seta, which is basally divided into 2 setae (Figs 5–6). ***Gland-spine*** formula mainly 3-2-1; on first space rarely present only 2 gland spines, on second space occasionally only 1 and on third space sometimes 2. Other marginal gland spines on each side of body are: 1–3 on segment 5; 2–4 on segment 4; 1–5 on segment 3 with some element sometimes in submarginal position; submarginal gland spines 0–3 ventrally on segments 2, with some element occasionally in marginal position. Rarely, gland spine with two glandular ducts. Without gland spines between median lobes. ***Eyes*** absent.

Comments. In the genus *Carulaspis*, the more conspicuous antennal seta of the adult female is divided at the base (Figs 5, 6); it remains to be verified whether this is also the case in *C. taxicola*. For the latter, only a limited number of incompletely detailed photographs of two syntypes were available for observation. In Diaspididae, such an antennal feature is reported at least for: *Crassaspis multipora* (Ferris), *Diaspis texensis* (Cockerell), *Furchadaspis zamiae* (Morgan) (Ferris 1937); *Getulaspis bupleuri* (Marchal), *Voraspis ceratoniae* (Marchal) and *Voraspis nerii* (Newstead) (Balachowsky 1954). Based on some occasional observations, it was found in: *D. boisduvalii* Signoret, *D. bromeliae* (Kerner), *D. echinocacti* (Bouché), *Epidiaspis gennadii* (Leonardi), *E. leperii* (Signoret) and *Mohelnaspis ampelodesmae* (Newstead).

Carulaspis silvestrii was confirmed on the host indicated by Lupo (1966) and recorded as a new host association on Leyland cypress, × *Cupressocyparis leylandii*.

Carulaspis silvestrii is close to *C. juniperi* and somewhat similar to *C. visci* and *C. minima*; it differs in having the body of the adult female more elongate and less turbinate, in the presence of three gland spines on the first spaces (between the median lobe and the second lobe), the absence of gland spines between median lobes. The gland spines between the median lobes are also lacking in *C. atlantica*, which generally looks more distant from its congeners;

it has a rounder body and different size and shape of median lobes. *Carulaspis silvestrii* differs from *C. atlantica* and *C. visci* also by the absence of submarginal dorsal macropores after segment 5 in adult females, and from *C. minima* in having a median macropore between the L1. The body shape of the adult female of *C. taxicola* greatly differs from that of *C. silvestrii*, with the prosoma and prepygidium tending to be wider, and the pygidium particularly acute. In addition, the number of marginal and submarginal ducts on the first abdominal segment is different in the two species.

The morphological similarity of adult females of the genus *Carulaspis* and the vagueness of their descriptions by previous authors have led to great nomenclatural confusion and unclear definitions (Danzig 1993). In addition, the intraspecific variability of its species may overlap among taxa, such as the number and arrangement of marginal and submarginal macroducts (Boratyński, 1957) and of gland spines, which show a small range of variability in number, which is reduced and becomes exceptional or null in the last segments of the pygidium.

Molecular characterization. Based on 28S sequence data, *C. silvestrii* and *C. juniperi* collected from different hosts in Sicily shared a haplotype with 99.02% identity. The resulting sequences were aligned to reference sequences from NCBI and compared with publicly available data on GenBank yielding an identity score of 99.2% and E-value = 0.0 with *C. juniperi* isolate from USA (Accession number DQ145301.2).

Key to adult females of *Carulaspis* species

While emphasising that a rather holistic taxonomic approach is useful for the morphological identification of species in the genus *Carulaspis*, we conclude that the species currently included in the genus are valid: each has its own morphological distinguishing characters, some of which are included in the following identification key.

1(0) With more than 3 dorsal ducts on each side of the marginal and submarginal area of first abdominal segment .... ***Carulaspis taxicola* (Vayssière)**
– With 0–3 ducts on each side of the marginal and submarginal area of first abdominal segment **2**
2(1) With a single gland spine between second lobe (L_2) and median lobe (L_1). L_2 not clearly bilobular, significantly larger than L_1 .... ***Carulaspis atlantica* (Lindinger)**
– With more than one gland spine between L_2 and L_1. L_2 clearly bilobular; medial lobule size close to L_1. .... **3**
3(2) With 3 gland spines between L_2 and L_1; without gland spines between median lobes... ***Carulaspis silvestrii* (Lupo)**
– With 2 gland spines between L_2 and L_1; with 2 gland spines between median lobes.. **4**
4(3) With marginal macroduct between median lobes **5**
– Without marginal macroduct between median lobes .... ***Carulaspis minima* (Signoret)**
5(4) With submarginal macroducts on segment 6 ...... ***Carulaspis visci* (Schrank)**
– Without submarginal macroducts on segment 6... .... ***Carulaspis juniperi* (Bouché)**

Conclusions

The redescription of *Carulaspis silvestrii* showed morphological details of the adult female that were not sufficiently highlighted in the original description, and the definition of the species has been enriched by molecular characterization. These acquisitions will allow the species to be correctly identified. *Carulaspis silvestrii* which is currently known only from Sicily, could have a much wider distribution in Italy and the Mediterranean, depending on the distribution of its host plants on which the armored scale can cause severe infestations, with possible economic consequences.

Acknowledgements

We are grateful to Dr Martin Husemann and Dr Eileen Nguyen (Zoologisches Museum von Hamburg, Germany), for allowing us to examine the holotype of *Carulaspis atlantica*; Dr Danièle Matile Ferrero, Dr Adeline Soulier-Perkins and Dr Laurent Fauvre (Muséum national d'Histoire naturelle, Paris, France), for the pictures of 2 syntypes of *C. taxicola*; Prof. Gian Pietro Giusso del Galdo (University of Catania) and Prof. Riccardo Guarino (University of Palermo), for checking our botanical determinations; Mrs Ambra Cucinotta, for the drawings support; Dr Salvatore Brunetti, for supporting use in SEM pictures. We wish also to thank Prof. Sebastiano Barbagallo (University of Catania), Prof. Juan Manuel Nieto Nafría (University of León), Dr Danièle Matile Ferrero, Dr Takumasa Kondo (Subject editor) and anonymous reviewers, for their constructive comments and suggestions.

Additional information

Conflict of interest

The authors have declared that no competing interests exist.

Ethical statement

No ethical statement was reported.

Funding

The work was carried out within the project COSOFI, University Research Incentive Plan 2020-22 (University of Catania).

Author contributions

Conceptualization: AR, MR, SN. Funding acquisition: AR, GM, MR, SN. Methodology: AR, GM, MBK, MR, SN. Field investigation: SN. Molecular studies: MR. Morphological studies: SN. Laboratory photos and figures editing: SN. Writing – original draft preparation: SN. Writing – review and editing: AR, GM, MBK, MR, SN.

Author ORCIDs

Salvatore Nucifora https://orcid.org/0000-0002-3627-683X
Gaetana Mazzeo https://orcid.org/0000-0002-6676-8077
Mehmet B. Kaydan https://orcid.org/0000-0002-0677-255X
Michele Ricupero https://orcid.org/0000-0001-5392-7553
Agatino Russo https://orcid.org/0000-0002-6949-397X

Data availability

All of the data that support the findings of this study are available in the main text.

References

Altschul SF, Gish W, Miller W, Myers EW, Lipman DJ (1990) Basic local alignment search tool. Journal of Molecular Biology 215 (3): 403–410. https://doi.org/10.1016/S0022-2836(05)80360-2

Balachowsky AS (1954) Les Cochenilles Paléarctiques de la Tribu des Diaspidini. Mémoires Scientifiques de l'Institut Pasteur, Paris, 450 pp.

Barbagallo S (2000) Ricordo di Vincenzo Lupo (1908–1999). Atti dell'Accademia nazionale italiana di entomologia 48: 67–80.

Biche M, Aroua K, Medani N, Belguendouz R, Boukhobza L, Zaabta I, Zakia K, Dahmani L, Ercan C, Tange DA, Kaydan MB, Chebli A (2022) The armored scales (Homoptera Diaspididae) of Algeria. Biodiversity Journal 13(3): 495–514. https://doi.org/10.31396/Biodiv.Jour.2022.13.3.495.514

Boratyński K (1957) On the two species of the genus *Carulaspis* MacGillivray (Homoptera: Coccoidea, Diaspidini) in Britain. Entomologist's monthly magazine 93: 246–251.

Bouché PF (1851) Neue arten der schildlaus-familie. Entomologische Zeitung, Stettin 12 (4): 110–112.

Danzig EM (1993) Fauna of Russia and Neighbouring Countries, Rhynchota. Vol. X. Scale Insects (Coccinea), Families Phoenicococcidae and Diaspididae. "Nauka" Publishing House, St. Petersburg, 452 pp.

Ferris GF (1937) Atlas of the Scale Insects of North America. Series I. Stanford University Press, Palo Alto, California.

García Morales M, Denno BD, Miller DR, Miller GL, Ben-Dov Y, Hardy NB (2016) ScaleNet: A literature-based model of scale insect biology and systematics. Database. https://doi.org/10.1093/database/bav118 [Accessed: July 2024]

Gómez-Menor Ortega J (1960) Adiciones a los "Cóccidos de España". V. (Superfamilia Coccoidea). EOS 36: 157–204.

International Commission on Zoological Nomenclature (1999) The International code of zoological nomenclature. Fourth edition. The International Trust for Zoological Nomenclature, London. [ISBN 0 85301 006 4] https://www.iczn.org/the-code/the-code-online/

Lindinger L (1911) Afrikanische Schildläuse. IV. Kanarische Cocciden. Ein Beitrag zur Fauna der Kanarischen Inseln. Jahrbuch der Hamburgischen Wissenschaftlichen Anstalten 28(3): 1–38.

Lupo V (1966) Il genere *Carulaspis* McGill. e le specie paleartiche ad esso appartenenti. Rendiconti dell'Accademia Nazionale Italiana di Entomologia 13: 34–48.

MacGillivray AD (1921) The Coccidae. Tables for the identification of the subfamilies and some of the more important genera and species together with discussions of their anatomy and life history. Scarab Company Urbana, Illinois, 502 pp. https://doi.org/10.5962/bhl.title.30504

Miller DR, Davidson JA (2005) Armored Scale Insect Pests of Trees and Shrubs. Cornell University Press, Ithaca and London, NY, Hong Kong, 442 pp.

Normark BB, Okusu A, Morse GE, Peterson DA, Itioka T, Schneider SA (2019) Phylogeny and classification of armored scale insects (Hemiptera: Coccomorpha: Diaspididae). Zootaxa 4616(1): 1–98. https://doi.org/10.11646/zootaxa.4616.1.1

Nucifora S, Watson GW (2001) Armoured scale insects (Hemiptera: Coccoidea: Diaspididae) new to Sicily: records and observations. Entomologica 33: 207–211.

Ricupero M, Biondi A, Russo A, Zappalà L, Mazzeo G (2021) The cotton mealybug is spreading along the Mediterranean: first pest detection in Italian tomatoes. Insects 12(8): 675. https://doi.org/10.3390/insects12080675

Schrank F (1781) Enumeratio Insectorum Austriae Indigenorum. Augustae Uindelicorum, apvd Vidvam Eberhardi Klett et Franck, 555 pp. https://www.biodiversitylibrary.org/bibliography/15091

Signoret V (1869) Quelques observations sur les cochenilles connues sous le nom de Pou à poche blanche qui ravagent les plantations de cannes a sucre a l'Ile Maurice et a l'Ile de la Réunion. Annales de la Société Entomologique de France (quatrième série) 9: 93–96.

Suh SJ, Evans GA (2016) A new record of the armored scale genus *Carulaspis* MacGillivray (Hemiptera: Diaspididae) from Korea and its aphelinid parasitoids (Hymenoptera: Aphelinidae). Insecta Mundi 0466: 1–6.

Vayssière P (1913) Cochenilles nouvelles de l'Afrique française. La revue de phytopathologie appliquée 1: 124.

Watson GW (2002) Arthropods of economic importance: Diaspididae of the world. Series Title: World Biodiversity Database. Expert Center for Taxonomic Identification (ETI) Bioinformatics, Leiden. UNESCO Publishing, Paris. CD-Rom. [ISBN: 90-75000-48-0] https://diaspididae.linnaeus.naturalis.nl/linnaeus_ng/app/views/introduction/topic.php?id=3377&epi=155

Williams DJ, Watson GW (1988) The Scale Insects of the Tropical South Pacific Region. Part. 1. The Armoured Scales (Diaspididae). CAB International, Wallingford, U.K., 290 pp.

ZooKeys

ZooKeys 1228: 139–159 (2025)
DOI: 10.3897/zookeys.1228.139654

Research Article

A new flea beetle genus from sub-Saharan Africa, and taxonomic remarks on the *Blepharida* genera group in the Afrotropical region (Chrysomelidae, Galerucinae, Alticini)

Paola D'Alessandro[1], Maurizio Biondi[1]

[1] Department of Health, Life and Environmental Sciences, University of L'Aquila, 67100 L'Aquila, Italy
Corresponding author: Paola D'Alessandro (paola.dalessandro@univaq.it)

Abstract

Cladocera fulvipennis Jacoby is transferred to *Afrotropicaltica* **gen. nov.**, here described. The new genus belongs to the group of Afrotropical genera traditionally attributed to the *Blepharida* group: *Blepharidina* Bechyné, *Calotheca* Heyden, *Diamphidia* Gerstaecker, *Polyclada* Chevrolat, and *Xanthophysca* Fairmaire. A diagnostic key to these genera, and the list of species currently attributed to *Diamphidia* and *Polyclada* are provided based on type material and original species descriptions. Species and genera whose taxonomic position needs a revision were identified. Finally, the following synonymy is proposed: *Cladocera fulvipennis* Jacoby, 1895 = *Blepharida favareli* Achard, 1922, **syn. nov.**

Key words: *Afrotropicaltica*, *Blepharidina*, *Calotheca*, *Cladocera fulvipennis*, *Diamphidia*, new synonymy, *Polyclada*, *Xanthophysca*

Academic editor:
Alexander Konstantinov
Received: 18 October 2024
Accepted: 5 December 2024
Published: 20 February 2025

ZooBank: https://zoobank.org/B4C6A019-EA05-4955-BCB0-159CE81B345C

Citation: D'Alessandro P, Biondi M (2025) A new flea beetle genus from sub-Saharan Africa, and taxonomic remarks on the *Blepharida* genera group in the Afrotropical region (Chrysomelidae, Galerucinae, Alticini). ZooKeys 1228: 139–159. https://doi.org/10.3897/zookeys.1228.139654

Introduction

The term *Blepharida* group refers to a group of approximately 21 genera from the Afrotropical, Nearctic, Neotropical, and Oriental regions (Furth 1992, 1998, Medvedev 1999; Furth and Lee 2000; Biondi et al. 2017; Calcetas and Staines 2024). Various authors discussed similarities and affinities between the genera based on adult and larval morphology, molecular markers, and ecology, and established new nomenclatural acts, generally focusing on one subset of taxa: Furth (1992, 1998), Medvedev (1999), Furth and Lee (2000), Becerra (2004), Takizawa (2005), Chaboo et al. (2007), Lee and Cheng (2007), Prathapan and Chaboo (2011), Biondi et al. (2017). Furth and Lee (2000) provided a morphological synthesis of the group based on adult characters (tarsal claws, procoxal cavities, head, pronotum, hind femora, eye, proepimeron, and metatibia) and larval characters (antenna, mandible, labrum, stemmata, endocarina, coronal suture, frontal suture), but highlighted that some characters are not shared by all the genera.

The Afrotropical region hosts five genera traditionally considered to belong to the *Blepharida* group, sensu Furth and Lee (2000): *Blepharidina* Bechyné, 1968; *Calotheca* Heyden, 1887; *Diamphidia* Gerstaecker, 1855; *Polyclada* Chevrolat, 1837, and *Xanthophysca* Fairmaire, 1901 (Biondi and D'Alessandro 2010, 2012; Biondi et al. 2017, 2022). Genus *Blepharidina* has recently been the object of a deep taxonomic revision (Biondi et al. 2017, 2019; D'Alessandro et al. 2018a, 2019). It includes 32 species, of which 12 are in the subgenus *Afroblepharida* Biondi & D'Alessandro, 2017, and 20 in the subgenus *Blepharidina* s. str. The genus mainly occurs in the intertropical area of Africa, with *Blepharidina* primarily distributed in the south and *Afroblepharida* largely in the central-eastern area, including Socotra Island, with extensions towards the north and in the west. Moreover, *Blepharidina* s. str. species generally occur in mesic environments, while *Blepharidina* (*Afroblepharida*) species are generally associated with more xeric conditions (D'Alessandro et al. 2018b; Iannella et al. 2021). *Calotheca* comprises 37 described species (Biondi et al. 2017; D'Alessandro et al. 2020, 2021, 2022, 2023a, 2023b). Some species groups have been revised recently, while others are still under investigation by the authors. The genus is widespread in sub-Saharan Africa, and particularly common in the eastern and southern parts of its distribution range, with limited extensions into Israel and the Arabian Peninsula (Iannella et al. 2021). *Calotheca* species are generally associated with savannas and forests, or with the typical South African vegetation, such as Albany thicket and Fynbos (D'Alessandro et al. 2018b; Iannella et al. 2021; Biondi et al. 2024). Many records reported *Searsia* species (Anacardiaceae) as the primary host plants (Koch 1958; Furth and Young 1988; MB, pers. data; E. Grobbelaar, pers. comm. 10 September 2024). *Polyclada* occurs in sub-Saharan Africa and the Arabian Peninsula with ~ 15 species (Biondi and D'Alessandro 2010, 2012; D'Alessandro and Biondi 2023). Species are associated with Anacardiaceae and Burseraceae and are found in various woodland and savannah ecosystems (Chaboo et al. 2007; Prathapan and Chaboo 2011; Biondi et al. 2022). *Diamphidia* comprises ~ 17 species, widespread in central, eastern, and southern-western Africa (Biondi and D'Alessandro 2010, 2012) and associated with *Commiphora* shrubs and trees (Burseraceae) (Chaboo et al. 2007; Biondi and D'Alessandro 2012). *Xanthophysca* is endemic to Madagascar, and currently includes 5–7 species (Biondi and D'Alessandro 2010, 2012; Biondi et al. 2017).

Diamphidia, *Polyclada*, and *Xanthophysca* have not been revised recently. *Polyclada* and *Diamphidia* species, previously described also under the generic names *Cladocera* Hope, 1840 and/or *Cladotelia* Kolbe, 1894, created a certain confusion in the generic name usage and, regarding *Polyclada*, also the genus author (Baly 1861; Chapuis 1875; Achard 1922; Laboissière 1941, 1942; Bryant 1942). In addition, discordances in the identification and description of key diagnostic characters for the genera *Diamphidia* and *Polyclada* have led to uncertainty in the attribution of some species and/or the transferring from one genus to the other (Baly 1861; Chapuis 1875; Achard 1922; Laboissière 1941, 1942; Bryant 1942).

In this paper, we establish the synonymy *Cladocera fulvipennis* Jacoby, 1895 = *Blepharida favareli* Achard, 1922, syn. nov., designate the lectotype of *Blepharida favareli*, and provide a reassessment of the taxonomic position of *Cladocera fulvipennis* by transferring it to *Afrotropicaltica* gen. nov. This new flea beetle genus has been established after the revision of the diagnostic characters of the Afrotropical genera traditionally attributed to the *Blepharida* group, specifically the adult morphological characters. Based on this revision, a diagnostic key to the genera is also provided. Since *Blepharidina* and most *Calotheca* species were revised and listed in recent papers (Biondi et al. 2017; D'Alessandro et al. 2018a, 2019, 2020, 2021, 2022, 2023a, b), particular attention is paid to *Diamphidia*, *Polyclada*, and *Xanthophysca*. The list of species attributed to these three genera is provided. Since the most recent taxonomic literature does not agree on some synonymies and/or the status of some taxa, possible synonyms are listed as separated species. Species whose generic attribution needs further investigation are reported. *Cladocera* and *Cladotelia* are currently considered as synonyms of *Polyclada* (Biondi and D'Alessandro 2012).

Materials and methods

Material examined consisted of dried pinned specimens preserved in the depositories listed in the "Abbreviations" section; abbreviations followed the list on the website The Insect and Spider Collections of the World (Evenhuis 2021). Species are attributed to the genera *Diamphidia*, *Polyclada*, and *Xanthophysca* focusing on type material and original species descriptions. Species whose taxonomic position at the genus level needs a revision are listed separately. Exact label data are cited for all type specimens; a double slash (//) divided the data on different labels and a single slash (/) divided the data in different rows. Information included in square brackets has been added to the label data using the Google Earth website for coordinates and geographic information. Geographic coordinates for the localities were reported in Degrees and Decimal Minutes (DDM) format using the WGS84 datum. [?] refers to undetectable or doubtful locality or illegible handwriting. Specimens were examined, measured, and dissected using a Leica M205C stereomicroscope. Photographs were taken using a Leica DMC5400 camera and compiled using Zerene Stacker software, v. 1.04. Scanning electron micrographs were taken using a Hitachi TM-1000. Terminology for genitalia follows Döberl (1986), Schmitt and Uhl (2015: fig. 1), and D'Alessandro et al. (2016: figs 10E, 11E). Terminology for the metafemoral spring or metafemoral extensor tendon (Nadein and Betz 2016) follows Furth (1982).

Abbreviations

Collections and depositories

BAQ	Italy, University of L'Aquila, Collection of M. Biondi;
MCZC	USA, Massachusetts, Cambridge, Harvard University, Museum of Comparative Zoology;
MNHN	France, Paris, Muséum National d'Histoire Naturelle;
MSNG	Italy, Genova, Museo Civico di Storia Naturale di Genova;
NHMUK	United Kingdom, London, The Natural History Museum;
NMPC	Czech Republic, Prague, National Museum (Natural History);
RMCA	Belgium, Tervuren, Musée Royal de l'Afrique Centrale.

Biometrics

LA	numerical sequence from base to apex of each antennomere, proportional to the length of the first antennomere;
LAED	length of median lobe of the aedeagus;
LAN	length of antennae;
LB	total body length (from apical margin of head to apex of elytra);
LE	length of elytra;
LF	maximum length of hind femora;

LP	medial length of pronotum;
LSP	maximum length of spermatheca, including ductus;
WE	maximum width of elytra combined;
WF	maximum width of hind femora;
WP	maximum width of pronotum.

Taxonomic account

Afrotropicaltica gen. nov.

https://zoobank.org/011F6C24-9303-4535-9952-09533542B544
Fig. 1

Description. Body subelliptical-elongate in dorsal view, with subparallel sides (Fig. 1A, B), distinctly convex in lateral view. Dorsal surface glabrous, bicoloured in the only known species, with yellowish head and pronotum, and reddish brown elytra. Head (Fig. 1E) with frontal grooves, frontal carina, and frontal calli barely distinguishable; surface smooth or micropunctate, with rounded punctures approx. as large as the supraorbital setiferous pore; puncture absent on the middle of front and vertex; eyes large, ovoidal; minimum distance between eyes on vertex, as wide as 2 × the interantennal space; interantennal space prominent compared to the clypeus, as wide as ~ 2/3 the length of the first antennomere; maxillary palpi three-articulated, and labial palpi bi-articulated, both with slender, subcylindrical segments. Antennae (Fig. 1A, B) with 11 antennomeres, filiform, longer than 1/2 the body length in both sexes, but slightly shorter in female; antennomere II slightly shorter than 1/2 of antennomere I and as long as 1/2 of antennomere III; antennomere IV as long as (female) or slightly longer (male) than antennomere III; antennomeres V–IX generally slightly longer than antennomere I (male) or approximately as long as antennomere I (female); antennomere X slightly shorter than antennomere I, especially in female; antennomere XI distinctly longer than antennomere I. Prothorax distinctly depressed dorsally (not subcylindrical). Pronotum (Fig. 1D) subrectangular, slightly convergent anteriorly, with curved, moderately expanded lateral margins, clearly visible in dorsal view; basal margin moderately arched; surface smooth to micropunctate without any groove or depression; anterior angles barely prominent; posterior angles widely obtuse; punctation rounded, quite sparse and irregularly distributed. Scutellum subtriangular. Elytra (Fig. 1A, B, D) subparallel, with base as wide as pronotal base; lateral margins finely bordered, barely visible in dorsal view; punctation rounded, variably arranged in numerous rows or bands, or almost confused. Epipleurae oblique, clearly visible in lateral view. Procoxal cavities open posteriorly; prosternum approx. as wide as the procoxal cavities; intercoxal prosternal process quite narrow; mesosternum slightly wider than prosternum, and distinctly wider than mesocoxal cavities; metasternum wider than mesosternum, twice the width of the metacoxal cavities; first abdominal ventrite as wide as metacoxal cavities. Posterior femora elliptical-elongate, moderately swollen; dorsal margin of middle and hind tibiae with distinct ciliate emargination, acute apically; hind tibiae straight in dorsal view; apical spur of hind tibiae simple; third visible metatarsomere deeply incised; fourth visible tarsomere of metatarsus simple, not swollen in both male and female; claws appendiculate. Metafemoral extensor tendon (Fig. 1H) with extended arm (ea: Fig. 1H) as long as ~ 1/2 the dorsal lobe (dl: Fig. 1H); dorsal-basal angle (dba: Fig. 1H)

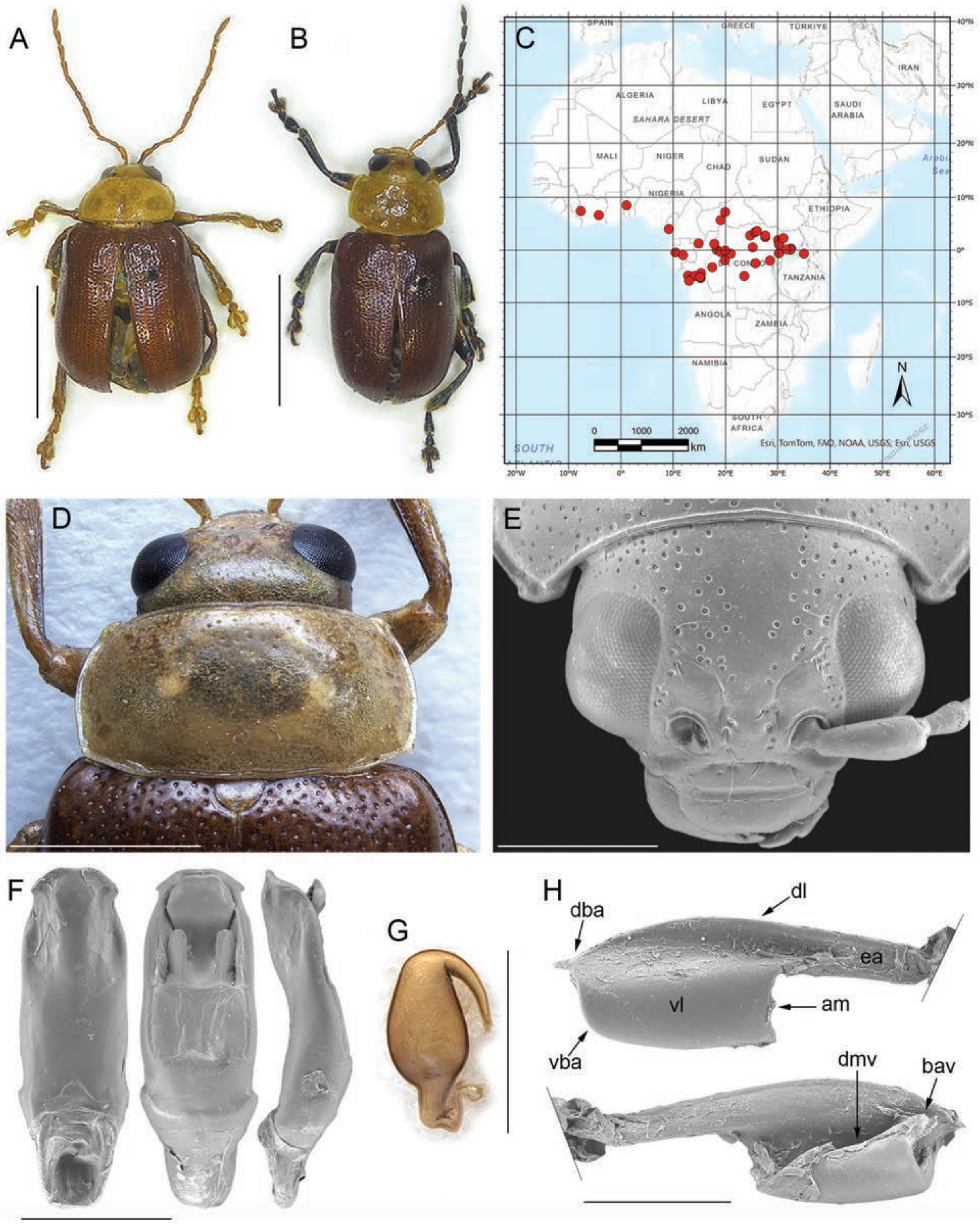

Figure 1. *Afrotropicaltica fulvipennis* (Jacoby) comb. nov. **A** lectotype of *Blepharida favareli* Achard, male, Ogooué, Sam-Kita, habitus **B** holotype of *Cladocera fulvipennis* Jacoby, male, habitus **C** distribution **D** head, pronotum, and base of elytra, male, Cameroun, Victoria **E** head, Republique du Congo, P.N. d'Odzala, Mbandza **F** median lobe of the aedeagus, from left to right in ventral, dorsal, and lateral view, Republique du Congo, P.N. d'Odzala, Mbandza **G** spermatheca, paralectotype of *Blepharida favareli* Achard, Democratic Republic of the Congo, Eala **H** metafemoral extensor tendon, Camerun, Victoria. Abbreviations: am: apical margin; bav: basal angle of the ventral lobe; dba: dorsal-basal angle; dl: dorsal lobe; dmv: dorsal margin of the ventral lobe; ea: extended arm; vba: ventral-basal angle; vl: ventral lobe. Scale bars: 3 mm (**A**, **B**); 1 mm (**D**, **E**, **F**, **G**); 500 μm (**H**).

approx. right angled, moderately prominent apically; ventral-basal angle (vba: Fig. 1H) distinctly obtuse and moderately rounded; apical margin of the tendon (am: Fig. 1H) slightly C-shaped; dorsal margin of ventral lobe (dmv: Fig. 1H) oblique; basal angle of ventral lobe (bav: Fig. 1H) quite close to the dorsal-basal angle of the tendon. Median lobe of the aedeagus (Fig. 1F) mostly subparallel in ventral view, with truncated apex, and curved in lateral view; dorsal ligula formed by a wider central lobe, and two lateral lobes. Spermatheca (Fig. 1G) with subovate basal part, narrowing towards ductus attach; distal part thin, without a distinct collum.

Type species. *Cladocera fulvipennis* Jacoby, 1895.

Etymology. The name of the new genus refers to flea beetle with strictly Afrotropical distribution. Gender feminine.

Distribution. Cameroon, Central African Republic, Democratic Republic of the Congo, Gabon, Ivory Coast, Kenya, Republic of South Africa, Togo, Uganda (Fig. 1C).

Afrotropicaltica fulvipennis **(Jacoby, 1895), comb. nov.**

Fig. 1

Cladocera fulvipennis Jacoby, 1895: 179.
= *Blepharida favareli* Achard, 1922: 8, syn. nov.
Blepharida fulvipennis (Jacoby, 1895): Achard 1922: 9, Bryant 1942: 161.
Diamphidia fulvipennis (Jacoby, 1895): Bechyné 1960: 111, Scherer 1969: 371.
Diamphidia fulvipennis favareli (Achard, 1922): Bechyné 1960: 111, Scherer 1962: 78, Scherer 1972: 16.
Diamphidia favareli (Achard, 1922): Laboissière 1941: 240, Biondi et al. 2017: 112.

Comments. Achard (1922) described *Blepharida favareli* and transferred *Cladocera fulvipennis* Jacoby to the genus *Blepharida*, due to the similarities with *B. favareli*. Bryant (1942) transferred *Cladocera fulvipennis* to *Blepharida*, as already proposed by Achard (1922). Bechyné (1960) established the combination *Diamphidia fulvipennis* (Jacoby, 1895) and considered the species described by Achard, *Blepharida favareli*, as a geographic form of *D. fulvipennis*. Scherer (1969) erroneously reported *Diamphidia fulvipennis* (Jacoby, 1895) as *Diamphidia fulvipennis* Jacoby, 1893. We formalize here the synonymy between *Cladocera fulvipennis* Jacoby, 1895 and *Blepharida favareli* Achard, 1922.

Type material examined. ***Holotype*** ♂ of *Cladocera fulvipennis*: "Type H.T // Togo / Africa // 42 // Type // Jacoby Coll. / 1909–28a. // *Cladocera* / *fulvipennis* / Jac. / Type" [8° 31.995'N 1° 5.853'E] (NHMUK). MCZC hosts the following specimen: "Type / 18327 // Boma / M. Tschoffen // Jacoby 2nd / Coll. // fulvipennis Jac." [Democratic Republic of the Congo, Boma, 5° 50.762'S 13° 4.296'E 5°52'32"S, 13°02'00"E] (photos available at https://mczbase.mcz.harvard.edu/guid/MCZ:Ent:18527). Lectotype ♂ of *Blepharida favareli* Achard, here designated: "Type // B. Favareli / Type / J. Achard det. // Ogooué / Sam-Kita" [Gabon, Samkita, 0° 26.516'S 10° 27.247'E] (NMPC). Paralectotype ♀ of *Blepharida favareli* Achard, here designated: "Type // B. Favareli / Type / J. Achard det. // Fort-Sibut / Oubanghi-Chari" [Central African Republic, Fort-Sibut, 5°43.57140'N 019°05.11590'E] (NMPC). Paralectotype ♀ of *Blepharida favareli* Achard, here designated: "Type // B. Favareli / Type / J. Achard det. // Musée du Congo / Eala / IX 1912 / R. Mayré" [Democratic Republic of Congo, Eala, 0° 2.441'N 18° 20.149'E] (NMPC).

Other material. CAMEROON • 16 specs, Victoria [= Limbé 4°1.917'N, 9°11.122'E], Jun.–Jul.1902, L. Fea leg. (MSNG). CENTRAL AFRICAN REPUBLIC • 1♀, Bamingui-Bangoran Pr., 45 km SSW Bamingui [7°16.400'N, 19°55.580'E], 450 m, 13–15 May 2009, A. Kudrna Jr leg. (BAQ). DEMOCRATIC REPUBLIC OF CONGO • 1 spec., Boma [5°50.762'S, 13°4.296'E], M. Tschoffen leg., Jacoby Coll. 1909-28a (NHMUK); 2 specs, ibid (RMCA); 1 spec., Eala [0°2.441'N, 18°20.149'E], Oct. 1935, J. Ghesquière leg. (RMCA); 1 spec., P.N. d'Odzala [1°16.167'N, 14°52.299'E], Mbandza, Nov. 1992, G. Carpaneto leg. (BAQ); 1 spec., Ekoiongouma, N1.20279 E17.88032 [1°12.16740' N, 17°52.81920' E], 341 m, 14 Feb. 2022, canopy light trap (-10 m), C.N. Hackfort & A. Tsoumou leg. (NHMUK); 1 spec., Lokandu [2°31.228'S, 25°44.566'E], Mar.1939, [Capt.] Marée leg. (NHMUK); 13 specs, ibid (RMCA); 1 spec., ibid, 1939 (RMCA); 3 specs, Equateur, Flandria [0°22.775'S, 19°5.500'E], 27 Oct.1932, R.P. Hulstaert leg. (RMCA); 1 spec., ibid, 31 Mar. 1932; 1 spec., Flandria, 15 Mar. 1932; 1 spec., ibid, 1931; 1 spec., Cataractes de Luozi [Luozi 4°54.711'S, 14°9.842'E], Dec. 1898, E. Luja leg. (RMCA); 1 spec., Bas-Congo, Lemfu [5°21.206'S, 15°15.709'E], Jun. 1945, Rév. P.L. De Reir leg. (RMCA); 1 spec., Tshuapa, Bokuma [0°40.648'S, 21°1.305'E], Dec. 1951, R.P. Lootens leg. (RMCA); 10 specs, Kisantu [5°7.473'S, 15°7.749'E], P. Goossens leg. (RMCA); 1 spec., ibid, ex col. Seeldrayers; 3 specs, ibid, 1905, col. Clavareau; 1 spec., Uelé, Dingila [3°38.633'N, 26°3.515'E], Jun. 1933, J.V. Leroy leg. (RMCA); 1 spec., Uelé, Paulis [= Isiro 2°46.212'N, 27°37.242'E], 1947, Abbeloos leg. (RMCA); 1 spec., Uelé, Bambesa [3°27.170'N, 25°41.579'E], 15 Sept. 1933, Lefèvre leg. (RMCA); 1 spec., Stanleyville [= Kisangani 0°30.542'N, 25°13.409'E], 1924, J. Ghesquière leg. (RMCA); 3 specs, Dima [3°16.47444'S, 17°28.99290'E], 14 Sept. 1908, A. Koller leg. (RMCA); 1 spec., Congo da Lemba [Lemba 4°24.598'S, 15°20.277'E], Jan. 1913, R. Mayné leg. (RMCA); 1 spec., ibid, 1–15 Apr. 1913; 7 specs, ibid, oct.–Dec.1911; 1 spec., Mongbwalu (Kilo) [1°55.640'N, 30°2.904'E], 1939, Mme Scheitz leg. (RMCA); 1 spec., Kilo [Kilo-Etat 1°49.738'N, 30°9.391'E], Dr. Abetti leg. (RMCA); 1 spec., Ganda Sundi [4°52.000'S, 12°52.000'E], [Comte J.] de Briey leg. (RMCA); 1 spec., Mahagi-Niarembe [between Mahagi and Niarembe 2°16.917'N, 31°3.371'E], 1935, Ch. Scops leg. (RMCA); 3 specs, Sud Ogowé, 'Ngomo [4°57.378'S, 23°37.289'E], [H.A.] Junod leg. (RMCA); 2 specs, Bas Congo, Maydi [5°11.958'S, 15°9.195'E], 1945, Rév. P. Van Eyen leg. (RMCA); 21 specs, ibid; 28 specs, ibid, 1942; 2 specs, ibid, 1943; 3 specs, Kivu, Kavumu à Kabunga, km 82 (Mingazi) [2°1.870'S, 28°30.949'E], Apr.–Jul.1951, H. Bomans leg. (RMCA); 1 spec., ibid, Nov.–Dec. 1951; 1 spec., ibid, 1951; 1 spec., Bas-Uele, Buta [2°47.787'N, 24°44.473'E], 1926, Fr. Joseph leg. (RMCA); 1 spec., Mayumbe, Makaia N'Tete [Mayumbe 2°30.000'N, 27°37.000'E], 24 Nov. 1915, R. Mayné leg. (RMCA); 1 spec., Busira [0°5.233'S, 19°55.086'E], 18 Oct.1905, Waelbroeck leg. (RMCA); 1 spec., Equateur, Bohuma [1°8.099'N, 30°13.892'E], 1938, R.P. Hulstaert leg. (RMCA); 1 spec., Ilenge [1°58.940'S, 19°52.474'E], 30 Jan. 1913, R. Mayné leg. (RMCA). GABON • 1♀, Gabon Français [0°59.062'S, 11°54.238'E] (NMPC). IVORY COAST • 1 spec., Andé, Bongouanou [Bongouanou 6°39.047'N, 4°11.247W], Mar. 1962, J. Decelle leg. (RMCA); 1 spec., 1171 m, Mt Tonkoui Peak, 07°27'15.2"N, 07°38'12.5"W [7°27.230'N, 7°38.148'W], 1–8 Nov. 2015, general collecting, M. Aristophanous, P. Moretto, E. Ruzzier leg. (NHMUK). KENYA • 1 spec., Brit. E. Africa, Nyangori, N Kavirondo [0°41.195'S, 35°0.679'E], 4800 ft, 18–19 May 1911, S.A. Neave leg. (NHMUK). UGANDA • 1 spec., Mawakota [Mawokota region 0°36.800'S, 30°12.695'E], Nov. 1931, [V.G.L.] van Someren leg. (NHMUK); 1 spec., Boy [Bay (?)], Entebbe [0°3.290'N, 32°28.216'E], 2800-4000 ft, forest within four miles of Kitabi Hill, May–Jun. 1913, C.A. Wiggins leg. (NHMUK); 1 spec., Entebbe, 14 Aug. 1911, C.C. Gowdey leg. (NHMUK); 1 spec., Prot. Entebbe, 12–20 Jan. 1912, S.A. Neave leg. (RMCA); 1 spec., Kampala [0°19.253'N, 32°35.055'E], 1–10 Jan. 1918, C.C. Gowdey leg. (NHMUK); 1 spec., Shores of L. Isolt, or Wamala [Wamala 0°7.799'N, 31°38.115'E], 3800 ft, 7–8 Jan. 1912, S.A. Neave leg. (NHMUK).

Redescription. Body subelliptical-elongate in dorsal view with parallel sides (Fig. 1A, B), distinctly convex in lateral view; total length of the body (LB) = 8.10 ± 0.91 mm ($6.50 \leq LB \leq 9.70$ mm) in male, and 8.77 ± 0.65 mm ($7.52 \leq LB \leq 9.51$ mm) in female; maximum pronotal width in the middle: WP = 3.43 ± 0.29 mm ($2.86 \leq WP \leq 3.78$ mm) in male, and 3.71 ± 0.25 mm ($3.30 \leq WP \leq 3.98$ mm) in female; maximum width of elytra in the middle: WE = 4.37 ± 0.37 mm ($3.69 \leq WE \leq 4.85$ mm) in male, and WE = 4.94 ± 0.42 mm ($4.46 \leq WE \leq 5.72$ mm) in female; WE/WP = 1.27 ± 0.04 ($1.22 \leq WE/WP \leq 1.33$) in male, and WE/WP = 1.33 ± 0.05 ($1.29 \leq WE/WP \leq 1.44$) in female.

Head and pronotum yellowish (Fig. 1A, B, D); elytra reddish brown; scutellum paler than elytra, often of the same colour as the pronotum or slightly darker; underside yellowish to pale brown; mouthparts yellowish, with black distal part of mandibles; antennae and legs with two colour patterns: both antennae and legs rather homogenous, yellowish to reddish brown, at most with slightly paler tarsi; antennal segments 1–4 yellowish and 5–11 blackish, and legs mostly blackish with the exception of femora, paler in their proximal part. Head (Fig. 1E) with smooth to micropunctate surface and sparse, rounded punctures, denser on vertex and near the inner ocular margins; frontal grooves and frontal calli barely distinguishable; frontal carina wide, not raised; eyes large, ovoidal; interantennal space as wide as ~ 2/3 the length of the first antennomere. Antennae (Fig. 1A, B) filiform, longer than 1/2 the body length: LAN = 6.07 ± 0.44 mm ($5.43 \leq LAN \leq 6.69$ mm) in male, and 5.62 ± 0.39 mm ($5.04 \leq LAN \leq 6.31$ mm) in female, and LAN/LB = 0.75 ± 0.05 ($0.65 \leq LAN/LB \leq 0.84$) in male, and 0.64 ± 0.03 ($0.60 \leq LAN/LB \leq 0.68$) in female. LA = 100:42:83:92:117:117:117:108:100:92:125 in male, and 100:42:83:83:108:100:100:92:83:83:117 in female. Pronotum (Fig. 1D) distinctly transverse: LP = 1.79 ± 0.17 mm ($1.50 \leq LP \leq 1.94$ mm) in male, and 1.85 ± 0.12 mm ($1.65 \leq LP \leq 2.04$ mm) in female, and WP/LP = 1.91 ± 0.06 ($1.80 \leq WP/LP \leq 2.00$) in male, and 2.01 ± 0.03 ($1.95 \leq WP/LP \leq 2.05$) in female; lateral margins slightly convergent anteriorly, moderately to distinctly curved, moderately expanded, visible in dorsal view; basal margin moderately arched; surface smooth to micropunctate; main punctation formed by rounded punctures, clearly impressed, quite sparse and irregularly distributed. Scutellum subtriangular, laterally rounded. Elytra (Fig. 1A, B, D) subparallel, clearly longer than wide, jointly rounded apically. LE = 6.57 ± 0.54 mm ($5.43 \leq LE \leq 7.23$ mm) in male, and 7.21 ± 0.48 mm ($6.40 \leq LE \leq 7.86$ mm) in female; WE/LE = 0.67 ± 0.02 ($0.63 \leq WE/LE \leq 0.70$) in male, and 0.68 ± 0.02 ($0.66 \leq WE/LE \leq 0.73$) in female; LE/LP = 3.66 ± 0.12 ($3.50 \leq LE/LP \leq 3.91$) in male, and 3.90 ± 0.09 ($3.80 \leq LE/LP \leq 4.05$) in female. Lateral margins finely bordered, indistinctly visible in dorsal view; surface very finely micropunctate or microwrinkled; main punctation clearly impressed, dense, variably arranged in numerous rows or bands, or almost confused. Humeral calli distinctly raised. Macropterous. Posterior femora moderately swollen (WF/LF = 0.44 ± 0.01); apical spur of hind tibiae very short; first tarsomere of fore- and middle legs clearly enlarged in male. Median lobe of the aedeagus (Fig. 1F) in ventral view: outline mostly subparallel with slightly sinuate margins, and narrower subapical part; apex truncated, distinctly expanded laterally; surface smooth, concave laterally and prominent medially in the apical third; in lateral view median lobe distinctly curved, with slightly sinuate outline; dorsal ligula formed by a wide central lobe, and two shorter and thinner lateral lobes, with base at apical ~ 1/3; LAED = 2.26 ± 0.10 mm (2.13 ≤ LAED ≤ 2.43 mm); LE/LAED = 2.90 ± 0.19 (2.55 ≤ LE/LAED ≤ 3.17). Basal part of the spermatheca (Fig. 1G) subovate, abruptly narrowing towards the ductus insertion; ductus short, thick, uncoiled, ventrally inserted; distal part of the spermatheca clearly bent towards the basal part, thin, acute apically; LSP = 0.93 ± 0.05 mm (0.87 ≤ LSP ≤ 1.02 mm); LE/LSP = 7.78 ± 0.25 (7.33 ≤ LE/LSP ≤ 8.11).

Distribution. Cameroon, Central African Republic, Democratic Republic of the Congo, Gabon, Ivory Coast, Kenya, Republic of South Africa, Togo, Uganda (Fig. 1C).

Ecological notes. Ecology, including host plant, unknown.

Key to the Afrotropical genera of the *Blepharida* group

The combination of characters identifying *Blepharidina* and *Calotheca* was based on recent revisions (Biondi et al. 2017, 2019; D'Alessandro et al. 2018a, 2019, 2020, 2021, 2022, 2023a, 2023b). Regarding *Diamphidia*, *Polyclada*, and *Xanthophysca*, characters reported in the key were derived from the species whose genus attribution was unequivocal, due to their similarities with the type species.

1 Antennae filiform, at most with distal segments slightly enlarged (Figs 1A, B, 2A, 3A, 6A); segment 4 approx. as long as 3 .... **2**

– Antennae pectinate, serrate, or with middle segments clearly subtriangular (Figs 4A, 5A); segment 4 distinctly longer than 3 .... **5**

2 Pronotal punctation not homogenous, with at least some larger and more deeply impressed punctures arranged in lines (at least one line) or dense groups (Figs 2B, C, 3B, C).. **3**

– Pronotal punctation uniform in size, homogenously or slightly irregularly distributed (Figs 1D, 4B, 5B, 6B) **4**

3 Pronotum with main punctation arranged in two striae that are straight, L-, or C- shaped, running from the anterior margin towards the disc (ps: Fig. 3B, C); basal longitudinal furrows or small dimples are present in some species (bf: Fig. 3B). Frontal grooves elongate, sinuate, and deeply impressed from the superior ocular margin to the interantennal space (fg: Fig. 3E); frons surface not depressed between antennal sockets and clypeus. Extended arm of the metafemoral extensor tendon ~ 1/3 the length of the dorsal lobe; apical margin of the tendon clearly C-shaped (Fig. 3D) .... ***Calotheca* Heyden**

– Pronotum with main punctation arranged in patches, and oblique, transverse, or longitudinal lines (Fig. 2B, C). Frontal grooves, not distinguishable (Fig. 2E), or at most short and moderately impressed; frons surface depressed between antennal sockets and clypeus. Extended arm of the metafemoral extensor tendon slightly shorter than 1/2 the length of the dorsal lobe; apical margin of the tendon moderately C-shaped (Fig. 2D) .... ***Blepharidina* Bechyné**

4 Procoxal cavities closed posteriorly. Pronotal punctation mostly uniform and dense (Fig. 6B). Frontal grooves distinctly impressed, from the antennal sockets to the upper ocular margin (Fig. 6B). Hind femur with a distinct emargination on the posterior side in both sexes, but more evi-

dent and tooth-shaped in male (Fig. 6A). Ductus spermathecae sub-truncate, practically absent (Fig. 6E). General shape of the median lobe of the aedeagus roughly subcylindrical (Fig. 6D). Metafemoral extensor tendon as in Fig. 6C .... ***Xanthophysca* Fairmaire**

– Procoxal cavities open posteriorly. Pronotal punctation mostly uniform and sparse (Fig. 1D). Frontal grooves, if distinguishable, short and moderately impressed (Fig. 1E). Hind femur without a distinct emargination on the posterior side. Ductus spermathecae present (Fig. 1G). General shape of the median lobe of the aedeagus clearly flatter (Fig. 1F). Metafemoral extensor tendon as in Fig. 1H.............................. ***Afrotropicaltica* gen. nov.**

5 Eye large and generally distinctly convex (Fig. 5B). Antennae pectinate (generally in males) (Fig. 5A) or clearly serrate. Body distinctly elongate (Fig. 5A), with elytra subparallel laterally, or wider in the apical third. Extended arm of the metafemoral extensor tendon ~ 1/2 the length of the dorsal lobe; apical margin C-shaped (Fig. 5D). Median lobe of the aedeagus (Fig. 5C) straight in lateral view, with apical part thickset and bent ventrally. Spermatheca (Fig. 5E) with basal part roughly subcylindrical, and ductus apically inserted .... ***Polyclada* Chevrolat**

– Eye small and moderately convex (Fig. 4B). Antennae with subtriangular or moderately serrate middle segments (Fig. 4A). Body generally robust, elliptical, more or less elongate, with elytra rounded laterally (Fig. 4A). Extended arm of the metafemoral extensor tendon distinctly longer than 1/2 the length of the dorsal lobe; apical margin widely arched (am: Fig. 4E). Median lobe of the aedeagus (Fig. 4C) slightly curved in lateral view, with apical part flat, depressed on the ventral surface, and softly curved ventrally. Spermatheca (Fig. 4D) with basal part generally slightly sinuate, dorsally bent at the ductus attachment .... ***Diamphidia* Gerstaecker**

List of *Diamphidia* species

Diamphidia femoralis Gerstaecker, 1855, type species
Diamphidia angolensis Jacoby, 1882
Diamphidia brevis Laboissière, 1942
Diamphidia concinna Weise, 1906
Diamphidia curtula Achard, 1922
Diamphidia flaveola Laboissière, 1941
Diamphidia flaviceps (Allard, 1887)
Diamphidia jacobyi (Gestro, 1895)
Diamphidia lesnei Achard, 1922
Diamphidia limbata (Allard, 1887)
Diamphidia locusta Fairmaire, 1893
Diamphidia longula Weise, 1902
Diamphidia nigrifrons (Allard, 1887)
Diamphidia nigripennis (Jacoby, 1888)
Diamphidia nigroornata Stål, 1858
Diamphidia patricki Bryant, 1948
Diamphidia rhabdoscelis Laboissière, 1942
Diamphidia robusta (Allard, 1887)

Diamphidia rugipennis Laboissière, 1942
Diamphidia semiopaca Achard, 1922
Diamphidia simplex (Peringuey, 1892)
Diamphidia uniformis (Jacoby, 1903)
Diamphidia vittatipennis Baly, 1865

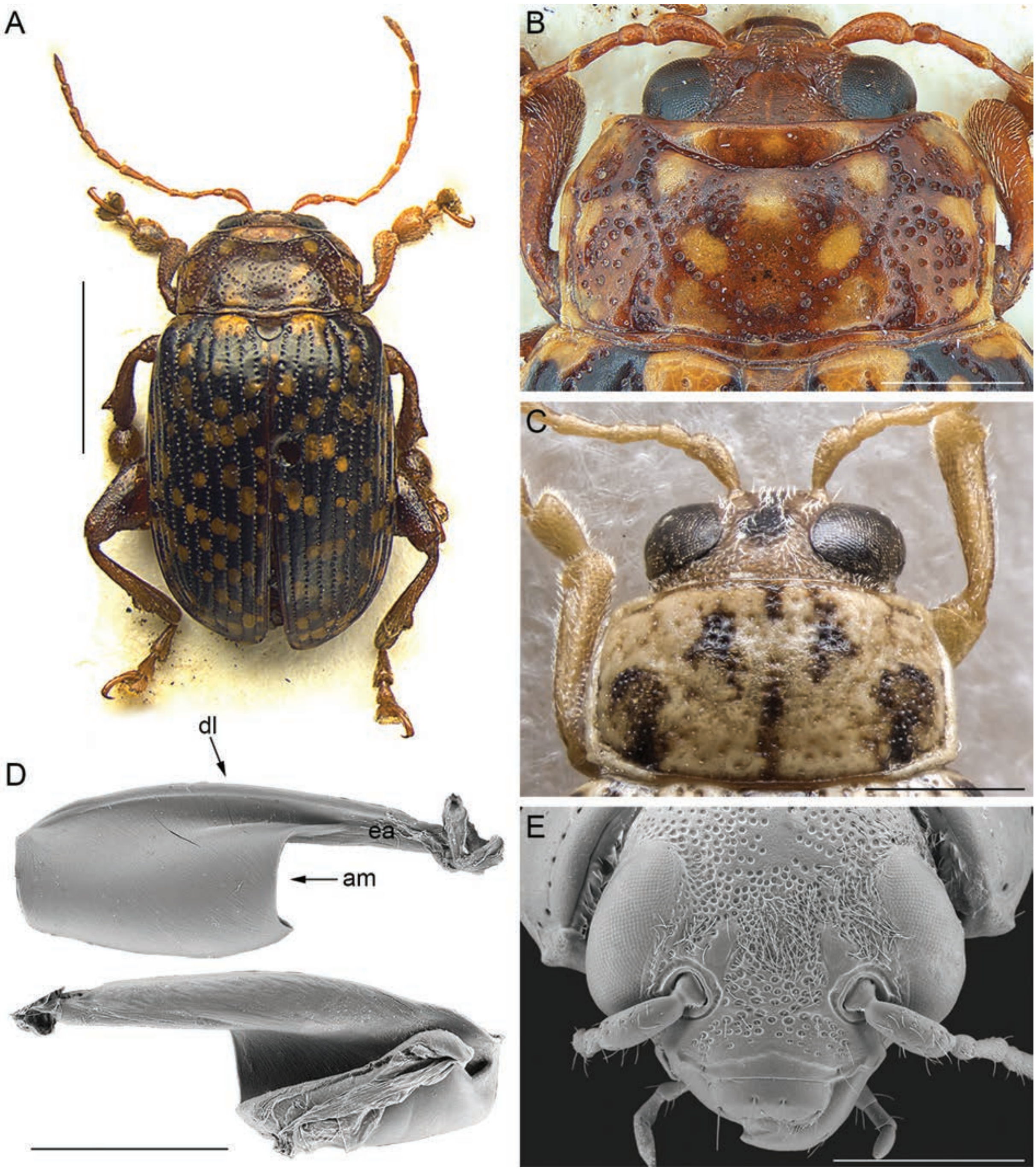

Figure 2. *Blepharidina* Bechyné **A** habitus of *Blepharidina* (*Blepharidina*) *guttulata* (Baly), male, modified from D'Alessandro et al. (2019) **B** ibid, head, and pronotum **C** head and pronotum of *Blepharidina* (*Afroblepharida*) *gedyei*, male, Kenya, Sosoma (BAQ) **D** metafemoral extensor tendon, modified from Biondi et al. (2017) **E** head of *Blepharidina intermedia*, modified from Biondi et al. (2017). Abbreviations: am: apical margin; dl: dorsal lobe; ea: extended arm. Scale bars: 3 mm (**A**); 1 mm (**B**, **C**, **E**); 500 µm (**D**).

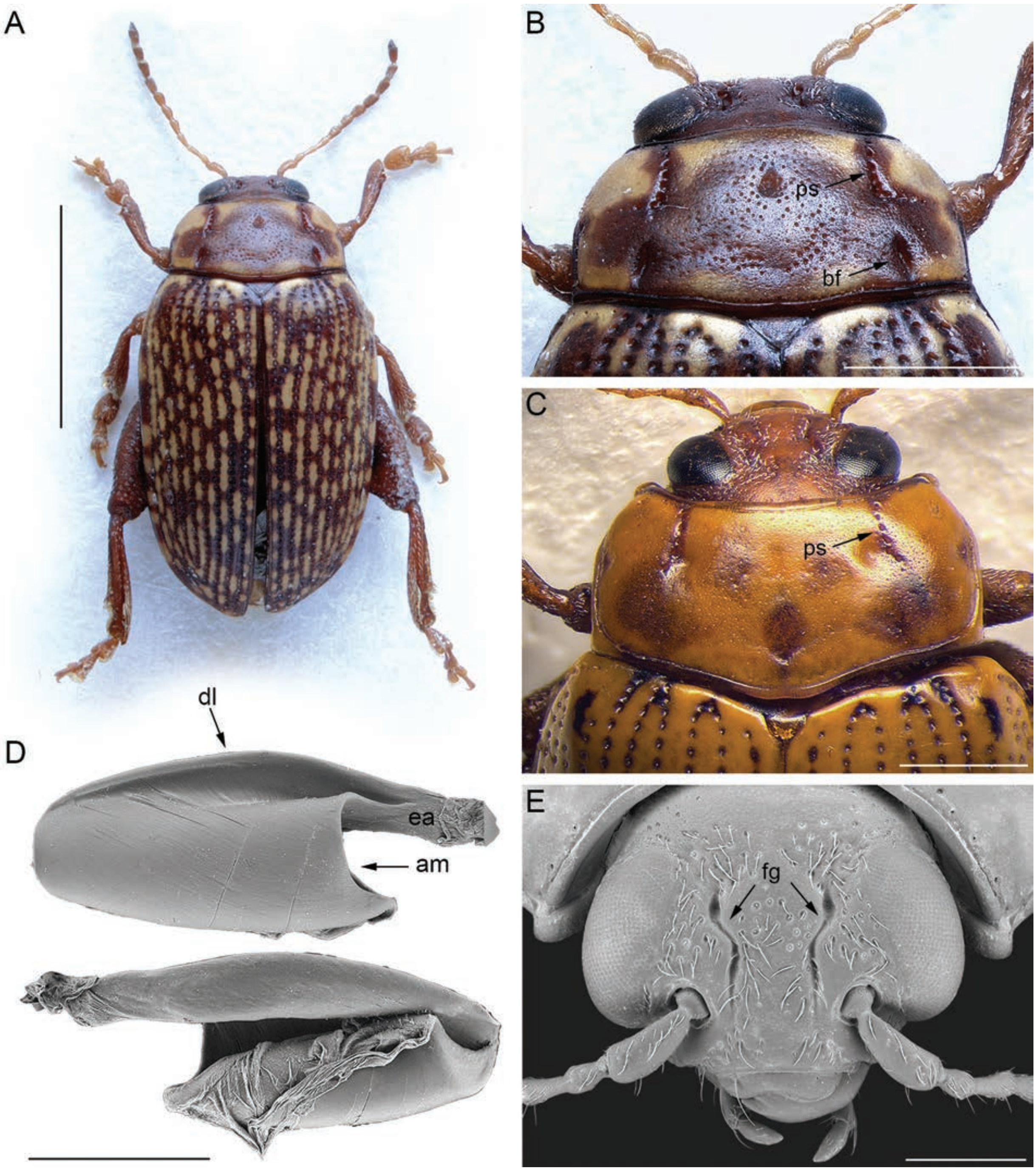

Figure 3. *Calotheca* Heyden **A** habitus of *Calotheca haroldi* (Baly), male, Republic of South Africa, Kranskloof (SANC) **B** ibid, head and pronotum **C** head and pronotum of *Calotheca marginalis*, modified from Biondi et al. (2017) **D** ibid, metafemoral extensor tendon **E** ibid, head. Abbreviations: am: apical margin; bf: basal furrow; dl: dorsal lobe; ea: extended arm; fg: frontal groove; ps: punctate stria. Scale bars: 3 mm (**A**); 1 mm (**B**, **C**); 500 µm (**D**, **E**).

List of *Polyclada* species

Polyclada pectinicornis (Olivier, 1791), type species
Polyclada benti Gahan, 1895
Polyclada bohemani (Baly, 1861)
Polyclada coriacea Achard, 1922
Polyclada kenyensis Bryant, 1942

Polyclada maculicollis Bryant, 1942
Polyclada ornata (Baly, 1861)
Polyclada ornatipennis Bryant, 1942
Polyclada somaliensis Bryant, 1948
Polyclada variegata (Weise, 1900)

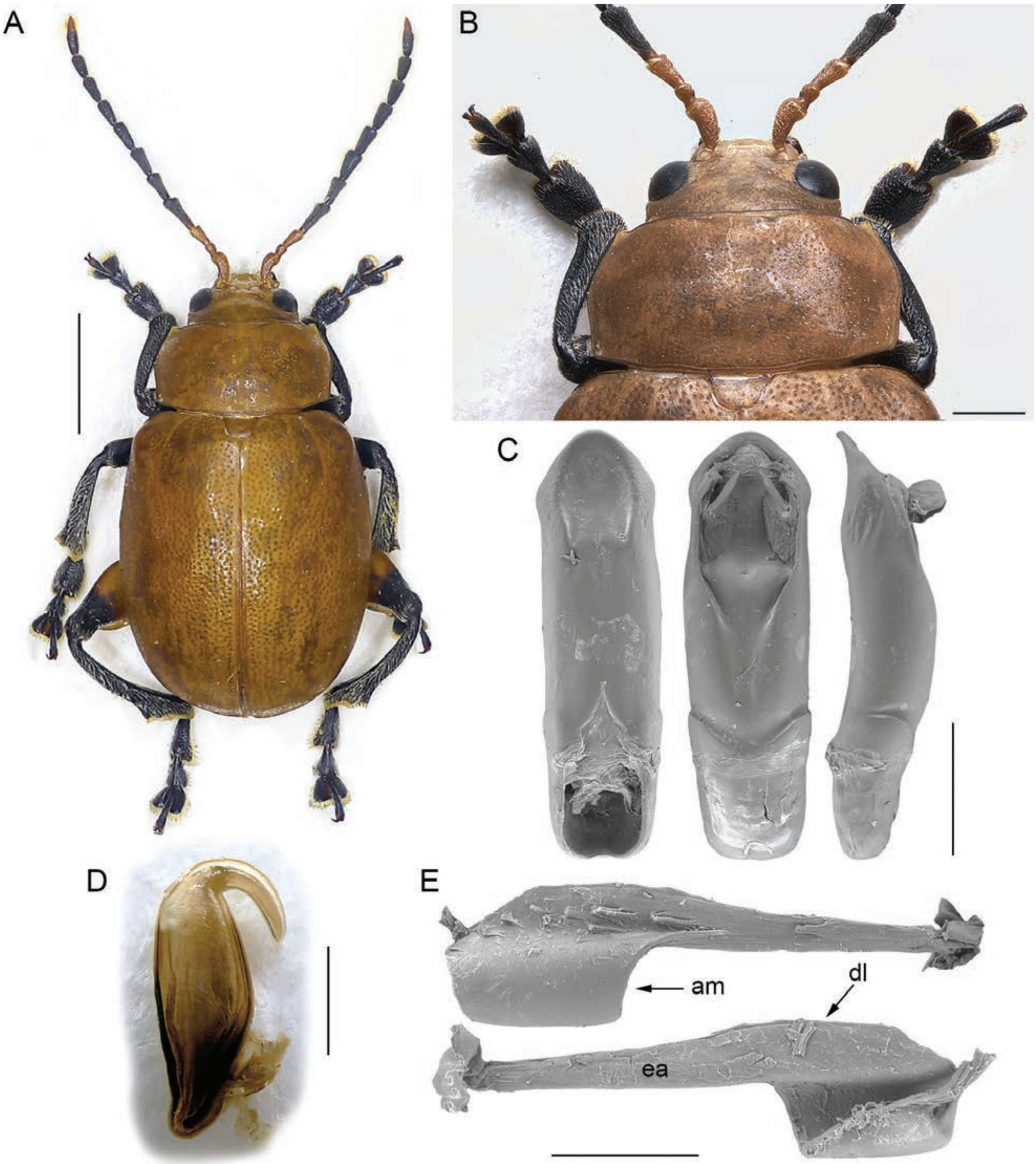

Figure 4. *Diamphidia* Gerstaecker **A** habitus of *Diamphidia femoralis*, male, Mozambique, 25 km N Tete (NMPC) **B** ibid, pronotum and base of elytra **C** ibid, median lobe of the aedeagus, from left to right in ventral, dorsal, and lateral view, Zambia, Victoria Falls (BAQ) **D** ibid, spermatheca, Transvaal, Pretoria (MSNG) **E** ibid, metafemoral extensor tendon, Republic of South Africa, Blyde River Canyon (BAQ). Abbreviations: am: apical margin; dl: dorsal lobe; ea: extended arm. Scale bars: 3 mm (**A**); 1 mm (**B**, **C**); 500 µm (**D**, **E**).

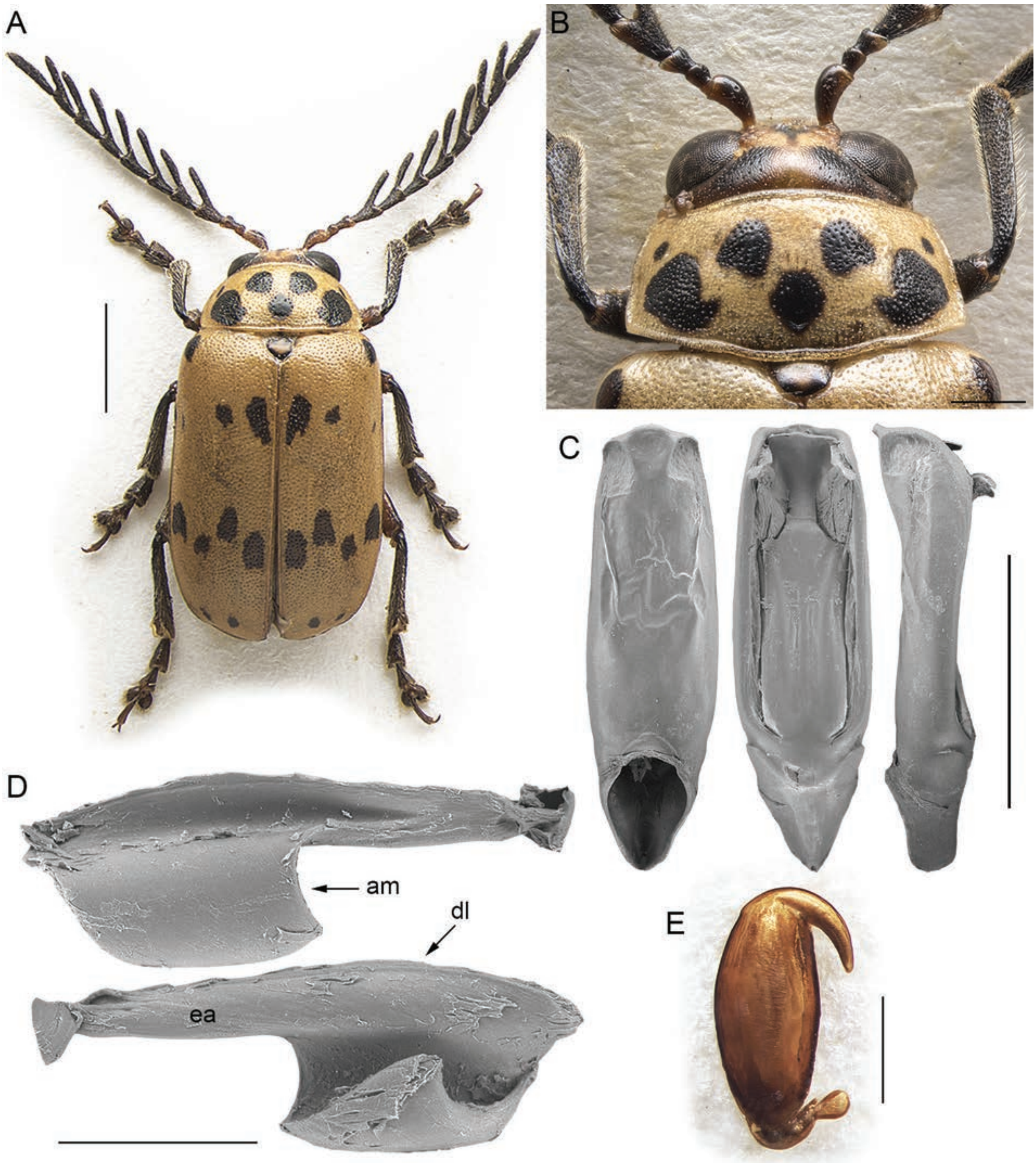

Figure 5. *Polyclada* Chevrolat **A** habitus of *Polyclada pectinicornis*, male, modified from Biondi et al. (2022) **B** ibid, pronotum and base of elytra, male, Somalia, Bardera (BAQ) **C** ibid, median lobe of the aedeagus, from left to right in ventral, dorsal, and lateral view, modified from Biondi et al. (2022) **D** ibid, spermatheca **E** ibid, metafemoral extensor tendon, Tanzania, Mto. Wa Mbu (BAQ). Abbreviations: am: apical margin; dl: dorsal lobe; ea: extended arm. Scale bars: 3 mm (**A**); 1 mm (**B**, **C**); 500 µm (**D**, **E**).

List of *Xanthophysca* species

Xanthophysca perrieri Fairmaire, 1901, type species
Xanthophysca androyana Achard, 1915
Xanthophysca donckieri Achard, 1915
Xanthophysca kolbei Weise, 1910
Xanthophysca variegata Achard, 1915

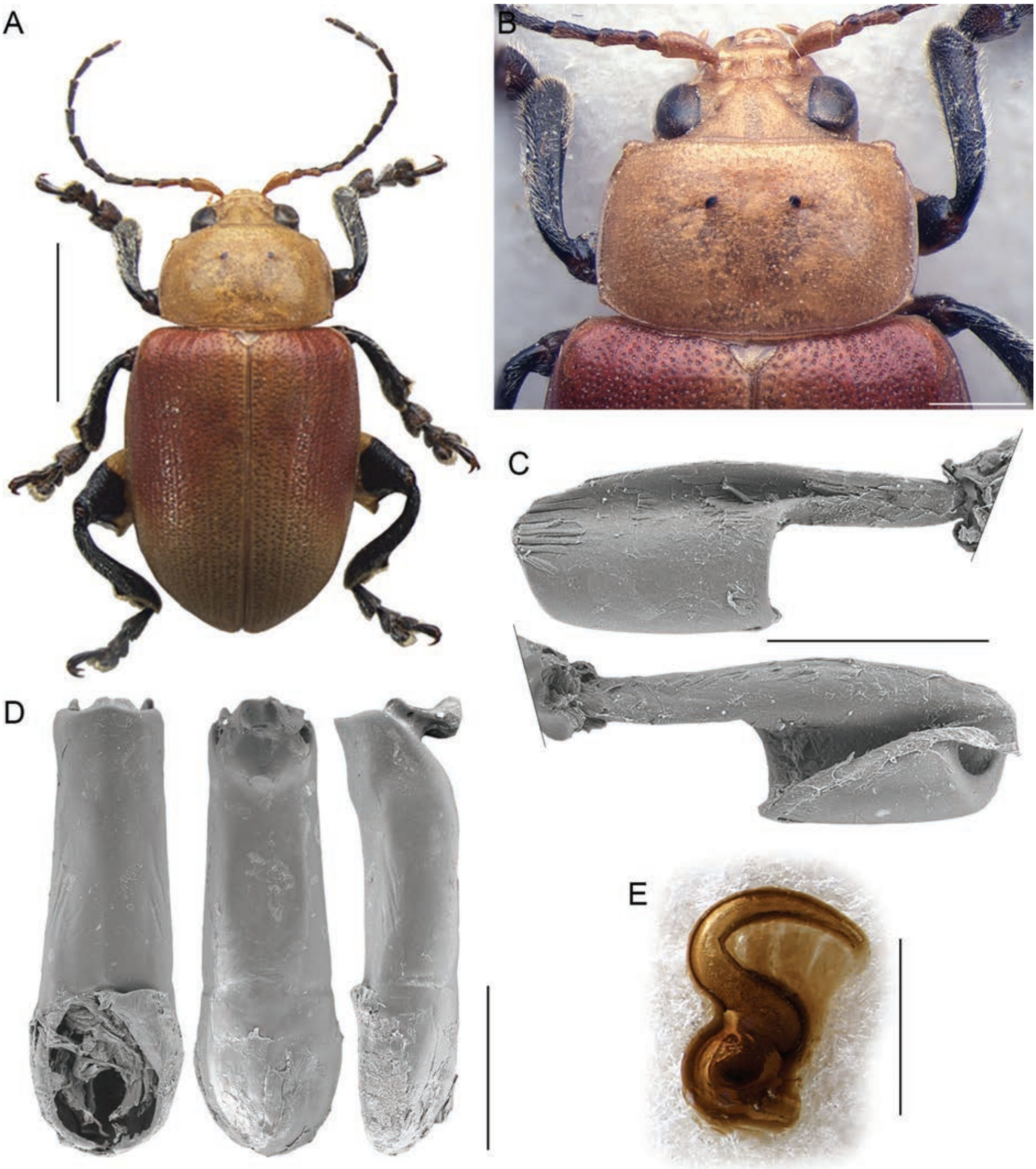

Figure 6. *Xanthophysca* Fairmaire **A** habitus of *Xanthophysca perrieri*, male, modified from Biondi and D'Alessandro (2012) **B** ibid, pronotum and base of elytra **C** metafemoral extensor tendon, Madagascar Ouest, Antsingy (MNHN) **D** ibid, median lobe of the aedeagus, from left to right in ventral, dorsal, and lateral view **E** ibid, spermatheca, Madagascar, Ankarafantsika Rés. nat. (MNHN). Scale bars: 3 mm (**A**); 1 mm (**B**, **D**); 500 µm (**C**, **E**).

The taxonomic position at genus level of some species is unclear because they lack one or more characters typical of *Diamphidia*, *Polyclada*, or *Xanthophysca*. These are *Polyclada bedeli* Achard, 1922 with antennae of the *Diamphidia* type; *Polyclada flavipennis* Bryant, 1942 and *P. marginata* Bryant, 1948 with antennae of the *Diamphidia* type and aedeagus lacking the typical *Polyclada* characters; *Polyclada flexuosa* (Baly, 1865) with aedeagus different from the typical *Polyclada* species; *Diamphidia ornaticollis* Bryant, 1948, with closed procoxal cavities and filiform antennae.

Discussion

Afrotropicaltica fulvipennis (Jacoby) comb. nov. was referred to different genera in the previous publications (*Cladocera*, *Blepharida*, *Diamphidia*). However, based on its unique combination of characters, it is not attributable to any of the known flea beetle genera. Considering the diagnostic characters used to identify the main groups of Afrotropical flea beetles (Biondi and D'Alessandro 2012), *Afrotropicaltica* gen. nov. can be grouped with *Diamphidia*, *Blepharidina*, *Calotheca*, *Polyclada*, and *Xanthophysca*, traditionally attributed to the *Blepharida* group sensu Furth and Lee (2000). The following traits characterise these genera: antennae with 11 antennomeres; apical tarsomere of metatarsus simple (not swollen); dorsal margin of middle and hind tibiae with distinct ciliate emargination, which is acute or subrounded apically; prothorax distinctly depressed dorsally (not subcylindrical); first metatarsomere as long as the second or longer, wide, subtriangular or subrounded; body length generally ≥ 4.00 mm; claws generally appendiculate; pronotal sculpture variable but without any ante-basal transverse sulcus. Differences in antennae, pronotum, and elytra are helpful for genera and subgenera identification, as reported in the diagnostic key above.

Genus *Xanthophysca* lacks a comprehensive revision, but the diagnostic characters are coherent among the species attributed to it. Differently, some species currently attributed to *Polyclada* and *Diamphidia* show a combination of characters that makes them not referrable as *Polyclada* or *Diamphidia*. Therefore, *Xanthophysca* and especially *Diamphidia* and *Polyclada* need a revision, also based on the undetermined material and undescribed species present in public and private collections.

Furth and Lee (2000), while providing their morphological synthesis of the *Blepharida* group of genera, stated that some characters are not shared by all the taxa. This is true also for the genera discussed here. Assessing the monophyly of the group and the evolutionary affinity among the included taxa requires a more extensive investigation, also requiring molecular data. The same problems are present for assessing the existence of a wider *Blepharida* group clade.

Acknowledgments

We are grateful to the collection managers and curators who enabled us to study the material preserved in their Institutions: Antoine Mantilleri (MNHN), Roberto Poggi (MSNG), Michael Geiser (NHMUK), Lukas Sekerka (NMPC), and Didier Van den Spiegel and Stéphane Hanot (RMCA). We sincerely thank Alexander S. Konstantinov (National Museum of Natural History, Washington DC, USA) and David G. Furth (Department of Entomology, Smithsonian Institution, Washington DC, USA) for spending time improving our manuscript.

Additional information

Conflict of interest

The authors have declared that no competing interests exist.

Ethical statement

No ethical statement was reported.

Funding

No funding was reported.

Author contributions

Conceptualization: MB, PD. Data curation: PD. Investigation: PD. Resources: PD, MB. Validation: MB. Visualization: PD, MB. Writing - original draft: PD. Writing - review and editing: MB.

Author ORCIDs

Paola D'Alessandro https://orcid.org/0000-0002-4481-9152
Maurizio Biondi https://orcid.org/0000-0003-2190-7376

Data availability

All of the data that support the findings of this study are available in the main text.

References

Achard J (1915) Halticides malgaches du genre *Xanthophysca* Fairm. [Col. Phytophaga]. Annales de la Société entomologique de France 84(4): 459–462. https://doi.org/10.1080/21686351.1915.12279409

Achard J (1922) Descriptions de nouveaux Halticini (Col. Chrysomelidae). Fragments Entomologiques 27(3): 3–10. https://doi.org/10.3406/bsef.1922.26922

Allard E (1887) Bulletin entomologique: diagnoses de quelques espèces nouvelles de Coléoptères Phytophages. Annales de la Société entomologique de France 7(6e serie): CC–CCI.

Baly JS (1861) Descriptions of new genera and species of Phytophaga. The Journal of Entomology 1: 193–206, 275–302, 450–459.

Baly JS (1865) LV.—Descriptions of new genera and species of Gallernucidæ. Annals and Magazine of Natural History 16: 402–410. https://doi.org/10.1080/00222936508679458

Becerra JX (2004) Molecular systematics of *Blepharida* beetles (Chrysomelidae: Alticinae) and relatives. Molecular Phylogenetics and Evolution 30: 107–117. https://doi.org/10.1016/S1055-7903(03)00158-1

Bechyné J (1960) Alticidae (Coleoptera, Phytophagoidea). Exploration du Parc National de l'Upemba. I. Miss. G.F. de Witte 59(3): 39–114.

Bechyné J (1968) Contribution à la faune du Congo (Brazzaville). Mission A. Villiers et A. Descarpentries. LXXXI. Coleopteres Alticidae. Bulletin de L'institut Francais d'Afrique Noire (série A) 30: 1687–1728.

Biondi M, D'Alessandro P (2010) Genus-group names of Afrotropical flea beetles (Coleoptera: Chrysomelidae: Alticinae): Annotated catalogue and biogeographical notes. European Journal of Entomology 107: 401–424. https://doi.org/10.14411/eje.2010.049

Biondi M, D'Alessandro P (2012) Afrotropical flea beetle genera: A key to their identification, updated catalogue and biogeographical analysis (Coleoptera, Chrysomelidae, Galerucinae, Alticini). Zookeys 253: 1–158. https://doi.org/10.3897/zookeys.253.3414

Biondi M, Frasca R, Grobbelaar E, D'Alessandro P (2017) Supraspecific taxonomy of the flea beetle genus *Blepharida* Chevrolat, 1836 (Coleoptera: Chrysomelidae) in the Afrotropical Region and description of *Afroblepharida* subgen. nov. Insect Systematics & Evolution 48: 97–155 https://doi.org/10.1163/1876312X-48022152

Biondi M, Iannella M, D'Alessandro P (2019) Unravelling the taxonomic assessment of an interesting new species from Socotra Island: *Blepharidina socotrana* sp. nov. (Coleoptera: Chrysomelidae). Acta Entomologica Musei Nationalis Pragae 59(2): 499–505. https://doi.org/10.2478/aemnp-2019-0040

Biondi M, D'Alessandro P, Cerasoli F, De Simone W, Iannella M (2022) Taxonomy, Habitat Preference, and Niche Overlap of Two Arrow-Poison Flea Beetle Species of the Genus *Polyclada* in Sub-Saharan Africa (Coleoptera, Chrysomelidae). Insects 13: 668. https://doi.org/10.3390/insects13080668

Biondi M, Iannella M, D'Alessandro P (2024) Ecological profile of the flea beetle genus *Calotheca* Heyden in South Africa (Chrysomelidae, Galerucinae, Alticinae). Insects 15: 994. https://doi.org/10.3390/insects15120994

Bryant GE (1942) New species of *Polyclada* (Coleoptera, Halticinae) from Africa. Proceedings of the Royal Entomological Society of London. Series B, Taxonomy 11(11): 161–165. https://doi.org/10.1111/j.1365-3113.1942.tb00716.x

Bryant GE (1948) XII.—New species of Chrysomelidæ (Halticinæ) from East Africa, Annals and Magazine of Natural History, Series 12, 1(3): 145–171. https://doi.org/10.1080/00222934808653898

Calcetas OA, Staines CI (2024) New Species of the Genus *Podontia* Dalman (Coleoptera: Chrysomelidae: Galerucinae: Alticini) in the Philippines and Redescription of *Podontia flava* Baly from Sarawak. Philippine Journal of Science 153 (3): 903–909. https://doi.org/10.56899/153.03.13

Chaboo CS, Grobbelaar E, Larsen A (2007) Fecal Ecology in Leaf Beetles: Novel Records in the African Arrow-Poison Beetles, *Diamphidia* Gerstaecker and *Polyclada* Chevrolat (Chrysomelidae: Galerucinae). The Coleopterist Bulletin 61: 297–309. https://doi.org/10.1649/0010-065X(2007)61[297:FEILBN]2.0.CO;2

Chapuis MF (1875) Histoire naturelle des Insectes. Genera des Coléopteres ou exposé méthodique et critique de tous les genres proposés jusqu'ici dans cet ordre d'Insectes. Par M. M. Lacordaire et F. Chapuis. Tome onzième. Famille des Phytophages. Paris, 420 pp. [+ pls 124–134]

Chevrolat (1837) Catalogue des Coléoptères de la collection de M. le Comte Dejean. Troisième édition, revue, corrigée et augmentée, livr. 5. Dejean PFMA (Ed.). Librairie Méquignon-Marvis Père et Fils, Paris, [i–xiv +] 385–503]. https://www.biodiversitylibrary.org/item/285852#page/390/mode/1up

D'Alessandro P, Biondi M (2023) Generic placement of the African flea beetle *Polyclada maculipennis* Bryant and the possible occurrence of the genus *Procalus* Clark in sub-Saharan Africa (Coleoptera, Chrysomelidae, Galerucinae, Alticini). ZooKeys 1145: 181–189. https://doi.org/10.3897/zookeys.1145.90667

D'Alessandro P, Samuelson A, Biondi M (2016) Taxonomic revision of the genus *Arsipoda* Erichson, 1842 (Coleoptera, Chrysomelidae) in New Caledonia. European Journal of Taxonomy 230: 1–61. https://doi.org/10.5852/ejt.2016.230

D'Alessandro P, Frasca R, Grobbelaar E, Iannella M, Biondi M (2018a) Systematics and biogeography of the Afrotropical flea beetle subgenus *Blepharidina* (*Afroblepharida*) Biondi & D'Alessandro, with description of seven new species (Coleoptera, Chrysomelidae, Galerucinae, Alticini). Insect Systematics & Evolution 49: 443–480. https://doi.org/10.1163/1876312X-00002182

D'Alessandro P, Iannella M, Frasca R, Biondi M (2018b) Distribution patterns and habitat preference for the genera-group *Blepharida* s.l. in Sub-Saharan Africa (Coleoptera: Chrysomelidae: Galerucinae: Alticini). Zoologischer Anzeiger 277: 23–32. https://doi.org/10.1016/j.jcz.2018.08.001

D'Alessandro P, Iannella M, Biondi M (2019) Revision of the Afrotropical flea beetle subgenus *Blepharidina* s. str. Bechyné (Coleoptera, Chrysomelidae). Zootaxa 4545(1): 032–060. https://doi.org/10.11646/zootaxa.4545.1.2

D'Alessandro P, Iannella M, Grobbelaar E, Biondi M (2020) Revision of the *Calotheca nigrotessellata* species group from southern Africa, with description of two new species (Coleoptera: Chrysomelidae: Galerucinae: Alticini). Fragmenta entomologica 52(2): 169–182. https://doi.org/10.4081/fe.2020.457

D'Alessandro P, Iannella M, Grobbelaar E, Biondi M (2021) Taxonomic revision of the *Calotheca parvula* species group from southern Africa, with descriptions of three new species (Coleoptera, Chrysomelidae). African Invertebrates 62(1): 315–337. https://doi.org/10.3897/AfrInvertebr.62.62426

D'Alessandro P, Iannella M, Grobbelaar E, Biondi M (2022) *Calotheca nigromaculata* species-group from sub-Saharan Africa with descriptions of two new species from KwaZulu-Natal (Chrysomelidae, Galerucinae, Alticini). ZooKeys 1084: 119–137. https://doi.org/10.3897/zookeys.1084.73175

D'Alessandro P, Grobbelaar E, Iannella M, Biondi M (2023a) *Calotheca borowieci* sp. nov. and *C. orophila* sp. nov. from southern Africa (Coleoptera, Chrysomelidae, Galerucinae, Alticini). Annales Zoologici 73 (3): 421–428. https://doi.org/10.3161/00034541 ANZ2023.73.3.006

D'Alessandro P, Grobbelaar E, Iannella M, Biondi M (2023b) *Calotheca leonardii*, a new flea beetle species from southern Africa (Coleoptera: Chrysomelidae: Galerucinae: Alticini) Natural History Sciences. Atti della Società italiana di Scienze naturali del Museo civico di Storia naturale di Milano 10(Supplement 1): 5–10. https://doi.org/10.4081/nhs.2023.681

Döberl M (1986) Die Spermathek als Bestimmungshilfe bei den Alticinen. Entomologische Blatter fur Biologie und Systematik der Kafer 82(1–2): 3–14.

Evenhuis NL (2021) The insect and spider collections of the world website. http://hbs.bishopmuseum.org/codens/ [Accessed 09 October 2024]

Fairmaire L (1893) Descriptión d'une nouvelle espèce de Chrysomélide de l'Afrique australe. Annales de la Société entomologique de France 62. Bulletin entomologique: CCCXLVII.

Fairmaire L (1901) Materiaux pour la faune coléoptérique de la région malgache (11° note) (fin). Revue d'Entomologie 20: 101–248.

Furth DG (1982) The Metafemoral Spring of Flea Beetles (Chrysomelidae: Alticinae). Spixiana 7: 11–27.

Furth DG (1992) The New World *Blepharida* group, with a key to genera and description of a new species (Coleoptera: Chrysomelidae). Journal of New York Entomological Society 100: 399–414. http://www.jstor.org/stable/25009970

Furth DG (1998) New World *Blepharida* Chevrolat 1836 (Coleoptera: Chrysomelidae: Alticinae). Memoirs of the Entomological Society of Washington 21: 1–109.

Furth DG, Lee JE (2000) Similarity of the *Blepharida*-group genera using larval and adult characters (Coleoptera: Chrysomelidae: Alticinae). Journal of the New York Entomological Society 108: 26–51. https://doi.org/10.1664/0028-7199(2000)108[0026:SOTBGG]2.0.CO;2

Furth DG, Young DA (1988) Relationships of herbivore feeding and plant flavonoids (Coleoptera: Chrysomelidae and Anacardiaceae: *Rhus*). Oecologia 74: 496–500. https://doi.org/10.1007/BF00380045

Gahan (1895) On the Coleoptera obtained by Dr. Anderson's Collector during Mr. T. Bent's Expedition to the Hadramaut, South Arabia. The Journal of the Linnean Society of London. Zoology 25(161): 285–291. https://doi.org/10.1111/j.1096-3642.1895.tb03418.x

Gerstaecker CEA (1855) Diagnosen der von Peters in Mossambique Gesammelten neuer Coleopteren und Lepidopteren. Monatsberichte der Akademie der Wissenschaften zu Berlin 1855: 636–639.

Gestro R (1895) Esplorazione del Giuba e dei suoi affluenti compiuta dal Cap. V. Bottego durante gli anni 1892-93 sotto gli auspici della Società Geografica Italiana. Risultati Zoologici. XVI. Coleotteri. Anali del Museo Civico di Storia Naturale di Genova, serie 2a, 15(35): 249–478. https://doi.org/10.5962/bhl.title.49163

Heyden von L (1887) Kleine coleopterologische Mitteilungen. Wiener Entomologische Zeitung 6: e98. https://doi.org/10.5962/bhl.part.17738

Hope FW (1840) The coleopterist's manual, part the third, containing various families, genera, and species, of beetles, recorded by Linneus and Fabricius. Also, descriptions of newly discovered and unpublished insects. Bowdery & Kerby, London, 191 pp.

Iannella M, D'Alessandro P, De Simone W, Biondi M (2021) Habitat Specificity, Host Plants and Areas of Endemism for the Genera-Group *Blepharida* s.l. in the Afrotropical Region (Coleoptera, Chrysomelidae, Galerucinae, Alticini). Insects 12: 299. https://doi.org/10.3390/insects12040299

Jacoby M (1882) Descriptions of new genera and species of phytophagous Coleoptera. Proceedings of the Zoological Society of London 50(1): 50–58. https://doi.org/10.1111/j.1096-3642.1882.tb02727.x

Jacoby M (1888) Descriptions of new or little-known species of phytophagous Coleoptera from Africa and Madagascar. Transactions of the Entomological Society of London 189–206. https://doi.org/10.1111/j.1365-2311.1888.tb01308.x

Jacoby M (1895) 179. Chrysomeliden von Togo (Bismarckburg). Deutsche Entomologische Zeitschrift, 165–188.

Jacoby M (1903) Descriptions of new genera and species of Phytophagous Coleoptera. Stettiner Entomologische Zeitung 64: 292–336.

Koch C (1958) Preliminary notes on the coleopterological aspect of the arrow poison of the bushmen. Pamphlet of the South African Biological Society 20: 49–54.

Kolbe HJ (1894) Der Pfeilgiftkäfer der Kalahari-Wüste, *Diamphidia* simplex Péring. (*Locusta* Fairm.). Entomologische Zeitung 55: 79–86.

Laboissière V (1941) Observations sur les Halticinae de la Collection du Musée du Congo et descriptions d'espèces nouvelles. Revue de Zoologie et de Botanique Africaines 34(2): 236–263.

Laboissière V (1942) Halticinae (Coleoptera, Phytophaga) Fam. Chrysomelidae. Exploration du Parc National Albert. Mission G.F. De Witte (1933–1935). Institut des Parcs Nationaux du Congo Belge 39: 1–131.

Lee CF, Cheng HT (2007) The Chrysomelidae of Taiwan Vol. 1. Sishou-Hills Insect Observation Network Press, Taipei, 199 pp.

Medvedev LN (1999) A revision of the group Blepharidiini (Chrysomelidae: Alticinae) from the Oriental region. Russian Entomological Journal 8: 175–184.

Nadein KS, Betz O (2016) Jumping mechanisms and performance in beetles. I. Flea beetles (Coleoptera: Chrysomelidae: Alticini). Journal of Experimental Biology 219: 2015–2027. https://doi.org/10.1242/jeb.140533

Olivier M (1791) Histoire Naturelle. Insectes. Tome VI. In: Encyclopédie Méthodique, Panckoucke, Paris, France, 368 pp.

Peringuey L (1892) On beetles collected in Tropical South-Western Africa. In: Peringuey L (Ed.) Third contribution to the South African Coleopterous fauna. Transactions of the South African Philosophical Society 6(2): 1–94. https://doi.org/10.1080/21560382.1889.9526255

Prathapan KD, Chaboo CS (2011) Biology of *Blepharida*-group flea beetles with first notes on natural history of *Podontia congregata* Baly, 1865 an endemic flea beetle from southern India (Coleoptera, Chrysomelidae, Galerucinae, Alticini). Zookeys 157: 95–130. https://doi.org/10.3897/zookeys.157.1472

Scherer G (1962) Beitrag zur kenntnis der Alticiden-fauna Zentral-Afrikas (Coleoptera Chrysomelidae Alticinae). Annales du Musée Royale de l'Afrique Centrale, Tervuren (Ser. 8, Zool.) 113: 1–82.

Scherer G (1969) Contributions à la connaissance de la faune entomologique de la Côte d'Ivoire (L. Decelle, 1961–1964) XLIII. Coleoptera Chrysomelidae Alticinae. Annales du Musée Royale de l'Afrique Centrale, Tervuren (Ser. 8, Zool.) 175: 365–371.

Scherer G (1972) Coleoptera aus Nordostafrika. Chrysomelidae: Alticinae. Notulae Entomologicae 52: 1–17.

Schmitt M, Uhl G (2015) Functional morphology of the copulatory organs of a reed beetle and a shining leaf beetle (Coleoptera: Chrysomelidae: Donaciinae, Criocerinae) using X-ray micro-computed tomography. In: Jolivet P, Santiago-Blay J, Schmitt M (Eds) Research on Chrysomelidae 5. ZooKeys 547: 193–203. https://doi.org/10.3897/zookeys.547.7143

Stål C (1858) Entomologiska bidrag. Öfversigt af Kongliga Vetenskaps-Akademiens Förhandlingar, 247–258.

Takizawa H (2005) Supra-generic subdivisions of the subfamily Alticinae based on larval characters, with descriptions of larvae of Hispaniolan species (Coleoptera: Chrysomelidae). Insecta Matsumurana 62: 187–206.

Weise J (1900) Beschreibungen africanischer Chrysomeliden nebst synonymischen Bemerkungen. Deutsche Entomologische Zeitschrift 2: 446–459. https://doi.org/10.1002/mmnd.48019000239

Weise J (1902) Afrikanische Chrysomeliden. Archiv für Naturgeschichte 68: 119–174.

Weise J (1906) Ostafrikanische Chrysomeliden und Coccinelliden. Deutsche entomologische Zeitschrift 1: 35–64.

Weise J (1910) Chrysomelidae von Madagaskar, der Comoren und der Inseln Ostafrikas. In: Reise in Ostafrika in den Jahren 1903–1905 mit Mitteln der Hermann und Elise geb. Heckmann Wentzel-Stiftung ausgeführt. Von Professor Dr. Alfred Voeltzkow. Wissenschaftliche Ergebnisse. Band ll. Systematische Arbeiten. Heft V, 419–506.

ZooKeys 1228: 161–172 (2025)
DOI: 10.3897/zookeys.1228.138084

Research Article

Phloeosinus metasequoiae sp. nov. (Coleoptera, Curculionidae, Scolytinae, Phloeosinini), a new insect pest of *Metasequoia glyptostroboides* in China

Hang Ning[1,2*], Ruixiong Deng[1,2*], Beibei Huang[1,2], Kaitong Xiao[1,2], Jingjing Huang[2,3], Jianfeng Hong[3], Yongmei Yi[2]

1 *Hubei Key Laboratory of Biological Resources Protection and Utilization (Hubei Minzu University), Enshi 445000, Hubei, China*
2 *College of Forestry and Horticulture, Hubei Minzu University, Enshi 445000, Hubei, China*
3 *Xingdoushan National Nature Reserve, Enshi 445000, Hubei, China*
Corresponding author: Hang Ning (ninghanghb@163.com)

Academic editor: Miguel Alonso-Zarazaga
Received: 28 September 2024
Accepted: 29 January 2025
Published: 20 February 2025

ZooBank: https://zoobank.org/F40984F7-8C3C-4AA4-9793-7A668CA84DE5

Citation: Ning H, Deng R, Huang B, Xiao K, Huang J, Hong J, Yi Y (2025) *Phloeosinus metasequoiae* sp. nov. (Coleoptera, Curculionidae, Scolytinae, Phloeosinini), a new insect pest of *Metasequoia glyptostroboides* in China. ZooKeys 1228: 161–172. https://doi.org/10.3897/zookeys.1228.138084

Abstract

We describe herein a previously unknown species of bark beetle, *Phloeosinus metasequoiae* Ning, **sp. nov.**, which was discovered in the Xingdoushan National Nature Reserve, Hubei Province, China. This new species can be distinguished from other species in the genus *Phloeosinus* Chapuis, 1869 by its deeply emarginate compound eyes, coarse frontal and prothoracic surfaces, reticulate texture, and deeply V-shaped basal margin of the elytra. Phylogenetic analyses based on the cytochrome oxidase I (COI) and the large nuclear ribosomal subunit (28S) genes indicated that the new species represents an independent lineage with the closely related *Phloeosinus aubei* (Perris, 1885), to which it has a 95% similarity. The new species is known only from the type locality. Diagnoses, descriptions, photographs, and a distribution map are presented, along with a description of host plant damage.

Key words: Bark beetle, *Metasequoia glyptostroboides*, morphology, molecular, new species, taxonomy

Introduction

Metasequoia glyptostroboides Hu & W.C.Cheng (Cupressaceae) is a typical relictual tree species with a native distribution limited to an extremely narrow triangular area encompassing Lichuan City, Hubei Province, and Shizhu County, Chongqing Municipality, and Longshan County, Hunan Province (Ma and Shao 2003; Wang et al. 2004). This deciduous conifera is an endangered species and the sole living representative of the genus *Metasequoia* Hu & W.C.Cheng, which was once believed to have become extinct during the Miocene epoch (Equiza et al. 2006). Currently, there are an estimated 5779 native mother trees of *M. glyptostroboides*, among which, 5746, 3, and 28 are distributed in Lichuan City, Longshan County, and Shizhu County, respectively (Wang et al. 2005). The specimens in Lichuan City grow in Jiannan, Moudao, Wangying, and Zhonglu towns and the Fubao Mountain Forest Management Area (Liu et al. 2023). As an important relictual

---

[*] These authors contributed equally to this work and should be considered co-first authors.

plant species, *M. glyptostroboides* has considerable ornamental, medicinal, and ecological value. The tree is characterized by an attractive pattern of growth and bears lush green leaves, and although the native population is now restricted to a very small area, it is widely cultivated for use as street and ornamental trees in parks and gardens. In China, the cultivation range of *M. glyptostroboides* extends across 26 provinces, with an estimated planting area of 1.08 × 10^4 hm (Leng et al. 2007). *Metasequoia glyptostroboides* is commonly found growing in wetland plains in the middle and lower reaches of the Yangtze River and coastal areas, and it has also been introduced to more than 50 countries worldwide, with a distribution range extending northward to 60°N in regions such as Volgograd and Alaska.

To date, comparatively few pests or diseases of the trunk have been reported for *M. glyptostroboides*, among which *Odontotermes formosanus* (Shiraki, 1909) is the most significant pest, and is considered to pose a threat to the survival of native mother trees (Wang et al. 2003). Given their weakened growth, mother trees that are characterized by hollow heartwood can be particularly vulnerable to infection by *O. formosanus*. Studies on pests that are detrimental impact to the growth of *M. glyptostroboides* have generally focused on defoliating insects, including *Ascotis selenaria* (Hubner, 1817), *Choristoneura metasequoiacola* (Liu, 1983), and *Ectropis obliqua* (Prout, 1915), whereas with respect to diseases, red blight, leaf blight, and leaf spot have been reported to be relatively common in *M. glyptostroboides* (Yang et al. 2021; Liang et al. 2023). However, previous studies tended to indicate that these pests and diseases are non-lethal and cause relative minor damage to the native mother trees. To date, however, there have been no reports of bark beetles feeding on *M. glyptostroboides*.

However, a recent survey of the pests of *M. glyptostroboides* in May to June 2024 in the Xingdoushan National Nature Reserve, Hubei Province, yielded what appeared to be a new species of bark beetle, which characterize here based on morphological observations and molecular analyses. Comparative morphological and molecular phylogenetic analyses provide evidence to indicate that the collected specimens represent a previously undescribed species, which we describe herein.

Materials and methods

Taxonomy

Specimens of the collected beetles were examined using a hand-held digital microscope (Aomekie A5; Aomekie, Ningbo City, China) and photographed using a DSLR camera (Canon EOS R6; Canon, Ota City, Kyoto, Japan) mounted on an Olympus BX53 compound microscope with ×5, ×10, and ×20 fluorite objectives (Olympus, Shinjuku City, Tokyo, Japan). Images were also obtained using a Canon EOS R6 camera equipped with a Godox Speedlite flash unit to provide additional lighting, with montage images being assembled using Adobe Photoshop 2023 (Adobe Inc., San Jose, California, USA). All measurements were made using a stereomicroscope (AxioVision SE64 v. 4.8.3) and are presented in millimeters. The descriptions and morphological terms used in the text are based on those adopted by Alonso-Zarazaga et al. (2023), Knížek (2011), Beaver (2011), Wood and Bright (1987, 1992), and Tsai and Yin (1964). Depositories of all specimens examined are abbreviated as:

ASM-HBMZU	Animal Specimens Museum, College of Forestry and Horticulture, Hubei Minzu University, Enshi, Hubei, China.

Abbreviations and terminology

NZMC	National Zoological Museum of China, Institute of Zoology, Chinese Academy of Science, Beijing, China
NMNS	National Museum of Natural Science, Taichung, Taiwan, China
NMNH	National Museum of Natural History, Washington, DC, USA
NHMW	Naturhistorisches Museum Wien, Austria
NHMUK	The Natural History Museum, London, UK

DNA extraction, PCR amplification, and sequencing

Live adult beetles were collected directly from beneath the bark of recently infested trees and preserved in 90% ethanol or stored at −80 °C until used for analyses. These specimens have been saved as vouchers in the Forest Conservation and Utilization Professional Laboratory, Hubei Key Laboratory of Biological Resources Protection and Utilization (Hubei Minzu University). DNA was extracted from specimens using a magnetic bead fresh tissue DNA extraction kit, according to the manufacturer’s instructions. Amplification and sequencing of partial cytochrome oxidase I (COI) and the large nuclear ribosomal subunit (28S) gene sequences were conducted using the primers pairs LCO1490 (5’-GGTCAACAAATCATAAAGATATTGG-3’), HCO2198 (5’-TAAACTTCAGGGTGACCAAAAAATCA-3’), 28S Rd 4.8a (5’-ACCTATTCTCAAACTTTAAATGG-3’), and 28S Rd 7b1 (5’-GACTTCCCTTACCTACAT-3’) described by Folmer et al. (1994) and Robertson et al. (2013), which were synthesized commercially by the General Biology Corporation (Anhui, China). Reads were assembled using DNAMAN 9.0.1 (www.lynnon.com)., and the obtained sequences were used to search the GenBank (www.ncbi.nlm.nih.gov/genbank) and BOLD (boldsystems.org) databases to identify potentially similar species. Sequences of the COI and 28S genes of *P. metasequoiae* sp. nov. have been deposited in the GenBank database to enable molecular diagnosis (COI: PQ276048, 28S: PQ278886).

Results

Taxonomy

Phloeosinus metasequoiae **Ning, sp. nov.**
https://zoobank.org/16EB30DA-8C67-4444-8719-69B8A1B3EA61
Fig. 1

Type material. *Holotype*: • female: China, Hubei Province: Enshi Tujia and Miao Autonomous Prefecture, Lichuan City, Xindoushan National Nature Reserve, Zhonglu Town, Shiziba Village; 30°7'1"N, 108°41'40"E; elev. 1123 m; all specimens were collected by HN, RD and KX; 5 June 2024; ASM-HBMZU, XDS-SZB007.

Paratypes: • 4 females, 5 males, with the same data as the holotype ASM-HBMZU, XDS-SZB003, XDS-SZB011–018 • 3 females, 4 males; Enshi Tujia and Miao Autonomous Prefecture, Lichuan City, Xindoushan National Nature Reserve, Fubao

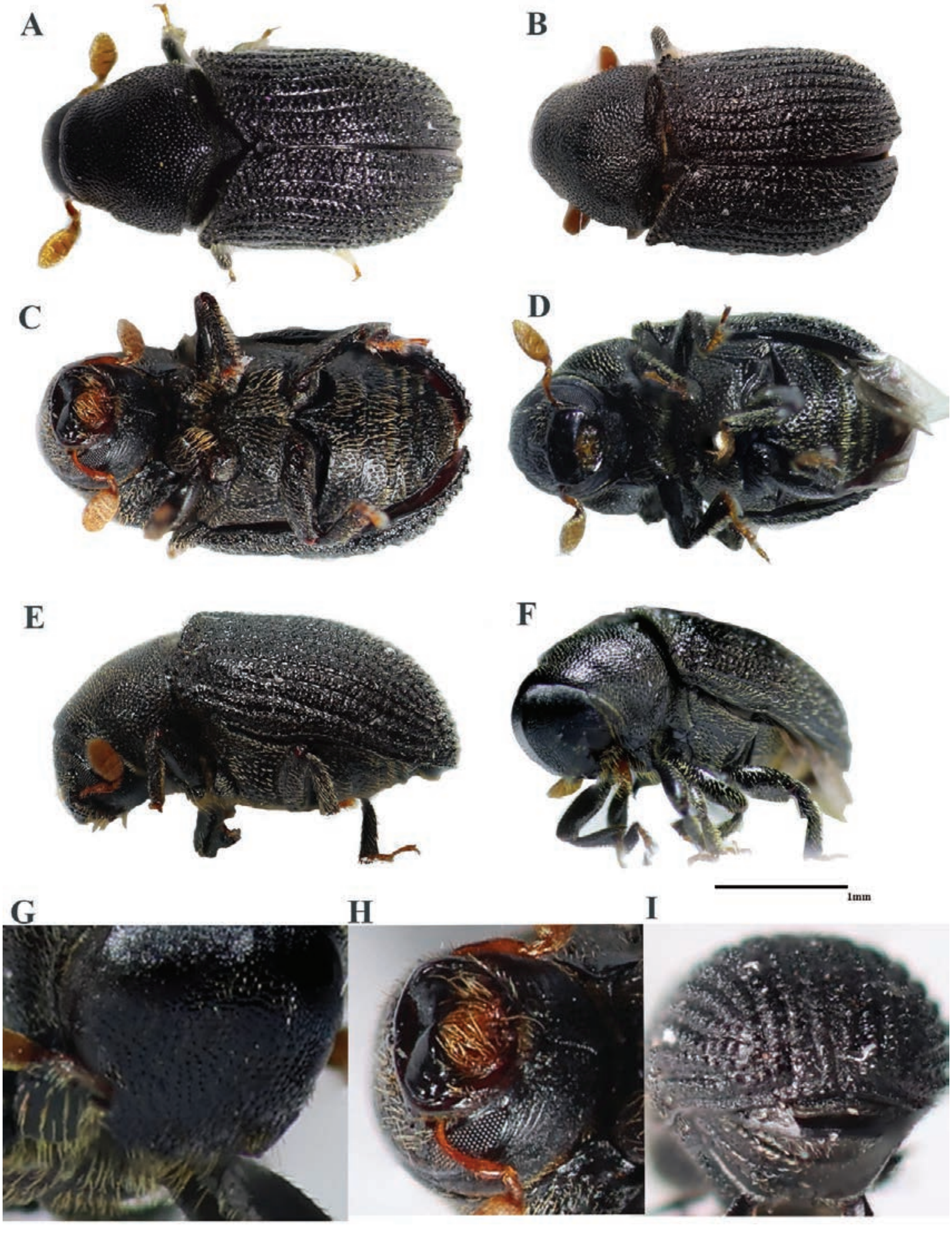

Figure 1. *Phloeosinus metasequoiae* sp. nov., holotype, female **A, B** dorsal view **C, D** ventral view **E, F** lateral view **G** head **H** mouthparts **I** elytra declivity.

Mountain Forest Management Area; 30°12'33"N, 108°42'26"E; elev. 1394 m; 5 June 2024; ASM-HBMZU, XDS-FBM017–023 • 7 females, 4 males; Enshi Tujia and Miao Autonomous Prefecture, Lichuan City, Xindoushan National Nature Reserve, Wangying Town; 30°16'N, 108°42'17"E; elev. 1130 m; 6 June 2024; ASM-HBMZU, XDS-WY003–008, XDS-WY015–019 • 5 females, 3 males; Enshi Tujia and Miao Autonomous Prefecture, Lichuan City, Xindoushan National Nature Reserve, Jiannan Town; 30°26'9"N, 108°32'15"E; elev. 974 m; 7 June 2024; ASM-HBMZU, XDS-JN010–017 • 7 females, 3 males; Enshi Tujia and Miao Autonomous Prefecture, Lichuan City, Xindoushan National Nature Reserve, Moudao Town; 30°26'N, 108°41'18"E; elev. 1377 m; 8 June 2024; ASM-HBMZU, XDS-MD015–024 • 1 female, 3 males; Enshi Tujia and Miao Autonomous Prefecture, Lichuan City, Xindoushan National Nature Reserve, Zhonglu Town; 30°"2'35"N, 108°44'20"E; elev. 829 m; 9 June 2024; ASM-HBMZU, XDS-ZL002, XDS-ZL008–0010.

Similar species. *Phloeosinus aubei* (Perris, 1855).

Diagnosis. 2.2–2.6 mm long (mean = 2.43 mm, *n* = 50); 2.59–2.65× as long as wide. *Phloeosinus metasequoiae* sp. nov. is similar to *P. aubei*, although the body is shorter and broader, with a notch in the middle of the anterior edge of the compound eye, and an oblong-ovate antennal club; the surface of the anterior thoracic dorsal plate is flat, and there are large tubercles on stripes 1 and 3 of the elytra, as shown in Fig. 1. *Phloeosinus metasequoiae* sp. nov. can be distinguished from other species of *Phloeosinus* based on two main differences. Firstly, the compound eyes of *P. metasequoiae* sp. nov. are notched, and the frontal and prothoracic surfaces are characterized by reticulations, which is a feature that can be used to distinguish this species from the most similar species, *P. aubei.* Secondly, *P. metasequoiae* sp. nov. and *P. aubei* differ significantly with respect to the basal margin of the elytra, with the basal margin of the *P. metasequoiae* sp. nov. elytra being characterized by its deep V-shape, whereas that of the *P. aubei* elytra is relatively flat, as shown in Figs 2, 3.

Description. Female: 2.2–2.6 mm long (mean = 2.43 mm, *n* = 50); 2.59–2.65× as long as wide. Body black or black-brown without luster, moderately densely covered with short, yellowish-brown, hair-like setae. ***Head***: epistoma entire, transverse, with a row of moderately long, sparse hair-like setae. Frons below upper margin of eye and above epistoma flat. Eye emargination (Fig. 4). Antennae with four funicle segments (including the pedicel). Antennal club with two procurved sutures. ***Pronotum*:** 0.96–1.14 (mean = 1.05, *n* = 50) × as long as wide. Pronotum widest at base, appearing almost triangular in profile. Surface of pronotal plate rough, reticular, with short yellow setae. Apparent triangular protrusion in the pronotum base, curved laterally. ***Elytra*:** 1.86–2.04× (mean = 2.0, *n* = 50) × as long as wide, 1.10–1.15 (mean = 1.12, *n* = 50) × as long as pronotum. Deeply V-shaped in the basal margin of elytra. Coarse surface with tubercles, dark-red declivity, and short, yellow setae. Two longitudinal tubercles present between each striae, with nine longitudinal interstriae on each elytra, larger tubercles at the base than at the front end, and larger tubercles in the 1st, 3rd, and 5th striae near the elytral striae. ***Legs*:** procoxae contiguous. Protibiae obliquely triangular, broadest at apical 1/3, densely covered with yellow setae. Posterior face of protibiae, with some small punctures near base and inner margin.

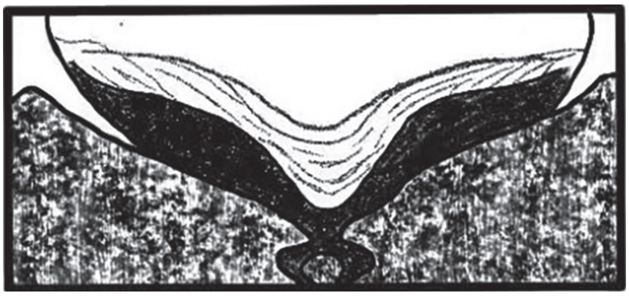

Figure 2. Morphological characteristics of the leading edge of elytra in *Phloeosinus metasequoiae* sp. nov.

Male. (Figs 5, 6). 2.0–2.5 mm long (mean = 2.38 mm, n = 50); 2.51–2.59× as long as wide. ***Pronotum*:** 0.89–1.10 (mean = 0.99, *n* = 50) × as long as wide. ***Elytra*:** 1.82–1.97 (mean = 1.91, *n* = 50) × as long as wide, 1.01–1.09 (mean = 1.06, *n* = 50) × as long as pronotum. Coarse surface with tubercles, tubercles in male elytral declivity larger than those in females (Fig. 7). Similar to females in most features except body size and size of tubercles in elytral declivity.

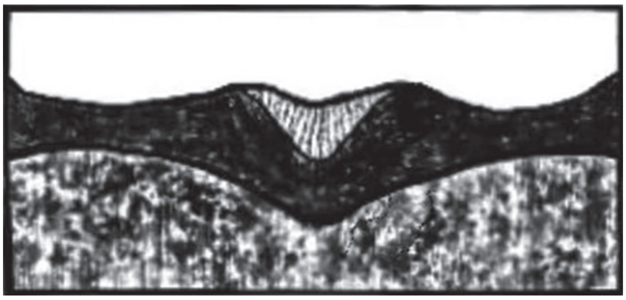

Figure 3. Morphological characteristics of the leading edge of elytra in *Phloeosinus aubei*.

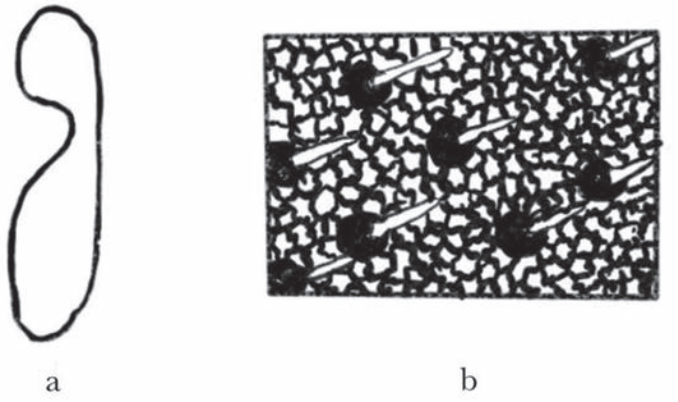

Figure 4. a compound eyes deeply emarginate **b** Surface of frons andprothorax not smooth but reticulate.

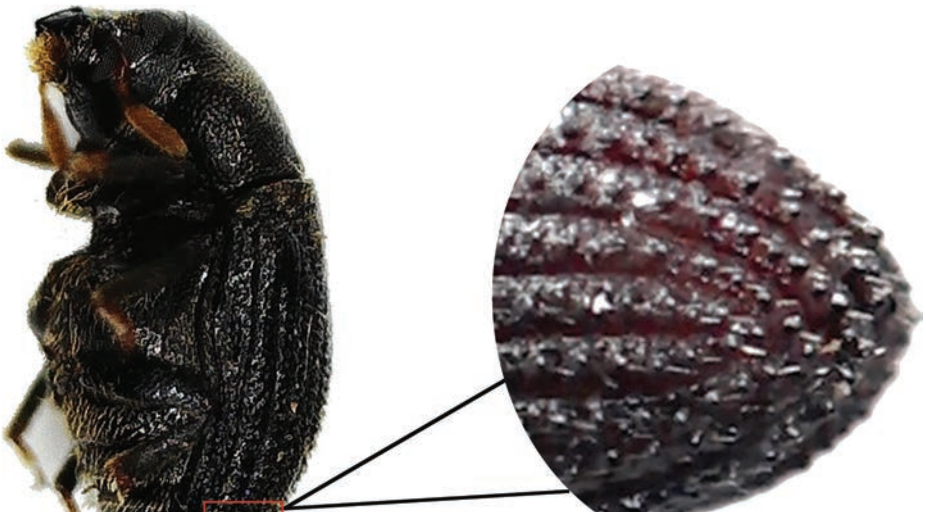

Figure 5. Elytral declivity in *Phloeosinus metasequoiae* sp. nov. male.

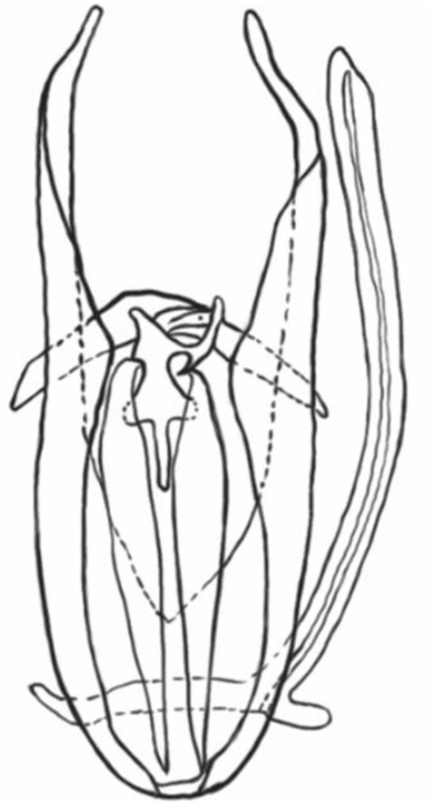

Figure 6. Aedeagus of *Phloeosinus metasequoiae* sp. nov. male.

Figure 7. Elytral declivity of *Phloeosinus metasequoiae* sp. nov. **a** male **b** female.

Etymology. The specific epithet *metasequoiae* is the genitive of the genus name of the host plant, *Metasequoia*, indicating that this new species is associated with this plant.

Host. *Metasequoia glyptostroboides* Hu &W.C.Cheng

Distribution. Known only from the type locality (Fig. 8).

Biology. Unknown

Phylogeny

Phylogenetic results (Figs 9, 10) reveal that the closest matching sequences are those of *P. punctatus* (from NCBI, COI: MG054750.1, 86.45% similarity) and *P. aubei* (from NCBI, 28S: JX263746.1, 95.10% similarity). The latter species has a 95% similarly to the *P. metasequoiae* sp. nov., indicating that it is genetically most closely related to *P. aubei*.

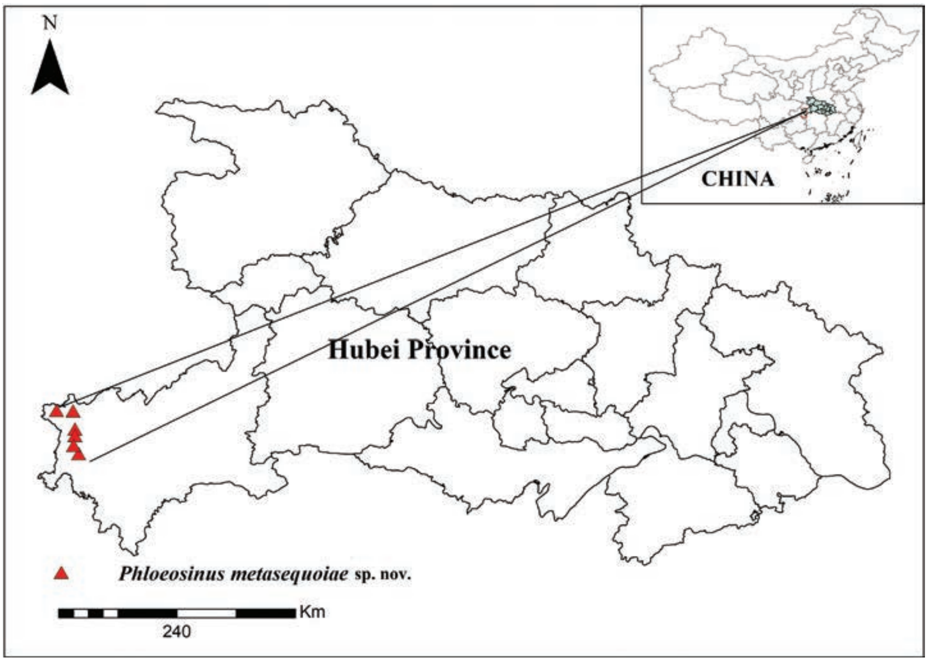

Figure 8. Distribution map of *Phloeosinus metasequoiae* sp. nov. in China.

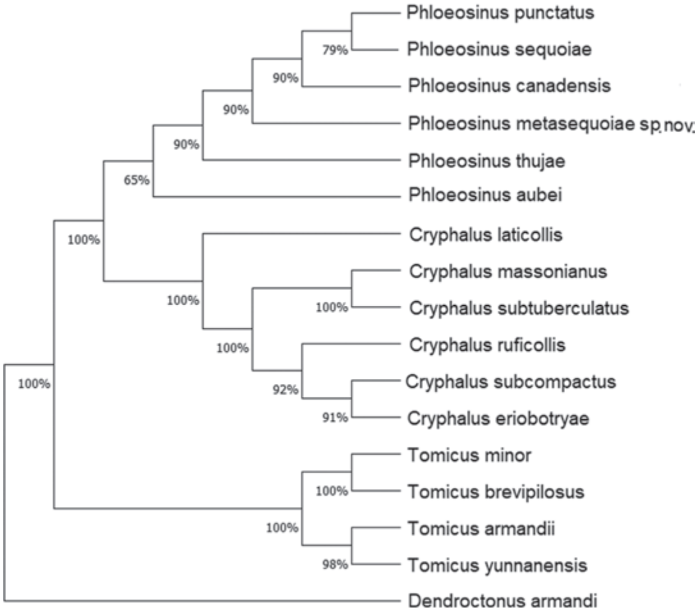

Figure 9. Neighbor-joining tree of analyzed CO1 sequences using the Kimura 2-parameter model, with *Dendroctonus armandi* as the outgroup.

Discussion

Bark beetles in the genus *Phloeosinus* are widely distributed worldwide. The recently published Cooperative Catalogue of Palaearctic Coleoptera Curculionoidea includes 956 species of Scolytinae in 107 genera and 21 tribes (Knížek 2011; Alonso-Zarazaga et al. 2023). In terms of morphological characteristics, *P*. *metasequoiae* sp. nov. is most similar to bark beetles within the genus *Phloeosinus*. Distinctive features include a comparatively short, broad body, an emargination in the middle of the anterior edge of the compound eye, and oblong-ovate antennal clubs. The surface of the anterior thoracic dorsal plate is

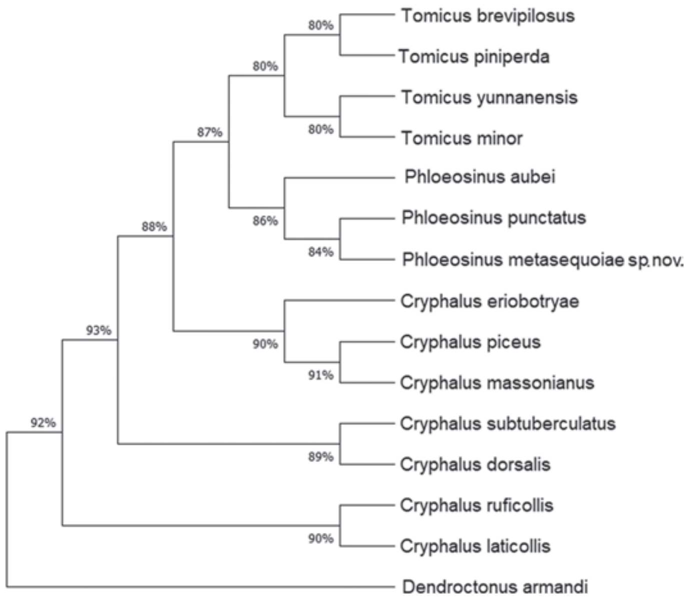

Figure 10. Neighbor-joining tree of analyzed 28S sequences using the Kimura 2-parameter model, with *Dendroctonus armandi* as the outgroup.

flat, with large tubercles on the first and third interstriae of the elytra. Males and females have concave and convex foreheads, respectively, and genetically, *P. metasequoiae* sp. nov. is most closely related *P. aubei*, with a similarity of 95%.

Having characterized this previously undescribed bark beetle, we immediately conducted an overall survey of *M. glyptostroboides* populations in the vicinity of Lichuan City, and to date, bark beetles have been found in the Xiaohe *M. glyptostroboides* Botanical Gardens, Zhonglu Town, and Jiannan Town. In Shiziba Village, near the Xiaohe *M. glyptostroboides* Botanical Gardens, our investigations revealed that at least seven mother trees were infected with the new species.

Our survey reveals that the initial invasion of *M. glyptostroboides* by *P. metasequoiae* sp. nov. can be detected by the appearance of small circular holes measuring less than 0.5 mm in the branches of host trees (Fig. 11B), and that as infestation progresses, the branches begin to show signs of decay, as evidenced by the gradual deterioration shown in Fig. 11E, G. Tunnels excavated by the adult beetles are longitudinal pits that extend primarily into the sapwood and, in most cases, terminate in a short horizontal pit. We established that the length of these tunnels tends to be proportional to the density of the invading bark beetles, typically ranging from 30 to 50 mm, with minimum and maximum lengths of 20 and 95 mm, respectively, and a width of approximately 1–2 mm (Fig. 11A, C, D). The most apparent symptom of the damage caused by this bark beetle is a reddening of the leaves during summer, which can be readily identified and is conducive to sampling by cutting branches (Fig. 11F). However, during the initial stages of infestation, symptoms are less apparent, and we thus speculate that there may have been more infected mother trees than those identified in our survey. Among cultivated *M. glyptostroboides*, we similarly detected the presence of this bark beetle in up to 20 infected trees, which, if we consider the occurrence of asymptomatic initially infected trees, could represent a minimum number. In addition, given the sporadic distribution of *M. glyptostroboides*, it is plausible that some trees may have been overlooked and, consequently, the actual number of infected trees may be considerably less significant.

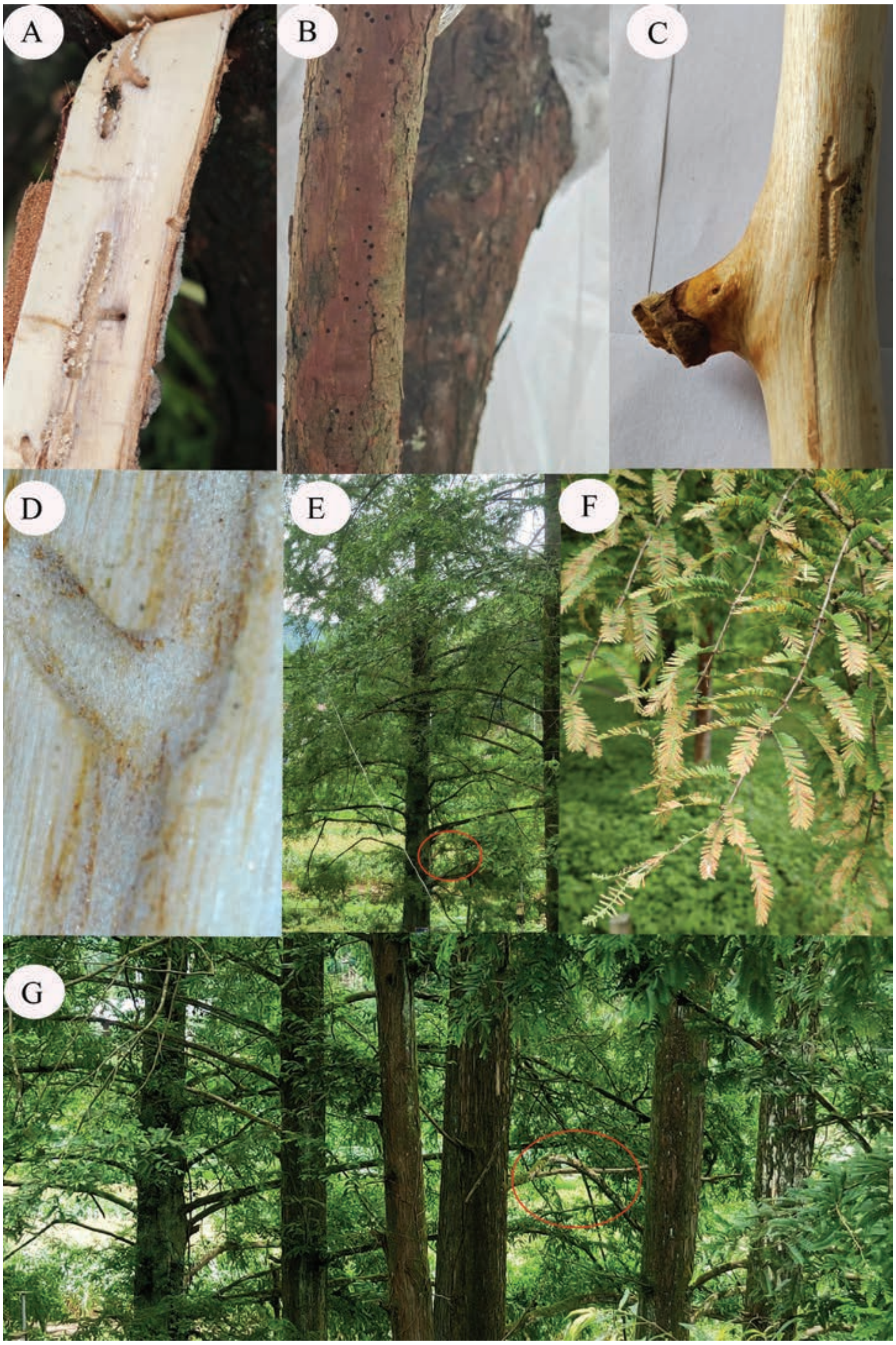

Figure 11. A galleries on the underside of bark **B** invasion holes in tree branches **C, D** *Phloeosinus metasequoiae* sp. nov. galleries in tree branches **E–G** trees infested with *P. metasequoiae* sp. nov.

We also conducted a comprehensive investigation of potential host trees, focusing primarily on species within the families Cupressaceae and Taxodiaceae. However, we failed to detect this beetle in any tree species other than *M. glyptostroboides*, thereby indicating that it may be an obligate pest of this tree. A further investigation assessing the environments surrounding infected trees reveals that damage was most severe among those trees growing along national roads, which were characterized by relatively poor vigor compared with *M. glyptostroboides* trees distributed in localities far from these roads. In this regard, we note that *M. glyptostroboides* growing along national roads tend to be regularly pruned, as excessively long branches can obstruct the view of vehicles, thereby influencing the growth of these trees, and we found that bark beetles preferentially invaded healthy trees with weaker vigor and diameter at breast height ranging from 50 to 80 cm (Fig. 11E–G).

Acknowledgements

We express their sincere gratitude to Dr Miguel Alonso-Zarazaga, Dr Michail Mandelshtam, and an anonymous reviewer for their constructive suggestions and valuable assistance, which have significantly improved this manuscript. Particular thanks go to Dr Colin for his meticulous revision of the English language in this work. Additionally, the authors express appreciation to Jianfeng Hong and Jingjing Huang (Xingdoushan National Nature Reserve, Hubei Province) helping collect specimens and taking photographs.

Additional information

Conflict of interest

The authors have declared that no competing interests exist.

Ethical statement

No ethical statement was reported.

Funding

This research was funded by the Natural Science Foundation of Hubei Province (Grant No. 2024AFB534).

Author contributions

Conceptualization: HN, RD. Data curation: HN, RD. Formal analysis: HN, RD, BH. Investigation: HN, RD, KX, JH. Supervision: HN, JH, YY. Visualization: RD, BH. Writing- original draft preparation: HN, RD. Writing- -review and editing: HN, RD.

Data availability

All of the data that support the findings of this study are available in the main text.

References

Alonso-Zarazaga M, Barrios H, Borovec R, Bouchard P, Caldara R, Colonnelli E, Gültekin L, Hlaváč P, Korotyaev B, Lyal CHC, Machado A, Meregalli M, Pierotti H, Ren L, Sánchez-Ruiz M, Sforzi A, Silfverberg H, Skuhrovec J, Trýzna M, Velázquez de Castro AJ, Yunakov NN (2023) Cooperative Catalogue of Palaearctic Coleoptera Curculionoidea. Monografias Electrónicas, Sociedad Entomológica Aragonesa 14: e780. http://www.sea-entomologia.org/monoelec14.html

Beaver RA (2011) New synonymy and taxonomic changes in bark and ambrosia beetles. Koleopterologische Rundschau 81: 277–289.

Equiza MA, Day ME, Jagels R (2006) Physiological responses of three deciduous conifers (*Metasequoia glyptostroboides*, *Taxodium distichum* and *Larix laricina*) to continuous light: adaptive implications for the early tertiary polar summer. Tree Physiology 26(3): 353–364. https://doi.org/10.1093/treephys/26.3.353

Folmer O, Black M, Hoeh W, Lutz R, Vrijenhoek R (1994) DNA primers for amplification of mitochondrial cytochrome coxidase subunit I from diverse metazoan invertebrates. Molecular Marine Biology and Biotechnology 3(5): 294–299. https://pubmed.ncbi.nlm.nih.gov/7881515/

Knížek M (2011) Scolytinae. In: Löbl I, Smetana A (Eds) Catalogue of Palaearctic Coleoptera (Vol. 7), Curculionoidea I. Apollo Books, Stenstrup, 86–87. [204–251] https://doi.org/10.1603/008.104.0301

Leng Q, Fan SH, Wang L, Yang H, Lai XL, Cheng DD, Ge JW, Shi GL, Jiang Q, Liu XQ (2007) Database of native *Metasequoia glyptostroboides* trees in hina based on new census surveys and expeditions. Bulletin of the Peabody Museum of Natural History 48(2): 185–233. https://doi.org/10.3374/0079-032X(2007)48[185:DONMGT]2.0.CO;2

Liang Y, Fang X, Zheng L, Wu H, He Z, Xiong Z, Hong J, Ai XR, Liang G (2023) The complete mitochondrial genome of *Choristoneura metasequoiacola* Liu, 1983 (Lepidoptera: Tortricidae). Mitochondrial DNA Part B, Resources 8(6): 653–657. https://doi.org/10.1080/23802359.2023.2221350

Liu BZ, Zhou Y, Hong JF, Wang SB, Li HP, Li H (2023) Current situation and countermeasures for the preservation of the native mother tree resources of *Metasequoia glyptostroboides* in lichuan. Hubei Forestry Science and Technology 52(4): 63–66. https://doi.org/10.3969/j.issn.1004-3020.2023.04.011

Ma J, Shao G (2003) Rediscovery of the first collection of the 'living fossil', *Metasequoia glyptostroboides*. Taxon 52(3): 585–588. https://doi.org/10.2307/3647458

Robertson JA, Slipiński A, Hiatt K, Miller KB, Whiting M, Mchugh J (2013) Molecules, morphology and minute hooded beetles: a phylogenetic study with implications for the evolution and classification of Corylophidae (Coleoptera: Cucujoidea). Systematic Entomology 38(1): 209–232. https://doi.org/10.1111/j.1365-3113.2012.00655.x

Tsai PH, Yin HF (1964) A study of chinese *Phloeosinus* Chap.(Coleoptera; Ipidae), with descriptions of new species. Acta Zootaxonomica Sinica 1: 84–99. https://www.cnki.net/

Wang BQ, Ai XR, Peng C, Yi YM, Fan SH, Zhang NW (2003) Diseases and insect pests of *Metasequoia glyptostroboides* and their control. Plant Protection 29(2): 42–43. https://doi.org/10.3969/j.issn.0529-1542.2003.02.012

Wang XQ, Ma LY, Guo BX, Ge JW, Fan SH (2004) The conservation of *Metasequoia glyptostroboides* and its current problems in China. Biodiversity Science 3: 377–385. https://doi.org/10.17520/biods.2004046

Wang XQ, Ma LY, Guo BX, Fan SH, Tan JX (2005) Analysis on the change of the original *Metasequoia glyptostroboides* populationand its environment in Lichuan City, Hubei from 1948 to 2003. Acta Ecologica Sinica 5: 972–977. https://doi.org/10.1007/s11461-006-0032-6

Wood SL, Bright DE (1987) A catalog of Scolytidae and Platypodidae (Coleoptera), Part 1: bibliography. Great Basin Naturalist Memoirs 11: 1–833. https://scholarsarchive.byu.edu/gbnm/vol11/iss1/1

Wood SL, Bright DE (1992) A catalog of Scolytidae and Platypodidae (Coleoptera), Part 2: taxonomic index, volumes A and B. Great Basin Naturalist Memoirs 13: 1–1553. https://biostor.org/reference/143868

Yang Y, Yang B, Ye J, Su L, Masutti L (2021) A study on the ecological control of red blight of *Metasequoia glyptostroboides* by integrated forest management. Journal of Nanjing Forestry University (Natural Sciences Edition) 45(6): 90–98. https://doi.org/10.12302/j.issn.1000-2006.202007069

ZooKeys

ZooKeys 1228: 173–183 (2025)
DOI: 10.3897/zookeys.1228.140176

Research Article

Two new species of *Stenoloba* Staudinger, 1892 from China (Lepidoptera, Noctuidae, Bryophilinae)

Jian Li[1], Chao Zhang[2], Hui-Lin Han[3,4], Vladimir S. Kononenko[5]

1 College of Forestry, Northeast Forestry University, Harbin 150040, China
2 Simianshan Forest Resource Service Center, Jiangjin District, Chongqing, 402296, China
3 Northeast Forestry University, Ministry of Education, Key Laboratory of Sustainable Forest Ecosystem Management, Harbin 150040, China
4 Northeast Asia Biodiversity Research Center, Northeast Forestry University, Harbin 150040, China
5 Laboratory of Entomology, Federal Scientific Center of the East Asia Terrestrial Biodiversity, Far Eastern Branch, Russian Academy of Sciences, Vladivostok-22, 690022, Russia

Corresponding authors: Hui-Lin Han (hanhuilin@aliyun.com); Vladimir S. Kononenko (vsk528217@gmail.com)

Abstract

Two new species of the moth genus *Stenoloba* Staudinger, 1892, *S. zhaotonga* **sp. nov.** and *S. oculibasis* **sp. nov.**, are described from China. The former includes photos of both female and male genitalia, while the latter only includes photos of male genitalia.

Key words: *Basiviridis* species-group, hyperdiverse, morphology, moth, *nigrabasalis* species-group, taxonomy

Academic editor: Reza Zahiri
Received: 8 November 2024
Accepted: 13 January 2025
Published: 21 February 2025

ZooBank: https://zoobank.org/0994DFBA-A473-4409-924E-8CE3EA4CBF7F

Citation: Li J, Zhang C, Han H-L, Kononenko VS (2025) Two new species of *Stenoloba* Staudinger, 1892 from China (Lepidoptera, Noctuidae, Bryophilinae). ZooKeys 1228: 173–183. https://doi.org/10.3897/zookeys.1228.140176

Introduction

Stenoloba Staudinger, 1892 (type species *Dichagyris jankowskii* Oberthür, 1884) represents a genus exclusively found in East Asia within the subfamily Bryophilinae, as established by Staudinger (1892). In the early 19th century, several species belonging to this genus were described by various scholars (Moore 1888; Leech 1889; Hampson 1910; Warren 1914; Mell 1943; Draudt 1950). Currently, it is recognized as a large and relatively well-studied group, acknowledged as one of the most diverse within the subfamily Bryophilinae. Its distribution extends from India to Indonesia and includes regions such as China, the Korean Peninsula, Japan, and the southern part of the Russian Far East.

The taxonomic position of this genus has undergone several revisions over the years. Earlier classifications placed it within the subfamily Acontiinae [Acontianae] or Sarrothripinae (Hampson 1910; Warren 1914; Mell 1943; Draudt 1950). It was not until Sugi (1970) conducted a revision of the genus in Japan that *Stenoloba* was officially assigned to the subfamily Bryophilinae. Since the beginning of this century, a significant global revision of *Stenoloba* has been carried out by Kononenko and Ronkay (2000, 2001). Subsequently, the genus *Stenoloba* has demonstrated a sporadic pattern of development. Notably, significant contributions to the description and revision of new species within the genus from China (including Taiwan Island) and other regions of Southeast Asia, have been progressively undertaken by Chen (1999); Yoshimoto (1992, 1994); Kononenko and Ronkay (2000, 2001); Ronkay (2001); Sohn and Han (2005); Han and Lü (2007); Han and Kononenko (2009, 2015, 2018, 2021); Han and Kononenko et al (2020); Holloway (2009); Behounek and Kononenko (2010); Han et al. (2011); Pekarsky (2011); Sohn and Tzuoo (2012); Pekarsky and Saldaitis (2013); Pekarsky et al. (2013); Pekarsky (2018, 2019); and Saldaitis and Volynkin (2020). To date, a total of 103 species and 22 species groups of *Stenoloba* have been recognised. This genus exhibits amazing diversity in China, with 69 species classified into 19 species groups recorded here.

In the course of the inventory of Chinese Noctuoidea fauna, we investigated the diversity of *Stenoloba* in the southeastern part of China. Extensive material on the genus has been collected. Among them, two new species of *Stenoloba* from two species groups are described below.

Material and methods

Specimens for this study were collected from the southern and southwestern regions of China using light traps. Adult specimens were prepared according to the standard Lepidoptera wing-spreading method. Dissection and slide preparation of the genitalia followed the techniques outlined by Kononenko and Han (2007). Adult images were captured using a Nikon D700 camera, while genitalia images were obtained with an Olympus BX51 microscope and the Qcapture Pro system. Image processing was conducted using Helicon Focus v. 7.0 and Adobe Photoshop 2023. The type specimens of the new species are deposited in the collection of Northeast Forestry University, Harbin, China.

Abbreviations used

NEFU	Northeast Forestry University, Harbin, China
HT	holotype
PT	paratype
HHL	slide made by Hui-Lin Han
LJ	slide made by Jian Li

Taxonomic account

Genus *Stenoloba* Staudinger, 1892

Stenoloba Staudinger, 1892, in Romanoff, *Mémoires sur les Lépidoptéres* 6: 381. Type-species: *Dichagyris jankowskii* Oberthür, 1884, *Etudes d'Entomologie* 10: 28, pl. 3: 5, by monotypy. Syntypes: [Russia, Primorye terr.] Sidemi (BMNH).

= *Neothripa* Hampson, 1894, *Fauna British India* (*Moths*) 2: 366, 382. Type species: *Neothripa punctistigma* Hampson, 1894, ibidem 2: 382, by original designation. Type(s): India: [Punjab] Simla (BMNH).

= *Lepidopyrga* Warren, 1914, *Novitates zoologicae* 21: 405. Type-species: *Stenoloba viridimicta* Hampson, 1910, *Catalogue of the Lepidoptera Phalaenae in the British Museum* 10: 369, pl. 159: 31, by original designation. Holotype: [India] Assam, Khasis (BMNH).

= *Conicochyta* Hampson, 1918, *Novitates zoologicae* 25: 137. Type-species: *Chytonis olivacea* Wileman, 1914, *Entomologist* 47: 165, by original designation. Holotype: [Taiwan] Formosa: Rantaizan (BMNH).

Stenoloba zhaotonga Li, Han & Kononenko, sp. nov.

https://zoobank.org/5A48B7A5-EC48-4A24-B3CA-0AED98FCCABA
Figs 1, 2, 7, 11, 13

Type material. ***Holotype:*** • 1♂, China, Prov. Yunnan, Zhaotong, Huangshadi, 22 July 2023, RT. Xu, MX. Han leg., slide LJ-128-1, coll. NEFU. ***Paratype:*** • 1♀, China, Prov. Yunnan, Zhaotong, Sanjiangkou, 21 July 2023, RT. Xu, MX. Han leg., slide LJ-127-2, coll. NEFU.

Diagnosis. The new species belongs to the *S. nigrabasalis* species-group. This group includes six species: *S. nigrabasalis* Chang, 1991, *S. ochribasis* Kononenko & Ronkay, 2001, *S. nora* Kononenko & Ronkay, 2001 (Figs 5, 8 12), *S. uncata* Han & Kononenko, 2018, *S. herbacea* Saldaitis & Volynkin, 2020 and *S. zhaotonga* Li, Han & Kononenko, sp. nov.

Stenoloba zhaotonga sp. nov. shares several important characteristics with other species that are typical of the *S. nigrabasalis* species-group. The structure of the male genitalia reveals that the uncus is usually shorter; both sacculus and costa exhibit different shapes and are asymmetrical. The valve is relatively wide from the base to the middle, displaying strong hardening, with narrowing commences at the cucullus, where the outer edge is nearly straight; the costa features a protrusion resembling a finger or hill shape; additionally, the cucullus generally possesses a protruding structure that extends outward and includes cornua of varying lengths; finally, the juxta is large and either diamond-shaped or lingual.

In contrast to all species in the *S. nigrabasalis* species-group, *S. zhaotonga* is very similar to *S. nora*. In terms of adult features, *S. zhaotonga* has the head and thorax brown-yellow (in *S. nora* ochreous-green); forewing is overall brown-yellow (in *S. nora* more greyish); the basal area is yellow, with some filamentous dark brown stripes (in *S. nora* darkened, with a conspicuous wide blackish streak); reniform stigma is preceded by some irregular black spots (in *S. nora* dark spot behind reniform small or missing); and costal margin has dense dark brown stripes (in *S. nora* sparse). For male genitalia, uncus of the new species is clavate, relatively wide, short and flattened (in *S. nora* long and thin); juxta is elongate, shovel-like (in *S. nora* fusiform); apex of valva thin, straight, pointed, with a rectangular subapical process and both sides are densely covered with hairs (in *S. nora* cucullus has a small hook-like process); sacculus with elongated hill-like extension on outer margin, straighter (in *S. nora* more rounded); vesica sickle-shaped, dorsal side has cornuti and a granulation area, and cornuti are densely distributed, with cornute longer (in *S. nora* broadly tubular, recurved, ends have cornuti and granulation areas, cornute shorter). For the female genitalia, apophysis anteriores longer and much thicker (in *S. nora* shorter and thinner); tubular part of corpus bursae relatively long (in *S. nora* shorter).

Description. ***Adult*** (Figs 1, 2). Wingspan 24–27 mm. Head brown-yellow, with dense olive scales. Antennae filiform both in male and female. Labial palps

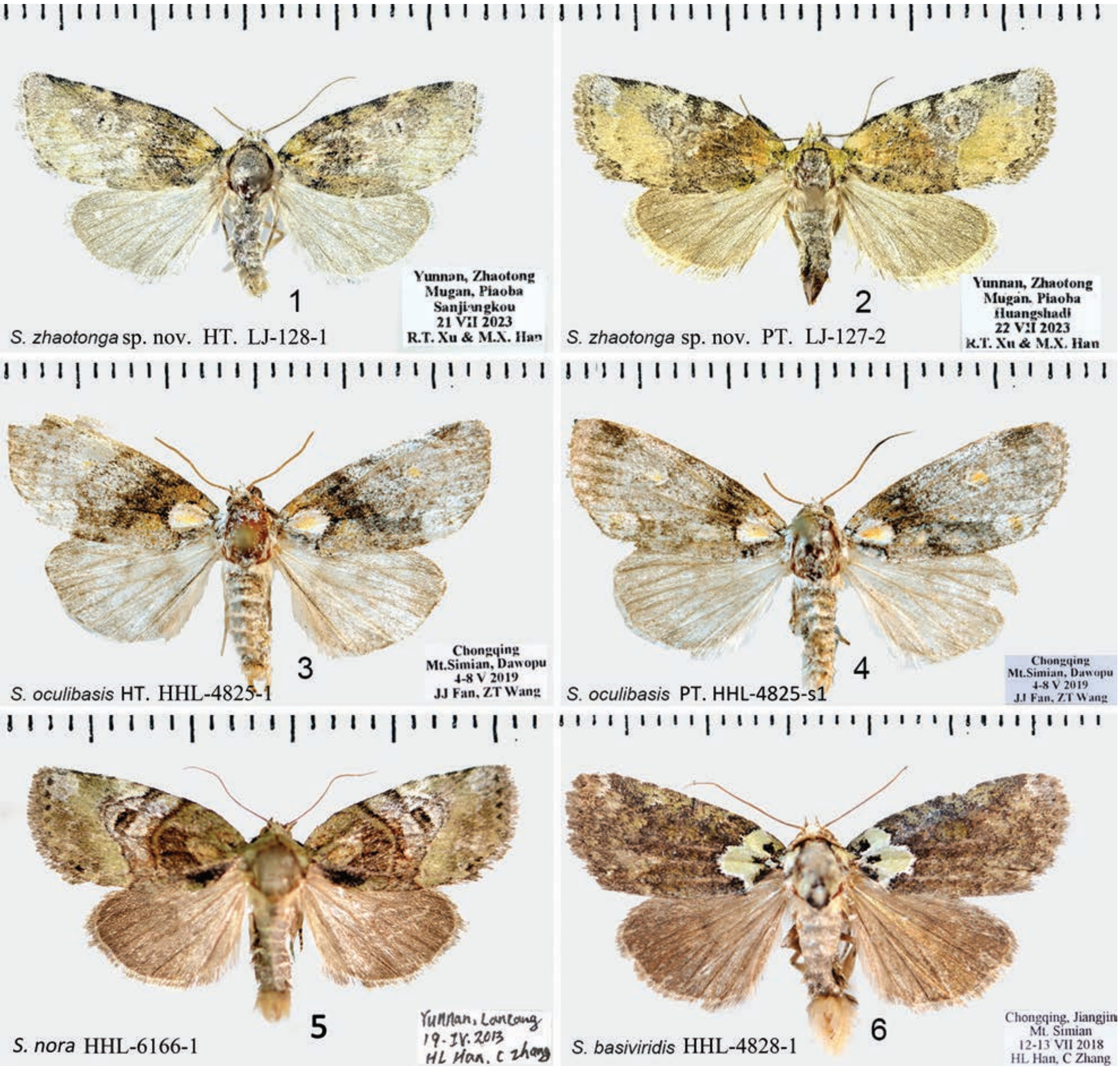

Figures 1–6. *Stenoloba* spp., adults. **1** *S. zhaotonga* sp. nov., male, HT, slide LJ-128-1 **2** *S. zhaotonga* sp. nov., female, PT, slide LJ-127-2 **3** *S. oculibasis* sp. nov., male, HT, slide HHL-4825-1 **4** *S. oculibasis*, sp. nov., male, PT, slide HHL-4825-s1 **5** *S. nora*, male, slide HHL-6166-1 **6** *S. basiviridis*, male, slide HHL-4828-1 [All materials from the collection of NEFU].

sickle-shaped. Thorax brown-yellow, mixed with white. Abdomen brown-yellow with grayish-white scales. Ground colour of forewings brown-yellow, scattered with smoky gray and coffee tones. Costal and inner margins almost parallel. Wing veins visible; milky white between vein R_2 and costal margin, with wavy brown markings. Apex slightly rounded, with gray spots; basal spots grayish-white; basal line blurred, jagged, tan; subbasal line sepia; antemedial line brown; medial area with irregular gray brown spots; reniform stigma brown, preceded by some irregular black spots, periphery with grayish-white radial stripes; postmedial line wavy, brown; subterminal line serrated, grayish-brown; terminal area with broken grayish-brown spots; fringe long, brown. Hindwing smoky gray, deeper in colour towards termen; outer margin decorated with grayish-brown fringe and brown discal spot.

Male genitalia (Fig. 7). Uncus wide, short, mallet-shaped, about 1/3 length of tegumen; tegumen narrow, V-shaped, about 1.5 times shorter than vinculum; saccus V-shaped, strongly sclerotized; valva slightly asymmetric with mid of costal margin near straight and wide base, gradually narrowing to cucullus; cucullus bifurcated and extends outward vertically, forms conical protrusion, approximately same length as uncus; sacculus wide, sclerotised, with elongated hill-like extension on outer margin, blunted apically, strongly sclerotised; juxta elongate, shovel-like, extends posteriorly, approximately as long as tegumen. Aedeagus slender, almost straight, tubular; caecum slightly enlarged, strongly sclerotised in carinal plate; vesica sickle-shaped, covered in medial part with scobinate area in distal part, dorsal side has cornuti field and granulation area, and cornuti densely distributed.

Female genitalia (Fig. 11). Papillae anales broad and conical; apophysis posteriors longer than apophysis anteriores, blunt, slightly extended proximally, anterior apophysis thicker, shorter; antrum large, deep, funnel-like; ductus bursae long, strongly sclerotized, with membranous ring in joining with ductus bursae; corpus bursae membranous, elongated sack-like, with strongly sclerotised appendix bursa at junction with ductus bursae.

Bionomics. This species is known in Southwest China only from its type locality in Zhaotong, Prov. Yunnan, where it was collected in the mountainous regions at an altitude of about 1700 m. Both a male and a female specimen were collected in July.

Distribution. (Fig. 13) Southwest China (Prov. Yunnan).

Etymology. The species name refers to its collection site, Zhaotong area in Prov. Yunnan.

Stenoloba oculibasis Li, Zhang, Han & Kononenko, sp. nov.

https://zoobank.org/C49C097A-5327-46AB-BBCC-0D016A2F9D94
Figs 3, 4, 9, 13

Type material. ***Holotype:*** • 1♂, China, Chongqing Municipality, Mt. Simian, 4–8 May 2019, JJ. Fan, ZT Wang leg., slide HHL-4825-1, coll. NEFU. ***Paratype:*** • 1♂, China, Chongqing Municipality, Mt. Simian, 4–8 May 2019, JJ. Fan, ZT Wang leg., slide HHL-4825-s1, coll. NEFU.

Diagnosis. The new species belongs to the *S. basiviridis* species-group. This group includes 10 species: *S. basiviridis* Draudt, 1950 (Figs 6, 10), *S. assimilis* (Warren, 1909), *S. assimilina* Han & Kononenko, 2018, *S. gaoligonga* Han & Kononenko, 2018, *S. domina* Kononenko & Ronkay, 2000, *S. dominula* Kononenko & Ronkay, 2000, *S. siamensis* Behounek & Kononenko, 2010, *S. mossy* Behounek & Kononenko, 2010, *S. lampra* Kononenko & Ronkay, 2000 and *S. oculibasis* Li, Zhang, Han & Kononenko, sp. nov.

In comparison to several other species within the *S. basiviridis* species-group, *S. oculibasis* exhibits several distinctive characteristics, specifically: the uncus is generally elongated; the valva is long and rod-like, nearly straight, with a base that maintains approximately equal width only at its terminal end. The cucullus is rounded and features dense, long, and strongly sclerotized (or hardened) cornua. The juxta is typically spindle-shaped. Furthermore, the terminal vesica of the aedeagus possesses a long, spiky basal plate associated with the ductus ejaculatorius.

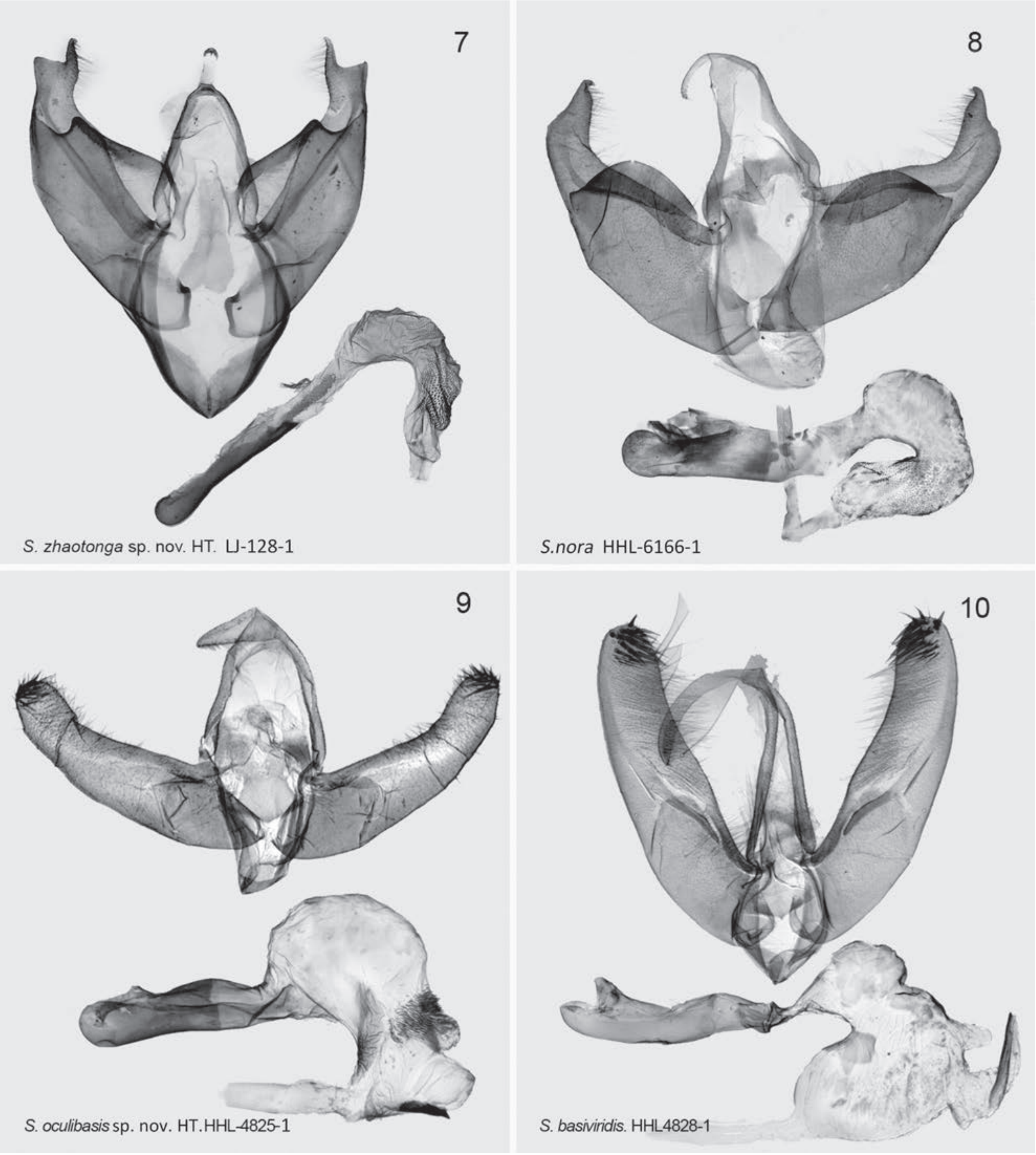

Figures 7–10. *Stenoloba* spp., male genitalia. **7** *S. zhaotonga* sp. nov., HT, slide LJ-128-1 **8** *S. nora*, slide HHL-6166-1 **9** *S. oculibasis* sp. nov., HT, slide HHL-4825-1 **10** *S. basiviridis*, male, slide HHL-4828-1 [All materials from the collection of NEFU].

From the perspective of wing surface characteristics, *S. oculibasis* is different from other species in this species-group. In the base area of the forewing, there exists a large oval spot. The center of this spot is orange-yellow, surrounded by gray-white. The middle part of the wing is darker and brown, while it turns to gray-white in the outer edge area. An orange-yellow reniform stigma is behind the submedial line. The male genitalia of *S. oculibasis* have similarities with both *S. assimilina* and *S. basiviridis*. It differs from *S. assimilina* by the shorter and tapered uncus and the missing strong ventro-subapical spine in

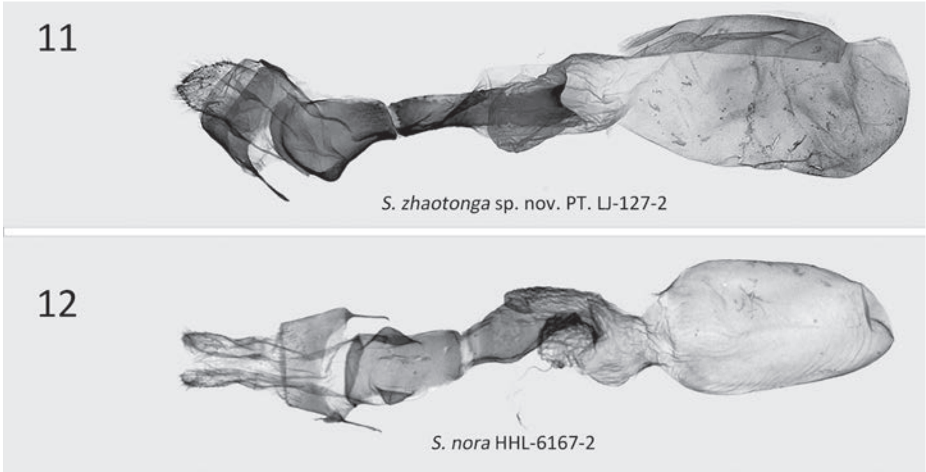

Figures 11, 12. *Stenoloba* spp., female genitalia. **11** *S. zhaotonga* sp. nov., PT, slide LJ-127-2 **12** *S. nora*, slide HHL-6167-2 [all materials from coll. NEFU].

the apical part of the valva [in *S. assimilina* (Han and Kononenko 2018, fig. 43) spine is present and the uncus short, flattened, rather massive, but not triangulate]. Compared with *S. basiviridis*, in *S. oculibasis* sp. nov. the uncus is short, pyramidal, sharp (in *S. basiviridis* long rod-like, tip fine); the vesica is generally kidney-shaped, with a wide base, oval shape, and a narrow middle and cornuti field is with intensive cornuti on the dorsal side (in *S. basiviridis* the vesica armed with one large spine-like cornutus).

Description. ***Adult*** (Figs 3, 4). Wingspan 26–27 mm. Forewing overall grayish-white with ochre tint. Head grayish-white. Thorax grayish-white, mixed with taupe. Abdomen gray, mixed with brown. Forewing basal area with grayish-white scales, there is an oval spot at the base, orange yellow in the middle, gray white around, and black brown on the outer edge; basal line brown; subbasal line distinct, russet; antemedial line tan; antemedial area darker, brownish-yellow; median line and postmedial line tan; reniform stigma yellow surrounded by light grayish-white; postmedial area with longitudinal stripes along veins; apex rounded, with irregular tan apical patch; tornal patch orange; terminal line serrated, brown; fringe trim, brown. Hindwing, light coloured, grayish-white; discal spot brown. Forewing underside colour grayish-white, with different shades, scattered brown stripes, and wing veins clearly visible.

Male genitalia (Fig. 9). Uncus relatively short, tapered, with wide base, pointed apically; tegument U-shaped; saccus V-shaped; valva long, almost equal in width from base to apex, slightly convex from base, sclerotised in apical half; sacculus wide, extending to about 1/3 length of valva, cucullus smooth, circularly arched, apex of cucullus armed with thorns and surrounded by long hair-like seta; juxta approximately pentagonal, extending upwards, sclerotised. Aedeagus straighter; caecum round; vesica reniform, cornuti field has dense cornutus, ventral area wrinkled and sclerotised, dorsally armed with large, wide, nail-like cornutus, and terminal has a long spiky basal plate of ductus ejaculatorius.

Female genitalia. Unknown.

Bionomics. The species is known only from its type locality in Southwest Chongqing Municipality, where it occurs in mountains at an altitude of 1100 m. Both male specimens were collected in May.

Distribution. (Fig. 13) Southwest China (Chongqing Municipality).

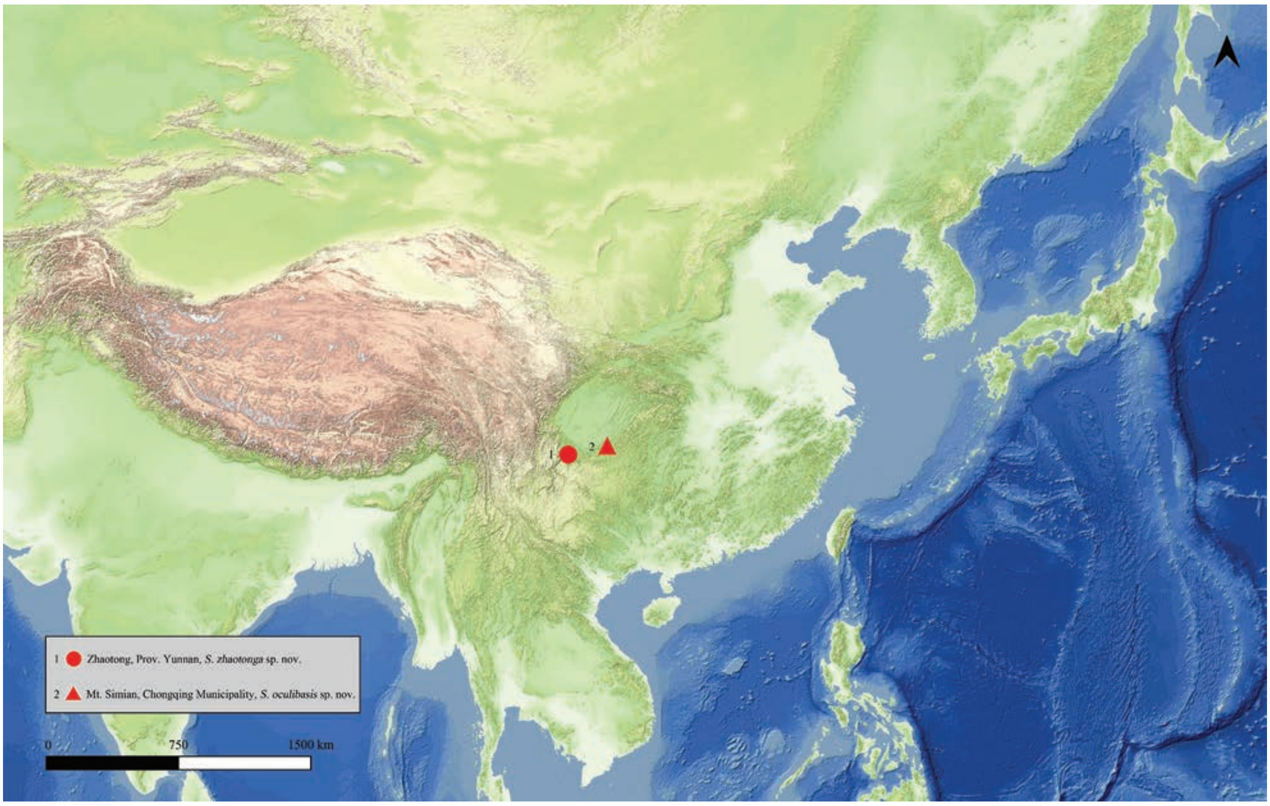

Figure 13. Map of collecting sites. **1** Zhaotong, Prov. Yunnan, *S. zhaotonga* sp. nov. **2** Mt. Simian, Chongqing Municipality, *S. oculibasis* sp. nov.

Etymology. The species name "*oculibasis*" refers to one of the two main distinguishing characters: the presence of the large white with a creamy centre rounded spot in the basal part of the forewing.

Acknowledgements

Xinyu Zhang provided tremendous assistance for the smooth collection of specimens.

Additional information

Conflict of interest

The authors have declared that no competing interests exist.

Ethical statement

No ethical statement was reported.

Funding

The present study was supported by the National Natural Science Foundation of China (No. 31872261), the project of the Northeast Asia Biodiversity Research Center (2572022DS09) and the Fundamental Research Funds for the Central Universities (No. 2572019CP11). Vladimir S. Kononenko carried out this research within the state assignment of Ministry of Science and Higher Education of the Russian Federation (theme No. 121031000151-3).

Author contributions

Conceptualization: HLH and VSK. Data curation: JL. Investigation: JL, HLH, CZ. Resources: JL, HLH, CZ. Supervision: HLH and VSK. Visualization: JL and VSK. Writing – original draft: JL. Writing – review and editing: HLH and VSK.

Author ORCIDs

Jian Li https://orcid.org/0009-0002-4428-0617
Chao Zhang https://orcid.org/0000-0001-6069-1059
Hui-Lin Han https://orcid.org/0000-0002-2045-6182
Vladimir Kononenko https://orcid.org/0000-0001-6103-4800

Data availability

All of the data that support the findings of this study are available in the main text.

References

Behounek G, Kononenko VS (2010) Fourteen new species of the genus *Stenoloba* Staudinger, 1892 from South East Asia (Lepidoptera: Noctuidae, Bryophilinae). Zootaxa 2679: 1–31. https://doi.org/10.11646/zootaxa.2679.1.1

Chang BS (1991) Illustration of moths in Taiwan (5). Taiwan Museum, Taiwan, 336 pp.

Chen YX (1999) Lepidoptera, Noctudae. In: Zhu HF, Wang LY (Eds) Fauna Sinica, Insecta, Vol. 16. Science Press, Beijing, 1596 pp.

Draudt M (1950) Beiträge zur Kenntnis der Agrotiden-Fauna Chinas aus den Ausbeuten Dr. H.Höne's. Mitteilungen der Münchener Entomologischen Gesellschaf 40(1): 1–174.

Hampson GF (1894) The fauna of British India, including Ceylon and Burma. Moths, Vol. 2. London, Taylor and Francis, xxii, 609 pp.

Hampson GF (1910) Catalogue of the Lepidoptera Phalaenae in the British Museum, Vol. 10. Taylor and Francis, London, i–xix, 829 pp.

Hampson, GF (1918) Description of a new species of Amatidae, Lithosiidae and Noctuidae. Novitates Zoologicae 25: 93–217. https://doi.org/10.5962/bhl.part.29763

Han HL, Kononenko VS (2009) A review of the genus *Stenoloba* Staudinger, 1892 from China, with description of 6 new species and 7 new records for China (Lepidoptera: Noctuidae, Bryophilinae). Zootaxa 2268: 1–22. https://doi.org/10.11646/zootaxa.2268.1.1

Han HL, Kononenko VS (2015) *Stenoloba ronkayi* Sohn & Tzuoo, 2012 – a new homonym of *S. ronkayi* Behounek & Kononenko, 2010 and new synonym of *S. glauca* Kononenko & Ronkay 2001. A postscript to the revision of Chinese *Stenoloba* (Lepidoptera, Noctuidae). Zootaxa 4013(3): 440–442. https://doi.org/10.11646/zootaxa.4013.3.8

Han HL, Kononenko VS (2018) Twelve new species and four new records of *Stenoloba* Staudinger, 1892 from China (Lepidoptera, Noctuidae: Bryophilinae). Zootaxa 4388(3): 301–327. https://doi.org/10.11646/zootaxa.4388.3.1

Han HL, Kononenko VS (2021) Two new species of *Stenoloba* Staudinger, 1892 and one *Victrix* Staudinger, 1879 from East Asia and China (Lepidoptera, Noctuidae, Bryophlilinae). Zootaxa 4951(2): 342–352. https://doi.org/10.11646/zootaxa.4951.2.7

Han HL, Lü LS (2007) A new species, *Stenoloba motuoensis* sp. nov., from China (Lepidoptera, Noctuidae s.l.). Tinea 20(1): 6–8.

Han HL, Kononenko VS, Behounek G (2011) Three new species of the subfamily Bryophilinae from China (Lepidoptera, Noctuidae). Zootaxa 3108: 53–63. https://doi.org/10.11646/zootaxa.3108.1.4

Han HL, Kononenko VS, Li CD (2020) The Catalogue of the Noctuoidea in the Three Provinces of Northeast China I: Families Erebidae (part), Euteliidae, Nolidae and Noctuidae. Heilongjiang Science and Technology Press, Harbin, 560 pp.

Holloway JD (2009) The Moths of Borneo 13. Family Noctuidae, subfamilies Pantheinae (part), Bagisarinae, Acontiinae, Aediinae, Eustrotiinae, Bryophilinae, Araeopteroninae, Aventiinae, Eublemminae and further miscellaneous genera. Malayan Nature Journal 62(1–2): 1–240.

Kononenko VS, Han HL (2007) Atlas genitalia of the Noctuidae in Korea (Lepidoptera). In: Park K-T (Ed.) Insects of Korea, Series 11. Seoul, Korea, 464 pp.

Kononenko VS, Ronkay L (2000) A revision of the genus *Stenoloba* Staudinger, 1892 (Lepidoptera, Noctuidae, Bryophilinae) with description of 25 new species and 3 new subspecies from East Asia (I). Insecta Koreana 17(3): 137–174.

Kononenko VS, Ronkay L (2001) A revision of the genus *Stenoloba* Staudinger, 1892 (Lepidoptera, Noctuidae, Bryophilinae) with description of 15 new species and 3 new subspecies from East Asia (II). Insecta Koreana 18(2): 95–121.

Leech JH (1889) On the Lepidoptera of Japan and Korea. Part III. Heterocera, sect. II. Proceedings of the Zoological Society of London, 1889: 474–571. https://doi.org/10.1111/j.1469-7998.1889.tb06789.x

Mell R (1943) Beiträge zur Fauna sinica. XXIV. Über Phlogophorinae, Odontodinae, Sarrothripinae, Westermanniinae und Camptolominae (Noctuidae, Lepid.) von Kuangtung. Zoologische Jahrbücher 76: 171–226.

Moore F (1888) Description of new Indian Lepidopterous Insects from the Collection of the Late Mr. W. S. Atkinson. Heterocera (continued) (Pyralidae, Crambidae, Geometridae, Tortricidae, Tineidae). Taylor and Francis, London, pp. 199–299. [pls 7–8]

Oberthür Ch (1884) Lepidopteres de l'Asie Orientale. Etudes d'Entomologie 10: 134–135.

Pekarsky O (2011) A new *Stenoloba* Staudinger species from China (Lepidoptera, Noctuidae, Bryophilinae). ZooKeys 108: 67–72. https://doi.org/10.3897/zookeys.108.1208

Pekarsky O (2018) Two new *Stenoloba* Staudinger, 1892 species from China and Vietnam (Lepidoptera, Noctuidae, Bryophilinae). Entomofauna carpathica 30(2): 59–67.

Pekarsky O (2019) New Bryophilinae species from Central Asia and Vietnam (Lepidoptera, Noctuidae). Entomofauna carpathica 31(1): 27–37.

Pekarsky O, Saldaitis A (2013) A new species of *Stenoloba* Staudinger, 1892 from China (Lepidoptera, Noctuidae, Bryophilinae). Zookeys 310: 1–6. https://doi.org/10.3897/zookeys.310.5125

Pekarsky O, Dvořák M, Ronkay G (2013) Three new species of *Stenoloba* Staudinger, 1892 from Southeast Asia (Lepidoptera, Noctuidae, Bryophilinae). Fibigeriana Supplement 1: 165–170. https://doi.org/10.3897/zookeys.310.5125

Ronkay L (2001) New *Stenoloba* Staudinger, 1892 species from Taiwan and Vietnam (Lepidoptera: Noctuidae, Bryophilinae). Annales historico-naturales Musei nationalis hungarici 93: 219–229.

Saldaitis A, Volynkin AV (2020) Two new *Stenoloba* Staudinger, 1892 from Yunnan, southwestern China (Lepidoptera, Noctuidae, Bryophilinae). Zootaxa 4755(3): 545–552. https://doi.org/10.11646/zootaxa.4755.3.6

Sohn JC, Han HL (2005) A new species of *Stenoloba* Staudinger (Noctuidae, Bryophilinae) from Korea. Tinea 19(1): 22–27.

Sohn JC, Tzuoo HR (2012) Two new species of *Stenoloba* (Lepidoptera: Noctuidae) from East Asia with the first description of *S. nora* female genitalia. Journal of Asia-Pacific Entomology 15: 241–244. https://doi.org/10.1016/j.aspen.2011.11.005

Staudinger O (1892) Die Macrolepidopteren des Amurgebiets. I. Theil. Rhopalocera. Sphinges, Bombyces, Noctuae. In: Romanoff NM (Ed.) Mémoires sur les Lépidoptéres 6. Imprimerie de M.M. Stassuléwitch, St Petersburg, 83–658.

Sugi S (1970) Notes on the genus *Stenoloba*, with description of a new genus. Konty 38(2): 130–135.

Warren W (1914) New species of Drepanulidae, Noctuidae, and Geometridae in the Tring Museum. Novitates Zoologicae 21: 401–425. https://doi.org/10.5962/bhl.part.16333

Warren W (1909–1914) Die eulenartige Nachtfalter. In: Seitz A (Ed.) Die Gross-Schmetterlinge der Erde. Die Gross-Schmetterlinge des Palaearctischen Faunengebietes. Band 3. Alfred Kernen Verlag, Stuttgart, 511 pp, iv, 75 pl.

Yoshimoto H (1992) Noctuidae. In: Haruta T (Ed.) Moths of Nepal. Part 1. Tinea 13 (Supplement 2): 50–69.

Yoshimoto H (1994) Noctuidae. In: Haruta T (Ed.) Moths of Nepal. Part 3. Tinea 14 (Supplement 1): 95–139.

ZooKeys 1228: 185–195 (2025)
DOI: 10.3897/zookeys.1228.131341

Research Article

A new species of the rib-degenerated loach, genus *Protocobitis* (Cypriniformes, Cobitidae), from Guangxi, China

Zhi-Xian Qin[1,2*], Ye-Wei Liu[3*], Si-Yu Zhang[1,2], Jing-Song Shi[4,5], Li-Na Du[1,2], Jia-Jun Zhou[6,7]

1 *Key Laboratory of Ecology of Rare and Endangered Species and Environmental Protection (Guangxi Normal University), Ministry of Education, Guilin, Guangxi 541004, China*
2 *Guangxi Key Laboratory of Rare and Endangered Animal Ecology, College of Life Science, Guangxi Normal University, Guilin, Guangxi 541004, China*
3 *Guangxi Key Laboratory for Forest Ecology and Conservation, College of Forestry, Guangxi University, Nanning, Guangxi 530004, China*
4 *Institute of Zoology, Chinese Academy of Sciences, Beijing 100101, China*
5 *Institute of Vertebrate Paleontology and Paleoanthropology, Chinese Academy of Sciences, Beijng 100044, China*
6 *Zhejiang Forest Resource Monitoring Center, Hangzhou, Zhejiang 310020, China*
7 *Zhejiang Forestry Survey Planning and Design Company Limited, Hangzhou 310020, China*
Corresponding authors: Li-Na Du (dulina@mailbox.gxnu.edu.cn); Jia-Jun Zhou (cnwaters@foxmail.com)

Abstract

A new species of the genus *Protocobitis* is described based on morphological comparisons and molecular analyses from specimens of a subterranean tributary of the Hongshui River, Lingyun County, Baise City, and a cave in Jinya Township, Fengshan County, Hechi City, Guangxi, China. Both morphological and molecular data support the validity of *Protocobitis longibarba* **sp. nov.** The new species can be distinguished from congeners by the following combination of characteristics: whole body except for head and area between pectoral-fin and pelvic-fin origin sparsely covered with minute scales; barbels elongate; five or six branched pectoral-fin rays and four branched pelvic-fin rays; vertebrae 4+42. Maximum-likelihood and Bayesian-inference phylogenetic trees exhibited congruent topological structures, exhibiting high node support for the monophyly of *Protocobitis longibarba* (BPP = 1; BS = 100), which was clustered with the other congeners.

Key words: Cavefish, mitochondrial gene, Pearl River, taxonomy

Academic editor: Bruno Melo
Received: 5 July 2024
Accepted: 8 January 2025
Published: 21 February 2025

ZooBank: https://zoobank.org/02EA0884-4F6B-45E7-B3CE-30D1641EBB19

Citation: Qin Z-X, Liu Y-W, Zhang S-Y, Shi J-S, Du L-N, Zhou J-J (2025) A new species of the rib-degenerated loach, genus *Protocobitis* (Cypriniformes, Cobitidae), from Guangxi, China. ZooKeys 1228: 185–195. https://doi.org/10.3897/zookeys.1228.131341

Introduction

The unique karst landforms of the Guangxi Zhuang Autonomous Region (hereinafter referred to as Guangxi) have resulted in extensive surface water and ground water systems, providing ideal conditions for the evolution and adaptive radiation of cavefish species. The perpetual absence of light in caves prevents photosynthesis, leading to a limited food supply primarily sourced from surface water exchange. This scarcity of food presents considerable challenges in providing adequate nutrition for fish reproduction. Consequently, populations of karst cavefish, such as *Sinocyclocheilus hyalinus* Chen & Yang, 1993, are extremely rare (Chen et al. 1994; Jeffery 2001, 2009; Zhao and Zhang 2009; Liang et al. 2011; Fan et al. 2024).

---

[*] These authors contributed equally to this work.

The genus *Protocobitis* Yang, Chen & Lan, 1994 was initially described based on specimens collected from Du'an County, Guangxi, with the type species *Protocobitis typhlops* Yang, Chen & Lan, 1994 (Yang et al. 1994). Endemic to Guangxi, this genus is a typical cave-dwelling fish species, displaying distinctive characteristics such as the absence of eyes, pigment degeneration leading to transparency or semitransparency, elongate barbels, reduction or absence of body scales, and tiny cranial bones (Zhao and Zhang 2006); thus, it demonstrates a high degree of adaptation to cave life. Four valid species have been recognized within the genus, including *P. anteroventris* Lan, 2013 and *P. longicostatus* Zhou, Qin, Du &Wu, 2024 from Baise City, *P. typhlops* from Hechi City, and *P. polylepis* Zhu, Lv, Yang & Zhang, 2008 from Nanning City (Yang et al. 1994; Zhu et al. 2008; Lan et al. 2013; Zhou et al. 2024). All known *Protocobitis* species are eyeless and exhibit varying degrees of rib degeneration.

Five specimens of *Protocobitis* were collected in February 2024 from a subterranean tributary of the Hongshui River in Luolou Town, Lingyun County, Baise City, and two collected in May 2024 from a cave in Jinya Township, Fengshan County, Hechi City, Guangxi, China. Results of our morphological and molecular analyses indicate that these loach specimens represent a new species of *Protocobitis*, which is described herein.

Materials and methods

All field collections abided by the rules of the Fisheries Law of the People's Republic of China. All activities conformed to the Laboratory Animal Guidelines for the Ethical Review of Animal Welfare (GB/T 35892-2018). After euthanizing the collected fish specimens with excessive anesthetic clove oil, the right pelvic fins were excised and placed in 95% alcohol for subsequent DNA sequencing, then the whole-body specimens fixed in 10% formalin and transferred to 75% ethanol for morphological study. Specimens were preserved at the Kunming Natural History Museum of Zoology, Kunming Institute of Zoology (**KIZ**), Chinese Academy of Sciences (CAS), and Zhejiang Forest Resource Monitorign Center (ZJFRF), Hangzhou, Zhejiang. Counts and measurements followed Yang et al. (1994). All measurements were taken point-to-point with dial calipers to the nearest 0.1 mm. X-ray scanning and three-dimensional (3D) reconstructions were conducted using nano-computerized tomography (CT) with a GE V|tome|X m dual tube 300/180 kV system at the Key Laboratory of Vertebrate Evolution and Human Origins, Institute of Vertebrate Paleontology and Paleoanthropology (IVPP), CAS. The specimens were scanned with an energy beam of 80 kV and a flux of 80 × μA using 360° rotation, then reconstructed into a 4 096 × 4 096 matrix of 1 536 slices. The final CT reconstructed skull images were exported with a minimum resolution of 8.9 μm. Skull images were exported from the virtual 3D model reconstruction using Volume Graphics Studio v. 3.4.0.

The extraction, amplification, and sequencing of genomic DNA were conducted by Tsingke Biotechnology Co., Ltd (China). Partial sequences of the mitochondrial *cytochrome c oxidase subunit I* (COI) and cytochrome *b* (cyt *b*) were sequenced and submitted to GenBank (accession: PP866712–PP866715 for COI, and PP868402–PP868405 for cyt *b*). The sequencing results were manually checked, corrected, and assembled using SeqMan within the Lasergene v. 7.1.0 package, DNASTAR, Inc., Madison Wis. The assembled sequences were aligned using MEGA v. 7.0 (Kumar et al. 2016) for multiple comparisons, and redundant segments were trimmed to obtain consistent sequences for further analysis. Genetic diversity analyses and haplotype filtering were performed using DnaSP v. 5 (Librado and Rozas 2009).

The complete mitochondrial genomes of 14 cobitid species and two botiid species (*Parabotia fasciata* Dabry de Thiersant, 1872 and *Leptobotia elongata* Bleeker, 1870) were retrieved from GenBank to serve as the outgroup. The phylogenetic placement of *Protocobitis longibarba* was determined using maximum likelihood (ML) and Bayesian inference (BI) implemented in the CIPRES Science Gateway (Miller et al. 2010). The ML tree was reconstructed using RAxML-HPC v. 8 (Stamatakis 2014), with 1,000 rapid bootstrapping iterations. The BI tree was constructed using MrBayes in XSEDE v. 3.2.7a (Ronquist et al. 2012). Two parallel runs were performed, with four Markov chains starting from a random tree. The chains were run for five million generations and sampled every 100 generations. The first 25% of sampled trees were discarded as burn-in, and the remaining trees were used to obtain a consensus tree and estimate Bayesian posterior probabilities (BPPs). The phylogenetic trees were viewed and edited using FigTree v. 1.4.4 (Rambaut 2009). Uncorrected pairwise distances (1000 replicates) based on concatenated dataset of mitochondrial COI and cyt *b* sequences was estimated using MEGA v. 7.0 (Kumar et al. 2016).

Results

Protocobitis longibarba **sp. nov.**

https://zoobank.org/50F311B3-8458-426E-A76B-808847C94DB3
Fig. 1, Table 1

Type material. ***Holotype*****.** • KIZ2024000004, male, 44.0 mm standard length (SL), Yangcun Village, Luolou Town, Lingyun County, Baise City, Guangxi, China, from a subterranean tributary of the Hongshui River; 24.4392°N, 106.7409°E, collected by J.J. Zhou, Y.W. Liu & S.P. Zhou; 15 February 2024. ***Paratypes*****.** • KIZ2024000001–3, female, 51.1–51.9 mm SL, KIZ2024000005, male, 44.0 mm SL, ZJFRF2402010, male, 53.5 mm SL; five specimens, collected with holotype • KIZ2024000006–7, male, 39.5–43.1 mm SL, two specimens, Liangfeng Cave, Shima Lake, Jinya Township, Fengshan County, Hechi City, Guangxi, China; 24.5587°N, 106.8655°E; collected by Y.W. Liu; 23 May 2024.

Diagnosis. *Protocobitis longibarba* can be distinguished from all other species of *Protocobitis* by the following combination of characteristics: whole body, except for head and abdomen, sparsely covered with minute scales (vs scaleless in *P. anteroventris*, scales present along midline of body in *P. typhlops*; barbels elongate; 5–6 branched pectoral fin rays (vs seven in *P. anteroventris*, *P. longicostatus*, and *P. polylepis*); four branched pelvic-fin rays (vs five in other *Protocobitis* species); caudal-peduncle height 34.9%–58.6% of its length (vs 64.1%–65.7% in *P. polylepis*, 27.9%–43.3% in *P. anteroventris*); head width 7.3%–10.3% of SL (vs 5.4%–6.6% in *P. anteroventris*); head height 50.2%–80.6% of lateral head length (vs 45.7%–49.5% in *P. longicostatus*, 43.8%–46.8% in *P. anteroventris*).

Description. Body elongate; maximum body width located immediately anterior to dorsal fin. Dorsal and ventral profiles almost straight except for slightly convex anus and base of fin. Snout obtuse. Head short, higher than width, roughly

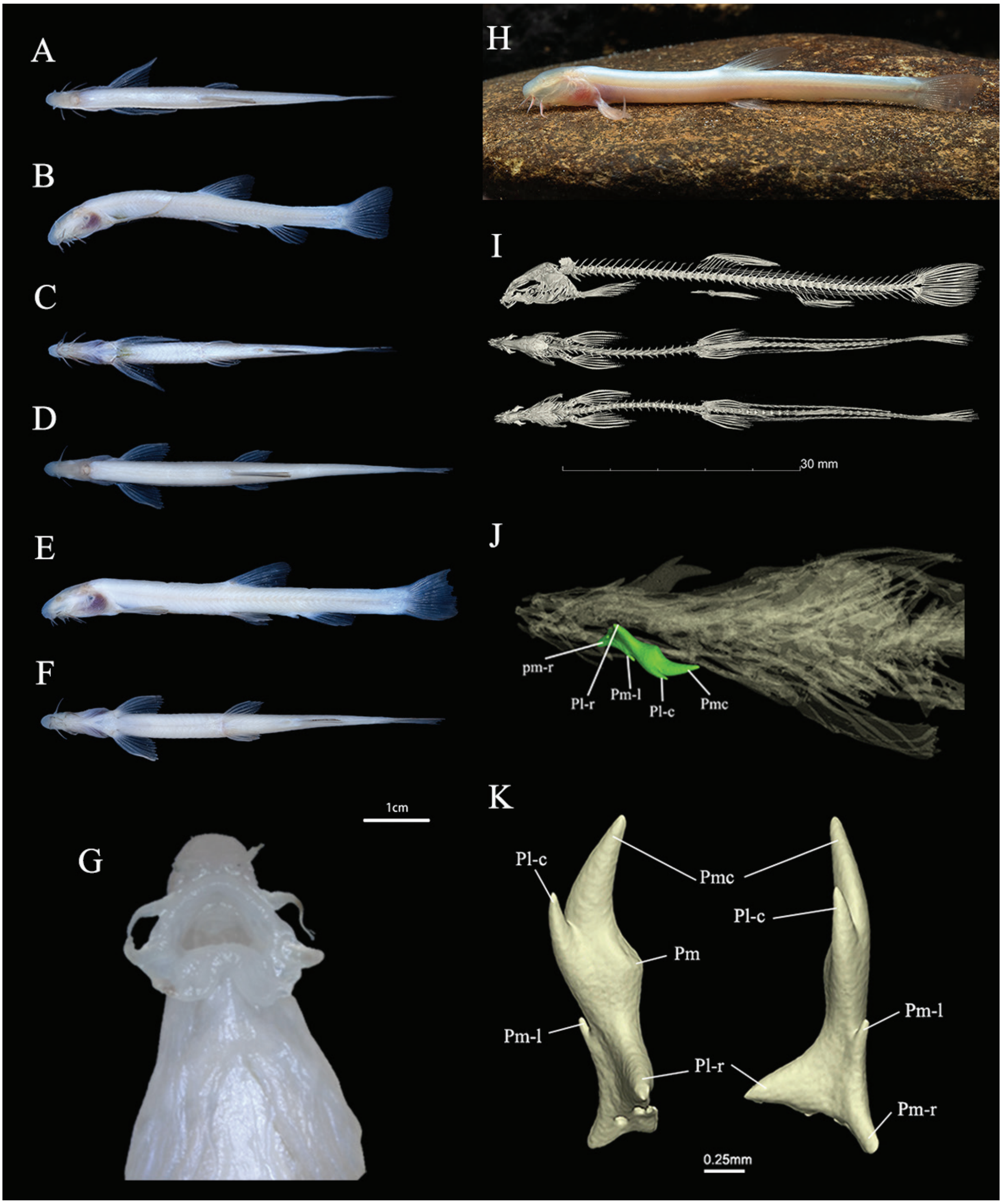

Figure 1. Morphometric characters of *Protocobitis longibarba* sp. nov. **A–C** lateral, dorsal and ventral views of male, holotype KIZ2024000004 **D–F** lateral, dorsal and ventral views of female, paratype KIZ2024000003 **G** ventral view of mouth **H** live male **I** lateral and ventral views of skeleton, paratype ZJFRF2402010 **J, K** suborbital spines (Abbreviations: Pmc, Processus mediocaudalis; Pl-c, Processus latero-caudalis; Pm, Processus medialis; Pm-l, Processus medio-lateralis; Pl-r, Processus latero-rostralis; Pm-r, Processus medio-rostralis).

triangular in dorsal view. Nostrils closely set, nearer to snout tip than to the operculum, anterior nostril in short tube. Eyeless. Suborbital spine bifid, relatively thick and short, with strong mediolateral process in front of cavity of eye, length of laterocaudalis processus nearly half of mediocaudalis process, four strumae in

Table 1. Morphometric and meristic data of *Protocobitis longibarba* sp. nov.

Characters	Holotype	Paratypes (mean ± SD)
Total length (mm)	53.5	43.7–61.7 (54.8 ± 7.1)
Standard length (mm)	44.0	39.5–51.9 (46.9 ± 5.4)
Percent of standard length (%)		
Deepest body depth	8.4	7.6–9.4 (8.8 ± 0.8)
Head width	7.3	7.7–10.3 (8.7 ± 0.9)
Head depth	14.3	9.9–15.1 (13.1 ± 2.2)
Lateral head length	20.4	17.2–21.9 (19.7 ± 1.8)
Prepelvic length	50.9	47.5–52.1 (50.7 ± 1.7)
Preanal length	78.2	71.2–76.7 (74.0 ± 1.9)
Preanus length	71.2	62.9–70.7 (67.9 ± 3.0)
Caudal-peduncle length	17.5	16.8–19.9 (18.1 ± 1.5)
Caudal-peduncle depth	7.2	6.2–9.8 (7.9 ± 1.3)
Percent of lateral head length (%)		
Head width	35.8	38.9–55.1 (44.7 ± 6.1)
Head depth	70.2	50.2–80.6 (66.8 ± 11.4)
Percent of caudal-peduncle length (%)		
Caudal-peduncle depth	41.1	34.9–58.6 (44.0 ± 9.9)
Fin-ray counts		
Dorsal-fin rays	iii, 7	iii, 7
Pectoral-fin rays	i, 6	i, 5–6
Pelvic-fin rays	i, 4	i, 4
Anal-fin rays	iii, 5	iii, 5
Branched caudal-fin rays	13	12–13

base of mediorostralis process (Fig. 1J, K). Mouth inferior and arched, in vertical line of nostrils. Lips thin and smooth, each side of middle of lower lip with pair of developed fleshy mental lobes (Fig. 1G). Inner surface of mouth densely covered with numerous papillae, and outer edge of upper jaw neatly arranged with row of small nodules. Three pairs of barbels, inner rostral barbel reaching corner of mouth, outer rostral barbel reaching tip of suborbital spine, maxillary barbel extending almost to vertical line at junction of head and dorsum.

Morphometric data of the type specimen of *P. longibarba* are given in Table 1. Dorsal fin with three unbranched and seven branched rays; pectoral fin with one unbranched and 5–6 branched rays; pelvic fin with one unbranched and four branched rays; anal fin with three unbranched and five branched rays; caudal fin with 12–13 branched rays. Dorsal-fin base short, originating at midpoint of body length, with tip of dorsal fin extending to vertical of anus origin; in male, the first branched pectoral fin ray elongated posteriorly and thicker, with a pointed tip; pelvic-fins origin closer to anal-fin origin than to pectoral-fin base, not reaching anus; anus elongated posteriorly into tube and closer to anal-fin origin; caudal fin emarginate, margins of lobes uneven.

Except for head and abdomen, whole body covered with sparse and minute scales, shallowly embedded in skin surface. Cephalic lateral-line and lateral-line pores absent. Nine to 10 inner gill rakers on first gill arch. Chest and abdominal walls thick and rich in fat. Air bladder absent, no bony bladder. Intestine straight, leading directly to anus. Ribs degenerate, each vertebra with only short and simple parapophysis (Fig. 1I). Vertebrae (from radiograph) 4+42.

Coloration. In life, body generally pale, without pigment, head and all fins transparent, outline of skull visible through skin, barbels exhibit distinct blood vessels (Fig. 1H). Whole body after preservation in formalin pale white, without pigment.

Sexual dimorphism. Male smaller than females, with longer pectoral fin. First branched pectoral fin ray in male thickened and elongated but without the lamina circularis, longest fin ray reaching midpoint between origin of pectoral fin and anus (Fig. 1A–C). First branched pectoral fin ray in females as long as second branched ray (Fig. 1D–F).

Etymology. The specific epithet is a combination of the Latin words *long-* (long) and *-barba* (barbel), indicating its long maxillary barbel, which extends almost to the vertical line at the junction of the head and dorsal body, feminine. We suggest the common Chinese name "Cháng Xū Yuán Huā Qiū (长须原花鳅)" and English name "long-barbal protocobitis".

Distribution and habitat. The new species is currently known from a cave located in Yangcun Village, Luolou Town, Lingyun County, Baise City and Jinya Township, Fengshan Country, Hechi City (Fig. 2A). In Fengshan County, this species occurs in a pool at the end of cave, which, in the dry season, has an area of approximately 100 m^2; the water surface is about 15 m from the ground. The

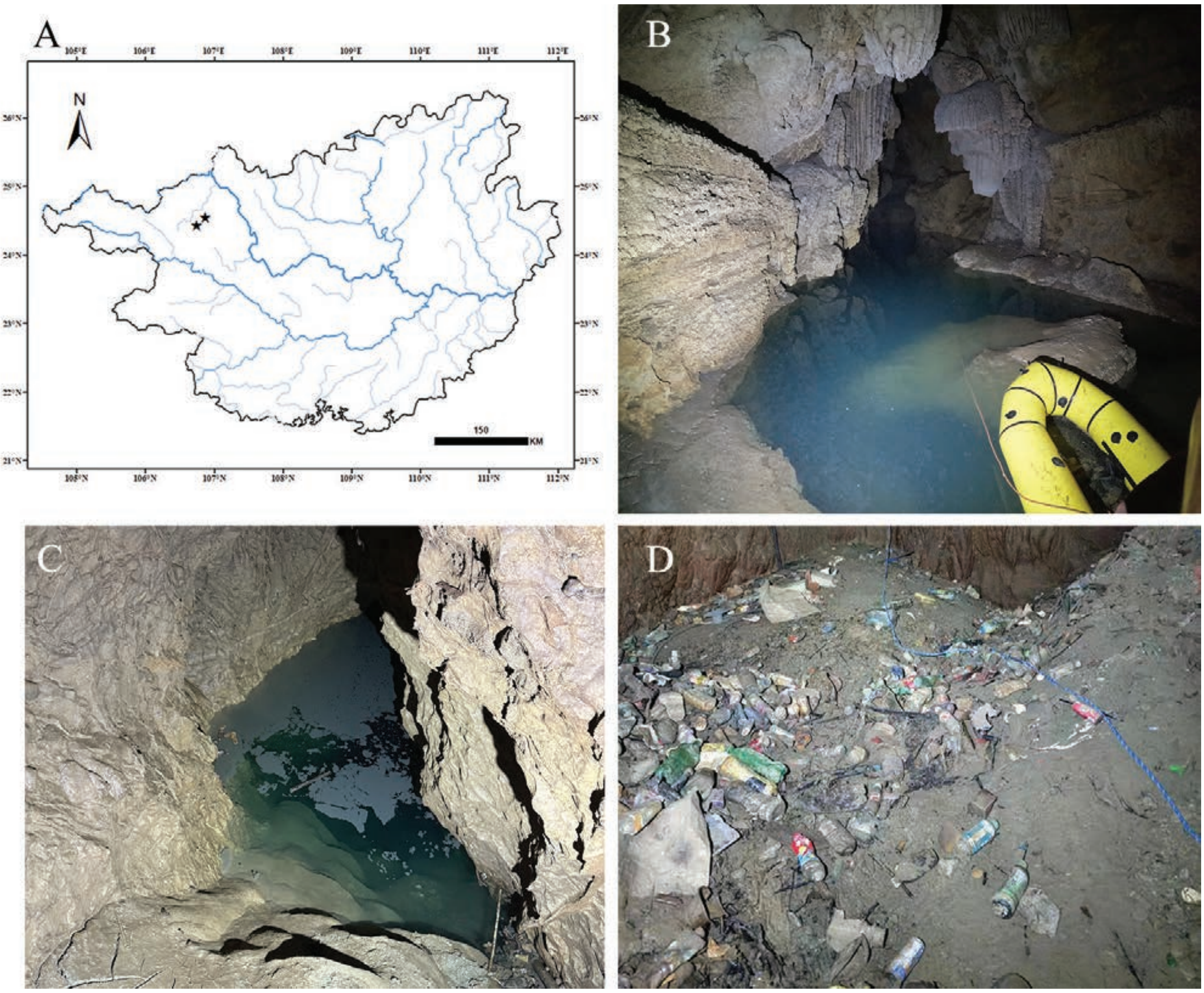

Figure 2. Distribution of *Protocobitis longibarba* sp. nov. and the environment of the cave at the time of collection **A** distribution map of *Protocobitis longibarba* sp. nov. **B** Liangfeng Cave in Fengshan County **C, D** cave in Lingyun County.

water depth is more than 30 m, and the water is clear and unpolluted (Fig. 2B). The pool belongs to the Poxin subterranean river system. Sympatric species include *Sinocyclocheilus lingyunensis* Li, Xiao & Luo, 2000, *Sinocyclocheilus microphthalmos* Li, 1989, *Sinocyclocheilus anshuiensis* Gan, Wu, Wei & Yang, 2013, and *Triplophysa lingyunensis* Liao,Wang & Luo, 1997. The cave in Lingyun County is approximately 300 m long, inclined downward at a 45° angle. The water pool located at the end of the cave is connected to the Shuiyuan Cave subterranean river system, which are, in turn, connected to a tributary of the Hongshui River. During the dry season, the water level area fluctuates from 5 to 50 m^2 (Fig. 2C). The cave acts as a conduit for surface water, domestic waste, and mud during the rainy season (Fig. 2D). As such, the primary substrate within the cave is mud. *Protocobitis longibarba* mainly feeds on algae and organic detritus and prefers to burrow into the muddy substrate. Sympatric species include *S. lingyunensis*, *S. microphthalmos*, and *S. anshuiensis*.

Genetic comparisons. Four sequences totaling 1775 bp in from *P. longibarba* were amplified, resulting in the detection of 14 haplotypes. The haplotype matrix consisted of 1,071 invariable sites, 704 variable sites, 387 parsimony informative sites, and 43 singletons.

The ML and BI phylogenetic trees exhibited congruent topological structures (ML tree see Fig. 4), exhibiting high node support for the monophyly of *P. longibarba* (BPP = 1; BS = 100), which was clustered with the other congeners. *Protocobitis* was sister to the lineage composed of species from *Paramisgurnus* Guichenot, 1872, *Misgurnus* Lacepède, 1803, and *Cobitis* Linnaeus, 1758 (Fig. 3). In the phylogenetic tree, *P. anteroventris* diverged earliest, followed by *P. longicostatus*, while *P. typhlops* was identified as sister group to *P. longibarba*. Additionally, pairwise comparisons of the concatenated dataset of mitochondrial COI and cyt *b* sequences revealed that the uncorrected *p*-distance between species of *Protocobitis* ranged from 6.25% to 16.45%. The minimum uncorrected *p*-distance is between *P. longibarba* and *P. typhlops* (6.25%), and the maximum uncorrected *p*-distance is between *P. longibarba* and *P. anteroventris* (16.45%) (Table 2).

Table 2. Uncorrected pairwise distances between species of *Protocobitis* based on concatenated dataset of mitochondrial COI and cyt *b* sequences.

ID	Species	1	2	3
1	*P. typhlops*			
2	*P. longibarba* **sp. nov.**	0.0625		
3	*P. longicostatus*	0.1166	0.1352	
4	*P. anteroventris*	0.1514	0.1645	0.1442

Discussion

Both morphological and molecular data support the validity of *Protocobitis longibarba*. The genus *Protocobitis* is typically characterized by the presence of degenerate ribs, with *P. anteroventris*, *P. longicostatus*, and *P. longibarba* showing progressively shorter ribs and *P. typhlops* and *P. polylepis* lacking ribs entirely. Vertebral counts also show variation among the species, with *P. anteroventris* having the highest count (4+57), *P. polylepis* having the lowest count (4+38), and the other three species ranging from 4+42 to 4+43. The

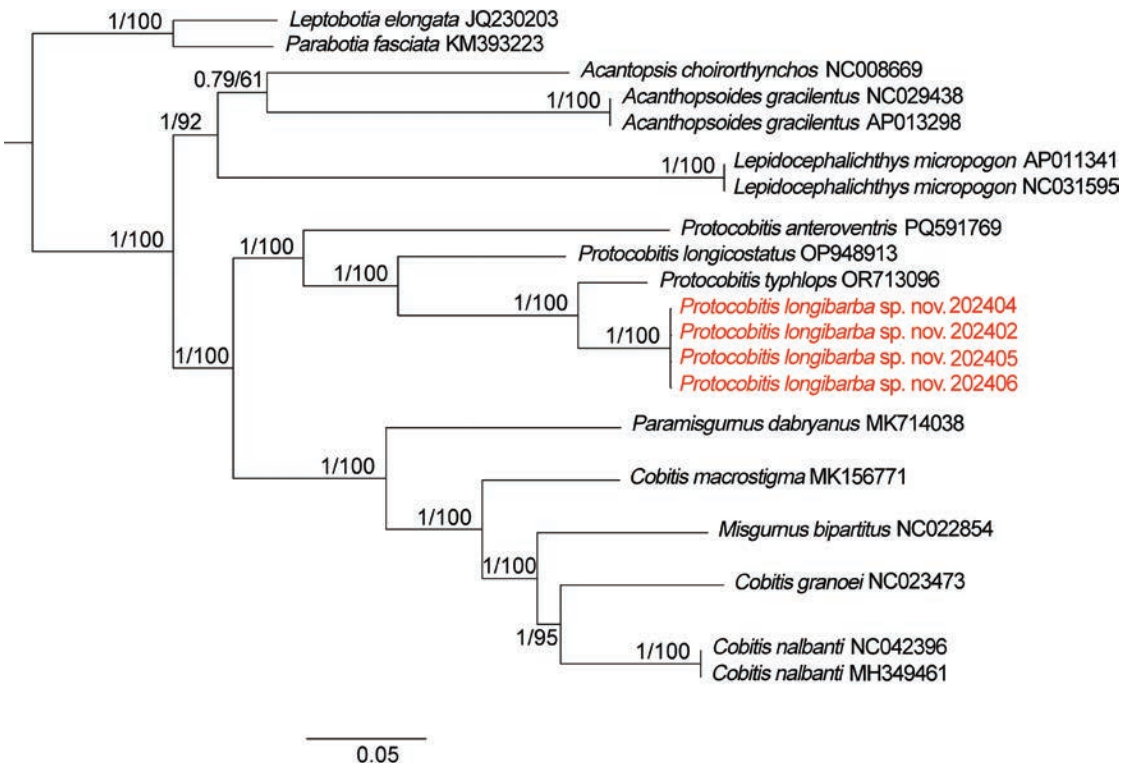

Figure 3. Bayesian phylogram of *Protocobitis* based on concatenated dataset of mitochondrial COI and cyt *b* sequences. The numbers on the nodes represent BPPs from BI and BS from ML.

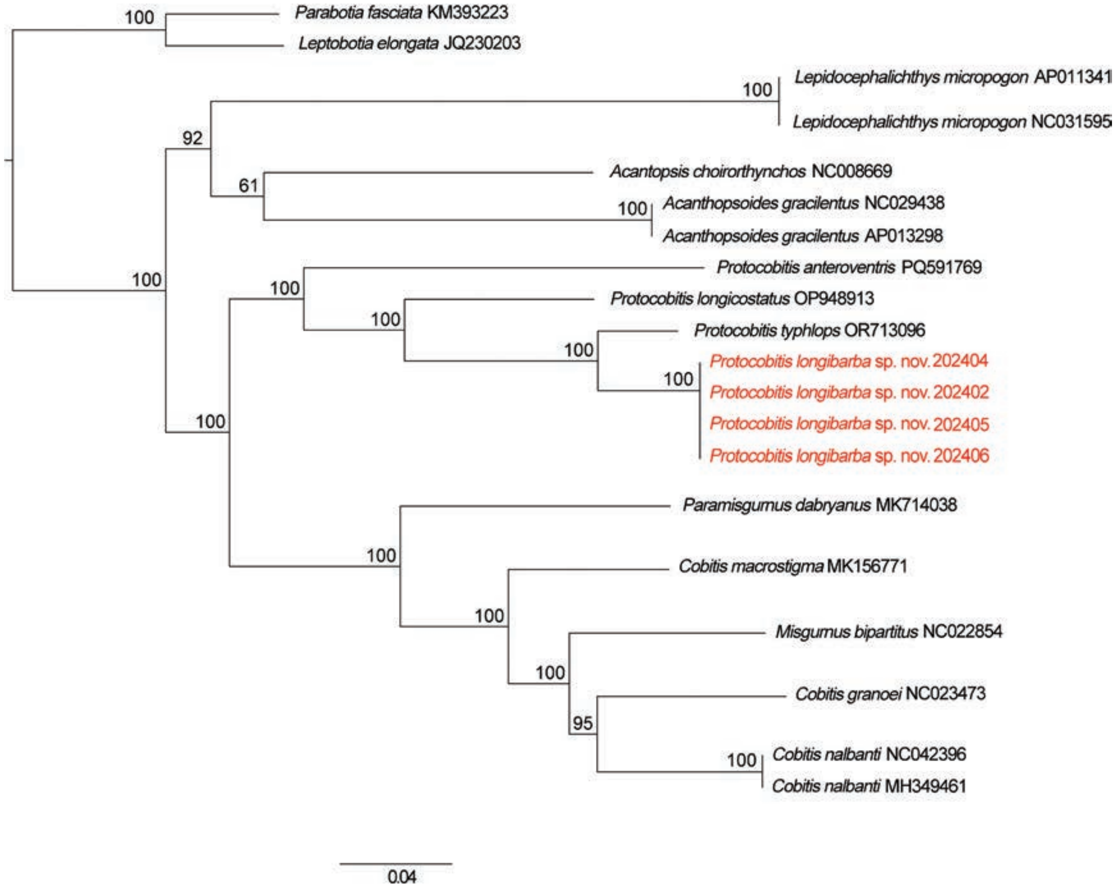

Figure 4. Maximum-likelihood tree of *Protocobitis* based on concatenated dataset of mitochondrial COI and cyt *b* sequences. Numbers near branches indicate bootstrap supports.

differences in vertebral count and rib degeneration indicated adaptations to cave environments. Morphologically, the new species can be distinguished from all other congeners based on a combination of the following characteristics: whole body covered with scales except for head and area between pectoral-fin origin and pelvic-fin origin (vs scaleless in *P. anteroventris*, scales present along midline of body in *P. typhlops*, 5–6 branched pectoral-fin rays (vs seven in *P. anteroventris*, *P. longicostatus*, and *P. polylepis*), and four branched pelvic-fin rays (vs five in other species within the genus). Furthermore, the new species can be distinguished from *P. polylepis* by the absence of pigmentation (vs black pigmentation present), from *P. anteroventris* and *P. polylepis* by caudal peduncle length 17%–20% of SL (vs 25%–28% in *P. anteroventris* and 15%–16% in *P. polylepis*), from *P. longicostatus* and *P. typhlops* by head height 50%–81% of lateral head length (vs 46%–50% in *P. longicostatus* and 52%–61% in *P. typhlops*), and from *P. polylepis* and *P. typhlops* by body height 8%–9% of SL (vs 17%–18% in *P. polylepis* and 9%–14% in *P. typhlops*).

This study provides a comprehensive morphological characters and x-ray scanning and three-dimensional (3D) reconstructions analysis of *P. longibarba*, contributing to the understanding of systematics and adaptations within this genus. The species exhibits distinct morphological characteristics, including rib reduction, which appears to be a consistent and diagnostic feature in *Protocobitis*. This structural adaptation may reflect an evolutionary shift away from reliance on ribs, potentially influencing body stability or flexibility. Additionally, we observed thickening of the chest and abdominal walls and absence of an air bladder, both of which are typical adaptations associated with benthic or bottom-dwelling species. The lack of an air bladder might indicate an ecological specialization, as reduced buoyancy is often advantageous for organisms that inhabit substrates or demonstrate sediment-burrowing behaviors (Longley 1993; Myhre and Klepaker 2009). These morphological traits raise the hypothesis that *P. longibarba* may engage in substrate penetration or mud-burrowing activities, behaviors warranting further ecological investigation to confirm.

Cavefish species exhibit high diversity, making them valuable for studying animal adaptations to extremely dark environments. Cavefish populations are extremely rare and highly sensitive to human disturbances due to their specialized habitats. Minor environmental changes, such as water pollution or extensive human activity, can lead to population extirpation or species extinction. During our field investigation, we observed that the karst cave inhabited by *P. longibarba* functions as a ponor cave in Lingyun City, leading to significant amounts of waste being transported into the cave by the river. This contamination has substantially impacted the habitat, hindering efforts to protect the cave-dwelling organisms. Consequently, establishing effective protection measures is crucial not only for preserving biodiversity but also for safeguarding the natural heritage and potential scientific value represented by cave-dwelling organisms.

Acknowledgements

We thank C. Watts for English corrections and suggestions. We thank S.P. Zhou for assistance in collecting specimens. We thank Y.M. Hou and P.F. Yi for their assistance with the CT scanning of the specimens.

Additional information

Conflict of interest

The authors have declared that no competing interests exist.

Ethical statement

No ethical statement was reported.

Funding

This study was funded by the Guangxi Natural Science Foundation Project (2022GXNSFAA035563), Project of the Innovation Team of Survey and Assessment of the Pearl River Fishery Resources (2023TD-10), Key Laboratory of Ecology of Rare and Endangered Species and Environmental Protection (Guangxi Normal University), and Ministry of Education, China (ERESEP2022Z05), Karst Landship National park of Southwest China comprehensive scientific investigation project. Small Grants Program for New Records and Rediscoveries of Rare Species initiated by Tencent Foundation and Shan Shui Conservation Center.

Author contributions

Z.X.Q. and L.N.D. conceived and designed the study, performed molecular experiments, and prepared the manuscript. Z.X.Q. and S.Y.Z. measured specimens and analyzed the molecular data. J.J.Z. and Y.W.L. collected the specimens and took specimen photographs. J.S.S. performed X-ray scanning and 3D reconstructions. All authors read and approved the final version of the manuscript.

Author ORCIDs

Zhi-Xian Qin https://orcid.org/0009-0001-7271-813X
Jing-Song Shi https://orcid.org/0000-0001-9168-1734
Li-Na Du https://orcid.org/0000-0002-2246-643X
Jia-Jun Zhou https://orcid.org/0000-0003-1038-1540

Data availability

All of the data that support the findings of this study are available in the main text.

References

Chen YR, Yang JX, Zhu ZG (1994) A new fish of the genus *Sinocyclocheilus* from Yunnan with comments on its characteristic adapation (Cypriniformes: Cyprinidae). Acta Zootaxonomica Sinica 19(2): 246–253. [In Chinese]

Fan C, Wang M, Wang JJ, Luo T, Zhou JJ, Xiao N, Zhou J (2024) *Sinocyclocheilus xiejiahuai* (Cypriniformes, Cyprinidae), a new cave fish with extremely small population size from western Guizhou, China. ZooKeys 1214: 119–141. https://doi.org/10.3897/zookeys.1214.127629

Jeffery WR (2001) Cavefish as a Model System in Evolutionary Developmental Biology. Developmental Biology 231(1): 1–12. https://doi.org/10.1006/dbio.2000.0121

Jeffery WR (2009) Regressive evolution in Astyanax cavefish. Annual Review of Genetics 43: 25–47. https://doi.org/10.1146/annurev-genet-102108-134216

Kumar S, Stecher G, Tamura K (2016) MEGA7: molecular evolutionary genetics analysis version 7.0 for bigger datasets. Molecular Biology and Evolution 33(7): 1870–1874. https://doi.org/10.1093/molbev/msw054

Lan JH, Gan X, Wu TJ, Yang J (2013) Cave Fishes of Guangxi. Science Press, Beijing. [In Chinese]

Liang XF, Cao L, Zhang CG (2011) Molecular phylogeny of the *Sinocyclocheilus* (Cypriniformes: Cyprinidae) fishes in northwest part of Guangxi, China. Environmental Biology of Fishes 92: 371–379. https://doi.org/10.1007/s10641-011-9847-6

Librado P, Rozas J (2009) DnaSP v5: a software for comprehensive analysis of DNA polymorphism data. Bioinformatics 25: 1451–1452. https://doi.org/10.1093/bioinformatics/btp187

Longley LG (1993) Morphological adaptations of the Texas blind catfishes *Trogloglanis pattersoni* and *Satan eurystomus* (Siluriformes: Ictaluridae) to their underground environment. Copeia 1993(4): 976–986. https://doi.org/10.2307/1447075

Miller MA, Pfeiffer W, Schwartz T (2010) Creating the CIPRES Science Gateway for inference of large phylogenetic trees. In: Proceedings of the Gateway Computing 349 Environments Workshop (GCE), 14 Nov. 2010, New Orleans, LA, 1–8. https://doi.org/10.1109/GCE.2010.5676129

Myhre F, Klepaker T (2009) Body armour and lateral-plate reduction in freshwater three-spined stickleback *Gasterosteus aculeatus*: adaptations to a different buoyancy regime? Journal of Fish Biology 75: 2062–2074. https://doi.org/10.1111/j.1095-8649.2009.02404.x

Rambaut A (2009) FigTree. Version 1.4.4. http://tree.bio.ed.ac.uk/software/figtree

Ronquist F, Teslenko M, van der Mark P, Ayres DL, Darling A, Höhna S, Larget B, Liu L, Suchard MA, Huelsenbeck JP (2012) MrBayes 3.2: efficient Bayesian phylogenetic inference and model choice across a large model space. Systematic Biology 61(3): 539–542. https://doi.org/10.1093/sysbio/sys029

Stamatakis A (2014) RAxML Version 8: a tool for phylogenetic analysis and post-analysis of large phylogenies. Bioinformatics 30(9): 1312–1313. https://doi.org/10.1093/bioinformatics/btu033

Yang JX, Chen YR, Lan JH (1994) *Protocobitis typhlops*, a new genus and species of cave loach from China (Cypriniformes: Cobitidae). Ichthyological Exploration of Freshwaters 5: 91–96.

Zhao YH, Zhang CG (2006) Cavefishes: concept, diversity and research progress. Biodiversity Science 5: 451–460. [In Chinese] https://doi.org/10.1360/biodiv.050226

Zhao Y, Zhang C (2009) An Endemic Cavefish Genus *Sinocyclocheilus* in China—Species Diversity, Systematics and Zoogeography (Cypriniformes: Cyprinidae). Science press, Beijing. [In Chinese]

Zhou JJ, Qin ZX, Du LN, Wu HY (2024) A new species of the blind cave loach genus *Protocobitis* (Cypriniformes: Cobitidae), *Protocobitis longicostatus* sp. nov., from Guangxi, China. Zoological Science 41(2): 210–215. https://doi.org/10.2108/zs230104

Zhu Y, Lv YJ, Yang JX, Zhang S (2008) A new blind underground species of the genus *Protocobitis* (Cobitidae) from Guangxi, China. Zoological Science 29: 452–454. https://doi.org/10.3724/SP.J.1141.2008.00452

ZooKeys 1228: 197–223 (2025)
DOI: 10.3897/zookeys.1228.141682

Research Article

Revision of the North American genus *Supralathosea* Barnes & Benjamin (Lepidoptera, Noctuidae, Oncocnemidinae) with description of two genera and three species

Lars G. Crabo[1], Kevin Keegan[2]

1 Adjunct Faculty, Department of Entomology, Washington State University, Pullman, Washington, USA
2 Carnegie Museum of Natural History, Pittsburgh, Pennsylvania, USA
Corresponding author: Lars G. Crabo (larscrabo@gmail.com)

Abstract

The noctuid genus *Supralathosea* Barnes & Benjamin (Noctuidae, Oncocnemidinae) is revised to include three species for the United States of America, *Supralathosea baboquivariensis* Barnes & Benjamin from southeast Arizona, *Supralathosea yavapai* **sp. nov.** from central Arizona, and *Supralathosea solastella* **sp. nov**. from Texas. Two genera are described for species formerly included in *Supralathosea*. *Infralathosea* **gen. nov.** includes *Infralathosea pronuba* **comb. nov.** from Arizona and New Mexico and *Infralathosea unicornis* **sp. nov.** from west Texas. *Eulathosea* **gen. nov.** contains only *Eulathosia obtusa* Smith, **comb. nov.** from Arizona. A key to genera and species is presented and adults and genitalia of all taxa are illustrated. *Infralathosea* and *Eulathosea* are assigned to Oncocnemidinae based on molecular evidence.

Key words: Amphipyrinae, Chihuahuan desert, DNA barcode, key, Madrean Archipelago, Oncocnemidinae, owlet moths

Academic editor: José Luis Yela
Received: 12 November 2024
Accepted: 7 January 2025
Published: 21 February 2025

ZooBank: https://zoobank.org/9AB9D46E-C3CA-4832-BE1A-C900F4AE9B18

Citation: Crabo LG, Keegan K (2025) Revision of the North American genus *Supralathosea* Barnes & Benjamin (Lepidoptera, Noctuidae, Oncocnemidinae) with description of two genera and three species. ZooKeys 1228: 197–223. https://doi.org/10.3897/zookeys.1228.141682

Introduction

Supralathosea Barnes & Benjamin, 1924 (Lepidoptera, Noctuidae) species are relatively nondescript medium-sized noctuid moths that are known from Arizona, New Mexico, and Texas in the United States but undoubtedly also occur in Mexico. The males of all species have bipectinate antennae and forewings with a nearly uniform pale to dark gray ground color, usually with faint noctuiform patterning modified with a black line along the trailing margin, and white or off-white hindwings. Females are darker gray, with more pronounced forewing patterning and gray suffusion on the hindwings. *Supralathosea* are uncommon in collections despite flying during much of the year, including in wintertime.

Supralathosea was described for *Supralathosea baboquivariensis* Barnes & Benjamin, 1924 (Barnes and Benjamin 1924). The genus remained monotypic until 1989 when *Catabena pronuba* Barnes & McDunnough, 1916 and *Cucullia obtusa* Smith, 1909 were reassigned to *Supralathosea* from the genera in which they were originally described in the non-annotated

Lepidopterorum Catalogus series (Poole 1989). *Supralathosea* has not been formally revised, and these three species were retained in the genus in subsequent North American check lists (Lafontaine and Schmidt 2010; Pohl and Nanz 2023). Although they share superficial similarities, these species are structurally distinct, differing in the morphology of the male antennae, male genital capsules and vesicae, and female bursae and egg laying apparatuses. Here we describe two new genera, *Infralathosea* gen. nov. and *Eulathosea* gen. nov., to provide a more cogent arrangement of these taxa. In addition, we describe two new species of *Supralathosea* and one new species of *Infralathosea*, all from southwestern United States.

Barnes and Benjamin (1924) placed *Supralathosea* in Cuculliinae (sensu Hampson 1903) where it was retained by McDunnough (1938) and Hodges et al. (1983). Cuculliinae is now defined more narrowly (Poole 1995), and most genera included in it historically have been dispersed to a number of different subfamilies (Lafontaine and Schmidt 2010; Pohl and Nanz 2023). *Supralathosea* was reassigned from Cuculliinae to Psaphidinae by Troubridge (2008), and shortly thereafter to Amphipyrinae, Psaphidini, Feraliina by Lafontaine and Schmidt (2010). Keegan et al. (2019, 2021) subsequently showed Amphipyrinae to be polyphyletic based on an analysis of nuclear and mitochondrial DNA sequences, and they reassigned *Supralathosea* to Oncocnemidinae as part of a massive restructuring of Amphipyrinae and related taxa.

Materials and methods

Wing pattern and genitalia structure terminology follow Lafontaine (2004). Deep lateral invaginations forming a transverse channel across abdominal segment A1 dorsal to the tympanum, typically found in many oncocnemidine genera (Troubridge 2008; Keegan et al. 2021), is herein called the “A1 transverse channel.” A spike-like extension from the ventral cucullus in *Supralathosea* is the pollex. Forewing lengths were measured from base to apex to the nearest half millimeter, excluding the fringe. All measurements and ratios in the genus and species descriptions and Diagnosis sections are based on the examined material, and are approximations. For readability we have omitted a “~” as an indicator of uncertainty prior to any numerical values. It is likely that individual specimens will be found that vary slightly from the descriptions.

Genitalia were prepared using standard methods (Hardwick 1950, Lafontaine 2004). Abdomens were macerated in hot 10% potassium hydroxide for 25–30 minutes. Initial dissections were performed in water followed by hardening in 95% isopropyl alcohol. Male vesicae and female bursae were inflated. Preparations were stained with orcein (Sigma Chemical Company, St. Louis, Missouri) and mounted in Euparal (Bioquip Products Inc., formerly of Rancho Dominguez, California) on glass slides with elevated cover glass to preserve the three-dimensional configuration of the structures. Some illustrated genitalia preparations from NMNH are stained blue, likely using Chlorazol black. Unless specified otherwise, female genitalia comparisons to “A8” refer to the anteroposterior length of segment A8.

The 658 base pair DNA “barcode region” of the mitochondrial cytochrome *c* oxidase subunit 1 (CO1) (“barcode”) was used to assess intra- and interspecific molecular variation within each genus. Legs from dried specimens were submitted to the Barcodes of Life Data System (BOLD) at the University of Guelph (Ontario, Canada) where they were subjected to standard DNA extraction, amplification, and sequencing protocols (Hebert et al. 2003) or sequenced by KK as described in Keegan et al. (2019). Barcodes were compared to pre-existing material at BOLD using the Kimura-2-Parameter distance model as implemented on http://www.barcodinglife.org.

Intergeneric phylogenetic relationships were evaluated by inferring a phylogeny in RAxML v. 8.2.12 (Stamatakis et al. 2008) with 1000 non-parametric bootstraps (BS) on CIPRES (Miller et al. 2010) based on previously available and newly generated sequences of five nuclear genes and mitochondrial CO1 as described in Keegan et al. (2019). We considered clades with BS ≥ 70 to be well supported (Hillis and Bull 1993; Lemoine et al. 2018).

Distribution data includes coordinates associated with photographs of live moths on the websites iNaturalist (iNaturalist community 2024) and BugGuide (VanDyk et al. 2024), vetted by LGC. Distribution data obtained from internet photographs are depicted as squares to distinguish them from data from examined specimens (circles) on the maps (Figs 33, 34).

Repository abbreviations

AMNH	American Museum of Natural History, New York, New York, USA
CMNH	Carnegie Museum of Natural History, Pittsburgh, Pennsylvania, USA
CNC	Canadian National Collection of Insects, Arachnids, and Nematodes, Ottawa, Ontario, Canada
DLW	Dave Wikle personal research collection, Whittier, California, USA
JV	James Vargo personal research collection, Mishawaka, Indiana, USA
LACM	Natural History Museum of Los Angeles County, Los Angeles, California, USA
LGC	Lars Crabo personal research collection, Bellingham, Washington, USA
NMNH	National Museum of Natural History, Washington, D. C., USA

Results

Our molecular dataset consisted of at most six genes and 5539 base pairs for 23 taxa. Represented among these taxa were three non-Oncocnemidinae outgroups representing the noctuid subfamilies Plusiinae, Acontiinae, and Cuculliinae. The genera *Eulathosea*, *Infralathosea*, and *Supralathosea* formed a well-supported group (BS = 91) (Fig. 35). We found *Supralathosea* to be monophyletic (BS = 100) with *Eulathosea* sister to it (BS = 85), and we recovered *Infralathosea* as a clade (BS = 69) sister to other two genera. Within *Supralathosea*, we found *S. baboquivariensis* sister to the remaining taxa in the genus that formed a well-supported clade (BS = 83). The relationship between these remaining *Supralathosea* taxa (*Supralathosea yavapai* sp. nov. and *Supralathosea solastella* sp. nov.) is unresolved in our tree.

Key to adults of *Supralathosea* sensu Pohl and Nanz (2023) for North America north of Mexico

1 Hindwing two toned, white with broad uniform blackish gray marginal band; forewing gray with orange-tan scales in cell near reniform spot (Figs 17, 18) .... ***Eulathosea obtusa***

– Hindwing white, off white, or gray, at most with a weak marginal band of powdery gray scales intermixed with the ground color; forewing gray, lacking warm colors (Figs 1–16) **2**

2 Male antenna bipectinate; anterior female ductus bursae > 1.5 × width of A8, thickened, crenulate (Figs 26–29); FW transverse lines either obsolete or normal, extending completely across wing when visible (Figs 1–12)........ **3 (*Supralathosea*)**

– Male antenna beaded; anterior female ductus bursae tubular, < 1 × width of A8 (Figs 30, 31); FW antemedial and postmedial line segments fused to form arcs from anterior and posterior margins (Figs 13–16)........ **5 (*Infralathosea*)**

3 Pollex of male valve triangular, length 2 × base width (Fig. 22); thick anterior segment of female ductus bursae wider than anteroposterior length of corpus bursae (Fig. 29); central Arizona........ ***Supralathosea yavapai***

– Male pollex rod-like, slender from base to apex (Figs 19–21); anterior female ductus bursae width less than anteroposterior length of corpus bursae (Figs 26–28); southern Arizona and Texas........ **4**

4 Male forewing grainy charcoal gray with dark veins, darker gray scales in subterminal area and on trailing margin in some individuals (Figs 1, 3); female hindwing with uniform dark marginal shade (Fig. 2); Madrean Archipelago of southeast Arizona .... ***Supralathosea baboquivariensis***

– Male forewing smooth medium to pale gray with black trailing margin or distinct black transverse lines (Figs 4, 5, 7); female hindwing marginal area variable, white or with patchy gray suffusion (Figs 6, 8, 9); Texas........ ***Supralathosea solastella***

5 Male vesica without apical stout cornutus (Fig. 23b); female hindwing gray (Fig. 14); Arizona and New Mexico .... ***Infralathosea pronuba***

– Male vesica with apical stout cornutus (Fig. 24b); female hindwing white (Fig. 16); west Texas .... ***Infralathosea unicornis***

Genus *Supralathosea* Barnes & Benjamin, 1924

Type species. *Supralathosea baboquivariensis* Barnes & Benjamin, 1924; by monotypy.

Diagnosis. *Supralathosea* species are pale to dark gray moths with forewings of 12.0–18.5 mm in length, adorned with very narrow scales. Males can usually be recognized by the combination of broad bipectinate antenna, relatively unmarked forewing with black posterior margin, and white hindwing with black thin incomplete terminal line and veins. Females are less distinctive, with filiform antenna, mottled darker gray forewing with more distinct transverse lines, pale-filled orbicular and reniform spots lacking dark outlines, and white hindwing often heavily dusted with gray. Although similar, males of the

Supralathosea species can be identified by their superficial appearance. The females are more similar and are best identified by association with the males or by locality.

Male genitalia have an uncus that is bent nearly 90° at the base. The valve is bluntly pointed near the apex, has a spike-like pollex but no corona, and the clasper ampulla is cow-horn-shaped. The vesica of the phallus is bulbous with multiple spike-like setae, resembling a medieval mace.

Females have a unique broad, thick, crenulate anterior segment of the ductus bursae abutting the corpus bursae, somewhat like beet or walnut half. The corpus bursae is asymmetric, pear-shaped with narrower right side directed slightly posteriad, and lacks signa.

Below we provide a redescription for *Supralathosea* in light of the recognition of *Eulathosea* and *Infralathosea*, and descriptions for the new species of *Supralathosea*.

Redescription. Adults medium size (FW length 12.0–18.5 mm) with pale to dark gray forewings, usually with very faint noctuiform patterning (lines distinct in south Texas populations) and black posterior margin. ***Head*** – Male antenna broadly bipectinate, rami 2.5–3.0 × central shaft width, covered densely except on dorsum with short cilia; female antenna filiform. Eye lacking interommatidial setae, strongly lashed posteriorly. Frons bulging slightly; dorsal head scales projecting slightly over frons with small paramedian tufts. Haustellum present. Labial palpus with short strap-like and long ventral and lateral black hair-like scales. ***Thorax*** – Collar with median crest, prominent in resting live moths, thin, white-edged black line across base; tegulum and dorsum gray, darkest dorsally. ***Wings*:** Forewing elongate with slightly pointed apex in males, slightly wider and rounder in females. Scales long, narrow, finely serrate, gray, translucent white, and gray-edged or gray-tipped white; ground color uniform pale gray to charcoal gray, posterior margin usually dark gray or black; subterminal area with three indistinct dark patches. Lines variable, very faint or limited to indistinct oblique dark marks on costa and vestiges of the postmedial line on the veins in males; those of some male *Supralathosea solastella* and all females are dark gray to black; basal line absent or a dark spot on costa; antemedial line double, inner component weak, pale filled, sinuous, convex with apex in fold; postmedial line similar, outer component weak, sinuous or dentate, prominently convex around cell with notch opposite reniform, segment posterior to Cu drawn basad in fold then perpendicular to posterior margin; medial line dark gray, nearly parallel to postmedial line; subterminal line pale, indistinct; terminal line of intervenal dark spots. Orbicular and reniform spots pale with dark centers, small and inconspicuous; claviform spot absent. Hindwing scales small translucent and long hair-like, pure white or off white, darker gray scales on portions of veins and terminal line in males; similar white or pale gray with discal spot, medial line, and distal gray suffusion in females. ***Legs*:** Scales mostly dark gray, scattered white; lacking tibial claw or other modifications; tarsal segments with three rows of setae, dark gray with distal white rings. ***Abdomen*** – Lacking A1 transverse channel, brush organs, and coremata. Scales pale to brownish gray; weak darker dorsal tufts on proximal segments. ***Male genitalia*:** Uncus relatively short, directed posteriad at base then bent 90° ventrad, cylindrical with small apical hook. Juxta broad, shield shaped with variable length ventral extension. Valve rhomboid, length 2.8–3.8 × width, distal 1/3 broadest, tapered to a subapical point with spike-like pollex at anal margin, lacking expanded cucullus or corona. Sacculus strong, extending to mid-valve, convex to near costa. Clasper base a bar near ventral margin distal to sacculus, ampulla arising at valve distal 1/3, cow-horn-shaped with > 90° curve dorsad and basad. Phallus length 3.5–4 × width, dorsal apex with sclerotized crenulate band with minute spikes. Vesica with 90° subbasal and mesial bends, apex posterior to proximal phallus, mesial segment ballooned posterior and leftward, covered by 50–70 spike-like cornuti, longest 6–7 at dorsal margin; subapical vesica with smaller patch of shorter thinner cornuti on convex segment or small diverticulum. ***Female genitalia*:** A7 tergite thick, large, lateral margins converging at ventral midline, covering small weakly sclerotized sternite; A7 pleural membranes leathery, redundant, covered densely with dark scales. Segment A8 width 1.4–1.9 × length. Papilla analis 1 × A8, mesiolaterally compressed, apex blunt, covered sparsely with uniform hair-like setae; not protruding in situ. Posterior apophysis 1.9–2.8 × A8; anterior apophysis 0.6–0.8 × posterior apophysis. Ostium bursae U-shaped, leathery with crenulate margin and lightly sclerotized broad V-shaped dorsal and ventral postvaginal plates. Ductus bursae with distinct anterior and posterior segments: shorter posterior ductus segment membranous, conical, broadest at ostium; longer anterior segment irregular, thick, rubbery, bulb-like with broad base at transverse or slightly angled junction to corpus bursae, length 1.7–2.2 × A8, width 1.0–1.2 × length, internally amorphous, seemingly lacking a lumen. Corpus bursae membranous, lacking signa, length 2–2.5 × A8, width 1.2–1.5 × length, pear shaped, apex right posterior with ductus seminalis at tip.

Higher classification. *Supralathosea* is assigned to Oncocnemidinae (Keegan et al. 2021).

Distribution and biology. This genus occurs in southwestern United States, where it has been found in Arizona and Texas. Several of the species undoubtedly occur in Mexico. Adults of most *Supralathosea* species fly throughout much of the year, but many records are from winter, December through February. Females are found much less commonly than males. The larva of *S. solastella* feeds on ash (*Fraxinus* sp., Oleaceae) (D. Wagner, pers. comm.). The early stages of the other species are unknown.

Discussion. United States populations of *Supralathosea* are distributed in four seemingly allopatric populations, three of which abut the border with Mexico. We have no information about the distribution of the genus in northern Mexico, but it seems certain that at least one or two *Supralathosea* species also occur there based on their known distributions in the United States. With this in mind, we arrange the United States populations into three species. Two relatively uniform and superficially distinctive species from separate parts of Arizona are supported by several characters, including distinct DNA sequences (*S. baboquivariensis*) or male genitalia (*Supralathosea yavapai*). The other two populations from Texas are treated as a third species (*Supralathosea solastella*). While these Texas populations are relatively distinct superficially, there are no significant genitalic or barcode differences between them to indicate that they are separate species. We suspect that the superficial differences represent clinal variation, but this can be neither confirmed or refuted until more is known about *Supralathosea* in northern Mexico.

Supralathosea baboquivariensis is relatively distinct genetically, with barcodes differing from those of other *Supralathosea* species by almost 4% and strong support in our RAxML maximum-likelihood analysis (Fig. 35). The other two species have several barcode haplotypes differing by less than 1.5%, and are unresolved in our multi-gene analysis. This is not unusual, as distinct species of other noctuid genera have similar or identical barcodes, including many species of *Euxoa* Hübner, *Abagrotis* Smith, and *Lasionycta* Aurivillius (Zahiri et al. 2014).

Supralathosea species lack a dorsal A1 transverse channel, an anatomic feature common to many Oncocnemidinae genera. Troubridge (2008) considered this to be the defining character of the subfamily, although he noted that it is also occurs in some diurnal species of Agaristinae (e.g., *Alypia* Hübner) and Stiriinae (e.g., *Annaphila* Grote). He moved several genera that lack this character to various non-oncocnemidine subfamilies, including assigning *Supralathosea* to Psaphidinae (now Psaphidini). Based on the DNA-based studies of Keegan et al. (2019, 2021) it is now clear that not all genera in the subfamily express this character, including *Supralathosea*, *Infralathosea*, *Eulathosea*, and at least some species of *Leucocnemis* Hampson.

Supralathosea baboquivariensis Barnes & Benjamin, 2024

Figs 1–3, 19, 26, 33 (Map)

Supralathosea baboquivariensis Barnes & Benjamin, 1924: 133.

Type material. Holotype male. USA, Arizona, Pima County, Baboquivari Mountains. NMNH [examined].

Diagnosis. *Supralathosea baboquivariensis* can be distinguished from the only other *Supralathosea* species in Arizona, *S. yavapai*, by its slightly smaller size (FW length of *S. baboquivariensis* < 15.5 mm; *S. yavapai* > 16.5 mm) and its pure white rather than off white hindwing ground color. The male pollex is thin and spike-like in *S. baboquivariensis*, shorter and broadly triangular in *S. yavapai*. The female bursa of *S. baboquivariensis* is rounder than that of *S. yavapai*.

Supralathosea baboquivariensis is similar in size to *S. solastella*, found in Texas. The forewing of male *S. baboquivariensis* is dark charcoal gray with a rough texture; that of *S. solastella* is smoother, either medium gray with thick black posterior margin (west Texas) or pale gray with distinct noctuiform pattern of transverse lines (south Texas). The hindwing ground color of both species is white, but the veins of *S. baboquivariensis* are nearly completely dark gray, whereas those of *S. solastella* are white or have less extensive gray scales limited to the positions of the postmedial and terminal lines. Females of *S. solastella* are more similar to *S. baboquivariensis* than the males, but tend to be paler gray with paler hindwings, especially in south Texas. The male valve and vesica and female bursa copulatrix of *S. baboquivariensis* are less massive than those *S. solastella*. This is evident in the figures, but the differences are subtle and difficult to appreciate without a side-by-side comparison.

Barcodes of *S. baboquivariensis* (BOLD:ADP1765) differ from those of other *Supralathosea* species by approximately 4%.

Distribution and biology. *Supralathosea baboquivariensis* is uncommon in collections. It occurs in the mountains of southeastern Arizona, with almost all examined specimens from the Baboquivari Mountains. A single male (Fig. 3) from Ash Canyon on the east slope of the Huachuca Mountains (NMNH) is slightly

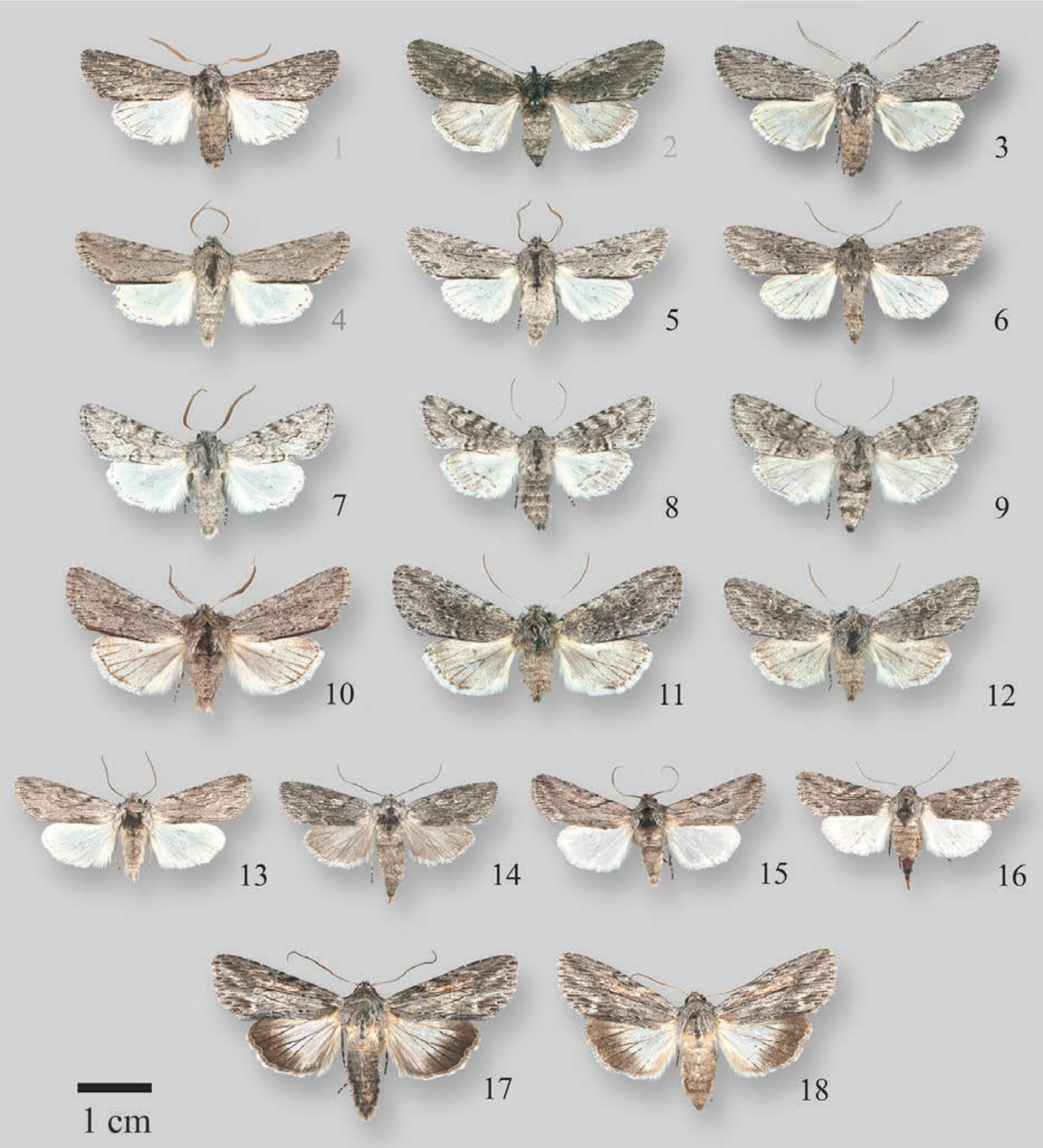

Figures 1–18. *Supralathosea*, *Infralathosea*, and *Eulathosea* adults **1** *Supralathosea baboquivariensis* male, USA, Arizona, Pima County **2** *S. baboquivariensis* female, USA, Arizona, Pima County **3** *S. baboquivariensis* male, USA, Arizona, Cochise County **4** *Supralathosea solastella* HT male, USA, Texas, Brewster County **5** *S. solastella* male, USA, Texas, Brewster County **6** *S. solastella* female, USA, Texas, Brewster County **7** *Supralathosea solastella* male, USA, Texas, Zapata County **8** *S. solastella* female, USA, Texas, Zapata County **9** *S. solastella*, USA, Texas, Zapata County **10** *Supralathosea yavapai* USA, Arizona, Yavapai County **11** *S. yavapai* USA, Arizona, Yavapai County **12** *S. yavapai* USA, Arizona, Yavapai County **13** *Infralathosea pronuba* male, USA, Arizona, Yavapai County **14** *I. pronuba* female, USA, New Mexico, Lincoln County, **15** *Infralathosea unicornis*, male, USA, Texas, Brewster County **16** *I. unicornis*, female, USA, Texas, Brewster County **17** *Eulathosea obtusa* male, USA, Arizona, Cochise County **18** *Eulathosea obtusa* female, USA, Arizona, Yavapai County.

smoother dark gray than topotypical specimens (Fig. 1). It is assigned to *S. baboquivariensis* until more material is available for examination. Adults fly throughout the year, mostly during summer and winter. Examined specimens were collected during June, July, October, and December. The early stages are unknown.

Supralathosea solastella **sp. nov.**

https://zoobank.org/25A24221-E5C1-4B18-8900-32B39F849B3C
Figs 4–9, 20, 21, 27, 28, 33 (Map)

Type material. ***Holotype*****, male.** [USA]: Texas: [Brewster County]: Big Bend Nat[ional] Park, Gov[ernment] Spring, 31 III [19]65, A. & M. E. Blanchard. NMNH. ***Paratypes*****.** 26 males, 5 females. **USA: Texas:** Brewster County: Big Bend Nat[ional] Park, Basin, A. & M. E. Blanchard, 8 VII [19]64 (1 male); 10 VII [19]64 (1 male); 10 VII [19]64 / Genitalia slide by RWP [female] USNM 45184 (1 female); 11 VII [19]64 (3 males, 2 females); 11 VII [19]64 / Barcode of Life, DNA voucher specimen CCDB-20821-C12, BOLD Proc. ID LNAU55033-13 / USNMENT 00906843 (1 male); 29 III [19]65 (1 male); 1 VII [19]65 (1 male, 1 female); 27 IX [19]65 (1 male); 2 X [19]66 (1 male); 9 IV 1967 (1 male); Big Bend Nat. Park, The Basin, 9 V 1959, M. R. MacKay / Genitalia CNC slide # 13940 male (1 male); Big Bend Nat[ional] P[ar]k, Chisos Basin, 30 V [19]81, Leg. E. C. Knudson / Barcode of Life, DNA voucher specimen CCDB-20821-C08, BOLD Proc. ID LNAUS 5029-13/USNMENT 00906839 (1 male); Big Bend Nat[ional] Park, Gov[ernment] Spring, A. & M. E. Blanchard, 31 III [19]65 / Genitalia slide by RWP [male] USNM 45183 (1 male); Big Bend Nat[ional] Park, Grapevine Hill, 2 X [19]65, A. & M. E. Blanchard (1 male); Big Bend Nat[ional Park], Green Gulch, A. & M. E. Blanchard, 3 IV [19]65 (1 male); 1 VII [19]65 (1 male); 30 XI [19]65 / Barcode of Life, DNA voucher specimen CCDB-20821-C07, BOLD Proc. ID LNAUS 5029-13 / USNMENT 00906838 (1 male); Big Bend Nat[iona]l P[ar]k, Green Gulch, 30 XI [19]85, leg. E. C. Knudson / Barcode of Life DNA voucher specimen, SmpleID CCDB-20821-C07, BOLD Proc. ID LNAUS5028-13 / USNMENT 00906838 (1 male); Big Bend National Park, Oak Spring, 8 V 1959, M. R. MacKay (1 male); 4 X [19]65, A. & M. E. Blanchard (1 male); Terlingua Ranch, 29.43–[29].47° -103.38–[103].41°, 9 IV 2016, 1090–1135 m, LG Crabo/BC Schmidt (1 male); Jeff Davis County: Ft. Davis, 3 V 2000, J. Vargo / Database # CNCLEP 00113220 / Barcode of Life, DNA voucher specimen, SmplID CNCLEP 00113220, BOLD Proc. ID: CNCLB906-14 (1 male); W[est] Davis M[oun]t[ain]s/R[ou]te 166, 30.685° -104.244°, 11 IV 2016, 1888 m, L G Crabo/B C Schmidt (1 male); Terrell County: Sanderson, J. Vargo, 2 V 2000 / *Supralathosea* sp. det. Ed Knudson / Database # CNCLEP 00113933 / Barcode of Life Project Leg removed DNA extracted (1 male); 2 V 2000 / Database # CNCLEP 00114076 (1 female); Val Verde County: 29.805° -101.556°, 17 III 2018, J. Vargo leg. (1 male). CNC, JV, LGC, NMNH.

The type series is restricted to west Texas.

Etymology. The species name is Latin, meaning lone star. This species occurs in Texas, the Lone Star State.

Diagnosis. This species is geographically variable with distinct phenotypes in west Texas and south Texas. All populations have paler gray forewings than those of *S. baboquivariensis*, and lack the rough texture of that species. Males of *S. solastella* from west Texas are dull medium gray with a black posterior margin; other markings are limited to slightly darker gray spots on the costa and terminal area patches. The populations from south Texas (Live Oak, Starr, and Zapata counties) are paler gray with a slight sheen, with distinct black transverse lines unlike males of any other *Supralathosea*. Like *S. baboquivariensis*, the male hindwing ground color of *S. solastella* is pure white, but dark scaling along the veins is less extensive in *S. solastella* than in *S. baboquivariensis*, with only a few dark scales on the veins at the positions of the postme-

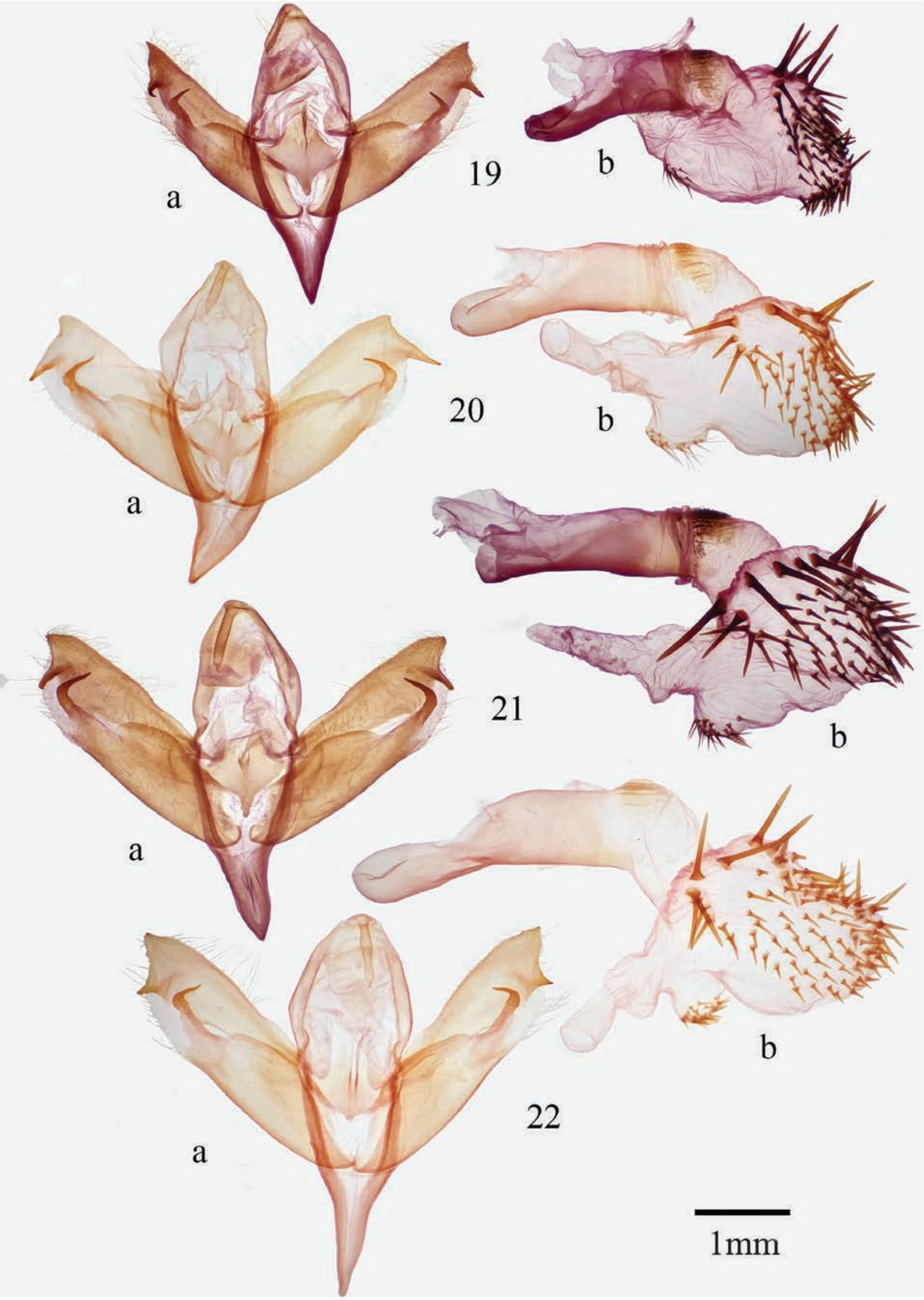

Figures 19–22. *Supralathosea* male genitalia **19** *Supralathosea baboquivariensis* **20** *S. solastella* (Brewster County, Texas) **21** *S. solastella* (Zapata County, Texas) **22** *S. yavapai*.

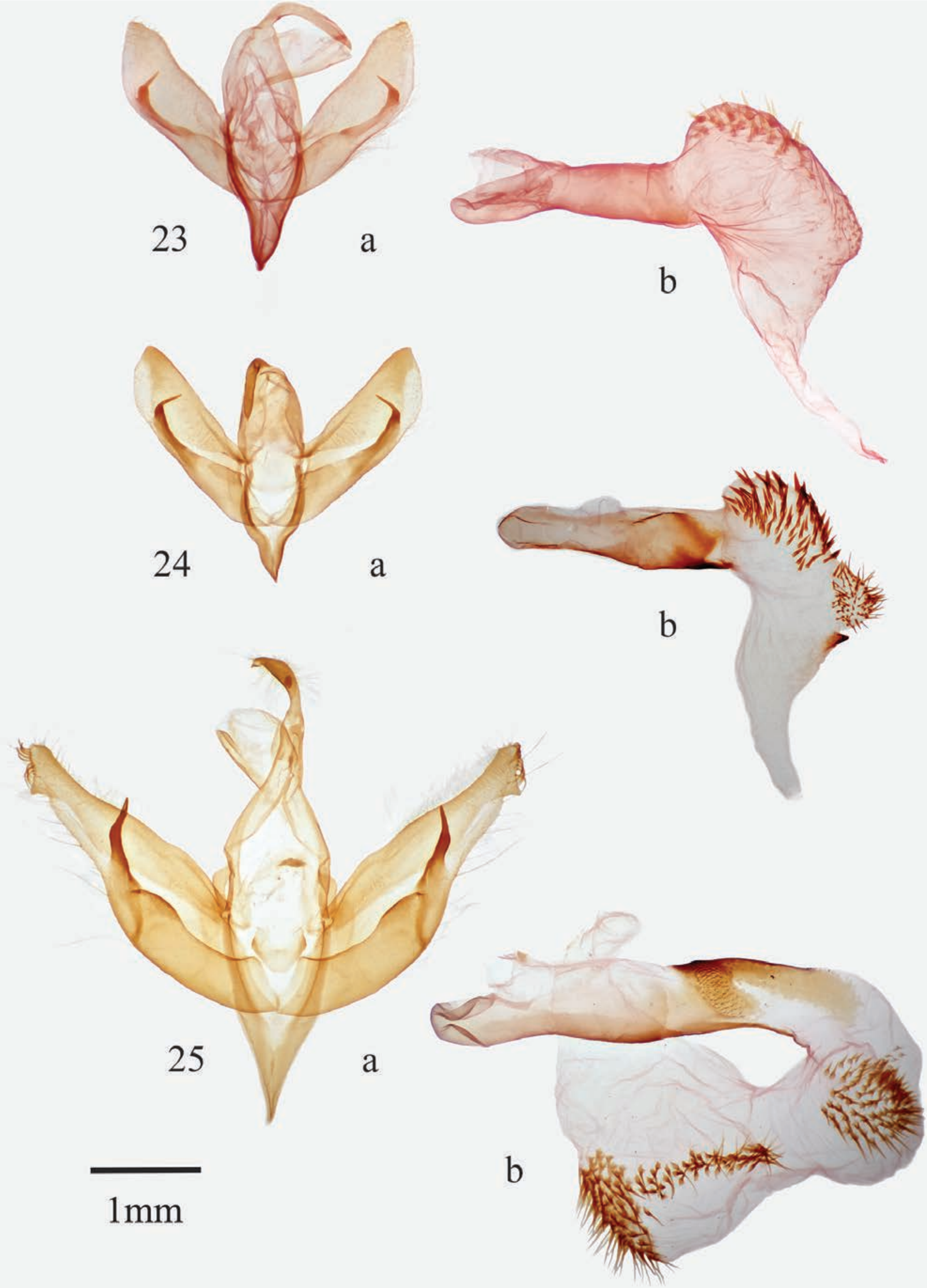

Figures 23–25. *Infralathosea* and *Eulathosea* male genitalia **23** *Infralathosea pronuba* **24** *I. unicornis* **25** *Eulathosea obtusa*.

dial and terminal lines. Females of *S. solastella* are darker and more mottled than the males, but the differences between the sexes are less pronounced than in *S. baboquivariensis*. As in the males, the forewing transverse lines are most prominent in the south Texas populations. Differences in size and habitus between *S. solastella* and *S. yavapai* are the same as those between *S. baboquivariensis* and *S. yavapai* as noted in the *S. baboquivariensis* Diagnosis section.

The male of *S. solastella* has a longer thinner pollex than that of *S. yavapai*. The valve and phallus of *S. solastella* are similar to those of *S. baboquivariensis* but are slightly more massive. These subtle differences are best appreciated when compared side-by-side. The female corpus bursae of *S. solastella* is larger than that of *S. baboquivariensis*, and has a longer rightward extension. It is slightly more globular than that of *S. yavapai*.

Supralathosea solastella is the only known *Supralathosea* in Texas.

The barcodes of *S. solastella* (*n* = 13) are assigned to four BINs in BOLD (BOLD:AAH5315, *n* = 9; BOLD:ADP4071, *n* = 1; BOLD:ADO7461, *n* = 1; BOLD:ADP4451; *n* = 2), and are not reliably differentiated from the single known haplotype of *S. yavapai* (*n* = 3). The two *S. solastella* specimens from the singleton BINs are from the same localities as some of the AAH5315 samples and the moths associated with these samples are not distinguishable by appearance, indicating that the genetic differences represent intraspecific variation. BOLD samples demonstrate minor barcode differences of approximately 1.4% between *S. solastella* populations from south Texas and those from west Texas (accessed May 2024); however, we did not recover each of these populations as monophyletic in our RAxML analysis (Fig. 35).

Description. Adults. ***Head*** – Male antenna rami up to 2.5 × shaft width. Scape short, white, and dark gray. Labial palpus scales mostly flat dark gray and white, few hair-like. Frons white with black dorsal transverse bar; dorsum scales white-tipped gray and white. ***Thorax*** – Scales mostly white-tipped dark gray trifurcate, few gray hair-like, appearing powdery medium gray with black and pale gray transverse band on collar base and dark tuft on metathorax; venter gray. ***Legs*:** Scales mixed mostly dark gray and scattered white; tarsal segments dark gray ringed with white. ***Wings*:** Forewing length 12.0–15.5 mm (males); 14.5–16.5 mm (females), length 2.5 × width, scales, white, black-rimmed white, silvery gray, and black; male ground color uniform slightly powdery medium gray (west Texas) or uniform slightly glossy pale to medium gray (south Texas); posterior margin black, thickest in west Texas populations; three ill-defined gray patches in terminal area; veins slightly darker, powdery; antemedial and postmedial lines variable, often limited to gray marks on costa and a series of dark lines on the veins at the postmedial line (west Texas) or complete, black, sinuous, thickest anteriorly (south Texas); subterminal line faint, pale, strongest proximal to three ill-defined gray patches in terminal area; terminal line dark gray, strongest between veins; fringe weakly checkered ground color and dark gray; orbicular spot oval, faint, pale with punctate or linear ocellus; reniform spot absent or a pale smudge. Female forewing ground color slightly darker than that of males of the same population, less uniform with pale mottling near costa and on distal wing. Hindwing ground color pure white; males with scattered dark gray scales on distal veins and terminal line; females with variable powdery gray scales (most numerous in south Texas populations) forming diffuse discal spot, thin postmedial line and broad marginal band ending short of margin; fringe white. ***Abdomen*** – Vestiture mostly mixed gray and white flat scales with fewer white hair-like scales. ***Male genitalia*:** Uncus and juxta as for genus. Valve shape as for genus, length 2.7 × width; sacculus 0.75 × valve length and 0.8 × valve width, dorsal margin broadly convex; ampulla length 0.5 × valve width; pollex spike-like, 0.5 × valve width. Phallus tubular, length 4 × width, apex as for genus. Vesica as for genus, slightly larger with longer stouter cornuti than that of *S. baboquivariensis*. ***Female genitalia*:** Papilla analis shape and vestiture as for genus, length 2 × width. Segment A8 and apophyses as for genus. Ostium bursae and ductus bursae as for genus, rubbery bulb-like anterior ductus segment 2.1–2.3 × A8, about as wide as long, with perpendicular junction to corpus bursae. Corpus bursae shape as for genus, length 2.1–2.3 × A8, width 1.6–1.8 × length, globular, rightward conical projection 1.5 × A8.

Distribution and biology. This species occurs in Texas. Examined specimens from west Texas are from the Chihuahuan Desert in the Big Bend region as far east as Terrell and Pecos counties. Examined specimens from south Texas are from Starr and Zapata counties. Many distribution records of *S. solastella* are from near the Rio Grande River indicating that this species undoubtedly occurs in adjacent Mexico, although its distribution south of the United States is unknown to us. Additional photographed live moths on iNaturalist (iNaturalist community 2024) likely representing this species from central Texas were examined from Bosque County (e.g., iNat/146854080), Hamilton County (e.g., iNat/146544200), and Val Verde County (e.g., iNat/104607005). These moths are most similar to west Texas populations of *S. solastella*, but their identification is hampered because the hindwings are not visible. In contrast, iNaturalist images from Live Oak County (e.g., iNat/214922172) are a close match to *S. solastella* from south Texas. The iNaturalist localities are included on the *S. solastella* distribution map (as squares) because they are the only known *Supralathosea* records from several parts of Texas (Fig. 35). *Supralathosea solastella* flies during most of the year. The examined specimens were collected during March–April, June–early August, and late September–November. Most iNaturalist photographs of *Supralathosea* from Texas were taken during mid-winter, December–February. The larva feeds at night on new ash foliage (*Fraxinus* sp., Oleaceae) (David L. Wagner, unpub. data).

Discussion. How to best classify the superficially distinctive *Supralathosea* populations from west and central Texas from those from south Texas was a difficult problem. We considered treating them as two species, subspecies of the same species, or—as presented—as distinctive unnamed populations of a single species. We hope that this paper will stimulate sampling of *Supralathosea* from regions between these populations, particularly from central Texas and northern Mexico, to corroborate or refute our thesis.

***Supralathosea yavapai* sp. nov.**

https://zoobank.org/F8189AAC-49AF-478C-A472-58F5F63136FB
Figs 10–12, 22, 29, 33 (Map)

Type material. *Holotype*, male. [USA]: ARIZ[ONA]: Yavapai Co[unty], 5 mi. [8.0 km] N[orth] [of] Prescott, 5450 ft [1661 m], 24 IV 1973, Lloyd M. Martin. CNC. ***Paratypes*,** 83 males, 5 females. [**USA**]: **Arizona:** Yavapai County: Prescott, collected by Lloyd M. Martin: 31 I 1970 (1 male); 6 II 1970 (1 male); 7 II 1970 (1 male); 8 II 1970 (1 male); 9 II 1970 (1 male); 10 II 1970 (1 male); 11 II 1970 (1 male); 13 II 1970 (1 male); 17 II 1970 (1 male); 23 II 1970 (1 male); 24 II 1970 (1 male); 28 II 1970 (1 male); 8 III 1970 (1 female); 21 III 1970 (1 male); 23 III 1970 (1 male); 25 III 1970 (1 male); 7 IV 1970 / Genitalia slide by RWP [female] USNM 45182 (1 female); 8 IV 1970 / Genitalia slide by RWP [male] USNM 45181 (1 male); 9 IV 1970 (1 female); 10 IV 1970 (1 female); Prescott, collected by Lloyd M. Martin, 29 I 1970 / Granite Dells, 4 mi. [6.4 km] N[orth] of (1 male); 4 mi. [6.4 km] N[orth] of Prescott, Lloyd M. Martin: 16 II 1972 / Genitalia slide #NOC17486 / Specimen voucher #CNCLEP00140439 (1 female); 18 II 1972 (1 male); 21 II 1972 (9 males); 23 II 1972 (5 males); 25 II 1972 (2 males); 8 III 1972 (2 males); 9 III 1972 (1 male); 10 III 1972 (3 males); 17 III 1972 (3 males); 17 III 1972 / [Crabo genitalia slide] 658 male (1 male); 19 III 1972 (1 male); 20 III 1972 (2 males); 22 III 1972 (1 male); 5 mi. [8.0 km] N[orth] [of] Prescott, 5450 ft [1661 m], Lloyd M. Martin: 23 IV 1973 (2 males); 23 IV 1973 / CNC / Genitalia Slide by RWP, USNM 41,553 (1 male); 24 IV 1973 (5 males); 24 IV 1973 / Specimen ID CNCLEP 00119516 / Barcodes of Life Project Leg removed DNA extracted (1 male); 24 IV 1973 / Specimen ID CNCLEP 00119514 / Barcodes of Life Project Leg removed DNA extracted (1 male); 24 IV 1973 / Genitalia CNC slide # 13942 male (1 male); 25 IV 1973 (5 males); 25 IV 1973 / Genitalia CNC slide # 13548 male (1 male); 26 IV 1973 (2 males); 27 IV 1973 (7 males); 27 IV 1973 / Genitalia CNC slide # 17796 male (1 male); 28 IV 1973 (3 males); 28 IV 1973 / CNC / Genitalia Slide by RWP, USNM 41,569 (1 male); 5 V 1973 (3 males); 5 V 1973 / Specimen ID CNCLEP 00119515 / Barcodes of Life Project, Leg removed, DNA extracted (1 male). CMNH, CNC, LACM, LGC, NMNH.

Etymology. The species epithet is the name of the people who inhabited Arizona between the Gila and Colorado rivers for hundreds of years prior to the colonization of the West by Caucasians of European descent. All examined specimens of this species are from Yavapai County, Arizona.

Diagnosis. *Supralathosea yavapai* males are distinguished by their off-white hindwing ground color, pure white in other *Supralathosea* species. The male antenna is the widest in the genus, rami 3.0 × shaft width (2.5 × in the other species). It is the largest *Supralathosea*, forewing length at least 16.5 mm (< 15.5 mm in the other species).

Males of *S. yavapai* have a relatively short broad-based triangular pollex. Those of other *Supralathosea* species are longer and thinner. The female genitalia of *S. yavapai* are only subtly different from those of other *Supralathosea* species. The crenulate anterior segment of the ductus bursae is relatively large compared to the bursa copulatrix in *S. yavapai*, and the membranous bursa is wider than long in *S. yavapai*, longer than wide in the other *Supralathosea* species.

The barcode of *S. yavapai* (BOLD:ADP3298; $n = 3$) is similar to several barcode haplotypes of *S. solastella*, clustering with them on similarity trees. These species are not recovered as distinct in our RAxML analysis (Fig. 35).

Description. Adults. ***Head*** – Male antennal rami up to 3 × central shaft width. Scape pale gray, tuft long, loose. Labial palpus as for genus, flat scales mixed dark gray and white. Frons scales gray, with a loose median ridge; dorsum scales long, pale gray, white-tipped gray, and black, darkest centrally; loose tufts anterior and posterior to antenna. ***Thorax*** – Scales long, white-tipped gray

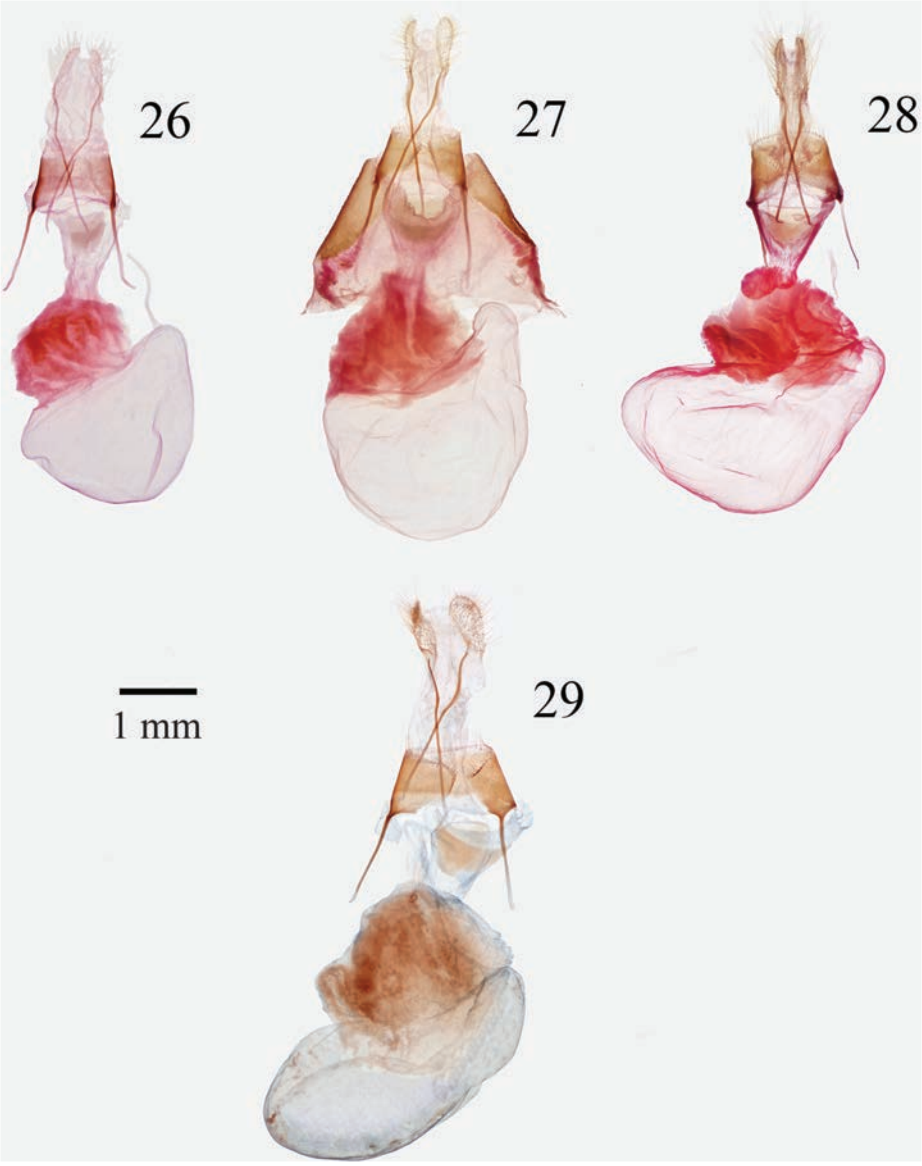

Figures 26–29. *Supralathosea* female genitalia **26** *Supralathosea baboquivariensis* **27** *S. solastella* (Brewster County, Texas) **28** *S. solastella* (Zapata County, Texas) **29** *S. yavapai*.

and scattered black or white, long hair-like black scattered on tegula and dense on dorsum, appearing medium gray (male) or charcoal gray (female) with black and pale gray bands across collar base and loose dark tuft on metathorax; venter densely hairy, dark gray. ***Legs*:** As for genus. ***Wings*:** Forewing length 16.5–18.5 mm (males); 17.5–18.0 mm (females), length 2 × width; scales white, black-rimmed white, and medium to dark gray; male ground color uniform slightly powdery medium gray with slight brownish tint, terminal area slightly darker, trailing margin blackish gray; veins slightly darker, powdery; basal line absent; antemedial line an oblique gray smudge on costa, occasionally dark marks on veins; medial line a gray smudge on costa or absent; postmedial line small dark marks on costa and series of dark lines on M3 to 1A+2A, strongly oblique basad posterior to cell; subterminal line absent or ill-defined, pale gray, with or without faint proximal darker shade; faint darker patches in terminal area; terminal line dark gray, strongest between veins; fringe weakly checkered ground color and slightly darker gray; orbicular and reniform spots absent or very faint; female ground color powdery charcoal gray, darkest centrally; with indistinct intervenal dark gray in terminal area; antemedial, medial, postmedial, and subterminal lines present, stronger than in males; orbicular and reniform spots evident as pale filling against dark ground color. Hindwing pale yellowish gray, gray suffusion along anterior margin (male) or diffuse (female); veins powdery gray; discal spot small, gray; terminal line powdery gray, thicker between veins; fringe white (male), white with incomplete gray base (female). ***Abdomen*** – Scales flat and hair-like, gray. ***Male genitalia*:** Uncus as for genus, mesial and subapical segments widest. Juxta ventral extension long. Valve shape as for genus, length 3.6 × width, sacculus 0.75 × valve length, dorsal margin broadly convex; clasper as for genus; pollex relatively short, triangular with broad base, length 0.25 × valve width. Phallus length 4 × width. Vesica relatively large, similar to that of *S. solastella* but slightly more massive. ***Female genitalia*:** Papilla analis as for genus, length 2 × width. A8 length 0.5 × width. Posterior apophysis 2.3 × A8; anterior apophysis 0.6 × posterior apophysis. Ostium bursae and ductus bursae as for genus, anterior segment as long as wide, 2 × A8, broad junction to corpus bursae angled 30°. Corpus bursae as for genus, width greater than length, with relatively long rightward extension.

Distribution and biology. This species is known from nearly 100 specimens collected by Lloyd Martin at his home north of Prescott, Arizona in the early 1970s, most of which are now at CNC and LACM. The habitat is dry ponderosa pine forest (J. D. Lafontaine pers. comm. 2018). All specimens were collected from late January to early May. This species might be more widespread in the Southwest United States but might elude detection due to its early flight period. The early stages of *S. yavapai* are unknown.

Discussion. The dense vestiture of the moth is probably an adaptation to cold temperatures during its spring flight.

Genus *Infralathosea* gen. nov.

https://zoobank.org/7DD5A023-E8DE-4CAE-A3BE-EBDBDA5C0D60

Type species. *Catabena pronuba* Barnes & McDunnough, 1916.

Gender. Feminine.

Etymology. The name is derived from the Latin prefix *infra* meaning below, and *Lathosea*, the genus included in the name *Supralathosea*. *Lathosea* is a junior subjective synonym of *Cucullia* Schrank (Noctuidae, Cuculliinae).

Diagnosis. *Infralathosea* adults are relatively small noctuid moths, forewing lengths 12.0–14.5 mm, with streaky pale gray forewings. The antemedial and postmedial lines are fused in the anterior and posterior medial area, forming thin black arcs based on the costa and posterior margin. The anterior arc is strongest and is diagnostic. Other markings include a thin basal dash, subterminal intervenal black lines, and indistinct darker gray patches on the costa (especially at the medial line origin), apex, and trailing margin. The orbicular and reniform spots are reduced to small pale patches. The hindwings are nearly pure white, except gray in the female of one species. The antennae of both sexes are thin, beaded in males.

Infralathosea species resemble *Catabena* Walker and *Catabenoides* Poole species (both Noctuidae, Oncocnemidinae). *Infralathosea* species have the forewing lines fused into arcs; lines absent or typically noctuiform in *Catabena* and *Catabenoides*, extending from the costa to the posterior margin when visible.

Males of *Infralathosea* have a cylindrical arced uncus, lacking a focal bend like those of *Supralathosea* and *Eulathosea*. The valves are simple, strap-like with a weak sacculus, thin curved thorn-like ampulla, and bluntly pointed apex lacking an expanded cucullus, pollex, or corona. Patches of short cornuti on the tubular vesica are arranged in patches on subbasal and medial bulges, with a stout subapical cornutus in one species. Females have a long conical papilla analis. The distal abdominal intersegmental membranes and apophyses are long and the ovipositors protrude from the distal abdomen in situ. The ductus bursae is tubular, membranous except for sclerotized postvaginal plates, and the corpus bursae is elongate, slightly asymmetric with the ductus seminalis joined to the posterior end. *Infralathosea* females differ from *Supralathosea* and *Eulathosea* females in many respects, including the elongate posterior abdominal structures; those of both other genera have nonprotruding pad-like papillae, short intersegmental membranes, and short apophyses.

Description. Adults. ***Head*** – Male antenna bead-like, setose ventrally; female antenna filiform, setae sparse. Scape medium length. Labial palpus as in *Supralathosea*, white and gray. Frons convex, scales white with dorsal transverse black line. Head scales white, gray, and white-tipped gray. Haustellum present. ***Thorax*** – Scales dimorphic, long narrow flattened or hair-like; white, gray, or white-tipped gray; forming slight hoary medium gray crest; venter pale gray. ***Wings*:** Forewing length 12.0–14.5 mm (males), 13.5–14.5 mm (females), apex blunt; scales strap-like white, gray, and black, appearing slightly streaky pale gray; lines black, thin, indistinct except on costa, anterior segments of antemedial and postmedial lines fused posterior to Cu and posterior segments fused near posterior margin, forming anterior and posterior arcs; orbicular spot small pale with central dark line; reniform spot a pale smudge or absent; claviform spot absent. Male hindwing ground color pure white; thin band of off-white scales along dorsal anterior margin towards apex; Female hindwing ground color either white with scattered gray scales near margin and on veins in some individuals (1 species) or medium gray (1 species). ***Legs*:** Lacking spines or claws; scales dark gray and white; tarsi dark gray with distal white rings; ventral tarsal segments except distal segment with three regular rows of uniform spiniform setae. ***Abdomen*** – Lacking dorsal A1 transverse channel, brush organs, and coremata. Scales mostly flat, fewer hair-like, medium gray. ***Male genitalia*:** Uncus thin, arced. Juxta shield-shaped, ventral margin broadly V-shaped. Valve simple, strap-like, length 3.5 × width; apex pointed bluntly, lacking corona or pollex; sacculus length 0.4 × valve length, width 0.5 × valve width, dorsum straight or weakly convex; clasper base a sclerotized rod at ventral margin distal to sacculus, ampulla thorn-like, base directed 45° dorsad from origin at valve distal ¹⁄₃, distal segment directed dorsad and slightly mesially beyond 90° bend. Phallus tubular, length 4 × width. Vesica length 1 × phallus length, diameter 0.4–0.5 × length, nearly straight beyond basal 90° bend; proximal vesica with broad-based dorsal bulge; bulge and adjacent posterior vesica surface covered by multiple porrect spine-like cornuti, much less massive than those of *Supralathosea*; mid vesica with broad posterior bulge or diverticulum covered by loose cluster of shorter thinner cornuti; single stout apical cornutus (1 species). ***Female genitalia*:** Segment A7 unmodified. Segment A8 elongate, width 0.6–0.7 × length, sparse short setae densest at posterior margin. Papilla analis 0.6–0.7 × A8, width 0.3–0.4 × length, mediolaterally compressed, apex pointed bluntly; sparse long hair-like setae at base and multiple short thin setae on distal third; membrane to A8 long, 1.8 × A8. Posterior apophysis 2.5–3.0 × A8; anterior apophysis 0.65–0.7 × posterior apophysis. Ostium bursae shallow, quadrate, membranous. Ductus bursae tubular, slightly expanded mesially in 1 species, length 2 × A8, weakly sclerotized except for strong quadrate ventral and dorsal postvaginal plates on posterior 1/5 to 1/3, joined broadly to left posterolateral corpus bursae. Corpus bursae membranous, lacking signa, length 2.3–2.6 × A8 and width 0.33–0.5 × length, elongate, ovoid, ductus seminalis at medial posterior end.

Higher classification. *Infralathosea* is assigned to Oncocnemidinae (Keegan at el. 2021). The male genitalia, including the simple valve with thorn-like ampulla and tubular vesica with patches of cornuti, are typical of the subfamily.

Distribution and biology: Like *Supralathosea*, this genus has a limited distribution in the American Southwest, occurring in central Arizona, New Mexico, and west Texas. At least one of the species probably occurs in adjacent northern Mexico. Adults of *Infralathosea* fly during much of the year except in the winter, with most records from spring and fall. The early stages are unknown. The papilla analis shape and long eversible ovipositor suggest that the eggs might be inserted into its hostplant, and as such the larva may be an internal feeder for at least a portion of its larval stage.

Discussion. This genus includes two allopatric species, *Infralathosea pronuba* comb. nov. from central Arizona and New Mexico and *Infralathosea unicornis* sp. nov. from west Texas. The males are indistinguishable without dissection or barcoding, while females are best distinguished by superficial appearance. As discussed above under *Supralathosea*, *Infralathosea* species lack an A1 transverse channel. *Catabena pronuba* was associated with *Supralathosea* by Troubridge (2008) based on the absence of this character.

***Infralathosea pronuba* (Barnes & McDunnough, 1916), comb. nov.**

Figs 13, 14, 23, 30, 34 (Map)

Catabena pronuba Barnes & McDunnough, 1916: 10, pl. 3 fig. 11.
Cucullia nanuscula Dyar, 1922: 168.

Type material. *Catabena pronuba*: Holotype, male, USA, New Mexico, Jemez Springs. NMNH. [examined]. *Cucullia nanuscula*: Holotype, male, USA, New Mexico, Jemez Springs. NMNH. [examined].

Diagnosis. *Infralathosea pronuba* males are superficially identical to *I. unicornis*. Both are relatively small streaky gray moths with characteristic fused

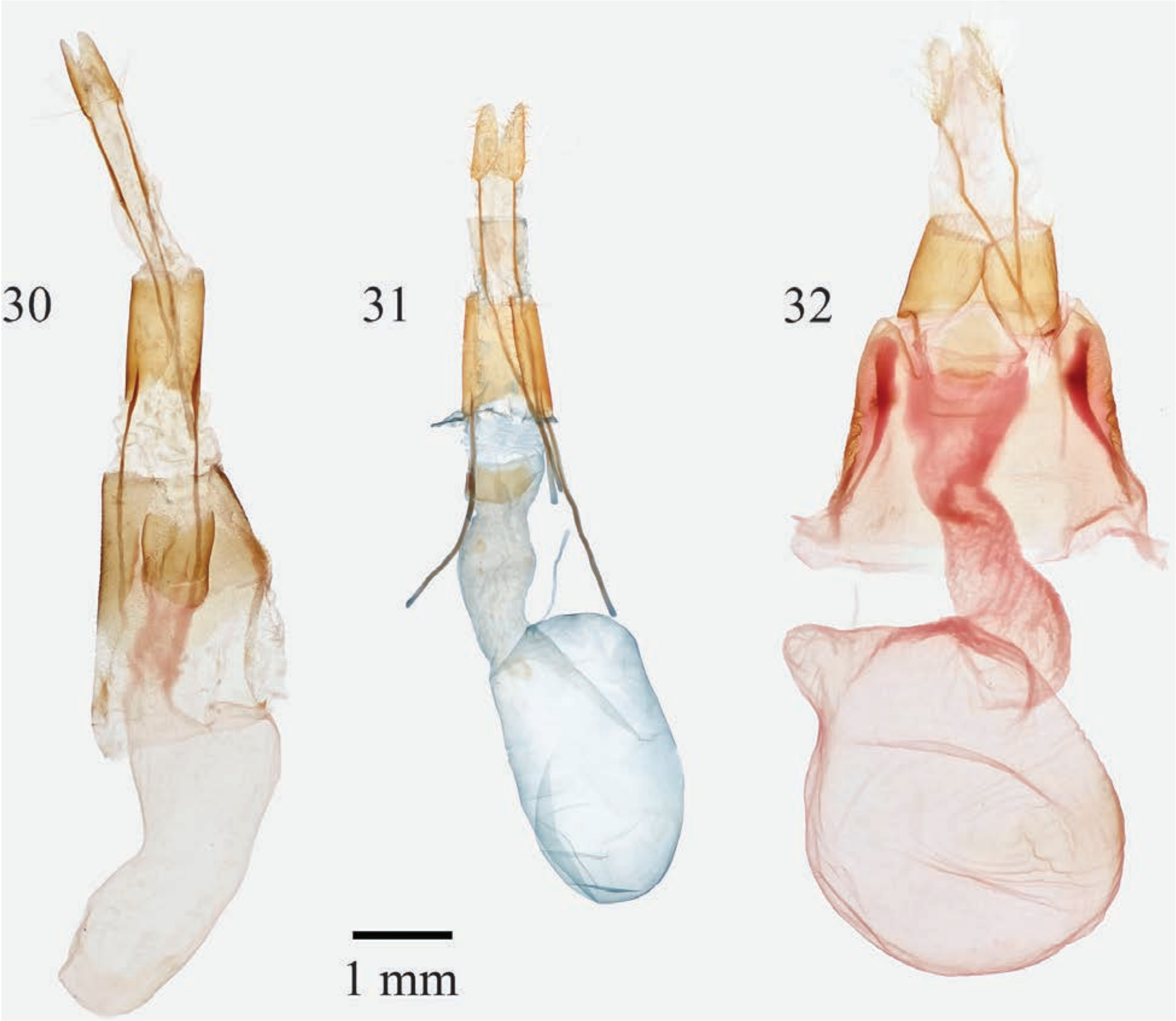

Figures 30–32. *Infralathosea* and *Eulathosea* female genitalia **30** *Infralathosea pronuba* **31** *I. unicornis* **32** *Eulathosea obtusa*.

forewing lines as described in the genus description and have nearly pure white hindwings. They are distinguishable by their genitalia. Males of *I. pronuba* lack an apical cornutus on the vesica, present in *I. unicornis*.

The females of *Infralathosea* species have identical forewings and similar genitalia, but are distinguished easily by their hindwings, gray in *I. pronuba* and white in *I. unicornis*.

Infralathosea pronuba is the only *Infralathosea* species in Arizona and New Mexico. *Infralathosea unicornis* occurs in west Texas.

The barcode of *I. pronuba* (BOLD:ACM7023, *n* = 13) differs by 5.3% from that of *I. unicornis*.

Distribution and biology. This species is known from north and central New Mexico and central Arizona (Yavapai County).

Infralathosea pronuba flies during spring and summer. Most examined specimens were collected from early March through April, with additional records from July. This species is not rare in central New Mexico, but there are relatively few specimens in examined collections. The early stages are unknown.

Infralathosea unicornis **sp. nov.**
https://zoobank.org/AC2731C6-182D-4963-B206-42764A7BDE95
Figs 15, 16, 24, 31, 34 (Map)

Type material. ***Holotype*****, female.** [**USA**]**: Texas:** [Brewster County]: Big Bend N[ational] P[ark], Chihuahuan Desert near Nugent M[oun]t[ai]n, 1 X [19]67, A. & M. E. Blanchard. NMNH. ***Paratypes***, 112 males, 49 females. **USA: Texas**: Brewster County: Big Bend N[ational] P[ark], Chihuahuan Desert near Nugent M[oun]t[ai]n., A. & M. E. Blanchard, 1 X [19]67 (2 males); 8 X [19]69 (1 female); Big Bend Nat[ional] Park, Dugout Wells, A. & M. E. Blanchard, 28 IX [19]65 (3 males, 5 females); 28 IX [19]65 / Genitalia slide by RWP [female] USNM 45299 (1 female); 3 X [19]66 (1 female); 30 III [19]71 (1 male); Big Bend National Park, Glenn Springs R[oa]d, near Nugent M[oun]t[ai]n., Leg. E. C. Knudson, 28 IX [19]81 (1 male); Big Bend Nat[ional] Park, Gov[ernment] Spring, A. & M. E. Blanchard, 29 IX [19]65 (7 males, 4 females); 29 IX [19]65 / [male] genitalia on slide A. B. 202 (1 male); 29 IX [19]65 / Genitalia slide by R. F. USNM 42,598 (1 female); 4 X [19]67 (1 male); 27 III [19]71 (2 males); Big Bend Nat[ional] Park, near Nugent M[oun]t[ai]n, leg. E. C. Knudson, 13 IX [19]82 (1 male); Big Bend Nat[ional] Park, Oak Spring, A. & M. E. Blanchard, 2 IV [19]65 (1 male); 6 X [19]65 (1 female); Big Bend Nat[ional] Park, K-Bar Res[earch] Sta[tion], A. & M. E. Blanchard, 23 III [19]71 (2 males, 1 female); 23 IX [19]71 (1 female); 25 IX [19]71 (1 female); Terlingua Ranch, 29.43–[29].47° -103.38–[103].41°, 1090–1135 m, 9 IV 2016, L. G. Crabo/B. C. Schmidt / Genitalia slide # 17800 [male] (1 male); Terlingua Ranch, guest cabin, 29.452° -103.393°, 1135 m, 9 IV 2016, UV lt., C. Schmidt, J. Dombroskie, L. Crabo CNC535745 (1 male); Terlingua Ranch, Church Rd., 29.442° -103.386°, 1092 m, 9 IV 2016, C. Schmidt/J. Dombroskie/L. Crabo / Database # CNCLEP 535915 / Barcodes of Life Project, Leg removed, DNA extracted (1 male); Terlingua Ranch Lodge, 29.453° -103.388°, 18 IX 2019, Limestone outcrop, C. Jaeger / CNCLEP numbers: 00232026–00232028, 00272842–0027845, 00272847, 00272848, 00272850–0027853, 00272885, 00272894, 00272895, 00272906, 00272907, 00272909, 00272912, 00272914, 00272915, 00272920, 00272929, 00272930, 00272958, 00272982, 00272988, 00272990, 00273064–00273067, 00273069, 00273070, 00273072–00273075, 00273742, 00273744–00273746, 00273784–0273786 (46 males); numbers: 00232025, 00272908, 00272910, 00272911, 00272927, 00272976, 00272980, 00272986, 00273062, 00273063, 00273068, 00273071, 273723, 00273726, 00273747, 00273748, 00273771, 00273787, 00272846, 00272849, 00272854, 00272855, 00272856 (23 females); Terlingua Ranch Lodge, Whitehouse Mtn saddle, 29.453° -103.388°, 22 IX 2023, Limestone outcrop, C. Schmidt, C. Jaeger / CNCLEP numbers 00335508, 00335510, 00335511, 00335513, 00335520, 00335537, 00335561, 00335562, 00335581, 00335582, 00335594, 00335620–003356213, 00335681, 00335685, 00335689, 00335719, 00335733, 00335734, 00335842 (22 males); Presidio County: Shafter, 9 IX [19]69, A. & M. E. Blanchard (4 males, 1 female); Terrell County: Sanderson, Desert Air Motel, N30.1453° W102.4059°, elev. 2810' [856 m], 27 + 28 IX 2024, to MV/BL, Leg. D. L. Wikle (11 males, 4 females); Val Verde County: Langtry, N29.804° W101.557°, 7 III 2016, J. Vargo (1 male); Same collection label / Crabo slide 629 [female] (1 female); Same locality, collector 17 III 2018 (1 male, 3 females); Seminole Canyon, 1400 ft. [427 m], N29.696° W101.324°, 22 III 2016, J. Vargo (2 males). CNC, DLW, JV, LGC, NMNH.

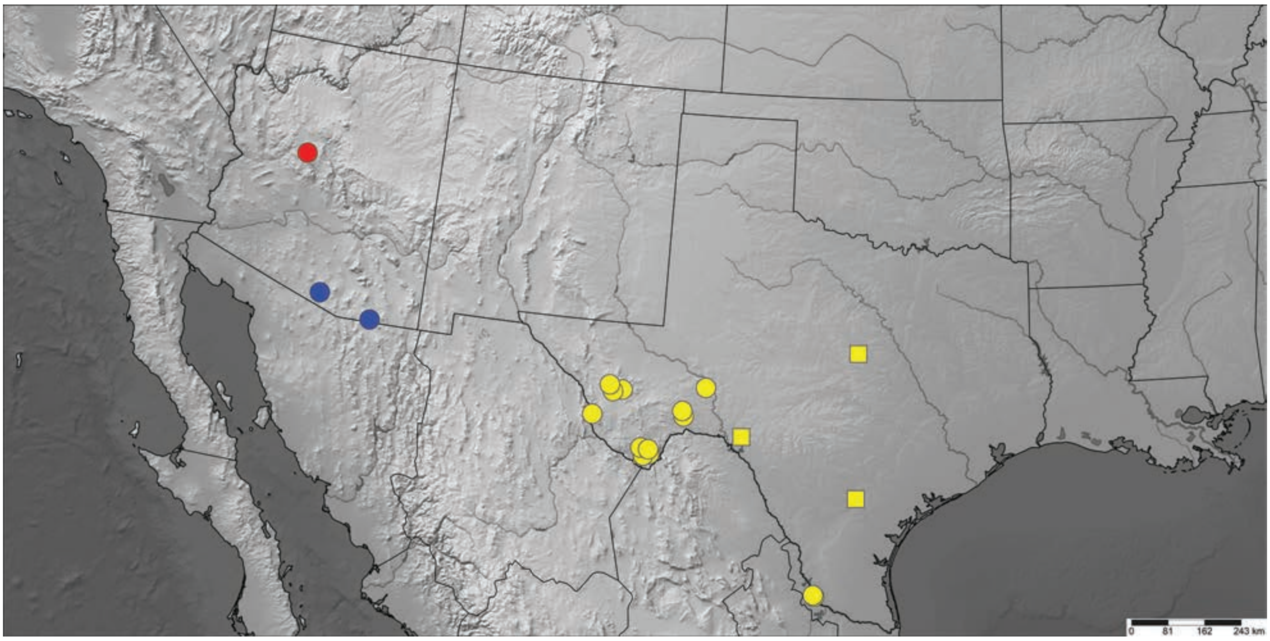

Figure 33. Distribution map of *Supralathosea* species. *Supralathosea baboquivariensis* (blue), *Supralathosea solastella* (yellow), and *Supralathosea yavapai* (red). Circles = examined specimens. Squares = iNaturalist records.

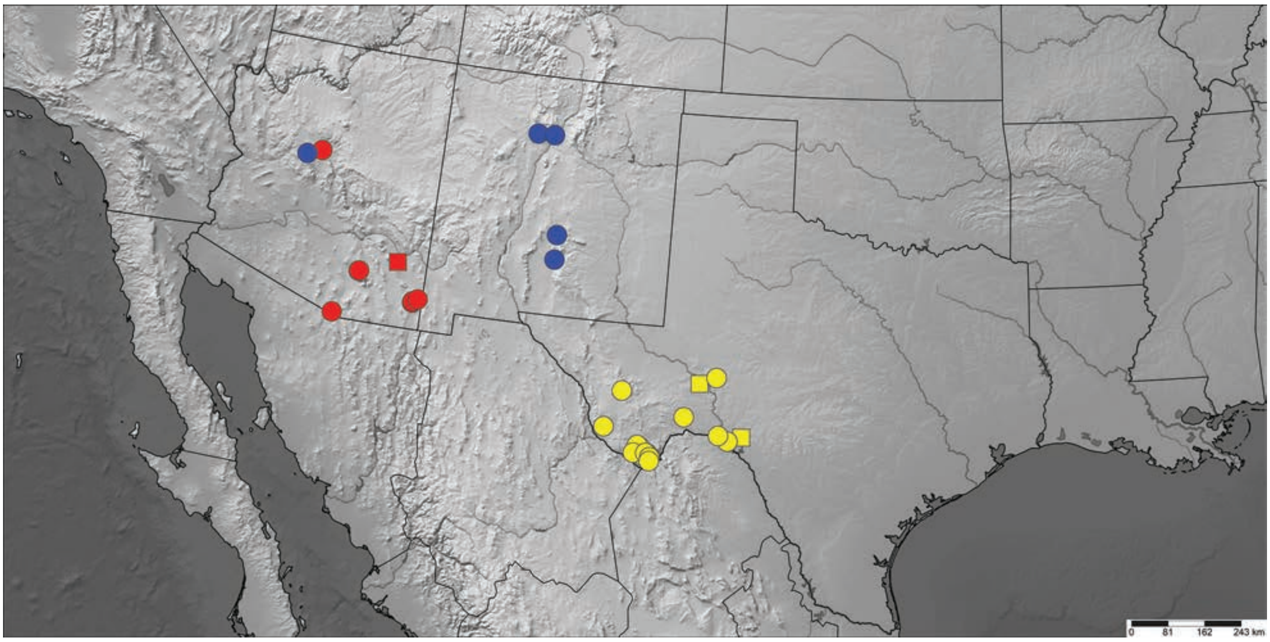

Figure 34. Distribution map of *Infralathosea* and *Eulathosea* species. *Infralathosea pronuba* (blue), *Infralathosea unicornis* (yellow), and *Eulathosea obtusa* (red). Circles = examined specimens. Squares = iNaturalist records.

Etymology. The name is Latin, meaning one horn. It refers to the diagnostic stout cornutus on the distal male vesica.

Diagnosis. This species resembles *I. pronuba* in habitus and structure. Males *I. unicornis* are superficially identical to those of *I. pronuba*, but can be identified by a stout cornutus on the distal vesica that *I. pronuba* lacks. The females of these species also have identical forewings, but the hindwing ground color is nearly pure white in *I. unicornis*, gray in *I. pronuba*.

Infralathosea unicornis is the only species in the genus in west Texas. The barcode of *I. unicornis* (BOLD:ADF0036; *n* = 1) differs from that of *I. pronuba* by 5.3%.

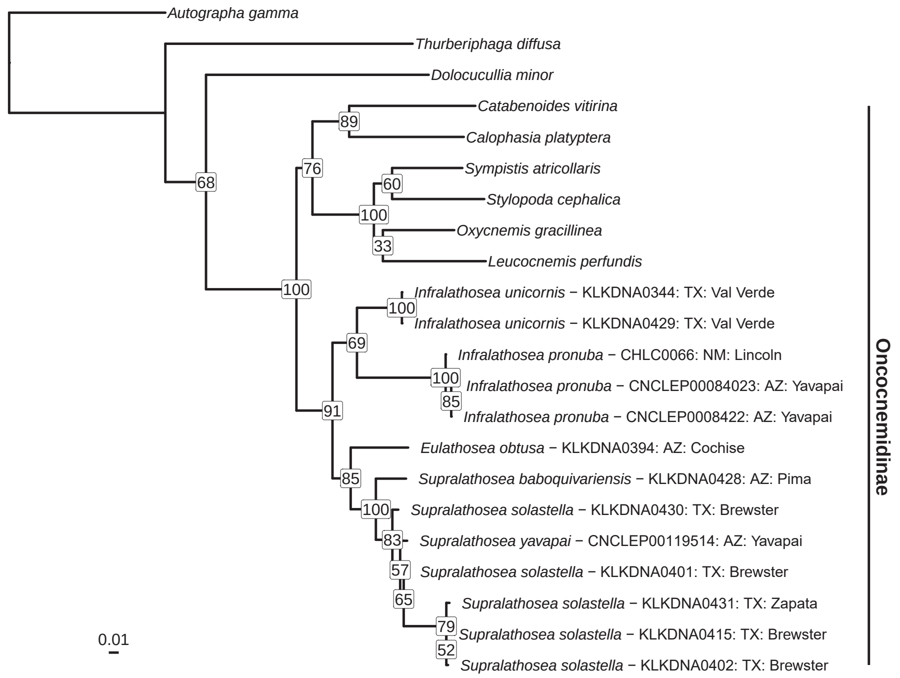

Figure 35. Maximum-likelihood tree inferred with RAxML based on five nuclear genes and CO1 of *Supralathosea*, *Infralathosea*, *Eulathosea*, selected Oncocnemidinae genera, and outgroups in other noctuid subfamilies (Plusiinae, Acontiinae, and Cuculliinae). Bootstrap values are shown over nodes. Tip labels for *Supralathosea*, *Infralathosea*, and *Eulathosea* provide additional identifying information in order to link specimens to full collection details.

Description. Adults. ***Head*** – Antennae of both sexes as for genus. Scape tuft medium dark gray. Labial palpus scales dark gray. Frons white, transverse black dorsally; dorsal head scales white and white-tipped gray, loose paramedian tufts anterior and posterior to antenna. ***Thorax*** – Patagium scales spatulate, white-tipped, appearing gray with weak dark basal line. Tegula scales long, spatulate, white, with fewer black of similar shape and hair-like, appearing pale gray; dorsal thorax charcoal; venter pale gray. ***Wings*:** Forewing length 13.0–14.0 mm; scales white, pale gray, dark gray; appearing slightly streaked medium gray, darkest on mesial posterior margin and in terminal area near apex and anal angle; veins and intervenal dark lines near apex dark gray; basal dash black; antemedial and postmedial lines fused as in genus description, anterior antemedial line and mesial fused segment darkest; medial line a gray smudge near costa; subterminal line diffuse, irregular, pale gray; fringe white and gray, slightly darker between veins; spots as for genus. Hindwing ground color pure white (male); uniform medium gray (female). ***Legs*:** As in genus description. ***Abdomen*** – Vestiture as for genus. ***Male genitalia*:** Uncus and juxta as for genus. Valve, including sacculus, clasper, and cucullus as for genus. Phallus length 4 × width. Vesica length 1 × phallus, width, diameter 0.4 × length; proximal cornuti patches as in genus description; mesial cornuti on distinct dome-shaped diverticulum; posterior apex with single stout cornutus. ***Female genitalia*:** Papilla analis, intersegmental membrane, and A8 as for genus. Posterior apophysis 3.0 × A8; anterior apophysis 0.65 × posterior apophysis. Ostium bursae as for genus; postvaginal plate length 0.2 × ductus bursae; ductus bursae 1.9 × A8, widest mesially. Corpus bursae shape as for genus, length 2.3 × A8 and width 0.5 × length.

Distribution and biology. This species occurs in Chihuahuan shrub desert in west Texas and is relatively common in collections. Most examined specimens are from the Big Bend region between Fort Davis and Big Bend National Park. Collection records suggest the presence of two broods, with records from spring (February to April) and fall (September and October). The early stages are unknown.

Genus *Eulathosea* gen. nov.

https://zoobank.org/D3BB84B1-B611-4BB6-8996-28F580FCF55A

Type species. *Cucullia obtusa* Smith, 1909.

Gender. Feminine.

Etymology. The name is derived from the Greek prefix *eu*, meaning good or pleasant, and *Lathosea*, the noctuid genus that is part of the names *Supralathosea* and *Infralathosea*. It refers to the attractive appearance of the only known species.

Diagnosis. *Eulathosea* is a monotypic genus which differs in many ways from *Supralathosea* and *Infralathosea*. Adults (forewing length 17.0–18.5 mm) are larger than all species in the other genera other than *S. yavapai*. They can be identified without dissection by the solid dark hindwing marginal band, marginal band absent or at most a powdery mixture of gray and whitish scales in *Supralathosea* and *Infralathosea*, and streaky pale gray forewing with orange-tan scales in the cell that extend nearly to the distal margin, forewing gray without warm colors in the other genera.

The male uncus of *Eulathosea* is bent ventrad at a sideways-D-shaped thickening, beyond which it is gracile and arced. The valve is rhomboid, broadest at the midpoint with a V-shaped bulge at the distal sacculus, gradually tapering to a weak cucullus with apical and anal points and partial corona of claw-like setae on the dorsal two-thirds, and a long acute ampulla that reaches the dorsal margin. The vesica is bent 270°, with dilated proximal and distal segments bearing cornuti shorter than those of *Supralathosea* and longer than those of *Infralathosea*. Females have a rounded corpus bursae with thick rippled membrane and a cone-shaped leftward process bearing the ductus seminalis. The undulating tubular ductus bursae is moderately thick and rubbery, but lacks the bulbous anterior segment that is present in *Supralathosea* females.

Description. Adults. Males and females superficially similar. ***Head*** – Antenna of both sexes filiform. Scape medium length, gray. Eyes lacking interommatidial setae, with few adjacent dark lash-like scales. Labial palpus distal segment length 0.4 × second segment, directed anterodorsad. Frons slightly convex, scales gray with black dorsal transverse line; dorsal head scales pale to dark gray, weak paramedian tufts gray anteriad and black posteriad to antenna. ***Thorax*** – Scales mostly long white-tipped pale gray, appearing pale gray; collar with basal tan, black, and pale gray lines, crest prominent in resting moths; weak tufts on metathorax; venter scales hair-like, white and pale gray. ***Legs*:** Tibia lacking spines or claws; tarsal segments with three regular rows of spine-like setae. ***Wings*:** Forewing length 17.0–18.5 mm, length 2.0–2.2 × width, outer margin smooth; scales strap-like white, pale to dark gray, tan; veins dark gray; appearing streaked and mottled medium gray, with dark patches on costa, distal posterior margin, and subterminal area, and pale orange-tan from cell base to wing apex; basal line absent; antemedial and medial lines dark oblique spots on costa; postmedial line with dark gray medial and whitish outer components, faint, irregular, drawn strongly basad in fold; subterminal line irregular, whitish, strongest between veins opposite cell and in fold; terminal line thin, dark gray; orbicular and reniform spots pale, small, faint; claviform spot absent; fringe weakly checkered ground color and dark gray. Hindwing ground color pearlescent white, veins and broad marginal band dark gray; fringe white, base striped ochre and dark gray. ***Abdomen*** – Lacking dorsal A1 transverse channel, brush organs, and coremata; scales gray; small dorsal tufts on segments A2 and A3. ***Male genitalia*: **Uncus base stout, cylindrical, directed posteriad, bent 90° ventrad at sideways-D-shaped subbasal bulge, mid and distal segments gracile, arced, tip with small downward tooth. Juxta V-shaped, dorsal arms curved mesially. Valve turkey-drumstick-shaped with strongly convex ventral margin to mid valve and undulating weakly convex dorsal margin, distal valve tapered to weak rhomboid cucullus with blunt triangular apex and acute granulose anal angle lacking a pollex, with corona of 10–15 long claw-like setae dorsal ⅔; sacculus 0.5 × valve length, proximal ⅔ uniform, 0.3 × valve width, distal ⅓ dorsally convex with thick sideways-V-shaped bulge; clasper base a thick bar at distal sacculus, clasper ampulla directed distal and 45° dorsad from origin on ventral third of valve distal to sacculus, slightly curved, slender, thorn-like, reaching valve dorsal margin. Phallus tubular, length 4 × width, spinulose apex bulging slightly leftward with ventral and dorsal extensions onto vesica. Vesica bent 90° ventrad at base, then curved dorsad 180° with apex to right of mid-phallus; subbasal and distal vesica dilated with intervening waist, subbasal bulge 1.8 × phallus diameter, distal bulge 2.5 × phallus diameter with smooth taper to apex; multiple similar needle-like cornuti in ovoid patch on left side of subbasal bulge and T-shaped patch on left and ventral sides of distal bulge. ***Female genitalia*: **A7 tergite normal size, pleural membrane thick, with anterior dark internally concave rugose structure (possibly a gland). Segment A8 width 1.5 × length. Papilla analis 0.8 × A8, width 0.3–0.4 × length, apex blunt, covered by uniform hair-like setae. Posterior apophysis 2.5 × A8; anterior apophysis 0.6 × posterior apophysis. Ostium bursae quadrate, width 0.5 × A8, ventral margin thin, sclerotized, postvaginal plates small; ductus bursae thick, rubbery, externally rugose, length 3 × A8, undulating, narrowest at midpoint, widest proximal to 90° ventrad bend at junction with corpus bursae. Corpus bursae globose, length and width 3 × A8, with short conical left ventral protrusion with ductus seminalis at apex and slightly thickened concentrically rippled membrane on right but lacking smaller distinct signum.

Higher classification. *Eulathosea* is assigned to Oncocnemidinae (Keegan et al. 2021).

Discussion. *Eulathosea* lacks an A1 transverse channel, as discussed under *Supralathosea*.

***Eulathosea* obtusa (Smith, 1909), comb. nov.**

Figs 17, 18, 25, 32, 34 (Map)

Cucullia obtusa Smith, 1909: 63.

Type material. *Lectotype*, male, designated by Todd 1982: 157. USA Arizona, Santa Catalina Mts. AMNH [examined from photograph].

Diagnosis. *Eulathosea obtusa* can be identified without dissection by the combination of streaky forewing pattern with orange-tan scales in and distal to the cell and white ground color hindwing with broad solid blackish marginal band that extends uninterrupted to the wing margin. It is most likely to be confused with streaky species of *Sympistis* Hübner (Noctuidae, Oncocnemidinae) or a *Cucullia* Shrank (Noctuidae, Cuculliinae) species with reddish brown on the anterior forewing (such as *Cucullia eucaena* Dyar). Most *Sympistis* species have a claw-like seta on the distal foretibia that *Eulathosea* lacks. Species of these genera lack the combination of genitalia characters described in the *Eulathosea* Diagnosis section, above.

The barcode BIN of *E. obtusa* is BOLD:AAH9892.

Distribution and biology. *Eulathosea obtusa* occurs in forests of eastern and central Arizona. It flies during late summer and fall, with records of examined specimens between late July and early October. The early stages are unknown.

Acknowledgements

This work is the culmination of a project initiated by LGC while visiting the CNC, during which he was hosted by J. D. Lafontaine and B. C. Schmidt. It would not have been possible without their encouragement and help. B. C. Schmidt gave constructive advice after reviewing the manuscript and also verified specimen data from the CNC. Jocelyn Gill photographed specimens and prepared preliminary illustrations. Chris Grinter, Chuck Harp, and Jim Vargo gave specimens to LGC. Merrill Peterson photographed adults and genitalia at Western Washington University, Bellingham, Washington, and received and cared for specimen loans on behalf of LGC. Paul Goldstein loaned specimens from NMNH, including type specimens, and Brian Brown and Weiping Xei loaned specimens from LACM.

Additional information

Conflict of interest

The authors have declared that no competing interests exist.

Ethical statement

No ethical statement was reported.

Funding

No funding was reported.

Author contributions

Conceptualization: LGC. Investigation: LGC, KK. Methodology: KK. Writing - original draft: LGC. Writing - review and editing: KK.

Author ORCIDs

Lars G. Crabo https://orcid.org/0009-0004-1089-5511
Kevin Keegan https://orcid.org/0000-0002-0872-7875

Data availability

All of the data that support the findings of this study are available in the main text.

References

Barnes W, Benjamin EH (1924) Notes and new species. Contributions to the Natural History of the Lepidoptera of North America 5: 99–199.

Barnes W, McDunnough J (1916) New species of North American Lepidoptera. Contributions to the Natural History of the Lepidoptera of North America 3: 5–34.

Dyar HG (1922) New American Moths (Lepidoptera). Insecutor Inscitiae Menstruus 10: 166–173.

Hampson GF (1903) Catalogue of the Noctuidae in the collection of the British Museum. Vol. 4. Taylor & Francis, London, 689 pp.

Hardwick DF (1950) Preparation of slide mounts of lepidopterous genitalia. The Canadian Entomologist 10: 231–235. https://doi.org/10.4039/Ent82231-11

Hebert PDN, Cywinska A, Ball SL, deWaard JR (2003) Biological identifications through DNA barcodes. Proceedings of the Royal Society of London. Series B. Biological Sciences 270: 313–321. https://doi.org/10.1098/rspb.2002.2218

Hillis DM, Bull JJ (1993) An empirical test of bootstrapping as a method for assessing confidence in phylogenetic analysis. Systematic Biology 42: 182–192. https://doi.org/10.1093/sysbio/42.2.182

Hodges RW, Dominick T, Davis DR, Ferguson DC, Franclemont JG, Munroe EG, Powell JA (1983) Check List of the Lepidoptera of America north of Mexico. E. W. Classey and The Wedge Entomological Research Foundation, Washington, DC, 284 pp.

iNaturalist community (2024) iNaturalist community. https://www.inaturalist.org [accessed 4 June 2024]

Keegan KL, Lafontaine JD, Wahlberg N, Wagner DL (2019) Towards resolving and redefining Amphipyrinae (Lepidoptera, Noctuoidea, Noctuidae). Systematic Entomology 44: 451–464. https://doi.org/10.1111/syen.12336

Keegan KL, Rota J, Zahiri R, Zilli A, Wahlberg N, Schmidt BC, Lafontaine JD, Goldstein PZ, Wagner DL (2021) Toward a stable global Noctuidae (Lepidoptera) taxonomy. Insect Systematics and Diversity 5: 1–24. https://doi.org/10.1093/isd/ixab005

Lafontaine JD (2004) The Moths of North America including Greenland, Fascicle 27.1, Noctuoidea Noctuidae (part) Noctuinae (part—Agrotini). The Wedge Entomological Research Foundation. Washington, DC, 385 pp.

Lafontaine JD, Schmidt BC (2010) Annotated check list of the Noctuoidea (Insecta, Lepidoptera) of North America north of Mexico. ZooKeys 40: 1–239. https://doi.org/10.3897/zookeys.40.414

Lemoine F, Domelevo Entfellner JB, Wilkinson E, Correia D, Dávila Felipe M, de Oliveira T, Gascuel O (2018) Renewing Felsenstein's phylogenetic bootstrap in the era of big data. Nature 556: 452–456. https://doi.org/10.1038/s41586-018-0043-0

McDunnough J (1938) Check list of the Lepidoptera of Canada and the United States of America. Memoirs of the Southern California Academy of Sciences 1: 1–272. https://doi.org/10.5962/bhl.title.146941

Miller MA, Pfeiffer W, Schwartz T (2010) Creating the CIPRES Science Gateway for inference of large phylogenetic trees. Proceedings of the Gateway Computing Environments Workshop (GCE). New Orleans, Louisiana, 14 November 2010. https://doi.org/10.1109/GCE.2010.5676129

Pohl GR, Nanz SR (2023) Annotated taxonomic checklist of the Lepidoptera of North America, north of Mexico. Wedge Entomological Research Foundation, Bakersfield, California, [xiv +] 580 pp.

Poole RW (1989) Lepidopterorum Catalogus. (New Series, Fasc. 118). Noctuidae. E. J. Brill, New York. 3 Vol., 1314 pp.

Poole RW (1995) Noctuoidea, Noctuidae (part), Cuculliinae, Stiriinae, Psaphidinae (part). In: Dominick RB, et al. (Eds) The Moths of America north of Mexico. Fascicle 26.1. The Wedge Entomological Research Foundation, Washington, DC, 249 pp.

Smith JB (1909) New species of Noctuidae for 1909. Journal of the New York Entomological Society 17: 57–71.

Stamatakis A, Hoover P, Rougemont J, Renner S (2008) A rapid bootstrap algorithm for the RAxML web servers. Systematic Biology 57: 758–771. https://doi.org/10.1080/10635150802429642

Todd EL (1982) The Noctuid type material of J. B. Smith (Lepidoptera). Unites States Department of Agriculture Technical Bulletin 1645: 228.

Troubridge JT (2008) A generic realignment of Oncocnemidini sensu Hodges (1983) (Lepidoptera: Noctuidae: Oncocnemidinae), with description of a new genus and 50 new species. Zootaxa 1903: 1–95. https://doi.org/10.11646/zootaxa.1903.1.1

VanDyk J, Sellers E, Bartlett T (2024) BugGuide - Identification, images, & information for insects, spiders & their kin for the United States & Canada. https://bugguide.net/ [accessed 4 June 2024]

Zahiri R, Lafontaine JD, Schmidt BC, deWaard JR, Zakharov EV, Hebert PDN (2014) A transcontinental challenge—A test of DNA barcode performance for 1,541 species of Canadian Noctuoidea (Lepidoptera). PLoS ONE 9(3): e92797. https://doi.org/10.1371/journal.pone.0092797

ZooKeys 1228: 225–273 (2025)
DOI: 10.3897/zookeys.1228.143007

Research Article

Centipedes (Myriapoda, Chilopoda) of Aldabra Atoll (Seychelles)

George Popovici[1,2], Gregory D. Edgecombe[3]

1 Department of Life Sciences, Imperial College London, London SW7 2AZ, UK
2 "Grigore Antipa" National Museum of Natural History, Pavel Dimitrievici Kiseleff St. 1, 011341, Bucharest, Romania
3 The Natural History Museum, Cromwell Road, London SW7 5BD, UK
Corresponding author: George Popovici (gp522@ic.ac.uk)

Abstract

Centipedes collected during Royal Society surveys of the arthropod fauna of the Aldabra Atoll in 1968–1975 are identified, described, and illustrated to provide the first checklist to the Aldabran centipede fauna, comprising 12 species. These newly include the lithobiomorph *Lamyctes tristani* (Pocock, 1893), the scolopendromorphs *Scolopendra morsitans* Linnaeus 1758, *Cryptops* cf. *japonicus* Takakuwa, 1934, *Cryptops mauritianus* Verhoeff, 1939, and *Cryptops nigropictus* Takakuwa, 1936, and the geophilomorphs *Ityphilus* cf. *taeniaformis* (Lawrence, 1960), *Mecistocephalus angusticeps* (Ribaut, 1914), *Mecistocephalus lohmanderi* Verhoeff, 1939, *Orphnaeus dekanius* Verhoeff, 1938, *Ribautia* cf. *paucipes* Attems, 1952, and *Tuoba sydneyensis* (Pocock, 1891). The geophilomorph genera *Hovanyx* Lawrence, 1960, **syn. nov.**, and *Mixophilus* Silvestri, 1929, **syn. nov.**, are revised in light of the examined material and hereby designated junior subjective synonyms of *Tuoba* Chamberlin, 1920 with the species *Geophilus lemuricus* Verhoeff, 1939, **syn. nov.**, and *Hovanyx waterloti* Lawrence, 1960, **syn. nov.**, designated as junior subjective synonyms of *T. sydneyensis*. The oryid genus *Nycternyssa* Crabill, 1959, **syn. nov.**, is revised and designated a junior subjective synonym of *Orphnaeus* Meinert, 1870. New data on intraspecific morphological variation are presented for *C. nigropictus*, with the validity of *Cryptops daszaki* Lewis, 2002 being questioned following examination of its type material. The affinities and possible origins of the Aldabran centipede fauna are found to be mainly East African, with several species occurring across other islands in the Western Indian Ocean.

Key words: Checklist, taxonomy, Western Indian Ocean

Academic editor: Pavel Stoev
Received: 28 November 2024
Accepted: 13 January 2025
Published: 21 February 2025

ZooBank: https://zoobank.org/3A5C895C-ACF6-4E44-BD53-6296E1F9EAB1

Citation: Popovici G, Edgecombe GD (2025) Centipedes (Myriapoda, Chilopoda) of Aldabra Atoll (Seychelles). ZooKeys 1228: 225–273. https://doi.org/10.3897/zookeys.1228.143007

Introduction

The Western Indian Ocean Islands, delimited at the north by Socotra and at the south by Madagascar, have been identified as a global biodiversity hotspot (Myers et al. 2000; Attorre and Van Damme 2020; Agnarsson et al. 2015). Although extremely variable in size, and geological origin and history, these islands harbour a terrestrial fauna notable for striking patterns of radiation and endemicity (Legros et al. 2020; Bergsten and Biström 2022; Sherlock et al. 2024). Despite being less intensively studied than their marine faunas, especially in smaller island groups, the terrestrial faunas of the Western Indian Ocean face significant risk of extinction due to the impacts of introduced species (Gerlach 2006; Griffiths and Florens 2006; Cheke 2010;

Hawlitschek et al. 2011) and habitat degradation (Haverkamp et al. 2017; Ibouroi et al. 2021). Smaller island groups can offer unique insights into understanding the patterns of colonisation and diversification in an area extensively shaped by eustatic changes (Camoin et al. 2004). The paleogeographic history of coral atolls in the Western Indian Ocean in particular has identified the present composition of terrestrial faunas on these islands as recent in origin (Austin et al. 2004; Agnarsson and Kuntner 2012; Steibl et al. 2024) and reflective of multiple colonisations from mainland populations and refugia (Nagy et al. 2003; Kehlmaier et al. 2023).

Aldabra Atoll is located in the Western Indian Ocean and has an area of approximately 155 km^2 and a maximum elevation of 8 m, being the second largest coral atoll in the world (Plummer 1995). It is composed of four main islands, Grand Terre (114 km^2), Malabar (26.5 km^2), Picard (9.28 km^2), and Polymnie (1.93 km^2), in addition to 40 small islets. The nearest large landmasses include the coast of Tanzania (640 km), the northern coast of Madagascar (425 km), Ngazidja (Comoros) (380 km), and Mahé (Seychelles) (1130 km). Palaeogeographical research on Aldabra has identified a complete submergence event during the last interglacial period, with any terrestrial fauna that had previously colonized the atoll having almost certainly disappeared approximately 125,000 years before the present (Warren et al. 2005). Re-emergence of a more permanent dry land area, together with signs of a terrestrial fauna including land snails is estimated to have occurred 118,000–80,000 years before the present, with continued fluctuations in the sea level exposing a dry land area twice as large as the current one ~ 27,000 years before the present. This was followed by dry land area reduction to its present condition after flooding of the inner lagoon ~ 5000 years before the present (Braithwaite et al. 1973; Hume et al. 2018). The faunal affinities of the Aldabra Atoll have been identified as predominantly East African, with general biogeographical patterns indicating dispersal and colonisation from continental East Africa, Madagascar, and the Seychelles (Cogan et al. 1971; Hill and Newbery 1982; Lawrence 2015), in contrast to the Mascarenes and Comoros, in which dispersal from Madagascar seemingly predominates (Agnarsson and Kuntner 2012). Given its young geological age and recent complete submergence, the fauna of Aldabra is comparatively less rich in endemic taxa than the granitic inner islands of the Seychelles (Agnarsson and Kuntner 2012).

Previous surveys of the centipede fauna of the Seychelles (Bonato and Minelli 2010; Lewis 2010b; Stoev and Gerlach 2010) have identified three species from Aldabra, *Australobius inflatitarsis* Eason, 1978, *Mecistocephalus angusticeps* (Ribaut, 1914), and *Tuoba sydneyensis* (Pocock, 1891). The threat level faced by endemic Myriapoda within the inner and outer islands of the Seychelles, including the Aldabra group, is significantly higher than the threat level faced by indigenous non-endemic (i.e., widespread) or introduced myriapods (Gerlach 2012). Observations on the natural history of large Scolopendromorpha in Mauritius and the Rodrigues provide circumstantial evidence on the vulnerability of island centipede populations to introduced predators (Lewis et al. 2010; Tercel et al. 2024).

We provide a comprehensive checklist and taxonomic revision of the centipedes from the Aldabra Atoll collected between 1968 and 1975 to provide historic baseline data to inform future conservation efforts of Aldabran terrestrial arthropods and shed light on the poorly known centipede fauna of the Western Indian Ocean.

Materials and methods

Morphological examination

Specimens were examined under a Nikon SMZ1270 stereomicroscope and a Leica DMR binocular microscope. Partial dissection was carried out as necessary according to the protocol outlined by Pereira (2000), with anatomical structures temporarily mounted in glycerol. Where necessary, specimens were cleared by temporary mounting in 80% lactic acid. Drawings were prepared with the aid of a camera lucida.

Specimen data

All specimens examined are part of the Myriapoda collection of the Natural History Museum, London (**NHMUK**). Collection data for a total of 181 specimens from the Aldabra Atoll are given in the Results section for each species. Sampling was undertaken in 1974 and 1975, apart from four specimens collected in 1968 and three from 1973. In addition to material collected from Aldabra, the following specimens have been examined, either as conspecifics from other geographic regions or for comparison to Aldabra samples:

Lamyctes tristani (Pocock, 1893)

NHMUK015626352, 2♀♀, Downtown, Diego Garcia, Chagos Archipelago, 7.263°S, 72.374°E, 26.06.2022, leg. W. Rabitsch, suction sampler; NHMUK015619670, 1♀, Diego Garcia, Chagos Archipelago, wetland site, 7.310°S, 72.419°E, 22.06.2022, leg. W. Rabitsch, suction sampler. NHMUK015087793, syntypes, Tristan da Cunha.

Ballophilus maldivensis Pocock, 1906

BMNH #200555, Chilo 1952-.12.11.102, 1 ♀ (holotype), Midu (މިޑޫ), Addu Atoll, Maldives, 1899–1900, Maldive-Laccadive Expedition 1899–1900.

Cryptops daszaki Lewis, 2002

1♂ (holotype, Spm. 1), Île aux Aigrettes, damp soil against wall of Warden's House, 19 October 1995, leg. S. J. Lewis. Spm 4 and 5, in soil under ebony litter, grid square E4, 18.10.1995, leg. J. G. E. Lewis.

Cryptops niloticus Lewis, 1967

BMNH(E)#200011 Chilo.1966.9.6.2, 1♀ (holotype), Blue Nile Bridge, Khartoum, Sudan, 28.09.1964, leg. J. G. E. Lewis, 1♂ (allotype), under stone, top of Nile Bank, Blue Nile Bridge, Khartoum, Sudan, 09.11.1962, leg. J. G. E. Lewis, BMNH(E) #200014 Chilo.1966.9.6.11, 1 juvenile (paratype), Blue Nile Bridge, Khartoum, Sudan, 09.11.1962.

Mecistocephalus glabridorsalis Attems, 1900

NHMUK015991408, 2 specimens, Serpent Island, Mauritius, 04.11.1995, leg. P. Daszak & J. Cottingham.

Orphnaeus brevilabiatus (Newport, 1845)

NHMUK015991423, 1♀, S. (South) Tenasserim (Great Tenasserim River, Myanmar), BM1889.7.15.73–4, leg. E. W. Oates; NHMUK015991422, 1♂, Rangoon (Yangon, Myanmar), BM1889.7.15.73–4, leg. E. W. Oates; NHMUK015991420, 1♀, Singapore, 18.10.1898, 98.10.18.53–55, leg. H. N. Hidley; NHMUK015991421, 1♀, Takhamen, Siam (Tak province, Thailand), 1897.9.7.34, leg. S. S. Flower; NHMUK015991412, 1♂2♀♀, Agraky Hills, Yemen, leg. G. W. Berry.

Orphnaeus dekanius Verhoeff, 1938

NHMUK015991413, 1♀, Ratnapura, Ceylon (Ratnapura, Sri Lanka), 19.08.1892, 92.8.19.6; NHMUK015991414, 1♂, Pundulaya, Ceylon (Pundaluoya, Sri Lanka), 13.12.1899, 1899.12.13.42; NHMUK015991415, 1♀, Nundulaya, Ceylon (Nuwara Eliya, Sri Lanka), 13.12.1899, 99.12.13.41; NHMUK015991416, 1♀, Ceylon (Sri Lanka), 88.55; NHMUK015991417, 2♂♂1♀, Singapore, 18.10.1898, 98.10.18.53–55, leg. H. N. Hidley; NHMUK015991418, 1♂1♀, Singapore, leg. H. N. Hidley; NHMUK015991419, 1♂, Kenurus, Maldives, 1951.12.11.100, Maldive-Laccadive Expedition 1899–1900.

Ribautia cf. *paucipes* Attems, 1952

NHMUK015991409, 1 specimen, fine soil overhanging rock surface, Coin de Mire, Mauritius, 19°56.5'S, 57°37'E, 27.10.1995, leg. J. G. E. Lewis & S. J. Lewis.

Tuoba sydneyensis (Pocock, 1891)

NHMUK015991411, 3♂♂3♀♀, under slabs of tuff rock, Serpent Island, Mauritius, 04.11.1995, P. Daszak & J. Cottingham.

Results

Checklist

Order Lithobiomorpha
Family Henicopidae
Genus *Lamyctes* Meinert, 1868

***Lamyctes tristani* (Pocock, 1893)**
Fig. 1

Examined material. 41 specimens: NHMUK015991449, 1♀, Cinq Cases, 16.03.1974; NHMUK015991450, 2♀, Malabar, 14.02.1975; NHMUK015991451

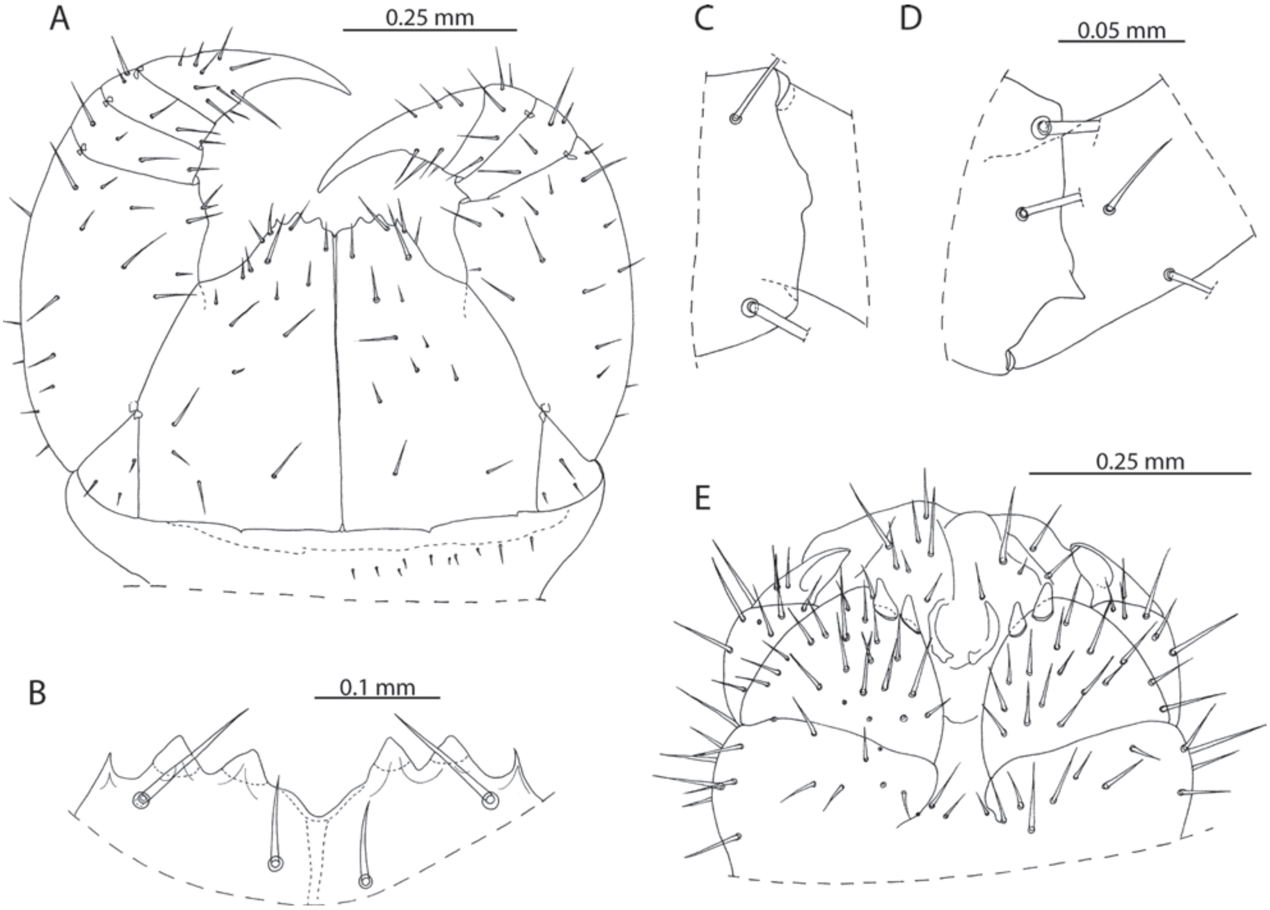

Figure 1. *Lamyctes tristani* (Pocock, 1893) **A, B, D** NHMUK015991452 **A** forcipular segment, ventral view **B** anterior margin of forcipular coxosternite, ventral view **C** NHMUK015991458, distal end of tibia of leg pair 12, lateral view **D** distal end of tibia of leg pair 12, lateral view **E** NHMUK015991456, Female gonopods, ventral view.

1♀, Picard, 28.02.1975; NHMUK015991452, 3♀, 1 juvenile, Cinq Cases B. F., 20.03.1974; NHMUK015991453, 2♀, Picard, 23.02.1974; NHMUK015991454, 2♀, Cinq Cases, 24.03.1974; NHMUK015991458, 3♀, Malabar, 08.06.1974; NHMUK015991455, 1♀, 1 juvenile, Aldabra, 30.01.1975; NHMUK015991456, 21♀, Picard, Summer 1975, leg. V. W. Spaull; NHMUK015991457, 2♀, 1 juvenile, Ochna litter, Cinq Cases B. F., 23.03.1974.

Remarks. The 38 specimens from the Aldabra Atoll (from Cinq Cases, Malabar, and Picard) for which sex can reliably be determined are all females, such that the population is parthenogenetic. They are likely conspecific with *L. tristani* as described from the Chagos Archipelago (Popovici et al. 2024), sharing the distinctly reduced spinous process on the tibia of leg pair 12, often taking the form of a rounded bump (Fig. 1C). The stability of this character is however uncertain as specimens from localities in the Aldabra Atoll exhibit conspicuous variation in the shape of the process (Fig. 1D, Table 1). Additional similarities between these two populations include the morphology of the forcipular coxosternite (Fig. 1A, B), the number of antennal articles, and the number and shape of the spurs on the female gonopods (Fig. 1E). Variability in the characters of antennal article number, number, and distribution of coxal pores and shape of the distal spinous process on the tibia of leg pair 12 are listed in Table 1 and compared with putatively conspecific individuals from the Chagos Archipelago, excluding anamorphic stages.

Table 1. Morphological variability of putative *L. tristani* specimens from Western Indian Ocean localities. Asterisk indicating regenerated appendage.

Locality	Body length (mm)	Antennal article number	Coxal pore formula (legs 12/12 – 13/13 – 14/14 – 15/15)	Shape of tibial spinous process on leg pair 12
Cinq Cases (Aldabra)	3.5	20	1/1 – 1/1 – 1/1 – 1/1	Rounded bump
Cinq Cases (Aldabra)	4	20	1/1 – 1/1 – 1/1 – 1/1	Rounded bump
Cinq Cases (Aldabra)	5	17	2/2 – 2/2 – 3/3 – 2/2	Acuminate, minute
Cinq Cases (Aldabra)	5	22	3/3 – 3/3 – 3/3 – 2/2	Acuminate, minute
Cinq Cases (Aldabra)	5	-	2/2 – 3/3 – 3/3 – 2/2	-
Cinq Cases (Aldabra)	5	22	2/2 – 3/3 – 3/3 – 2/2	Rounded bump
Cinq Cases (Aldabra)	6	23	3/3 – 3/3 – 3/3 – 3/3	Acuminate, minute
Malabar (Aldabra)	5.5	24	2/2 – 2/2 – 3/3 – 2/2	-
Malabar (Aldabra)	5.5	24	2/2 – 2/2 – 3/3 – 2/2	Rounded bump
Malabar (Aldabra)	6	(23)24	2/2 – 2/2 – 2/3 – 2/2	Rounded bump
Malabar (Aldabra)	6	15(20)	3/3 – 3/3 – 3/3 – 3/3	Asymmetrical, rounded bump on left tibia, acuminate spur on right tibia
Malabar (Aldabra)	6	24	3/3 – 3/3 – 3/3 – 3/3	-
Picard (Aldabra)	3.5	19	1/1 – 1/1 – 1/1 – 1/1	Rounded bump
Picard (Aldabra)	3.5	20	1/1 – 1/1 – 1/1 – 1/1	Rounded bump
Picard (Aldabra)	3.5	20	1/1 – 1/1 – 1/1 – 1/1	Rounded bump
Picard (Aldabra)	4	20	1/1 – 1/1 – 1/1 – 1/1	Rounded bump
Picard (Aldabra)	4	20	1/1 – 1/1 – 1/1 – 1/1	Rounded bump
Picard (Aldabra)	4	20	1/1 – 1/1 – 1/1 – 1/1	Rounded bump
Picard (Aldabra)	4	20	1/1 – 1/1 – 1/1 – 1/1	Rounded bump
Picard (Aldabra)	4	21	2/2 – 2/2 – 2/2 – 1/1	Rounded bump
Picard (Aldabra)	4	21	2/2 – 2/2 – 2/2 – 1/1	Rounded bump
Picard (Aldabra)	4	20	1/1 – 1/1 – 1/1 – 1/1	-
Picard (Aldabra)	4.5	24	2/2 – 2/2 – 3/3 – 2/2	Acuminate, minute
Picard (Aldabra)	4.5	(22)23	2/2 – 2/2 – 3/3 – 2/2	Rounded bump
Picard (Aldabra)	4.5	21	1/1 – 2/2 – 2/2 – 2/2	-
Picard (Aldabra)	5	(24)25	2/2 – 2/2 – 2/2 – 2/2	Rounded bump
Picard (Aldabra)	5	(22)23	3/3 – 3/3 – 3/3 – 2/2	Acuminate, minute
Picard (Aldabra)	5	15*	3/3 – 3/3 – 3/3 – 2/2	Acuminate, minute
Picard (Aldabra)	5	24	2/2 – 3/3 – 3/3 – 2/2	Acuminate, minute
Picard (Aldabra)	5	(21)24	2/2 – 3/3 – 3/3 – 2/2	Acuminate, minute
Picard (Aldabra)	5	-	2/2 – 3/3 – 3/3 – 2/2	Acuminate, minute
Picard (Aldabra)	5	24	2/2 – 3/3 – 3/3 – 2/2	Acuminate, minute
Picard (Aldabra)	5	20	2/2 – 2/2 – 3/3 – 2/2	Rounded bump
Picard (Aldabra)	5.5	24	3/3 – 3/3 – 3/3 – 3/3	Acuminate, minute
Picard (Aldabra)	6	24	3/3 – 3/3 – 3/3 – 3/3	Acuminate, reduced in size
Picard (Aldabra)	7	(24)25	3/3 – 3/3 – 3/3 – 3/3	Acuminate, reduced in size
Diego Garcia (Chagos)	6	27	3/3 – 3/3 – 3/3 – 3/3	Rounded bump
Diego Garcia (Chagos)	6.2	(18)20	3/3 – 3/3 – 3/3 – 3/3	Rounded bump
Diego Garcia (Chagos)	6.5	(21)24	3/3 – 3/3 – 3/4 – 4/4	Rounded bump

Order Scolopendromorpha
Family Cryptopidae
Genus *Cryptops* Leach, 1815

Cryptops cf. *japonicus* Takakuwa, 1934
Fig. 2

Examined material. 35 specimens: NHMUK015991425, 4 specimens, Black Path, Picard, Summer 1975, leg. V. W. Spaull; NHMUK015991429, 1 specimen,

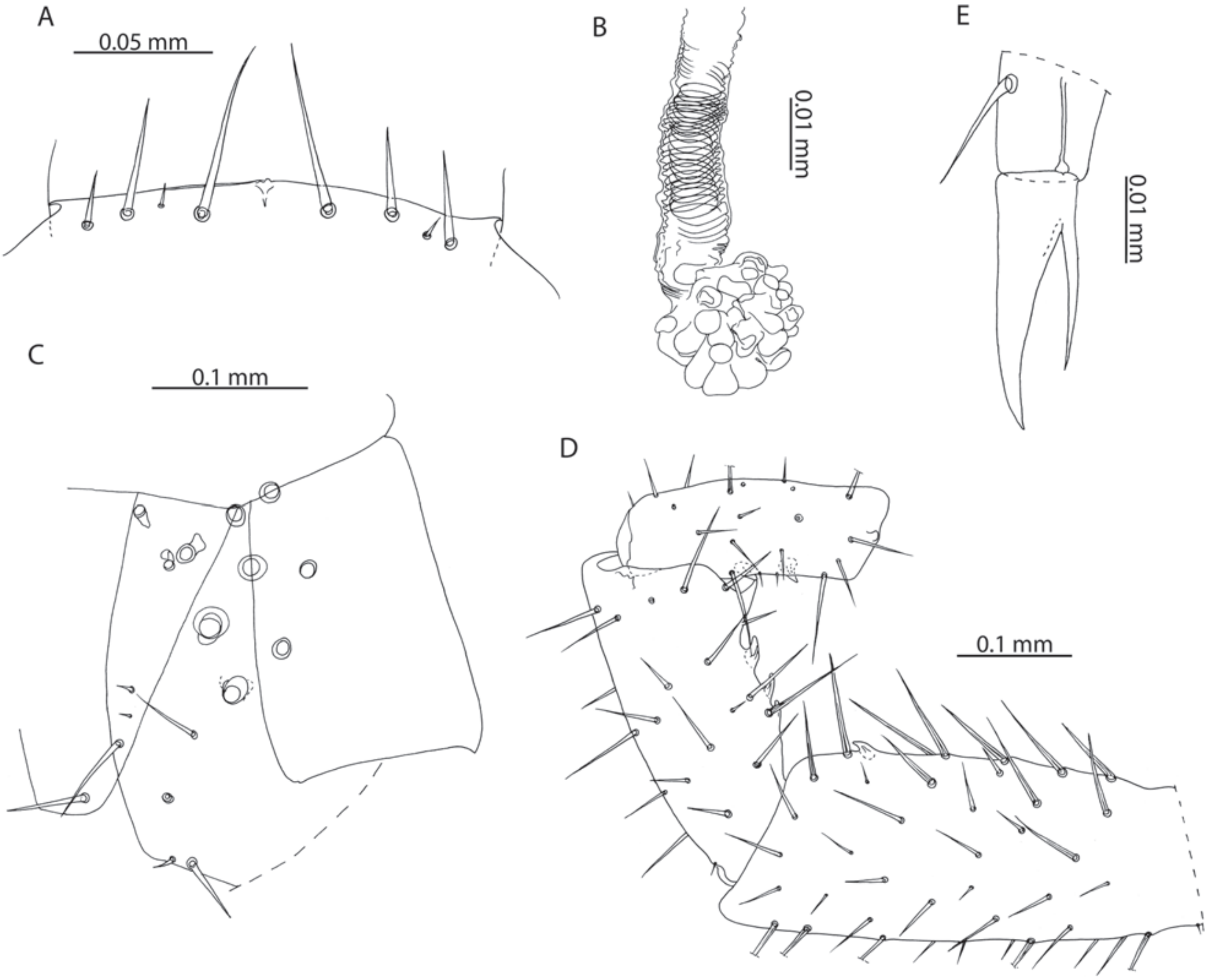

Figure 2. *Cryptops* cf. *japonicus* Takakuwa, 1934 **A, B, D** NHMUK015991433 **A** anterior margin of forcipular coxosternite, ventral view **B** Calyx of venom gland, lateral view **C** NHMUK015991430, coxopleuron of ultimate leg-bearing segment, lateral view **D** femur, tibia, and tarsus 1 of ultimate leg telopodite, lateral view **E**. NHMUK015991429, pretarsus of leg pair 8, lateral view.

Aldabra, 10.11.1973; NHMUK015991430, 6 specimens, Point Hodoul, Grande Terre, 22.03.1974; NHMUK015991431, 2 specimens, Ile. Malabar, 08.06.1974; NHMUK015991432, 18 specimens, *Casuarina* and *Sideroxylon* litter, Anse Cedres, 12.02.1974; NHMUK015991433, 4 specimens, Esprit, 14.12.1974.

Remarks. *Cryptops* cf. *japonicus* collected in Aldabra is an unexpected occurrence for a species otherwise restricted to localities in southern Japan, the Korean peninsula, Manchuria (Takakuwa 1936) and Taiwan (Chao 2008). Despite the description of the morphologically similar *C. doriae* Pocock, 1891 from nearby localities in the Seychelles (Lewis 2007a), consistent diagnostic morphological characters separate these two populations. Most prominently, specimens from Aldabra only have one pretarsal accessory spur on legs 1–20, > 1/2 the length of the pretarsus (Fig. 2E), in contrast to *C. doriae* from the Seychelles which has been described with two generally subequal, conspicuous, accessory spurs that are much shorter relative to the pretarsus, on the same leg pair range (Lewis 2007a). The examined specimens agree with the description provided by Chao (2008) based on specimens collected in Taiwan, in which he notes the low number of coxopleural pores (9) in the immature ("larva") stages, which overlaps with the condition of Aldabra specimens (Fig. 2C), the presence of 4 setae along the anterior margin of the forcipular coxosternite (Fig. 2A), and the ovoid shape of the calyx of the venom gland (Fig. 2B).

All specimens from Aldabra Atoll range from 3–10 mm and exhibit several traits characteristic of juvenile specimens including reduced number of pores on the coxopleuron, indistinct paramedian sutures on tergites, and a reduced number of tibial and tarsal saw teeth (Fig. 2D). Following clearing, no spermatozoa or oocytes could be observed in the posterior trunk of specimens. Without additional sampling to confirm the condition of adult specimens it is not possible to comment on the presence or absence of sexually mature adults in the present sample. Introduced populations of *C. doriae* have been described bearing similar neotenic characteristics (reduced body size, number of coxal pores, number of saw teeth), even in sexually mature adults (Lewis 2007b), potentially explaining the morphology of the Aldabra specimens in light of possible introduction to the atoll. Nevertheless, in the absence of additional material and molecular data, our assignment to *Cryptops japonicus* is only tentative. The status and relationships of different populations identified as *C. doriae* and related taxa remains to be clarified.

Cryptops mauritianus **Verhoeff, 1939**
Fig. 3

Examined material. NHMUK015991434, 1 specimen, *Sideroxylon* litter, Anses Coco & Porche, Aldabra, 03.12.1974, V. W. Spaull. leg.

Remarks. *Cryptops mauritianus* has been described by Verhoeff (1939) from Mauritius. Subsequent taxonomic revision of Mauritian *Cryptops* species (Lewis 2002) completed the summary original description and provided additional illustrations of material from near the type locality. In the singular Aldabra specimen examined, the presence of minute accessory spurs on the pretarsus of leg pairs 1–20 (Fig. 3G) clearly delimits it from all other *Cryptops* species known from localities in the Western Indian Ocean (Lewis 2011). Subsequent re-description by Lewis (2002) provided data on an immature (“adolescens”) specimen which matches the condition of the material presently examined (body length 8 mm), allowing us to confidently refer it to *C. mauritianus*.

Cryptops nigropictus **Takakuwa, 1936**
Fig. 4

Examined material. 12 specimens: NHMUK015991424, 3 specimens, Black Path, Picard, Aldabra, Summer 1975; NHMUK015991426, 3 specimens, *Calophyllum* litter, Takamaka, Grande Terre, 14.01.1975; NHMUK015991427, 2 specimens, *Sideroxylon* litter, Au Parc, Aldabra, 14.02.1975. V. W. Spaull leg; NHMUK015991428, 1 specimen, Picard, Aldabra, 28.02.1975; NHMUK015991445, 1 specimen, *Sideroxylon* litter, Ile. Michel, Aldabra, 28.03.1975; NHMUK015991446, 2 specimens, *Casuarina* litter, Picard, Aldabra, 08.05.1974.

Remarks. Taxonomic revision of *Cryptops* species belonging to the “*hortensis* group” identified *C. decoratus* Lawrence, 1960, *C. melanotypus* Chamberlin, 1941, and *C. nigropictus* Takakuwa, 1936 as a potential species complex, raising doubts on the taxonomic validity of many morpholog-

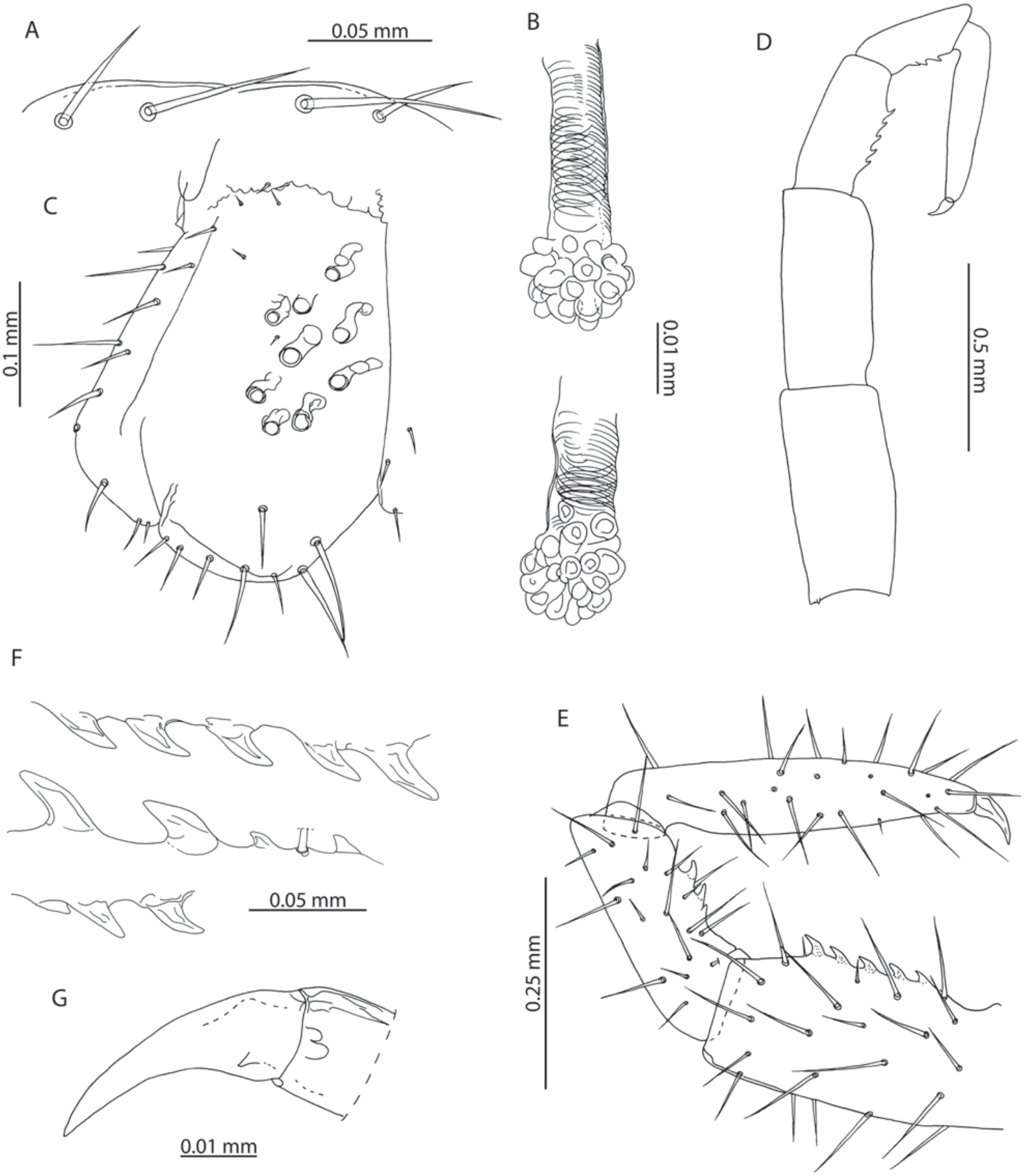

Figure 3. *Cryptops mauritianus* Verhoeff, 1939. NHMUK015991434 **A** anterior margin of forcipular coxosternite, ventral view **B** calyx of venom gland. Left forcipule (top), right forcipule (bottom) **C** coxopleuron of ultimate leg-bearing segment, lateral view **D** Ultimate leg telopodite, lateral view **E** tibia and tarsal articles of ultimate leg, lateral view **F** tibial comb (top), tarsal comb of left ultimate leg (middle), tarsal comb of right ultimate leg (bottom) **G** pretarsus of leg pair 18, lateral view.

ically similar species (Lewis 2011). A reliable diagnostic trait mentioned by Lewis (2011) is the presence of a single long pretarsal accessory spur in *C. nigropictus* (Fig. 4K), differentiating it from *C. decoratus* and *C. melanotypus* which bear two small pretarsal accessory spurs on leg pairs 1–20. The Aldabra specimens key out to *C. nigropictus* in the key provided within the

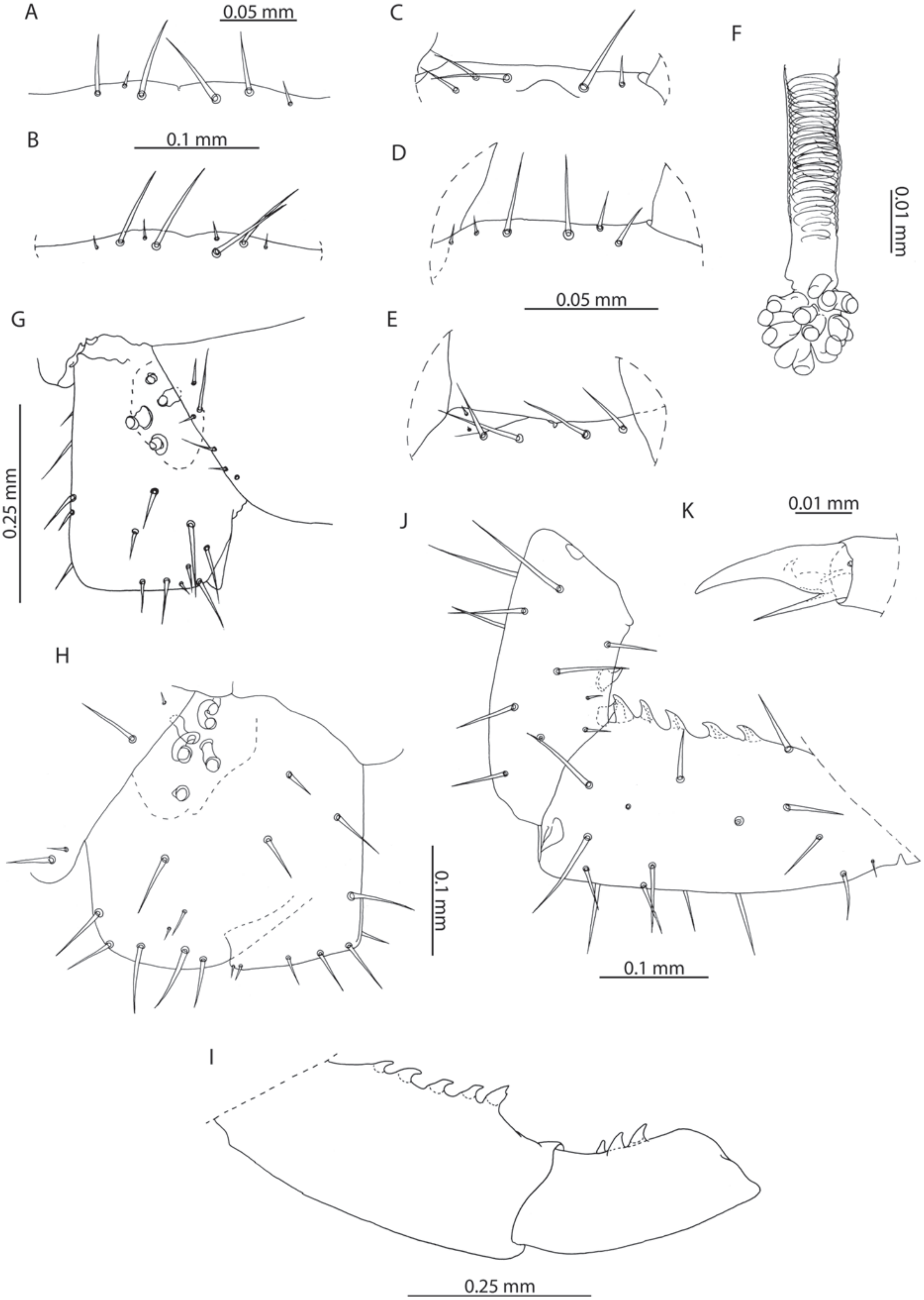

Figure 4. *Cryptops nigropictus* Takakuwa, 1936 **A, F, K, I, B** NHMUK015991426 **H, J** NHMUK015991446 **G** NHMUK015991424 **C** "*Cryptops daszaki*" holotype, Île aux Aigrettes, 19.10.1995 **D, E** paratype, Île aux Aigrettes, 18.10.1995 **A, B, C, D, E** anterior margin of forcipular coxosternite, ventral view **F** calyx of venom gland, lateral view **G, H** coxopleuron of ultimate leg-bearing segment, lateral view **I, J** tibia and tarsus of ultimate leg telopodite, lateral view **K** pretarsus of leg pair 8, lateral view.

same article and agree with its revised description. Although originally described from East Asia, various nominal taxa recorded from East Africa and islands of the Indian Ocean (including Mauritius and Rodrigues) have been placed in synonymy with *C. nigropictus* (Lewis 2011).

Cryptops daszaki Lewis, 2002 was described from several localities in Mauritius. Lewis (2002) remarked on the small body size (4.5–7.5 mm) of sexually mature specimens and their apparent juvenile characteristics (low number of coxal pores, reduced setation). The specimens collected from Aldabra with a similar body length to specimens assigned by Lewis to *C. daszaki* overlap in morphology with respect to the usual lack of subcuticular dark pigment, the number of setae on the anterior margin of the forcipular coxosternite (2 or 3 on each side in *C. daszaki*, 3 or 4 on each side in *C. nigropictus*; Fig. 4C versus Fig. 4A, B, D, respectively), the relative length of the single pretarsal accessory spur on legs 1–20 (> 1/2 the length of the pretarsus) and the number of coxal pores (5 or 6 in *C. daszaki*, 4–9 in *C. nigropictus*) but show greater variation than *C. daszaki* in the number of saw teeth on the tibia (3–5) and tarsus (2 or 3). The number of tibial and tarsal saw teeth is known to be intraspecifically variable in *Cryptops* (Iorio and Geoffroy 2003; Lewis 2009) and scales allometrically with body size, as exemplified by the largest *C. nigropictus* specimen in our sample (12 mm, NHMUK015991426; Fig. 4I).

The only other diagnostic trait given by Lewis (2011) separating *C. daszaki* and *C. nigropictus* is the position of the setae near the anterior margin of the forcipular coxosternite, being described as “marginal” in *C. daszaki* and “submarginal” in *C. nigropictus*. Re-examination of the type specimens of *C. daszaki* revealed that these setae occupy a submarginal position (Fig. 4C), which may be misinterpreted as marginal depending on the orientation of the specimens. As both of the two putative diagnostic traits separating *C. daszaki* and *C. nigropictus* are fully encompassed by intraspecific variation within *C. nigropictus* and the latter species has been recorded from nearby localities (Lewis 2002), we consider *C. daszaki* a likely junior subjective synonym of *C. nigropictus*, from which it cannot be reliably distinguished by morphology alone. Similarly, the presence of subcuticular dark pigment cannot be reliably used to separate putative *Cryptops* species in Western Indian Ocean and Eastern African localities. This character is variable within our sample, with all specimens with the exception of NHMUK015991428 lacking dark subcuticular pigment. Dark pigmentation is also variable in the type specimens of *Cryptops niloticus* Lewis, 1967 (present in male allotype but absent in female holotype and in juvenile paratype), a species previously recorded from the Western Indian Ocean (Lewis 2002) but subsequently synonymised with *C. nigropictus* (Lewis 2011).

Family Scolopendridae
Genus *Scolopendra* Linnaeus, 1758

Scolopendra morsitans Linnaeus, 1758

Examined material. 52 specimens: NHMUK015991435, 33 juveniles; *Casuarina* litter, Picard, Aldabra, 18.04.1974, leg. V. W. Spaull; NHMUK015991436, 1 specimen, *Casuarina*, Picard, Aldabra, 04.02.1974; NHMUK015991437, 1 specimen, *Ochna* soil, Picard, Aldabra, 15.02.1974; NHMUK015991438; 2 specimens, mixed scrub, Picard, 24.12.1974; NHMUK015991439, 1 specimen, *Thespesia* litter, Cinq Cases, Aldabra, 15.11.1973; NHMUK015991441, 5 specimens, Black Path, Picard, 1975; NHMUK015991442, 1 specimen, Picard, 03.12.1973; NHMUK015991443, 1 specimen, Picard, 18.01.1974; NHMUK015991440, 4 specimens, Picard, 18.11.1974; NHMUK015991444, 1 specimen, Pitfall trap 5, 08.12.1974; NHMUK015991447, 1 specimen, South Island, Aldabra, 13–20.03.1968, leg. B. Cogan & A. Hutson; NHMUK015991448, 1 specimen, Ile. Michel, 02.1968, leg. B. Cogan & A. Hutson.

Remarks. Specimens of *S. morsitans* Linnaeus, 1758 collected from mainland Africa, originally identified as *Scolopendra amazonica* Bücherl, 1946 overlap with the specimens from the Aldabra Atoll in several characters (Table 2) (Lewis 1966, 1967, 1968, 1969), but generally have a greater number of glabrous basal antennal articles, a character in which specimens from the Aldabra Atoll more closely match Indian specimens of *S. morsitans* previously assigned to *S. amazonica* (Jangi 1955, 1959). In the absence of newly collected material from which molecular data can be collected to evaluate possible interspecific delimitation between different population of *S. morsitans*, we assign material collected in the Aldabra Atoll to *S. morsitans*, following the conclusions on interspecific variation within this taxon reached by Würmli (1975). Subsequent phylogenetic analyses of molecular data for *S. morsitans* identified multiple lineages within this taxon (Joshi and Karanth 2011; Siriwut et al. 2016), potentially indicating the existence of a cryptic species complex as suggested by recent taxonomic review (Lewis 2010a). Until the global taxonomy of *S. morsitans* is interrogated using molecular data to establish if this is the case, we classify the examined material as *S. morsitans*.

Additionally, specimens were compared to the original description of the morphologically similar and geographically proximate *Scolopendra antananarivoensis* Kronmüller, 2010. Material from the Aldabra Atoll did not exhibit the characters given as diagnostic for *S. antananarivoensis*, lacking a longitudinal median depression on sternite 21 and not having a distinctly more elongate coxopleural process (Kronmüller 2010).

Table 2. Morphological variability in *Scolopendra morsitans* populations obtained from literature data (Lewis 1966, 1967, 1969) and examined specimens.

Character	***Scolopendra morsitans*** **(India)**	***Scolopendra amazonica*** **sensu Jangi (=** ***Scolopendra morsitans*****) (India)**	***Scolopendra amazonica*** **sensu Lewis (=** ***Scolopendra morsitans*****) (Africa)**	***Scolopendra morsitans*** **(Aldabra)**
Subadult and adult body length (mm)	18–113	15–65	13–100	13–78
Number of antennal articles	20	19	18–21	(17)18–19
Number of glabrous antennal articles	Can be > 6	≤ 6	5–7	(3.5)4
Complete paramedian sutures begin	Mostly T3	Mostly T2	TT2–4	T3
Lateral margination	May begin more anteriorly	Generally last 5 tergites	Last 2–15 tergites	Last 4–10 tergites
Coxopleural process spines	5	4	2–6	(3)4–5
Lateral coxopleural spine	Present	Present or absent	Present or absent	Present
Leg 20 tarsal spur	Present	Absent	Absent	Absent

Order Geophilomorpha
Family Geophilidae
Genus Ribautia Brölemann, 1909

Ribautia cf. *paucipes* Attems, 1952
Fig. 5

Examined material. NHMUK015991467, 1 juvenile, *Casuarina* litter, Picard, Aldabra, 10.12.1974, leg. V. W. Spaull.

Remarks. The sexually immature specimen found in the present sample displays all diagnostic characters that support its assignment to *Ribautia*, comprising an elongate cephalic shield, lack of lappets on the first maxillae, the two halves of the second maxillary coxosternite being united by a sclerotised isthmus and the pleural sutures of the forcipular coxosternite being parallel to its lateral edge distally. A potentially novel ontogenetic observation is the incomplete separation of the two halves of the second maxillary coxosternite by an isthmus (Fig. 5B), as is a characteristic of *Ribautia*. Taking into account the very small size (length 7 mm) and sexual immaturity of the specimen, this may be a character state that becomes more conspicuous in older individuals.

Beside the very low number of leg-bearing segments (37), which is shared with *R*. cf. *paucipes* reported from the Seychelles (Bonato and Minelli 2010), the developmental stage of the present specimen does not allow for satisfactory evaluation of potential morphological differences between

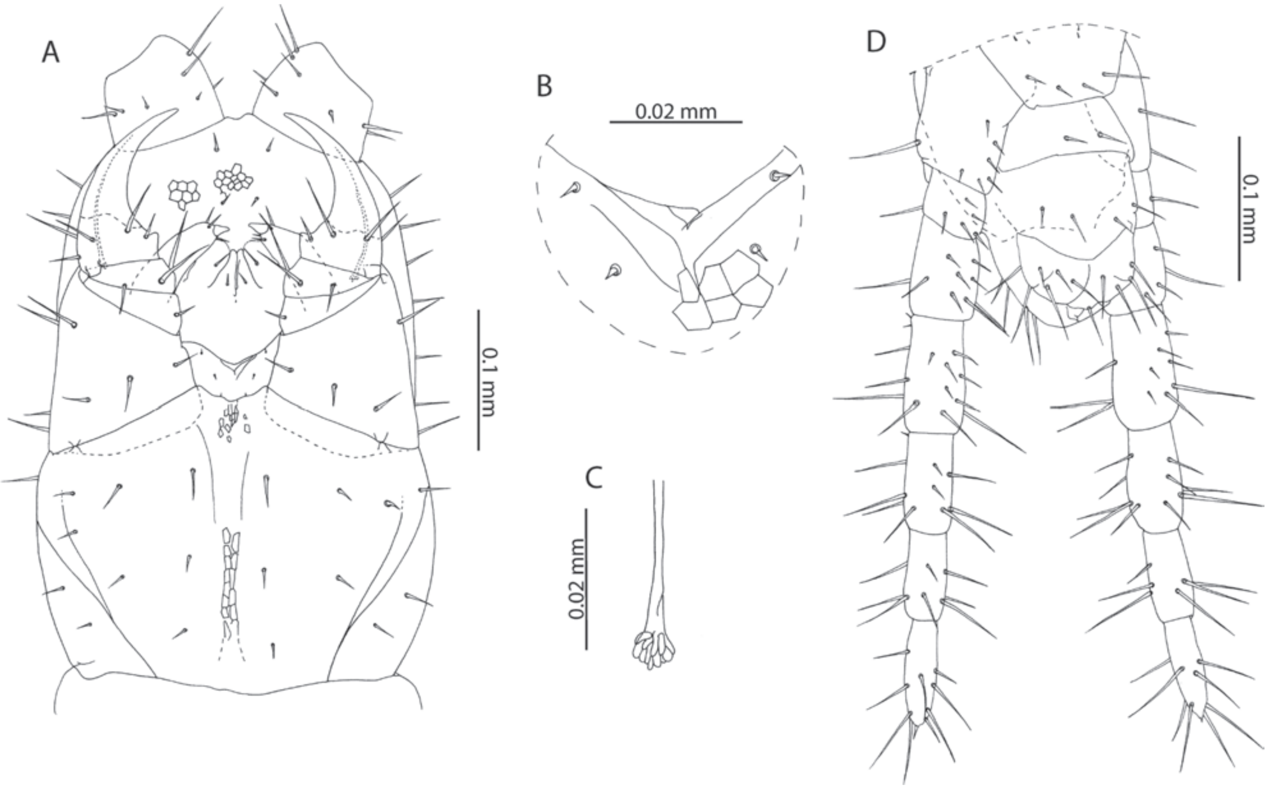

Figure 5. *Ribautia* cf. *paucipes* Attems, 1952. NHMUK015991467 **A** head and forcipular segment, ventral view **B** anterior margin of second maxillary coxosternite, ventral view **C** calyx of venom gland, lateral view **D** ultimate leg-bearing and postpedal segments, ventral view.

Ribautia specimens described from Western Indian Ocean localities and type material of *Ribautia paucipes* described from the environs of Lake Kivu in Central Africa. Notably, the Aldabra specimen lacks evident denticles on the anterior margin of the forcipular coxosternite and the interior margin of the forcipular trochanteroprefemur, although these are clearly illustrated in the original description of *R. paucipes* (Attems 1952: fig. 203). The specimen also lacks conspicuous coxal organs or coxal pores, a character state not noted in *R.* cf. *paucipes* recorded from the Seychelles. Ontogenetic variation in the number of coxal pores has been well-documented for other geophilid centipedes (Horneland and Meidell 2009; Gregory and Barber 2010; Brena 2014; Stojanović et al. 2020), increasing with body size at each postembryonic stage, and being absent in comparably sized adolescens stages of some species (Gregory and Barber 2010). Additionally, the second maxillary pretarsus of the present specimen is markedly shorter and less acuminate than illustrated for *R. paucipes* from continental Africa. As the ontogenetic variation of the morphology of the second maxillae in *Ribautia* is not presently known and in other characters the specimen strongly resembles individuals described from the Seychelles, we maintain its presently assigned identity.

Genus *Tuoba* Chamberlin, 1920
Hovanyx Lawrence, 1960, syn. nov.

Mixophilus Silvestri, 1929, syn. nov.

Remarks. The monotypic genus *Mixophilus* was erected by Silvestri (1929) to place a new species of geophilomorph sampled from riparian sites in Madras (Chennai), Southern India. The original description of *Mixophilus indicus* includes illustrations of the head, forcipular apparatus and ultimate leg-bearing segment as well as detailed ecological observations concerning its preferred microhabitats in the type locality. Subsequent physiological investigations revealed a modified tracheal system, comprising possible adaptations to immersion for long periods of time (Rajulu 1970). An affinity to *Henia* and *Chaetechelyne* (Dignathodontidae) was suggested, however, within the same section Silvestri (1929) pointed to differences between *Mixophilus* and both of these genera in “the structure of the labrum” (tripartite in *M. indicus* but unipartite in Dignathodontidae), “the distribution of sternal pores” (transverse band in *M. indicus*, medial sub-circular/elliptical field in Dignathodontidae), in the last leg-bearing segment (telopodite composed of 7 articles in *M. indicus* but 6 in *Henia*), and in the elongation of the forcipular pretergite (longer in *M. indicus* than in *Chaetechelyne*). The structure of the labrum described and illustrated for *M. indicus*, comprising three conspicuous pieces, suggests a close affinity to other members of Geophilidae s. str. An estuarine habitat preference and multiple morphological characters show a near complete overlap between the diagnoses of *Tuoba* and *Mixophilus* (Table 3). Complete chitin lines in *M. indicus* may indicate intraspecific or interspecific variability which has been recorded in *Tuoba* (Jones 1998) or artifacts of examination under light microscopy. In light of this re-evaluation of its original description, we propose reassignment of *M. indicus* to *Tuoba* considering the available data on its morphology, with *Tuoba indica* comb. nov. as the valid name for specimens on which its original

Table 3. Taxonomically informative invariant and variable morphological characters for the genera *Hovanyx*, *Mixophilus*, and *Tuoba* based on literature data. Characters in boldface represent putative morphological differences.

Character	*Tuoba* Chamberlin, 1920	*Hovanyx* Lawrence, 1960	*Mixophilus* Silvestri, 1929
Head shape	Subquadrate	**Longer than wide**	Subquadrate
Setation of clypeus	Three pairs of setae medially, flanked by a group of 2–4 setae on each side	10–11 setae	Four pairs of setae medially, flanked by a group of 3 or 4 setae on each side
Medial piece of labrum. Orientation of tubercles	Anteriorly recurved (variable)	Anteriorly recurved	Anteriorly recurved
Side pieces of labrum	With variable number of tubercles or plumose setae	-	Without tubercles or plumose setae
Maxillae I lappets	Absent. External corners with spiniform cuticular projections	Absent. External corners with spiniform cuticular projections	Absent
Maxillae II pretarsus	Simple, claw-shaped. Variably reduced in size	**Simple, claw-shaped**	Simple, claw-shaped. Reduced in size
Forcipular coxosternite chitin lines	Complete or nearly complete	Vanishing before reaching the condyles	Complete
Denticle at the base of the tarsungulum	Present	Present	Present
Carpophagus structures	**Present**	-	-
Metasternal pore field shape	Transverse band	Transverse band. Divides on LBS XI–XII	Transverse band (medially constricted)
Pretarsus of walking legs	Distinctly elongate	Distinctly elongate	Distinctly elongate
LLBS metasternite shape	Wider than long, trapezoidal	Wider than long, trapezoidal	Wider than long, trapezoidal
Coxal organs	Multiple opening in single pit	**Absent**	Multiple opening in single pit
LLBS pretarsus	Simple, claw-shaped	Simple, claw-shaped	Simple, claw-shaped

description was based. Consequently, we propose that *Mixophilus* is the junior subjective synonym of *Tuoba* syn. nov. Similarities between *Tuoba indica* comb. nov. and *T. sydneyensis* exist in elongation of the ultimate legs and reduction of the second maxillary pretarsus, however these characters are shared by several species of *Tuoba*. The incomplete original description provided by Silvestri does not allow for definitive assignment of *Tuoba indica* comb. nov. to another species of *Tuoba* until the type material can be adequately re-described.

Similarly, the genus *Hovanyx* was erected for the species *Hovanyx waterloti*, described in Lawrence's (1960) catalogue of Malagasy centipedes. An affinity to Dignathodontidae was again proposed based on similarities in the structure of the labrum, originally described for *H. waterloti* as composed of a single piece and bearing a small number of rudimentary, anteriorly oriented tubercles ("Labre […] à dents pas très distinctes, quatre courtes dents triangulaires dirigées vers l'avant, de chaque côté."). The diagnosis of *Hovanyx* singled out the absence of coxal organs ("[…] diffère de tous les autres membres de la sous-famille des Dignathodontinæ par l'absence de pores aux pattes terminales.") as the main distinguishing trait separating it from all other dignathodontid genera. However, both the original description and accompanying illustrations suggest a closer affinity to Geophilidae s. str., as multiple other morphological characters (shape of head, forcipular coxosternite, metasternal pore fields) are characteristic of the Geophilidae rather than the Dignathodontidae, and subsequent taxonomic revision of both families placed *Hovanyx* under Geophilidae (Bonato 2011). Furthermore, the incomplete original description overlaps almost entirely with that of *T. sydneyensis*, a wide-ranging geophilid encountered in littoral sites in the Seychelles (Bonato and Minelli 2010) and the Aldabra

Atoll (present records) close to the type locality of *H. waterloti*. Shared characters include range of leg bearing segment number (41–43), morphology of the labrum, condition of chitin lines on the forcipular coxosternite (incomplete) (Table 3). The only putative differences between *H. waterloti* and *T. sydneyensis* are the unipartite labrum and absence of coxal organs in the former (Table 3). These may however be unreliable characters because of inadequate documentation, as published illustrations of *Tuoba* specimens and the material here illustrated show great variability in the orientation and shape of the labral pieces, which depending on the degree of sclerotization seen in the specimen and shape and number of denticles on the side pieces, may resemble the labrum of Dignathodontidae under light microscopy. The absence of coxal organs has not been previously reported in any species of *Tuoba*, however this character shows extensive ontogenetic plasticity within Geophilidae (Horneland and Meidell 2009; Gregory and Barber 2010; Tuf and Dányi 2015; Peretti and Bonato 2016; Stojanović et al. 2020) and the small size of the holotype and only known specimen as well as variations in clearing and position of the coxopleuron may render the pit inconspicuous.

***Tuoba sydneyensis* (Pocock, 1891a)**

Figs 6–10

Geophilus (*Bothrogeophilus*) *lemuricus* Verhoeff, 1939, syn. nov.
Hovanyx waterloti Lawrence, 1960, syn. nov.

Examined material. 19 specimens: NHMUK015991475, 1 specimen, South Island, Aldabra, 13–20.03.1968, leg. B. Cogan & A. Hutson; NHMUK015991476, 1 juvenile, Cinq Cases/Point Hodoul Arga, 27.03.1974, leg. V. W. Spaull; NHMUK015991477, 1♀, inside fallen dead coconut tree, Picard, Aldabra, 23.02.1974, leg. V. W. Spaull; NHMUK015991478, 3♀, 1♂, 1 juvenile, Cinq Cases, Aldabra, 10–17.03.1974, leg. V. W. Spaull; NHMUK015991479, 1♀, *Cyperus ligularis* soil and litter, Dune Patates, Aldabra, 05.06.1974, leg. V. W. Spaull; NHMUK015991480, 1♂, 1 incomplete, *Mystroxylon* and *Dracaena* litter, Gionnet, 03.12.1974, leg. V. W. Spaull; NHMUK015991481, 1♀, 1♂, *Casuarina* litter, Picard, Aldabra, 08.05.1974, leg. V. W. Spaull; NHMUK015991482, 1♂, *Pemphis* litter, Dune D'Messe, Grande Terre, 29.01.1975, leg. V. W. Spaull; NHMUK015991483, 2♂, 1♀, *Casuarina*, Picard, 27.12.1974, leg. V. W. Spaull.; NHMUK015991484, 2♀, *Suriana* litter near Point Hodoul, Grande Terre, 22.03.1974, leg. V. W. Spaull; 1 juvenile, *Cocos* litter, Esprit, Aldabra, 14.12.1974, leg. V. W. Spaull.

Remarks. *Tuoba sydneyensis* has previously been reported from the Seychelles (Bonato and Minelli 2010). Material presently described from the Aldabra Atoll, as well as specimens collected on Serpent Island (Mauritius) and other islands of the Seychelles (Bonato and Minelli 2010) can be assigned as conspecific on the basis of the low number of leg-bearing segments (41–45), elongation of the antennal articles (Fig. 6A) and in the shape of the ultimate leg-bearing segment metasternite (Jones 1998).

The only other species of *Tuoba* hitherto reported from the East African coast are *Tuoba poseidonis* Verhoeff, 1901 (Zapparoli 1990) and *Tuoba sudanensis* Lewis, 1963. The small number of diagnostic characters separating these two species

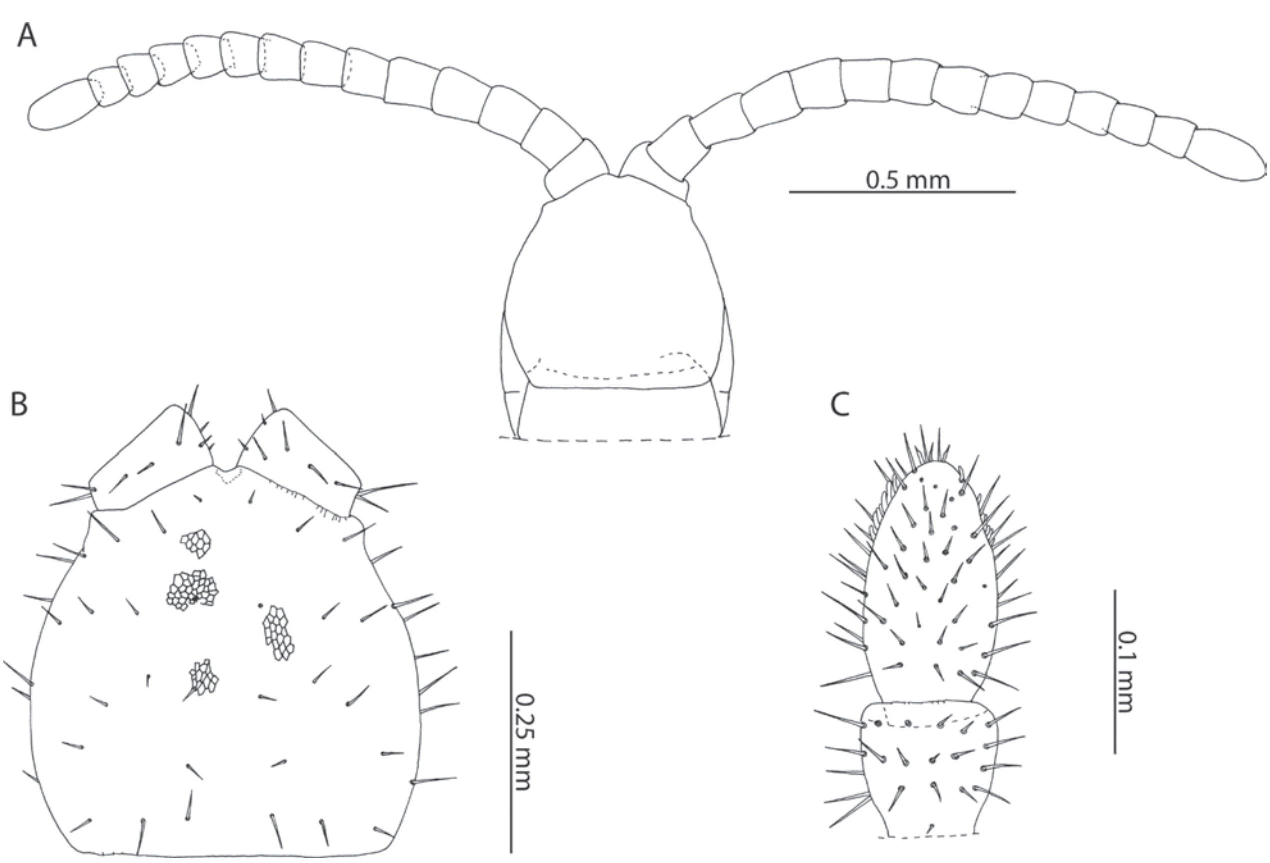

Figure 6. *Tuoba sydneyensis* (Pocock, 1891a). NHMUK015991484 **A** head and antennae, dorsal view **B** cephalic shield, dorsal view **C** antennal article XIV, dorsal view.

casts doubt on the validity of *T. sudanensis* or on the Somali record of *T. poseidonis*. Examination of additional material from the East African coast would be necessary to elucidate the diversity of *Tuoba* in Northern and Eastern Africa.

Both species can be reliably differentiated from *T. sydneyensis* in the Western Indian Ocean by the larger number of leg-bearing segments (51–53 in *T. sudanensis* compared to 41–45 in *T. sydneyensis*), greater elongation of the telopodal lappets of the first maxillae (30% of the length of the telopodite as illustrated for *T. sudanensis*; compared to minute in *T. sydneyensis* (Fig. 8B)), shape of the carpophagus structure (with a distinct median “hump” in *T. sudanensis*; lacking any “hump” medially in *T. sydneyensis*), point of the midbody transition (sternites 20–22 in *T. poseidonis* and *T. sudanensis*; sternites 14–15 in *T. sydneyensis*) and the shape of the ultimate leg-bearing segment metasternite (1.6 × wider than long as illustrated for male *T. sudanensis*; 1.9 × wider than long in male *T. sydneyensis*, Fig. 10A). The combination of diagnostic characters presented clearly unify the Western Indian Ocean populations of *Tuoba* under one morphospecies, closely matching the description of *T. sydneyensis*, which is distinct from *Tuoba* species recorded in continental Eastern and Northern Africa.

Verhoeff (1939) described *Geophilus* (*Bothrogeophilus*) *lemuricus* from La Ponce, Mauritius and remarked that it is closely related to (“[…] nahe verwandt […]”) *Geophilus carpophagus* Leach, 1815. Although incomplete, the description provides several characters that allow reliable assignment to *T. sydneyensis*, with which it agrees in number of leg-bearing segments (47 in *G. lemuricus*,

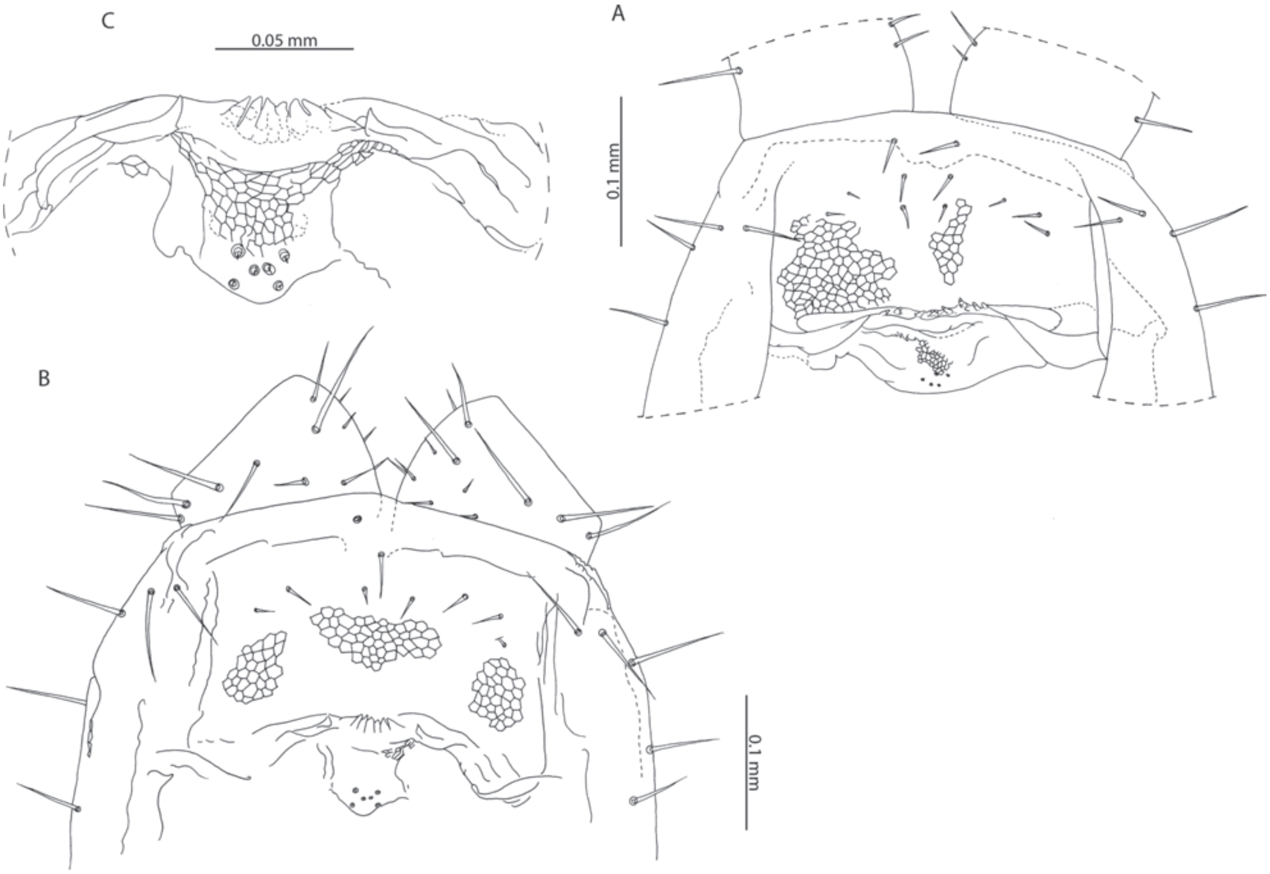

Figure 7. *Tuoba sydneyensis* (Pocock, 1891a) **B, C** NHMUK015991478 **A** NHMUK015991484 **B** clypeus and labrum, ventral view **C** labrum, ventral view.

41–45 in *T. sydneyensis* from the Western Indian Ocean), the apical claw of the second maxillae being reduced in size and not overtaking surrounding setae in length ("[...], überragt nicht die Nachbarborsten.") (Fig. 8B, C), and in the arrangement of the coxal organs on the coxopleuron of the last leg-bearing segment, which are arranged into a rosette opening in a pouch near the edge of the metasternite ("[...] neben dem Endbeinsternit mündet eine Tasche und in diese eine Rosette von Drüsen") (Figs 9A, 10A). We consider *G. lemuricus* to be a junior subjective synonym of *T. sydneyensis*, which has been subsequently collected from Mauritius (NHMUK015991411).

Family Mecistocephalidae
Genus *Mecistocephalus* Newport, 1843

Mecistocephalus angusticeps (Ribaut, 1914)
Fig. 11B

Examined material. 11 specimens: NHMUK015991461, 1♂, *Pandanus tectorius* soil and litter, Cinq Cases, 24.03.1974, leg. V. W. Spaull; NHMUK015991462, 1♀, 2 km N of Cinq Cases, 11.03.1974, leg. V. W. Spaull; NHMUK015991463, 6 juveniles, *Sideroxylon* litter, Cinq Cases, 10–17.03.1974, leg. V. W. Spaull; NHMUK015991464, 1♀, *Pandanus tectorius* soil and litter, Cinq Cases/Point Hodoul, 27.03.1974, leg. V. W. Spaull; NHMUK015991465, 1♂, Gionnet, Aldab-

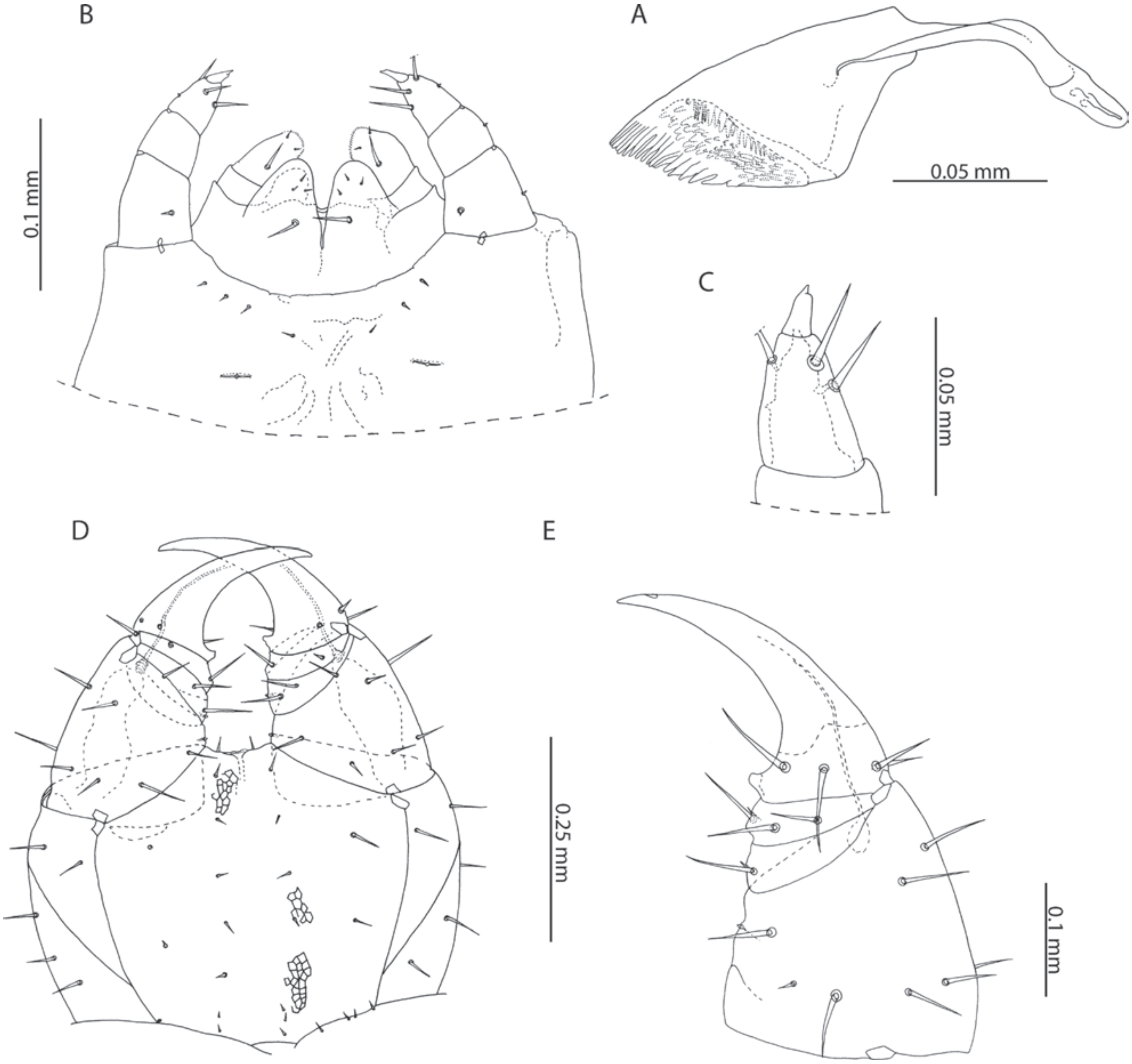

Figure 8. *Tuoba sydneyensis* (Pocock, 1891a). NHMUK015991484 **A** Mandible, lateral view **B** First and second maxillae, ventral view **C** second maxillary article III and pretarsus, ventral view **D** forcipular segment, ventral view **E** right forcipule, ventral view.

ra, 03.12.1974, leg. V. W. Spaull; NHMUK015991466, 1♂, Casuarina, Aldabra, 04.02.1974, leg. V. W. Spaull.

Remarks. Previously recorded from multiple localities near the East African Coast and the Western Indian Ocean (Ribaut 1914; Bonato and Minelli 2010; Popovici et al. 2024), making natural dispersal a likely explanation for the presence of *M. angusticeps* in Aldabra. Presently examined specimens are morphologically indistinguishable from conspecifics recorded from the Seychelles and the Chagos Islands. Although not previously noted, the forcipular cerri were found to be absent in examined specimens (Fig. 11B). In combination with other diagnostic characters (47 leg-bearing segments, conspicuous medial reduction in clypeal reticulation, large distal trochanteroprefemoral denticle and sternal sulcus not furcate), this allows for easy separation from other syntopic *Mecistocephalus* spp. within its range.

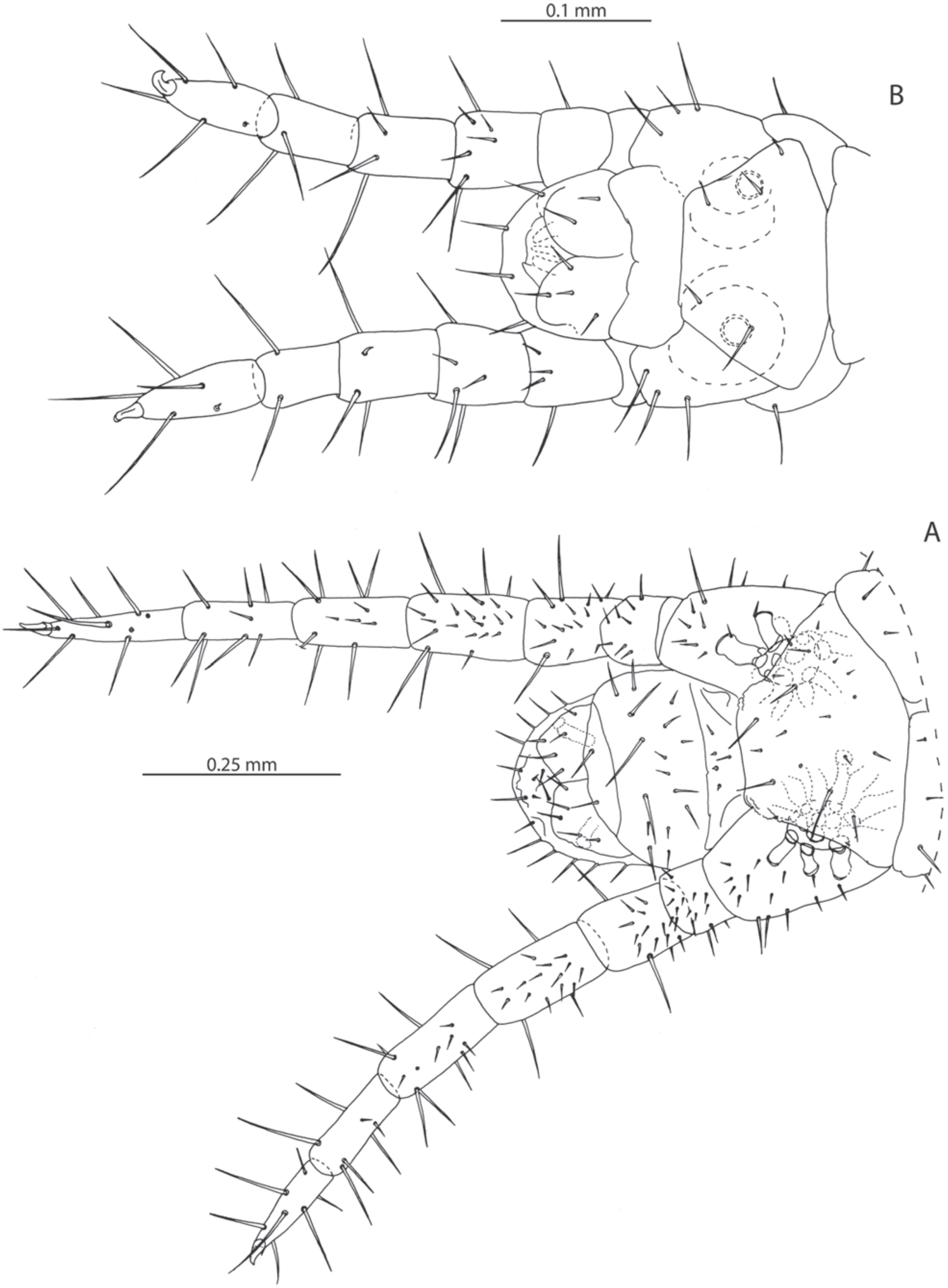

Figure 9. *Tuoba sydneyensis* (Pocock, 1891a) **A** NHMUK015991484, female ultimate leg-bearing and postpedal segments, ventral view **B** NHMUK015991478, juvenile ultimate leg-bearing and postpedal segments, ventral view.

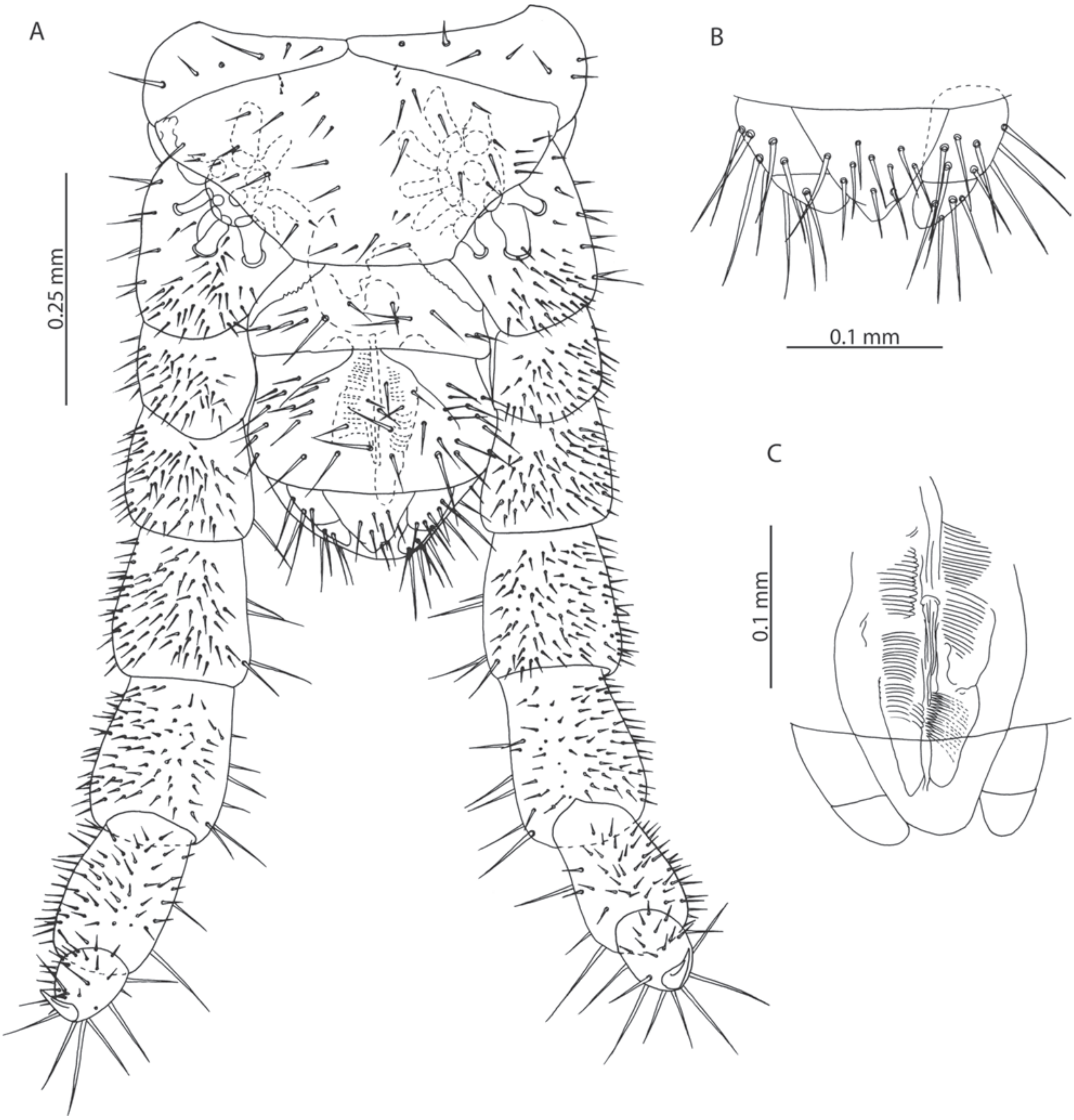

Figure 10. *Tuoba sydneyensis* (Pocock, 1891a), NHMUK01591483 **A** male ultimate leg-bearing and postpedal segments, ventral view **B** male gonopods, ventral view **C** penis, ventral view.

Mecistocephalus lohmanderi Verhoeff, 1939

Fig. 11A

Examined material. 2 specimens: NHMUK015991459, 1♀, Black Path, Picard, Aldabra, Summer 1975, leg. V. W. Spaull; NHMUK015991460, 1♂, *Casuarina* litter, Picard, 10.12.1974, leg. V. W. Spaull.

Remarks. Originally described from Mauritius (Verhoeff, 1939), *M. lohmanderi* has been found on other Western Indian Ocean Islands (Bonato and Minelli 2010; Popovici et al. 2024). Similarly to *M. angusticeps* (Fig. 11B), examined

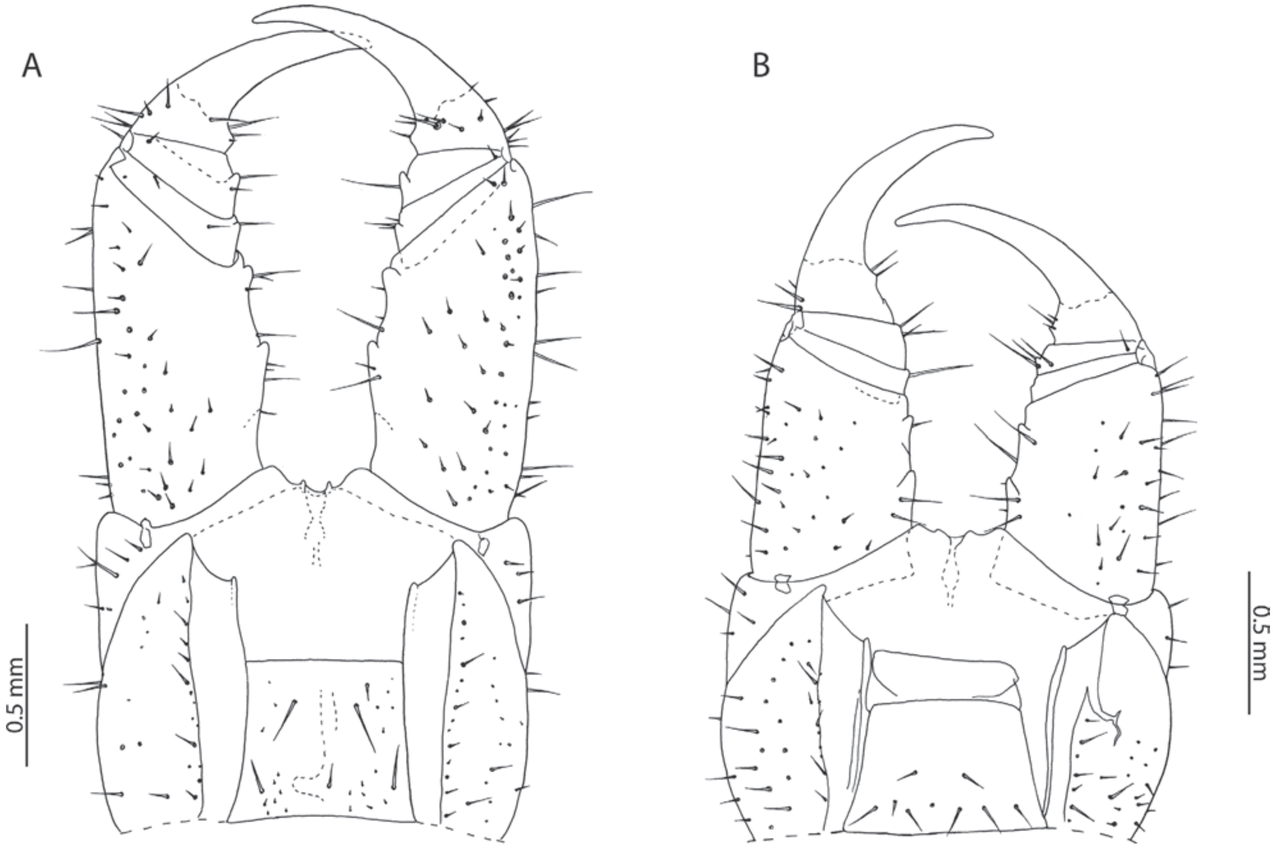

Figure 11. A *Mecistocephalus lohmanderi* Verhoeff, 1939, NHMUK015991460, forcipular segment, dorsal view **B** *Mecistocephalus angusticeps* (Ribaut, 1914), NHMUK015991466, forcipular segment, dorsal view.

specimens lack forcipular cerri (Fig. 11A). Presently examined specimens are most similar to *M. lohmanderi* specimens collected from the Diego Garcia atoll (Popovici et al. 2024). Adults (female 34 mm body length, male 34 mm body length) in the Aldabra sample lack dark subcutaneous pigment patches and maintain the characteristic clypeal setation pattern described in *M. lohmanderi* from other localities (Bonato and Minelli 2010; Popovici et al. 2024). Similarly, specimens assigned to *M. insularis* described from Socotra (Lewis and Wranik 1990) match all diagnostic characters outlined for *M. lohmanderi*, and can be referred to this taxon, thus extending its range to island localities in the Northwestern Indian Ocean.

Records of large adult specimens (70–91 mm) assigned to *Mecistocephalus insularis* from the Arabian Peninsula (Lewis 1996) are fully consistent with the revised description of *Mecistocephalus glabridorsalis* Attems, 1900 from the Seychelles (Bonato and Minelli 2010) and are almost certainly misidentified *M. glabridorsalis*. In particular, the clypeal morphology illustrated for specimens from Saudi Arabia shares the presence of a small non-areolate insula anterior to the plagulae with specimens from the Seychelles and the arrangement of setae in a transverse line on the areolate part of the clypeus. This morphology has hitherto only been recorded in *M. glabridorsalis* and *M. punctifrons* Newport, 1843 (Bonato and Minelli 2004), casting further doubt on the true identity and distribution of *M. insularis*. Insufficient data on morphological variability in *M. lohmanderi* and the uncertain status of *M. insularis* records from past literature prevent further inferences on the taxonomic validity and relationships between these species.

Family Oryidae
Genus *Orphnaeus* Meinert, 1870
Nycternyssa Crabill, 1959 syn. nov.

Orphnaeus dekanius Verhoeff, 1938

Figs 12–16, 18D–H

Examined material. 6 specimens: NHMUK015991469, 1♂, 40 mm, 73 leg-bearing segments, Picard, Aldabra, 08.10.1974; NHMUK015991470, 1♂, 35 mm, 75 leg-bearing segments, Picard, 09.04.1974; NHMUK015991471, 1♀, 24 mm, 81 leg-bearing segments, Grande Terre, Aldabra, 03.1974, leg. J. Wilson; NHMUK015991472, 1 juvenile, 13 mm, 81 leg-bearing segments, Grande Terre, Aldabra, 05.1974, leg. J. Wilson; NHMUK015991473, 1♂, 37 mm, 75 leg-bearing segments, *Pandanus* litter, Aldabra, 22.03.1974; NHMUK015991474, 1♀, 51 mm, Takamaka (Anse Takamaka), 23–27.02.1968, leg. B. Cogan & A. Hutson.

Diagnosis. Medium to large size *Orphnaeus* species, with 73–81 leg-bearing segments and variable but generally present longitudinal bands of dark pigment flanking the central vessel. Mandible with three or four pectinate lamellae. First maxillae with both telopodal and coxosternal lappets present and uniarticulate telopodite. Second maxillary pretarsus spatulate, fringed by acuminate hyaline projections. Posterior trunk metasternites with paired pore fields at the posterior end. Pore fields on posterior metasternites, procoxae and metacoxae bordered by dense groups of setae-like projections. Female gonopods uniarticulate, medially overlapping, with angled, rounded external margin.

Description. ***Head and antennae*.** Cephalic plate with broadly rounded anterior margin and straight posterior margin, overlapping the forcipular tergite. Head approximately as broad as long (NHMUK015991473) to 1.2 × broader than long (NHMUK015991474). Antennae approximately 2.5 × longer than head, weakly tapering distally (Fig. 12A). In older specimens, the tapering of antennae and dorsoventral compression of proximal antennal articles are more clearly visible (Fig. 12C). Antennal article XIV 1.9 × longer than the penultimate, with two clusters of sensilla basiconica arranged in lateral pits. Small, spear-like sensilla present at apical end.

***Mandibles*.** Of typical aspect for the genus (Fig. 13C, D). Four conspicuous pectinate lamellae evident, arranged concentrically around distal edge. Proximal to the outermost lamella, isolated projections resembling those on the lamellae are present. Two minute sensilla present laterally.

***Labrum and clypeus*.** Labrum of typical oryid aspect, with short hairlike hyaline projections on middle part (Fig. 13B). Lateral parts incompletely separated from middle part and clypeus by evident sutures. Clypeus with two pairs of postantennal sensilla, a median field of sensilla spanning its mediolateral axis and one pair of prelabral sensilla posterior to these (Fig. 13A). Polygonal reticulation evident.

***Maxillae*.** First maxillae with apically rounded, short coxal projections, bearing 8–11 sensilla (Fig. 14A). Telopodite broadly rounded, uniarticulated, of similar size to the coxal projection, bearing 7–12 sensilla. Both telopodal and coxosternal pairs of lappets present, with distinct spinous reticulation (Fig. 14C). Coxosternal pair of lappets completely obscured by second maxillary telopodite in ventral view. Second maxillary coxosternite with shallow, concave, rounded anterior margin bordered by a row of trichoid sensilla and two groups of trichoid

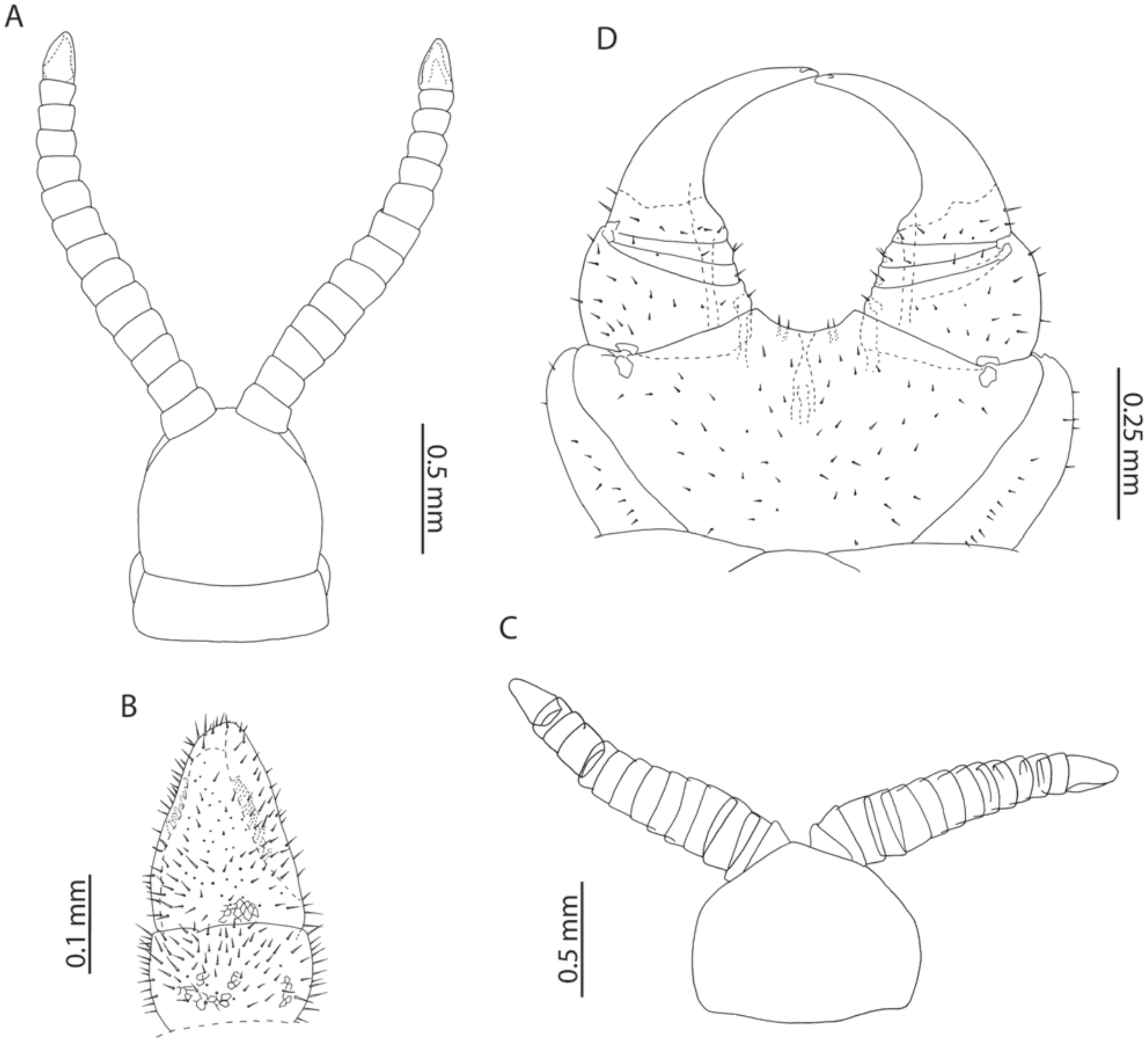

Figure 12. *Orphnaeus dekanius* Verhoeff, 1938 **A, B, D** NHMUK015991470 **A, C** NHMUK015991474. Head and antennae, dorsal view **B** antennal article XIV, dorsal view **D** forcipular segment, ventral view.

sensilla proximally (Fig. 14A). Metameric pore conspicuous, surrounded by sclerotised rim. Telopodal articles stout. Pretarsus with spine-like projections around entire exterior margin and two pores opening on its dorsal surface (Fig. 14D, E).

***Forcipular segment*.** Forcipular tergite 3.2 × broader than long. Exposed surface of forcipular coxosternite 2.2 × broader than long (Fig. 12D). Chitin lines absent. Anterior margin rounded, deeply concave. Pleural sutures strongly converging posteriorly. Trochanteroprefemur ~ 1.5 × broader than long, with evidently rounded external face. Tarsungulum stout, large, entirely covered by anterior edge of cephalic plate, with smooth inner concavity. Opening of venom gland channel immediately proximal to tip of tarsungulum. All forcipular articles without denticles.

***Trunk*.** Last five or six trunk metasternites with two posteriorly located pore fields (Fig. 15D), anteriorly bordered by dense clusters of hairs (Fig. 15A). All other trunk metasternites with four pore fields, two anterior and two posterior, of equal size on metasternites 2–46, the anterior gradually decreasing in size until

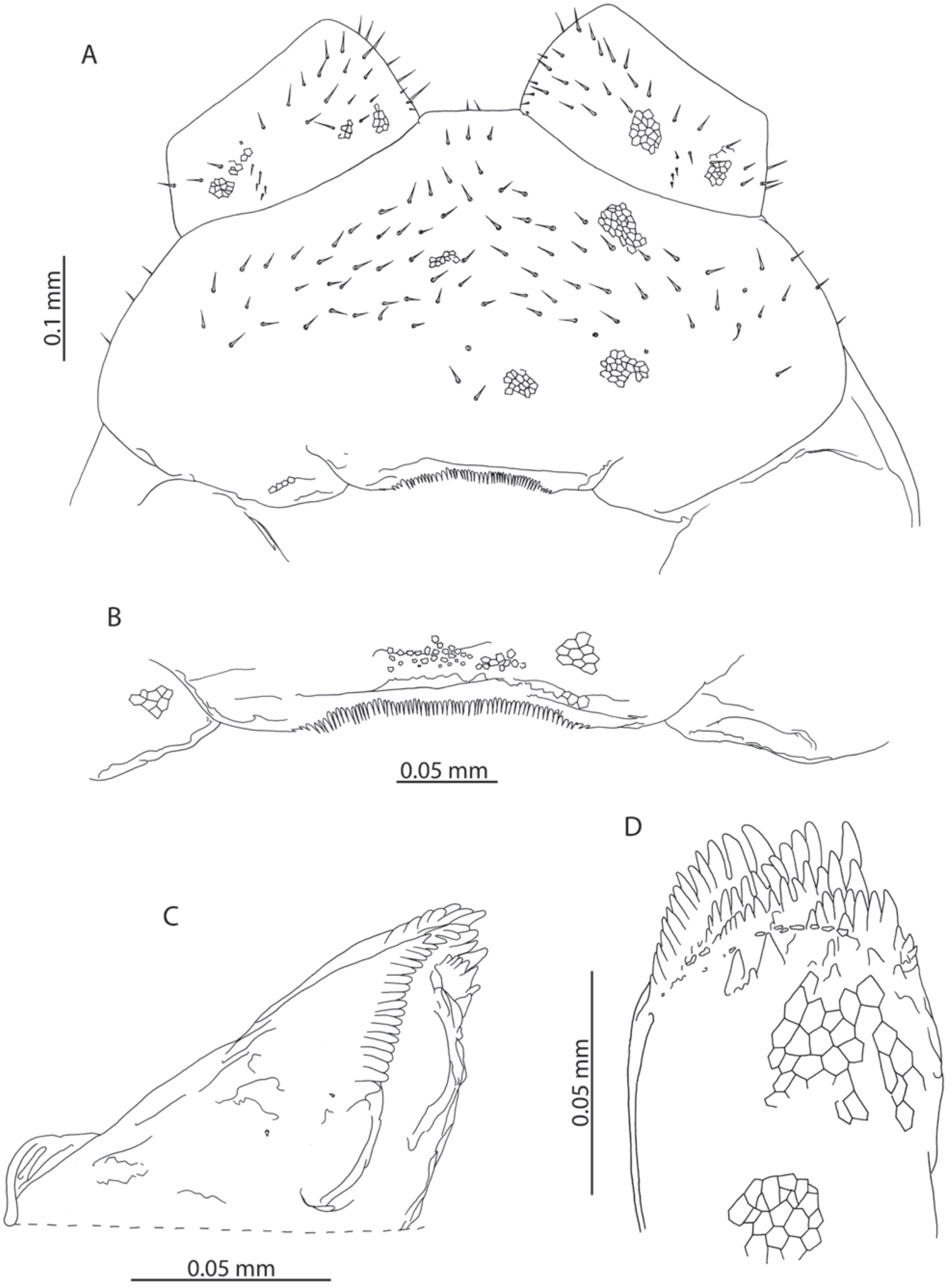

Figure 13. *Orphnaeus dekanius* Verhoeff, 1938. NHMUK015991470 **A** clypeus and labrum, ventral view **B** labrum, ventral view **C, D** Mandible, lateral and dorsal views.

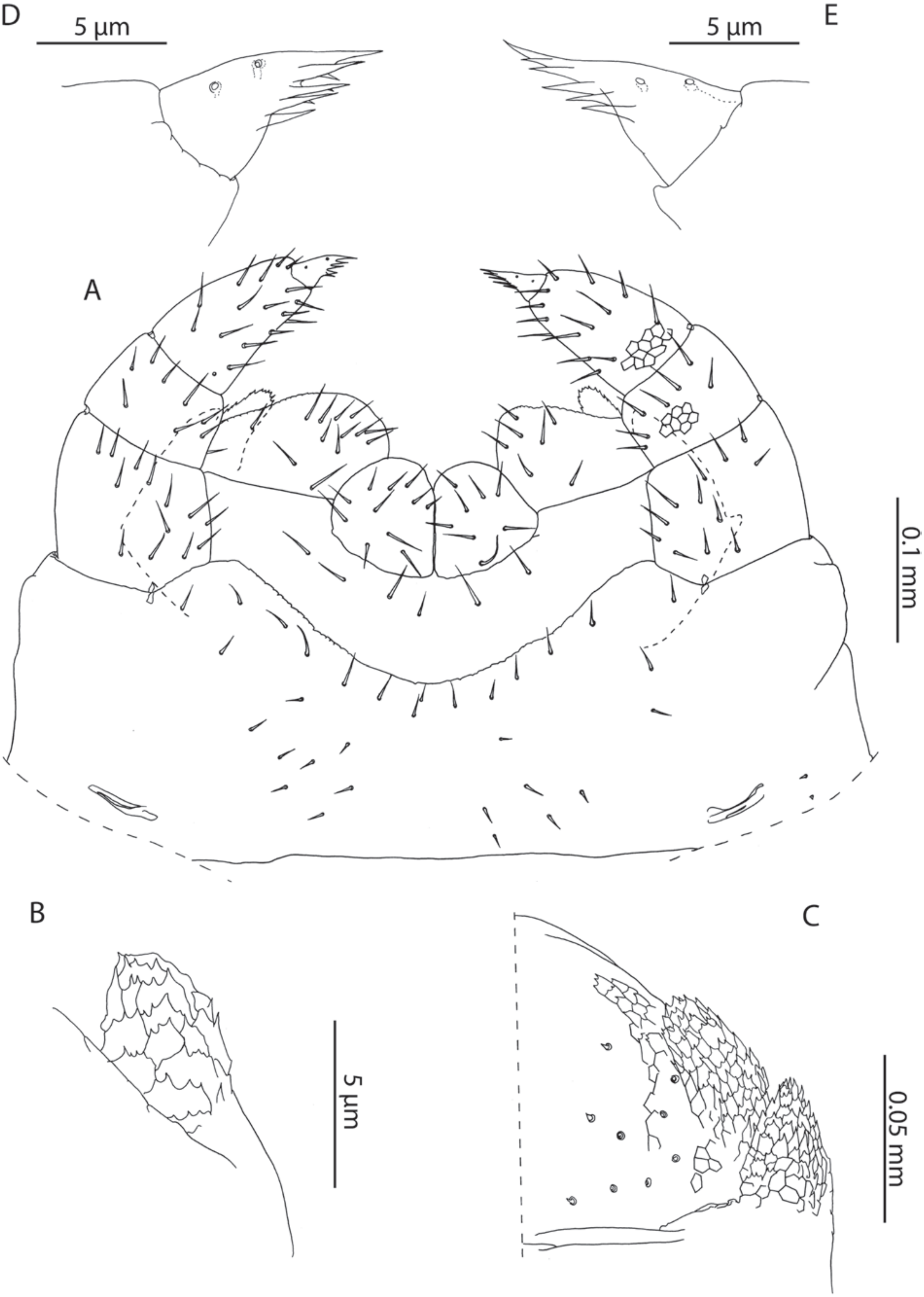

Figure 14. *Orphnaeus dekanius* Verhoeff, 1938 NHMUK015991470 **A** first and second maxillae, ventral view **B** first maxillary right telopodal lappet, ventral view **C** first maxillary left telopodal and coxosternal lappets, dorsal view **D, E** left and right second maxillary pretarsi, ventral view.

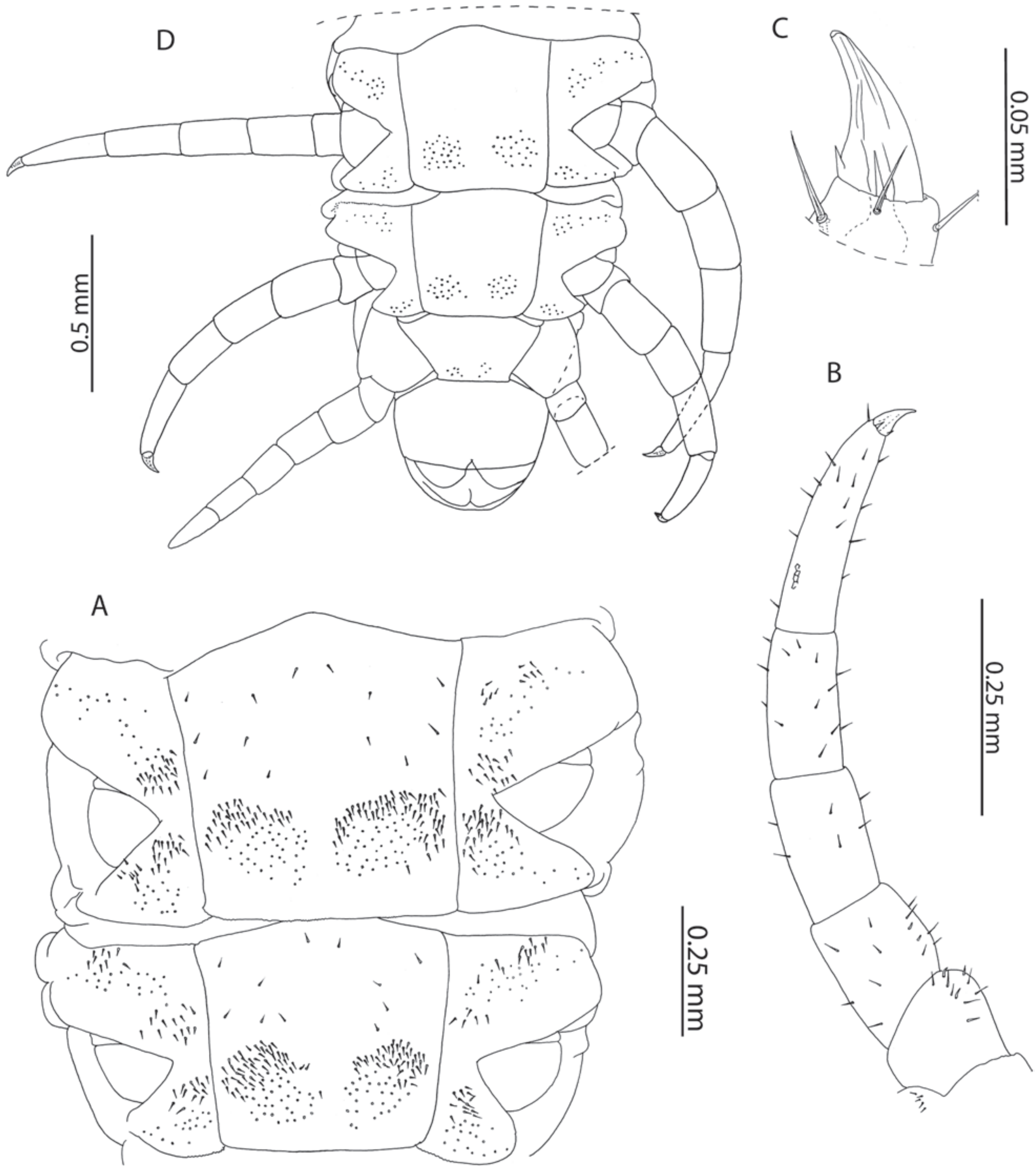

Figure 15. *Orphnaeus dekanius* Verhoeff, 1938 **A, D** NHMUK015991474 **B, C** NHMUK015991470 **A** metasternites of leg-bearing segments 79 – 80, ventral view **B** walking leg, pair 74, lateral view **C** Walking leg pair 74 pretarsus, lateral view **D** Leg-bearing segments 79 – 81, ventral view.

disappearing on metasternites 74–76. One single row of paratergites present beginning from the second leg-bearing segment, becoming very conspicuous on the eighth leg-bearing segment. General setation of sclerites sparse.

***Ultimate leg-bearing and postpedal segments*.** Ultimate leg-bearing segment metasternite variably trapeziform, 2.3 × broader than long (Fig. 16A, B). Posterior edge with dense field of hairs and occasionally small clusters of pores. Coxopleuron stout, without coxal organs. Telopodite of ultimate leg-pair only

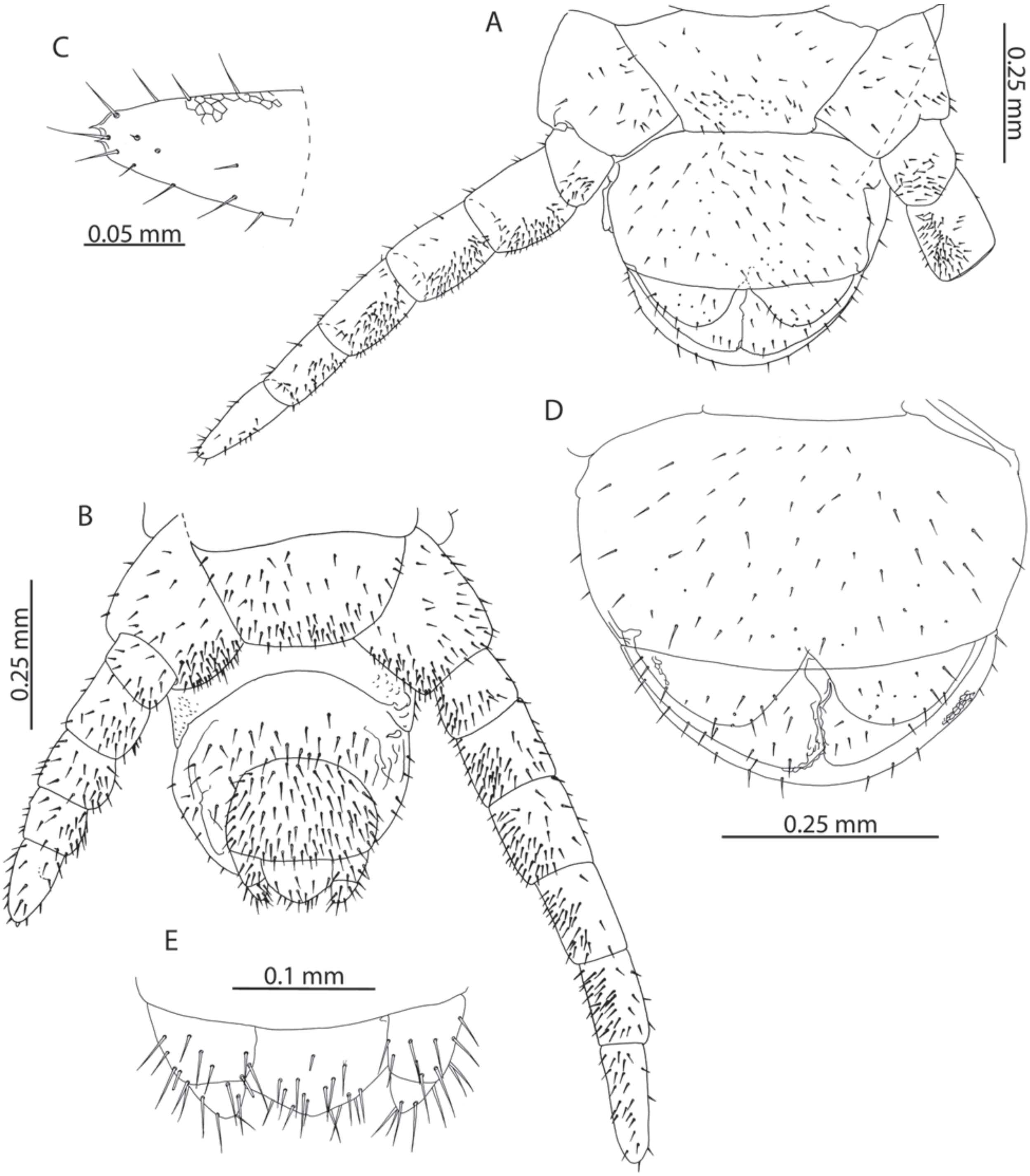

Figure 16. *Orphnaeus dekanius* Verhoeff, 1938 **A, C, D** NHMUK015991471 **B, E** NHMUK015991470 **A, B** ultimate leg-bearing and postpedal segments, ventral view **C** ultimate leg pair metatarsus, lateral view **D** female gonopods, ventral view **E** male gonopods, ventral view.

moderately inflated in both males (Fig. 16B) and females (Fig. 16A), with dense fields of hairs present on the ventral side of all articles. Pretarsus absent (Fig. 16C). Metatarsus with small hair-like projections at its apical edge.

Female gonopods usually uni-articulated (Figs 15D, 16D), occasionally with an anterior notch or asymmetrical articulation. Lateral edge smooth, rounded, forming strongly acute angle with posterior edge of first genital sternite. Male gonopods biarticulated, bearing 16 setae (Fig. 16E).

Remarks. *Orphnaeus dekanius* was originally described from Trivandrum (Thiruvanathapuram), India (Verhoeff 1938), and maintained as a valid species under *Orphnaeus* until its reassignment to *Nycternyssa*, justified by the description of the female gonopods as “uni-articulate”. A detailed re-evaluation of the status of *Nycternyssa* is provided below.

Subsequent to its original description, there is no evidence that other specimens had been assigned to either *O. dekanius* or *N. dekania* prior to recent records from the Chagos Archipelago (Popovici et al. 2024). Based on morphology alone, the present specimens are considered conspecific with those collected in the Chagos Archipelago and match the original description of *O. dekanius*. The most salient diagnostic trait allowing for reliable differentiation of *O. dekanius* from *O. brevilabiatus* is the presence of dense clusters of minute setae bordering the posterior pore fields of the former (Fig. 15A). Although this character was illustrated by Verhoeff in the original description of *O. dekanius* (Verhoeff 1938: tafel 8, fig. 61), no mention was made of it in the text of the description. It is unambiguously shared by all specimens studied here from near the type locality of *O. dekanius* (specimens from Sri Lanka listed above under “Specimen data”), and from other localities in the Western Indian Ocean, and is consistent in both sexes in specimens. Setae are sparse in the smallest studied Aldabra specimen (13 mm) but are clustered by a body length of 24 mm. As these clusters of setae are completely absent in specimens identified as O. *brevilabiatus* from near its type locality in Myanmar (Fig. 17) and other localities in mainland and maritime Southeast Asia, we maintain the validity of *O. dekanius* and *O. brevilabiatus* even in light of the variability of female gonopodal articulation in the latter (Fig. 18A–C). The incomplete description of *Orphnaeus meruinus* Attems, 1909 does not allow for reliable separation from *O. dekanius*, given the inconsistencies in how diagnostic characters for these two taxa are coded in past literature. One salient difference from all *O. dekanius* specimens in our sample is the greatly inflated ultimate leg telopodite in males assigned to *O. meruinus* collected in Oman (Lewis and Gallagher 1993), a character that separates these species even when accounting for body size.

Family Schendylidae
Genus *Ityphilus* Cook, 1899

Ityphilus cf. *taeniaformis* (Lawrence, 1960)
Figs 19–23

Examined material. NHMUK015991468, 1♂, Aldabra, 21.03.1974., V. W. Spaull leg.

Description. ***Head and antennae*.** Antennae conspicuously claviform in shape, medially weakly geniculate, with articles IX–XIV widened (Figs 19A, 20A, C). Articles IX and XIII with clusters of type c sensilla (*sensu* Pereira 2017) on the distal edge of the dorsal side (Fig. 19C, D). Article XIV with two lateral clusters of sensilla basiconica and a small number of spear-shaped sensilla at its apex (Fig. 19B). Head approximately as wide as forcipular tergite, 1.14 × broader than long. Curved sulcus near posterior margin. Chaetotaxy of head as in Fig. 20B.

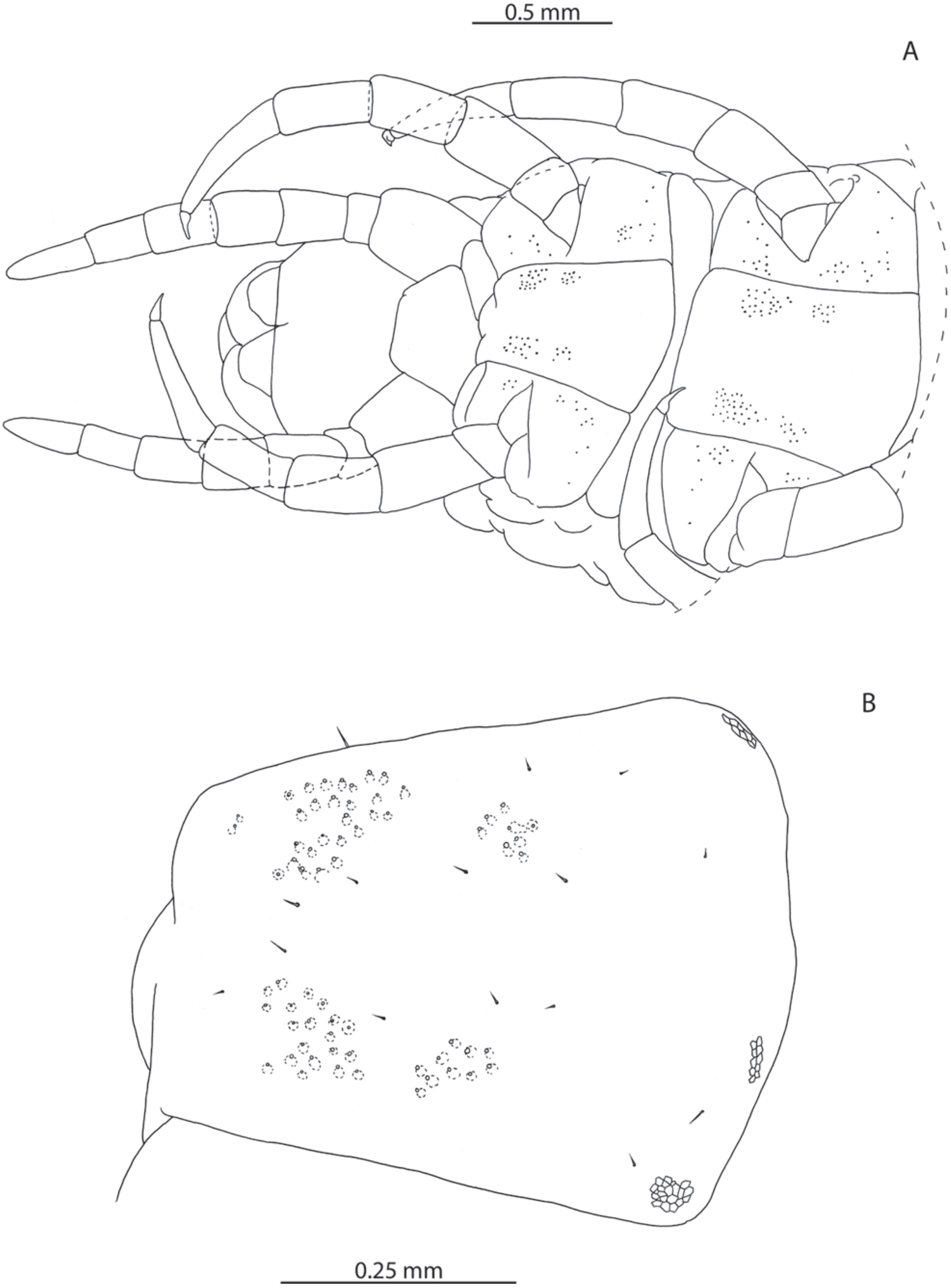

Figure 17. *Orphnaeus brevilabiatus* (Newport, 1845). NHMUK015991423 **A** leg bearing segments 77 – 79, ventral view **B** metasternite of leg-bearing segment 78, ventral view.

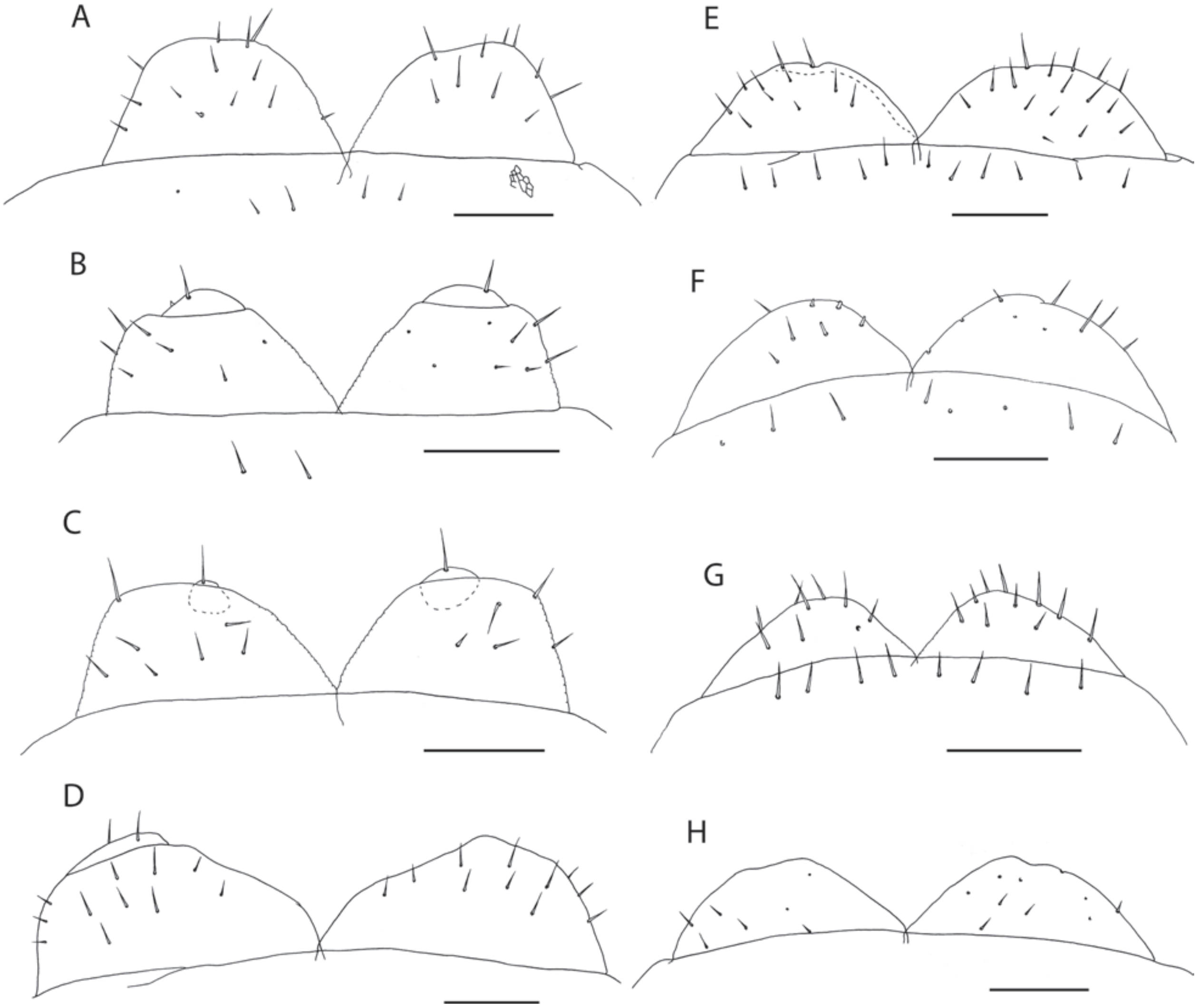

Figure 18. Female gonopods of *Orphnaeus* Meinert, 1870 species **A, B, C** *Orphnaeus brevilabiatus* (Newport, 1845). (A = NHMUK015991423 (Myanmar), B = NHMUK015991421 (Thailand), C = NHMUK015991420 (Singapore)) **D, E, F, G, H** *Orphnaeus dekanius* Verhoeff, 1938. (D = NHMUK015991415 (Sri Lanka), E = NHMUK015991413 (Sri Lanka), F = NHMUK015991417 (Singapore), G = NHMUK015991418 (Singapore), H = NHMUK015991416 (Sri Lanka)). Scale bars: 0.1 mm.

Mandibles. Dentate lamella with seven denticles, only six conspicuous in lateral view. Pectinate lamella with approximately 22 hyaline projections (Fig. 21A).

Labrum and clypeus. Clypeus with a pair of postantennal setae, a cluster of seven medial setae and one prelabral seta. Lateral pieces of labrum narrow, conspicuously sclerotised, lacking any fringes or projections. Medial piece contiguous with clypeus, poorly sclerotised, membranous and lacking conspicuous hairs or projections.

Maxillae. First maxillae with evident, triangular coxal projections, each bearing one sensillum. Telopodites bearing one sensillum each, conspicuously larger than coxal projections and partly covering them (Fig. 21B). Lappets absent. Second maxillary coxosternite with evident but incomplete medial suture, extending for half of its length (Fig. 21C). Each side of the suture bearing one sensillum. Telopodite stout, terminating in large pretarsus. Second maxillary pretarsus spatulate, lateral edges densely fringed (Fig. 21D, E).

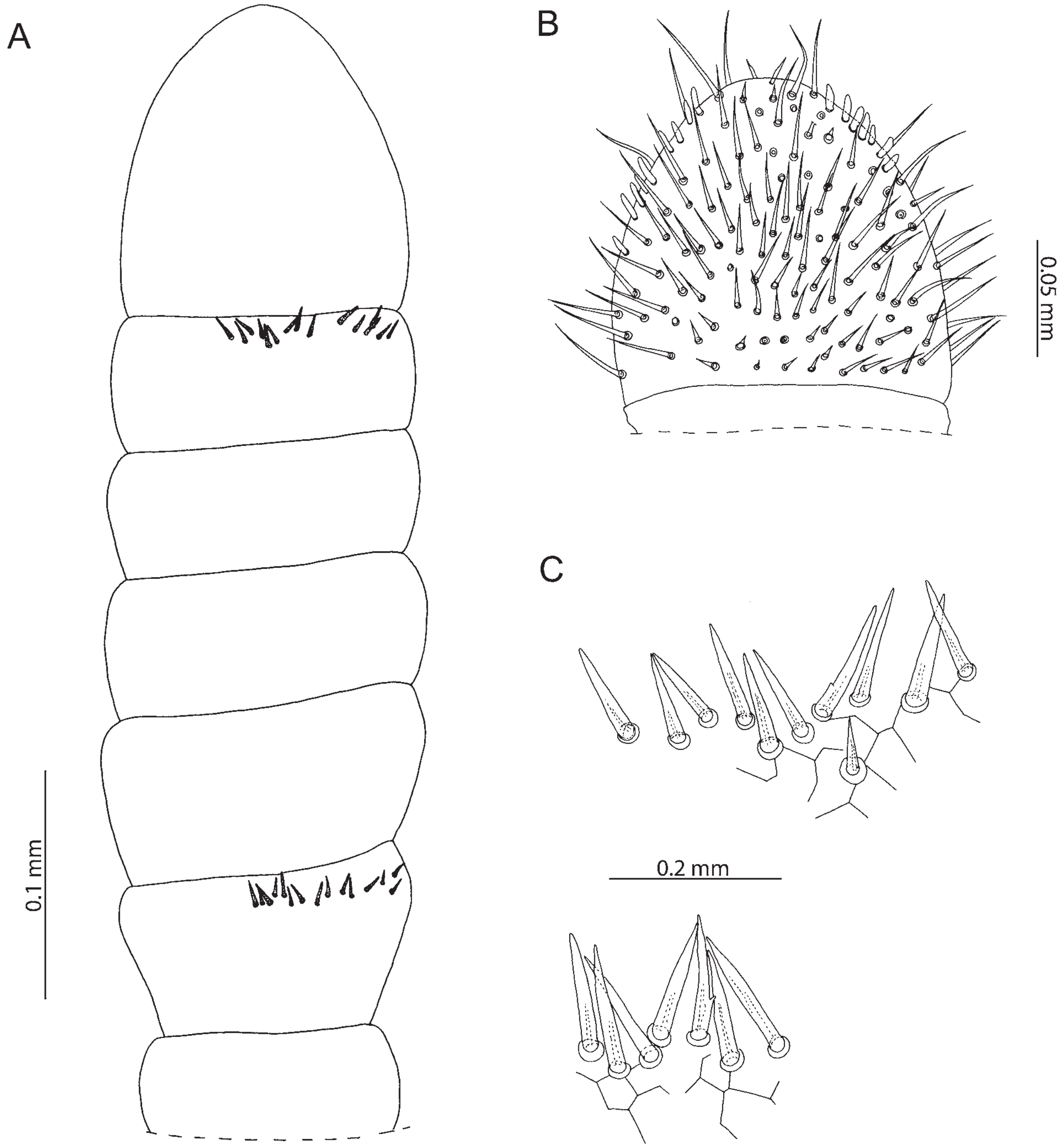

Figure 19. *Ityphilus* cf. *taeniaformis* (Lawrence, 1960). NHMUK015991468 **A** right antenna, dorsal view **B** antennal article XIV, ventral view **C** clusters of type c sensilla on antennal article XIII (top) and IX (bottom), dorsal view.

Forcipular segment. Exposed face of forcipular coxosternite 2.2 × broader than long (Fig. 22A). Chitin lines present, reaching the condyles. Forcipular trochanteroprefemur 1.25 × longer than broad. Calyx of venom gland elongated, ovoid in shape (Fig. 22C). All forcipular articles without denticles (Fig. 22B). Internal margin of tarsungulum smooth. Extended, forcipules do not reach the anterior margin of the head.

Trunk. 75 leg-bearing segments. Pore fields located on raised areas in the middle of all metasternites excluding those of leg-bearing segments 1, 74, and 75. Shape of pore field oval, medially constricted and anteriorly bordered by a line of setae (Fig. 22D). Colour of pore field bluish grey, conspicuously pigment-

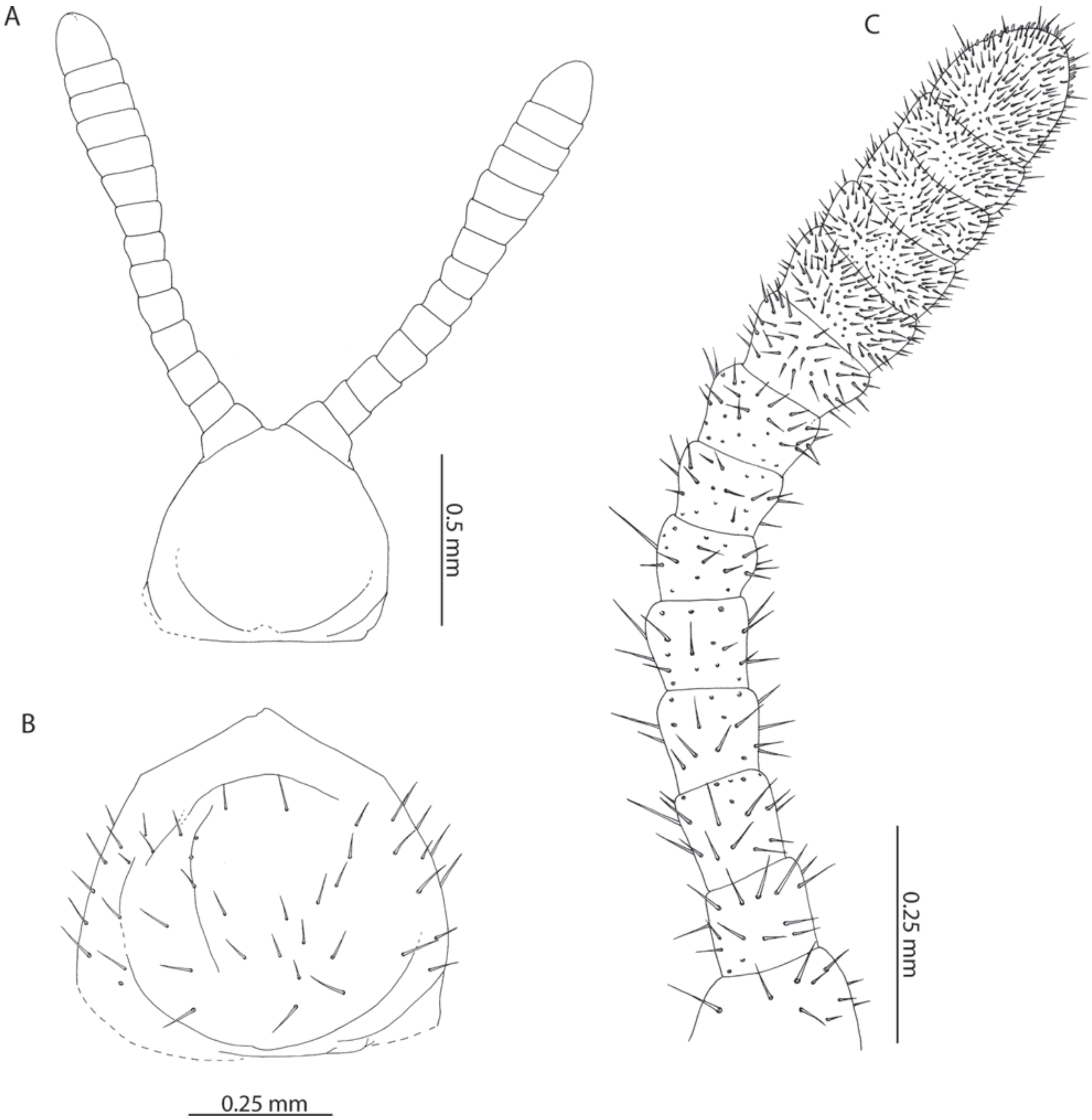

Figure 20. *Ityphilus* cf. *taeniaformis* (Lawrence, 1960) NHMUK015991468 **A** head and antennae, dorsal view **B** cephalic shield, dorsal view **C** right antenna, ventral view.

ed relative to surrounding cuticle. Despite the faded colour of the ethanol-preserved specimen, pigmentation of the pore field is conspicuous and the trunk is generally greenish grey in appearance.

Ultimate leg-bearing and postpedal segments. Intercalary pleurites separated from ultimate pretergite by evident sutures. Ultimate metasternite trapezoidal, 1.3 × longer than broad. Coxopleura each with two distinct coxal organs, partially covered by the ultimate metasternite (Fig. 23A). Entire ventral side of ultimate leg-bearing segment covered in setae. Ultimate leg telopodite composed of seven articles, all distinctly thickened. Pretarsus absent (Fig. 23B). Metatarsus with a small spine subapically. Intermediate sternite indistinct. First genital sternite with straight posterior margin. Gonopods uni-articulate, flanking penis (Fig. 23C).

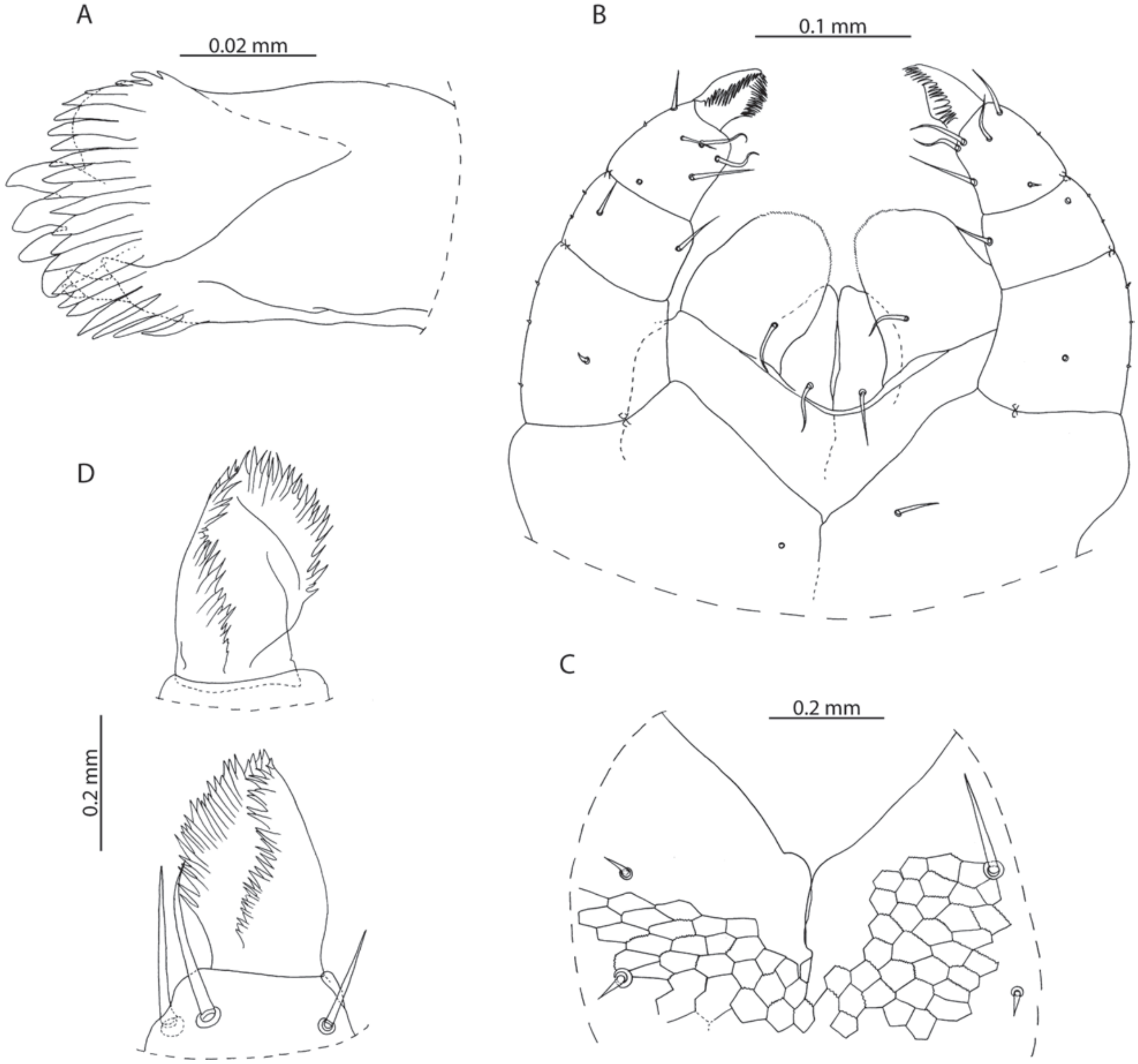

Figure 21. *Ityphilus* cf. *taeniaformis* (Lawrence, 1960). NHMUK015991468 **A** mandible, lateral view **B** first and second maxillae, ventral view **C** anterior margin of second maxillary coxosternite, ventral view **D** second maxillary pretarsus left (top), right (bottom), ventral view.

Remarks. The taxonomy of *Ityphilus* remains largely unresolved, especially outside of South America, where different authors have disagreed on its relation to *Ballophilus*, alternatively considering it a different genus (Attems 1929) or a synonym of *Ballophilus* (Verhoeff 1939). Recent revision of the genus (Bonato et al. 2007) has maintained the distinction between *Ityphilus* and *Ballophilus*, but remarked on the close relationship between the two, and on cases in which the presence of complete or nearly complete chitin lines is doubtful, such as in *Ityphilus boteltobogensis* (Wang, 1955), despite this character being predominantly used to distinguish the two genera. Similarly, several *Ballophilus* species are described as bearing a cuticular thickening in the usual position of the chitin line (Demange 1963; Pereira et al. 1997), further confounding the utility of this character in taxonomy within the Ballophilidae. The presence of a median sulcus in the second maxillary coxosternite has been shown to be unreliable

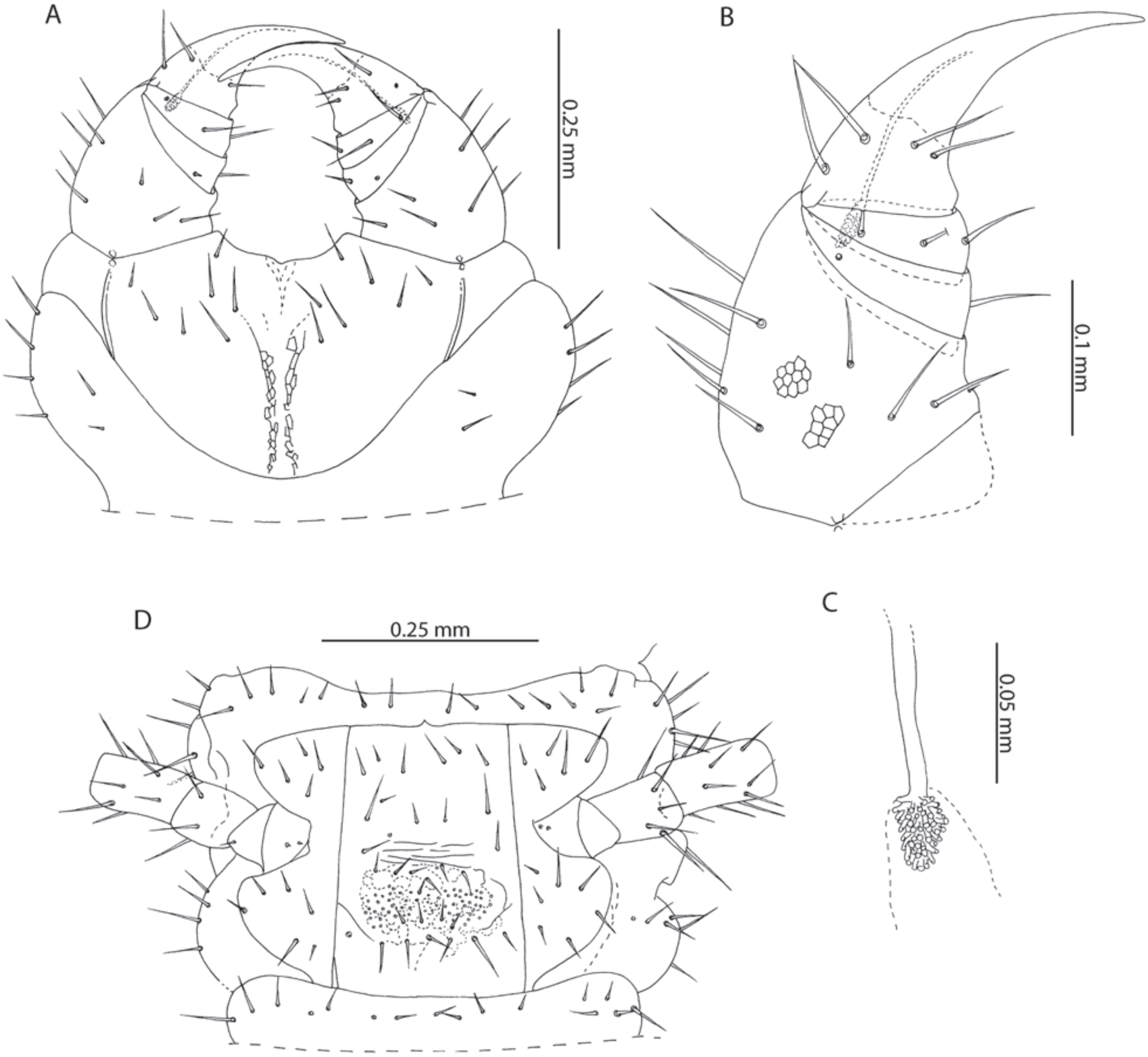

Figure 22. *Ityphilus* cf. *taeniaformis* (Lawrence, 1960). NHMUK015991468 **A** forcipular segment, ventral view **B** left forcipule, ventral view **C** calyx of venom gland, ventral view **D** leg-bearing segment 9, ventral view.

in separating *Ballophilus* and *Ityphilus*. This character has been described in both *Ballophilus* (Ribaut 1914; Pereira et al. 1997) and *Ityphilus* (Pereira et al. 2000), in some cases as incomplete (Brölemann 1909) (Fig. 21B, C), and is not included in the most recent diagnosis of the latter genus (Bonato et al. 2007).

Verhoeff (1939) described two *Ballophilus* species from Mauritius, *B. lawrencei* Verhoeff, 1939 and *B. mauritianus* Verhoeff, 1939. Both are known from single specimens but, according to their original description, compare closely with *Ballophilus allauadi* Ribaut, 1914 described from Eastern Africa. The Aldabra specimen differs from these species in the presence of pore fields on all but the first and last two leg-bearing segment metasternites (contrasting with the absence of the pore field on the first and the last four metasternites). Additionally, the distal end of the antenna of *B. lawrencei* is illustrated as markedly less clavate than observed for the Aldabra specimen. Despite this, the *Ityphilus* specimen collected in Aldabra overlaps in the shape of the metasternal pore field, its position on a raised area and in the relative elongation of the ultimate

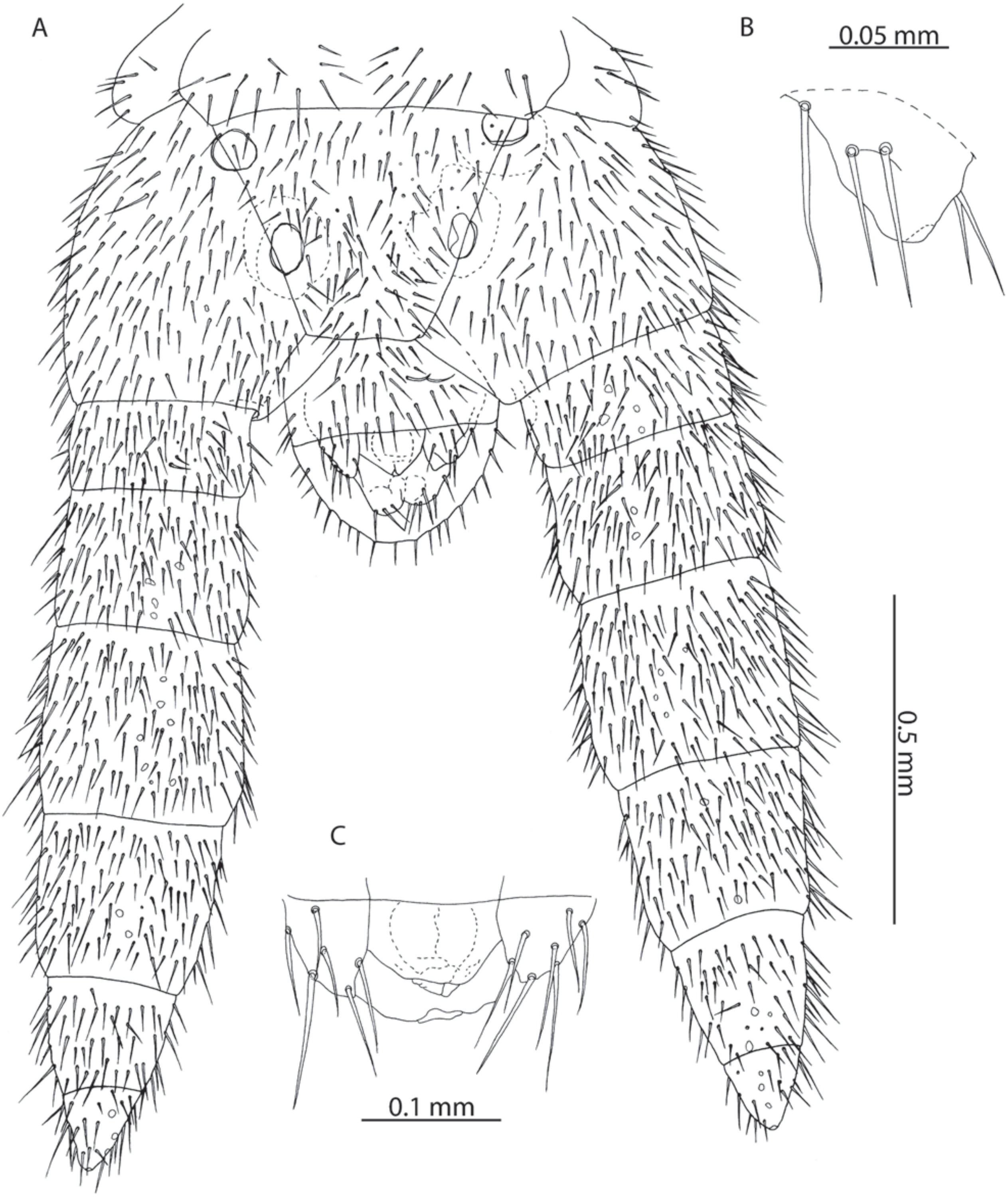

Figure 23. *Ityphilus* cf. *taeniaformis* (Lawrence, 1960). NHMUK015991468 **A** ultimate leg-bearing and postpedal segments, ventral view **B** tip of right ultimate leg telopodite, ventral view **C** male gonopods, ventral view.

leg-bearing segment telopodite and the number of leg-bearing segments with *B. lawrencei*. As all Mauritian *Ballophilus* species are known solely from their holotypes, it is not possible to comment on intraspecific variability that may account for the overlap in these traits.

Ballophilus maldivensis Pocock, 1906, described from the Maldives, similarly resembles the Aldabra specimen in the shape of the metasternal pore fields and their pigmentation. The incomplete original description did not allow for comparison of any other putative diagnostic characters beside the number of leg-bearing segments (67 in the female holotype), which is lower than that of the Aldabra specimen (75 in a male). Re-examination of the holotype (Fig. 24), the sole known specimen, revealed several features that further distance it from the Aldabra specimen and bring it closer to the currently accepted diagnosis of *Ballophilus*. *Ballophilus maldivensis* lacks chitin lines

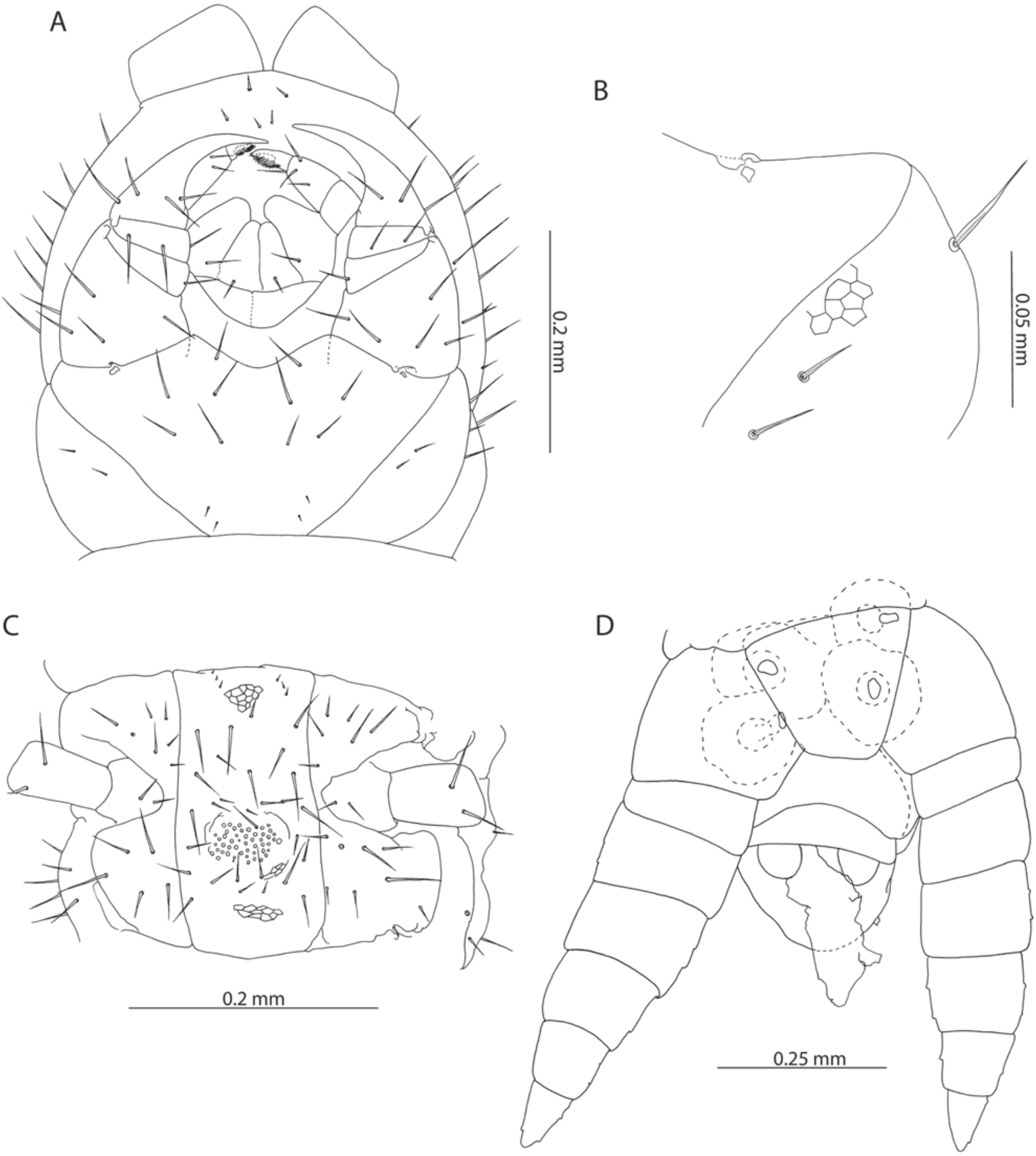

Figure 24. *Ballophilus maldivensis* Pocock, 1906. BMNH #200555 **A** head and forcipular segment, ventral view **B** magnified view of forcipular coxosternite showing lateral pleurite and condyle, right side, ventral view **C** metasternite of leg-bearing segment 7, ventral view **D** ultimate leg-bearing and postpedal segments, ventral view.

or any cuticular thickenings near their position (Fig. 24A, B). Other important differences from *I.* cf. *taeniaformis* from Aldabra include the absence of the metasternal pore field from the last four leg-bearing segments and a more strongly enlarged ultimate leg telopodite (Fig. 24D).

Lawrence (1960) described three species assigned to *Ballophilus* from Madagascar, of which *Ballophilus taeniaformis* Lawrence, 1960 overlaps in nearly all diagnostic traits with the Aldabra material examined, differing only in the number of teeth on the dentate lamella of the mandible (7 in the Aldabra specimen compared to eight or nine in *B. taeniaformis*). Lawrence made no comment on the presence or absence of the chitin line on the forcipular coxosternite for the species he assigned to *Ballophilus*. As noted above, this character has been used to differentiate between the genera *Ballophilus* and *Ityphilus*, although its variability as discussed above and the lack of consensus on the status of *Ityphilus* at the time of Lawrence's original description of *B. taeniaformis* prompt us to refer the examined specimen from Aldabra to *Ityphilus*.

In nearly all characters examined, the singular specimen from Aldabra agrees with the description of *Ityphilus melanostigma* (Attems 1900) and the subsequent redescription of this species from specimens collected in the Seychelles (Bonato and Minelli 2010). However, the greatly reduced number of leg-bearing segments (75) relative to the presently known range within *I. melanostigma* (95–101) suggest specific distinction, as extensive variation in leg-bearing segment number is not generally known from other species of *Ityphilus*. Other putative differences to the original description of *I. melanostigma* include the greater relative enlargement of the ultimate leg pair telopodites in the Aldabra specimen, relative to *Ityphilus* specimens illustrated from the Seychelles (Bonato and Minelli 2010).

Discussion

Composition and affinities of the Aldabran centipede fauna

With the exception of *Australobius inflatitarsis*, all centipede species previously recorded from Aldabra are represented in the examined sample. This includes nine species new to the atoll, raising the total number of centipede species known from Aldabra to 12. The high abundance of *L. tristani* and *Cryptops* specimens in the examined sample is surprising given the lack of previous mentions of their presence on the atoll.

Of the recorded species, half are shared with other islands of the Seychelles (Lewis 2010b; Stoev and Gerlach 2010) and approximately a third with both Mauritius and the Chagos Archipelago (Table 4; Verhoeff 1939; Lewis and Daszak 1996; Lewis 2002; Popovici et al. 2024). Some have a wide to near-cosmopolitan distribution and have been recorded from mainland localities in East Africa (*Cryptops nigropictus*, *Mecistocephalus angusticeps*, *Scolopendra morsitans*; Ribaut 1914; Lewis 1969; Zapparoli 1990) and the Indian subcontinent (*Orphnaeus dekanius*, *Scolopendra morsitans*; Verhoeff 1938; Joshi and Karanth 2011) or have been recorded from coastal localities across the entire Indian Ocean (*Orphnaeus dekanius*, *Tuoba sydneyenis*; Bonato and Minelli 2010; Popovici et al. 2024). The new records of *S. morsitans* from Aldabra confirm its presence in the outer islands of the Seychelles, which was previously suggested as likely despite the lack of known specimens (Lewis 2007a).

Table 4. Occurrence data of centipede species found on the Aldabra Atoll and in nearby areas. Asterisk indicates that morphologically similar congeners have been recorded from the locality but taxonomic revision is required to confirm their identity.

Species	Locality					
	Chagos Archipelago	**Madagascar**	**Maldives**	**Mauritius**	**Seychelles (inner islands)**	**East Africa (mainland)**
Australobius inflatitarsis	Not recorded	Not recorded	Not recorded	Not recorded	**Recorded**	Not recorded
Lamyctes tristani	**Recorded**	**Recorded**	Not recorded	Not recorded*	Not recorded	Not recorded
Cryptops cf. *japonicus*	Not recorded	Not recorded	Not recorded	Not recorded	Not recorded*	Not recorded
Cryptops mauritianus	Not recorded	Not recorded	Not recorded	**Recorded**	Not recorded	Not recorded
Cryptops nigropictus	Not recorded	Not recorded	Not recorded	**Recorded**	**Recorded**	**Recorded**
Scolopendra morsitans	Not recorded	Not recorded	Not recorded	**Recorded**	Not recorded	**Recorded**
Ityphilus cf. *taeniaformis*	Not recorded	**Recorded**	Not recorded	Not recorded	Not recorded*	Not recorded
Mecistocephalus angusticeps	**Recorded**	Not recorded	Not recorded	Not recorded	**Recorded**	**Recorded**
Mecistocephalus lohmanderi	**Recorded**	Not recorded*	**Recorded**	**Recorded**	**Recorded**	Not recorded
Orphnaeus dekanius	**Recorded**	Not recorded*	**Recorded**	Not recorded	Not recorded	Not recorded*
Ribautia cf. *paucipes*	Not recorded	Not recorded	Not recorded	Not recorded	**Recorded**	Not recorded
Tuoba sydneyensis	Not recorded	**Recorded**	Not recorded	**Recorded**	**Recorded**	Not recorded

Comparison with literature data and specimens from Mauritius in the NHM collection reveals that there are no centipedes endemic to Aldabra that are obviously diverging in morphology, and most species occur throughout the Western Indian Ocean islands. Overviews of diagnostic morphological characters given above and in previous surveys of Western Indian Ocean centipedes (Bonato and Minelli 2010; Popovici et al. 2024) strongly suggest that these populations may be closely related and part of a distinctive centipede fauna unique to the Western Indian Ocean, characterised by strong dispersive potential rather than localised radiations within island groups. In the absence of molecular data that would allow for the interrogation of population structure as well as additional vetting of the proposed identifications, and a more complete sample of centipedes from the Comoros and Mascarene island groups, these conclusions are only tentative and based on morphological examination of collected specimens. Similarly, the unresolved taxonomy of the genera *Cryptops*, *Ityphilus*, and *Lamyctes*, particularly in the Western Indian Ocean, makes the apparent absence of *L. tristani* and *Ityphilus* cf. *taeniaformis* potentially doubtful from islands in which morphologically similar congeners have been recorded (Bonato and Minelli 2010; Stoev and Gerlach 2010), as future taxonomic revision may reveal that these populations are conspecific.

Human-mediated introduction of centipedes to the Aldabra Atoll is difficult to assess in light of the patchy information on its early human habitation (Stoddart 1971). The atoll was apparently uninhabited when a hydrographic survey was conducted in 1878, and settlement at Picard has been continuous but sparsely populated since 1890. Plantings of coconut, maize, sisal, cotton and other crops by the late 19th Century may account for some soil invertebrate introductions, including centipedes. Approximately 20% of plant species known from Aldabra are considered to be human-mediated introductions, despite a small area devoted to plantations (Renvoize 1971). Human introductions of terrestrial invertebrates are generally poorly characterised across the Western Indian Ocean but have been recorded for the terrestrial gastropod *Achatina fulica* Férussac, 1821 (Peake 1971) and for terrestrial invertebrates in the Chagos Islands (https://chagosinformationportal.org/uploads/Terrestrial_Inverts_of_BIOT_21_03_18_1.xlsx), where 50% of recorded species are listed as introduced and 2.8% as potentially invasive, as well as suggested for the geophilomorph *Tygarrup javanicus* Attems, 1929 in the granitic inner islands of the Seychelles (Bonato and Minelli 2010).

Being comprised of low to mid-elevation atolls, we consider the Chagos islands a useful guidepost for evaluating the possibility of centipede introductions to Aldabra. The cryptic habits of most centipedes pose challenges to accurately assessing present diversity, let alone introduction potential. One isolated record in Feasibility Study for the Resettlement of the British Indian Ocean Territory Draft Report (https://data.parliament.uk/DepositedPapers/Files/DEP2014-1543/Feasibility_Study_for_the_Resettlement_of_the_BIOT_Draft_Report.pdf) attests to the import of soil from Sri Lanka on some islands, potentially representing a channel for centipede introduction. The morphological similarity of Chagossian *Rhysida longipes* to Sri Lankan populations of this species (Popovici et al. 2024) well as its classification as a likely invasive (https://chagosinformationportal.org/uploads/Terrestrial_Inverts_of_BIOT_21_03_18_1.xlsx) both indicate that introduction of this species to its Western Indian Ocean locality may have been human-mediated, in association with ballast or imported soil. The lack of any comprehensive historical record of such soil or vegetation transfers on Aldabra makes it difficult to ascribe the presence of any presently reported centipede species to human introduction.

The status of *Nycternyssa*

The genus *Nycternyssa* was erected by Crabill (1959), comprising the newly described *Nycternyssa stheno* Crabill, 1959 from Okinawa, Japan and four other taxa previously included in *Orphnaeus*, namely *Nycternyssa conspersa* (Verhoeff, 1937a), *Nycternyssa dekania dekania* (Verhoeff, 1938), *Nycternyssa dekania singaporiensis* (Verhoeff, 1937b) and *Nycternyssa eidmanni* (Verhoeff, 1942). The original generic diagnosis states “*Orphnaeus* differs from *Nycternyssa* in that the female gonopod is divided into two distinct articles while it is simple and undivided in *Nycternyssa*”, with both genera being distinguished from all other related oryids by having only one row of paratergites. No comment was made on characters that differ between male specimens of *Orphnaeus* and *Nycternyssa*. Additional characters listed in the diagnosis of *Nycternyssa*, based on the description of *N. stheno*, are of ambiguous significance or shared by *Orphnaeus*. Crabill (1959) remarked that the first maxillary telopodite is “bipartite”, although the accompanying illustrations provided for *N. stheno* show it as unambiguously uniarticulated and otherwise identical in aspect to illustrations of this structure given for *Orphnaeus* (Fig. 14A). The antennae of *Nycternyssa* are described as barely attenuate and barely flattened proximally, in contrast to the diagnosis of *Orphnaeus* in which the proximal end of the antennae is described as flattened ("plattgedrückt") (Attems 1929). This difference of appearance is likely a result of the time since collection and fixation medium of examined specimens, as variation within it can be observed within conspecific individuals from the same locality (Fig. 12A, C), and similar deformations of antennal shape in other geophilomorph taxa have likewise been treated as carrying dubious taxonomic value (Dányi and Tuf 2017; Popovici 2024).

Subsequent mentions of *Orphnaeus* restate the biarticulate nature of the female gonopods as characteristic for the genus (Crabill 1968), or do not comment on this character specifically, but stress the uniarticulate female gonopods of *Nycternyssa* as diagnostic (Bonato 2011). Although this character is regarded as fixed in *Orphnaeus* in the monograph on Geophilomorpha compiled by Attems (1929), several earlier accounts of the type species, *O. brevilabiatus*, do not clearly illustrate biarticulate female gonopods (Saussure and Humbert 1872; Haase 1887), incorrectly identify male specimens as female (Pocock 1889), do not mention the female gonopods in generic keys (Pocock 1893), or illustrate unambiguously uniarticulate female gonopods (Pocock 1896, Saussure and de Zehntner 1902). Although the type material for this species is presumed to be lost, we examined and illustrate the two specimens mentioned by Pocock (1891b) from areas near the type locality in present-day Myanmar (Burma) (Figs 17, 18A–C). One of the two specimens with provenance given as S. Tenasserim is an adult female with unambiguously uniarticulate gonopods (Fig. 18A). Notably Pocock (1891b) mentioned, "I have carefully compared the types of *brevilabiatus* and *lineatus* […]", implying that the condition of the gonopods in the female specimen from S. Tenasserim and that of the type material did not raise any doubt with respect to the identity of these specimens. As no other morphological characters of the near-topotypic specimens illustrated here suggest they are different from *O. brevilabiatus* as originally described, we consider that the articulation of the female gonopods is likely variable within *Orphnaeus*. Given that there are no characters to support the reciprocal monophyly of both genera, *Nycternyssa* is here placed in junior subjective synonymy.

Specimens identified as *O. brevilabiatus* from other localities displayed variably biarticulate female gonopods, a state previously considered typical for this species (Fig. 18A–C). The present observations rise further doubt on the identity of old records of *O. brevilabiatus* and agree with the reserve of other authors in continuing to treat *O. brevilabiatus* as a single, pantropical species (Würmli 1974). As intraspecific variation in the articulation of the female gonopods is not known in Oryidae, it is possible that the specimens assigned to *O. brevilabiatus* are part of a complex of morphologically similar species.

Acknowledgements

We thank Jan Beccaloni (The Natural History Museum) for curatorial support and providing access to the collection. We are grateful to Lauren Hughes (The Natural History Museum) for kindly providing lab space, and to Lucio Bonato (Università degli Studi di Padova) and Pavel Stoev (National Museum of Natural History, Bulgarian Academy of Sciences) for constructive reviews of the manuscript.

Additional information

Conflict of interest

The authors have declared that no competing interests exist.

Ethical statement

No ethical statement was reported.

Funding

No funding was reported.

Author contributions

Conceptualization: GP, GDE. Investigation: GP. Writing – original draft: GP, GDE. Writing – review and editing: GDE, GP.

Author ORCIDs

George Popovici https://orcid.org/0000-0003-0662-7472
Gregory D. Edgecombe https://orcid.org/0000-0002-9591-8011

Data availability

All of the data that support the findings of this study are available in the main text.

References

Agnarsson I, Kuntner M (2012) The Generation of a Biodiversity Hotspot: Biogeography and Phylogeography of the Western Indian Ocean Islands. In: Anamthawat-Jonsson K (Ed.) Current Topics in Phylogenetics and Phylogeography of Terrestrial and Aquatic Systems. InTech, 33–82. https://doi.org/10.5772/38958

Agnarsson I, Jencik B, Veve G, Hanitriniaina S, Agostini D, Goh S, Pruitt J, Kuntner M (2015) Systematics of the Madagascar *Anelosimus* spiders: remarkable local richness and endemism, and dual colonization from the Americas. ZooKeys 509: 13–52. https://doi.org/10.3897/zookeys.509.8897

Attems C (1909) Myriopoda. In: Sjöstedt Y (Ed.) Wissenschaftliche Ergebnisse der Schwedischen Zoologischen Expedition nach dem Kilimandjaro, dem Meru und den umgebenden Massaisteppen Deutsch-Ostafrikas 1905–1906. Palmquists, Stockholm 19: 1–64.

Attems C (1929) Geophilomorpha. Das Tierreich, 52. W. de Gruyter & Co., Berlin/Leipzig. [XXIII +] 388 pp.

Attems C (1952) Neue Myriopoden des Belgischen Congo. Annales du Musée Royal du Congo Belge, Tervuren (Belgique) 18: 1–139.

Attorre F, Van Damme K (2020) Twenty years of biodiversity research and nature conservation in the Socotra Archipelago (Yemen). Rendiconti Lincei. Scienze Fisiche e Naturali 31: 563–569. https://doi.org/10.1007/s12210-020-00941-7

Austin JJ, Arnold EN, Jones CG (2004) Reconstructing an island radiation using ancient and recent DNA: the extinct and living day geckos (*Phelsuma*) of the Mascarene islands. Molecular Phylogenetics and Evolution 31(1): 109–122. https://doi.org/10.1016/j.ympev.2003.07.011

Bergsten J, Biström O (2022) Diversification in the Comoros: Review of the *Laccophilus alluaudi* Species Group with the Description of Four New Species (Coleoptera: Dytiscidae). Diversity 14(2): 81. https://doi.org/10.3390/d14020081

Bonato L (2011) Chilopoda – Taxonomic Overview. Order Geophilomorpha. In: Minelli A (Eds) Treatise on Zoology – Anatomy, Taxonomy, Biology. The Myriapoda, Vol. 1. Leiden, The Netherlands: Brill. 538 pp. https://doi.org/10.1163/9789004188266

Bonato L, Minelli A (2004) The centipede genus *Mecistocephalus* Newport 1843 in the Indian Peninsula (Chilopoda Geophilomorpha Mecistocephalidae). Tropical Zoology 17(1): 15–63. https://doi.org/10.1080/03946975.2004.10531198

Bonato L, Minelli A (2010) The geophilomorph centipedes of the Seychelles (Chilopoda: Geophilomorpha). Phelsuma 18: 9–38.

Bonato L, Pereira LA, Minelli A (2007) Taxonomic and nomenclatural notes on the centipede genera *Chomatobius*, *Ityphilus*, *Hapleurytion*, *Plateurytion*, and *Steneurytion* (Chilopoda: Geophilomorpha). Zootaxa 1485: 1–12. https://doi.org/10.11646/zootaxa.1485.1.1

Braithwaite CJR, Taylor JD, Kennedy WJ (1973) The evolution of an atoll: the depositional and erosional history of Aldabra. Philosophical Transactions of the Royal Society of London B 266: 307–340. https://doi.org/10.1098/rstb.1973.0051

Brena C (2014) The embryoid development of *Strigamia maritima* and its bearing on post-embryonic segmentation of geophilomorph centipedes. Frontiers in Zoology 11: 58. https://doi.org/10.1186/s12983-014-0058-9

Brölemann H (1909) À propos d'un système des géophilomorphes. Archives de Zoologie Expérimentale et Générale 5(3): 303–340.

Bücherl W (1946) Novedades sistematicas na ordem Scolopendromorpha. Memórias do Instituto Butantan 19: 135–158

Camoin GF, Motaggioni LF, Braithwaite CJR (2004) Late glacial to postglacial sea level changes in the Western Indian Ocean. Marine Geology 206(1–4): 119–146. https://doi.org/10.1016/j.margeo.2004.02.003

Chamberlin RV (1920) The Myriopoda of the Australian region. Bulletin of the Museum of Comparative Zoology, Harvard College 64: 1–269.

Chao JL (2008) Scolopendromorpha (Chilopoda) of Taiwan. VDM Verlag Dr. Müller Aktiengesellschaft & Co. KG, Saarbrücken, Germany, 94 pp.

Cheke A (2010) The timing of arrival of humans and their commensal animals on Western Indian Ocean oceanic islands. Phelsuma 18: 38–69.

Cogan BH, Hutson AM, Shaffer JC (1971) Preliminary observations on the affinities and composition of the insect fauna of Aldabra. Philosophical Transactions of the Royal Society of London B 260: 315–325. https://doi.org/10.1098/rstb.1971.0017

Cook OF (1899) The Geophiloidea of the Florida Keys. Proceedings of the Entomological Society of Washington 4: 303–312.

Crabill RE (1959) A new centipede from Okinawa (Chilopoda: Oryidae). Pacific Insects 1: 173–176.

Crabill RE (1968) A New Oryid Genus and Species from Africa, with Generic Key and Notes on Evolution within the Family Oryidae (Chilopoda: Geophilomorpha). Entomological News 79: 246–253.

Dányi L, Tuf IH (2017) On the identity of *Photophilus* Folkmanová, 1928: A new generic synonymy (Chilopoda: Geophilomorpha: Geophilidae). Zootaxa 4347(2): 361–370. https://doi.org/10.11646/zootaxa.4347.2.10

Demange JM (1963) Chilopoda. La réserve naturelle integrale du Mont Nimba – Mémoires de l'Institut Française d'Afrique Noire 5: 41–118.

Eason EH (1978) On Lithobiidae from the Seychelles with description of two new species of the subgenus *Australobius*, genus *Lithobius* (Chilopoda: Lithobiomorpha). Journal of Zoology 184: 21–34. https://doi.org/10.1111/j.1469-7998.1978.tb03263.x

Gerlach J (2006) Terrestrial and Freshwater Mollusca of the Seychelles islands. Backhuys, Leiden 1–117.

Gerlach J (2012) Red Listing reveals the true state of biodiversity – a comprehensive assessment of Seychelles biodiversity. Phelsuma 20: 8–22.

Gregory SJ, Barber AD (2010) Observations of a population, including juveniles, of *Geophilus carpophagus* Leach, 1815, sensu stricto from Oxfordshire. Bulletin of the British Myriapod and Isopod Group 24: 2–15.

Griffiths OL, Florens VFB (2006) A Field Guide to the Non-Marine Molluscs of the Mascarene Islands (Mauritius, Rodrigues and Réunion) and the Northern Dependencies of Mauritius. Bioculture Press, Mauritius 1–185.

Haase E (1887) Die Indisch-Australischen Myriopoden. Pt. I. Chilopoden. Abhandlungen und Berichte des Königl. Zoologischen und Anthropologisch-Etnographischen Museums zu Dresden 5: 1–118.

Haverkamp PJ, Shekeine J, de Jong R, Schaepman M, Turnbull LA, Baxter R, Hansen D, Bunbury N, Fleischer-Dogley F, Schaepman-Strub G (2017) Giant tortoise habitats under increasing drought conditions on Aldabra Atoll—Ecological indicators to monitor rainfall anomalies and related vegetation activity. Ecological Indicators 80: 354–362. https://doi.org/10.1016/j.ecolind.2017.05.029

Hawlitschek O, Brückmann B, Berger J, Green K, Glaw F (2011) Integrating field surveys and remote sensing data to study distribution, habitat use and conservation status of the herpetofauna of the Comoro Islands. ZooKeys 144: 21–78. https://doi.org/10.3897/zookeys.144.1648

Hill MG, Newbery DM (1982) An Analysis of the Origins and Affinities of the Coccid Fauna (Coccoidea; Homoptera) of Western Indian Ocean Islands, with Special Reference to Aldabra Atoll. Journal of Biogeography 9(3): 223–229. https://doi.org/10.2307/2844665

Horneland EO, Meidell B (2009) Postembryonic development of *Strigamia maritima* (Leach, 1817) (Chilopoda: Geophilomorpha, Linotaeniidae) with emphasis on how to separate the different stadia. Soil Organisms 81(3): 373–386. https://soil-organisms.org/index.php/SO/article/view/34

Hume JP, Martill D, Hing R (2018) A terrestrial vertebrate palaeontological review of Aldabra Atoll, Aldabra Group, Seychelles. PLoS ONE 13(3): e0192675. https://doi.org/10.1371/journal.pone.0192675

Ibouroi MT, Dhurham SAO, Besnard A, Lescureux N (2021) Understanding Drivers of Unsustainable Natural Resource Use in the Comoro Islands. Tropical Conservation Science 14(1). https://doi.org/10.1177/19400829211032585

Iorio E, Geoffroy J-J (2003) Etude des Scolopendromorphes français du genre *Cryptops* Leach 1814 – Première partie: *Cryptops parisi* Brolemann, 1920 et *C. parisi* var. *cristata* Ribaut, 1925 (Chilopoda, Scolopendromorpha, Cryptopidae). Bulletin de Phyllie n° 18–4^{e} trimestre: 28–37.

Jangi BS (1955) Some aspects of the morphology of the centipede *Scolopendra morsitans* Linn. (Scolopendridae). Annals and Magazine of Natural History 8(92): 597–607. https://doi.org/10.1080/00222935508655671

Jangi BS (1959) Further notes on the taxonomy of the centipede *Scolopendra morsitans* Linnaeus (Scolopendridae). Entomological News 70: 253–257.

Jones RE (1998) On the species of *Tuoba* (Chilopoda: Geophilomorpha) in Australia, New Zealand, New Caledonia, Solomon Islands and New Britain. Records of the Western Australian Museum 18: 333–346.

Joshi J, Karanth KP (2011) Cretaceous-Tertiary diversification among select Scolopendrid centipedes of South India. Molecular Phylogenetics and Evolution 60(3): 287–294. https://doi.org/10.1016/j.ympev.2011.04.024

Kehlmaier C, Graciá E, Ali JR, Campbell PD, Chapman SD, Deepak V, Ihlow F, Jalil NE, Pierre-Huyet L, Samonds KE, Vences M, Fritz U (2023) Ancient DNA elucidates the lost world of western Indian Ocean giant tortoises and reveals a new extinct species from Madagascar. Science Advances 9(2): eabq2574. https://doi.org/10.1126/sciadv.abq2574

Kronmüller C (2010) *Scolopendra antananarivoensis* spec. nov. – a new species of *Scolopendra* Linnaeus, 1758 related to *Scolopendra morsitans* Linnaeus, 1758 from Madagascar (Myriapoda, Chilopoda, Scolopendridae). Spixiana 33: 281–288.

Lawrence RF (1960) Myriapodes – Chilopodes. Faune de Madagascar 12: 1–123.

Lawrence JM (2015) A short note on the biogeography of the rarely observed Seychelles butterflies. Phelsuma 23: 1–5.

Legros V, Rochat J, Reynaud B, Strasberg D (2020) Known and unknown terrestrial arthropod fauna of La Réunion Island, Indian Ocean. Journal of Insect Conservation 24: 199–217. https://doi.org/10.1007/s10841-019-00188-0

Lewis JGE (1963) On *Clinopodes poseidonis* (Verhoeff) (Chilopoda: Geophilomorpha: Geophilidae) with a description of a new subspecies from the Red Sea littoral. Annals and Magazine of Natural History 13(6)(B): 49–55. https://doi.org/10.1080/00222936308651322

Lewis JGE (1966) The taxonomy and biology of the centipede *Scolopendra amazonica* in the Sudan. Journal of Zoology, London 149: 188–203. https://doi.org/10.1111/j.1469-7998.1966.tb03893.x

Lewis JGE (1967) The scolopendromorph centipedes of the Sudan with remarks on taxonomic characters in the Scolopendridae. Proceedings of the Linnean Society of London 178: 185–207. https://doi.org/10.1111/j.1095-8312.1967.tb00973.x

Lewis JGE (1968) Individual variation in a population of the centipede *Scolopendra amazonica* from Nigeria and its implications for methods of taxonomic discrimination in the Scolopendridae. Journal of the Linnean Society (Zoology) 47: 315–326.

Lewis JGE (1969) The variation of the centipede *Scolopendra amazonica* in Africa. Zoological Journal of the Linnean Society 48: 49–57. https://doi.org/10.1111/j.1096-3642.1969.tb00704.x

Lewis JGE (1996) Further records of scolopendromorph and geophilomorph centipedes from the Arabian Peninsula with a note by Dr. E. H. Eason on *Lithobius erythrocephalus cronebergii* Sseliwanoff. Fauna of Saudi Arabia 15: 137–156.

Lewis JGE (2002) The scolopendromorph centipedes of Mauritius and Rodrigues and their adjacent islets (Chilopoda: Scolopendromorpha). Journal of Natural History 36: 79–106. https://doi.org/10.1080/00222930110098508

Lewis JGE (2007a) Scolopendromorph centipedes from Seychelles with a review of previous records (Chilopoda: Scolopendromorpha). Phelsuma 15: 8–25.

Lewis JGE (2007b): On *Cryptops doriae* Pocock, from the wet tropical biome of the Eden Project, Cornwall (Chilopoda, Scolopendromorpha, Cryptopidae). Bulletin of the British Myriapod and Isopod Group 22: 12–16.

Lewis JGE (2009) A review of some characters used in the taxonomy of *Cryptops* (subgenus *Cryptops*) (Chilopoda: Scolopendromorpha: Cryptopidae). Soil Organisms 81: 505–518.

Lewis JGE (2010a) A key and annotated list of the *Scolopendra* species of the Old World with a reappraisal of *Arthrorhabdus* (Chilopoda: Scolopendromorpha: Scolopendridae). International Journal of Myriapodology 3: 83–122. https://doi.org/10.1163/187525410X12578602960380

Lewis JGE (2010b) Order Scolopendromorpha Pocock, 1895. In: Gerlach J, Marusik Y (Eds) The Arachnida and Myriapoda of the Seychelles Islands. Siri Scientific Press, Manchester, 379–386.

Lewis JGE (2011) A review of the species in the genus *Cryptops* Leach, 1815 from the Old World related to *Cryptops* (*Cryptops*) *hortensis* (Donovan, 1810) (Chilopoda, Scolopendromorpha). International Journal of Myriapodology 4: 11–50. https://doi.org/10.3897/ijm.4.1116

Lewis JGE, Daszak P (1996) On centipedes collected on the Raleigh International Expedition to Mauritius and Rodrigues 1993, with a description of a new species of *Scolopendra* (Scolopendromorpha; Scolopendridae). Journal of Natural History 30: 293–297. https://doi.org/10.1080/00222939600771161

Lewis JGE, Gallagher MD (1993) Scolopendromorph and Geophilomorph centipedes from Oman and the United Arab Emirates. Fauna of Saudi Arabia 13: 55–62.

Lewis JGE, Wranik W (1990) On the centipedes of Yemen. Zoology in The Middle East 4: 61–70. https://doi.org/10.1080/09397140.1990.10637589

Lewis JGE, Daszak P, Jones CG, Cottingham JD, Wenman E, Maljkovic A (2010) Field observations on three scolopendrid centipedes from Mauritius and Rodrigues (Indian Ocean) (Chilopoda: Scolopendromorpha). International Journal of Myriapodology 3: 123–137. https://doi.org/10.1163/187525410X12578602960425

Linnaeus C (1758) Systema naturae. Editio Decima. Holmiae: 1–824.

Meinert F (1868) Danmarks Scolopender og Lithobier. Naturhistorisk Tidsskrift 5: 241–268.

Meinert F (1870) Myriapoda Musei Hauniensis. Bidrag til myriapodernes morphologi og systematik. I. Geophili. Naturhistorisk Tidsskrift 7: 1–128.

Myers N, Mittermeier RA, Mittermeier CG, da Fonseca GA, Kent J (2000) Biodiversity hotspots for conservation priorities. Nature 403(6772): 853–858. https://doi.org/10.1038/35002501

Nagy ZT, Joger U, Wink M, Glaw F, Vences M (2003) Multiple colonization of Madagascar and Socotra by colubrid snakes: evidence from nuclear and mitochondrial gene phylogenies. Proceedings of the Royal Society of London B 270: 2613–2621. https://doi.org/10.1098/rspb.2003.2547

Newport G (1843) On some new genera of the class Myriapoda. Proceedings of the Zoological Society of London, 10 (1842): 177–181.Newport G. 1844. A list of the species of Myriapoda, order Chilopoda, contained in the cabinets of the British Museum, with a synoptic description of forty-seven species. Annals and Magazine of Natural History 13: 94–101. https://doi.org/10.1080/03745484409442576

Newport G (1845) XXVIII. Monograph of the Class Myriapoda, Order Chilopoda. Transactions of the Linnean Society of London 19(4): 349–439. https://doi.org/10.1111/j.1096-3642.1842.tb00370.x

Peake JF (1971) The Evolution of Terrestrial Faunas in the Western Indian Ocean. Philosophical Transactions of the Royal Society of London, B 260(836): 581–610. https://doi.org/10.1098/rstb.1971.0027

Pereira LA (2000) The preparation of centipedes for microscopical examination with particular reference to the Geophilomorpha. Bulletin of the British Myriapod Group 16: 22–25.

Pereira LA (2017) A new miniature species of geophilomorph centipede from the Ecuadorian Amazon rainforest (Chilopoda: Geophilomorpha: Ballophilidae). Studies on Neotropical Fauna and Environment *53*(2): 91–106. https://doi.org/10.1080/01650521.2017.1412687

Pereira LA, Foddai D, Minelli A (1997) First Record of a Ballophilid Centipede from Argentina with a Description of *Ballophilus ramirezi* n.sp. (Chilopoda: Geophilomorpha: Ballophilidae). Studies on Neotropical Fauna and Environment 31(3–4): 170–178. https://doi.org/10.1076/snfe.31.3.170.13335

Pereira LA, Foddai D, Minelli A (2000) New taxa of Neotropical Geophilomorpha (Chilopoda). Amazoniana 16: 1–57.

Peretti E, Bonato L (2016) *Geophilus pygmaeus* (Chilopoda: Geophilidae): clarifying morphology, variation and geographic distribution. Zootaxa 4139(4): 499–514. https://doi.org/10.11646/zootaxa.4139.4.3

Plummer P (1995) Planet Aldabra. In: Amin M, Willetts D, Skerrett A, editors. Aldabra—World Heritage Site. Nairobi: Camerapix International & Seychelles Islands Foundation: 1995 49–70.

Pocock RI (1889) Report on the Myriopoda of the Mergui Archipelago collected by Dr. Anderson F.R.S. Journal of the Linnean Society of London, Zoology 21: 287–303. https://doi.org/10.1111/j.1096-3642.1889.tb00980.x

Pocock RI (1891a) Descriptions of some new Geophilidae in the collection of the British Museum. Annals and Magazine of Natural History 6(8): 215–227. https://doi.org/10.1080/00222939109460423

Pocock RI (1891b) On the Myriopoda of Burma. Part 2. Report upon the Chilopoda collected by Sig. L. Fea and Mr. E. W. Oates. Annals and Magazine of Natural History 8(6): 152–164. https://doi.org/10.1080/00222939109460410

Pocock RI (1893) Report upon the Myriopoda of the ‘Challenger’ Expedition, with remarks upon the fauna of Bermuda. Annals and Magazine of Natural History 6(6): 121–142. https://doi.org/10.1080/00222939308677479

Pocock RI (1896) Chilopoda. In: Godman F, Salvin O (Eds) Biologia Centrali-Americana, London 12: 1–40.

Pocock RI (1906) Chilopoda and Diplopoda. In: Gardiner JS (E.) The Fauna and Geography of the Maldive and Laccadive Archipelagoes 2, Supplement 2. Cambridge University Press, 1042–1045.

Popovici G (2024) A review of the genus *Pachymerium* C. L. Koch, 1847 (Geophilomorpha, Geophilidae) from Romania. Zootaxa 5406(4): 588–600. https://doi.org/10.11646/zootaxa.5406.4.7

Popovici G, Edgecombe GD, Hall DW (2024) New Chilopoda from the Chagos Archipelago. Journal of Natural History 58(41–44): 1885–1915. https://doi.org/10.1080/00222933.2024.2395903

Rajulu GS (1970) Tracheal pulsation in a marine centipede *Mixophilus indicus*. Current Science 39(17): 397–398.

Renvoize SA (1971) The origin and distribution of the flora of Aldabra. Philosophical Transactions of the Royal Society of London, B 260: 227–236. https://doi.org/10.1098/rstb.1971.0012

Ribaut H (1914) Voyage de Ch. Alluaud et R. Jeannel en Afrique Orientale (1911–1912). Résultats Scientifiques. Myriapodes. I. Chilopoda. Libr. A. Schulz, Paris 1–35.

Saussure H, Humbert A (1872) Études sur les Myriapodes. In: Milne Edwards H (Ed.) Mission scientifique au Mexique et dans l’Amérique Centrale. Recherches zoologiques. Mémoires du Muséum national d’Histoire naturelle, Paris 6(2): 1–211.

Saussure H, de Zehntner L (1902) Histoire naturelle des Myriapodes. In: Grandidier A (Ed.) Histoire physique naturelle et politique de Madagascar. Mémoires du Muséum national d'Histoire naturelle, Paris 37(53): [VIII +] 356.

Sherlock MB, Streicher JW, Gower DJ, Maddock ST, Nussbaum RA, Oommen OV, Serra Silva A, Day JJ, Wilkinson M (2024) Genomic SNPs resolve the phylogeny of an ancient amphibian island radiation from the Seychelles. Molecular Phylogenetics and Evolution 198: 108130. https://doi.org/10.1016/j.ympev.2024.108130

Silvestri F (1929) Description of a new genus and species of Geophilidae (Myriapoda Chilopoda) from Madras (India). Records of the Indian Museum, Calcutta 31(4): 263–267. https://doi.org/10.26515/rzsi/v31/i4/1929/162537

Siriwut W, Edgecombe GD, Sutcharit C, Tongkerd P, Panha S (2016) A taxonomic review of the centipede genus *Scolopendra* Linnaeus, 1758 (Scolopendromorpha, Scolopendridae) in mainland Southeast Asia, with description of a new species from Laos. ZooKeys 590: 1–124. https://doi.org/10.3897/zookeys.590.7950

Steibl S, Bunbury N, Young H, Russell J (2024) A renaissance of atoll ecology. Annual Review of Ecology Evolution and Systematics 55: 301–322. https://doi.org/10.1146/annurev-ecolsys-102722-013447

Stoddart DR (1971) Settlement, development and conservation of Aldabra. Philosophical Transactions of the Royal Society of London, B 260: 611–628. https://doi.org/10.1098/rstb.1971.0028

Stoev P, Gerlach J (2010) Lithobiomorpha Pocock, 1895 and Scutigeromorpha Pocock, 1895. In: Gerlach J, Marusik Y (Eds) Arachnida and Myriapoda of the Seychelles Islands. Siri Scientific Press, Manchester, 376–378.

Stojanović DZ, Mitić BM, Dudić BD, Gedged AM, Tomić VT, Antić DŽ, Makarov SE (2020) Early development of the centipede *Geophilus serbicus* (Chilopoda: Geophilomorpha: Geophilidae) from the Balkan Peninsula. Invertebrate Reproduction & Development 64(2): 115–125. https://doi.org/10.1080/07924259.2020.1726514

Takakuwa Y (1934) Sechs neue Arten der Chilopoden aus Japan. Transactions of the Sapporo Natural History Society 13: 398–406.

Takakuwa Y (1936) Über die japanischen *Cryptops*-Arten. Transactions of the Sapporo Natural History Society 14: 236–241.

Tercel MPTG, Cuff JP, Vaughan IP, Symondson WOC and others (2024) Ecology, natural history, and conservation status of *Scolopendra abnormis*, a threatened centipede endemic to Mauritius. Endangered Species Research 54:181–189. https://doi.org/10.3354/esr01337

Tuf IH, Dányi L (2015) True identity of *Folkmanovius paralellus* Dobroruka (Chilopoda: Geophilomorpha: Geophilidae). Zootaxa 4058(3): 444–450. https://doi.org/10.11646/zootaxa.4058.3.11

Verhoeff KW (1901) Beiträge zur Kenntnis paläarktischer Myriopoden. XVI. Aufsatz: zur vergleichenden Morphologie, Systematik und Geographie der Chilopoden. Nova Acta Abhandlungen der Kaiserlichen Leopoldinisch-Carolinisch Deutschen Akademie der Naturforscher 77: 369–465.

Verhoeff KW (1937a) Über einige Chilopoden aus Australien und Brasilien. Zoologische Jahrbücher, Abteilung für Systematik 70: 1–16.

Verhoeff KW (1937b) Chilopoden aus Malacca nach den Objecten des Raffles Museum in Singapore. Bulletin of the Raffles Museum 13: 198–270.

Verhoeff KW (1938) Chilopoden-Studien zur Kenntnis der Epimorphen. Zoologische Jahrbücher, Abteilung für Systematik 71: 339–388.

Verhoeff KW (1939) Chilopoden der Insel Mauritius. Zoologische Jahrbucher, Abteilung für Systematik, Ökologie und Geographie der Tiere 72: 71–98.

Verhoeff KW (1942) Myriopoden der Insel Fernando Po und über den Ankerapparat und die Spermaleitung der Spirostreptoideen XVI. Beitrag zu den Wissenschaftlichen Ergebnissen der Forschungsreise H. Eidmann nach Spanisch-Guinea – Zeitschrift für Morphologie und Ökologie der Tiere 39: 76–97. https://doi.org/10.1007/BF00403132

Wang YM (1955) Serica 1b. A preliminary report on the Myriapoda and Arachnida of Lan Yu Islets (Botel Tobago) China. Quarterly Journal of the Taiwan Museum 8: 195–201.

Warren BH, Bermingham E, Prys-Jones RP, Thebaud C (2005) Tracking island colonization history and phenotypic shifts in Indian Ocean bulbuls (Hypsipetes: Pycnonotidae). Biological Journal of the Linnean Society 85: 271–287. https://doi.org/10.1111/j.1095-8312.2005.00492.x

Würmli M (1974) Ergebnisse der Österreichischen Neukaledonien-Expedition 1965 Chilopoden. Annalen des Naturhistorischen Museums in Wien 78: 523–533.

Würmli M (1975) Systematische Kriterien in der Gruppe von *Scolopendra morsitans* Linné, 1758 (Chilopoda: Scolopendromorpha: Scolopendridae). Deutsche Entomologische Zeitschrift 22: 201–206.

Zapparoli M (1990) Note sui Chilopodi della Somalia. Biogeographia – The Journal of Integrative Biogeography 14: 125–147. https://doi.org/10.21426/B614110330

ZooKeys 1228: 275–286 (2025)
DOI: 10.3897/zookeys.1228.143710

Research Article

Three new species of Batrisini (Coleoptera, Staphylinidae, Pselaphinae) from southeast Xizang, China

Yong-Qin Zhang[1], Zi-Wei Yin[1]

1 *Laboratory of Systematic Entomology, College of Life Sciences, Shanghai Normal University, Xuhui District, Shanghai 200234, China*
Corresponding author: Zi-Wei Yin (pselaphinae@gmail.com)

Abstract

Three new species of the ant-loving beetle tribe Batrisini, Reitter, 1882 (Pselaphinae: Batrisitae) from southeast Xizang, China are described: *Arthromelodes lhunzensis* **sp. nov.**, *Tribasodites liangi* **sp. nov.**, and *Tribasodites yumaicus* **sp. nov.** Illustrations of the habitus and diagnostic features of these species are provided to aid identification. With these additions, the number of batrisine species known from Xizang increases to 83.

Key words: Ant-loving beetles, *Arthromelodes*, distribution, new taxa, taxonomy, *Tribasodites*

Academic editor: Jan Klimaszewski
Received: 6 December 2024
Accepted: 17 January 2025
Published: 21 February 2025

ZooBank: https://zoobank.org/2A22CD92-3BC6-40B2-A4BB-260FA831D8E1

Citation: Zhang Y-Q, Yin Z-W (2025) Three new species of Batrisini (Coleoptera, Staphylinidae, Pselaphinae) from southeast Xizang, China. ZooKeys 1228: 275–286. https://doi.org/10.3897/zookeys.1228.143710

Introduction

A recent monograph on the pselaphine tribe Batrisini Reitter, 1882 of Xizang has unveiled a previously undocumented yet diverse fauna, describing two new genera and 68 new species primarily distributed along the Himalaya and its southeastern region (Yin 2022). In this study, we report three new species belonging to the genera *Arthromelodes* Jeannel, 1954 and *Tribasodites* Jeannel, 1960, collected by Prof. Hong-Bin Liang and his team from a previously unsampled valley in Yümai, Xizang, China. These new findings increase the number of known Batrisini species in the region to 83 and highlight its potential for future discoveries, particularly in remote, underexplored areas.

Material and methods

The material treated in this paper is deposited in the Insect Collection of Shanghai Normal University, Shanghai, China (SNUC), and the Institute of Zoology, Chinese Academy of Sciences, Beijing, China (IZCAS). The label data of the material are quoted verbatim. Dissected parts were mounted in Euparal on plastic slides pinned with the specimen. The habitus images of the beetles were taken using a Canon EOS R5 camera, equipped with a 7.5× Mitutoyo M Plan Apo lens, with a Raynox DCR-150 macro lens in between serving as the tube lens; and three 10W LED bulbs (5500 K) were used as the light source. Images of morphological details were produced using a Canon G9 camera mounted to an Olympus CX31 compound microscope under reflected or transmitted light.

Helicon Focus Pro v. 8.2.0 was used for image stacking. All images were modified and grouped into plates using Adobe Photoshop CC 2020.

Measurements were taken as follows: total body length was measured from the anterior margin of the clypeus to the apex of the abdomen; head length was measured from the anterior margin of the clypeus to the head base, excluding the cervical constriction; head width was measured across the eyes; the length of the pronotum was measured along the midline, the width of the pronotum equals the maximum width; the length of the elytra was measured along the suture; the width of the elytra was measured as the maximum width across both elytra; the length of the abdomen is the length of the dorsally exposed part of the abdomen along its midline, the width is the maximum width. The terminology follows Chandler (2001) and Yin (2022). Abdominal tergites and sternites are numbered in Arabic (starting from the first visible segment) and Roman (reflecting true morphological position) numerals, e.g., tergite 1 (IV), or sternite 1 (III). Paired appendages in the descriptions are treated as singular.

Taxonomy

Arthromelodes lhunzensis sp. nov.

https://zoobank.org/BBDF3698-E89C-4C79-A7B8-C80E7E0280A2
Figs 1, 4
Chinese common name: 隆子丽蚁甲

Type material (1 ex.). ***Holotype*****:** China: • ♂: ‘China: Xizang, Shannan, Lhünzē County, Yümai Town, Jianzhejinzhe, 28°30'21"N, 93°07'07"E, 2930 m, in wood, 5.ix.2023, Hong-Bin Liang leg., 西藏隆子县玉麦乡件哲金哲’ (SNUC).

Diagnosis. Male. Body elongate, length 2.1 mm. Head, pronotum and abdomen much darker in color than elytra. Head sub-rectangular; vertex finely punctate, with transverse sinuate sulcus between antennal tubercles, foveae asetose. Antenna elongate, antennomeres more or less elongate, lacking obvious modifications; antennomere 11 approximately as long as 9 and 10 combined. Discal striae of elytra extending to approximately apical 4/5 of elytral length. Protibia with shallow disc-like impression at apical 2/5 of ventral surface; mesotibia with distinct apical spine. Abdomen with large tergite 1 (IV) longer than tergites 2–4 (V–VII) combined in dorsal view, simple. Aedeagus strongly asymmetric, median lobe with moderately large basal capsule and subtriangular foramen, ventral stalk much shorter than dorsal lobe. **Female.** Unknown.

Description. Male. Body (Fig. 1A) length 2.10 mm; head, pronotum and abdomen darkish-brown, elytra and legs reddish-brown, tarsi and mouthparts lighter in color. Dorsal surface finely punctate, covered with short pubescence.

Head (Fig. 1B) sub-rectangular, rounded at base, slightly wider than long, length 0.39 mm, width across eyes 0.41 mm; vertex finely punctate, with widely separated foveae (dorsal tentorial pits), with short, transverse sinuate sulcus at apical portion, lacking mediobasal carina; tempora slightly shorter than eyes, convergent posteriorly; antennal tubercles moderately raised; frons slightly impressed medially, confluent with clypeus; clypeus smooth, anterior margin carinate and moderately raised; ocular-mandibular carinae complete, distinct. Venter with small gular foveae (posterior tentorial pits) in single pit, with distinct median carina extending from pit anteriorly to mouthparts. Compound eyes prominent, composed of approximately 32 ommatidia. Maxillary palpus with palpomere 1 minute, 2 elongate, curved, pedunculate basally and enlarged apically, 3 short, sub-trapezoidal, 4 fusiform, widest near middle. Antenna moderately elongate, length 0.99 mm; club loosely formed by enlarged apical three antennomeres (Fig. 1C); antennomere 1 thick, subcylindrical, 2–7 each elongate, successively longer, 8 shortest, 9 much longer and broader than 8, 10 broader than 9, 11 longest, approximately as long as 9 and 10 combined (1:1), subfusiform.

Pronotum (Fig. 1B) slightly longer than wide, length 0.48 mm, width 0.44 mm, widest at middle; lateral margins rounded; disc moderately convex, finely punctate, with median longitudinal sulcus slightly longer than semicircular lateral sulci in dorsal view; lacking median antebasal fovea, with complete, deep transverse antebasal sulcus connecting lateral antebasal foveae; outer and inner pair of basolateral foveae distinct. Prosternum with basisternal (precoxal) portion longer than procoxal rests; with small lateral procoxal foveae; hypomeral grooves moderately long, extending from base anteriorly for almost entire length of hypomeron, lacking lateral procoxal pits, hypomeral ridges short, close to margins of coxal cavities.

Elytra slightly wider than long, length 0.70 mm, width 0.77 mm; moderately constricted and truncate at bases; each elytron with two large, asetose basal foveae; discal striae long, curved, extending from outer basal foveae posteriorly to 4/5 of elytral length; humeri moderately raised, small subhumeral foveae present, thin marginal striae extending posteriorly from foveae to posterior margins of elytra. Metathoracic wings fully developed.

Mesoventrite short, laterally fully demarcated from metaventrite by oblique ridges; median mesoventral foveae widely separated, originating from shared setose, transverse opening, lateral mesoventral foveae large and setose, broadly forked internally; prepectus massive, collar-shaped; mesoventral intercoxal process short, apically blunt; marginal striae complete. Metaventrite broadly and distinctly impressed at middle and densely setose at lateral portions of impression, with large, setose lateral mesocoxal foveae and pair of smaller, setose lateral metaventral foveae, metaventral intercoxal process with small and narrow split at middle.

Legs moderately elongate; protibia with disc-like impression at apical 2/5 of ventral surface (Fig. 1D); mesotibia with distinct spine at apex (Fig. 1E); mesofemur widened to middle.

Abdomen slightly narrower than elytra, widest at lateral margins of tergite 1(IV), length 0.62 mm, width 0.71 mm; lacking modifications. Tergite 1 (IV) longer than 2–4 (V–VII) combined, setose basal sulcus separated by mediobasal and one pair of basolateral foveae, lacking discal carinae; tergites 2–4 (V–VII) each with one pair of basolateral foveae, tergite 4 (VII) slightly shorter than 2 and 3 combined along middle, tergite 5 (VIII) semicircular, posterior margin roundly emarginate at middle. Sternite 2 (IV) with large mediobasal and broad basolateral foveae, lacking lateral carinae; midlength of sternite 2 (IV) slightly shorter than sternites 3–5 (V–VII) combined, 3–5 each with one pair of tiny basolateral foveae, sternite 6 (VIII) transverse, posterior margin sinuate, sternite 7 (IX) (Fig. 1F) suboval, weakly sclerotized, with scattered long setae along apical margin.

Aedeagus (Fig. 1G, H) 0.35 mm in length, moderately sclerotized, dorso-ventrally strongly asymmetric; median lobe with large, extended basal capsule and roundly triangular foramen, ventral stalk dorso-ventrally broadened at base and with pointed apex; dorsal lobe extremely elongate and evenly curved ventrally; parameres reduced to single broad membranous structure.

Figure 1. Morphology of *Arthromelodes lhunzensis* sp. nov., male **A** dorsal habitus **B** head and pronotum **C** antennal club **D** protibia **E** mesotibia **F** sternite 7 (IX) **G, H** aedeagus, lateral (**G**), and ventral (**H**). Scale bars: 0.5 mm (**A**); 0.3 mm (**B**); 0.2 mm in (**C, D, E**); 0.1 mm in (**F, G**); 0.05 mm (**A**).

Female. Unknown.

Comparative notes. The male of this species exhibits morphological similarities to *A. nepaeformis* Yin, 2022 distributed in Cona and Nyingchi counties, particularly in the general appearance and position of sexual characters on the male protibiae. However, these two species can be readily distinguished by the structure of their aedeagi. Additionally, *A. nepaeformis* is characterized by markedly modified protibiae and significantly more elongated apical spines of the mesotibiae. In contrast, the new species displays only a subtle impression on the protibia, and the apical spine of the mesotibia is notably shorter. A total of 28 species of this genus are known from Xizang.

Distribution. Southwest China: Xizang (Lhünzē County) (Fig. 4).

Etymology. The name is a toponymy referring to the type locality of this species, Lhünzē County.

Tribasodites liangi **sp. nov.**

https://zoobank.org/ED8AA4E3-AE72-4B95-98A3-1C02B340AF46
Figs 2, 4
Chinese common name: 梁氏脊胸蚁甲

Type material (4 exx.). ***Holotype*****:** China: • ♂: 'China: Xizang, Shannan, Lhünzē County, Yümai Town, Jianzhejinzhe, 28°30'21"N, 93°07'07"E, 2930 m, in wood, 5.ix.2023, Hong-Bin Liang leg., 西藏隆子县玉麦乡件哲金哲' (SNUC). ***Paratypes*****:** China: • 3 ♀♀, same collecting data as for holotype (SNUC, IZCAS).

Diagnosis. Male. Body length approximately 2.4 mm. Head subglobose, slightly narrower than pronotum; vertex with complete reversed U-shaped sulcus connecting small, asetose foveae, with distinct mediobasal carina extending from head base anteriorly to level of middle length of eyes. Antenna elongate, lacking modifications. Pronotum lacking marginal spines, with distinct median and lateral longitudinal sulci, with pairs of big discal and antebasal spines. Discal striae of elytra shallow, extending posteriorly approximately to half of elytral length. Metatrochanter with large projection on ventral margin. Aedeagus strongly asymmetric; median lobe with large basal capsule and broad foramen, ventral stalk greatly broadened at base, dorsal lobe slender and widely forked in apical portion, parameres reduced and forming single membranous structure. **Female.** Body length approximately 2.6 mm; legs simple, genitalia as in Fig. 2G.

Description. Male. Body (Fig. 2A) 2.42 mm long, reddish-brown, elytra slighter darker, with tarsi and mouthparts lighter in color. Dorsal surface of body covered with relatively long pubescence.

Head (Fig. 2B) subglobose, rounded at base, slightly wider than long, length 0.49 mm, width across eyes 0.51 mm; vertex finely punctate, with small, asetose vertexal foveae (dorsal tentorial pits), with complete, reversed U-shaped sulcus connecting foveae, mediobasal carina distinct, extending from head base anteriorly to level of eye midlength, lateral carinae complete; tempora rounded; frons anteriorly fused with clypeus at middle, anterolaterally with thin oblique carinae; area between moderately raised antennal tubercles weakly impressed; clypeus with smooth surface, entire anterior margin strongly carinate and moderately raised; ocular-mandibular carinae complete; Venter with small gular foveae (posterior tentorial pits) originating from shared transverse opening, with thin median carina extending from opening anteriorly to mouthparts. Compound eyes moderately prominent, composed of approximately 43 small ommatidia. Antenna elongate, length 1.30 mm, indistinct club loosely formed by slightly enlarged apical three antennomeres; antennomere 1 thick, subcylindrical, antennomeres 2–8 each slightly elongate, 8 shortest, 9 wider and longer than 8, 10 wider and slightly longer than 9, 11 largest, slightly longer than 9 and 10 combined (25:22), subconical, anterolateral margin slightly impressed.

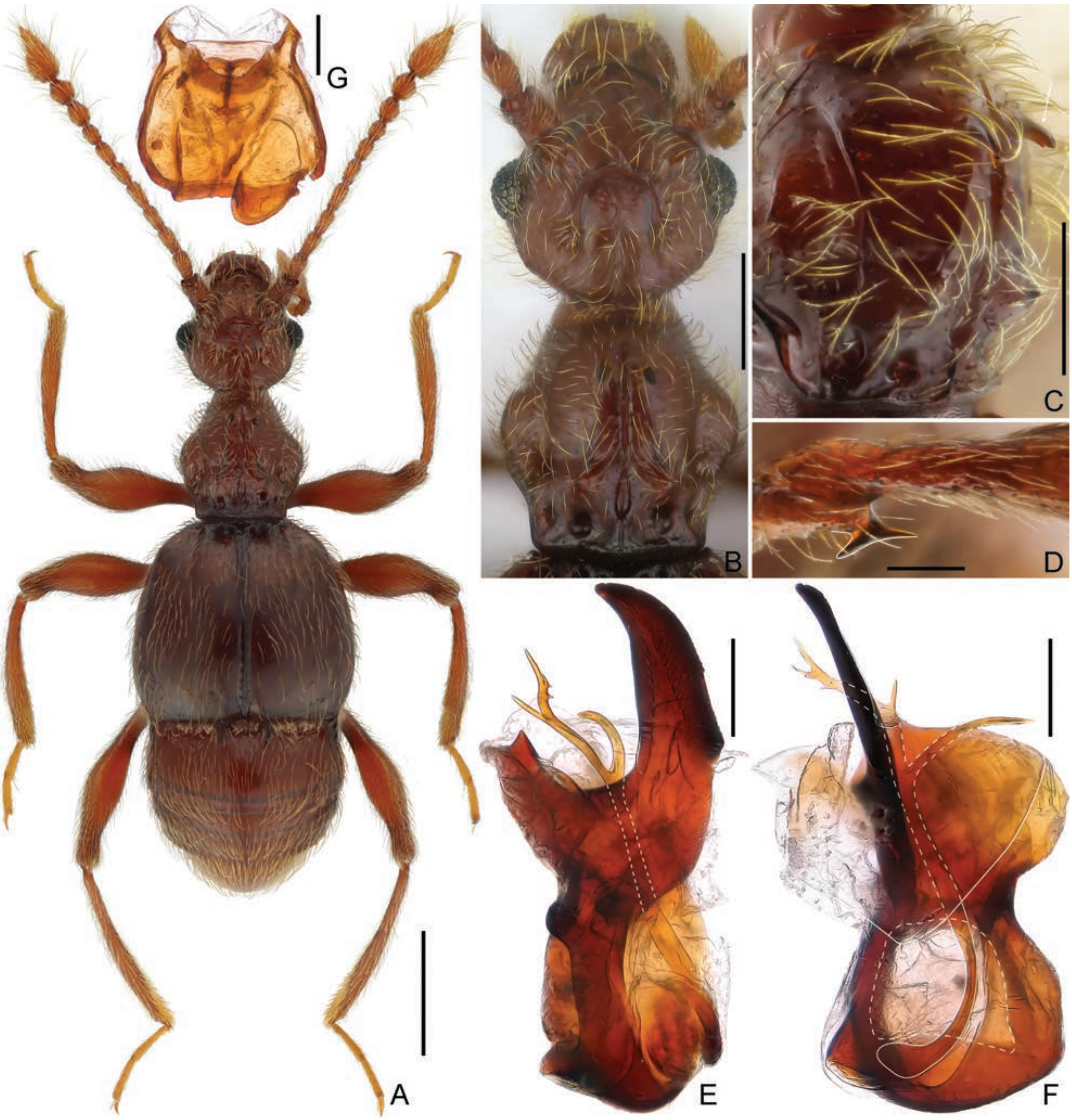

Figure 2. Morphology of *Tribasodites liangi* sp. nov. (**A–F** male **G** female) **A** dorsal habitus **B** head and pronotum **C** pronotum, in dorsolateral view **D** metatrochanter **E, F** aedeagus, lateral (**E**), and dorsal (**F**) **G** genitalia. Scale bars: 0.5 mm (**A**); 0.3 mm (**B**); 0.2 mm (**C**); 0.1 mm (**D, E, F, G**).

Pronotum (Fig. 2B) slightly longer than wide, length 0.48 mm, width 0.44 mm, widest at middle; lateral margins lacking spines, rounded, convergent basally and parallel at basal 1/5; disc convex, finely punctate, distinct median longitudinal sulcus with slightly carinate margins, posteriorly confluent with oval antebasal impression and short mediobasal carina, with pair of thin lateral longitudinal sulci, and pairs of discal and antebasal spines (Fig. 2C); lateral antebasal foveae distinct and setose; with distinct outer and inner pair of basolateral foveae. Prosternum with basisternal (precoxal) portion longer than procoxal rests, with large lateral procoxal foveae; hypomeral grooves obliquely extending from base anteriorly to half-length of hypomera, with lateral antebasal hypomeral impression, hypomeral ridges close to margins of coxal cavities, extending anteriorly to meet hypomeral grooves.

Elytra slightly wider than long, length 0.75 mm, width 0.90 mm; each elytron with three moderately large, asetose basal foveae; discal striae extending posteriorly from outer basal foveae to half of elytral length; humeri moderately prominent, subhumeral foveae present, carinate marginal stria extending from foveae to posterior margins of elytra.

Mesoventrite short, demarcated from metaventrite by oblique ridges; median mesoventral foveae broadly separated, originating from shared setose, transverse opening, large lateral mesoventral foveae forked internally; prepectus massive, collar-shaped; mesoventral intercoxal process short, apically acute; marginal striae complete. Metaventrite prominent admesally, inclined towards middle, with well-developed lateral mesocoxal and two lateral metaventral foveae, metaventral intercoxal process with small and narrow split at middle.

Legs elongate; procoxa with exceptionally long seta at base; mesotrochanter with tiny ventral tubercle; metatrochanter (Fig. 2D) with distinct ventral projection greatly broadened at apex.

Abdomen widest at lateral margins of tergite 1 (IV), length 0.76 mm, width 0.80 mm. Tergite 1 (IV) more than twice as long as 2 (V), setose basal sulcus separated by two mediobasal and two pairs of basolateral foveae, with pair of short discal carinae, inner marginal carinae thin and complete, outer carinae present for basal 1/2; tergite 2 (V) slightly longer than 3 (VI), 4 (VII) as long as tergites 2 and 3 combined; tergites 2–4 (V–VII) each with one pair of small basolateral foveae, tergite 5 (VIII) semicircular, transverse, posterior margin roundly emarginate at middle. Sternite 2 (IV) with one pair of small mediobasal and three pairs of basolateral foveae, lacking lateral carina; midlength of sternites 2–4 (IV–VI) gradually shorter, 5 (VII) slightly longer than 4, 3–5 lacking basolateral foveae, sternite 6 (VIII) transverse, posterior margin broadly emarginate at middle.

Aedeagus (Fig. 2E, F) elongate, length 0.54 mm, dorso-ventrally strongly asymmetric; median lobe with large basal capsule and broad foramen, ventral stalk broadest at base, narrowing towards apex; dorsal lobe long and broadly forked apically, left fork (orientation according to Fig. 2F) split into four spines at apex, and one longer spine before middle; parameres fused, broad and flattened, membranous.

Female. Similar to male in external morphology; antenna slightly shorter, simple, legs lacking tubercles or projections; each compound eye composed of approximately 38 ommatidia; humeri weakly raised; metathoracic wings fully developed. Measurements (as for male): body length 2.56–2.60 mm; length/width of head 0.50–0.51/0.52–0.53 mm, pronotum 0.52–0.53/0.51–0.52 mm, elytra 0.72–0.80/0.91–0.92 mm; abdomen 0.83–0.90/0.81–0.83 mm; length of antenna 1.24–1.27 mm; genitalia (Fig. 2G) moderately sclerotized, broad, maximum width 0.32 mm.

Comparative notes. This species closely resembles several congeners from Xizang due to the presence of discal and antebasal spines of the pronotum, as well as the simple antennae of the male. However, *Tribasodites liangi* sp. nov. is distinguished by the lack of marginal spines of the pronotum and its uniquely structured aedeagus, characterized by an elongate, slender, and apically serrate dorsal lobe.

Distribution. Southwest China: Xizang (Lhünzē County) (Fig. 4).

Etymology. This species is named after Hong-Bin Liang, collector of the type series.

***Tribasodites yumaicus* sp. nov.**

https://zoobank.org/A01F5C1C-D138-4F31-B23C-2318757CEA2C
Figs 3, 4
Chinese common name: 玉麦脊胸蚁甲

Type material (6 exx.). ***Holotype*:** China: • ♂: 'China: Xizang, Shannan, Lhünzē County, pass to Yümai Town, 28°38'18"N, 93°4'23"E, 3660 m, under stone, 4.ix.2023, Hong-Bin Liang leg., 西藏隆子县玉麦北1公里处观景台' (SNUC). ***Paratypes*:** China: • 1 ♂, 4 ♀♀, same collecting data as for holotype (SNUC, IZCAS).

Diagnosis. Male. Body length approximately 2.5 mm. Head roundly rectangular, slightly narrower than pronotum; vertex with shallow reversed U-shaped sulcus connecting small, asetose foveae, with distinct mediobasal carina extending from head base anteriorly to slightly below level of middle length of eyes. Antenna elongate, lacking modifications. Pronotum with small, acute marginal spines, with two pairs of antebasal spines. Discal striae of elytra long, extending posteriorly to apical 4/5 of elytral length. Protibia with small apical tubercle; mesotrochanter with distinct ventral spine, mesotibia with short spine at apex; metatrochanter with hook-like projection. Aedeagus strongly asymmetric; median lobe with subtriangular basal capsule and foramen, ventral stalk split to two projections, dorsal lobe plate-like. **Female.** Body length approximately 2.2–2.4 mm; legs lacking spines, tubercles, or projections, genitalia as in Fig. 3K, greatly transverse.

Description. Male. Body (Fig. 3A) length 2.51–2.52 mm; color reddish-brown, tarsi and mouthparts lighter. Dorsal surface of body covered with relatively dense pubescence.

Head (Fig. 3B) roundly rectangular, truncate at base, slightly wider than long, length 0.47–0.50 mm, width across eyes 0.50–0.51 mm; vertex finely punctate, with small, asetose vertexal foveae (dorsal tentorial pits), with shallow, complete, reversed U-shaped impression connecting foveae, mediobasal carina distinct, extending from head base anteriorly to below level of eye midlength, lateral carinae present only posterior to antennal tubercles; tempora rounded; frons anteriorly fused with clypeus at middle, anterolaterally with thin oblique carinae; area between moderately raised antennal tubercles weakly impressed; clypeus with smooth surface, entire anterior margin strongly carinate and moderately raised; ocular-mandibular carinae complete. Venter with small gular foveae (posterior tentorial pits) originating from shared oval opening, with weak median carina present only for short distance near mouthpart. Compound eyes moderately prominent, composed of approximately 45 small ommatidia. Antenna elongate, length 1.54–1.60 mm, indistinct club formed by slightly enlarged apical three antennomeres; antennomere 1 thick, subcylindrical, 2–7 each slightly elongate, 3 and 8 shortest, 9 slightly wider and longer than 8, 10 wider than 9, subconical, 11 largest, longer than 9 and 10 combined (34: 27), subfusiform, anterolateral margin impressed.

Pronotum (Fig. 3B) slightly longer than wide, length 0.56–0.57 mm, width 0.53–0.54 mm, widest slightly anterior to middle; lateral margins rounded, convergent basally and parallel at basal 1/5, with pair of small, acute spines; disc slightly convex, finely punctate, distinct median longitudinal sulcus with slightly carinate margins, posteriorly confluent with oval antebasal impression and

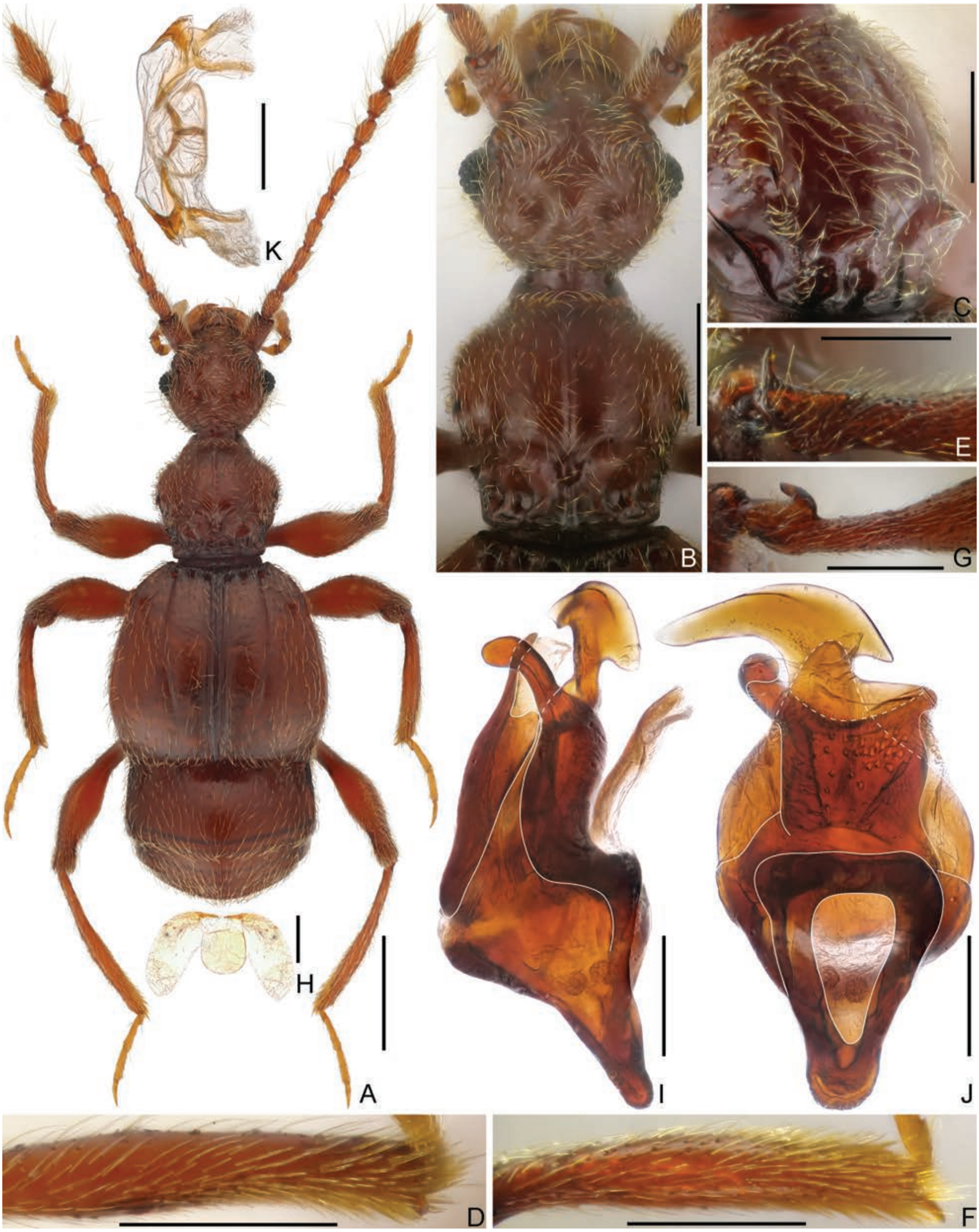

Figure 3. Morphology of *Tribasodites yumaicus* sp. nov., (**A–J** male **K** female) **A** dorsal habitus **B** head and pronotum **C** pronotum, in dorsolateral view **D** protibia **E** mesotrochanter **F** mesotibia **G** metatrochanter **H** sternite 7 (IX) **I, J** aedeagus, lateral (**I**), and ventral (**J**) **K** genitalia. Scale bars: 0.5 mm (**A**); 0.3 mm (**B**); 0.2 mm (**C, D, E, F, G**); 0.1 mm (**H, I, J, K**).

distinct mediobasal carina, with pair of thin lateral longitudinal sulci and two pairs of antebasal spines (Fig. 3C); lateral antebasal foveae distinct and setose; with distinct outer and inner pair of basolateral foveae. Prosternum with basisternal (precoxal) portion longer than procoxal rests, with small lateral procoxal foveae; hypomeral grooves obliquely extending from base anteriorly to half-length of hypomera, with lateral antebasal hypomeral impressions, hypomeral ridges close to margins of coxal cavities, extending anteriorly to meet hypomeral grooves.

Elytra much wider than long, length 0.81–0.84 mm, width 0.95–0.97 mm; each elytron with three large, asetose basal foveae; long discal striae extending posteriorly from outer basal foveae posteriorly for 4/5 elytral length; humeri moderately prominent, subhumeral foveae present, carinate marginal striae extending from foveae to posterior margins of elytra. Metathoracic wings fully developed.

Mesoventrite short, demarcated from metaventrite by oblique ridges; median mesoventral foveae moderately separated, originating from shared setose, transverse opening, large lateral mesoventral foveae unforked internally; prepectus massive, collar-shaped; mesoventral intercoxal process short, apically acute, marginal striae complete. Metaventrite prominent admesally, inclined towards middle, with well-developed lateral mesocoxal and two lateral metaventral foveae, metaventral intercoxal process with small and narrow split at middle.

Legs elongate; procoxa with exceptionally long seta at base, protibia (Fig. 3D) with small apical tubercle; mesotrochanter (Fig. 3E) with distinct ventral spine, mesotibia (Fig. 3F) with small spine at apex; metatrochanter (Fig. 3G) with hook-like projection.

Abdomen widest at lateral margins of tergite 1 (IV), length 0.76–0.78 mm, width 0.81–0.84 mm. Tergite 1 (IV) more than twice as long as 2 (V), thin basal sulcus interrupted by one pair of mediobasal and one pair of basolateral foveae, with pair of short discal carinae, oblique inner marginal carinae thin and complete, outer carinae present for basal 1/2; tergite 2 (V) slightly longer than 3 (VI), 4 (VII) shorter than tergites 2 and 3 combined, 2–4 (V–VII) each with one pair of small basolateral foveae; tergite 5 (VIII) semicircular, transverse, posterior margin roundly emarginate at middle. Sternite 2 (IV) with one pair of mediobasal and three pairs of basolateral foveae, lacking lateral carina; mid-length of sternites 2–4 (IV–VI) gradually shorter, 5 (VII) slightly longer than 4, 3–5 each with two pairs of small basolateral foveae, sternite 6 (VIII) transverse, posterior margin broadly emarginate at middle, sternite 7 (IX) (Fig. 3H) membranous, composed of pair of lateral lobes and one oval median plate.

Aedeagus (Fig. 3I, J) length 0.45 mm, dorso-ventrally strongly asymmetric; median lobe with subtriangular basal capsule and elongate foramen, ventral stalk divided into two parts in apical portion, one lobe short, rounded at apex, another greatly expanded at apex, dorsal lobe broad, plate-like, surrounding ventral stalk, parameres fused and reduced to ventral membrane.

Female. Similar to male in external morphology; antenna slightly shorter, simple, legs lacking tubercles, spines or projections; each compound eye composed of approximately 35 ommatidia; humeri weakly raised; metathoracic wings fully developed. Measurements (as for male): body length 2.21–2.38 mm; length/width of head 0.46–0.51/0.47–0.52 mm, pronotum 0.51–0.56/0.48–0.55 mm, elytra 0.76–0.84/0.87–0.96 mm; abdomen 0.56–0.61/0.67–0.71 mm; length of antenna 1.37–1.56 mm; genitalia (Fig. 3K) slightly sclerotized, greatly transverse, maximum width 0.28 mm.

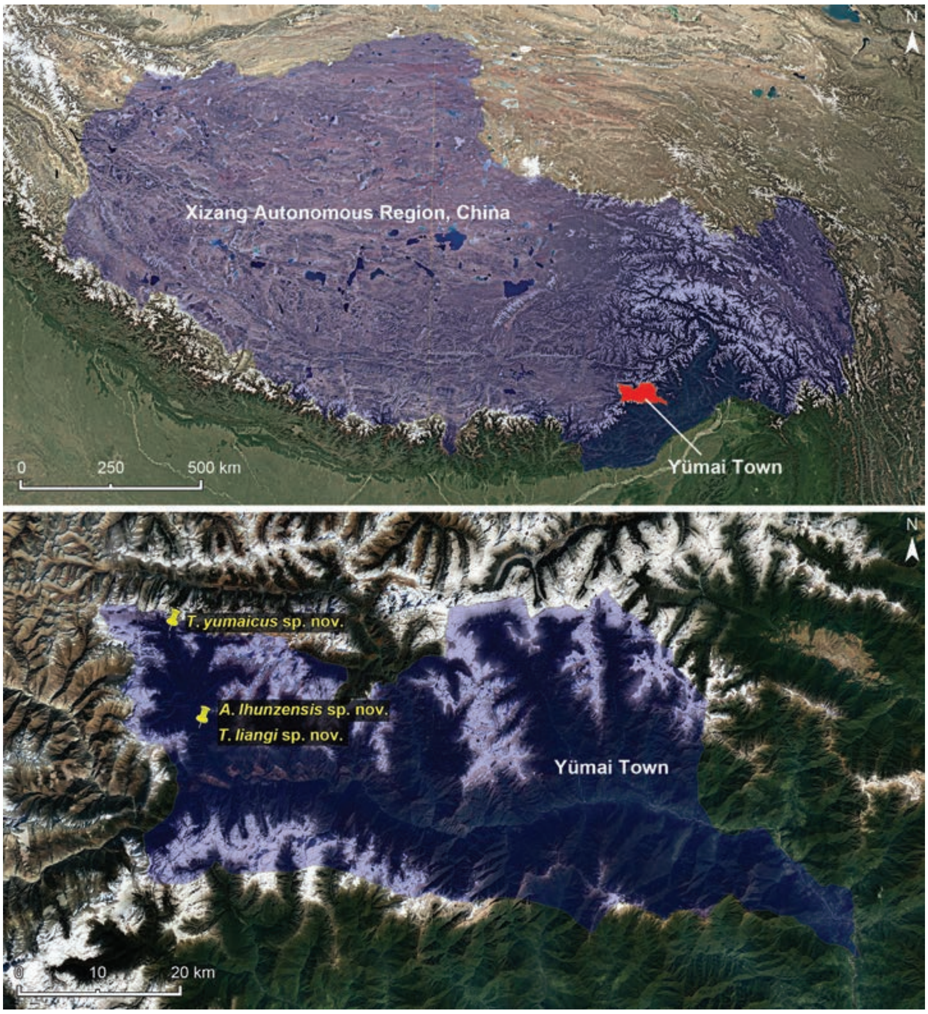

Figure 4. Distribution of the three species in Yümai Town, Xizang. **A** location of Yümai Town in Xizang **B** distribution of *Arthromelodes lhunzensis* sp. nov., *Tribasodites liangi* sp. nov. and *Tribasodites yumaicus* sp. nov. in a north-south valley located at western Yümai Town.

Comparative notes. This species closely resembles several congeners from Xizang due to the similarly structured aedeagus, i.e., dorsal lobe of the aedeagus broadened and encircling the ventral stalk. However, *Tribasodites yumaicus* sp. nov. can be readily distinguished by the simple male antennae and the unique configuration of the aedeagus. With the addition of the two new species described here, the total number of known species of this genus occurring in Xizang has increased to 15.

Distribution. Southwest China: Xizang (Lhünzē County) (Fig. 4).

Etymology. The name is a toponymy referring to the type locality of this species, Yümai Town.

Acknowledgments

We are grateful to Hong-Bin Liang (梁红斌, IZCAS) for providing the specimens used in this study. Rostislav Bekchiev (National Museum of Natural History, Sofia, Bulgaria) and Shûhei Nomura (National Museum of Nature and Science, Tsukuba, Japan) critically read the draft manuscript which improved the paper.

Additional information

Conflict of interest

The authors have declared that no competing interests exist.

Ethical statement

No ethical statement was reported.

Funding

Financial support was provided by the National Natural Science Foundation of China (no. 32370465), and the Second Tibetan Plateau Scientific Expedition and Research Program (no. 2024QZKK020200).

Author contributions

Conceptualization: ZWY. Funding acquisition: ZWY. Investigation: YQZ. Methodology: YQZ. Supervision: ZWY. Writing - original draft: YQZ. Writing - review and editing: YQZ, ZWY.

Author ORCIDs

Zi-Wei Yin https://orcid.org/0000-0001-6659-9448

Data availability

All of the data that support the findings of this study are available in the main text.

References

Chandler DS (2001) Biology, morphology and systematics of the ant-like litter beetles of Australia (Coleoptera: Staphylinidae: Pselaphinae). Memoirs on Entomology, International 15: 1–560.

Yin Z-W (2022) The Batrisini of Tibet: unveiling an enigmatic ant-loving beetle diversity at Earth's "Third Pole" (Coleoptera, Staphylinidae, Pselaphinae). Zootaxa 5111(1): 1–211. https://doi.org/10.11646/zootaxa.5111.1.1

ZooKeys 1228: 287–294 (2025)
DOI: 10.3897/zookeys.1228.142968

Short Communication

A new species of *Pseudodendroides* Blair, 1914 (Coleoptera, Pyrochroidae, Pyrochroinae) from China, with a key to the species

Qi Gao[1,2], Xin-Mei Yang[1], Daniel K. Young[3], Zhao Pan[1]

1 *Key Laboratory of Zoological Systematics and Application of Hebei Province, School of Life Sciences, Institute of Life Science and Green Development, Hebei University, 071002, Baoding, Hebei Province, China*
2 *Department of Entomology, College of Plant Protection, Nanjing Agricultural University, 210000, Nanjing, Jiangsu Province, China*
3 *Department of Entomology, University of Wisconsin, Madison, WI 53706, USA*
Corresponding author: Zhao Pan (panzhao86@yeah.net)

Abstract

Pseudodendroides Blair, 1914 is distributed in East Asia, with five described species. Currently, a new species, *Pseudodendroides frontalis* Gao & Pan, **sp. nov.**, is described and illustrated from Yunnan Province, China. A key to the species of *Pseudodendroides* is provided and the phylogenetic relationships among *Pseudodendroides* and related genera are briefly discussed.

Key words: China, fire-colored beetle, identification key, new species, *Pseudodendroides*, taxonomy

Academic editor: Dmitry Telnov
Received: 28 November 2024
Accepted: 15 January 2025
Published: 21 February 2025

ZooBank: https://zoobank.org/837AEBB5-A660-41CF-AC8D-60EF8C74B45E

Citation: Gao Q, Yang X-M, Young DK, Pan Z (2025) A new species of *Pseudodendroides* Blair, 1914 (Coleoptera, Pyrochroidae, Pyrochroinae) from China, with a key to the species. ZooKeys 1228: 287–294. https://doi.org/10.3897/zookeys.1228.142968

Introduction

The pyrochroine *Pseudodendroides* Blair, 1914 was redefined by Young (1999, 2015) and may be distinguished from other pyrochroine genera by the following character combination: compound eyes large; cranial pits (male) well developed and usually paired; antennal scape long and parallel-sided; posterior margin of abdominal sternite VIII widely emarginate and conspicuously concave (male); parameres of male genitalia short and widely separated for approximately half their length (Young 1999). Young (2015) reviewed the taxonomic history of this genus and transferred two species to the genera *Himalapyrochroa* Young, 2004 and *Sinodendroides* Young, 2005. The following year, he transferred *Dendroides madurensis* Pic, 1912 from *Pseudodendroides* to the new genus *Pyroghatsiana* (Young 2016). Currently, five extant species of *Pseudodendroides* are known (Young et al. 2020 recorded six species in error) from Japan and southern China (Lewis 1887; Kôno 1935, 1936; Pic 1955; Nakane 1988).

Three of the five *Pseudodendroides* species have been recorded from China up to now: *Ps. sulcatithorax* Pic, 1955, *Ps. umenoi* (Kôno, 1936), and *Ps. uraiana* Kôno, 1935. During the examination of specimens from Yunnan Province, we discovered a new species, *Pseudodendroides frontalis* Gao & Pan, sp. nov.. The new species is described and illustrated herein, and a key to *Pseudodendroides* species is provided.

Material and methods

The type material is deposited in the Museum of Hebei University, Baoding, China [MHBU (MHBUa = material preserved in 95% ethyl alcohol)]. The specimens were studied using a Nikon SMZ1500 stereomicroscope, and the images were taken using a Canon EOS 5D Mark III (Canon Inc., Tokyo, Japan) with a Laowa FF 100 mm F2.8 CA-Dreamer Macro 2× or Laowa FF 25 mm F2.8 Ultra Macro 2.5–5× (Anhui Changgeng Optics Technology Co., Ltd, Hefei, China). Figures of the antennae were hand drawn using the Nikon SMZ1500 with a camera lucida. Label data are presented verbatim. Line breaks on labels are denoted by a single slash (/).

Most of the terms in the description are from previous literature (e.g., Young 1975). The ocular index (OI) = 100× minimum dorsal distance between compound eyes / maximal dorsal width across compound eyes (Campbell and Marshall 1964).

Results

Genus *Pseudodendroides* Blair, 1914

Pseudodendroides Blair, 1914: 314; Young 1999: 1; 2015: 195; Pollock and Young 2008: 415; Young et al. 2020: 566.

Type species. *Dendroides niponensis* Lewis, 1887, by original designation.

Key to the species of *Pseudodendroides*

1 Male: eyes larger, OI usually less than 25 (Fig. 2), except *Ps. amamiana* and *Ps. umenoi* (figs 15–16 in Nakane 1988), rami of antennal flagellomeres longer (Fig. 4), posterior margins of abdominal sternites VII and VIII mesally emarginate (fig. 4 in Young 1999) **2**

– Female: eyes smaller, OI greater than 30 (Fig. 3), rami of antennal flagellomeres shorter (Fig. 5), posterior margins of abdominal sternites VII and VIII almost straight **7**

2 Frons with one sub-rounded shallow depression (Fig. 2); pronotum orange-yellow; China: Yunnan .... ***Ps. frontalis* Gao & Pan, sp. nov.**

– Frons with cranial pits at least partially divided mesally by well-developed carina; pronotum black **3**

3 Compound eyes large, OI less than 25; cranial pits paired, with at most a feeble additional transverse ridge **4**

– Compound eyes relatively smaller than above, OI greater than 30 (fig. 8 in Young 1999); frons with two distinct cranial pits and a transverse ridge, making pits nearly four chambered **6**

4 Cranial pits deep, bordered posteriorly by slightly elevated rim, rim slightly emarginate mesally; China: Sichuan .... ***Ps. sulcatithorax* (Pic, 1955)**

– Cranial pits broad, shallow, their posterior margin not elevated **5**

5 Cranial pits separated posteriorly by mesal carina, pits confluent anteriorly; Japan .... ***Ps. niponensis* (Lewis, 1887)**

– Cranial pits completely separated by mesal carina; China: Taiwan .... ***Ps. uraiana* (Kôno, 1935)**

6 Cranial pits subquadrate (fig. 15 in Nakane 1988); Japan: Amami-Oshima .... ***Ps. amamiana* (Nakane, 1988)**

– Cranial pits, especially posterior pits, ovate-rounded; China: Taiwan .... ***Ps. umenoi* (Kôno, 1936)**

7 Pronotum orange-yellow; flagellomere I without ramus; China: Yunnan .... ***Ps. frontalis* Gao & Pan, sp. nov.**

– Pronotum black, at most with red-orange margin; flagellomere I with short ramus **8**

8 Compound eyes large, OI less than 40........ **9**

– Compound eyes relatively smaller than above, OI greater than 45........ **11**

9 Flagellomere I with dorsal face, including ramus flat to slightly concave, foliaceous; China: Sichuan........ ***Ps. sulcatithorax* (Pic, 1955)**

– Flagellomere I sub-cylindrical........ **10**

10 Frons between antennal insertions very sparsely punctate; Japan .... ***Ps. niponensis* (Lewis, 1887)**

– Frons between antennal insertions moderately sparsely punctate; China: Taiwan........ ***Ps. uraiana* (Kôno, 1935)**

11 Frons densely covered with moderately long, golden setae; Japan: Amami-Oshima........ ***Ps. amamiana* (Nakane, 1988)**

– Frons moderately sparsely covered with short, mostly decumbent setae, especially between compound eyes; China: Taiwan .... ***Ps. umenoi* Kôno, 1936**

***Pseudodendroides frontalis* Gao & Pan, sp. nov.**

https://zoobank.org/D522CD7B-C7F2-4721-BD19-8EBC31B7F2DC
Figs 1–10

Type locality. China: Yunnan, Nujiang Lisu Autonomous Prefecture, Lanping Bai and Pumi Autonomous County, Zhongpai Township, Biyuhe Village.

Type specimens. *Holotype*: • ♂, labeled “2023.V / 云南兰坪中排乡碧玉河村 [China, Yunnan, Lanping, Zhongpai Township, Biyuhe Village / elev. 2600–2900 m / 河北大学博物馆 [Museum of Hebei University]”, “HOLOTYPE / *Pseudodendroides frontalis* sp. nov. / Det. Gao & Pan” (MHBU). ***Paratypes*:** • 1 ♂ 1 ♀, with same label as the holotype (MHBU); 6 ♂♂, labeled “2023.VI / 云南兰坪中排乡碧玉河村 [China, Yunnan, Lanping, Zhongpai Township, Biyuhe Village / elev. 2700–3000 m / 河北大学博物馆 [Museum of Hebei University]”, 5 alcohol specimens additionally with a label of Sample ID for each: “P2J9, P2J10, P3B2, P3B3, P3B4” (1 MHBU, 5 MHBUa); • 1 ♀, “2023.X / 云南怒江福贡石月亮乡 [China, Yunnan, Nujiang, Fugong, Shiyueliang Township / elev. 2500–2700 m / 河北大学博物馆 [Museum of Hebei University]” (MHBU). All paratypes with the label “PARATYPE / *Pseudodendroides frontalis* sp. nov. / Det. Gao & Pan”.

Diagnosis. This new species can be easily distinguished from other *Pseudodendroides* species by its orange-yellow pronotum (entirely to largely black in other species). Additionally, males of *Ps. frontalis* lack distinct cranial pits, exhibiting only a shallowly depressed region between the antennal insertions, and the compound eyes are very large, similar to those of *Ps. niponensis* (OI = 17.4–18.5). By contrast, the frons of other species possesses two distinct cranial pits. The compound eyes of *Ps. umenoi* and *Ps. amamiana* are relatively smaller than those of *Ps. frontalis* (OI ≥ 30). The females of all *Pseudoden-*

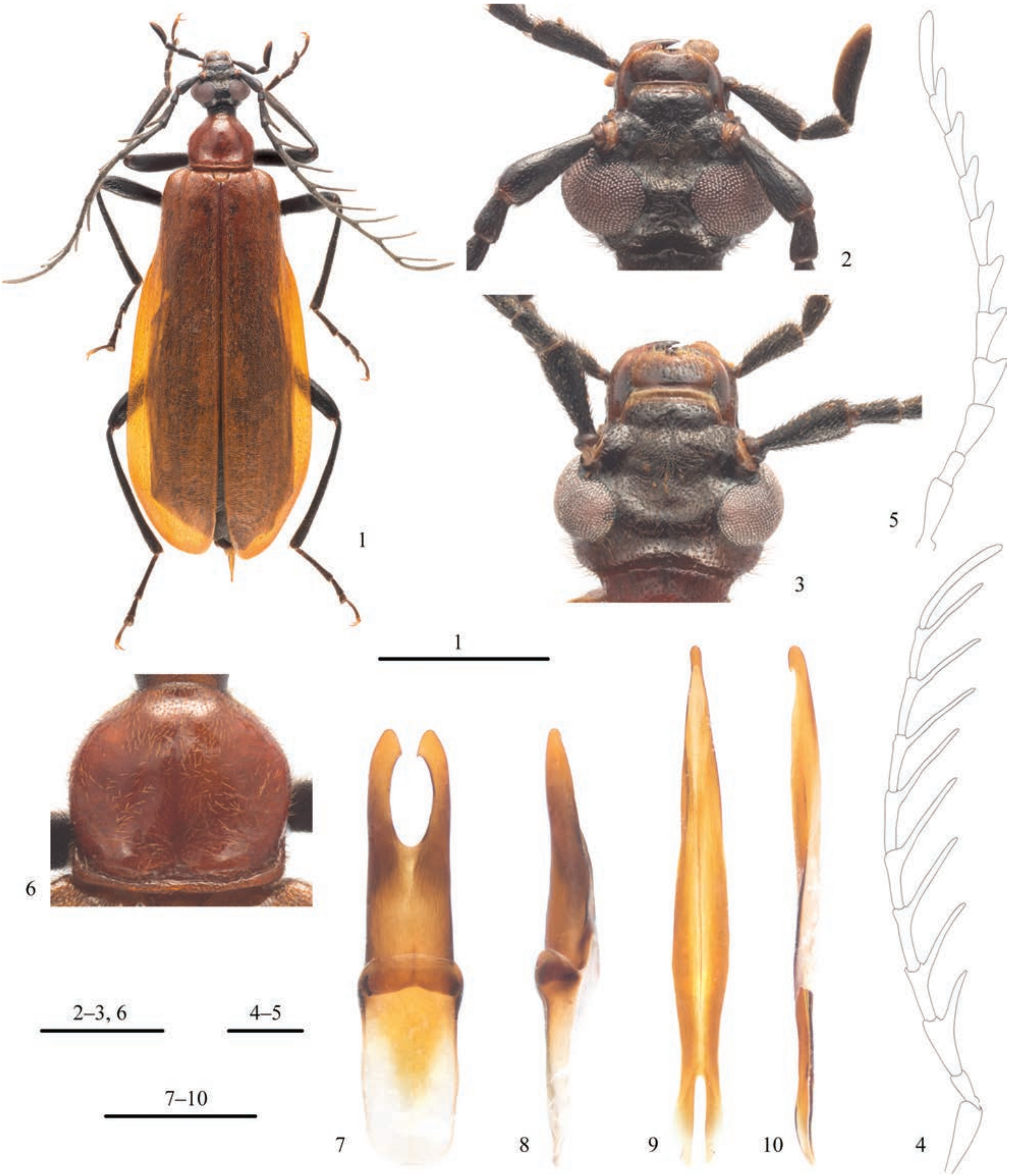

Figures 1–10. *Pseudodendroides frontalis* Gao & Pan, sp. nov., paratypes **1** habitus, male, dorsal view **2, 3** head, dorsal view: **2** male **3** female **4, 5** antenna: **4** male **5** female **6** pronotum, male, dorsal view **7, 8** tegmen: **7** dorsal view **8** lateral view **9, 10** penis: **9** dorsal view **10** lateral view. Scale bars: 5 mm (**1**); 1 mm (**2–10**).

droides species are morphologically similar. However, the female of the new species differs from those of the other species in the shape of flagellomere I, which is almost without any ramus; there is at most a slight apical prominence in *Ps. frontalis*, with a long or short ramus in the other species.

Description. Body length: 16.3–16.8 mm; humeral width: 3.2–3.8 mm.

Male: Body (Fig. 1) black, except pronotum, prosternum, and elytra orange-yellow; apex of clypeus, labrum, and mandibles yellow-brown to dark brown. Body covered with medium-length yellow-brown setae; those of antennae and legs short (except coxae, trochanters, and ventral sides of femora); setation sparse on head and pronotum, dense on elytra, and very dense at basal half of depression on frons.

Head (Fig. 2) widest at level of eyes, with irregular small punctures, diameter of punctures less than spacing of punctures; punctures on vertex each bearing a very fine, long seta. Compound eyes large, dorsal distance between eyes narrow (OI = 17.4–18.5). Clypeus and labrum flattened; labrum with anterior margin slightly emarginate. Frons with one sub-rounded large depression between antennal insertions; occiput sharply, transversely concave; genae reduced, short. Antennae (Fig. 4) long, extending back to near middle of elytra; scape slightly and gradually widened apically; pedicel short, approximately half length of scape; flagellomere I shortest; flagellomeres II–IV subequal in length, approximately as long as scape; rami of flagellomeres sub-cylindrical, ramus of flagellomere I shortest, approximately half as long as flagellomere I, rami of flagellomeres I–IV with gradually increasing lengths, rami of flagellomeres IV–VIII subequal in length and shorter than flagellomere IX.

Pronotum (Fig. 6) widest in anterior 2/5, slightly and gradually narrowed posteriad and sharply narrowed anteriad; approximately as wide as head, 0.80–0.90× as long as wide; disc shining, sparsely covered with very small punctures, diameter of punctures distinctly less than spacing of punctures; disc with a shallow, longitudinal mesal groove, a shallow depression at center of base, and a transverse groove along posterior margin. Scutellar shield rounded apically, densely and finely punctate. Legs slender; prothoracic tarsomere V longest, I second longest, II–IV gradually shorter; mesothoracic tarsomere V subequal in length to I, II–IV gradually shorter; metathoracic tarsomere I longest, IV second longest, II–III gradually shorter. Pretarsal claws simple.

Posterior margins of abdominal sternites III–VI subparallel, VII–VIII with posterior margin acutely emarginate mesally. Parameres distinctly longer than phallobase (Figs 7, 8), basal half of parameres fused, each lateral lobe of parameres with a small, subapical tooth on inner margin, in dorsal view (Fig. 7). Penis elongate, somewhat dorsoventrally flattened, gradually narrowed apically, apex nodular-shaped with a small recurved hook (Figs 9, 10).

Female: Similar to male, except as follows: depression on frons shallower than that of male and without dense setae inside; compound eyes relatively small (OI = 34.7–42.9), with wider range than male; genae slightly prominent (Fig. 3); antennal rami distinctly shorter than those of male, flagellomere I almost without ramus, only slightly prominent apically (Fig. 5); pronotum slightly wider than that of male, aspect ratio ca. 0.82; posterior margin of abdominal sternite VII straight, that of sternite VIII slightly convex mesally.

Etymology. The specific name comes from the Latin adjective “*frontalis*” meaning “frontal”, in reference to the unique characteristic of the frons of this species in the male, bearing a transverse shallow depression instead of paired cranial pits.

Distribution. China: Yunnan.

Discussion

According to the redefinition of *Pseudodendroides* (Young 1999), the male head has paired cranial pits on the frons. However, the frons of the new species, *Ps. frontalis*, is only shallowly depressed. We propose that this new species belongs to the genus *Pseudodendroides* because it fits most of the diagnostic characters of the genus, e.g., the shape of the antennal scape, the abdominal sternite VIII, and the parameres of male genitalia. Thus, *Pseudodendroides* may not be distinguished from other genera based on the shape of the frons in males.

As mentioned in previous literature (Gao et al. 2024a, b), Pyrochroinae is currently known to consist of 15 genera worldwide, but their phylogenetic relationships remain unclear. A preliminary phylogenetic analysis of the subfamily Pyrochroinae based on mtDNA *COI* barcode sequences found that *Pseudodendroides* has very close relationships with the genera *Himalapyrochroa* and *Phyllocladus* Blair, 1914 (Gao, unpubl. Masters thesis). Unfortunately, the relationships among these three genera have still not been resolved on this basis or by results based on morphological comparisons (also see Young 2004, 2013, 2015; Gao et al. 2023).

These three genera share the following morphological characters: the male genitalia are similar, with the fused portions of the parameres being relatively short (approximately half of the total length); the penis is nodular-shaped apically; the antennal scape is elongate and slightly clavate, while the pedicel is elongate and sub-cylindrical. For differences, *Phyllocladus* may generally be distinguished from the other two by the flattened rami of its flagellomeres (versus cylindrical in *Himalapyrochroa* and *Pseudodendroides*). *Pseudodendroides* and *Phyllocladus* share a putative apomorphy associated with the abdominal sternite VIII: the apical margin is widely emarginate and conspicuously concave. However, it is interesting that the cranial pits and the size of the compound eyes in the male are polymorphic in *Phyllocladus* and *Pseudodendroides*. The frons of *Ps. frontalis* n. sp. and all species of *Himalapyrochroa* lacks distinct cranial pits, bearing only a shallow depression (distinct paired cranial pits in other *Pseudodendroides* species and all species of *Phyllocladus*). *Phyllocladus grandipennis* (Pic, 1906), *Ps. frontalis* n. sp., and *Ps. niponensis* have very large eyes (the minimum dorsal distance between the eyes is distinctly less than the transverse width of each eye); whereas the other species of both *Phyllocladus* and *Pseudodendroides* have smaller eyes (the minimum dorsal distance between the eyes is at most as wide as the transverse width of each eye), which is shared with *Himalapyrochroa* species.

Acknowledgements

We wish to thank Prof. Darren A. Pollock (Eastern New Mexico University, Portales, USA) and one anonymous reviewer for constructive comments.

Additional information

Conflict of interest

The authors have declared that no competing interests exist.

Ethical statement

No ethical statement was reported.

Funding

This study was supported by the Special Program for Basic Resource Investigation of the Ministry of Science and Technology, China (No. 2022FY202100).

Author contributions

Resources: ZP. Validation: ZP. Visualization: QG. Writing – original draft: QG, XMY. Writing – review and editing: DKY, ZP.

Author ORCIDs

Qi Gao https://orcid.org/0000-0002-5902-9276
Xin-Mei Yang https://orcid.org/0009-0008-4480-7371
Daniel K. Young https://orcid.org/0000-0002-5711-2519
Zhao Pan https://orcid.org/0000-0001-7798-0009

Data availability

All of the data that support the findings of this study are available in the main text.

References

Blair KG (1914) A revision of the family Pyrochroidae (Coleoptera). Annals and Magazine of Natural History 13(75): 310–326. https://doi.org/10.1080/00222931408693484

Campbell JM, Marshall JD (1964) The ocular index and its application to the taxonomy of the Alleculidae (Coleoptera). The Coleopterists Bulletin 18(2): 42. https://doi.org/10.5962/p.372397

Gao Q, Zhan ZH, Pan Z (2023) Taxonomy of genus *Himalapyrochroa* (Coleoptera: Pyrochroidae), with description of a newly recorded species from China. Sichuan Journal of Zoology 42(2): 213–218. https://doi.org/10.11984/j.issn.1000-7083.20220324

Gao Q, Young DK, Pan Z (2024a) *Oblatopyrochroa bellula*, an enigmatic new genus and species of Pyrochroinae (Coleoptera, Pyrochroidae) from Xizang, China. ZooKeys 1191: 369–377. https://doi.org/10.3897/zookeys.1191.118653

Gao Q, Young DK, Zhan ZH, Cheng HY, Pan Z (2024b) Revision of *Eupyrochroa* Blair, 1914 (Coleoptera: Pyrochroidae) based on morphological comparison and molecular phylogenetics. Zootaxa 5406(2): 238–252. https://doi.org/10.11646/zootaxa.5406.2.2

Kôno H (1935) Drei neue Heteromeren aus Japan und Formosa, mit einer Liste der geographischen Verbreitung der japanischen Pyrochroiden und Pediliden. Insecta Matsumurana 9(4): 157–161.

Kôno H (1936) Über die Käfersammlung des Museums "Umeno Konchû Kenkiujo" I. Pyrochroidae, Meloidae, Rhipiphoridae. Bulletin of the Umeno Entomological Laboratory, Kurume 3: 1–6.

Lewis G (1887) On the Pyrochroidae of Japan. Annals and Magazine of Natural History, Series 5, 20: 165–175. https://doi.org/10.1080/00222938709460033

Nakane T (1988) Notes on some little-known beetles (Coleoptera) in Japan, 2. Kita-Kyūshū no Konchū 35(1): 3–5. [pl. 1]

Pic M (1955) Descriptions et notes. Diversités Entomologiques 15: 9–16.

Pollock DA, Young DK (2008) Family Pyrochroidae Latreille, 1807. In: Löbl I, Smetana A (Eds) Catalogue of Palaearctic Coleoptera. Vol. 5: Tenebrionoidea. Apollo Books, Stenstrup, 414–417.

Young DK (1975) A revision of the family Pyrochroidae (Coleoptera: Heteromera) for North America based on the larvae, pupae, and adults. Contributions of the American Entomological Institute 11(3): 1–39. https://doi.org/10.25335/zj0y-nf23

Young DK (1999) Transfer of the Taiwanese *Pseudopyrochroa umenoi* and the Japanese *P. amamiana* to *Pseudodendroides*. The Pan-Pacific Entomologist 75(1): 1–7.

Young DK (2004) *Himalapyrochroa gibbosa*, a new genus and species of fire-colored beetle (Coleoptera: Pyrochroidae: Pyrochroinae) from Darjeeling, India. Oriental Insects 38: 189–196. https://doi.org/10.1080/00305316.2004.10417386

Young DK (2013) Two new species of *Phyllocladus* (Coleoptera: Pyrochroidae: Pyrochroinae) from China, with a key to males of the Chinese species. Zootaxa 3669(1): 56–64. https://doi.org/10.11646/zootaxa.3669.1.6

Young DK (2015) Nomenclatural Changes in Pyrochroinae: three Maurice Pic types of *Pseudodendroides* Blair (Coleoptera: Pyrochroidae). The Coleopterists Bulletin 14 (mo4): 191–195. https://doi.org/10.1649/0010-065X-69.mo4.191

Young DK (2016) *Pyroghatsiana*: a new genus of fire-colored beetles (Pyrochroinae) from the Southern Ghats, India. Insecta Mundi 0468: 1–8.

Young DK, Pollock DA, Telnov D (2020) Family Pyrochroidae Latreille, 1806. In: Iwan D, Löbl I (Eds) Catalogue of Palearctic Coleoptera. Vol. 5. Tenebrionoidea. Revised and Updated 2nd edn. Brill Publishers, Leiden, 565–569.

ZooKeys 1228: 295–306 (2025)
DOI: 10.3897/zookeys.1228.140752

Research Article

Revision of the genus *Ninomimus* Lindberg, 1934 (Hemiptera, Lygaeoidea, Ninidae), with the description of a new species from China

Cuiqing Gao[1], Suyan Cao[1]

1 *Co-Innovation Center for Sustainable Forestry in Southern China, College of Forestry and Grassland, Nanjing Forestry University, Nanjing, Jiangsu 210037, China*
Corresponding author: Cuiqing Gao (cqgao@njfu.edu.cn)

Abstract

The species of *Ninomimus* Lindberg, 1934 are reviewed. A new species, *Ninomimus fuscus* **sp. nov.**, is described from Hunan Province, China. It differs from its two congeners in its shiny body and translucid hemelytra. A diagnosis of the genus, a key to the included species, photographs of habitus and male genitalia of selected species, and micrographs of the pruinose area of the type species are also presented.

Key words: Heteroptera, identification key, *Ninomimus fuscus*, taxonomy, true bugs

Academic editor: Jader Oliveira
Received: 2 November 2024
Accepted: 25 January 2025
Published: 21 February 2025

ZooBank: https://zoobank.org/9A4AD403-5C8C-426F-B657-02726AF1C86F

Citation: Gao C, Cao S (2025) Revision of the genus *Ninomimus* Lindberg, 1934 (Hemiptera, Lygaeoidea, Ninidae), with the description of a new species from China. ZooKeys 1228: 295–306. https://doi.org/10.3897/zookeys.1228.140752

Introduction

The Ninidae (Hemiptera, Heteroptera, Lygaeoidea) are a small family comprising five genera and 14 species worldwide (Slater 1964; Dellapé and Henry 2024). This family was erected by Barber (1956) as a tribe within Cyminae (Lygaeidae) and elevated to family level by Henry (1997). Prior to this study, the genus *Ninomimus* Lindberg, 1934 comprised of two species, *N. assamensis* (Distant, 1901), distributed in Japan and India, and *N. flavipes* (Matsumura, 1913), distributed in Russia, Korea, Japan, and China (Zheng and Zou 1981; Péricart 2001).

In this study, a new species, *Ninomimus fuscus* sp. nov., is identified and described from Hunan Province, China. As a result, three species are now included in the genus, with two of them occurring in China. A key to all known species of the genus is given. In addition, the ultrastructure of the cuticular pruinose area of the type species is also explored using scanning electron microscopy.

Materials and methods

Images of the specimens were captured using a Canon EOS R6 camera mounted on a Wemacro focus stacking rail, equipped with a Laowa 25 mm f/2.8 2.5–5× Ultra Macro lens and then z-stacked using Helicon Focus v. 8.1.0. Images of the genital segments were obtained using MSHOT Image Analysis System v. 1.1.4. A female of *N. flavipes* was sputter-coated with gold and observed using a scanning electron microscope (SEM, FEI Quanta 200). Figures were post-processed with Adobe Photoshop CC 2023.

Details of male dissection methods and terminologies used in this article are those given in Ashlock (1957). All measurements in the text are given in millimeters.

Abbreviations of institutions where the material were deposited:

IZAS	Institute of Zoology, Academia Sinica, Beijing, China
NKUM	Institute of Entomology, Nankai University, Tianjin, China
NJFU	Nanjing Forestry University, Nanjing, China

Results

Ninomimus **Lindberg, 1934**

Figs 1–7

Ninomimus: Lindberg 1934: 8; Scudder 1957: 106–107; Stichel 1958: 318; Slater 1964: 425–426; Zheng and Zou 1981: 40–41; Péricart 2001: 70.

Type species. *Ninomimus lundbladi* Lindberg, 1934 (= *N. flavipes*), by original monotypy.

Diagnosis. Body elongate, nearly parallel-sided, covered with long setae. Head wider than long; eyes sessile and large; first antennal segment short and thick, with length close to eye width; second longest, third and fourth nearly equal in length; labium with apical half of first segment swollen. Pronotum slightly widened posteriorly, wider than long; humeral angles rounded; posterior margin shallowly concave before scutellum; posterolateral angle of metapleuron acute. Scutellum with tip slightly bifid. Hemelytra extending to tip of abdomen; clavus with three rows of punctures, one along of corium incomplete, the other two extending to apex. Membrane with a central longitudinal dark brown stripe. Femora slender and unarmed; posterior tarsi with first segment slightly longer than combined length of the other two.

Ninomimus is distinguished from *Cymoninus*, *Paraninus*, and *Neoninus* by the swollen apical half of the first labial segment. *Ninomimus* is distinguished from *Ninus* by the punctae on the apical half of the clavus and the corium, which bear a dense series of punctures extending anterior to the R+M veins as well as along these veins, whereas in *Ninus*, the apical half of the clavus is impunctate, and the corium is punctate only along the R+M veins.

Key to species of *Ninomimus* Lindberg

1 Head, scutellum and pronotum except middle of anterior margin and postero-lateral spots covered with thick white pruinosity; ground color of pronotum yellowish brown (Figs 1, 4) **2**

– Head, scutellum and pronotum shining, without thick white pruinosity; ground color of pronotum blackish brown (Fig. 6a, d).... ***N. fuscus*** **sp. nov.**

2 Hemelytra opaque; membrane with longitudinal fuscous stripe at apex only; middle spot at humeral angle slightly fuscous, and inner anterior angles

of large spot on humeral angle usually anteriorly pointed (Figs 1a, d, 4); second antennal segment conspicuously longer than fourth .... ***N. flavipes*** **(Matsumura, 1913)**

– Hemelytra semitranslucid; membrane with longitudinal fuscous stripe extending along whole length of membrane and broader at middle; humeral angle not fuscous, and both medial and lateral angles of anterior margin of large spot on humeral angle bluntly extended anteriorly (Fig. 5a); second antennal segment only very slightly longer than fourth .... ***N. assamensis*** **(Distant, 1901)**

Ninomimus flavipes (Matsumura, 1913)

Figs 1–4

Lygaeosoma flavipes Matsumura, 1913: 142.
Ninomimus lundbladi Lindberg, 1934: 9.
Ninus flavipes: Esaki 1950: 223.
Cymoninus flavipes: Kormilev 1955: 4.
Ninomimus flavipes: Scudder 1957: 107; Stichel 1958: 318; Slater 1964: 426; Zheng and Zou 1981: 40–41; Péricart 2001: 70.

Material examined. China – Anhui Prov. • 8 ♂ 6 ♀; Shucheng County, Wanfo Mountain; 31.0753°N, 116.5628°E; alt. 465 m; 18 May 2024; S.Y. Cao & C.Q. Gao leg.; NJFU. – Heilongjiang Prov. • 1 ♂ 1 ♀; Hailin City, Hengdaohezi Town, Weihu Mountain; 25–30 Jul. 2003; Y.L. Ke leg.; NKUM. – Jilin Prov. • 1 ♀; Erdaobaihe Town; alt. 740 m; 7 Jul. 1986; Li leg.; NKUM. – Henan Prov. • 3 ♀; Nanyang City, Huangshi'an; 17 Jul. 1998; H.F. Zhang leg.; NKUM. – Shaanxi Prov. • 1 ♂; Feng County, Qinling Railway Station; alt. 1400 m; 28 Jul. 1994; W.J. Bu leg.; NKUM. • 22 ♂ 26 ♀; Foping Nature Reserve; alt. 1100 m; 19–20 Jul. 2006; D. Ding & J.Y. Xu leg.; NKUM. – Zhejiang Prov. • 10 ♂ 10 ♀; Qingyuan County, Baishanzu; alt. 550–1650 m; 15–16 Jul. 1994; H. Wu leg.; NKUM. • 6 ♂ 13 ♀; Taishun County, Wuyanling Nature Reserve; 4–5 Aug. 2007; Z.H. Fan & W.B. Zhu leg.; NKUM. • ♀; Lin'an District, Changhua Town, Qingliangfeng Mountain; alt. 1000 m; 17 May 2012; W.B. Yin leg.; NKUM. – Hubei Prov. • 7 ♂ 6 ♀; Fang County; 14–17 Jun. 1977; L.Y. Zheng & Q. Mu leg.; NKUM. • 5 ♂ 3 ♀; Shennongjia Nature Reserve; 22 Jun.–9 Jul. 1977; L.Y. Zheng & H.G. Zou leg.; NKUM. • 13 ♂ 15 ♀; Lichuan City, Xingdou Mountain; 31 Jul. 1999; H.J. Xue leg.; NKUM. • 6 ♂ 6 ♀; Tongshan County, Jinjigu Valley; alt. 450 m; 30 Jul.–11 Aug. 2010; Y. Wang leg.; NKUM. – Jiangxi Prov. • 2 ♂; Lushan Botanical Garden; 21–25 Jul. 1957; S.H. Ying leg.; NKUM. • 3 ♀; Jiulian Mountain; 16 Jul. 2002; H.J. Xue leg.; NKUM. – Hunan Prov. • 1 ♀; Huaihua City; 20 Jul. 1995; W.J. Bu leg.; NKUM. • 10 ♂ 13 ♀; Yanling County, Taoyuandong; alt. 1000 m; 17–18 Jul. 2004; Y.L. Ke & J.Y. Xu leg.; NKUM. • 1 ♂ 3 ♀; Dong'an County, Shunhuang Mountain; alt. 1200 m; 28 Jul. 2004; Y.L. Ke leg.; NKUM. – Fujian Prov. • 2 ♂ 1 ♀; Shanghang County, Buyun Village; 6 May 1993; W.J. Bu leg.; NKUM. • 1 ♂; Dehua County, Shangyong Town, Houzhai Village; 15 Sep. 2022; W.L. Zhang leg.; NKUM. – Hainan Prov. • 6 ♂ 3 ♀; Wanning City, Jianling Nature Reserve; 28–29 Jul. 2008; C.Q. Gao, Z.H. Fan & X. Zhang leg.; NKUM. • 1 ♀; Wanning City, Xinglong District; alt. 100 m; 1 Aug. 2008; Z.H.

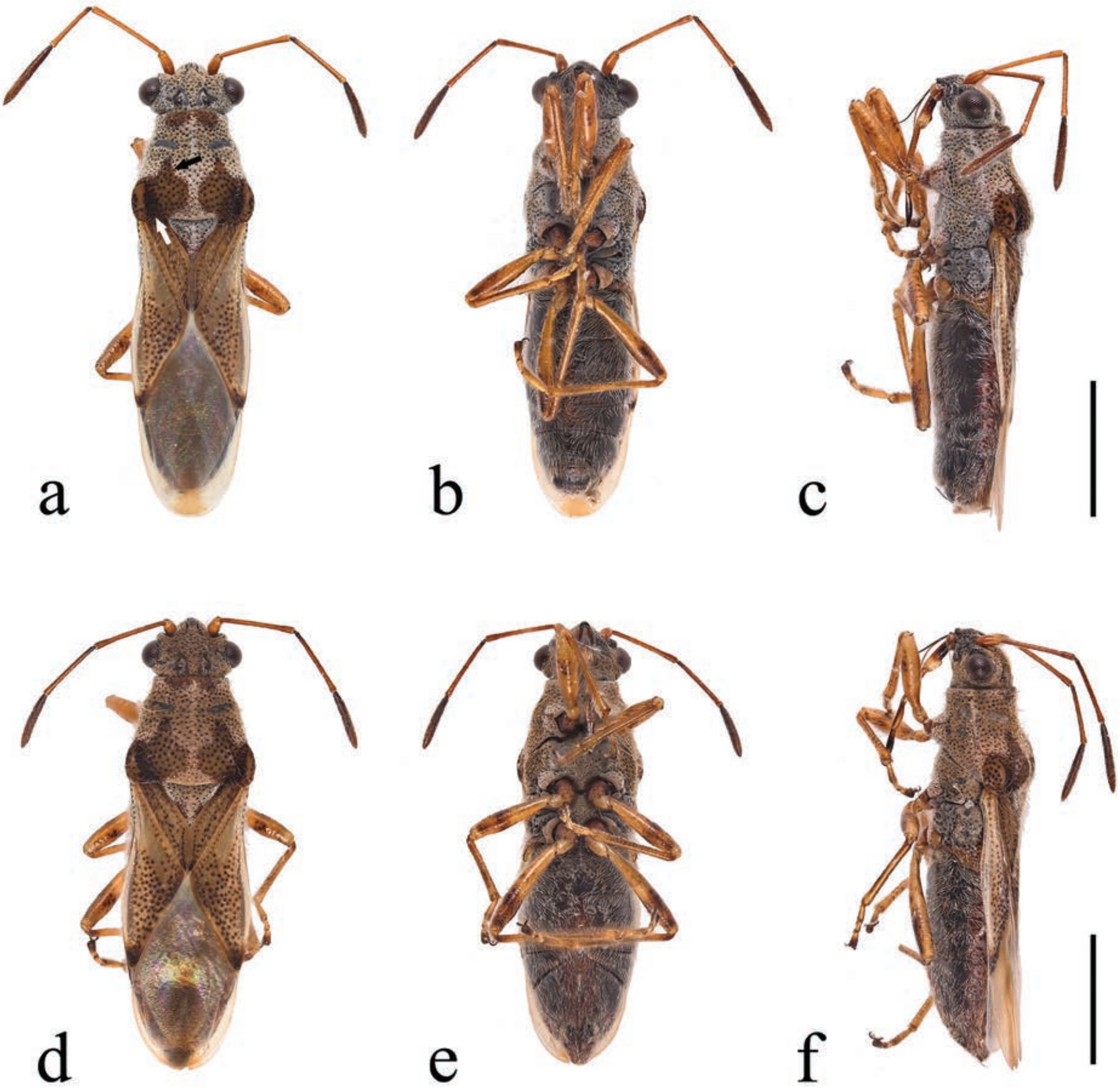

Figure 1. *Ninomimus flavipes* (Matsumura, 1913) **a** male in dorsal view; black arrows, indicating inner anterior margin of large spot at humeral angle pointed anteriorly; white arrows, indicating middle spot at humeral angle slightly fuscous **b, c** male in ventral and lateral views, respectively **d–f** female in dorsal, ventral, and lateral views, respectively. Scale bars: 1.0 mm.

Fan leg.; light trap; NKUM. – Guangxi Prov. • 1 ♂ 2 ♀; Longsheng Autonomous County; 25–28 Aug. 1964; L.C. Wang & S.L. Liu leg.; NKUM. • 18 ♂ 14 ♀; Mao'er Mountain; alt. 1100 m; 20 Apr. 2002; H.J. Xue leg.; NKUM. – Sichuan Prov. • 2 ♀; Dujiangyan City, Gaoyuan Village; alt. 1100 m; 15 Aug. 2011; Y. Liu leg.; NKUM. – Guizhou Prov. • 5 ♂ 7 ♀; Xishui County; 1 Jun. 2000; H.J. Xue leg.; NKUM. • 14 ♂ 18 ♀; Suiyang County, Kuankuoshui Nature Reserve; alt. 850–1700 m; 4–8 Jun. 2010; K. Dang leg.; NKUM. • ♀; Suiyang County, Kuankuoshui Nature Reserve; alt. 1300 m; 16 Aug. 2010; Y.H. Wang & X. Sun leg.; NKUM.

Redescription. Body slender, covered with long, yellowish-white setae, densest at basal part of hemelytra. Head (except for tylus and a pair of large spots anterior to ocelli), pronotum (except of two spots at middle of anterior margin, calli, and a pair of large spots at humeral angles), and scutellum bearing a thick white pruinosity (Figs 1, 3, 4).

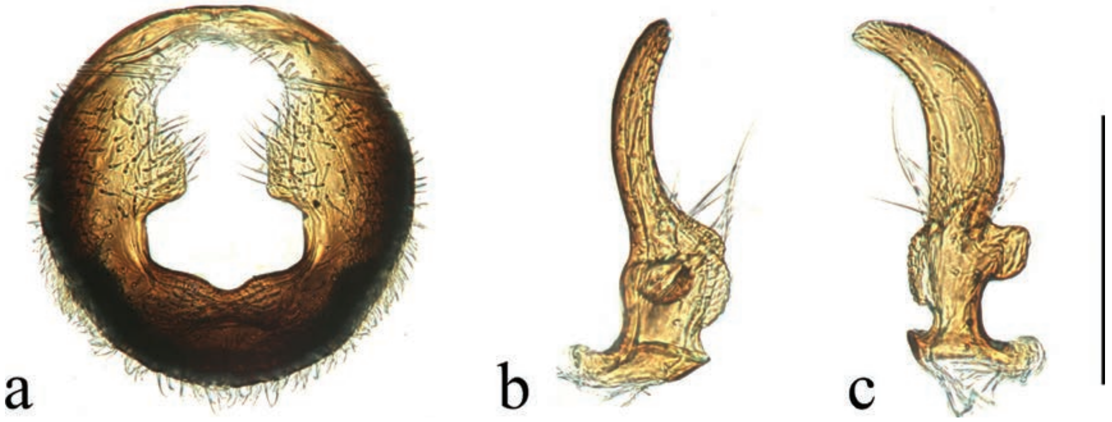

Figure 2. Genitalia of *Ninomimus flavipes* (Matsumura, 1913) **a** pygophore, inposterodorsal view **b, c** right paramere, in dorsal and ventral view. Scale bars: 0.2 mm.

***Head*:** greyish brown; eyes large and rounded; setae on third and fourth antennal segments approximately twice of diameter of respective segments (Fig. 4); labium extending to mesocoxae, yellowish brown; basal part of first segment and fourth segment blackish brown; apical swollen part of first segment light brown.

***Thorax*:** pruinose area of pronotum greyish white, composed of dense, long, curly, hair-like microtrichia, as seen in the SEM micrographs (Figs 1, 3e, 4); calli black, two spots at middle of anterior margin and a pair of large spots at humeral angles brown, composed by short, erect microtrichia showed in SEM micrographs (Fig. 3b, f); middle spot at humeral angle slightly fuscous, and inner anterior angles of large spot on humeral angle usually pointed anteriorly (Figs 1a, d, 4); posterior margin of pronotum shallowly impressed anteriad of scutellum. Scutellum completely pruinose. Propleuron brown, with a large black spot on supracoxal lobes; meso- and metapleura mostly black, with supracoxal lobes and posterior margins of metapleuron yellowish brown; pro-, meso-, and metapleura covered with the same type of pruinosity as pronotum and scutellum.

***Hemelytra*:** clavus and corium pale brown, nearly opaque; apices of corium and punctures on hemelytra blackish brown; clavus with three distinct rows of punctures, with outermost row not extending to apex; punctures on corium usually not spreading to exocorium.

***Abdomen*:** blackish brown, covered with long setae.

***Legs*:** yellowish brown, with femora and distal tarsal segment darker.

Male genitalia (Fig. 2): pygophore covered with setae; apical part of dorsal opening with anterior margin rounded rhomboid; distal margin of lateral lobe parallel; and basal part nearly rectangular with a median indentation broadly rounded on posterior margin. Paramere with both dorsal and ventral lobes broadened, rectangular; middle part of blade not apparently broadened and tip of blade rounded.

Measurements (in mm; male / female, *n* = 6). Body length 3.28–3.46 / 3.37–3.53. Head length 0.39–0.40 / 0.40–0.42; width across eyes 0.78–0.85 / 0.81–0.92; eye length 0.13–0.14 / 0.13–0.15; eye width 0.20–0.22 / 0.21–0.22; eye–ocellus space 0.11–0.12 / 0.12–0.14; interocular space 0.44–0.47 / 0.45–0.48; interocellar space 0.12–0.13 / 0.12–0.13; length of antennal segments I–IV respectively 0.21–0.22 / 0.21–0.23, 0.67–0.70 / 0.68–0.73, 0.61–0.62 / 0.62–0.63, 0.66–0.67 / 0.66–0.67; length of labial segments respectively 0.31–0.32 / 0.32–0.33, 0.27–0.27 / 0.27–0.28, 0.23–0.24 / 0.24–0.25, 0.24–0.25 / 0.25–0.27. Pronotum length

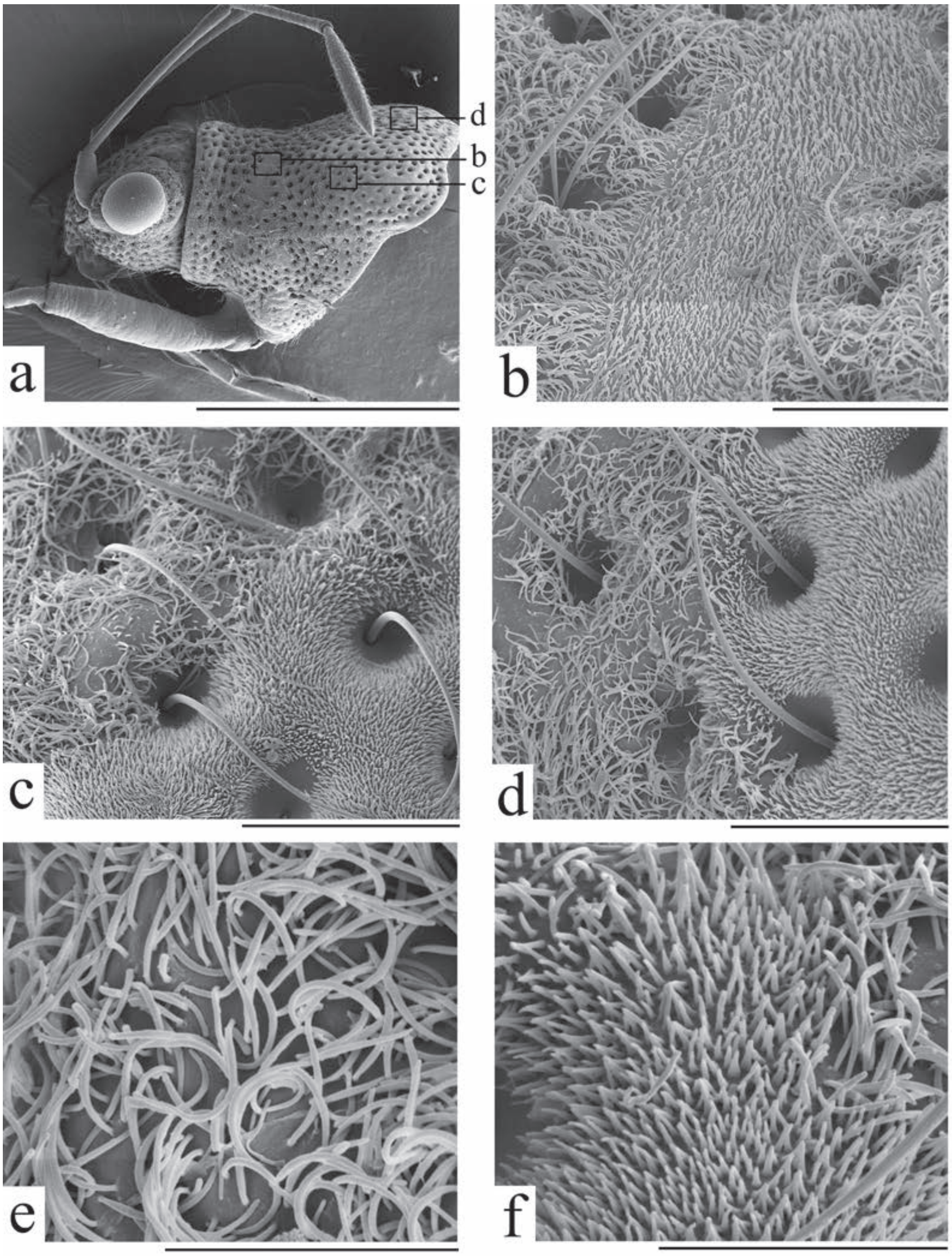

Figure 3. SEM micrographs of *Ninomimus flavipes* (Matsumura, 1913) **a** head and prothorax, lateral view **b** calli **c** edge of left humeral large spot **d** edge of right humeral large spot **e** dense, long, curly, hair-like microtrichia (pruinose area) **f** short, erect microtrichia (non-pruinose area). Scale bars: 1.0 mm (a); 0.05 mm (b–d); 0.02 mm (e, f).

0.71–0.75 / 0.74–0.79; width of anterior margin 0.51–0.54 / 0.53–0.56; width of posterior margin 0.80–0.83 / 0.82–0.88; scutellar length 0.28–0.30 / 0.30–0.34; scutellar width 0.40–0.41 / 0.40–0.42. Length of hemelytra 2.13–2.20 / 2.19–2.29; length of corium 1.39–1.43 / 1.40–1.47; length of claval commissure 0.30–0.31 / 0.33–0.34; distance of apex of clavus–apex of corium 0.67–0.69 / 0.70–0.73; distance of apex of corium–apex of membrane 0.72–0.76 / 0.76–0.79.

Distribution. China (Heilongjiang, Jilin, Henan, Shaanxi, Anhui, Zhejiang, Hubei, Jiangxi, Hunan, Fujian, Hainan, Guangxi, Sichuan, Guizhou); Russia (Vladivostok); Korea; Japan (Péricart 2001).

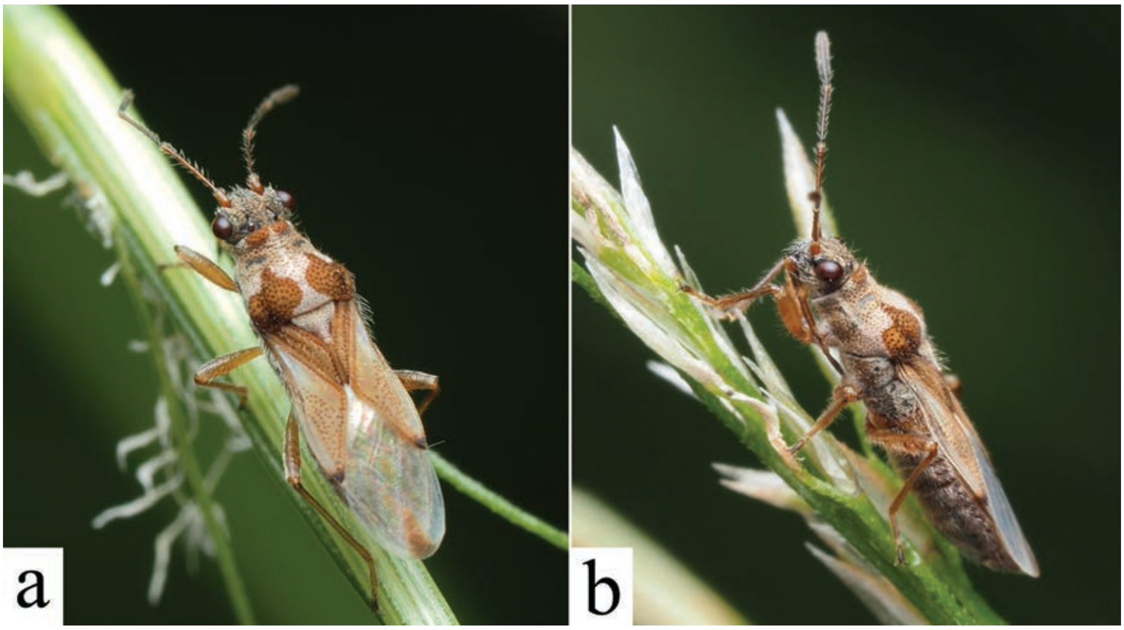

Figure 4. *Ninomimus flavipes* (Matsumura, 1913), live habitus. **a** dorsal view **b** lateral view.

Remarks. This species is characterized by the dense, white pruinosity on its head, pronotum, and scutellum (Scudder 1957; Zheng and Zou 1981). After observing it under SEM, we found that the pruinose areas are composed of dense, long, curly, hair-like microtrichia (Fig. 3e). The non-pruinose areas are also not completely smooth, and they are in fact covered with short, erect microtrichia (Fig. 3f).

***Ninomimus assamensis* (Distant, 1901)**

Fig. 5

Ninus assamensis Distant, 1901: 465.
Cymoninus assamensis: Bergroth 1921: 168.
Ninomimus assamensis: Scudder 1957: 107–108; Stichel 1958: 318; Slater 1964: 425–426; Péricart 2001: 70.

Type material examined. Syntype: India • ♂; *Ninus assamensis* Distant, 1901: 465 [printed]; Distant Coll., 1911-383 [printed]; Margherita [handwritten]; assamensis Dist. [handwritten]; Type [label with red ring, printed]; BMNH(E), 1340254 [printed]. We examined the type photo (Fig. 5b).

Diagnosis (modified from Scudder 1957). Head black; antennae yellowish brown, with fourth segment darkest; second antennal segment longest; labium yellowish brown, with dark brown tip. Pronotum yellowish brown with black calli, entirely pruinose except for two spots near middle of anterior margin and a pair of large spots covering most of hind lobes and including extreme lateral areas of posterior margin; humeral angles not fuscous, and both inner and lateral angles of anterior margin of spots on humeral angles bluntly extended anteriorly (Fig. 5a). Hemelytra pale brown with darker punctures; apices of clavus and corium dark brown; apical half of clavus semitranslucid; membrane with a longitudinal brown stripe running along entire length and broader in middle.

Distribution. Japan; India.

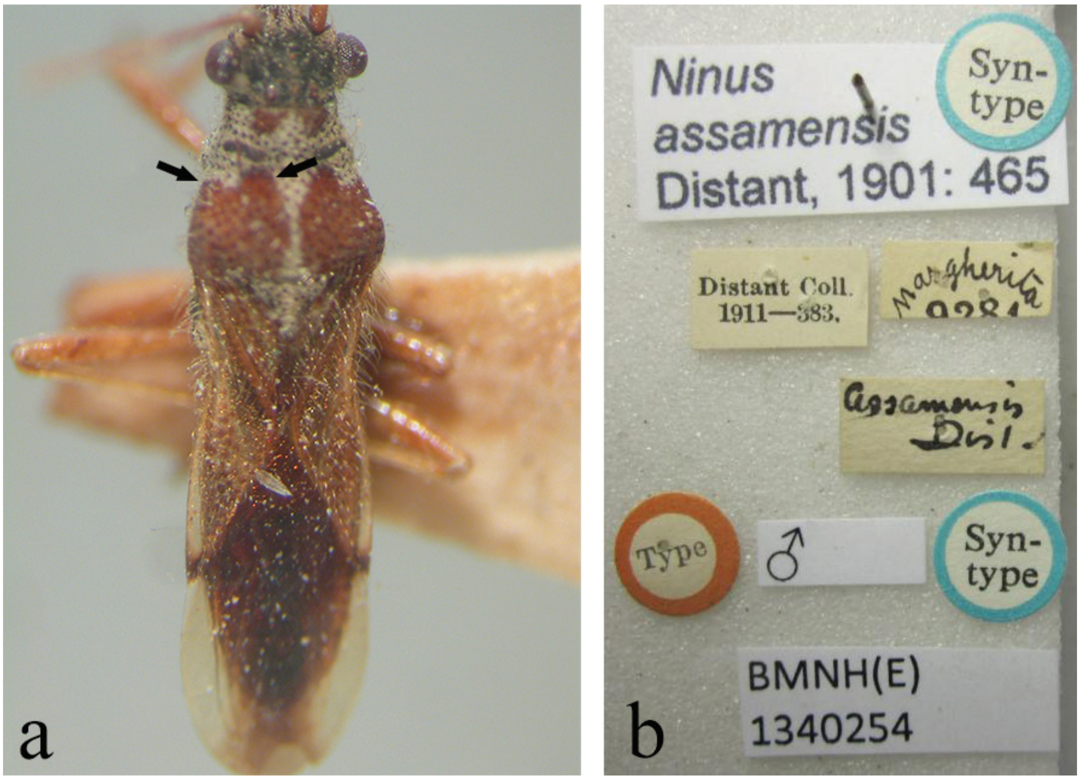

Figure 5. Type photographs of *Ninomimus assamensis* (Distant, 1901) **a** syntype, in dorsal view; black arrows indicate medial and lateral angles of anterior margin of spot on humeral angle bluntly extended anteriorly; **b,** labels (photographed by Előd Kondorosy).

Ninomimus fuscus **Gao & Cao, sp. nov.**

https://zoobank.org/7A8D0D6E-F45C-4C6C-A4C9-CE4FC7B6CF10

Figs 6, 7

Type material. ***Holotype*:** China • ♂; Hunan Prov., Chengbu County, Dankou Town, Taiping Village; 26.3495°N, 110.2397°E; alt. 479 m; 19 Nov. 2017; Kaidong Zhao leg.; IOZ(E)1429746, IZAS. ***Paratype*:** ♀; same collection data as for holotype; IOZ(E)1429745. All type specimens are deposited at IZAS.

Diagnosis. Body shiny, blackish brown, without thick, dense, white pruinosity, and pruinosity poorly visible; body more elongate than its congeners, with body length-to-width ratio across eyes reaching 4.6; hemelytra translucid; pygophore with anterior margin of dorsal opening rounded; paramere with base of dorsal lobe slightly constricted, and tip of blade sharp.

Description. Body shiny, without thick, dense, white pruinosity (Fig. 6).

***Head*:** black, covered with long, sparse setae; wider than long, slightly declivent; eyes large and sessile; antennae yellowish brown, with fourth segment dark brown; first segment stout, second and third segments slender, fourth segment spindle-shaped; antennal ratios I < III < IV < II; bucculae short, only extending to base of antenniferous tubercles; labium reaching mesocoxae, yellowish brown, with basal part of first segment and fourth segment blackish brown, apical part of first segment prominently swollen and light yellowish brown.

***Thorax*:** pronotum shiny, blackish brown, coarsely punctate except at calli and humeral angles, wider than long; lateral margins slightly convex in anterior

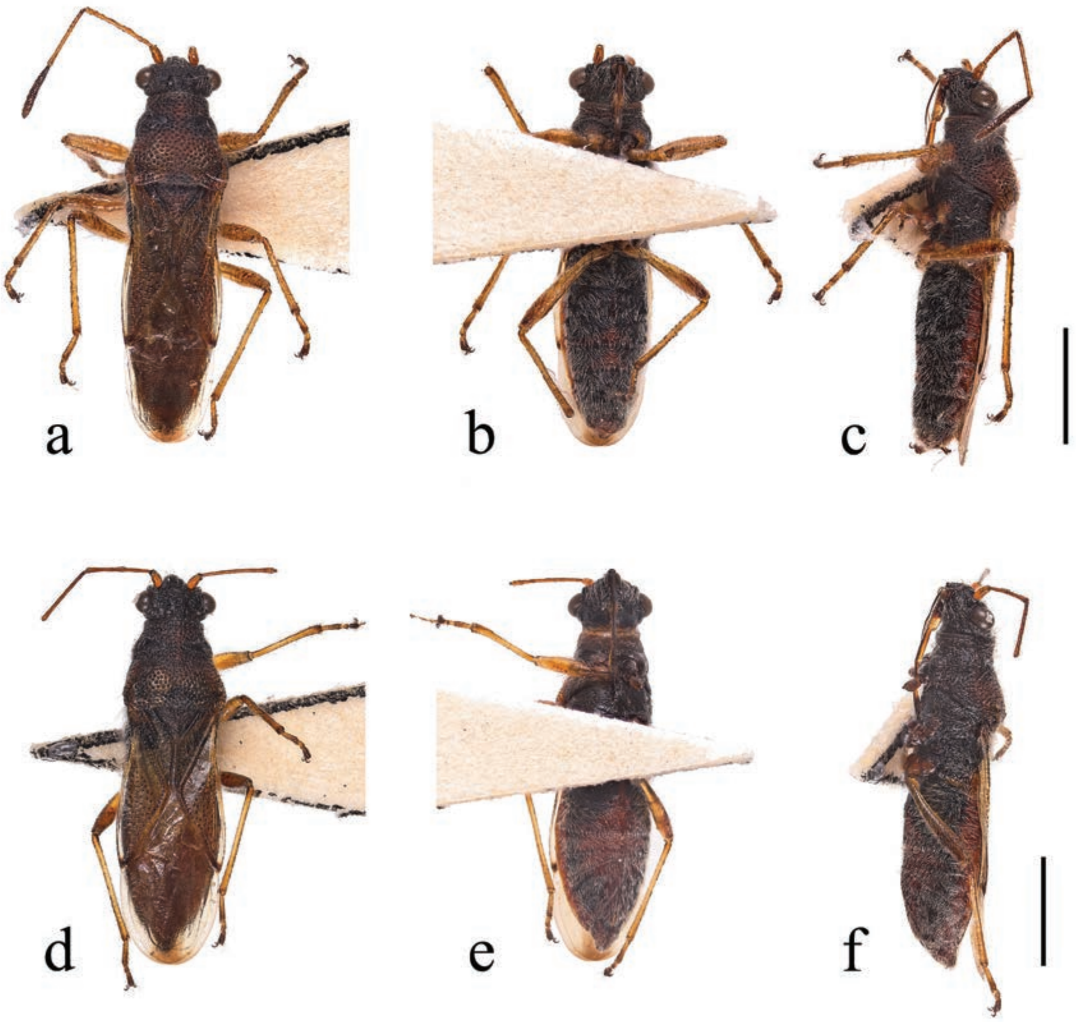

Figure 6. *Ninomimus fuscus* sp. nov. type photos **a–c** holotype, male, in dorsal, ventral, and lateral view, respectively **d** paratype, female, in dorsal, ventral, and lateral view, respectively. Scale bars: 1.0 mm.

half; posterior margin shallowly impressed anteriad of scutellum; humeral angles rounded; posterolateral angle of metapleuron acute. Scutellum blackish brown, with slightly darker margins; triangular, length equal to claval commissure; tip slightly bifid. Pro-, meso-, and metasterna blackish brown; pro-, meso-, and metapleura blackish brown except posterior margin of metapleura yellowish brown; supracoxal lobes yellowish brown.

***Hemelytra*:** translucid, extending to tip of abdomen and fully covering abdominal connexivum; constricted at base; inner margin of clavus, basal half and apex of corium blackish brown; clavus with three rows of punctures, one adjacent to scutellum extending along commissure, the other two near suture margin with inner row extending to apex; corium with punctures along suture and apical margins and irregular punctures along R vein, scattered across disc to apex of R+M; membrane with longitudinal dark brown stripe extending from middle to apex, basal half of the stripe thin, widening to form a triangle towards apex.

***Abdomen*:** blackish brown, with semi-erect and decumbent setae.

***Legs*:** yellowish brown, covered with long setae; femora slender and unarmed; first segment of posterior tarsus longer than combined length of distal two segments; distal tarsal segment blackish brown.

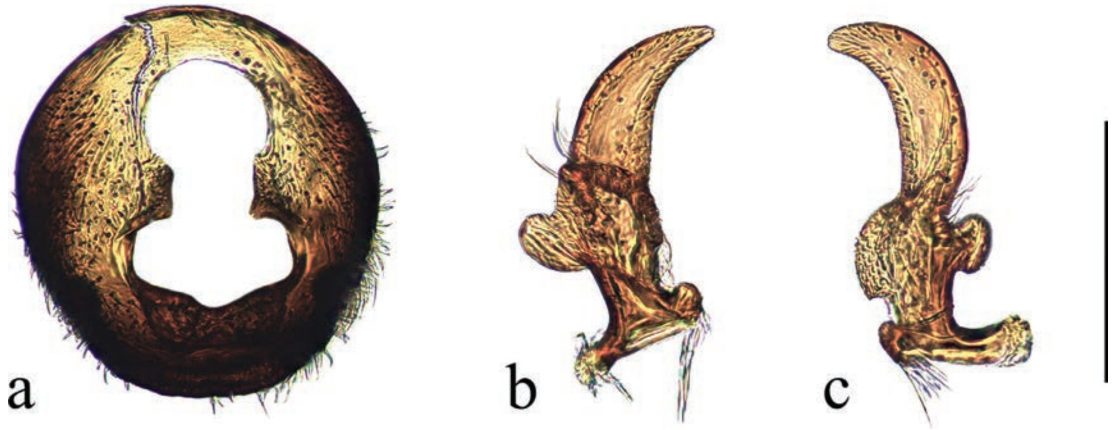

Figure 7. Genitalia of *Ninomimus fuscus* sp. nov. **a** pygophore, in posterodorsal view **b, c** right paramere, in dorsal and ventral view, respectively. Scale bars: 0.2 mm.

Male genitalia (Fig. 7): pygophore covered with suberect setae; apical part of dorsal pygophore opening with anterior margin rounded; distal margin of lateral lobe parallel; and basal part nearly rectangular with a median indentation broadly rounded on posterior margin. Paramere with both dorsal and ventral lobes broadened, with base of dorsal lobe slightly constricted; middle part of blade not apparently broadened and tip of blade sharp.

Measurements (in mm, holotype ♂ / paratype ♀). Body length 3.34 / 3.59. Head length 0.41 / 0.53, width across eyes 0.73 / 0.77; eye length 0.15 / 0.16; eye width 0.20 / 0.22; eye–ocellus space 0.11 / 0.12; interocular space 0.44 / 0.44; interocellar space 0.12 / 0.13; length of antennal segments I–IV respectively 0.18 / 0.17, 0.65 / 0.59, 0.57 / 0.52, 0.61 / ?; length of labial segments respectively 0.39 / 0.39, 0.32 / 0.33, 0.25 / 0.26, 0.25 / 0.27. Pronotum length 0.78 / 0.82; width of anterior margin 0.50 / 0.54; width of posterior margin 0.87 / 0.89; scutellar length 0.30 / 0.31; scutellar width 0.37 / 0.41. Length of hemelytra 2.17 / 2.33; length of corium 1.39 / 1.45; length of claval commissure 0.36 / 0.42; distance of apex of clavus–apex of corium 0.71 / 0.79; distance of apex of corium–apex of membrane 0.80 / 0.87.

Etymology. The species epithet, *fuscus*, is Latin meaning “brown” and is in reference to the new species’ dark-brown body colour, without the thick, dense white pruinosity of its congeners.

Distribution. Only known from the type locality.

Remarks. *Ninomimus fuscus* sp. nov. can be easily distinguished from its two congeners by its shiny and overall blackish-brown body, without a thick white pruinosity, and its clavus and corium completely translucid, while the other *Ninomimus* species show dense, thick, white pruinosity patterns, and the hemelytra are nearly opaque. The body of the new species is more slender than that of its congeners, with a body length-to-width across the eyes ratio exceeding 4.6, while this ratio in *N. flavipes* is < 4.2 and in *N. assamensis* it is approximately 4.4. The pygophore of *N. fuscus* has a rounded anterior margin of the dorsal opening, not rhomboid as in *N. flavipes*; the paramere of *N. fuscus* has the base of the dorsal lobe slightly constricted, and the tip of the blade is sharp, which contrasts with the less constricted dorsal lobe base and rounded blade tip in *N. flavipes*. Since we only examined the photographs of the type of *N. assamensis*, we were unable to compare its male genitalia morphology with those of the other species.

Acknowledgements

We thank Hong Liu (IZAS) and Wenjun Bu (NKUM) for the loan of specimens. We are grateful to Előd Kondorosy (Hungarian University of Agriculture and Life Sciences, Hungary) for sharing the type photographs of *Ninomimus assamensis*. We are grateful to reviewers for their valuable detailed comments on the manuscript.

Additional information

Conflict of interest

The authors have declared that no competing interests exist.

Ethical statement

No ethical statement was reported.

Funding

This study was supported by the National Natural Science Foundation of China (grant no. 31402010), and the Highly Educated Talents Foundation in Nanjing Forestry University (grant no. G2014002).

Author contributions

Conceptualization, CQ Gao and SY Cao; methodology, CQ Gao; software, SY Cao; validation, CQ Gao; formal analysis, SY Cao; data curation, SY Cao; writing—original draft preparation, SY Cao; writing—review and editing, CQ Gao; visualization, SY Cao; supervision, CQ Gao; project administration, CQ Gao; funding acquisition, CQ Gao.

Author ORCIDs

Cuiqing Gao https://orcid.org/0000-0002-0177-5161
Suyan Cao https://orcid.org/0009-0008-4432-234X

Data availability

All of the data that support the findings of this study are available in the main text.

References

Ashlock PD (1957) An investigation of the taxonomic value of the phallus in the Lygaeidae (Hemiptera-Heteroptera). Annals of the Entomological Society of America 50: 407–426. https://doi.org/10.1093/aesa/50.4.407

Barber HG (1956) A new arrangement in the subfamily Cyminae (Hemiptera, Lygaeidae). Proceedings of the Entomological Society of Washington 58: 282.

Bergroth E (1921) Notes on some Cyminae (Hem., Myodochidae). Annales de la Société Entomologique de Belgique 61: 165–168.

Dellapé PM, Henry TJ (2024) Lygaeoidea Species File. Version 5.0. https://lygaeoidea.speciesfile.org [Accessed on 25 Sep 2024]

Distant WL (1901) Rhynchotal notes. XI.—Heteroptera: Fam. Lygaeidae. Annals and Magazine of Natural History (series 7) 8: 464–486. https://doi.org/10.1080/03745480109443351

Esaki T (1950) Iconographia insectorum Japonicorum. Editio secunda, reformata. Hokuryukan Ltd., Tokyo, 1738 pp.

Henry TJ (1997) Phylogenetic analysis of family groups within the infraorder Pentatomomorpha (Hemiptera: Heteroptera), with emphasis on the Lygaeoidea. Annals of the Entomological Society of America 90: 275–301. https://doi.org/10.1093/aesa/90.3.275

Kormilev NA (1955) Notas sobre Lygaeidae neotropicales I (Hemiptera): la subfamilia Cyminae (Stål) en la Argentina. Instituto de Ciencias Naturales, San Miguel 2: 3–8.

Lindberg H (1934) Verzeichnis der von R. Malaise im Jahre 1930 bei Vladivostok gesammelten Heteropteren. Notulae Entomologicae 14: 1–23.

Matsumura S (1913) Illustrated 1000 Insects of Japan. Volume 1. Rhynchota. Tokyo, 183 pp.

Péricart J (2001) Lygaeidae. In: Aukema B, Rieger C (Eds) Catalogue of the Heteroptera of the Palaearctic Region. Volume 4. Pentatomomorpha I. The Netherlands Entomological Society, Amsterdam, 35–220.

Scudder GGE (1957) A revision of Ninini Hemiptera-Heteroptera, Lygaeidae including the description of a new species from Angola. Publicações Culturais da Companhia de Diamantes de Angola 34: 93–108.

Slater JA (1964) A Catalogue of the Lygaeidae of the World. University of Connecticut, Storrs, 1668 pp.

Stichel W (1958) Illustrierte Bestimmungstabellen der Wanzen. II. Europa (Hemiptera-Heteroptera Europae). Published privately, Berlin, 318 pp.

Zheng LY, Zou HG (1981) Lygaeidae. In: Hsiao TY, Ren SZ, Zheng LY, Jing XL, Zou HG, Liu SL (Eds) A Handbook for the Determination of the Chinese Hemiptera-Heteroptera. Volume 2. Science Press, Beijing, 1–114. [in Chinese, English summary]

ZooKeys 1228: 307–313 (2025)
DOI: 10.3897/zookeys.1228.146632

Corrigendum

Addenda and corrigenda: Angus RB, Maté JF, Angus EM, Král D (2024) Towards a revision of the Palaearctic species of *Aphodius* Hellwig, 1798, subgenus *Liothorax* Motschulsky, 1860 (Coleoptera, Scarabaeidae, Aphodiinae). ZooKeys 1207: 205–299. https://doi.org/10.3897/zookeys.1207.117225

Robert B. Angus[1], Jason F. Maté[2], Elizabeth M. Angus[3], David Král[4]

1 Department of Life Sciences (Insects), The Natural History Museum, Cromwell Road, London SW7 5BD, UK
2 c/Henares 16, Velilla de San Antonio, Madrid, 28891, Spain
3 Biomedical Imaging Unit, Level B South Block, Mail point 12, General Hospital, Southampton SO16 6YD, UK
4 Department of Zoology, Faculty of Science, Charles University, Viničná 7, CZ-128 00, Praha 2, Czech Republic
Corresponding author: Robert B. Angus (r.angus@rhul.ac.uk)

Abstract

Corrigenda to the abovementioned paper are given, as well as new data on *Aphodius* (*Liothorax*) *felix* Angus et al., 2024 and *A.* (*L.*) *bellumgerens* Angus et al., 2024

Key words: Corrections, *Liothorax*, new data

Academic editor: Andrey Frolov
Received: 13 January 2025
Accepted: 27 January 2025
Published: 21 February 2025

ZooBank: https://zoobank.org/69913A6D-AD4E-46B9-B7A1-DF6F062A3B30

Citation: Angus RB, Maté JF, Angus EM, Král D (2025) Addenda and corrigenda: Angus RB, Maté JF, Angus EM, Král D (2024) Towards a revision of the Palaearctic species of *Aphodius* Hellwig, 1798, subgenus *Liothorax* Motschulsky, 1860 (Coleoptera, Scarabaeidae, Aphodiinae). ZooKeys 1207: 205–299. https://doi.org/10.3897/zookeys.1207.117225. ZooKeys 1228: 307–313. https://doi.org/10.3897/zookeys.1228.146632

Addenda and corrigenda

Addenda

1. *Aphodius felix* Angus et al., 2024 and *A. bellumgerens* Angus et al., 2024 in Calabria.

Angus et al. (p. 268) mentioned newly acquired living material from Calabria, collected from the mud of a dried-out pool near Villagio Mancusa (39.107°N, 16.641°E). This material was collected by members of the Balfour-Browne Club (a water-beetle study group) in the course of a meeting in Calabria. Much of this material was moribund but karyotypes were obtained from three females. These are shown in Fig. 1, along with material from Campo Felice for comparison. Although identification of the X chromosomes is difficult when only females are available, the sequence of chromosomal sizes and shapes along the karyotype matches those of *A. felix*, but not those of either *A. bellumgerens* or the Sardinian *A. krelli* Angus et al., 2024, when their karyotypes are used as templates. The collecting site is shown in Fig. 2.

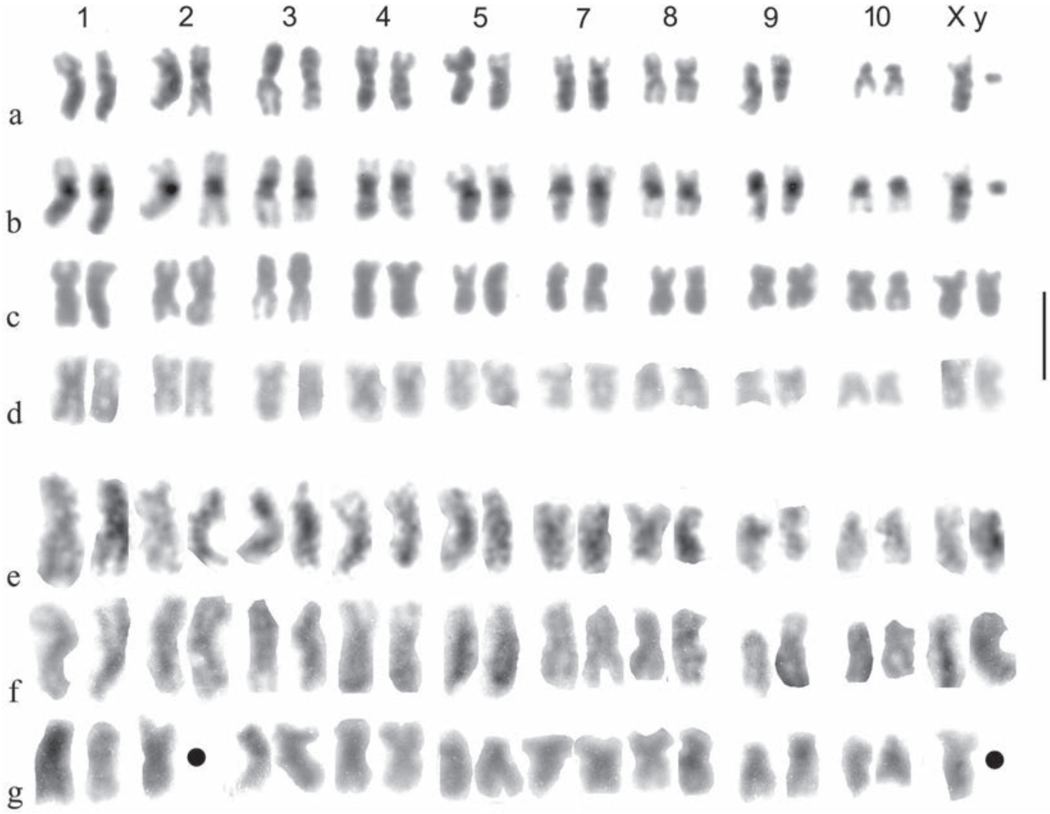

Figure 1. Mitotic chromosomes of *A. felix* Angus et al., 2024, arranged as karyotypes **a**, **b** Campo Felice, ♂♂, **a** Giemsa stained **b** C-banded **c** Campo Felice, ♀, Giemsa stained **d**–**g** ♀♀, Calabria, Giemsa stained **d**, **e** ♀ 2 **f**, **g** ♀4. Missing chromosomes in **g** are indicated by heavy dots. Scale bar: 5 µm.

Figure 2. Members of the Balfour-Browne Club working the bottom of a dried-out pool near Villagio Mancusa. Photo courtesy of Zuqi Mai.

The possibility of *A. bellumgerens* occurring in the extreme toe of Calabria was suggested by Jason Maté after studying material borrowed from the Muséum d'histoire naturelle in Geneva, Switzerland.

We have been able to re-examine two of these specimens, a male and a female, collected by Paganetti. Both specimens were in the R. Petrovitz collection. The female has the data "Calabria/ Sta Christina/ lg Paganetti." and the male simply "Calabria/Paganetti". The aedeagus of the male was glued to the face of the card on which the beetle was mounted, but only the phallobase remained, the parameres and aedeagal tube having been broken off, probably long ago. However, floating the basal piece off the card and clearing it in KOH solution showed that the retracted endophallus was present, as were the two struts which arise from the base of the aedeagal tube. These parts are shown in Fig. 3, with the whole aedeagi of *A. bellumgerens* and *A. felix* for comparison. The endophallus (Fig. 3c), though contracted, is a better size match for that of *A. bellumgerens* (Fig. 3d) than the larger endophallus of *A. felix* (Fig. 3e).

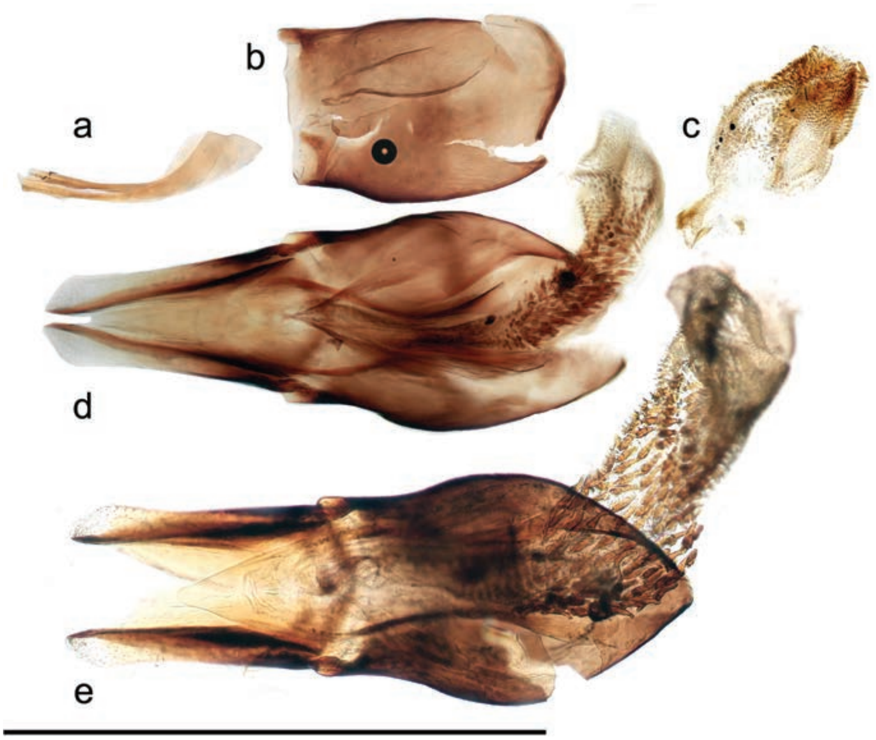

Figure 3. Aedeagi **a**–**c** *A. bellumgerens*, aedeagal fragments from a specimen labelled "Calabria, Paganetti" (MHNG) **a** aedeagal struts **b** phallobase **c** retracted endophallus **d** *A. bellumgerens*, paratype, IT, Sicily, Nebrodi **e** *A felix*, Calabria, Villagio Mancusa. Scale bar: 1 mm.

Any consideration of the beetles from the toe of Italy must address the possibility of Sardinian species being present in view of the close proximity of the Plateau della Sila to Sardinia during the Pliocene. (Foster 2024). This plateau (and its National Park) is adjacent to the Villagio Mancusa locality where the *A. felix* was taken. In the case of subgenus *Liothorax*, the species involved would be *A. krelli* Angus et al., 2024. Fortunately, the shape of the pronotum distinguishes this species from both *A. bellumgerens* and *A. felix*. In *A. felix* and *A. bellumgerens* the sides of the pronotum bulge outwards so that the lateral margin is to some extent obscured in dorsal view, and the pronotal sides appear somewhat rounded (Fig. 4a–d), whereas in *A. krelli* the pronotal sides are less bulging and the lateral margins are visible throughout, giving straighter sides to the pronotum (Fig. 4e). It thus seems unlikely that *A. krelli* occurs in this part of Italy.

Figure 4. Heads and pronota **a** *A. bellumgerens*, holotype, Sicily **b** *A. bellumgerens* ♂, Calabria (MNHG)) **c** *A. bellumgerens* ♀, Calabria (MNHG) **d** *A. felix*, paratype, IT, Campo Felice **e** *A. felix* ♀ 2, Calabria **f** *A. krelli*, holotype, IT, Sardinia. Scale bar: 1 mm.

Although the identifications of *A. felix* and *bellumgerens* presented here appear to be reliable, it would be highly desirable to get better living material, including males, of both species so that totally unambiguous karyotypes could be obtained.

Corrigenda

1. Figs 8, 9. The published figures are from previous manuscript versions and are incorrect and do not match the captions. Corrected versions are given here.

2. p. 245, Fig. 29c. The *A. p. plagiatus*, apparently in China (Nei Mongol), is incorrectly plotted - it should be in Mongolia.

3. p.272, *A. isikdagensis*. Fig. 8c, d is omitted from the list of figures.

4. p. 275. *A. alberti*. Before “Remarks” should be “Etymology. Named after Prof. Alberto Ballerio who collected the type material.”

5. *A. alberti* and “*ballerioi*”. In the initial drafts of this paper we (reluctantly) treated *Liothorax* as a genus and named Alberto Ballerio’s species as

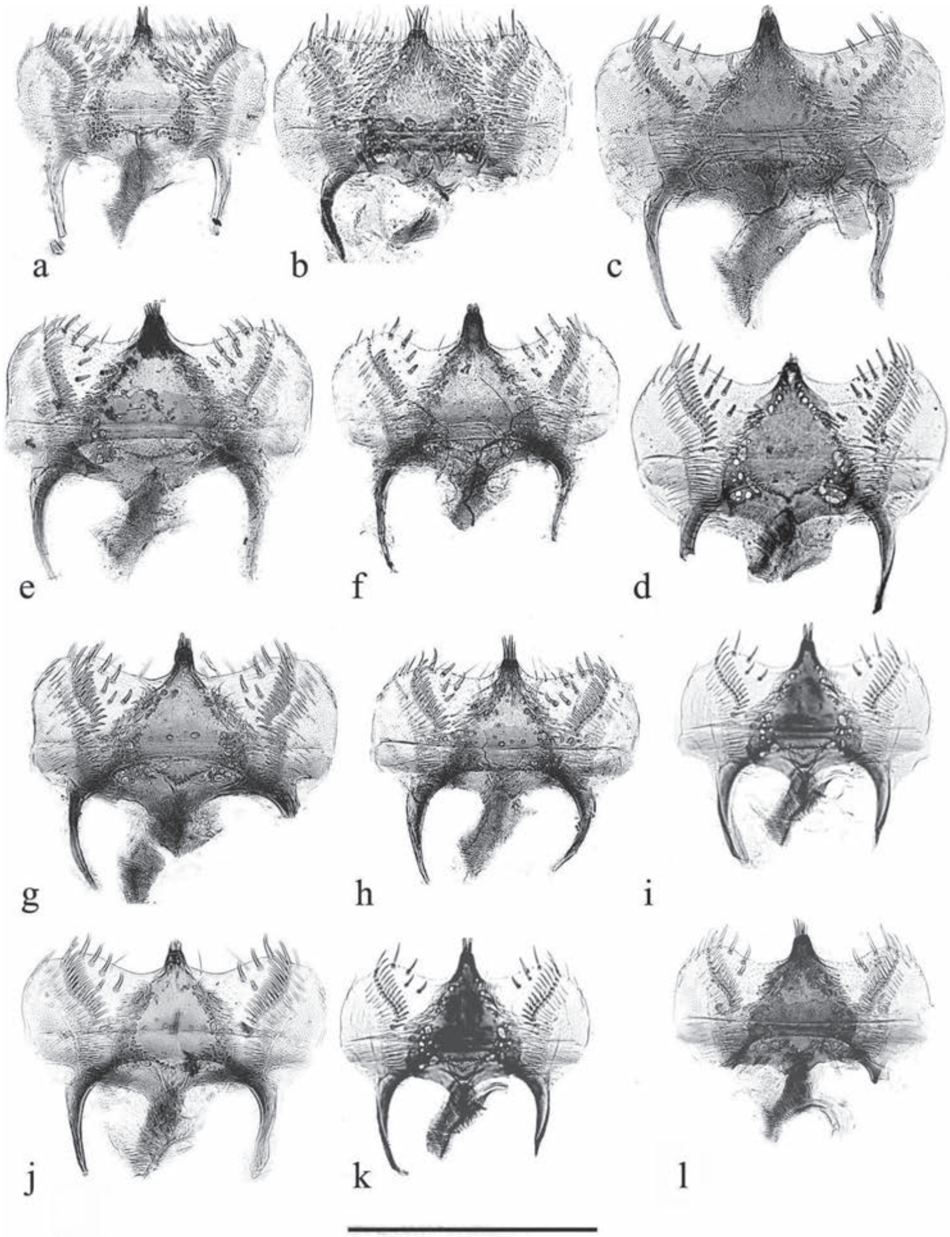

Figure 8. a–**l** epipharynxes **a**, **b** *A. kraatzi*, SV **c**, **d** *A. isikdagensis* paratypes, TR, Çamildere **e**, **f** *A. felix* sp. nov. paratypes **g**, **h** *A. bameuli* sp. nov. paratypes **i** *A. alberti*? AR **j** *A. krelli* sp. nov., paratype **k, l** *A. alberti* sp. nov., paratypes. Scale bar: 0.5 mm.

A. ballerioi. Then Prof. Ballerio cautioned that he did not regard the status of the genera/subgenera of *Aphodius* as stable and suggested using the name *alberti* to avoid future homonymy. In the event, we followed advice from two referees and treated *Liothorax* as a subgenus, so *ballerioi* was unavailable. Unfortunately, not all references were corrected, so *ballerioi* is listed in the captions to Figs 37 and 38 (p. 288) and 39A and B (pp. 289 and 290). This should be corrected to *alberti* here, as well as in any other places we still haven't noticed.

6. In the Acknowledgements Prof. Ballerio is listed as being located in Rome, but it should be Brescia. This is correctly given in the list of Material on p. 207.

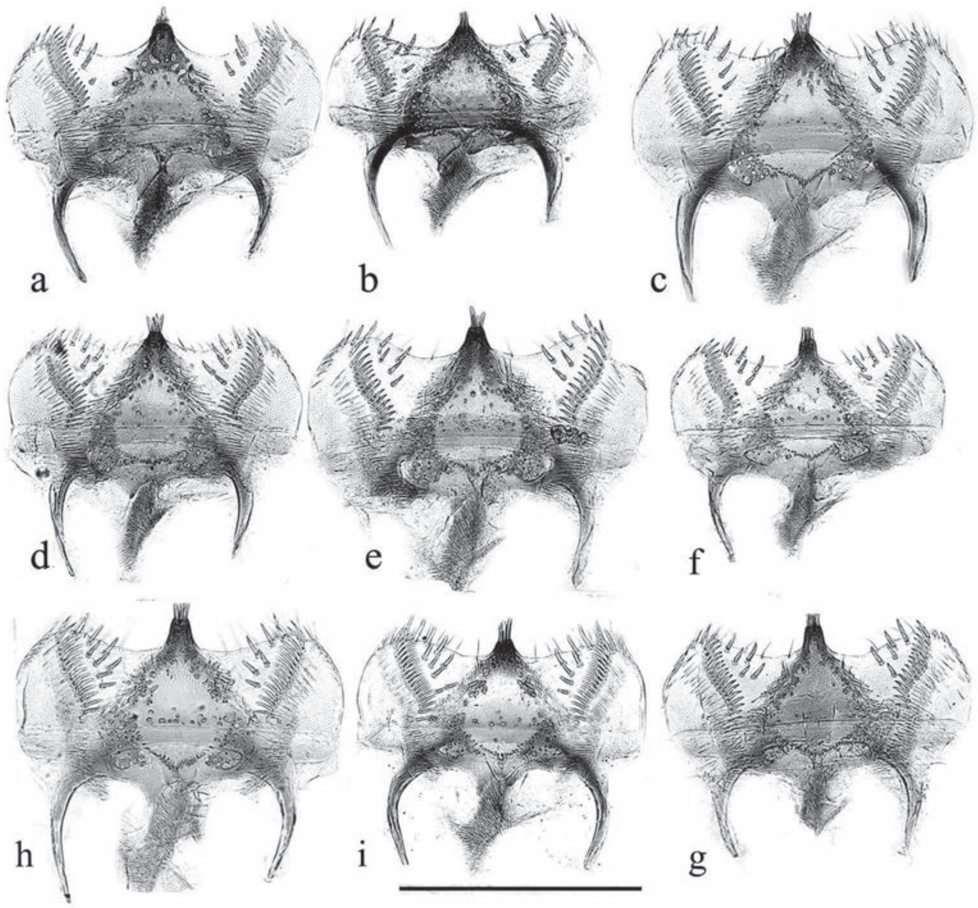

Figure 9. **a**–**i** epipharynxes **a**–**c** *A. niger* **a** SV, Tullgarn **b**, **c** GB, Hampshire, New Forest **d** *A niger*? CZ, Hradec Králové **e** *A. muscorum* HU, Hortobagyi **f**, **g** *A. bellumgerens* sp. nov. paratypes, IT, Piano Battaglia **h**, **i** *A. wilsonae* paratypes, SP **h** El Vellón **i** Manzanares el Real. Scale bar: 0.5 mm.

Acknowledgements

We thank Zuqi Mai for the use of his photograph shown in Fig. 2 and Clive Turner for the living *A. felix* from Calabria.

Additional information

Conflict of interest

The authors have declared that no competing interests exist.

Ethical statement

No ethical statement was reported.

Funding

No funding was reported.

Author contributions

All authors have contributed equally.

Author ORCIDs

Robert B. Angus https://orcid.org/0000-0002-3860-5617
Jason F. Maté https://orcid.org/0000-0002-2505-7113
David Král https://orcid.org/0000-0002-7930-1927

Data availability

All of the data that support the findings of this study are available in the main text.

References

Foster GN (2024) Italy 2024. Latissimus 57: 29–32.